DESIGN AND HYDRODYNAMIC PERFORMANCE OF TRIMARAN DISPLACEMENT SHIPS

by

Junwu Zhang

A thesis submitted for degree of

Doctor of Philosophy

Department of Mechanical Engineering

University College London

1997

ABSTRACT

To meet the demands for increasing the speed and improving the seakeeping behaviour of commercial and naval ships, this thesis investigates a new type of ship configuration - *The Trimaran Displacement Ship*, it features a slender centre hull and two small side hulls. The design methodology and hydrodynamic performance of this new ship concept has been investigated through design studies, model experiments and theoretical analysis. Potential advantages of the trimaran ship are, lower wavemaking resistance at high speed, larger deck area, and improved seakeeping behaviour compared with existing ship types.

Firstly, existing marine vessel types, both monohulls and multihulls, are reviewed with regard to their advantages and limitations. The new trimaran concept and its background is then described from its initiation by a desire of inheriting advantages and avoiding limitations of these existing ship types. Namely, achieving the low resistance of slender monohulls and large deck area of multihulls, whilst eliminating the speed limit of conventional monohulls and the stiff roll motion of catamarans. The review of the trimaran ships design studies shows the potential applications of this new concept in commercial and naval roles.

The feasibility of the new concept and the methodology required for its design are investigated through the concept design studies of.a trimaran fast ferry (Figure 1) and the hull form design for a trimaran model ship (Figure 2) for seakeeping experiments. This provides an initial view on the design procedure and basic design considerations for the trimaran ship. The parametric study in the trimaran ferry design gives the basic parameters for trimaran hull forms.

Hydrodynamic performance of the trimaran ship has been investigated through model experiments and theoretical analysis on seakeeping, resistance, and manoeuvrability. Good agreements between theoretical predictions and model experiments have been achieved. This shows the merit of the computer programs developed during the investigation so they can be used in future trimaran ship designs for hydrodynamic performance assessments. A three dimensional theory is used in the trimaran motion analysis. Roll damping characteristics of the trimaran ship has been examined by including viscous effects in roll damping which can be derived either by simulating damping data from free decay experiments or by direct computation, that has been shown to improve the roll motion predictions. Systematic investigation into the wavemaking resistance of the trimaran ship reveals the relationship between the side hull configuration

and the resistance performance. Wave cancellation effects can be achieved when the side hulls are appropriately located to further reduce the wavemaking resistance of the trimaran ship. A manoeuvrability study concentrated on the effect of the side hulls on the turning ability of the trimaran ship as well as the effect of side hull propulsion.

Following the hydrodynamic analysis of the trimaran ship, the design procedure and general considerations in trimaran ship design distinctive from other ship types are proposed and discussed with particular reference to stability and hydrodynamic performance. Trimaran hull form options are also discussed alongside some other design considerations.

The thesis concludes that the new trimaran displacement ship shows superior characteristics in some hydrodynamic aspects over existing marine vessels, particularly in resistance and seakeeping, and therefore there is no reason why this novel concept can not be translated into real ships.

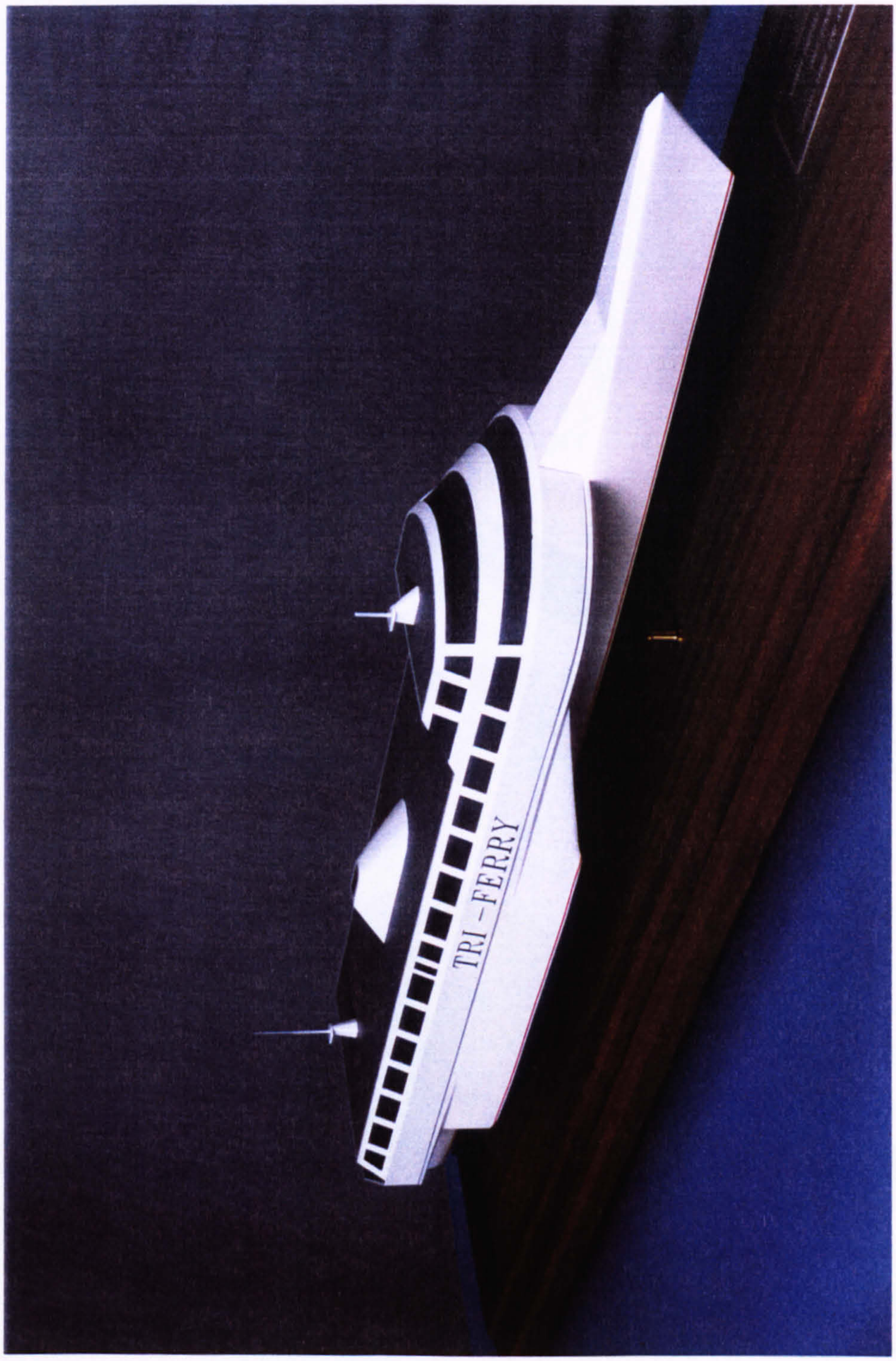

Figure 1 The 38 knot Trimaran Passenger/Car Ferry

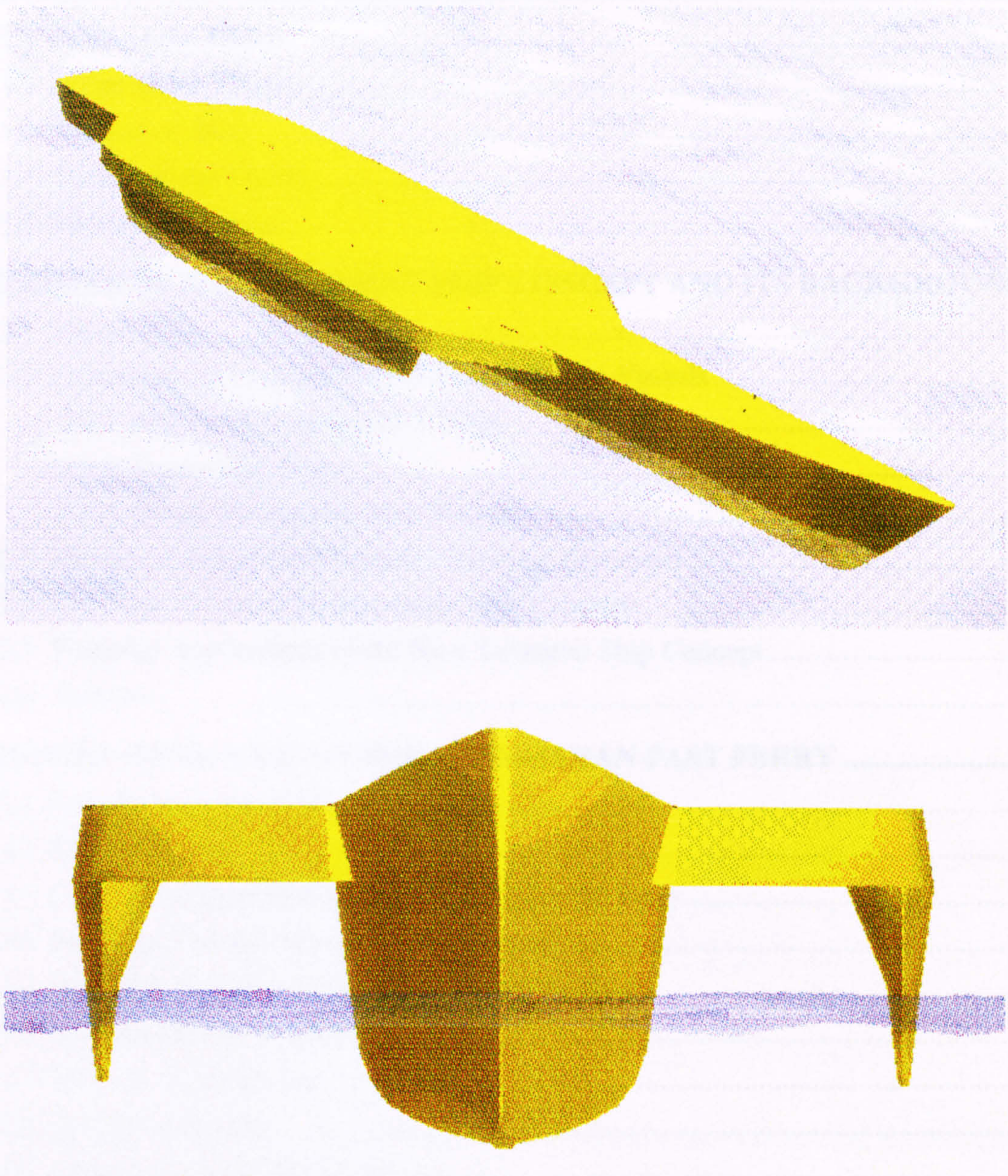

Figure 2 GODDESS model of the 5000t Trimaran Destroyer

CONTENTS

FIGURES

TABLES

ACKNOWLEDGEMENTS

Firstly, I would like to express my sincere gratitude to my first supervisor Douglas Pattison, formerly Professor of Naval Architecture of University College London (UCL), and now a Director in The Director General Surface Ship organisation of Bristol, for the inspiration and guidance he has given to me, which was enhanced when the trimaran introduction paper **(Pattison & Zhang 1994)** was awarded 'The Gold Medal of 1995' by RINA.

Next, I would like to express my sincere gratitude to my current supervisor David Andrews, Professor of Naval Architecture of UCL, not only for his constant encouragement and supervision but also for his patience to grill the details of my every research report and finally this thesis. The contents of three jointly authored papers **(Andrews & Zhang 1995a, 1995b & 1996)** on trimaran ship design considerations have been drawn on in the thesis' text.

In addition, I should like to thank Mr John Hall, Head of Surface Ship Hydrodynamics of DRA Haslar, for the valuable discussions and advice he provided on trimaran hull form design and analysis as well as for the financial support he managed for several of research tasks described in the thesis. I am also very grateful for the support provided by Dr Guoxiong Wu on CFD (Computational Fluid Dynamics) in trimaran seakeeping and wavemaking resistance analysis, valuable advice provided by Professor Roy Burcher on the manoeuvrability aspect, and the assistance by other staff in the Naval Architecture and Marine Engineering Office of UCL.

Finally, I should say the most influential and unconditional support comes from my family, my wife and my daughter, in a way the two side hulls have behaved, have never complained for not being in the centre, but provided the necessary stability to keep the centre hull afloat.

NOMENCLATURE

(a) Roman Symbols

A	mass inertia; area
a	effective aspect ratio of a lift surface
A'_{ws}	side hull waterplane area at wet deck
A_f	ship profile area
A_{jk}	added mass matrix
AP	Aft Perpendicular
A_R	rudder area
A_{wc}	centre hull waterplane area at design WL
A_{ws}	side hull waterplane area at design WL
B	beam on waterline; damping coefficient
B/T	length to draught ratio
B_1	linear roll damping coefficient
B_2	quadratic roll damping coefficient
B_3	cubic roll damping coefficient
B_a	appendage roll damping coefficient
B_{aD}	appendage roll damping due to drag force
B_{aL}	appendage roll damping due to lifting force
BAR	propeller Blade Area Ratio
B_e	eddy making roll damping coefficient
b_{ec}	sectional roll damping coefficient due to eddy making for centre hull
b_{es}	sectional roll damping coefficient due to eddy making for side hull
B_f	frictional roll damping coefficient
B_{jk}	damping coefficient matrix
BM	metacentric height above centre of buoyancy
B_s	side hull beam on waterline
B_w	wavemaking damping coefficient
C	hydrostatic restoring force coefficient
C'_{33}	heave restoring force coefficient due to side hull flare
C^*_{33}	heave restoring force coefficient includes side hull flare effect
C_A	appendage resistance coefficient
C_B	block coefficient
C_{DA}	appendage drag coefficient due to rolling
C_{DE}	eddy making drag coefficient due to rolling

C_{DF}	skin friction drag coefficient due to rolling
C_F	frictional resistance coefficient
C_{FC}	frictional resistance coefficient for centre hull
C_{FS}	frictional resistance coefficient for side hull
C_{jk}	restoring force coefficient matrix
C_L	lift coefficient
C_m	mid-ships coefficient
C_{p00}	prismatic coefficient
C_R	residual resistance coefficient
C_T	total resistance coefficient
C_t	propeller brake coefficient
C_w	wavemaking resistance coefficient
C_{w0}	wavemaking resistance coefficient without wave interaction
C_{wi}	wavemaking resistance coefficient due to wave interaction
D	depth; diameter; and restoring moment
e	error function
E	energy
F	force
F_j	total force and moment acting on ship in waves in *j*th mode
F_n	Froude number
FP	Fore Perpendicular
g	acceleration due to gravity
G	Green function
GM	metacentric height above centre of gravity
GZ	righting lever
H	Kochin function
$H_{1/3}$	significant wave height
H_a	air gap from waterline to wet deck
I	mass moment of inertia
I'	added mass moment of inertia
J	advance coefficient
k	wave number; roll decay coefficient
KB	vertical centre of buoyancy above keel
KG	vertical centre of gravity above keel
KM	height of metacentre above Keel
K_Q	propeller torque coefficient
K_T	propeller thrust coefficient
L	ship length on waterline

L/B	length to beam ratio
L_c	centre hull length on waterline
LCB	longitudinal centre of buoyancy
LCG	longitudinal centre of gravity
L_s	side hull length on waterline
l_s	side hull set back
L_w	wavelength
M_{jk}	mass matrix
N	moment
n	normal vector; propeller revolution
N_H	hydrodynamic moment
N_R	moment induced by side hull resistance differential
N_r	partial derivative of yaw moment with respect to yaw rate
N_{rc}	partial derivative of yaw moment with respect to yaw rate for centre hull
N_{rs}	partial derivative of yaw moment with respect to yaw rate for side hull
N_T	turning moment produced by wing propulsion
N_v	partial derivative of yaw moment with respect to sway velocity
N_{vc}	partial derivative of yaw moment with respect to sway velocity for centre hull
N_{vs}	partial derivative of yaw moment with respect to sway velocity for side hull
P	pressure
PE	effective power
PS	shaft power
P/D	propeller pitch diameter ratio
Q	propeller torque
QPC	quasi-propulsive efficiency
Q_i	rate of ship energy change
R	radius of steady turning
r	position vector; turning (yaw) rate
R_A	appendage resistance
RAO	Response Amplitude Operator
R_F	frictional resistance
R_{FC}	frictional resistance for centre hull
R_{FS}	frictional resistance for side hull
R_n	Reynolds number
R_{no}	Reynolds number associated with roll motion at zero forward speed
rpm	propeller revolution per minute
R_R	residual resistance
R_T	total resistance

R_w	wavemaking resistance
S	ship wetted surface
S_c	wetted surface of centre hull
S_s	wetted surface of side hull
T	ship draught; torque
t	time, tonnes
T_c	centre hull draught
T_e	encounter period of wave
T_{jk}	hydrodynamic force in jth direction due to kth oscillation
T_n	roll period
T_s	side hull draught
T_w	propeller thrust force
T_{wp}	thrust force of port side wing propeller
T_{ws}	thrust force of starboard side wing propeller
u	longitudinal velocity
U_h	horizontal linear velocity
v	lateral velocity
V	ships speed
V_A	propeller advance speed
VCG	vertical centre of gravity
W	steady velocity vector
WL	waterline
X	surge force
x_G	x coordinate of centre of gravity from amidships
x_r	distance from amidships to rudder
X_{RP}	resistance of port side hull
X_{RS}	resistance of starboard side hull
x_s	distance for amidships of the centre hull to that of side hull
Y	sway force
Y_δ	rudder force coefficient
Y_H	hydrodynamic force
Y_r	partial derivative of sway force with respect to yaw rate
Y_{rc}	partial derivative of sway force with respect to yaw rate for centre hull
Y_{rs}	partial derivative of sway force with respect to yaw rate for side hull
y_s	distance from central line of a side hull to that of centre hull
Y_v	partial derivative of sway force with respect to sway velocity
Y_{vc}	partial derivative of sway force with respect to sway velocity for centre hull
Y_{vs}	partial derivative of sway force with respect to sway velocity for side hull

Ⓜ ship length to volume of displacement ratio $(L/\nabla^{1/3})$

(b) Greek Symbols

α attack angle of a lift surface

μ ship's heading

μ_v coefficient of dynamic viscosity

Λ tuning factor

∇ ship's volume of displacement, vector differential operator

Δ ship's displacement

λ rudder sweep angle of quarter-chord line

δ rudder angle

Φ total velocity potential

$\tilde{\Phi}$ total unsteady velocity potential

$\bar{\phi}$ steady velocity potential

ϕ_0 potential of incident waves

ϕ_7 potential of diffraction waves

ϕ_j radiation velocity potentials of six modes (j = 1...6)

η_0 incoming wave amplitude; propeller open water efficiency

η_j motion amplitudes of six modes (j = 1...6)

θ phase angle

θ_h heeling angle

θ_r rolling angle

σ source strength

σ_t cavitation number

ω frequency, encounter frequency

ω_0 wave frequency

Ψ yaw angle

γ specific gravity

(c) Acronyms

ASNE	American Society of Naval Engineers
CASD	Computer Aided Ship Design
DNV	Det Norske Veritas
DRA	Defence Research Agency
DTp	Department of Transportation
GODDESS	Government Of Defence DEsign System for Ships
IMO	International Maritime Organisation
ITTC	International Towing Tank Conference
NARG	UCL's Naval Architecture Research Group
NES	Naval Engineering Standard
RINA	Royal Institute of Naval Architecture
SNAME	Society of Naval Architecture and Marine Engineers
UCL	University College London
WEGEMT	West European Graduate Education Marine Technology

(d) Subscripts

(Applicable to all symbols used within the thesis)

c	centre hull
cross	cross structure
s	side hull
sup	superstructure

CHAPTER 1

INTRODUCTION

1.1 Aims of the Thesis

The demands for increasing the speed and improving the seakeeping behaviour of commercial and naval ships has led to a rapid development of advanced marine vehicles during the recent decades. They include: the Small Waterplane Area Twin Hull (SWATH) ship, the fast catamaran ship, the Surface Effect Ship (SES), the planing craft, the Hydrofoil ship, and the Hovercraft ship. These advanced marine vehicles can achieve either higher speed or better seakeeping performance compared with the conventional monohull ship of equivalent size. However, these achievements are usually accompanied with some undesirable features or penalties such as, limited ship size due to displacement sensitivity for the planing craft; increased resistance in calm water for the SWATH ship; stiff roll motion in catamarans; or structure fatigue problems due to employing light aluminium materials **(WEGEMT 1989)**. Most importantly, they all demand higher building costs compared with the conventional monohull ships. It is, therefore, desirable to find a new type of ship configuration which would possess those advantages of the advanced marine vehicles but with minimal penalties.

This desire initiated a research program at University College London, as introduced in this thesis, into a new type of ship configuration - The Trimaran Displacement Ship, aimed to achieve higher speed and superior or equivalent seakeeping performance compared with monohull ships **(Pattison & Zhang 1994)**. The major feature of the proposed trimaran concept is a very slender central hull which will result in substantial reduction in wavemaking resistance, particularly at high speeds. Two additional small slender side hulls of each less than 5% of the total displacement, placed under the outer edge of the cross structure, to provide transverse stability and seakeeping and meet normal damage stability requirements.

The main potential advantage of the new concept is that the main hull may be optimised to the lowest resistance but not at the expenses of seakeeping and stability which will be achieved satisfactorily by the assistance of the two small side hulls. Furthermore, the three hull configuration will provide a larger deck area for flexible layout. It is anticipated that the increased cost over the conventional monohull ship due to the two additional small side hulls may be reasonable low compared with other types of advanced marine vehicles because it needs neither special building materials nor special propulsion equipment and arrangements.

However, conventional naval architecture practice tends not to build a very slender displacement ship with a length beam ratio beyond the normal range **(Kennell 1995)**. The trimaran concept is a radical departure from this conventional wisdom in having a

very slender hull form. The introduction of the two outriggers makes the flow around the ship more complicated compared with the monohull ship and so is the interaction between the hulls. These would certainly make the hydrodynamic performance of the trimaran ship different from any existing displacement vessels. Extensive research work is therefore necessary to identify any unforeseen effects of this radical departure.

The main objective of this research work is to perform an initial feasibility study to validate the potential of this new trimaran concept as well as to identify any possible flaws which may be associated with the new concept. To achieve this, methodologies required for the analysis of the hydrodynamic performance of and the design of the trimaran ship are developed and presented in the thesis.

Though the configuration of the trimaran concept provides great flexibility compared with the monohull ship, the benefit of a trimaran ship can only be achieved when the advantageous configurations of the central hull and the side hulls are found. The role of a vessel would also effect the choice of configuration. The final goal of this thesis is to provide some insight views on the configuration considerations for the trimaran displacement ship.

1.2 Scope of the Thesis

The analytical object in this work is the *'Sea-going Trimaran Displacement Ship'*, shortened as the *'Trimaran Ship'* or simply the *'Trimaran'* throughout the thesis. Trimaran itself is not a new concept as there are already some existing trimaran craft, such as trimaran sailing boats, trimaran yachts, and trimaran river boats, etc. By using the term *'Sea-going Trimaran Displacement Ship'*, it is intend to distinguish this new trimaran concept from those existing trimaran craft. The *'Sea-going'* distinguishes it from the restricted operation of existing small trimaran craft; and the *'Displacement'* trimaran means it is supported wholly by the static buoyancy of the hulls and requires no dynamic or powered lift to support its weight at any speeds. Thus the research results would not be applicable to any other existing trimaran craft or any dynamically supported multihull vessels. More specifically, two seagoing trimaran displacement ships have been designed and used here for analytical work; they are, a 1000 tonne cross-channel fast trimaran passenger/car ferry and a 5000 tonne trimaran frigate/destroyer (**Zhang 1992 & 1993**).

The research work undertaken and described in this thesis emphasises theoretical analyses and experimental studies of the hydrodynamic performance of the trimaran ship. Priority is given to validating the seakeeping performance to reveal the effects of the

trimaran configuration. The configuration of a trimaran displacement ship would also affect the wavemaking resistance as the three hulls generate a much more complex wave system compared with the monohull ship. Therefore, the wavemaking resistance analysis is a necessary part for the investigation into the trimaran ship to find the effects of the side hull configuration on the total resistance. A preliminary analysis on the turning ability of a trimaran ship is also included in the thesis to provide an initial view on this matter.

Essential considerations in the design of a trimaran ship are discussed through the thesis. These are based on the experience gained during the trimaran concept design studies, including the design procedure, choice of the hull forms, and intact and damage stability assessment.

The investigation into the effects of different trimaran configurations on hydrodynamic performance is concentrated on the side hull configurations. The predominant parameters are, the side hull displacement ratio to the total displacement of the trimaran, and the location of the side hulls.

The trimaran concept opens a wide range of new research areas for naval architects which is unlikely to be covered by a single project. The immediate areas of investigation, not covered by this thesis but which can be considered as essential future research topics for the development of the trimaran ship, would be: analysis of fluid loads on the trimaran ship particularly on the side hulls, structural responses, effects of trimaran configurations on its machinery systems, and cost analysis, etc.

1.3 Method of Study

There are three basic elements in this trimaran ship study, *Design, Experiment,* and *Theoretical Analysis*. The design is to explore the basic considerations in the choice of trimaran configurations and provide subject trimaran ship designs to enable analytical and experimental work to be undertaken. The theoretical analysis is to investigate the performance characteristics of trimaran ships. The experimental work is to validate the new trimaran concept and validate the theoretical predictions for the hydrodynamic performance of the trimaran ship.

Design Study

The objective of the thesis, as described in Section 1.1, is to validate the new trimaran concept by investigating the performance of the trimaran ships and the design considerations to be taken into account in trimaran design. Design study is an essential method used throughout the research work. The primary parameters of the trimaran configuration have been studied through designs to provide realistic data for experiments and theoretical analysis. Described in this thesis are the concept design of a fast passenger/car ferry and the hydrodynamic design of the trimaran hull form used in the model experiments and theoretical analysis. The concept design procedure for trimaran ships has been developed and presented in the thesis.

Experimental Study

At the early development stage of a new ship concept, it is always accompanied by extensive model experiments to get reliable performance data, such as the development work on SWATH ships, SES ships and fast catamarans. Although the modern numerical methods and computers provide powerful tools for theoretical predictions, it is still necessary to carry out model experiments on the hydrodynamic performance of the trimaran ship to achieve assurance of the viability of the new ship concept, as well as to validate the theoretical analysis tools. According to the scope of the research, as described in Section 1.2, the priority in the hydrodynamic model experiments was the seakeeping behaviour of the trimaran ship. The measurements taken were heave, pitch and roll motions of the trimaran models at various speeds and headings in regular waves. Free decay experiments have been conducted because it is a very efficient method to provide data for the roll motion analysis, as the roll prediction is still the weakest section of the current seakeeping theory. Self propelled trimaran models controlled by autopilot were used in the experiments. Resistance experiments were also conducted for some of the model configurations as well as turning ability tests. All the experiments were conducted by DRA Haslar **(DRA 1995)** for the trimaran model derived from the design study **(Zhang 1993)**.

Theoretical Analysis

The successful development of the two dimensional strip theory has made it the most commonly used technique for analysing ship motions for monohull and multihull ships **(Salvesen et al. 1970)**. Good agreement exists between strip theory predictions and experimental data for some catamarans, SWATH ships, and SES ships **(Nordenstrom et al. 1971) (McCreight 1987)**. Since the trimaran ship consists of three hulls and the side hulls and the central hull are normally of different sizes, unlike the twin-hull ships with

two equal length and form demi-hulls, a three dimensional theory is more suitable than a 2D strip theory for predicting the hydrodynamic forces and motions, particularly, for asymmetric motion predictions. A three dimensional method (**Wu & Eatock Taylor 1989**) has been adapted for this theoretical modelling. The velocity potential of the fluid around the trimaran hull surfaces is computed using the boundary element technique to derive the added mass and added damping coefficients. The 3D model allows the interactions between centre hull and the side hulls to be taken into account in the motion calculations. Since the wave potential theory alone is inadequate for roll motion predictions (**Lloyd 1989**), the roll damping characteristics of the trimaran ship have been investigated by analysing free decay test data using a nonlinear technique (**Haddara & Cumming 1992**). A theoretical method for direct computation of roll damping has been developed and is presented in the thesis.

For the computation of resistance, slender ship assumptions (**Wehausen 1973**) are used for the calculation of the wavemaking resistance components of the three hulls to investigate the effects of side hull configurations on wavemaking resistance. The approach for analysing turning ability is a combination of theoretical and empirical methods (**Jacobs 1964**), treating the trimaran ship as a combination of a slender hull with two fixed fins whilst ignoring the interaction between the hull and the fins.

1.4 Format of the Thesis

The results of the investigations and the underlying methodology are presented in the thesis in the following sequence:

Chapter Two of the thesis describes the concept of the new trimaran and its background. The review of the limitations of existing marine vessels shows the potential advantages of the new trimaran displacement ship concept. The trimaran designs carried out at UCL suggested this potential and also reveal new areas of research which needs to be accomplished to validate this concept.

Chapter Three describes the initial design study for a Fast Trimaran Car/Passenger Ferry. The aim is to reveal the basic design procedure and considerations for trimaran displacement ships, covering the initial sizing process, resistance prediction, structural design, and general arrangement. The design focused on finding appropriate configurations for the centre hull and the side hulls for the trimaran ship. Comparisons with other types of ships are also discussed.

As it was felt that the major uncertainty associated with this new concept would be its seakeeping performance, particularly the transverse motion of the hull in seaways, much of the thesis concentrates on trimaran seakeeping performance. Chapters Four to Six describe the theoretical studies and model experiments on the motion behaviour of the trimaran ship.

Chapter Four presents the experimental work on predicting the hydrodynamic performance of a trimaran ship. In order to obtain realistic predictions for trimaran ship performance, a detailed hull form design has to be conducted. The considerations studied for the hull form design are presented in detail. Two sets of trimaran ships were designed for the experiments. Five sets of model configurations were tested in regular waves at various speeds and headings for the measurement of heave, pitch, and roll motions. Other experiments, including resistance tests and manoeuvring tests, are also described.

Chapter Five presents the numerical method and results of theoretical seakeeping predictions for the trimaran models and comparisons with experimental results. Good agreements have been achieved between the predictions and the experiment data. Comparisons between the trimaran ship and the monohull ship for seakeeping performance are also presented.

Chapter Six describes the analytical work on the roll damping characteristics of the trimaran ship. Two methods for estimating roll damping coefficients for trimaran ships are presented, the estimation of the coefficients from free decay experiment data, and the theoretical prediction of the coefficients directly from the hull form configurations of the trimaran ship. The effects of nonlinear roll damping are analysed and discussed.

Chapter Seven studies the wavemaking resistance of the trimaran ship. The methodology for the prediction of trimaran wavemaking resistance is described. The investigation focuses on the effects of changes in the trimaran configuration on its wavemaking resistance.

Manoeuvrability was another unknown area for the trimaran displacement ship and Chapter Eight describes the study into its manoeuvrability characteristics. The major concern centred on the turning ability at speed, as the directional stability of a trimaran is enhanced by the two additional narrow side hulls. The chapter explains the numerical model produced to estimate the turning motion of the trimaran ship, the methods used to estimate the derivatives of the motion equation, and the turning ability of a trimaran ship using rudders as well as using the wing propellers fitted to the side hulls.

General discussions of design considerations and procedures for trimaran displacement ships, based on the experience gained from the design studies, are presented in Chapter Nine. A stability procedure is proposed for initial sizing and conceptual design process which is distinguished from that for conventional monohull design. Other considerations and design options covering various aspects in trimaran ship design for improving its performance are also discussed.

Finally, Chapter Ten presents the principal conclusions of the study and recommendations for future research work on this novel ship concept.

1.5 Glossary of Terms

Associated with the new trimaran concept, there are some new technical terms in the trimaran design and analysis which need to be clarified as they can not be found in the existing literature. This section summarises the definitions and explanations of these new technical terms as used in the following chapters. More detailed explanations can be found in the relevant chapters.

Trimaran

Triple hull displacement ship consists of a slender centre hull, two small side hulls, and a cross structure. It is restricted to the triple hull seagoing displacement ship configuration in this thesis.

Centre Hull

The slender main hull at the centre line of a trimaran ship contributes the majority of the buoyancy of the ship.

Side Hull

Two small outriggers on either side of the centre hull of a trimaran ship.

Cross Structures

The box structure connecting the centre hull and the two side hulls.

Side Hull Displacement Ratio

The percentage of displacement in one side hull to the total displacement of the ship.

Wet Deck

The exposed under deck of the cross structure between the hulls.

Air Gap

The distance between the deep displacement still waterline and the wet deck of the cross structure of a trimaran ship.

Side Hull Setback

The distance between the fore perpendicular of the centre hull and the fore perpendicular of the side hulls.

Side Hull Span

The distance between the centre line of the centre hull and the centre line of a side hull.

Side Hull Flare

The flare of a side hull, mostly at the inner side of the side hull above the design waterline, to compensate for the waterplane area losses of the other side hull due the heel of the ship to enable stability requirements to be met.

CHAPTER 2

TRIMARAN DISPLACEMENT SHIP CONCEPT AND ITS BACKGROUND

2.1 Introduction

As described by **Pattison & Zhang (1994)**, the development of the trimaran sea-going displacement ship concept is based on:-

- The idea that a slender monohull ship would produce less wavemaking resistance than a more conventional ship form.
- The experience gained in the development of other existing multihull vessels including some triple hull craft.

This chapter introduces the new trimaran concept by reviewing the merits and limitations of the other types of marine vehicles, and by reviewing the development of the triple hull craft. This showed that the idea of using the slender hull to increase the speed of the monohull ship would naturally lead to the trimaran concept and the limitations of the existing multihull vessels would also lead to the trimaran concept as one of the solutions.

Having introduced the background, the concept of the trimaran displacement ship is then explained followed by discussions of its potential advantages over existing ship types in the areas of resistance, seakeeping, stability, and layout.

The related activities of trimaran designs carried out at University College London (UCL) are also briefly reviewed to demonstrate the potential of the new concept and to illustrate its possible naval and commercial applications.

2.2 Limitations of Existing Displacement Marine Vessels

2.2.1 Monohull Displacement Ships

A monohull displacement ship is a single hull which is supported by static buoyant lift and requires no dynamic or powered lift to support its weight at any speed. Today, Monohull displacement ships represent all but a small fraction of both commercial and naval ships in service because of their desirable features: high payload carrying efficiency, ruggedness and simplicity, scope for growth, and low building cost. However, the attraction of the monohull ship leads to some undesirable characteristics **(Graham 1985)**:

- *Limited top speed*

  Monohulls have free buoyancy lift and require small propulsion power to move slowly. But, due to the nature of wavemaking resistance, power requirements increase rapidly with speed and few existing displacement monohull ships exceed a speed of 30 knots. Higher speed for a displacement monohull ship requires either a longer hull or a very high power to weight ratio. In either case, a speed of 40 knots appears to be an upper practical limit for a monohull frigate/destroyer **(Graham 1985). Oossanen (1989)** gave a similar speed limit for a monohull displacement ship at a Froude number (Fn) value of 0.5. This is because at these speeds the hull length is less than one bow wave length and the hull attains an unfavourable bow-up running trim with a high bow wave. Efforts had been spent to use a broad transom stern and flat buttocks to minimise this unfavourable trim and the height of the bow wave, but, the improvements are very limited. The most effective way to increase the speed of a monohull ship and minimise the required installed power at these speeds is to have a longer waterline length. **Parsons (1897)** went a long way toward this in 1895 with an extremely slender monohull, *Turbina*, which was 30.48 metres long and only 2.74 metres beam. It achieved 35 knots (Fn = 0.89) and was also the first vessel fitted with a steam turbine. More recently, in late 1940s, the 14.3 metres *Piquant* had a beam of 2.0 metres and reached speeds of over 20 knots (Fn = 0.87) **(Farrar 1989).** These have demonstrated that a longer slender hull can break the speed limitation of the monohull. However, the concept of these very slender crafts was not extended to any large seagoing ships because they would lack adequate transverse stability.

- *Sensitivity to sea state*

  A monohull ship of small size is also very sensitive to the sea state due to its short length and large waterplane area. This severely impairs operability of the monohull ship in rough seas. Considerable research has been devoted to improving the seakeeping performance of the monohull ship by varying the hull parameters **(Bales & Cummins 1970) (Lloyd 1991).** Improvements are modest if the size of the ship is not significantly increased. **Kennell, White & Comstock (1985)** showed this by designing a seakeeping monohull ship using modern seakeeping theory and compared it with a conventional monohull ship with the same payload. They showed that a monohull ship driven by seakeeping performance had to be 40% greater in length and 70% greater in displacement than that of the payload driven monohull.

These facts show that to significantly ease the speed and operability limitations of a monohull ship demands a longer hull. However, a longer hull would result in an increased displacement as one has to increase the beam of the ship to satisfy the stability

requirement, and this would demand higher power. So the issue is how to satisfy stability requirements without increasing the beam and the displacement as would be the case for a slender monohull.

2.2.2 Catamaran Ships

Catamaran is a name given to the twin-hull displacement ship and has a history of more than 400 years. Catamarans were considered second best to the monohull ships because their resistance qualities in the low speed range were much poorer than those of monohulls until the recent development of the modern fast catamarans **(Fry & Graul 1972) (Alaez 1989).** The modern fast catamaran ships have been attracting increasing attention in recent years because of their potential for large deck area, great roll stability, and the possibility of achieving higher speeds. The higher speed achieved is largely due the deployment of the light weight materials which presented an opportunity for great weight saving. The most effective of the fast catamarans so far is the wavepiercer catamaran SeaCat designed and built by INCAT in 1990. This 74 metres long passenger/car ferry with speeds of over 35 knots was then the largest catamaran ever built **(Jane's 1991).** The catamaran ferry has proved to be economically very successful and has attracted enormous attention world wide.

However, apart from the success and advantages of the fast catamaran ships, some limitations described by **Alaez (1989)** still remain:-

- The poor hydrodynamic feature of large total resistance at low speed due to the increased wetted hull surface.
- Uncomfortable ship motions limit the use of current designs on open water routes.

and also:-

- Structural fatigue problems resulted from the cross deck structure between the demi-hulls and machinery compartments due to the use of light weight materials.
- Requirements for extra fire protection due to the use of the light materials for hull structures compared with the steel structures.

When the SeaCat wavepiercing catamaran came in operation in the cross Channel service, the review of the operational experience issued by the INCAT designer (**Hercus**

1991) acknowledged some of the above limitations still existing even for the very successful modern fast catamaran:-

> *'The vessel's ride did not live up to public expectation and there was much adverse publicity attached to the incidence of seasickness.'*
>
> *'Cracking has also been encountered in the superstructure and in way of the superstructure mountings due to global deformation of the hull structure.' The 'hull structure is globally strong enough but it deflects under load and this deflection causes local problems in the superstructure and mounts.'*

This review of the limitations of the catamaran ships does not undermine the success of the fast catamarans. The question raised here is: is there any way to inherit the advantages of the catamarans - large deck area, possibility of high speed due to slender hulls, and great transverse stability, and at the same time, to overcome the limitations of excessive roll stiffness, and the problems caused by using light weight materials?

2.2.3 Small Waterplane Area Vessels

The small waterplane area vessels, particularly, the Small Waterplane Area Twin Hull (SWATH) ships, have been developed rapidly since its first appearance more than two decades ago. The first true SWATH, the *Kaimalino*, was designed in the USA and went to sea in 1973 **(Lang et al. 1974)**. A comprehensive review of the SWATH development history can be found in a paper by **Betts (1988)** and is not detailed further here. The primary attraction of the SWATH concept is its superior seakeeping performance compared with other displacement hull forms of equivalent size, which allows the SWATH ships to maintain higher speed in high sea states. **Kennell et al. (1985)** showed that a monohull needed to have 30 percent more displacement to achieve a SWATH ship's level of seakeeping performance in the North Atlantic all year round. If account is taken of the operability at high speed in rough seas, this percentage is increased further. Other advantages of SWATH include large deck area, high large-angle stability, good low-speed manoeuvrability, and low underwater noise.

The advantages of the SWATH concept are not attained free of charge. The unique configuration responsible for so many of its attributes also leads to a number of limitations **(Gore 1985)**. The principal limitations compared with other types of displacement ships are:-

- Very sensitive to weight changes due to its small waterplane area.

- Lower speed in calm water due to large wetted surface area.
- Higher building and operation costs due to greater structural complexity and weight.
- More void spaces in struts and demi-hulls.

Though the SWATH concept is aimed to improve seakeeping performance and not intended to compete with other displacement ships on speed in calm water, the above limitations have restricted the concept from a wide range of applications.

It is of interest to look at the evolution of the O'Neill Hull Form (OHF) concept originated by **O'Neill (1986)**. The OHF is a tri-strut small waterplane area ship that has the majority of its buoyancy concentrated in a centre hull. This promises to give better stability and operability in high seas than both monohulls and SWATH ships. The first proposed hull form had a small waterplane section shape for each of the three hulls as in Figure 2.1(a). The subsequent study and model tests **(Davis & Jones 1987)** revealed some flaws of the O'Neill hull form, among them were:-

- Overall resistance was excessive compared with the monohull and SWATH ships.
- Displacement was too great for the total waterplane area. The payload fraction and growth margin were too small.

The excessive overall resistance was due to increases in both wavemaking resistance and frictional resistance. The excessive wavemaking resistance of the OHF was due to the relatively large and long outboard hulls, as the displacement of the outboard hulls is over 18% of the total displacement, which resulted in adverse wave interaction effects. The deeper draft of the OHF resulted in a much greater wetted surface area compared with an equivalent monohull and resulted in a much greater frictional resistance. Hence, **Davis & Jones (1987)** suggested a configuration of the OHF without outboard hulls and just outboard struts as in Figure 2.1(b), because the *'outboard hulls are too costly in power compared to the advantages they provide in roll accelerations... to justify their inclusion in a design'*. This made the OHF concept one step closer to the trimaran concept introduced in this thesis, since the outriggers were no longer small waterplane area hulls.

Further study on exploring the wave cancellation effects of the OHF concept by **Wilson & Hsu (1992)** found out that the majority of the contribution to the wavemaking resistance of the OHF arose from the centre body and the centre body-centre strut interactions. They suggested that the centre body-centre strut combination be replaced by a tapered centre hull, with a trapezoidal cross section shape, as shown in Figure 2.1(c). It was claimed a reduction of 30% in wavemaking resistance due to this change at the speed

range above 24 knots. This improvement of the O'Neill hull form made it a step closer to the new trimaran concept.

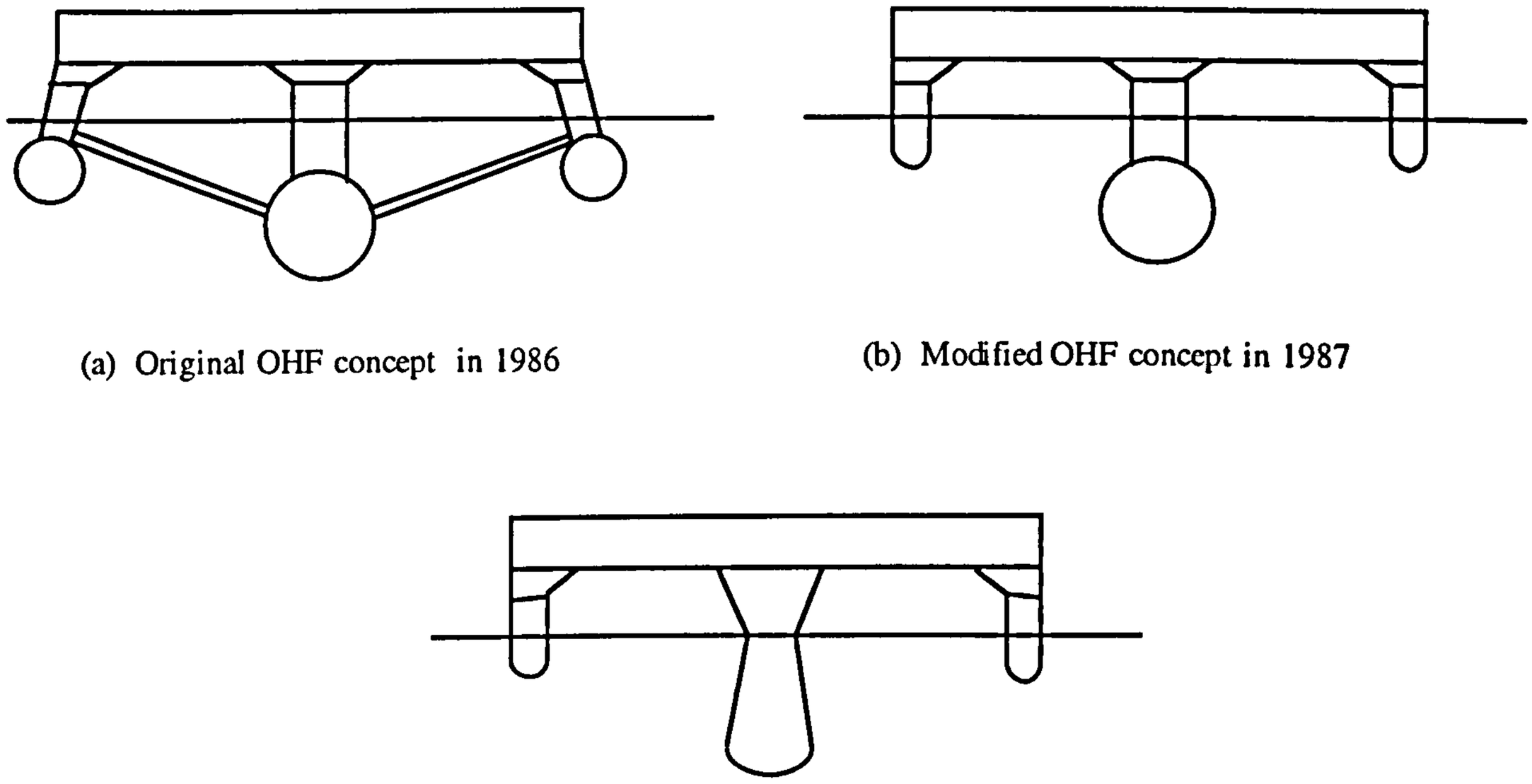

(a) Original OHF concept in 1986

(b) Modified OHF concept in 1987

(c) Wave Cancellation - The new OHF in 1992

Figure 2.1 The evolution of the OHF concept

The **Wilson & Hsu's (1992)** study did not make any proposals to reduce the excessive frictional resistance of the OHF. The most effective way to achieve this would be to reduce the wetted surface area of the submerged hulls. This can be achieved by reducing the draft of the centre hull and the length of the outer hulls if permitted. With this modification, the new OHF concept would become identical to the trimaran concept introduced in this thesis as shown later in Figure 2.7. The trimaran would have less resistance compared to the OHF concept.

2.3 History of Triple Hull Vessels - Existing Trimarans

The first recorded appearance of the word 'Trimaran' was about half century ago in a news report about a wind-sailing trimaran boat in 1949 **(Oxford 1986)**. As a technical term , it was used for the first time in a report on the **Engineering (1959)** to describe *'the trimaran configuration, that is a main hull and two outriggers'*. However, the triple hull craft had existed long before that. One of the earliest forms of seagoing vessel was the outrigger canoe originating in Indonesia **(Hornell 1946)**, with its slender main hull derived from a hollowed tree trunk, and widely spaced and even more slender side hulls as shown in Figure 2.2.

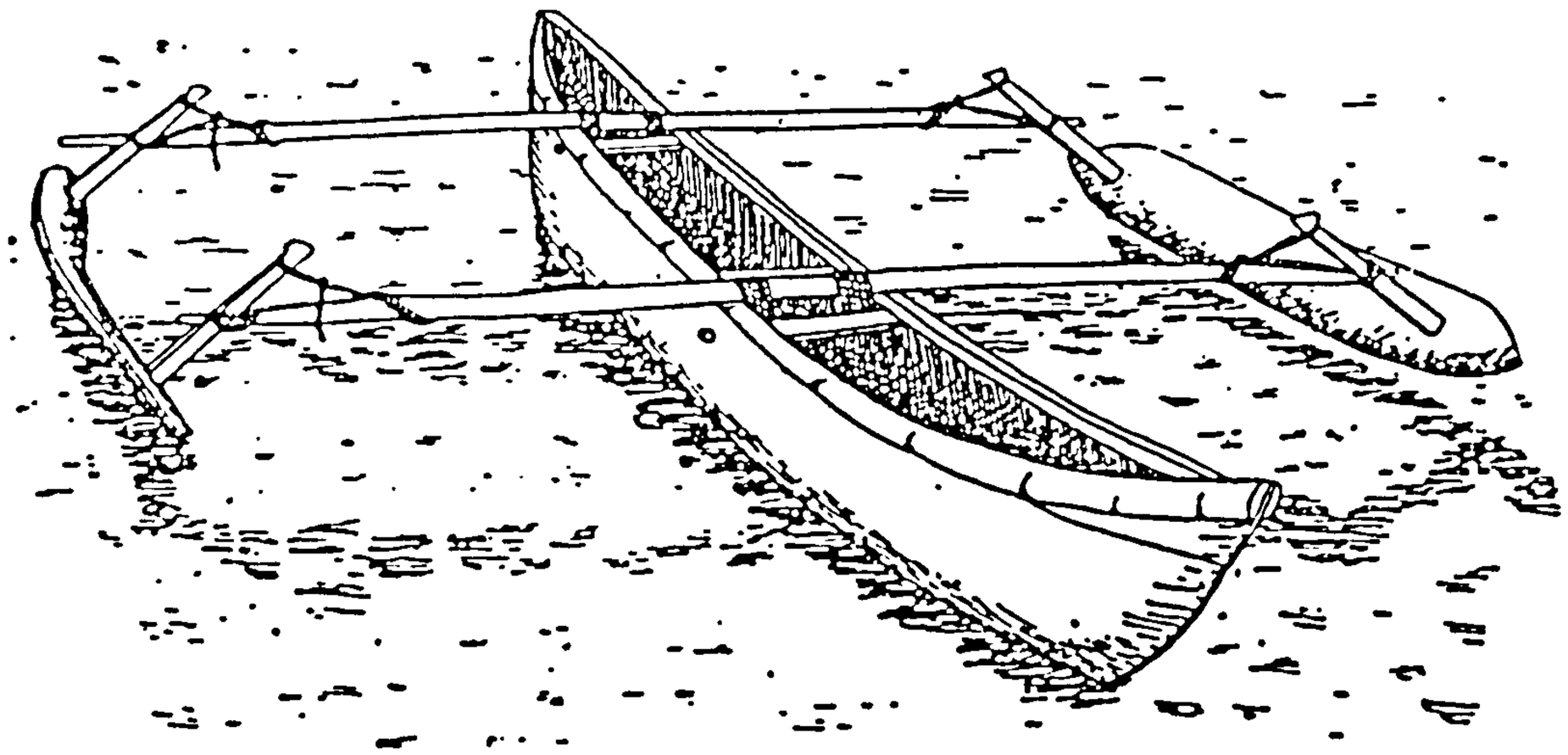

Figure 2.2 An African outrigger canoe of Indonesian Affinity, Dar-es-Salaam

More than two centuries ago, the drawing of a Triple Vessel named *Edinburgh* about 70 feet long was presented as an invention by Patrick Miller in 1787 **(Woodcroft 1848)**, which consists of three hulls of almost the same size, driven by wind sails and man-powered wheels. Figure 2.3 is the original drawings of the elevation, plan, and section views of the proposed triple vessel. The principle properties of *Edinburgh*, claimed by the author were:

- The mechanism of the wheels made it possible for the vessel to sail when there is no wind
- The small draught of the triple hulls made it suitable for shallow river or canal navigation.

- The vessel would be able to sail at a speed of fifteen to sixteen miles a hour which was an outstanding speed for a sail boat at the time.
- The transverse stiffness improved the stability.
- The transverse stiffness made the heel of the vessel inconsiderable when upon a wind, which was a great advantage for a sailing vessel.

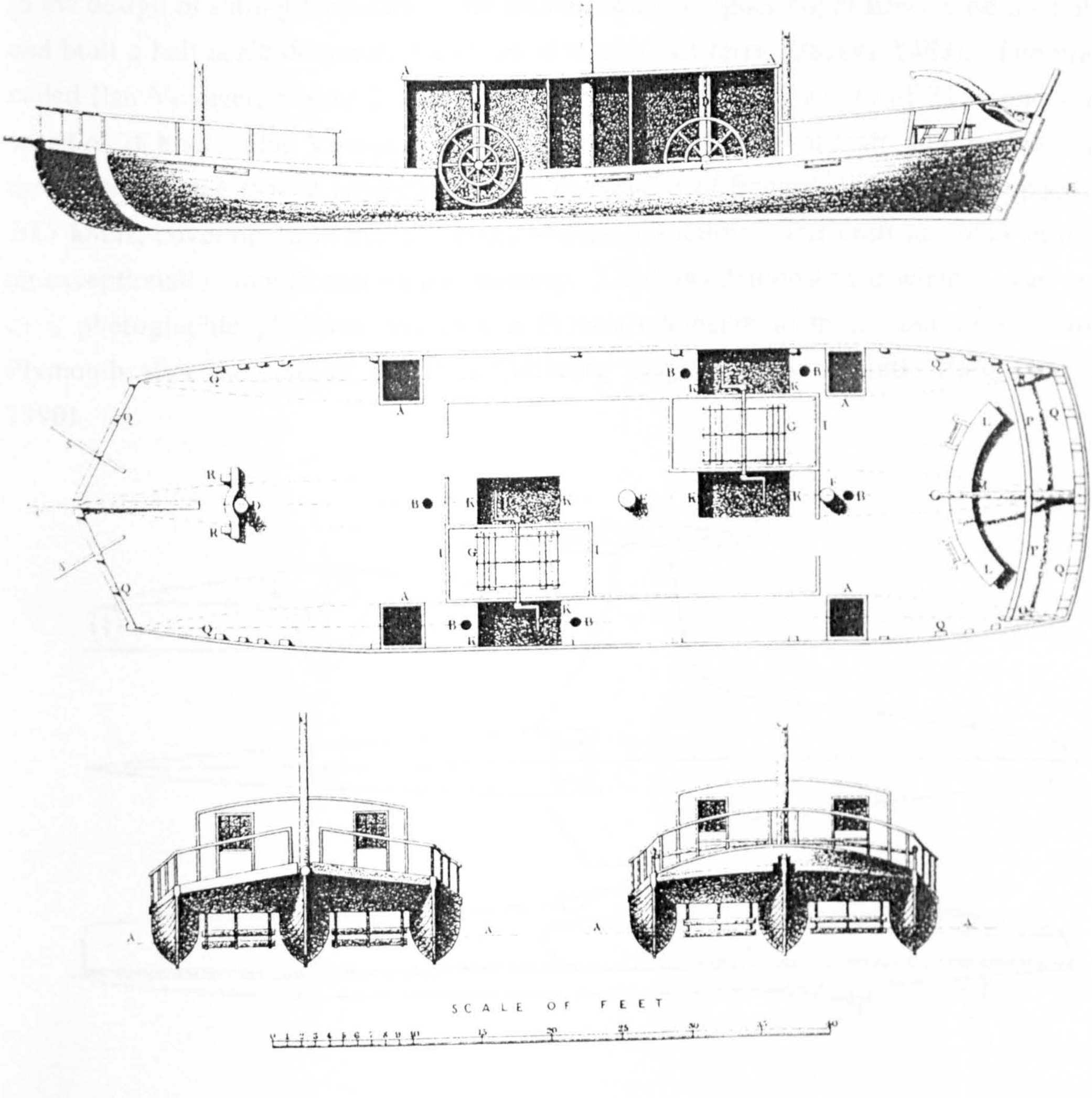

Figure 2.3 Triple hull sailing ship EDINBURGH

Of the above advantages, the most important one the triple vessel *Edinburgh* had was an increased speed compared with other sail vessels. However, it must be noted that there is a fundamental difference between the *Edinburgh* concept and the modern trimaran

concept investigated in the thesis: the speed increase of the former is because its transverse stiffness allows it to have more sails than other sail boats, and the latter is due to the decrease in resistance. However, it was a mystery why this boat was never built.

Over the decades, the trimaran form has been developed by the designers of offshore racing yachts into the fastest long distance sailing vessels ever seen. One of the leaders in the design of sailing trimarans is the Bristol-based designer Nigel Irens, who designed and built a half scale demonstrator of his idea of a fast ferry (**Farrar 1989**). The craft, called Ilan Voyager, Figure 2.4, displaces only 3.4 tonne on a length of 21m, and for a speed of 28 knots. Ilan Voyager proved to be a very fuel-efficient craft, and in 1990 won the trophy for the fastest powerboat circumnavigation of Britain at an average speed of 20.7 knots, covering 1568 nautical miles without refuelling. The craft has also showed an exceptionally smooth motion and stability. This was demonstrated when it was used as a photographic platform and took a French television team far out to sea from Plymouth after the start of the 1988 Carlsberg Single-Handed Atlantic Race (**Farrar 1990**).

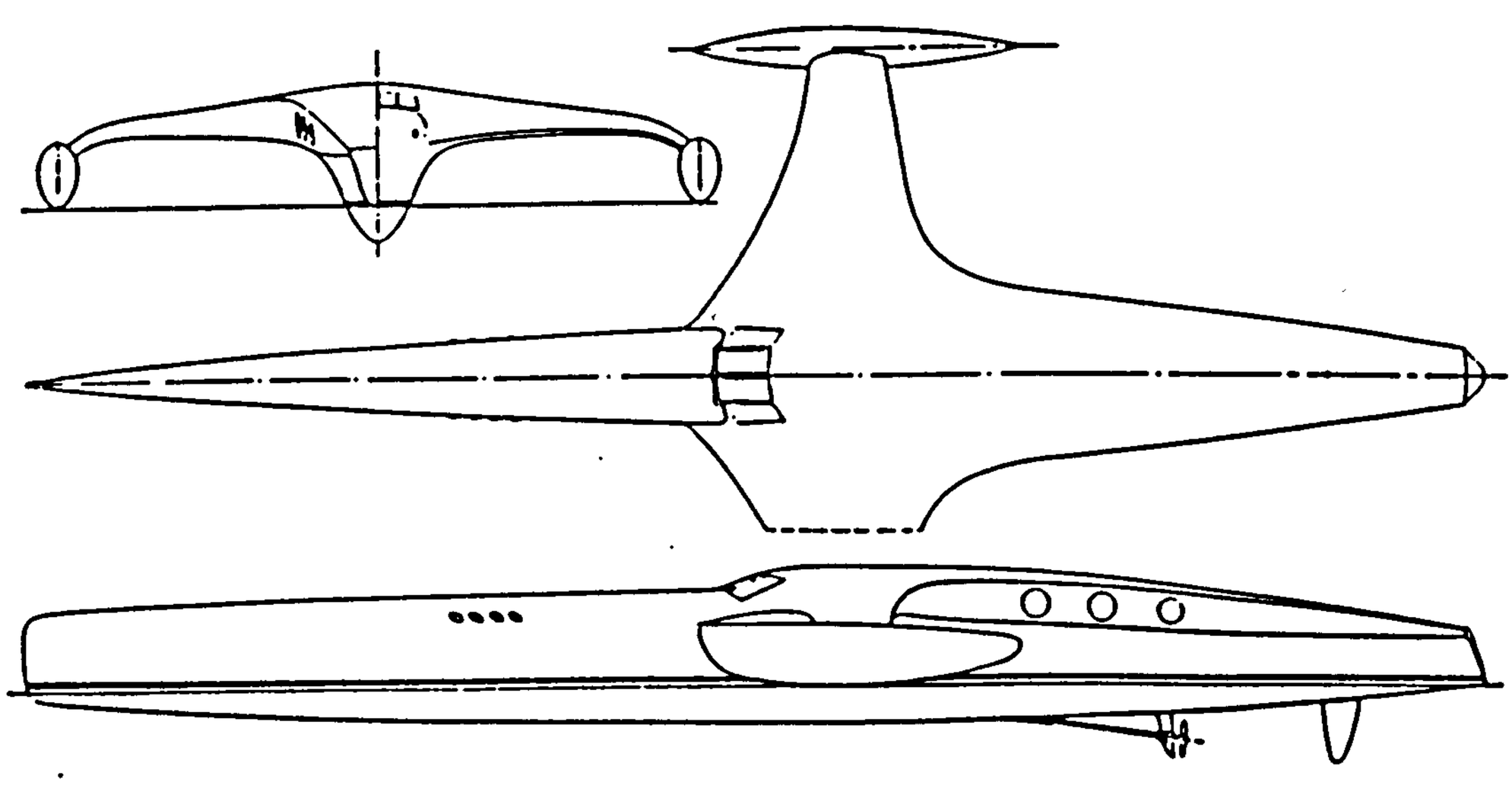

Figure 2.4 The 21m boat Ilan Voyager

More recently, a trimaran river passenger craft was developed by Griffon Hovercraft Ltd (**Gifford 1995**) for use in the River Thames. The purpose of adopting trimaran hull form for the craft was to achieve low-wash. A 12 seat version was built in 1993 and the design

study for a proposed 60 passenger version was presented in 1995. Figure 2.5 is the 60 passenger version of the ferry. It was claimed that low wash had been achieved and proved by experiments and the subsequent operation of the 12 seat ferry in the River Thames. It did not prove to have any advantages on powering and resistance. This, as the figure shows, may due to the relatively fat outriggers which would produce considerable added resistance to offset the benefit gained from the slender central hull. Had the outriggers be smaller or thinner, lower resistance and lower wash would have been achieved to further demonstrate the superiority of the hull form.

Figure 2.5 60 passenger ferry by White Horse Ferries Ltd

However, the existing triple hull craft and these proposed triple hull vessels have showed and suggested the potential of this hull form in reducing resistance and improving seaworthiness. Irens concept of a slender monohull stabilised by two side hulls of very low displacement was introduce to the MSc Ship Design Exercise at UCL in 1989 by Pattison with the proposal to design the first sea-going trimaran ship (**Bastisch & Peters 1990**). A similar idea had also been proposed by John Hall working at DRA Haslar on radical ways to reduce surface ship propeller noise. Hall suggested using tractor propellers working virtually in open water, mounted on the fore ends of the side hulls of a slender trimaran (**Hall 1988**).

2.4 The New Trimaran Displacement Ship Concept

Summarising the limitations of the existing ships types as discussed in the previous sections, the following measures are seen as desirable to exceed these limitations and improve the performance of marine vessels, if achievable:-

- to reduce the wavemaking resistance and exceed the top speed limits of monohull ships
- to reduce wetted surface area of the submerged hulls to reduce the frictional resistance of twin-hull ships
- to improve seakeeping performance, particularly to reduce the transverse stiffness and accelerations compared with catamaran ships
- to use steel materials for the hull structures to eliminate the fatigue problems associated with light weight materials and to reduce costs compared with the catamaran and SWATH ships.

One of the most effective ways to achieve these, particularly the low wavemaking resistance, is to use a very slender monohull ship. It has been known theoretically and experimentally that if a displacement vessel has a waterline beam of only approximately 6 percent of its length, the vessel makes hardly any waves **(Farrar 1990)**, and the resistance is almost entirely composed of surface friction. This was demonstrated by the slender boat *Turbinia* **(Parsons 1897)** a long time ago. But, a slender monohull has two distinct flaws; there is not much space in the hull for the payload of a sea-going ship since the hull is too narrow, and it lacks sufficient transverse stability.

One way to solve the space problem is to add a wider box structure on top of the narrow hull to provide space for the payload as shown in Figure 2.6, but the transverse stability of the ship would be even worse as the centre of gravity would be higher. Nevertheless this ship does have some advantageous features. Firstly, it would achieve higher speed compared with the conventional monohull as the wavemaking resistance would be much lower. Secondly, as the slender hull is much longer than an equivalent displaced catamaran, the vertical motion of the ship would be reduced compared with the catamaran and the less transverse stiffness would also result in some reduction in roll acceleration. Finally, the ship would be more structurally efficient than the catamaran and SWATH ship, in that it would be quite sensible to use steel material for the main structure. This would eliminate the structural problems associated with the light material

necessary for fast catamarans, and it would lack the demanding prying loads which drive up the structural weight of SWATH ships.

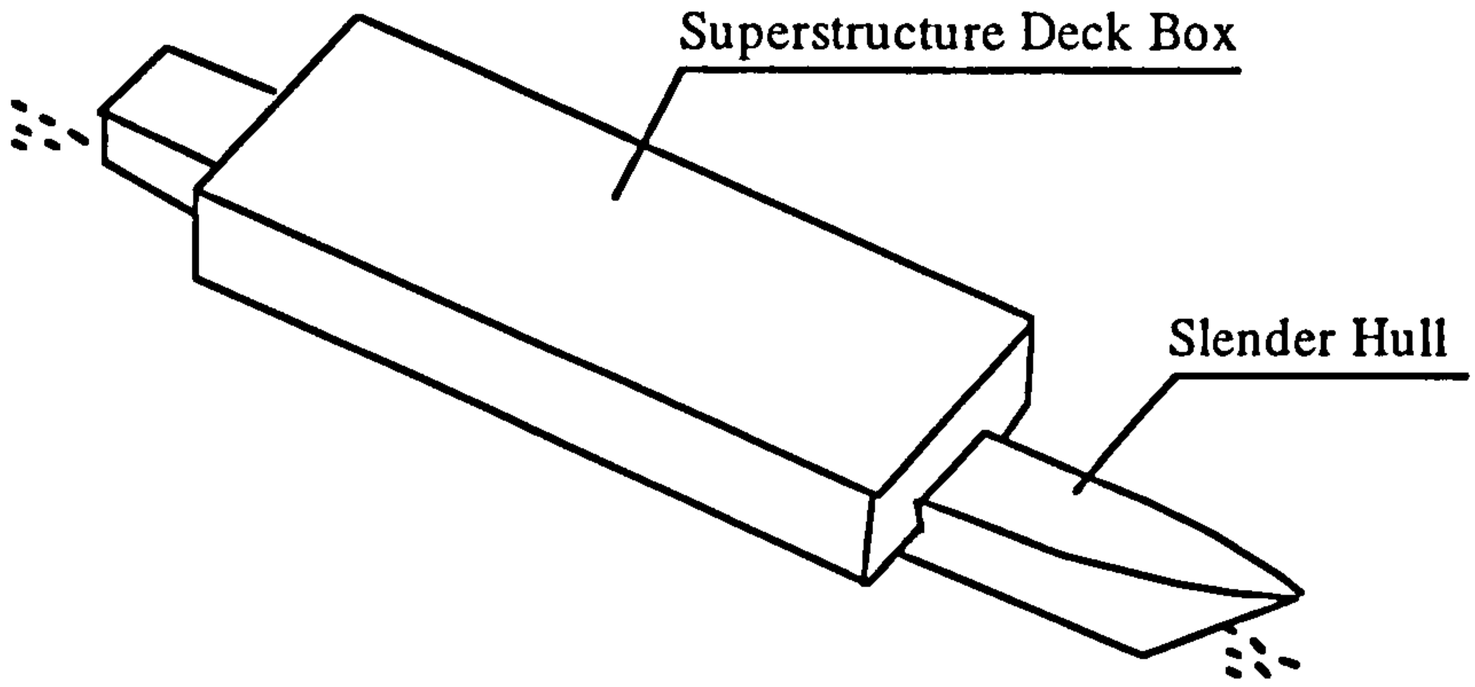

Figure 2.6 Idea of a slender monohull

However, a solution to the problem of transverse stability in the slender monohull must be found to make the idea feasible. One of the solutions proposed by Pattison and described subsequently in a paper **(Pattison & Zhang 1994)** is to apply the Irens idea of using two small outriggers to provide extra waterplane areas to ensure the slender monohull meets the stability requirements. The idea proved to be remarkably successful when it was first applied to a student frigate design as a subject for the UCL Ship Design Exercise as part of the MSc in Naval Architecture **(Bastisch 1992)**. It was found to have advantages in the areas of ship layout, survivability, and powering, with no obvious penalties. This has also led to several other ship types designed using the same concept which showed a wide range of possible applications of the concept. This is discussed in the next section.

This new concept is defined as the trimaran sea-going displacement ship and is shown in Figure 2.7. Its major feature is an extremely slender centre hull with a length-beam ratio above 14 which provides more than 90 percent of the total buoyancy of the ship. Two slender side hulls of about 30-40 percent of the centre hull length each of which provides less than 5 percent of the total displacement of the ship but double the transverse waterplane inertia thereby meeting the requirement for intact and damage stability. The centre hull and the side hulls are connected by a cross-structure supporting the superstructure which provides useful deck area and volume.

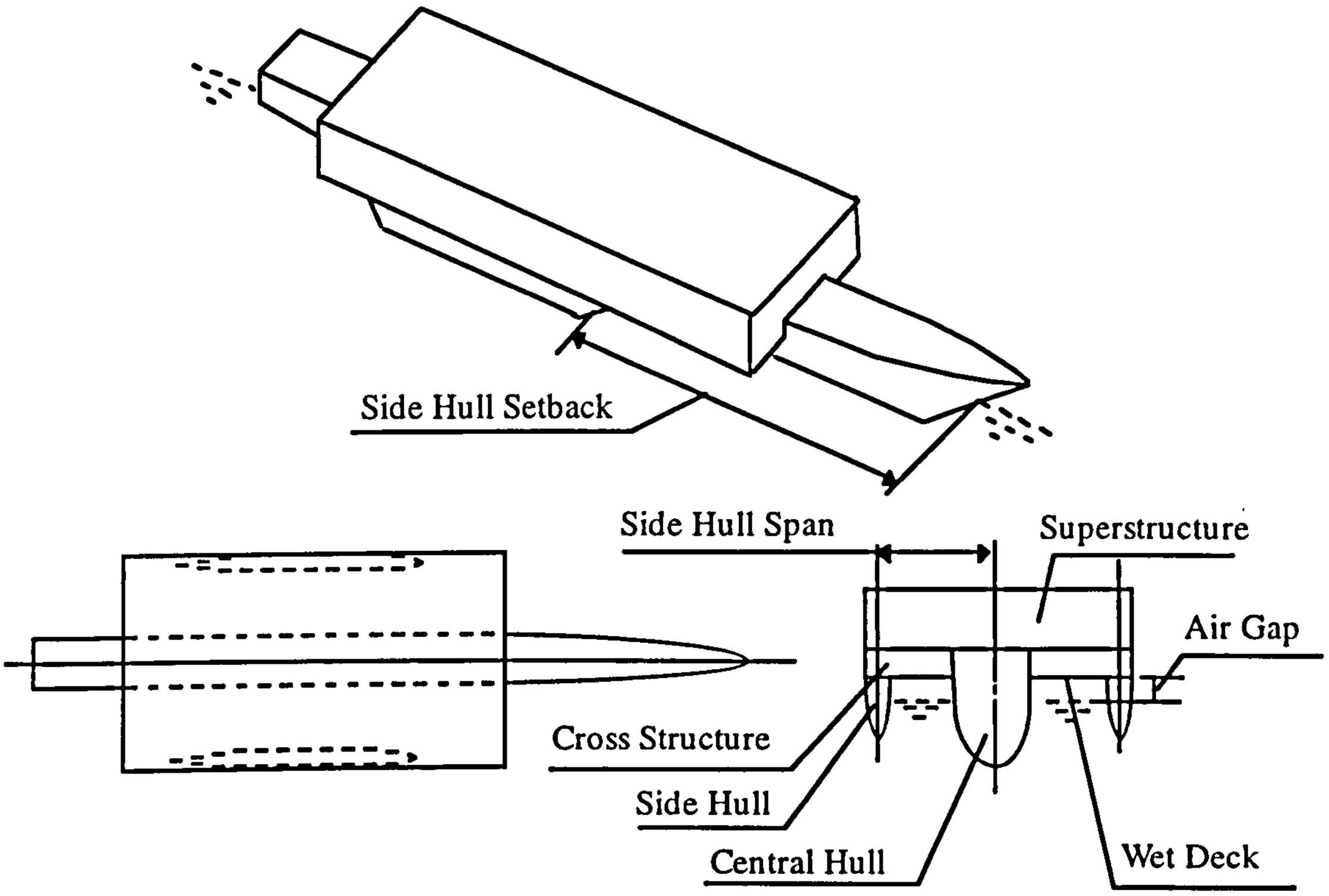

Figure 2.7 The trimaran ship concept

Having defined the concept of the new trimaran configuration, the possibilities of achieving the goals set at the beginning of this section can now be considered.

Lower resistance at high speed

At slow speeds, where skin friction dominates, the shorter monohull with less wetted surface is advantageous, but at higher speeds where wavemaking is more important the slender trimaran form would be less resistful. The Lloyds Sirius enquiry (**Lloyds Register of Shipping 1988**), compared the resistance of various hull shapes for high speed naval ships, and Figure 2.8 taken from that reference has the addition of predictions for two 2642 tonne trimaran designs, giving a band of possible trimaran predictions. The lower trimaran curve is for an 'Ilan Voyager' arrangement with side hulls clear of the water, and shows the gains that are possible with a single slender hull; the upper curve shows the effect of side hulls designed to meet the requirements for damage stability (each side hull is 5% of total displacement). This curve includes an arbitrary 10% addition for wave interference (it will be shown in Chapter 7 that the

wave cancellation effects may result in negative interference in certain speed ranges for some side hull configurations). At higher speeds the trimarans have lower resistance than monohulls. The length to beam ratios and displacements of these monohulls are listed in Table 2.1.

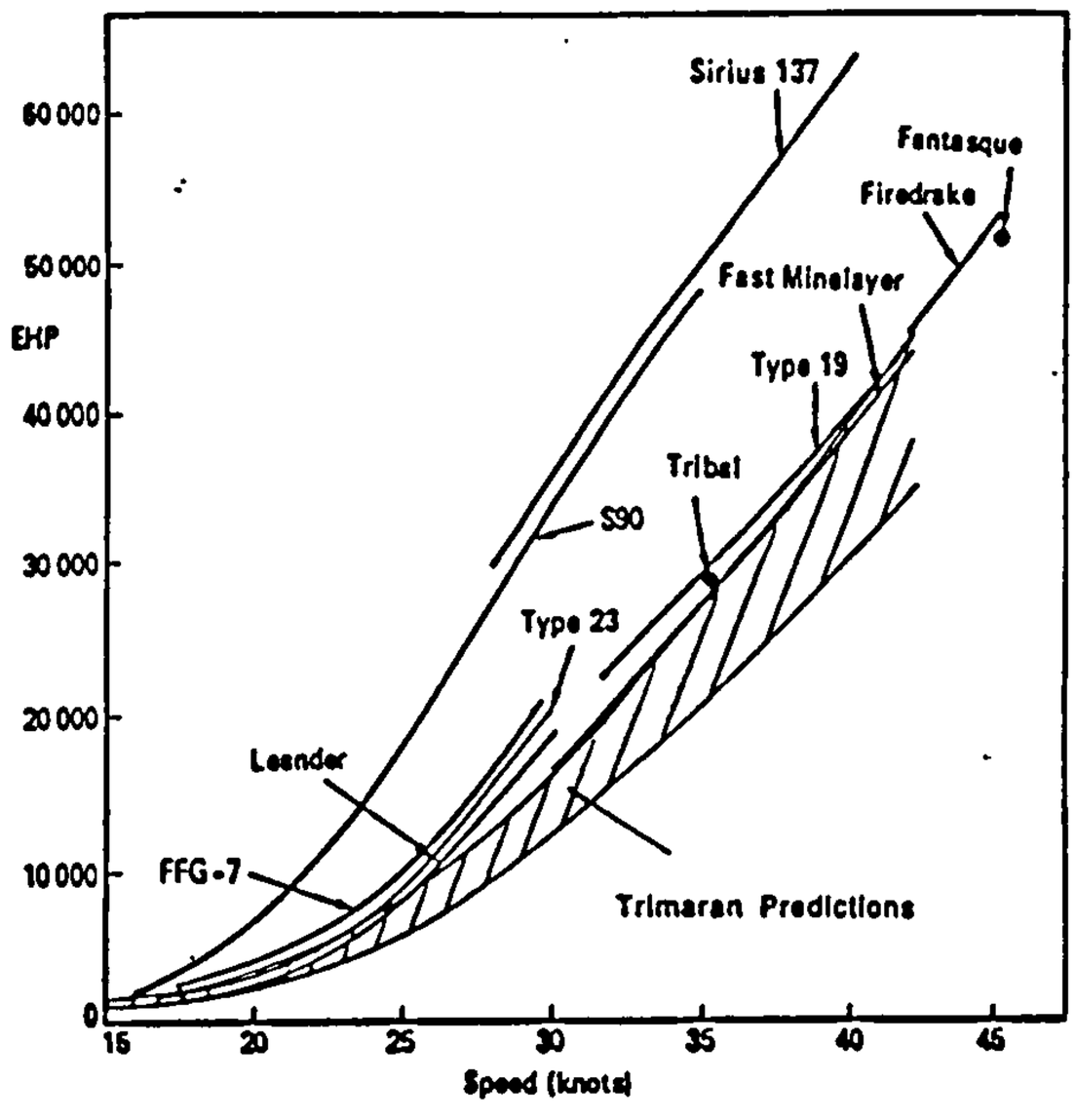

Figure 2.8 Comparison of EHP at a displacement of 2642 tonne based on Fig. 7.4.7 in Lloyds (1988) Enquiry

Table 2.1 List of the monohulls in Figure 2.8

Ship's Name	Displacement (t)	L/B
Fantasque	2642	10.1
Fast Minelayer	2642	10.5
FFG-7	2642	8.7
Firedrake	2642	10.3
Leander	2580	8.8
S90	2642	5.0
Sirius 137	2894	5.2
Tribal	2642	9.7
Type 19	2642	9.5
Type 23	2642	8.2

Less wetted surfaces area of the submerged hulls

There should be a significant reduction in frictional resistance for the trimaran ship when compared with twin hull ships, given that the wetted surface area of a trimaran ship should be less than that of an equivalent displacement catamaran ship and much less than that of an equivalent displacement SWATH ship. If we take into account of the structural efficiency of the trimaran, and compare its wetted surface with a twin hull ship of equivalent payload and built with the same structural material, there will be a greater reduction in frictional resistance. This comparison is discussed further in Chapter 7.

Improved seakeeping performance

The trimaran ship is not intended to compete with the SWATH ship on seakeeping as the later is an optimal form for seakeeping, albeit at the expense of high resistance in calm water **(Gore 1985)**. However, the trimaran would have improved seakeeping performance compared with monohulls and catamarans. The centre hull of a trimaran which contributes more than 90 percent of the total buoyancy will normally be about 40 percent longer than an equivalent monohull or catamaran. It has been proved that a longer ship would result in reduced heave and pitch motions because the exciting forces are relatively smaller than for a shorter one **(Bhattacharyya 1978)**. Figure 2.9, taken from **Moor (1966)**, illustrates the reduced heave and pitch motions as ship length increases.

The stiff roll motion of a catamaran ship is due to the high transverse inertia of its waterplane area which causes a reduction in roll amplitude but increases roll accelerations. The waterplane area inertia of a trimaran ship is much smaller and can be tuned to be very similar to that of a monohull ship and at the same time satisfy initial stability requirement. Thus the natural roll frequency of a trimaran can be tuned to avoid commonly encountered wave frequencies. Twin hull ships, catamarans and SWATH ships, may also experience unpleasant 'corkscrew motions' because their natural pitch period and roll period can be very close to each other; the corkscrew motion may, along with the linear and angular accelerations, cause severe seasickness **(Bhattacharyya 1978)**. The pitch motion period of a trimaran ship is similar to that of a monohull ship, is far away from the roll motion period, and thus severe corkscrew motions will be avoided.

Because the forward end of the cross structure of a trimaran can be located fairly well aft, compared with most catamarans, there should be less problem for trimarans than for catamarans in terms of slamming under the cross structure. This also means the

payload, crew, and passengers would be located further away from the bow of the ship, in a more comfortable position, as shown in Figure 2.13 of the trimaran ferry, where the motion amplitudes are much reduced. Moreover, collision protection of the passengers and cargo is improved.

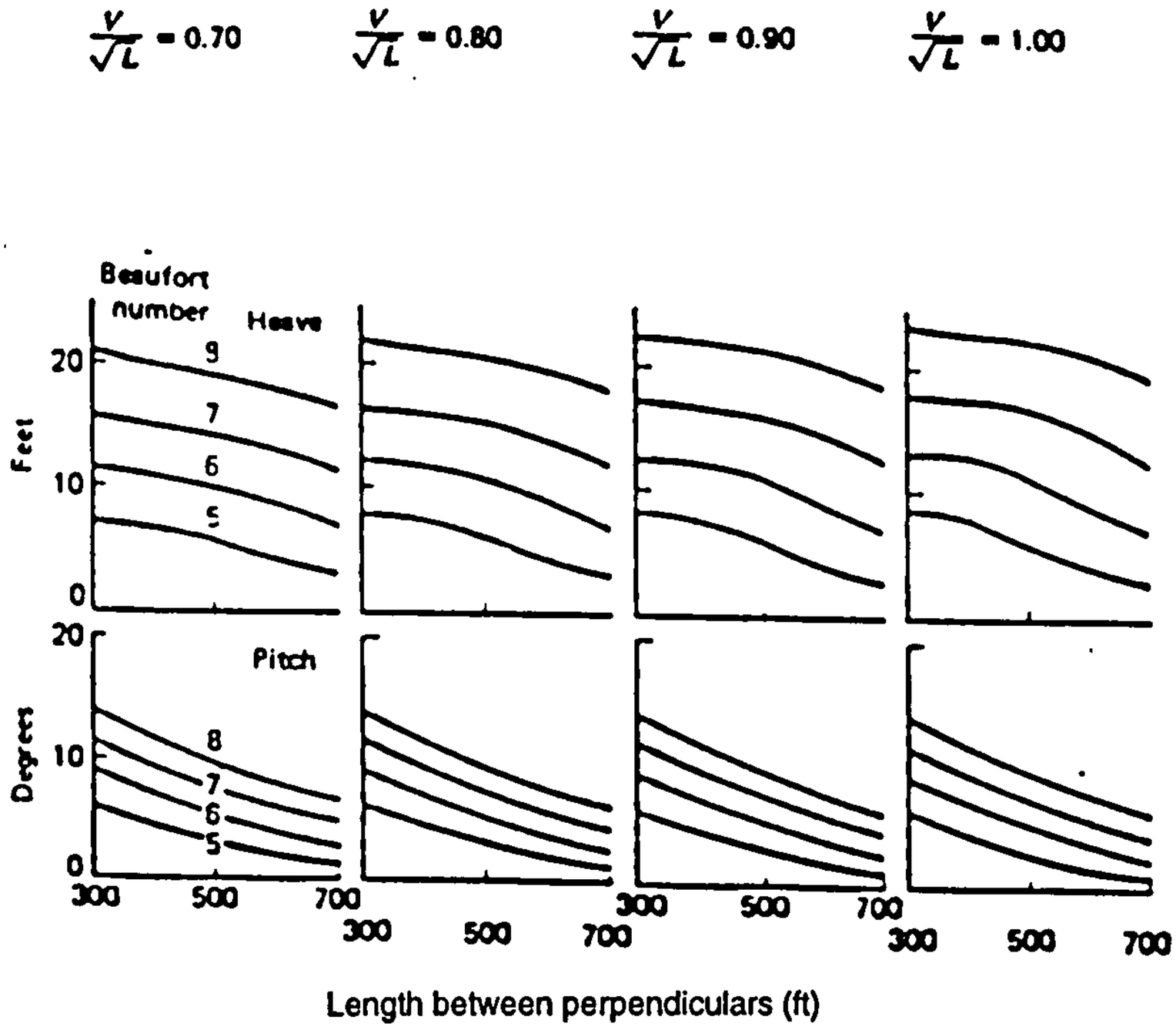

Figure 2.9 Seakeeping characteristics as function of ship length (Moor 1966)

Suitability for steel construction

To achieve high speeds, modern fast catamarans have to be built using light materials to reduce the structural weight and the total displacement. The new trimaran displacement ship is more weight efficient compared with the catamaran. Firstly, the span of the cross structure of the trimaran is about a quarter of that of an equivalent size catamaran, and should result in a significant save in structural weight; secondly, the propulsion machinery and system of a trimaran can be arranged efficiently in the central hull instead of two sets of propulsion machinery and systems to be located in the narrow demi-hulls of a catamaran. This should result in a significant reduction in machinery weight. It is possible to use steel to construct the centre hull and the cross structure for a trimaran as has been suggested for the fast ferry design **(Zhang 1992)**. The use of steel material for the main structure of a trimaran would make it less prone to structural fatigue problems suffered by the aluminium catamarans **(Hercus 1991)**,

and importantly, would reduce the building cost due to cheaper steel structures and less costly fire protection, albeit an aluminium structure might prove attractive in some very fast ferry applications.

In addition to the possibility of achieving the above goals, there are some further potential advantages for a trimaran compared with the existing hull types:-

Large deck area for flexible arrangement

As with twin hull ships, the trimaran ship provides a wider beam on the upper deck giving a flexible arrangement compared with a monohull ship. For a naval ship, the greater overall length gives benefits in weapon and sensor arcs of fire and improved clearances reducing sensor and weapon interference. The greater beam provides an excellent area for a flight deck near to the ship's pitch centre. The cross deck provides extra valuable 'real estate' in the centre of the ship where space is at a premium. For a commercial ship, such as a passenger/car ferry, the wider large deck area would make the vehicle deck and accommodation space arrangement more flexible and possibly a wider vehicle entry space which could shorten the harbour turn round time.

Improved survivability

For warships, survivability may be split into *susceptibility*, the probability of the ship being hit, and *vulnerability*, the probability of the ship's operational capability being reduced if it is hit **(Brown 1988)**. The major aspects of susceptibility affected by the ship type are associated with sonar and radar signatures, and these will be slightly different for a trimaran compared with a monohull. It is expected that the flow into the propeller will be less disturbed by the slender trimaran hulls, and shaft angles may be slightly less, thus delaying cavitation onset and reducing propeller noise. The trimaran will, however, be longer and will probably need greater freeboard, and this will presumably lead to a larger radar echoing area. Both effects are expected to be small. The small trimaran aircraft carrier design **(Cudmore 1992)** has no funnel, as the main engine exhausts have been led out into the space between the hulls. This idea would substantially reduce the infra-red signature of the ship. More than a third of the length of the main hull has been overlapped on each side by the side hulls. In a sea-skimming missile attack the extra protection given by these side hulls plus the extra beam of the ship, may be quite significant. In the aircraft carrier design all of the main operational spaces, the main machinery, and the air weapons magazines, were fitted between the side hulls.

Like existing ship types, there are likely to be some limitations for the new trimaran ship type. However, the potential advantages discussed above reveal the new trimaran concept is a strong contender for improving the performance of future marine vehicles.

2.5 Potential Applications of the New Trimaran Ship Concept

This section illustrates the potential applications of the trimaran concept by reviewing the eleven trimaran displacement ships designed at UCL in recent years, and discussing the various aspects of the naval architecture of this novel ship type. The design studies included the initial sizing of the ships, hull form development, and the preliminary design considerations of each vessel's stability, powering, strength, seakeeping and general arrangement. The principal characteristics of the designs are given in Table 2.2 and are briefly discussed below.

Table 2.2 Principal characteristics of UCL trimaran design studies

	ASW[4] Frigate	Fast Ferry	OPV[5]	Small Carrier	AAW[6] Destroyer	Canadian Ferry	Corvette	Small Support Vessel	LPH[7]	ASW[4] Frigate	Cruise Liner
Displacement[1]	4,200	1,130	514	16,657	4,978	1,350	1,777	234	11,850	4,300	9,050
Length extreme m	154.7	105.0	78.8	231.6	168.6	120.0	112	61.04	191.5	156.8	192.0
Beam extreme m	27.50	19.2	13.7	43.0	25.0	25.0	20	10.85	40	25.9	28.0
Depth m	10.23	8.5[2]	8.5	23.5	11.1	8.0[2]	8.85	4.3	23.35	12.1	13.2
Main Hull											
Length WL m	148.7	99.0	76.8	220	151.3	115	106.7	59.8	177.2	149.8	178.3
Beam WL m	10.4	6.8	4.2	14.5	10.8	6.5	8.5	4.2	13.5	10.8	13.0
Draught m	5.2	3.4	3.4	8.0	4.8	3.2	4.25	2.1	8.74	5.3	6.4
Side Hull											
Displacement[3]	5.5%	4.0%	3.1%	6.8%	4.7%	3.8%	4.3%	4.2%	5%	3.7%	3.0%
Length WL m	36.0	35.0	28.0	82.0	65.0	30	50	19.9	65.2	56.9	71.3
Beam WL m	3.0	1.5	0.74	4.0	2.5	2	2.7	1.06	3.65	2.0	2.8
Draught m	3.6	2.0	2.1	6.5	2.7	1.5	1.35	0.9	4.37	2.8	2.6
Max. Speed knots	28	38	25	27	28	36	30	25	18	28	26
P_S MW	24	20	4.3	70	29	20	20	2.14	16.8	26	31.5

Notes: [1] The data given in tonne for the deep or departure conditions,

[2] Depth to car deck,

[3] The side hull displacement is % of total displacement in one hull,

[4] ASW - Anti Submarine Warfare,

[5] OPV - Offshore Patrol Vessel,

[6] AAW - Anti Air Warfare,

[7] LPH - Landing Platform Helicopter

Advanced Technology ASW Frigate

This first design, Figure 2.10, was a futuristic attempt to carry out the role of the current frigate in the next century using the concept of a slender trimaran ship. The design **(Bastisch & Peters 1990)** generated considerable interest particularly because of the implications for reduced ship powering, and the excellent arrangement of the helicopter feature in this small ship. The project was also expected to explain why there are no trimaran ships, but no serious flaw in the concept was discovered.

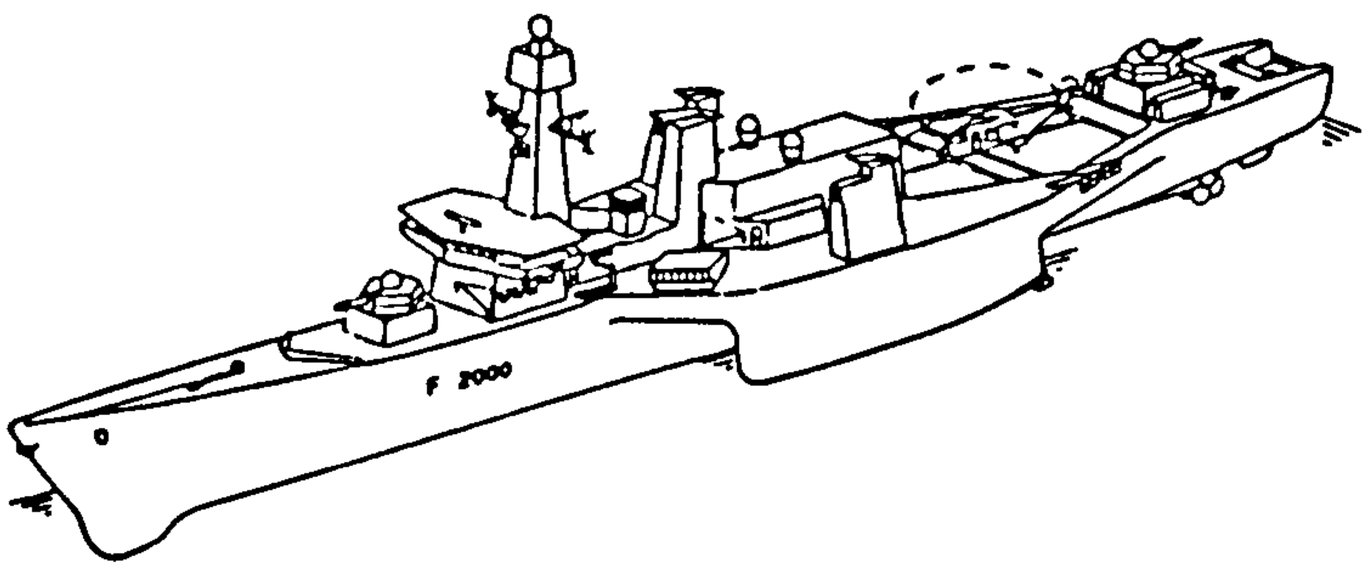

Figure 2.10 The Advanced Technology ASW Frigate

Cross Channel Ferry

This was the first task of the research work described in this thesis in investigating the trimaran concept and its design considerations through a design study **(Zhang 1992)**. The details of the study is presented in Chapter three. This high speed trimaran ferry is intended for cross-channel operation with the capacity for 450 passengers and 90 cars at a maximum speed of 38 knots. The requirement was chosen so as to be able to compare the design directly with large wavepiercing catamarans, and was developed with the advice of Three Quays Marine Services. The structure was designed with the majority in mild steel to reduce building costs and fatigue problems in service, and the ship was designed to meet normal RO/RO ferry safety standards **(DNV 1992)** **(DTp 1991)**. Extensive work was done to optimise the hull proportions for stability and powering, and despite adopting steel hull structure the power required was only slightly greater than that fitted to the aluminium wavepiercing catamarans. Conventional propulsion arrangements of twin shafts and propellers were used. A photograph of the ferry model is at page 4 of the thesis.

Offshore Patrol Vessel

In the 1992 Ship Design Exercise comparative designs of a trimaran (**Pearson & Schild 1992**) and a monohull OPV (**Machin 1992**) were produced to a common requirement, and the two design teams sought advice from Vosper Thornycroft (UK) Ltd. The trimaran, Figure 2.11, at 542 tonne, was heavier than the 498 tonne monohull, but with less power needed in the propulsion machinery the estimated unit production cost was no greater. The ship arrangement was more flexible, with much better helicopter arrangements, and the trimaran was estimated to provide better seakeeping in head seas, with a maximum sustainable speed 2 to 3 knots greater than the monohull in sea state 5 to 6.

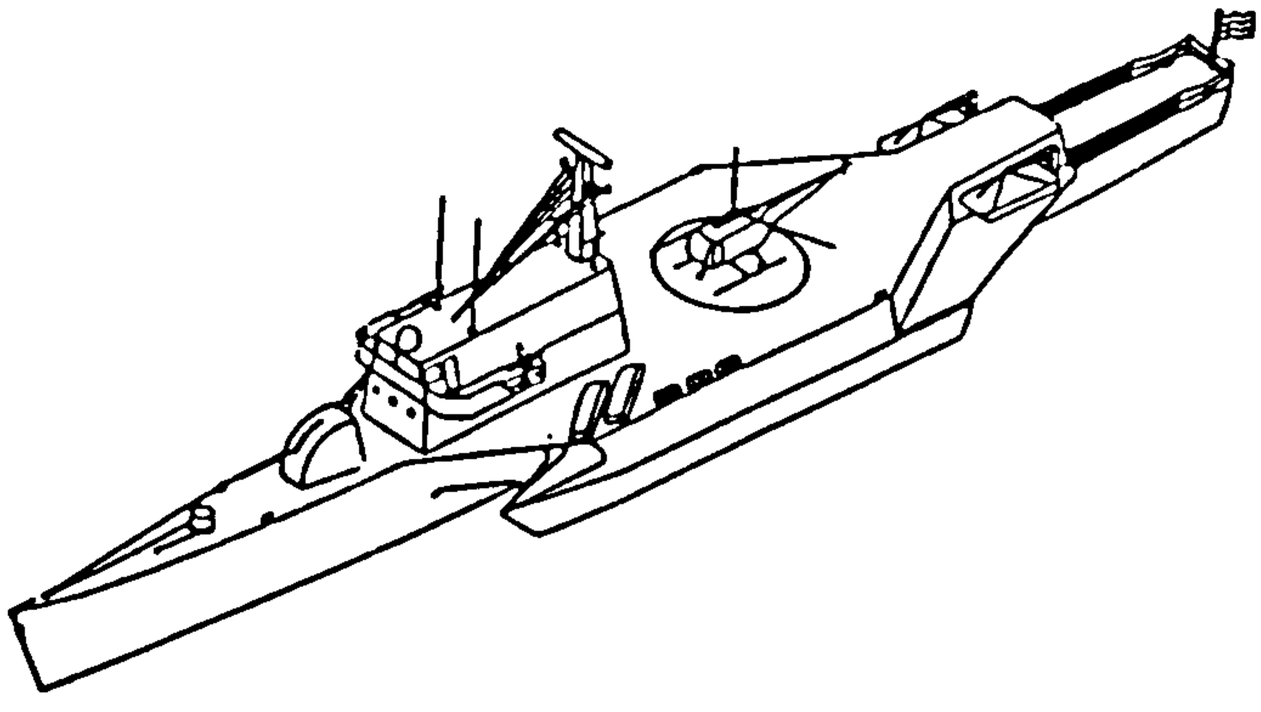

Figure 2.11 Trimaran Offshore Patrol Vessel

Small Aircraft Carrier

This design (**Cudmore & Best 1992**) was diverted away from a monohull design at the request of DRA Haslar, in order to test the suitability of this new concept for a future aircraft carrier. The design was surprisingly successful, not particularly in the areas of seakeeping or powering, but in the overall arrangement of the flight deck and hangar, and possibly in the ability to survive a missile hit.

There is a sensible lower limit to the size of aircraft carriers because the minimum length of flight deck is driven by the aircraft type, not aircraft numbers, and minimum hull beam and depth below the hangar are then driven by damage stability considerations. This design shown in Figure 2.12 produced a 16,700 tonne ship with a flight deck wide enough to keep the aircraft lifts off the runway, and suggested that the naturally long and wide trimaran form could fit a smaller displacement, and

cheaper hull beneath a given length of flight deck. This might make smaller carriers, if required, a practical proposition.

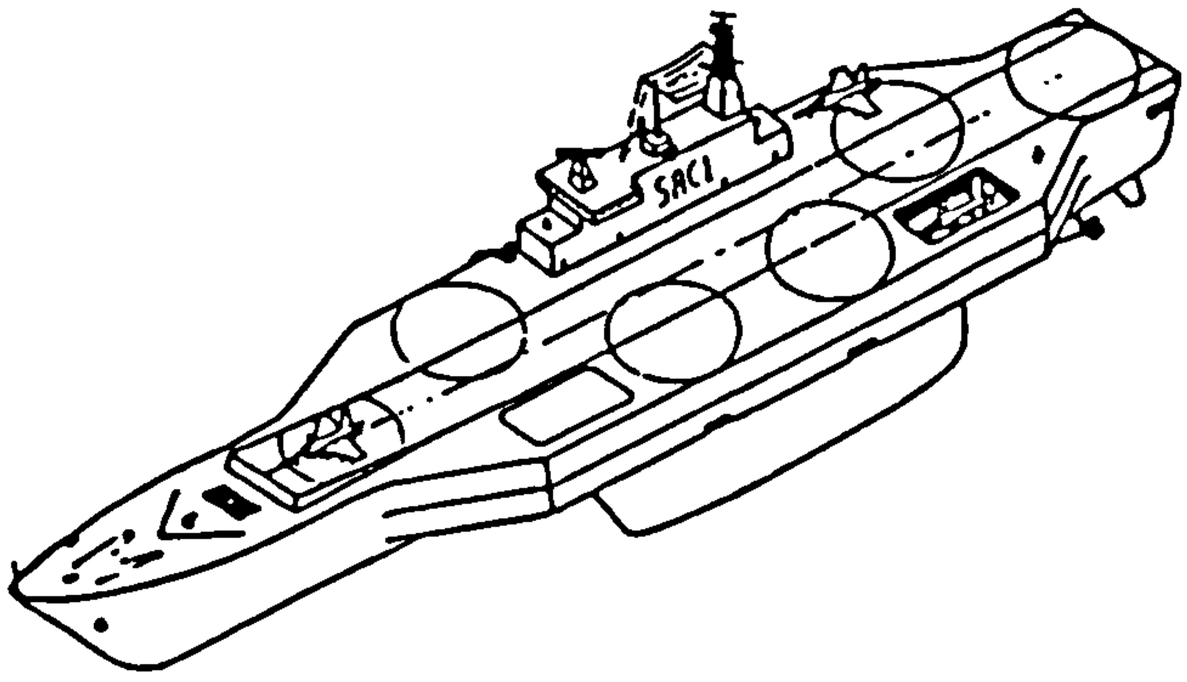

Figure 2.12 Trimaran Small Aircraft Carrier

AAW Destroyer

This design **(O'Brien & Russell 1993)** meets the requirements for a modern Anti-Air Warfare Destroyer, and shows benefits of increased flexibility in the layout of the accommodation and operations spaces from the wider upper decks. The reduced power needed for top speed led to an all electric CODLAGL (combined diesel-electric and gas turbine-electric) propulsion system using diesel generators for lower speeds and combining these with a single gas turbine generator for full speed. The extra cost associated with all electric drive was more than compensated for by the need for only one gas turbine due to the reduced high speed resistance of the trimaran configuration.

Canadian Coastal Ferry

The project **(Hill & Merchant 1993)** was to design a trimaran ferry of similar capacity to the cross channel ferry but with a longer range in order to operate on the west coast of Canada and the United States between Vancouver, Victoria and Seattle, with a capacity of 500 passengers and 85 cars. In contrast with other equivalent existing ferries, the location of passenger areas was further aft than in other ship types giving improved passengers comfort in terms of ship motion, possible only with a trimaran because of its greater length. Two propellers were used to drive the ship at speeds up to 25 knots and to provide good manoeuvring at lower speeds, and two

additional water jets gave the ferry a top speed of 36.3 knots. Figure 2.13 shows the general arrangement.

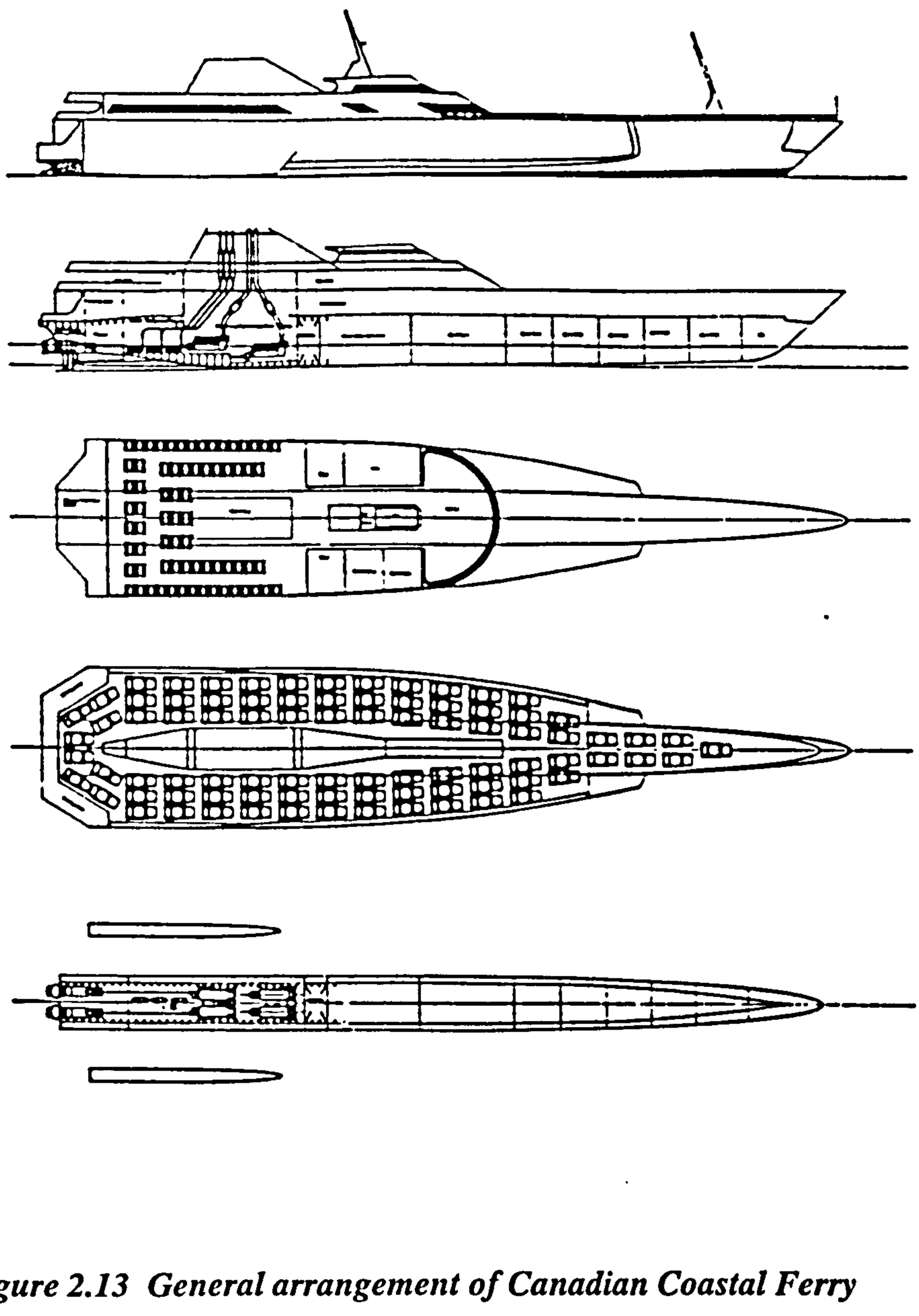

Figure 2.13 General arrangement of Canadian Coastal Ferry

Other trimaran ship designs

There have been a few more trimaran design studies conducted at UCL, as also listed in Table 2.1, to further explore the range of ship type for which the trimaran configuration may prove attractive. The corvette design **(Kamil & Burrows 1994)** and the small support vessel design **(Putnam 1995)** further proved that small trimaran

ships have similar advantages over the traditional monohull with regard to operating helicopters to those already identified with the SWATH ship **(Kennell et al. 1985).** The LPH design **(Mateus & Whatley 1995)** indicates distinct advantages over a monohull equivalent in terms of arrangement of flight deck and hanger, damaged stability and reduced installed power. A second trimaran ASW Frigate **(Smith 1996)** was designed to meet the same baseline requirements as that of the Type 23 frigate aimed to compare the performance of the two ship types. The trimaran option showed very promising characteristics, especially in seakeeping, helicopter availability, operational availability, and maximum speed range, though higher power was required for cruising speed. The cruise liner **(Frost & Palios 1996)** was designed to have a capability of 310 passengers (150 cabins) for world-wide cruise with a top speed of 28 knots. The layout study in the cruiser design suggested improved passenger comfort due to the wide superstructure decks allowing for spacious passenger cabins, and convenient access/service routes when compared with a monohull cruiser of similar displacement.

The potential of the trimaran concept has also attracted a few other ship design and research institutes to start design and research work on this hull form configuration recently. A concept study was carried out by **Summers & Eddison (1995)** of MoD Future Project Directorate (Naval) to use the trimaran configuration as a variant for a Future Escort. The ship displaces 5,800 tonnes, 160 metres in length, a single shaft in the centre hull powered by 2 gas turbines, and with a small electric propulsion motor in each side hull. The top speed is 30 knots. Though the study was not involved very much in the design considerations of the seakeeping and resistance performance of the ship, it discussed in some detail the potential advantages of the trimaran concept in layout and survivability and claimed that the notional equivalent monohull and SWATH designs to the same requirement would displace some 6,300 and 7,200 tonnes respectively. The trimaran concept has also led to the proposal of a fast trimaran corvette by Vosper Thornycroft **(Scott 1995).** The 100 metre trimaran corvette powered by water jets is intended to achieve 30 knots with about half the installed power required for a equivalent 83 metre monohull. Additionally, both Basin des Carines **(Galtiev 1994)** and the Finnish Hydrodynamic Research Centre **(Helasharju 1994)** have published initial details on high speed (40 knot) trimaran container ship model tests.

2.6 Summary

This chapter has reviewed the limitations of existing monohull and multihull vessels and introduced the new displacement trimaran concept. It is postulated would this overcome some of these limitations and possess advantages in the areas of:-

- Less power at high speed due to slender hull form.
- Improved seakeeping quality due to longer waterline length and less transverse stiffness.
- Flexible layout due to wide overall beam and large deck areas.
- Improved survivability because the side hulls provide extra protection.
- Low building costs as a result of the possibility of using steel material and the reduction in propulsion machinery system.

The review of the concept designs of some trimaran ships demonstrated the potential for wide applications of this ship type for commercial and naval roles.

However, the discussion of the advantages of the trimaran concept so far has been largely qualitative. This obviously would not be sufficient to convince the naval architecture world to accept this new ship type. The performance of the trimaran ship, particularly the hydrodynamic performance, has to be analysed quantitatively to validate the feasibility this new concept. This has been briefly reported in two previous papers **(Andrews & Zhang 1995a & 1995b)**, and will be discussed in detail in the following chapters covering the model experiment work and the theoretical analytical work on a trimaran ship.

CHAPTER 3

INITIAL DESIGN STUDY FOR A TRIMARAN FAST FERRY

3.1 Introduction and Aims

Having introduced the trimaran concept and its potential applications, it is now necessary to describe how the trimaran ship design studies, the Cross-Channel Ferry (**Zhang, 1992**) and the DRA trimaran model (**Zhang, 1993**), were conducted and what was the design methodology behind the choices of the principal parameters of the trimaran ship. This is particularly important because some of these parameters, especially those associated with the geometry and the disposition of the side hulls, had not of course been previously encountered in the designs of monohull and other multihull vessels.

In the early stage of the research project, there were hardly any trimaran design data except the design of the Advanced Technology Frigate (ATF) (**Bastisch & Peters 1990**). The ATF design had broadly demonstrated the potential advantages of the trimaran concept, but as the very first attempt in the trimaran concept, the design did not get into details on the trimaran hull form which remained to be explored. It was therefore necessary to carry out more detailed design studies to look into the configuration of the trimaran ship and also to provide the bases for further investigations into the trimaran concept.

The first trimaran design study after the experimental design of the ATF was a fast cross channel passenger/car ferry (**Zhang 1992**) outlined in Section 2.4. The choice of a fast ferry for the design study was made because of the perceived potential advantages of the trimaran concept, namely, low resistance at high speed, large deck area, and good seakeeping performance as described in the previous chapter. Compared with other marine vessel applications, a fast passenger/car ferry has more demands in speed, passenger comfort, and large deck area for easy loading/unloading, which made it an ideal choice for the trimaran study. In addition, there is a growing market for fast ferries around the world. Though conventional monohull ferries are still a large proportion of the ferry fleet, advanced marine vessel concepts including multihull ships are playing an increasingly important role in the ferry market due to the increased demand for better seakeeping and higher speeds. These factors made the trimaran ship a very good contender for future fast ferries.

This chapter aims to reveal general considerations in the design of the trimaran ship including initial sizing, hull form, layout, stability, power/speed, and structural design, through the design process that was adopted for the trimaran ferry study.

3.2 Design Process

It is necessary first to discuss the design process for the trimaran ship. This should in principle be similar to that used in the design of monohull displacement ships. The process can be illustrated by the design spiral **(Andrews 1982)** as a gradually converging conical solid with various constraints impinging on the vessel. The ship synthesis process presented by **Andrews (1984)** is generally applicable to the concept design of the trimaran ship and will not be discussed in the thesis. Only those aspects related to the unique features of the trimaran ship design will be discussed.

The complex feature of the trimaran ship, compared with the monohull ship, gives the designer more choices in its design solution. One of the differences is with regard to stability. Unlike the monohull ship, the side hull parameters of a trimaran ship can not be completely determined along with the centre hull parameters in the initial sizing process. Otherwise, the initial sizing process would become unnecessarily laborious since the detailed side hull configuration requires extensive calculations which would have little influence on the determination of the centre hull parameters. The process of side hull configuration therefore could be divided into two stages, the initial side hull sizing together with the detailed centre hull sizing, and then detailed side hull shape. This procedure was followed.

Thus, for the first stage the initial parameters of the side hulls can determined by the following major factors:-

(a) Desired metacentric height (GM) to enable the ship to meet the intact initial stability requirements and be favourable for the seakeeping performance. This normally drives the side hull beam and span together with other constraints.

(b) Required side hull length as a proportion of main hull length. This is related to the required length of damage for the ship to survive according to the chosen damage stability criteria.

(c) Desired size and location of the cross structure. This is usually governed by the layout considerations necessary to meet the operational requirements.

(d) A favourable location for the side hulls to reduce wavemaking resistance of the ship, which is revealed through a compromise with factor (c).

The second stage is a process to refine the parameters of the side hulls carried out in conjunction with the detailed stability analysis. The damage stability assessment for a

monohull ship would usually affect the extent of subdivision of the ship but not alter the hull size determined from the initial sizing. However, this is not the case for trimaran ships because damage stability assessment would not only affect the subdivision of the ship but also affect the size and the shape of the side hulls. The tasks required to refine the side hulls can be summarised as:-

(a) Identify the worst damaged cases for the ship.

(b) Adjust the length of the side hulls.

(c) Determine the required side hull subdivision.

(d) Determine and adjust the shape of the side hulls taking into account of the effects of changes to the side hull displacement ratio on building cost and on satisfying the stability requirements

(e) Determine other measures to be taken to reduce the side hull length.

(f) Refinement of the side hull location to achieve better hydrodynamic performance.

These tasks are all related to each other and the final configuration would be the result of the interaction between these tasks. The resistance performance of a trimaran ship is greatly affected by the configuration of the side hulls, i.e., their size and location. Thus a reduced side hull displacement ratio would result in reduced resistance for the trimaran ship, as is discussed Section 3.4. Undertaking these tasks will produce a side hull configuration with less side hull displacement while satisfying stability requirements.[1]

[1] The details of these tasks and their relationship with other issues in hydrodynamic performance are discussed further in Chapter 9 when general considerations in trimaran ship design procedure are presented and after the hydrodynamic issues have been presented.

3.3 Design and Operational Requirements for the Ferry

Initially, the design and operational requirements for the fast ferry were agreed with the help of Three Quays Marine Services **(Pearson 1991)** as follows:-

Routes

The primary duty of the ferry is to operate on cross-channel services between Dover - Calais or Dover - Zeebruge. The ferry would also be suitable for operation on alternative short international voyages.

Capacities

The ferry will carry up to 450 passengers and 90 motor cars. The passenger number was decided by the upper-limit of the IMO Resolution A.373(X) 'Code for Dynamically Supported Craft' **(IMO 1977) (DTp 1991)**. The number of cars was chosen to be compatible to the passenger numbers. No provision was made for coaches or trailers.

Speed

According to the trend of ferry operations **(Pearson 1991)**, is was envisaged that the speed should be approximately twice that of existing monohull ferries to show benefit, that is, in the range of 36-40 knots. It appeared that the speed was also influenced by the necessity to keep the required power within the output range of relatively lightweight propulsion machinery.

Building Materials

In order to investigate , It was decided to use steel for the main structure of the ferry to achieve of reduced building cost and reduced fatigue because of the problems encountered by the light material built craft **(Hercus 1991)**. This also to investigate the suitability of the trimaran ship for steel construction.

Propulsion Machinery

Conventional propulsion machinery was the first choice for the ferry, i.e., diesel engine plus screw propellers. Firstly, this would reduce the capital and maintenance costs. Secondly, the expected benefits in such a design would indicate the consequences of the characteristics of the new hull form configuration rather than those achieved by employing sophisticated machinery systems.

3.4 Principal Considerations on Initial Sizing

This section describes the parametric studies carried out during the design of the trimaran fast ferry and reveals the principal considerations in choices of the trimaran parameters. The trimaran concept raised many new questions which need to be investigated in the initial sizing stage. The primary questions are:-

- The main feature of the trimaran ship is the slender centre hull, but how slender should the hull be to achieve desired low resistance?
- What is the best side hull displacement ratio?
- What is the required air gap between the water surface and the wet deck of the cross structure?
- What is the required size for the cross structure?
- What is the best location for the side hulls for the hydrodynamic performance of the ship including resistance and seakeeping?

Concept design may be carried out in either of two ways, the empirical approach relied upon accumulated experience and data for the type of ship being designed, or the parametric analysis approach **(Taggart 1980)**. As a novel ship type, it was not possible to rely on the first approach for the trimaran ship design. Parametric studies were therefore carried out for the trimaran ferry to investigate the primary questions listed above. A design model for the trimaran ferry were developed based on the concept illustrated in the previous chapter and with reference to the current design techniques for monohull ships and advanced marine vehicles (algorithms developed for the design model are illustrated in Appendix 1). The model was then implemented into an interactive computer program, TRIDES **(Zhang 1992)**. The program allows the user to input operational requirements, such as speed and payload, and to choose desired trimaran parameters. It then performs a initial design balance by estimating structural weights, machinery weights, outfitting weights, resistance, and speeds.

The design model defined in the program consists the following parameters:-

1) Operational parameters

   - Number of passengers
   - Number of cars

- Range of the ferry
- Maximum speed
- Service speed

2) Hull parameters

- Length beam ratio of centre hull
- Beam draft ratio of centre hull
- Minimum freeboard
- Block coefficient of centre hull
- Prismatic coefficient of centre hull
- Side hull displacement ratio
- Length beam ratio of side hulls
- Beam draft ratio of side hulls
- Block coefficient of side hulls
- Prismatic coefficient of side hulls

3) Arrangement aspects

- Number of car decks
- Number of passenger decks
- Length beam ratio of superstructure
- Span of side hull
- Longitudinal position of side hulls

4) Other parameters

- Choices of materials for centre hull, side hulls and cross structures
- Choices of propulsion engines
- Choices of propulsion devices

For the purpose of this initial design study, the crucial algorithms for design balance in the program are structural weight estimation and resistance prediction. In order to get reasonable confidence on the structural weight estimation, a basic midship section structure was designed using the DNV rules **(DNV 1992)** with the structural model described in Section 3.8. Separated structural weights for the centre hull, and the cross structure were obtained from the midship section structure by approximately distributing the weight along the ship. Using these weights as a basis, weights of the centre hull and side hulls were estimated using Watson's formula **(Watson & Gilfillan 1976)**. The cross structure weight and the superstructure weight were calculated by the deck area and

number of decks. The weights of the side hull structure were treated in the same way. The resistance for the centre hull and the side hulls were predicted using the Series 64 data **(Yeh 1965)** ignoring the interaction effects between the hulls. Details of these algorithms, a listing of the program menu and the program output of a sample run can be found in Appendix 1.

A series of studies were produced using the TRIDES program by varying hull parameters to investigate the performance trends of the trimaran ferry. As an initial design study, the intention was not to answer all the questions raised by the trimaran concept. The study concentrated on finding out the appropriate sizes of the three hulls. Thus, the parametric study was carried out by varying some but not all of the major hull parameters. The effects of the location of the side hulls on the hydrodynamic performance of the trimaran ship needed further intensive analysis and model experiments which is discussed in subsequent chapters.

Slenderness of The Centre Hull

As already described, the trimaran concept is characterised by its slender centre hull. The effect of varying length beam ratio of the centre hull was first studied under the following assumptions:

- The centre hull and the side hulls were of the same length beam ratio.
- The beam draught ratio of the centre hull was 2.0.
- The centre hull and cross structure were to be of steel material, and the superstructure and the side hulls were to be of light material - aluminium.
- The ship was driven by medium speed diesel engines and fixed pitch propellers.

The effects of the length beam ratio of the centre hull are reflected primarily on the ship's light weight and required propulsion power. In contrast to monohull ships, the light weight of the trimaran ferry decreases with an increasing length to beam ratio, even at a very high value of L/B = 12, until it reaches 14, as shown in Figure 3.1. This is because the machinery weight of a high speed ship contributes a very large portion to the total weight of the ship. As the hull length increases, although the structural weight increases, the required power drops very sharply (as shown in Figure 3.2), and this leads to a decrease in machinery weight as well as the total weight. When the length beam ratio exceeds 16, the reduction in powering stops and there is a sharp increase in the ship's lightweight. This is because the benefit of reduced wavemaking resistance has been traded off by the increase of the frictional resistance when the hull slenderness is further

increased. The machinery weight does not reduce further but a sharp increase in structural weight occurs due to the increase of the hull length. Taking into account both effects of the lightweight and required power, a length beam ratio of between 14 to 15 appeared to be beneficial for the trimaran ferry at its maximum speed (38 knots).

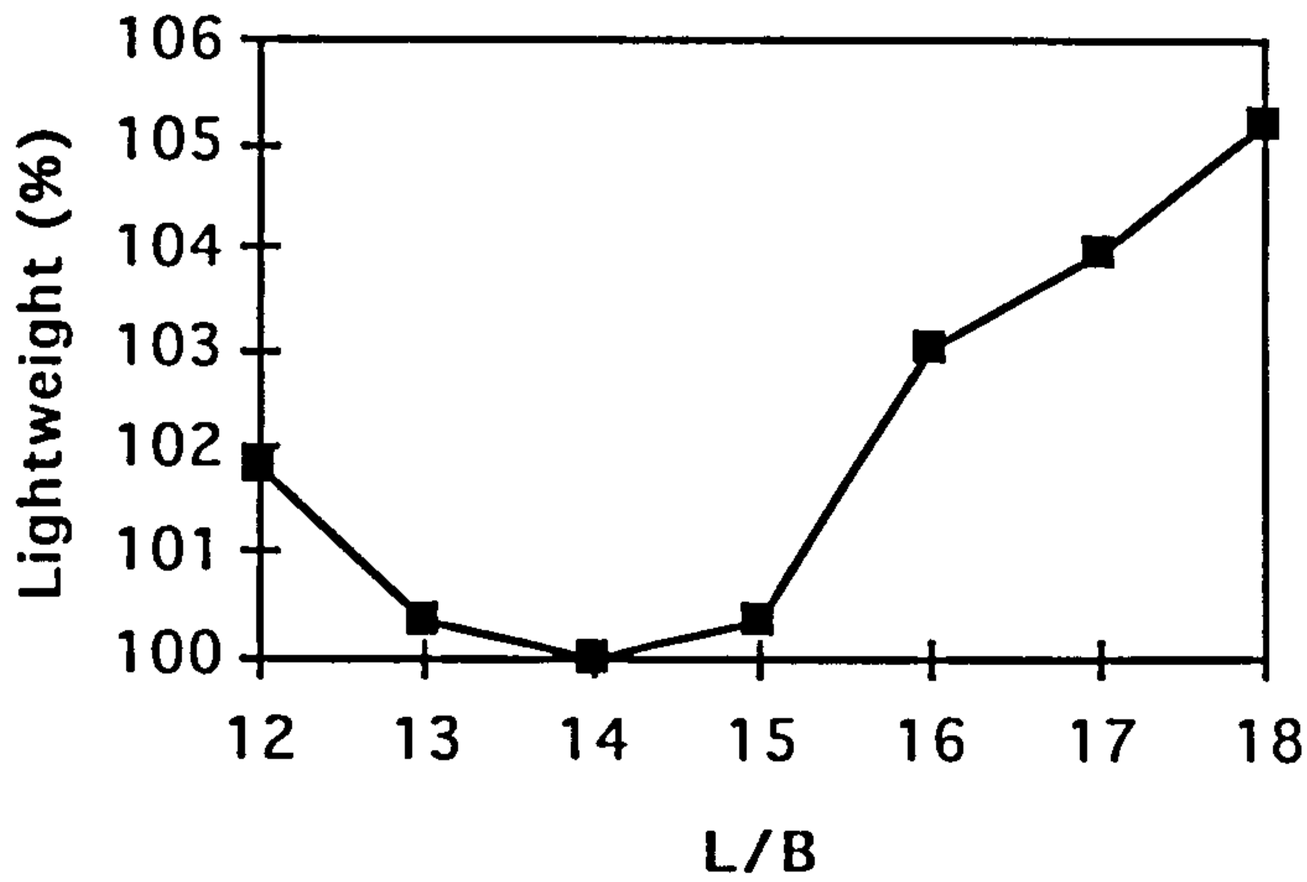

Figure 3.1 Effect of length beam ratio on lightweight

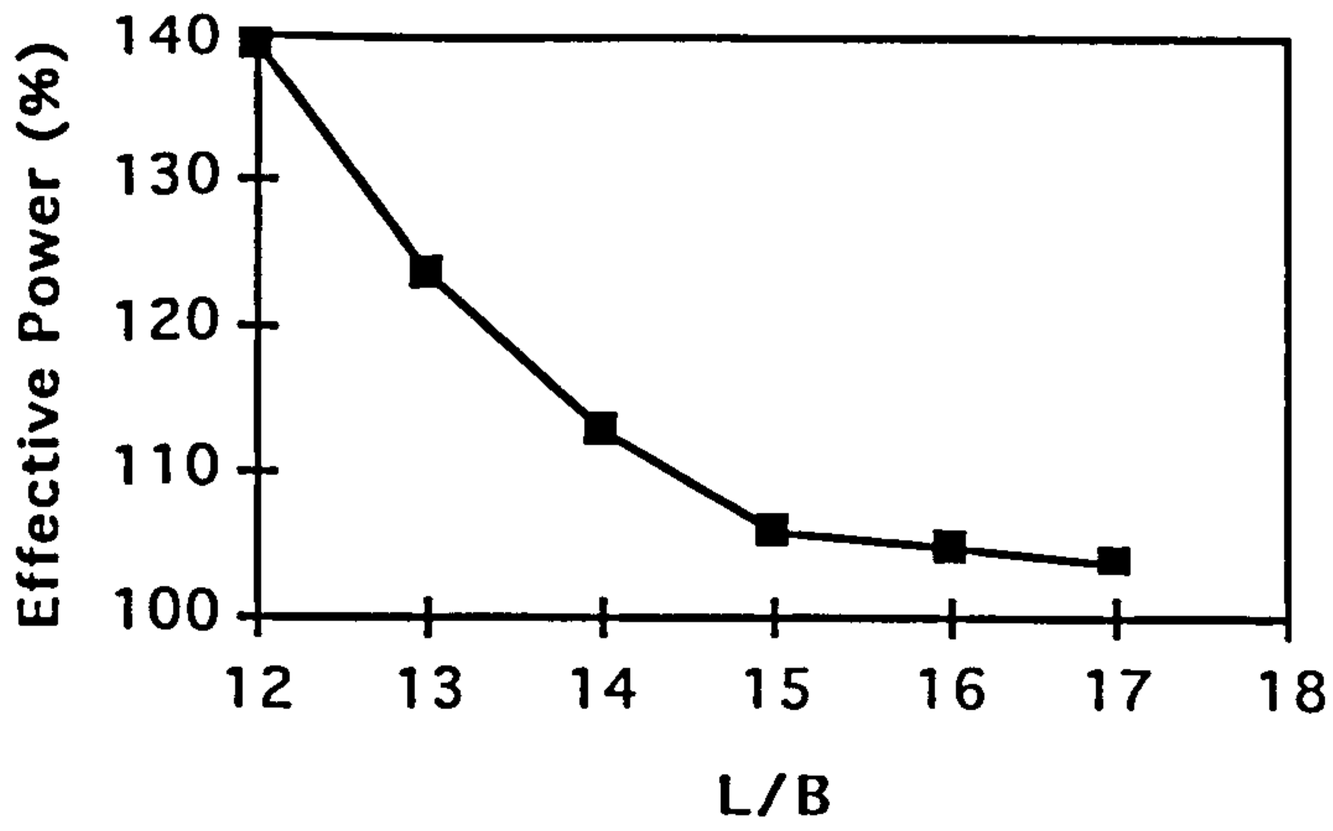

Figure 3.2 Effect of length beam ratio on effective power

Side Hull Displacement Ratio

The ratio of the side hull displacement to the total displacement would influence the performance of the trimaran very significantly. The study of the effects of varying side hull displacement ratio was carried out under the following assumptions:-

- the length to beam ratios was 15 for the centre hull and the side hulls,
- the length to beam ratio of the car deck box was 3.0,
- the beam to draught ratio of side hulls was 1.0,
- the transverse location of side hulls were right under the edges of the deck box,
- the side hull length was about 30 percent of the centre hull length ,
- the GM value was about 2.0m.

Figure 3.3 shows a very direct relationship between the side hull displacement ratio and the required power at a top speed of 38 knots. It can be seen that the smaller the side hull displacement ratio the less power is required. The same trend was found for the lightweight as shown in Figure 3.4. An extreme case occurs when the side hull displacement ratio tends to zero. Then the ship will become a slender monohull which is the most efficient in terms of powering and weight. Another extreme case occurs when the ratio approaches infinity, the ship becomes a catamaran. Thus we may also say that the trimaran ship is an intermediate design solution between the monohull and the catamaran displacement ship.

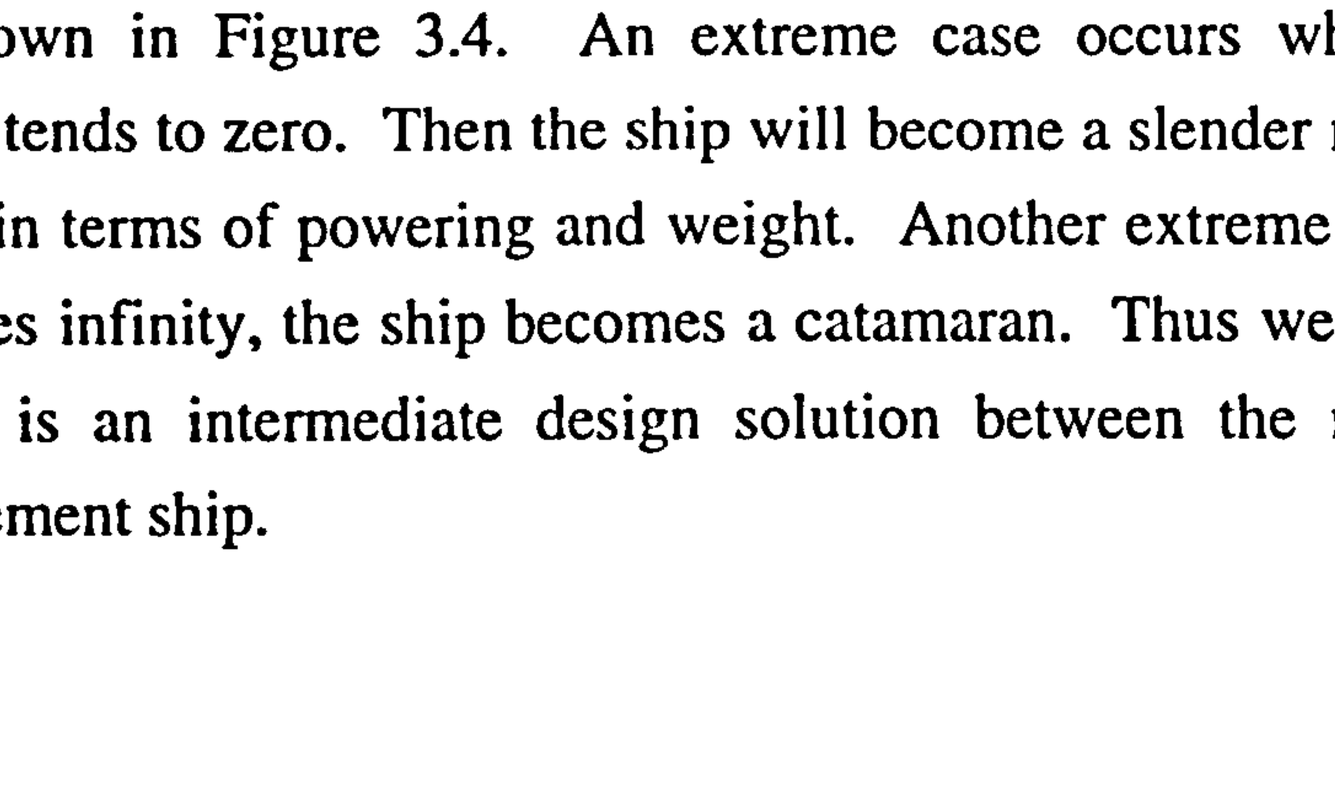

Figure 3.3 Relationship between side hull displacement ratio and powering

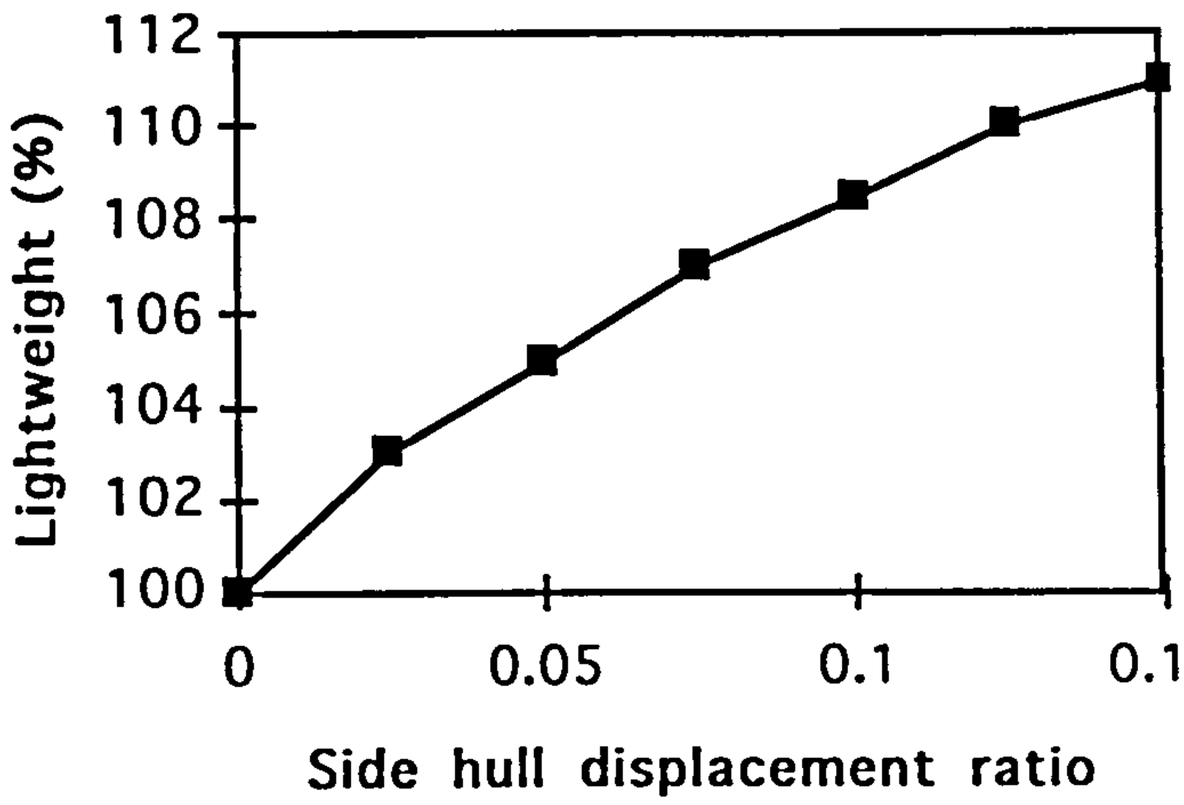

Figure 3.4 Relationship between side hull displacement ratio and lightweight

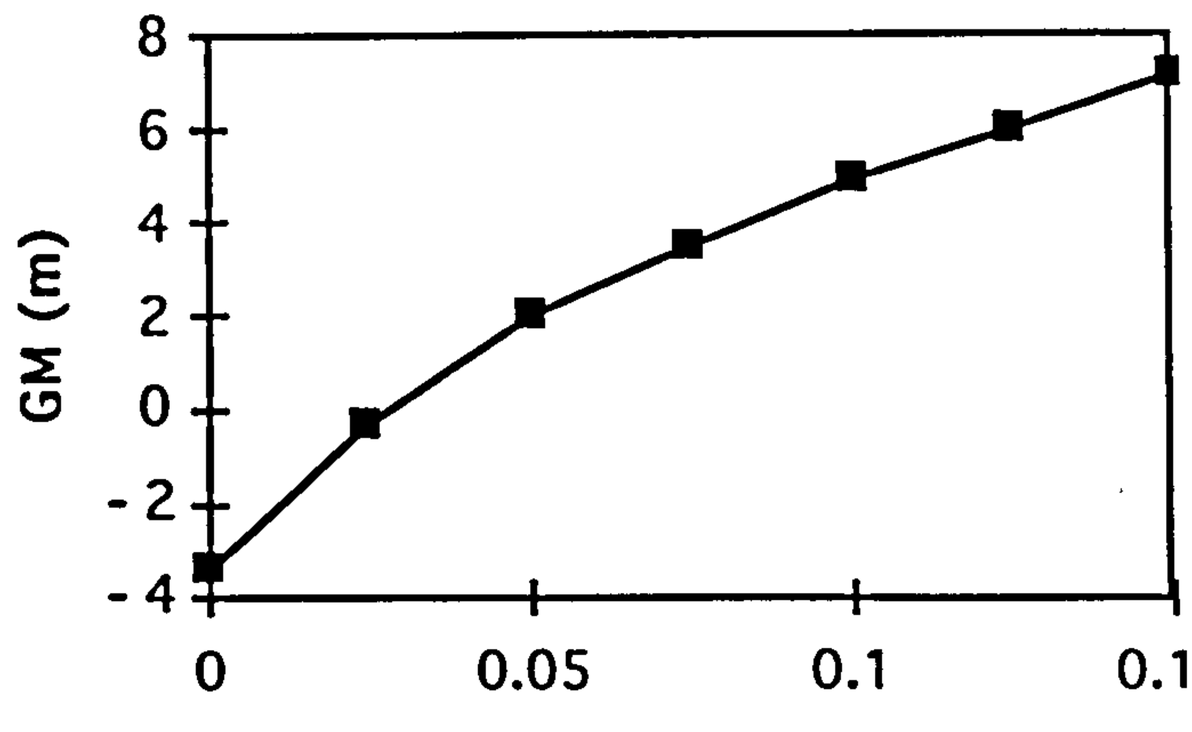

Figure 3.5 Relationship between side hull displacement ratio and GM

However, as explained above, the presence of the side hulls is necessary to provide extra waterplane area for the ship to meet the requirements of transverse stability. It is necessary to determine the required side hull displacement for a trimaran ship. At the initial study stage, the value of metacentric height (GM) was used to derive the side hull waterplane areas. Obviously, the required side hull displacement ratio will also depend on the requirements of large angle stability and damage stability, and this is discussed in Section 3.5. Using the TRIDES program, a relation between GM and side hull displacement ratio was derived as shown in Figure 3.5. It can be seen that, under the assumptions listed above, the GM value will go to negative if the side hull displacement ratio is below 0.02. A side hull displacement ratio of between 0.04 and 0.05 seems preferable to achieve required GM and keep the power and lightweight low. It should be noted that the GM value is not only a function of the side hull displacement ratio but is

actually dominated by the beam and span of the side hulls. The relationship between GM and the side hull ratio would vary for individual cases.

Size of The Deck Box

The size of the deck box, apart from the requirements of the transverse position of the side hulls, is dominated by the layout requirements. However, the cross structure was such located that its aft end was in line with the stern of the centre hull. The size of the cross structure was therefore longer than that of the side hulls. There are two advantages for a relatively long and narrow cross structure, firstly, to minimise its structural weight as the transverse loads to the cross structure reduces when its width reduces, secondly, to reduce harbour hours as an effective stern loading/unloading is provided for cars (see Section 3.7 General Arrangement).

Required Air Gap

The air gap between the wet deck of the cross structure and the water surface was determined by the probability of waves impacting the wet deck at the front end of the cross structure. Figure 3.6 shows the number of occurrences per hour where wave surfaces exceed the air gap at different sea state against varying height of air gap at a speed of 38 knots. For a sea state of significant wave height $H_{1/3}$ = 2.5m, an impacting frequency of less than 20 times per hour would be achieved with an air gap of 3.0m. In this initial design study, the seakeeping performance of the ship was analysed using a UCL strip theory program **(Bishop, Price & Tam 1977)** in which only the vertical motion was included. The effects of the side hulls on transverse motion of the ship was therefore not included here but is to be discussed in Chapters 5 and 6.

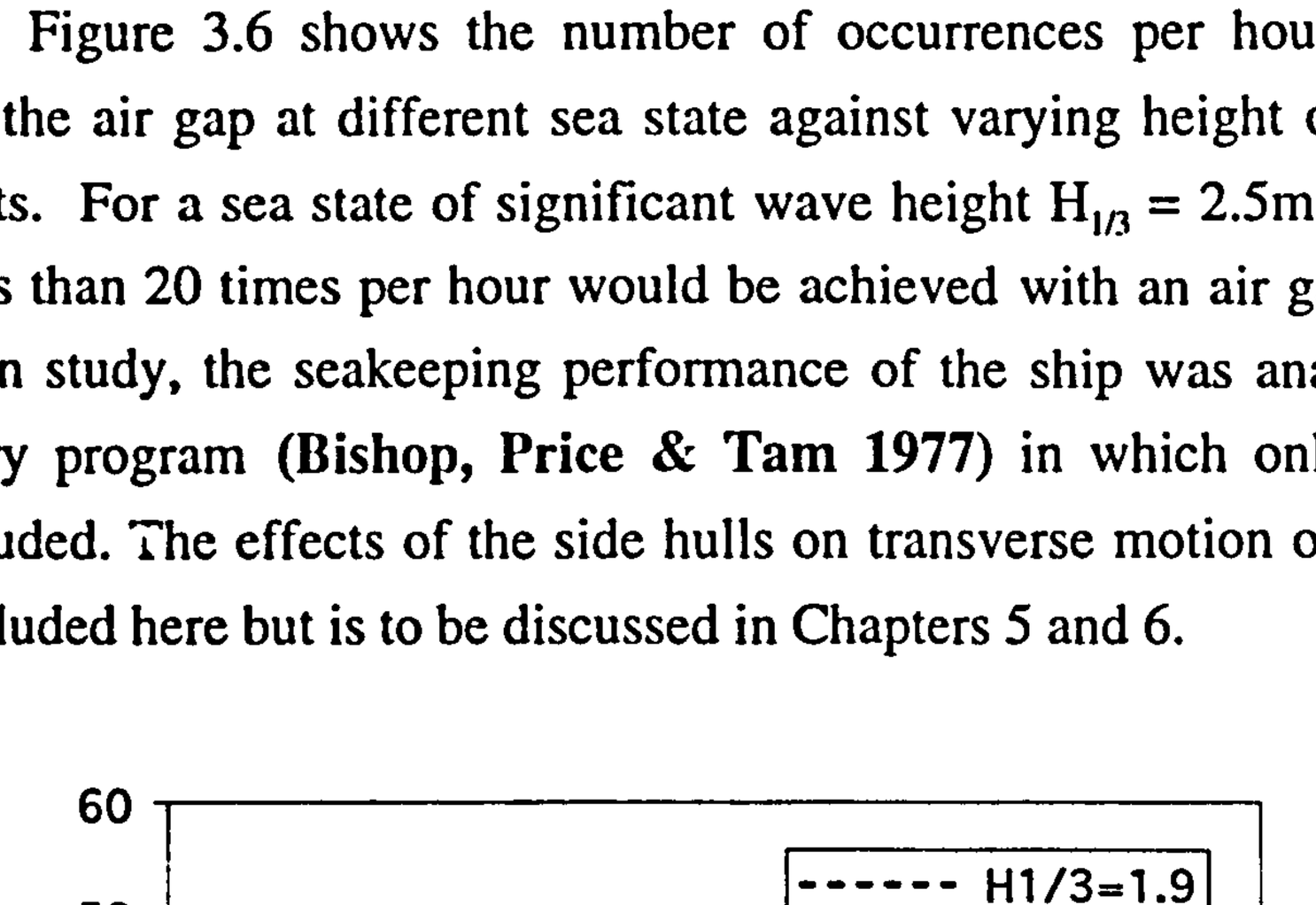

Figure 3.6 Effects of air gap

3.5 Side Hull Refinement through Stability Analysis

The task at this side hull refinement stage is to find a good choice of configuration for the side hulls which would not compromise the speed performance of the ship but provide sufficient transverse stability, in both intact and damaged conditions. The stability suit of programs in the GODDESS system **(Pattison et al. 1986)** were used in the stability analysis. Although the system was not designed for multihull ships, the flexibility of the programs allows users to add the side hulls as additional geometry modules. Figure 3.7 shows an isometric of the hull definition for a stability calculation model of the trimaran ferry created for GODDESS analysis.

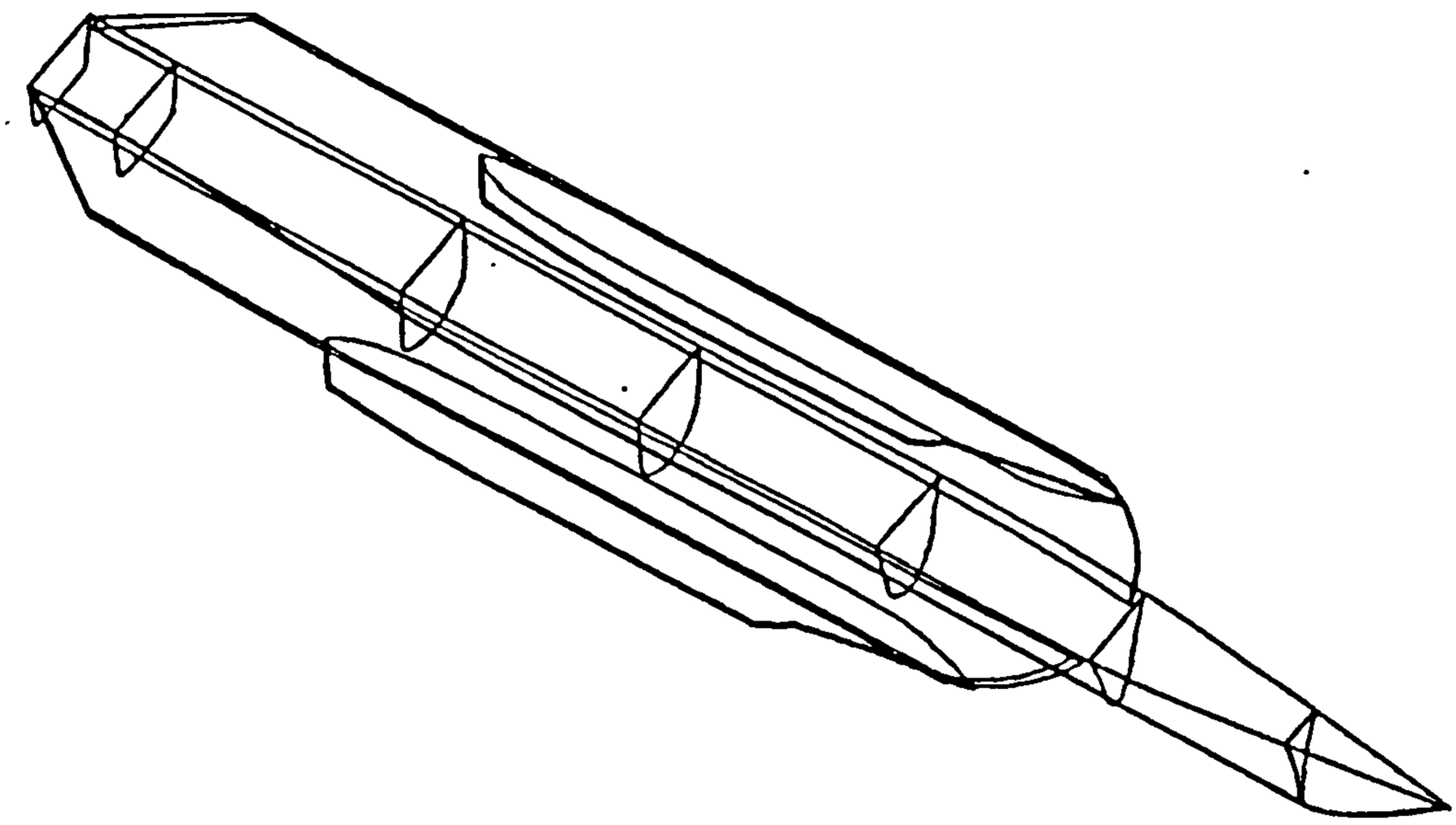

Figure 3.7 Stability calculation model by GODDESS

Stability criteria

There are no regulations for the stability of triple hulled ships to date. The existing IMO Resolution A.373(X) *Code of Safety for Dynamically Supported Craft* **(IMO 1977)** was used for the stability assessment of the trimaran ferry, together with the proposed review

by **DTp (1991)** which has now become part of the new code '*International Code of Safety for High Speed Craft*' **(IMO 1995).** Though the trimaran displacement ferry is not dynamically supported, the IMO code was considered to be the most applicable one to the fast ferry since there were no other safety codes suitable for high speed ships (details of stability criteria are given in Appendix 2).

Intact Stability

Initially, for the purpose of simplicity in construction, the side hulls were designed to have a zero flare above the waterline as in Figure 3.8,. It was soon found from the stability calculation that the ship did not meet the stability criteria. The heeling angles of the vessel due to beam wind and high speed turning exceeded the criteria as shown in Figure 3.9. This occurred because when the ship heels, one of the side hulls would begin to emerge from the water, causing the loss of waterplane area and inertia. Unlike monohulls, the increase of waterplane area at the centre hull due to heeling has little influence on the total transverse inertia of the waterplane because of the narrow beam. Also, there was little compensation to the waterplane area from the immersed side hull because of zero flare. This caused the GZ curve to flatten out beyond a heel angle of 10 degrees until the watertight cross structure touches the water at a heel angle of around 30 degrees.

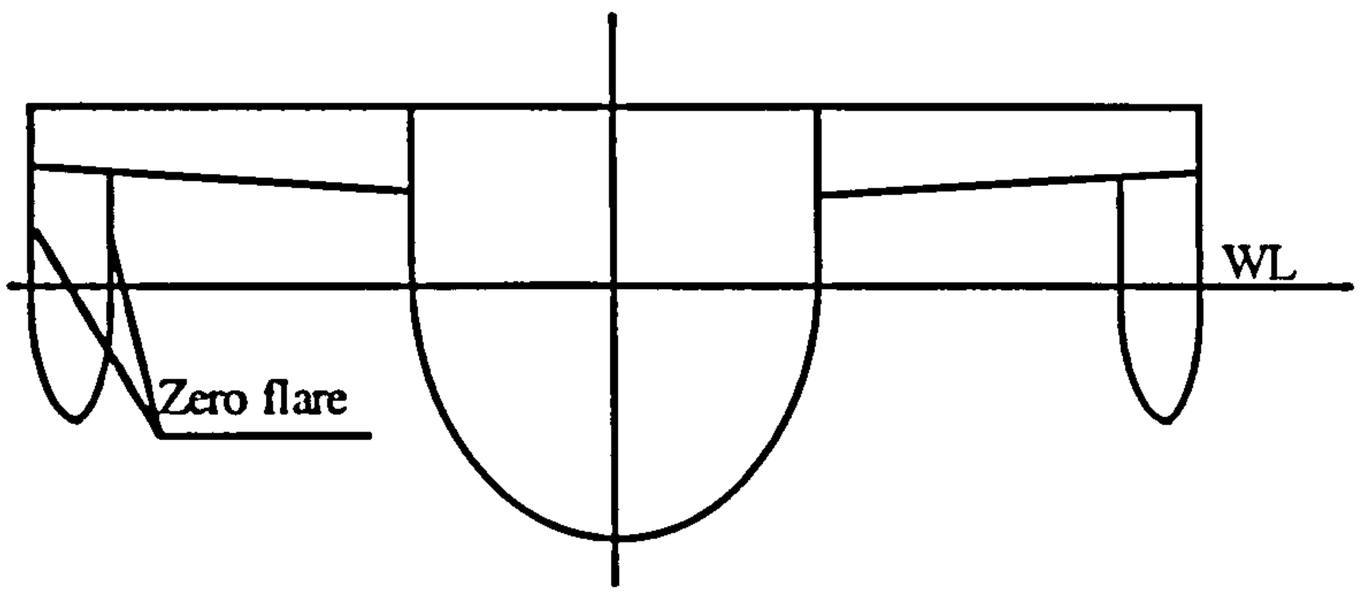

Figure 3.8 Side hulls with zero flare

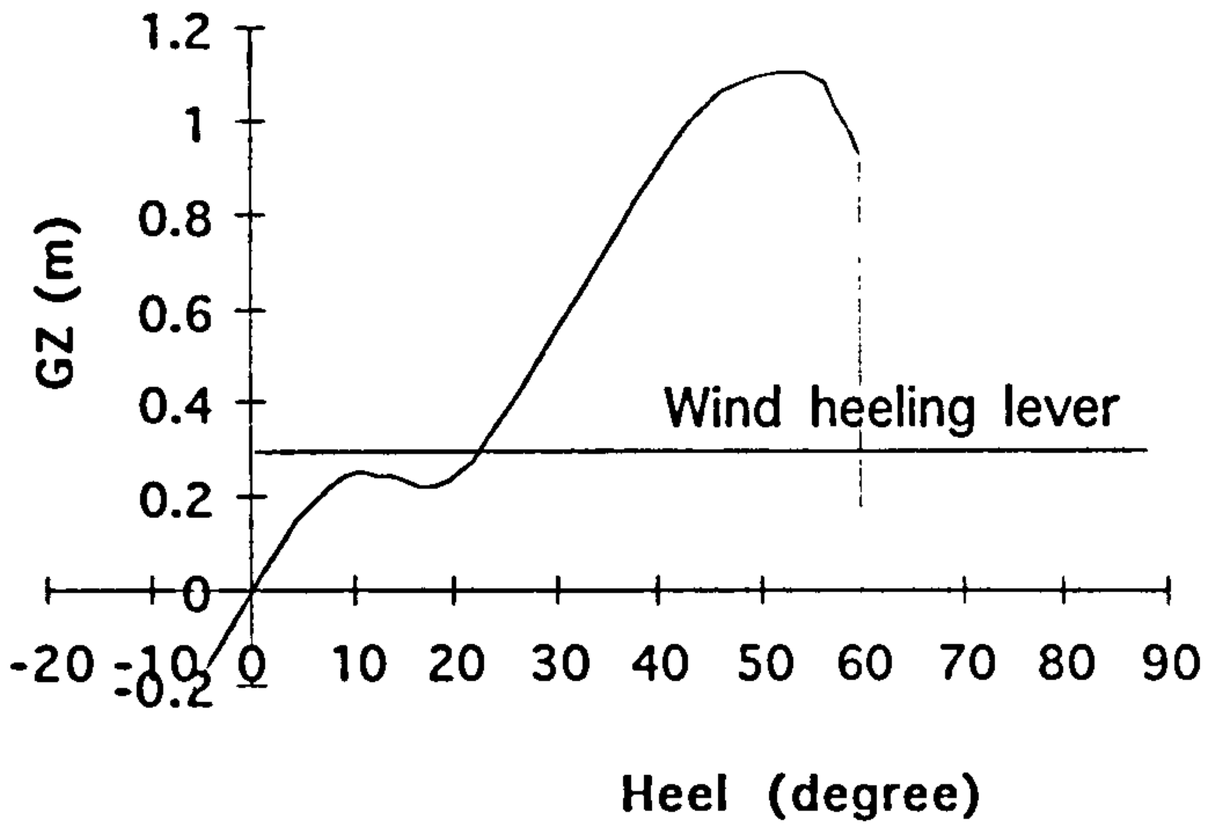

Figure 3.9 GZ curve with zero side hull flare

A few options were considered to solve this problem,

a Increase the beam or length of the side hulls.

b Stretch the side hulls further away from the centre hull, i.e. increase the span of the side hulls.

c Increase the flare of the side hulls (to an angle of 20°) as shown in Figure 3.10.

The first option would mean an increase in the displacement of the side hulls if the draught is be kept the same, which would lead to an increase in weight and powering. The parametric study showed that increase in displacement should be avoided as far as possible. The second option seemed acceptable because it would not adversely effect the resistance performance of the ship but could be beneficial due to the larger span between the hulls. It would, however, cause some increase to GM which is not desirable for the rolling motion, although the absolute value of GM would still be extremely low compared with catamarans.

The third option, increasing the flare of the side hulls, overcomes most of the undesirable features of the first two options. There would be no increase in GM, no increase in resistance, at least in calm water, and little influence on weights. Therefore, this option was used to make the ship meet the stability criteria. Figure 3.11 shows the final GZ curve with side hull flare which meets all intact criteria. The final side hull flare is tuned for the ship to meet the damaged stability criteria and is demonstrated in the following damaged stability analysis.

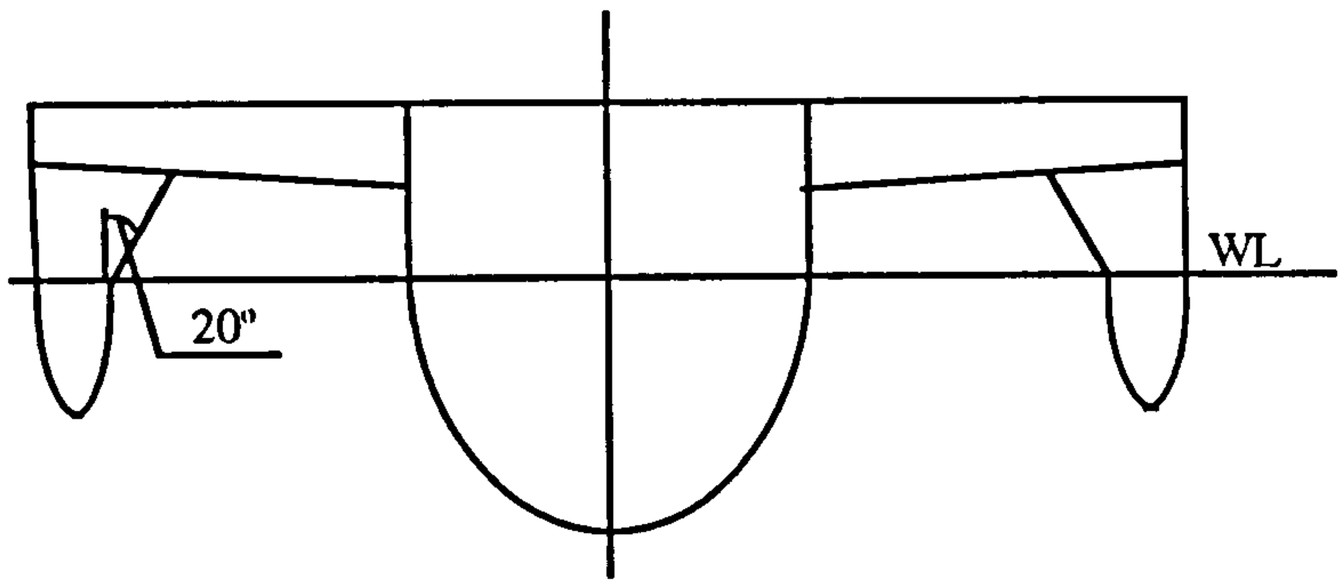

Figure 3.10 Side hulls with flare

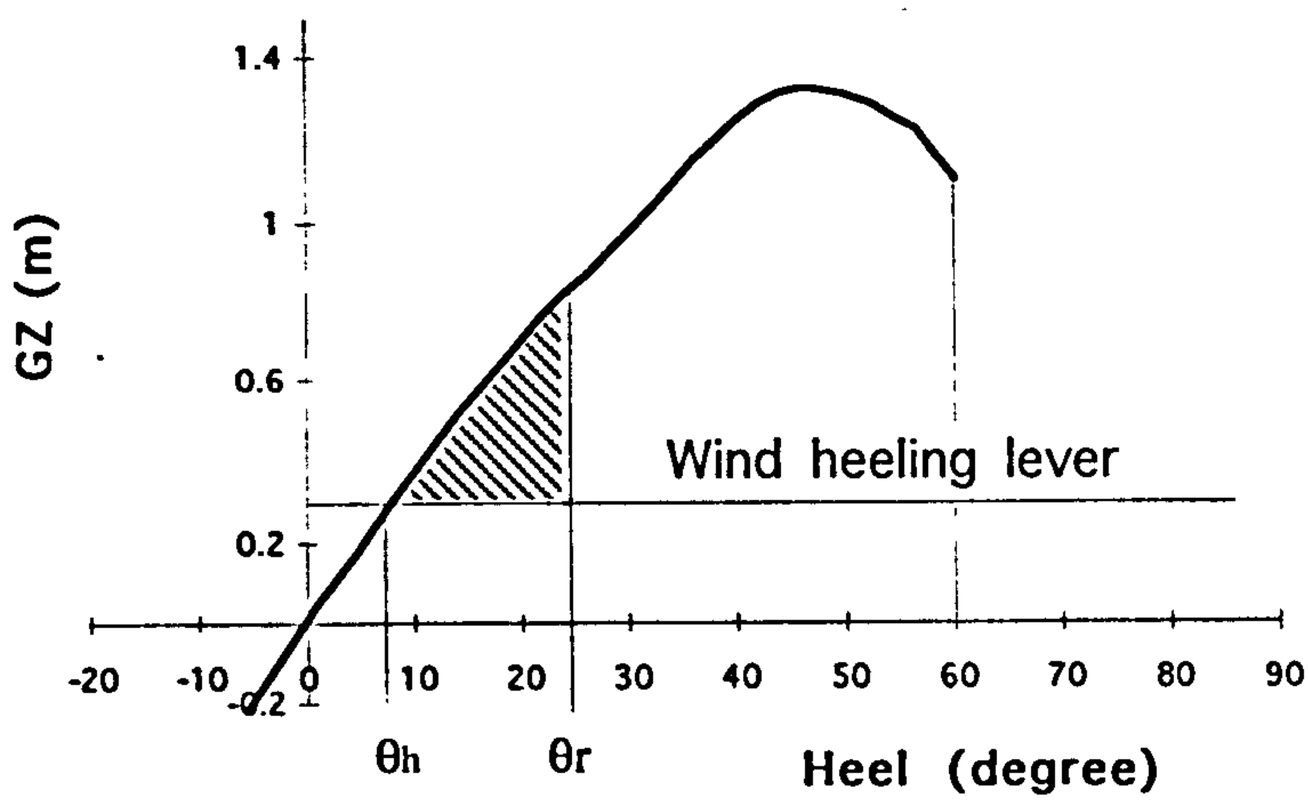

Figure 3.11 Intact GZ curve with side hull flare

Damaged Stability

According to the IMO code **(IMO 1977) (DTp 1991)** (details see Appendix 2), the extent of damage to the hulls was found as follows,

- Longitudinally, 5.97 metres (3 m + 0.03L) for side and bottom damage.
- Transversely, 3.8 metres (0.2B) for side damages and 12.0 metres for bottom damage.
- Vertically, full depth of the ship for side damages and 0.9 metre for bottom damage.

The subdivision of the centre hull was determined in accordance with the minimum requirement of **DNV (1992)** rules to the number of watertight transverse bulkheads and considerations in machinery layout. This resulted in 7 watertight bulkheads in the centre hull. The subdivision of the side hulls was determined by considering the damage extent of the hulls. Initially, a 6 metre long compartment was chosen for the side hulls, thus two

compartments (12 metres) were considered as flooded when damaged. Therefore, damage cases needed to be studied for the ferry were,

a Any two adjacent compartments of the centre hull flooded.

b Any two adjacent compartments of one side hull plus two adjacent compartments of one cross structure flooded, whilst the centre hull and the other side hull remain intact.

c Any two adjacent compartments of the centre hull plus two adjacent compartments of one side hull flooded.

d Any two adjacent compartments of the centre hull plus two adjacent compartments of both side hulls flooded.

All of the damaged cases were checked against the IMO criteria. The results showed that all of the cases in (a), (c) and (d) met the criteria for damaged stability quite comfortably. Figures 3.12 and 3.13 show two typical damaged cases (a) and (c).

But the damaged cases in (b) failed to meet the criteria. This was due to the heavy loss of buoyancy and waterplane area of the flooded side hull. So , the side hulls needed to be modified. The method discussed in solving the intact stability problems could also be used to tackle this problem, i.e., to increase the side hull length and flare. In addition, the following measures were considered,

- Further subdivision of the side hulls.
- Filling the side hulls with foam materials up to the design waterline to decrease the permeability.

The second option was dropped since it might make future structural survey and maintenance work difficult. The final refinement of the side hulls was through modifying the length , flare, and the subdivision of the side hulls. Firstly, the side hulls were further subdivided, the compartments being reduced from 6 m long to 3 m. This would not effect other features of the ferry very significantly, because the side hulls and the cross structures were transversely framed, and changing a few transverse webs in the side hulls into transverse bulkheads would give little increase in weight. Since the side hulls were not designed to accommodate any machinery equipment, smaller compartments should not cause any problems in layout. The side hull length was increased, to 35 percent of the central hull length following many calculations, and at the same time the flare of the side hulls was also adjusted (to 24 degrees).

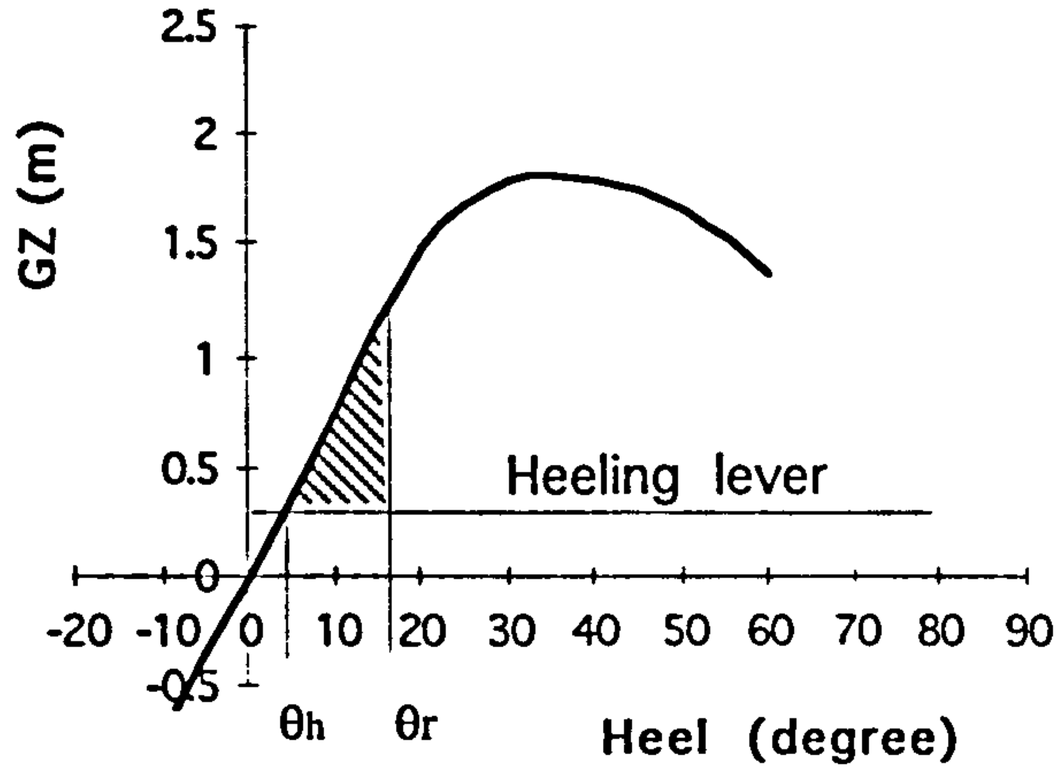

Figure 3.12 GZ curve with two centre hull compartments damaged (case a)

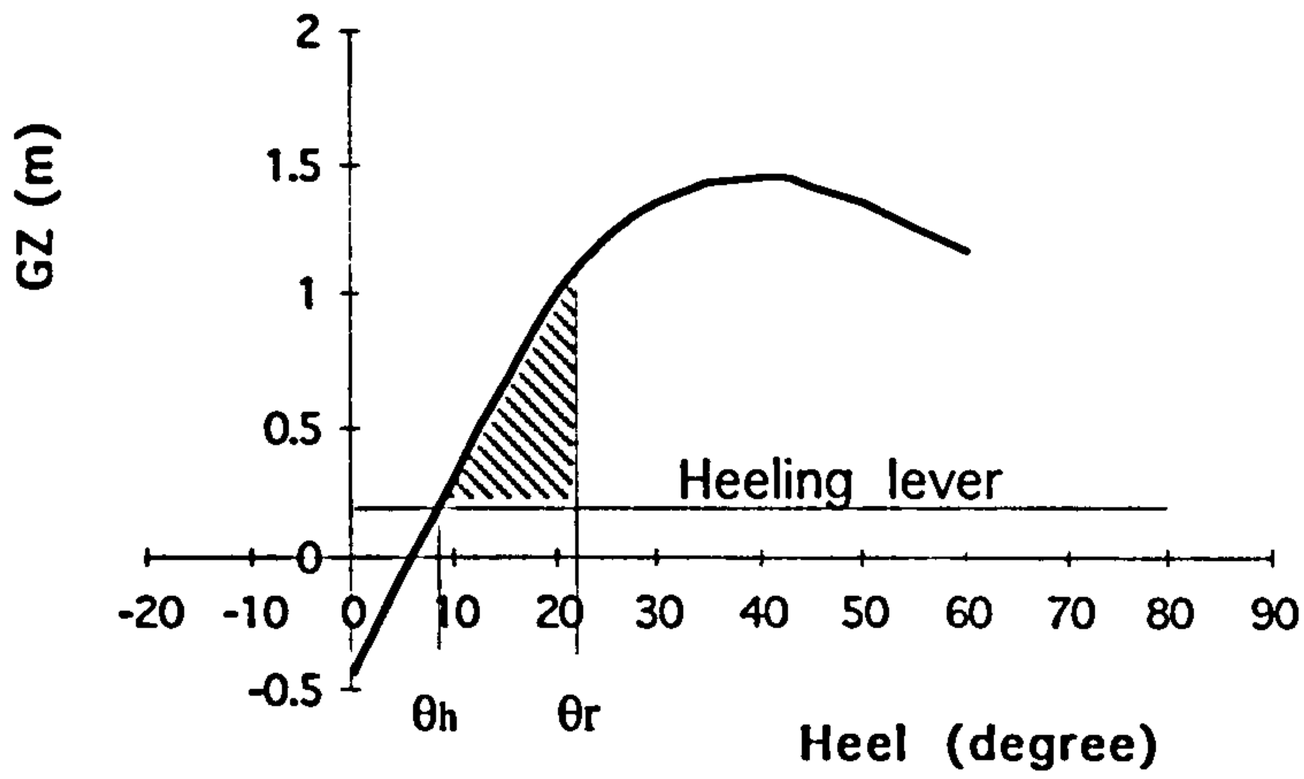

Figure 3.13 GZ curve with two centre hull compartments plus two compartments in a side hull damaged (case c)

Final calculations showed that, after the refinement of the side hulls, the ferry met all the damaged stability criteria. Figure 3.14 shows the GZ curve of a damaged case when three compartments (9 metres) at the middle section of a side hull plus cross structure are flooded.

The final configuration of the trimaran fast ferry is obtained and listed in Table 3.1.

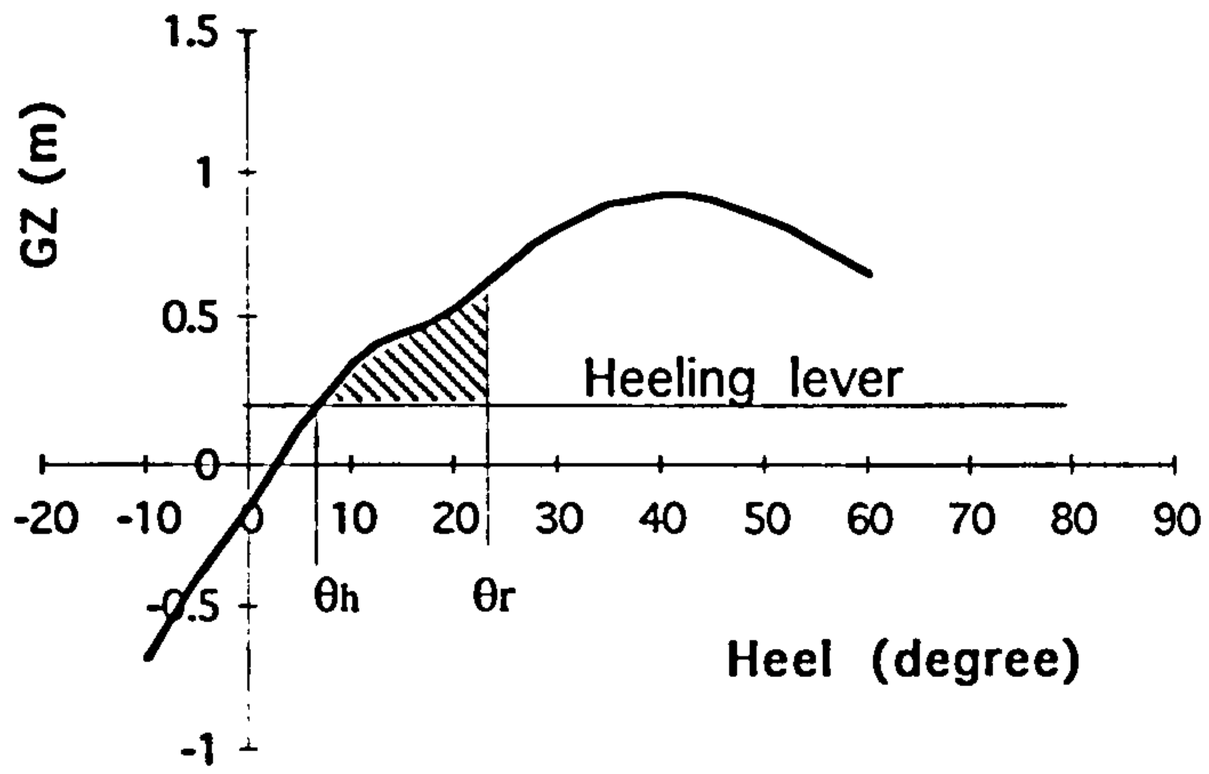

Figure 3.14 GZ curve with 9 metres of one side hull damaged

Table 3.1 Principal particulars of the Trimaran Ferry design

Overall Ship:		**Passenger/Car Capacity:**	
Length	105.00m	Passengers	450
Beam	19.20m	Car	90
Draught	3.40m		
Displacement	1130t	**Dead-weight**	
Centre Hull:		Passengers/Luggage	54t
		Cars	113t
Length WL	99.00m	Crew/Effects	2t
Beam WL	6.80m	Stores	5t
Draught Deep	3.40m	Duty-free Goods	8t
Displacement	1040t	Fuel	20t
		Fresh Water	8t
Side Hulls:			
		Total Dead-weight	210t
Length WL	35.00m		
Beam WL	1.50m	**Speed and Propulsion**	
Draught	2.00m		
Displacement	45t	Max. Speed (Full Loaded)	38knots
% Total Displacement	4.0		
		Main Engine	4 x RUSTON16RK270
Deck Box		MCR	4 x 5000kW x 1000 rpm
		Propulsion	2 x FPP
Length	80.00m		
Breadth	19.20m	Fuel Consumption	
Height of Car Deck	2.50m	(at Max. Speed 38kn)	104kg/n.mile
Height of Passenger Deck	2.70m		

3.6 Hull Forms and Powering

Hull Forms

The hull form of the centre hull was derived from Series 64 **(Yeh 1965)**, which is a US Navy high speed displacement form series based on destroyer forms with speed-length ratios up to 5.0 (knot/$\sqrt{\text{feet}}$). The variation of length to beam ratio in the series is from 8.5 to 18. The length beam ratio of the ferry's centre hull is 15, and the speed length ratio of the centre hull is 2.0, which are all well inside the range of the series data. The beam draught ratio was chosen as 2.0 to minimise the wetted surface area. The stern of the hull was slightly adjusted to accommodate propellers. The side hull forms were derived by distorting Series 64 forms with a smaller beam draught ratio. The increased draught was chosen to reduce the possibility of the bottom of the side hulls coming out of the water when the ship rolls in rough seas.

The hull form design is not further discussed here to avoid repetition, as the detailed considerations in trimaran hull form design are revealed in Chapter 4 where the hull form design of a trimaran model ship is considered.

Resistance

A computer program was developed, based on the Series 64 model experiment data, for the resistance prediction. Three parameters, beam-draught ratio, displacement-length ratio, and block coefficient were used to derive the coefficients of residuary resistance at various speed-length ratios. The friction resistance coefficient was calculated from ITTC 1957 line **(ITTC 1957)**. An allowance of 0.0004 was added to the coefficient of total resistance in keeping with normal practice **(Lewis 1989)**.

Figure 3.15 shows the predicted effective power of the trimaran ferry in the fully loaded condition. The effects of wave interaction between hulls were not taken into account at this stage of the trimaran study, although a early model test on multihull ships showed some negative effects on wave making resistance **(Everest 1968)**.

Propulsion

The propulsion system consisted of four RUSTON16RK270 medium speed diesel engines **(Ruston 1992)**, each providing 5000 kW at 1000 rpm. Two sets of GES gear boxes were used to reduce rpm to 455 to drive two fixed pitch **Newton-Rader (1960)** cavitating propellers with the characteristics listed in Table 3.2. Figure 3.15 also gives

the curve of shaft power for the ferry. Figure 3.16 shows the layout of the propulsion machinery.

Table 3.2 Propeller characteristics

Number of propellers	2
Diameter	2.20 m
Number of blades	3
Cavitation Number σ_t	0.67
BAR	0.95
P/D	1.44
rpm	455
η_o	0.68

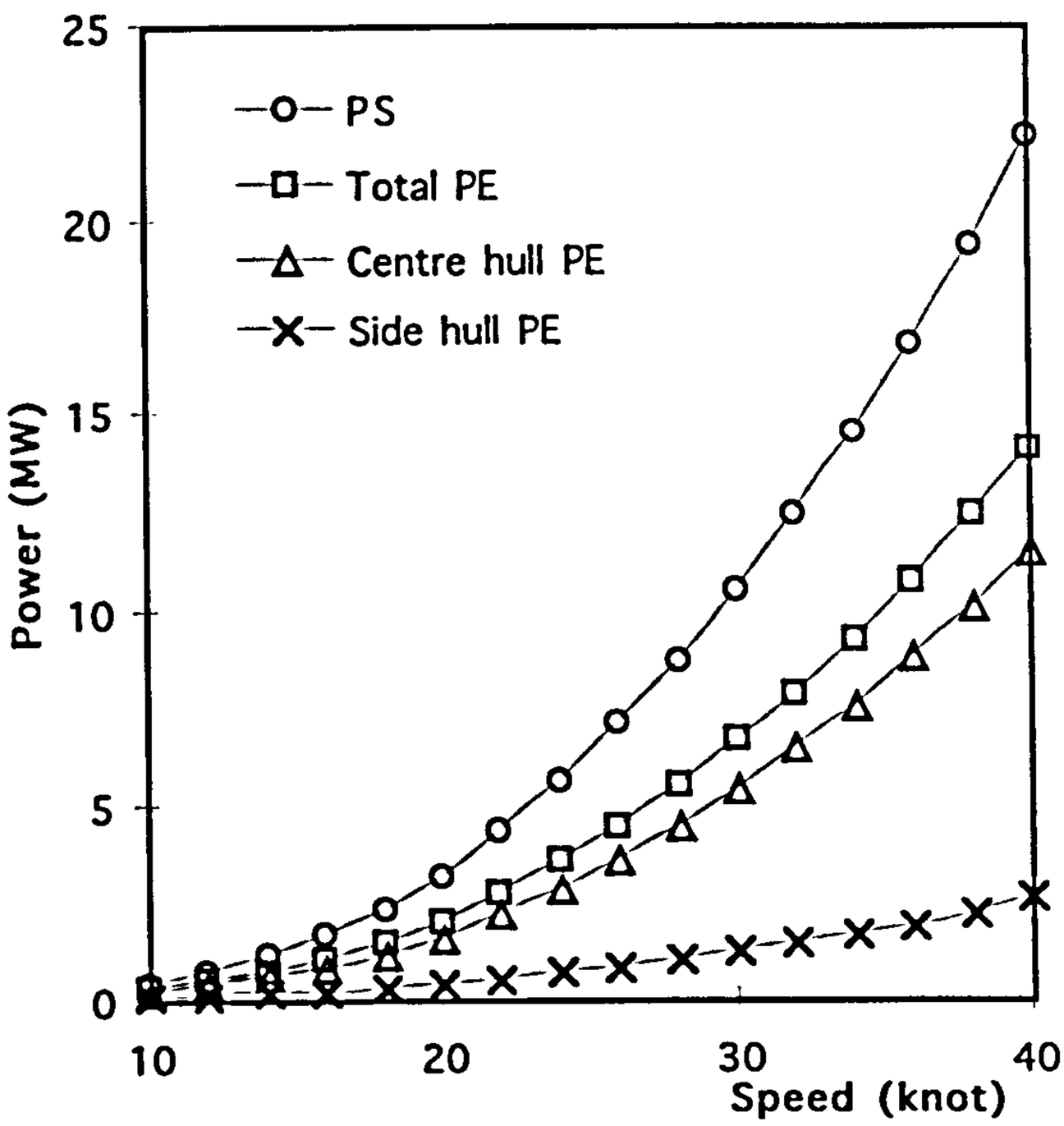

Figure 3.15 Power curves for the fast ferry

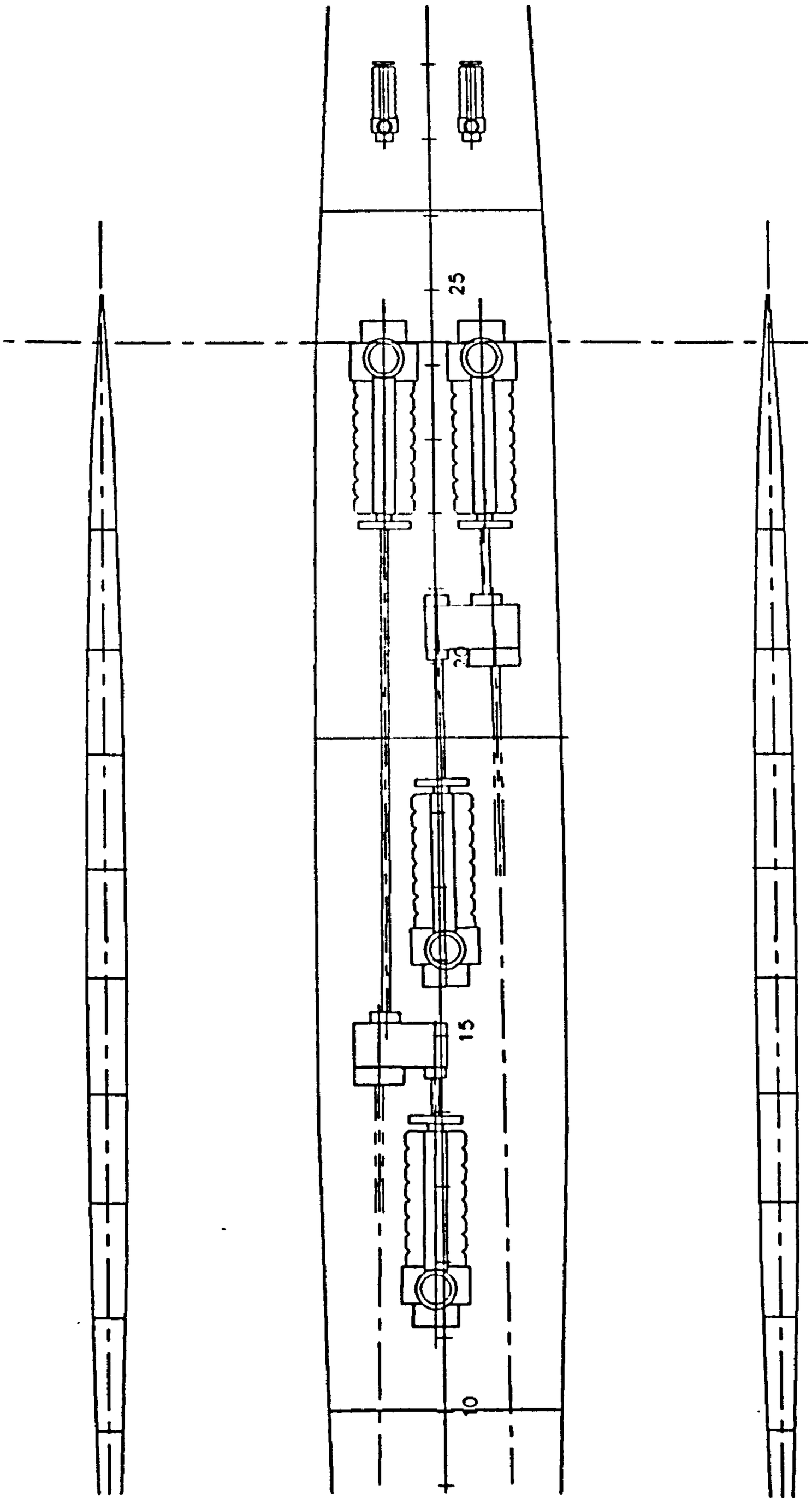

Figure 3.16 Layout of the propulsion machinery

3.7 General Arrangement

The general arrangement of the ferry is shown in Figure 3.17. The single car deck and the single passenger deck are located in the deck box. The propulsion machinery and the auxiliary machinery are accommodated in the centre hull. Trimming tanks are provided at the bow and stern of the centre hull. Heeling tanks are arranged in the side hulls.

Car Deck

The 1350 m^2 car deck offers a clear headroom of 2.2 m for cars of average required space of 2.8 x 5.9 m each. Cars are loaded from the stern of the ferry through a 2.2m high and 5 m wide opening. The 19.2 m beam of the deck box allows cars to U turn forward on the deck for efficient loading and unloading. The car deck is divided by a 2 m wide longitudinal trunk at the centre line, which eliminates any pillars on the car loads area and will make the traffic easy to organise. Stairways, engine casing, and store rooms are also accommodated in the trunk.

Passenger Deck

The passenger deck, total of 1180 m^2, is spilt into two compartments to comply with the requirements of fire control **(IMO 1977)**. Most of the passenger seats are arranged at the sides and the front of the deck box near to windows which would be taken as comfortable positions by most passengers. The spacious passenger deck can be arranged with various catering and leisure amenities. Accesses to the passenger deck are provided by internal stairways. Separate evacuation routes are provided for each compartments.

Machinery

The narrow beam of the centre hull requires some careful consideration for the machinery layout. The main propulsion machinery is located in the centre hull amidships. Two pairs of RUSTON RK270 diesel engines each drives a fixed pitch propeller at the stern via a GEC gear box. The narrow beam of the centre hull made the conventional symmetrical layout of the main engine groups impracticable. An asymmetric arrangement solution was found to solve the narrow beam problem as shown in Figure 3.16. The propulsion shafts run alongside the two aft engines. Each forward engine delivers power to a pinion at the bottom of the main wheel of the gear box, and this should also help to reduce the height of the engine room. A watertight transverse bulkhead divides the engine room into two to reduce the possibility of flooding causing shutdown of both shafts. Fuel and oil tanks are located in the double bottom. The

auxiliary machinery equipment has been arranged in the centre hull as well, and the two diesel generator units are located in the compartment forward of the main engine rooms.

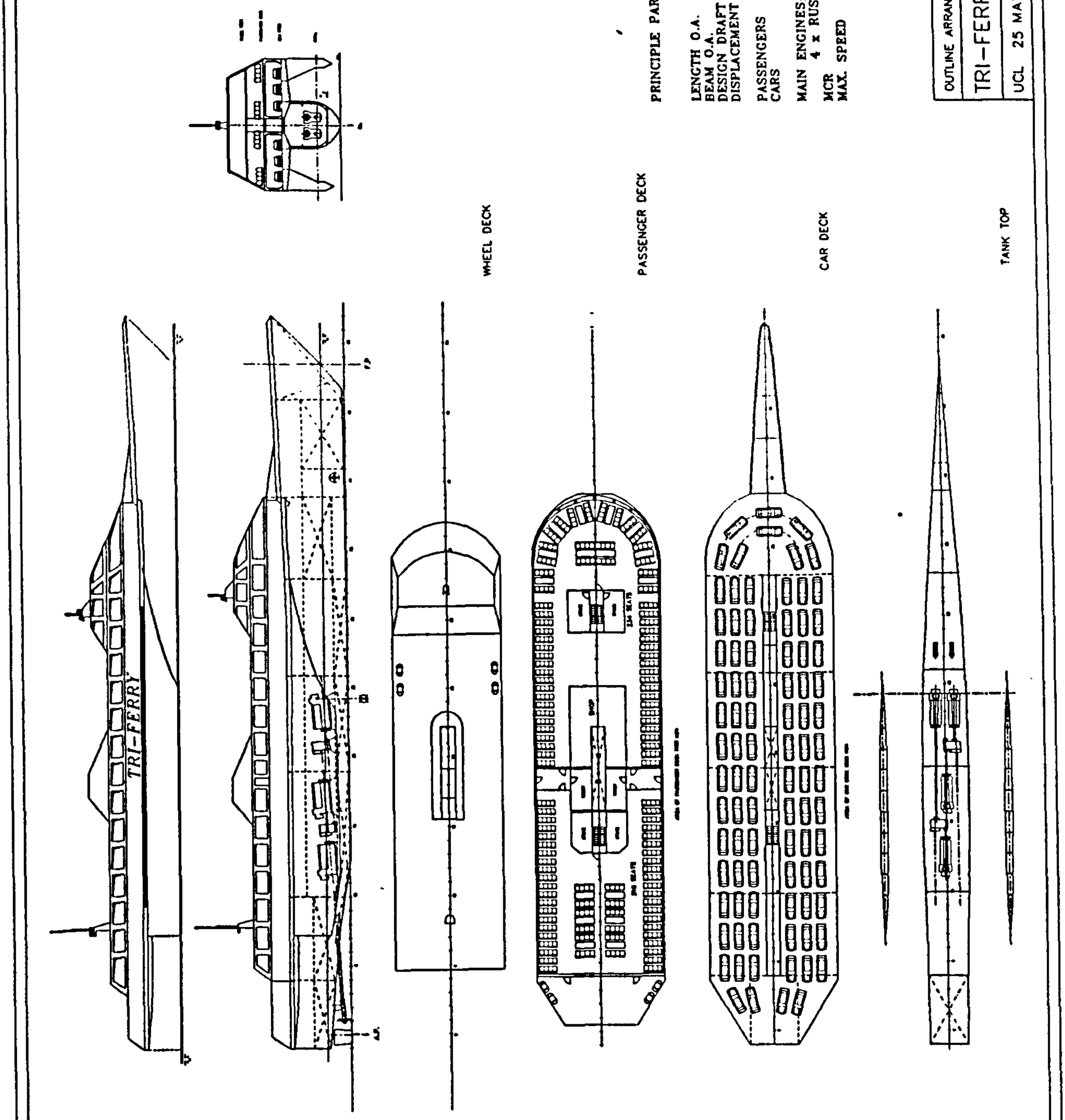

Figure 3.17 General arrangement drawings

3.8 Structural Design

The unique feature of the trimaran ship demands special considerations in its structural design. The main parts of a trimaran structure include the centre hull, side hulls, and the cross structure. These structural parts need to be designed with sufficient strength to resist the forces generated by the sea as well as the weight and internal loads from the ship itself. The aim is to keep the structure weight as low as possible.

The primary load for a trimaran is still the longitudinal wave load in head seas akin to the monohull, and its calculation is essentially straightforward and similar to that for the monohull. The transverse load on the side hulls and the cross structure can be considered as the secondary load, nevertheless, the design of the cross structure is still the key part of a trimaran structural design, because it is unique from any other existing ship types and also provides more choices for the designer for the structural modelling.

The structure of the ferry was designed in comply with the DNV rules for ships with length less than 100 metes **(DNV 1992)**. The rules were used for deriving the scantlings of platings, stiffeners, and frames for the main steel structure of the ferry. Since the rules were designated for monohull ships, the longitudinal strength calculations specified in the rules were not applicable to this three hull ship, therefore the GODDESS program **(Pattison et al 1986)** was used for direct calculation of the longitudinal loads of the ship balancing on a trochoidal wave. In addition, DNV rules for high speed light craft **(DNV 1985)** were also used in determining design loads on the cross structure.

Longitudinal Loads and Strength

Longitudinal loads on the hull girder were calculated for the fully loaded condition in terms of weight distribution, bending moments and shear forces. The ship was balanced on a trochoidal wave with the wave length equals to the length of the centre hull and the wave height equals to 5 percent of the wave length.

The centre hull, car deck, and the cross structures which extend 70 percent of the ship length, form the hull girder for the longitudinal strength calculation. The longitudinal load and strength calculation for the ferry is summarised in Table 3.3. The calculation was carried out using the GODDESS wave balance program. Appendix 3 shows the program results of the wave loading calculation for the ferry in sagging condition.

Table 3.3 Summary of longitudinal strength calculation

Wave Bending Moment:		
Still Water	9.70 MN-m	
Sagging	61.4 MN-m	
Hogging	25.9 MN-m	
Design bending moment	71.1 MN-m	
Required midsection modulus	4062 cm^2-m	
Calculated midsection modulus:		
Deck	11925 cm^2-m	
Bottom	8083 cm^2-m	
Stress at bottom	87.9 N/mm^2	(120)*
Stress at deck	59.5 N/mm^2	(120)*

* Figures in brackets indicate allowable stress

Transverse loads

The scantlings of the cross structure were decided by the transverse loading calculations. Two extreme static load conditions in beam seas were considered in this design. Firstly in the event of one side hull's total emergence from the water the cross structure needs to support the weights, and secondly in the event of the total immersion one side hull in the water the cross structure needs to resist the buoyancy force. The design was based on the first case as it turned out to be the limiting case.

The transverse load on the cross structure at the connection with the centre hull was calculated under the following assumptions:-

a The side hull came out of the water surface.

b Cars loaded on the car deck crowded to the ship side.

c The loads due to the weights of the superstructure and passengers above the car deck.

d Vertical acceleration was assumed for the average 1/100 highest accelerations **(DNV 1985).**

Figure 3.18 illustrates the loads on the cross structure. Where P_u represents the loads of passenger deck and structural weights, P_s is the weight of the cross structure, and p_c includes the loads of cars and the weight of the cross structure. The cross structure was

then designed by keeping the transverse stresses within the requirements of the rules **(DNV 1992).**

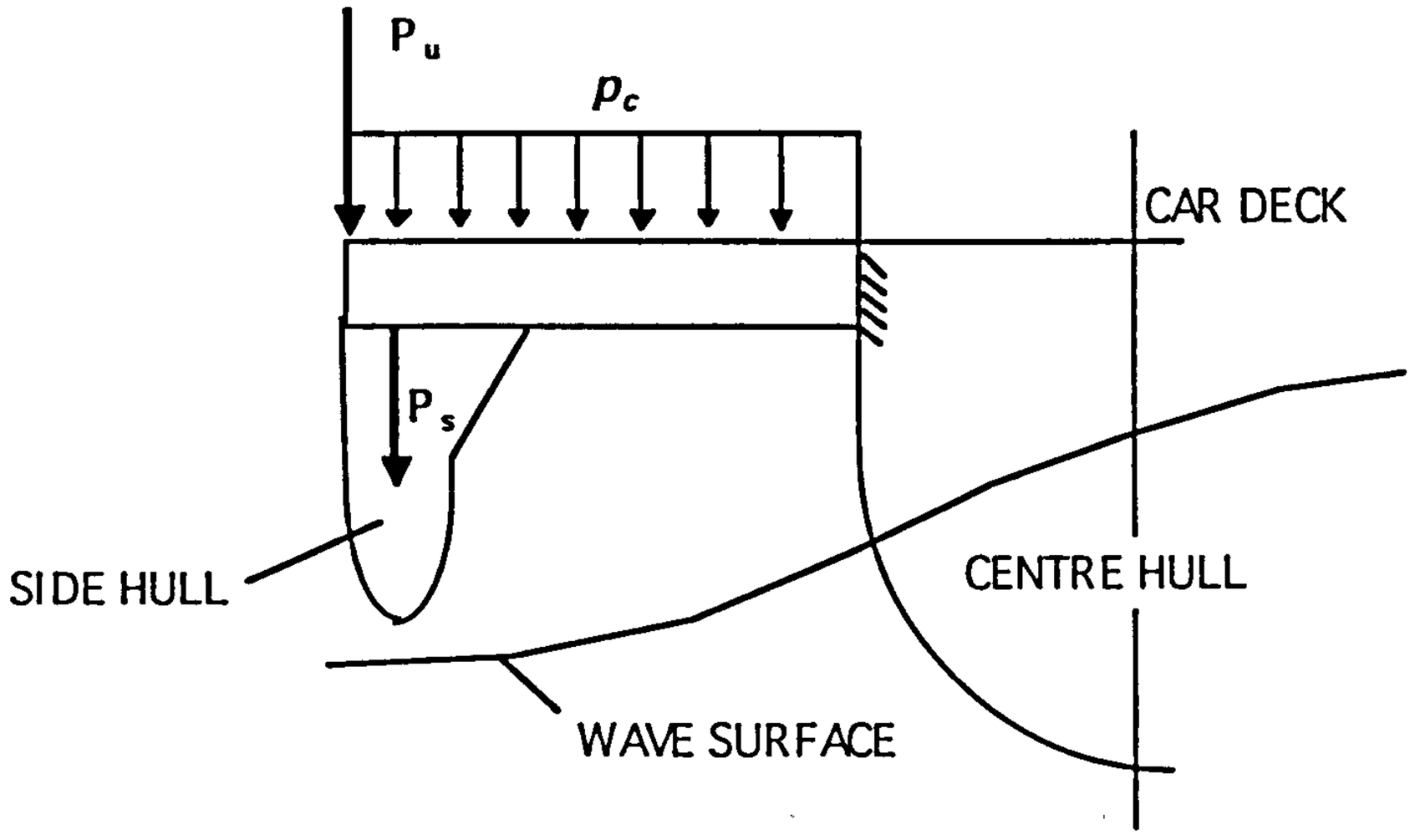

Figure 3.18 Loads on cross beam

Structural modelling

The main structure of a trimaran ferry may be described as two side hulls connected to a deck box supported by the centre hull. The structural model would neither be the same as monohull ships nor the same as existing twin hull ships. How the four main parts of structure, the main hull, deck box, and the two side hulls, should be connected together became the key question in the structural design.

Since the deck box is much wider than the centre hull and there should be no transverse bulkheads on the car deck for the purpose of easy loading and unloading, a transverse beam system of cross structure needs to be provided to support the deck box and the side hulls. Two forms of the transverse beams were considered. The first one was a double deck in the centre hull extended to the edges of the deck box as shown in Figure 3.19. It forms an integrated cross structure including the car deck. The advantage of this form was that, it would provide a very good support to the superstructure and the side hulls. But the scantling calculation and the longitudinal strength checks showed that the section modulus was far more than required by the longitudinal load. It would also be difficult to find a good value for the height of the cross structure. Deck heights between the car deck and the lower deck in the centre hull were investigated, and it was clear that a lower deck height would increase difficulties for construction and access to the centre hull due to the narrow space between decks, or the alternative of a higher double deck would mean increased material and weight.

Therefore , a second type of structural model was developed as shown in Figure 3.20. The lower deck within the centre hull was eliminated. The cross structure became two separate structures connecting the centre hull and the side hulls. The Longitudinal strength calculation showed that the hull girder strength was still sufficient for all loading conditions. The single car deck at the centre hull would make accesses to the compartments in the centre hull easier. The elimination of the lower deck at the centre hull would also reduce the structural weight.

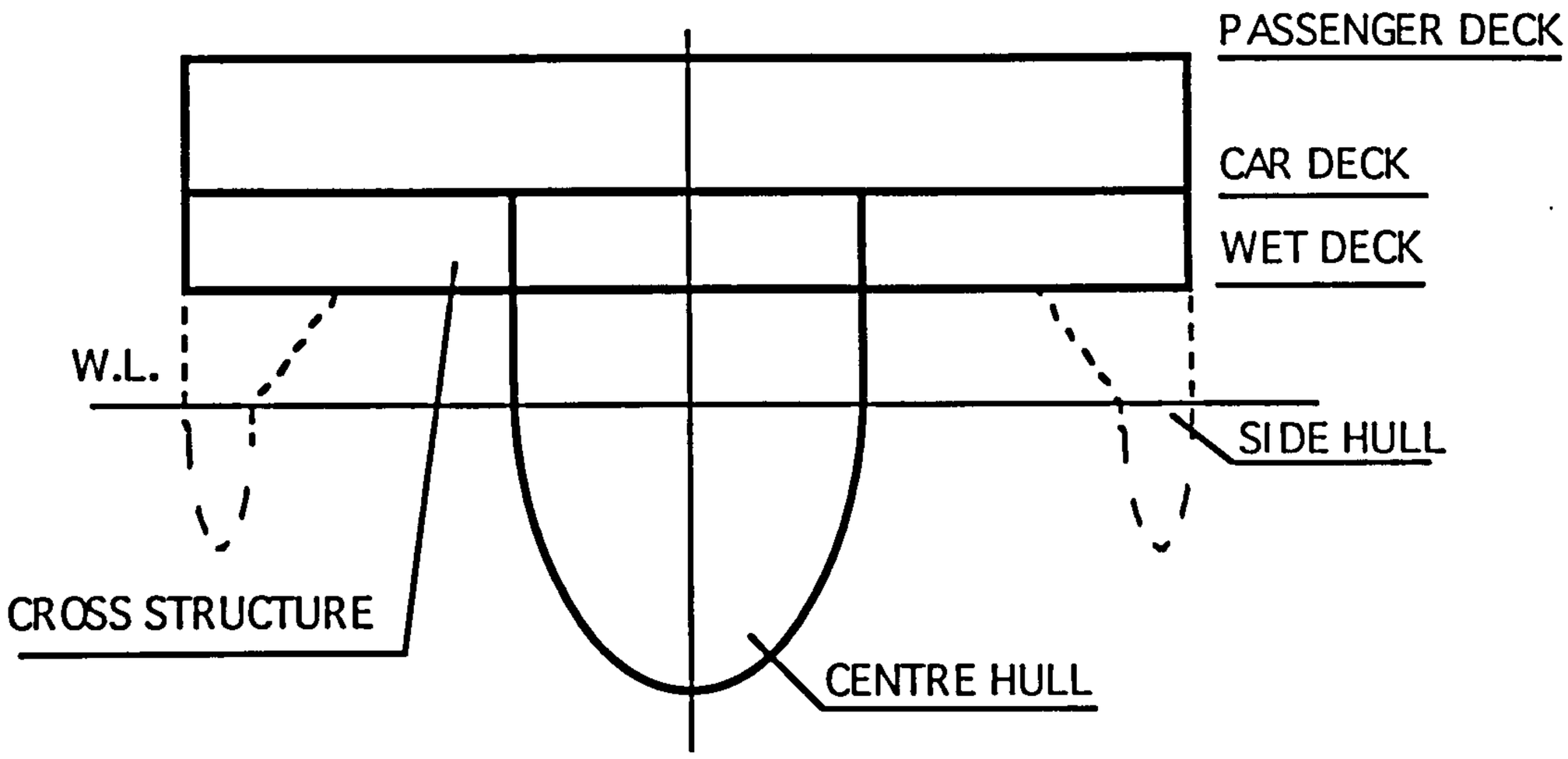

Figure 3.19 Structural model of double car deck

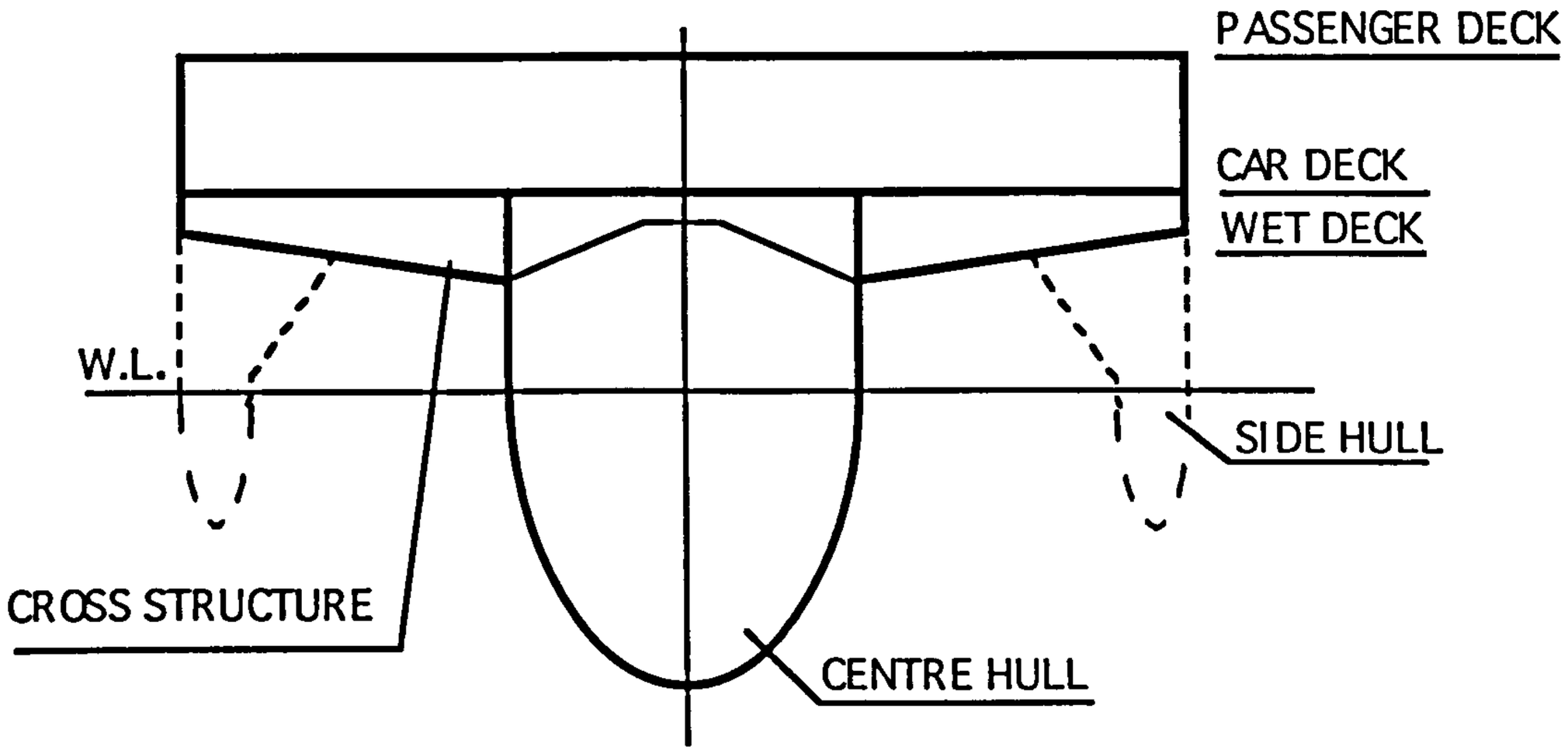

Figure 3.20 Structural model of single car deck at the centre hull

On comparing the two options, the second was chosen for the structural design of the trimaran due to its structural and space efficiency. The key area of this single deck option was the connection between the centre hull and the cross structures. Although the subsequent analysis showed that it would provide sufficient transverse strength even at the worst condition, special care would still be needed for the detailed structural design for the local structure to avoid stress concentrations.

The centre hull, the deck box up to the passenger deck and the cross structure were longitudinally framed with longitudinal spacing of 0.6 metre and transverse web spacing of 2.0 metres. The side hulls were transversely framed. All of the structures except the superstructure above the passenger deck are of mild steel. The longitudinal stresses either on the bottom of the keel or at the top of the car deck are low (see Table 3.3) and suitable for mild steel. DNV grade NVA mild steel was used except for those panels where higher grades of material are required by the rules. The superstructures above the passenger deck, which is not included in the sectional modulus calculation, are of aluminium alloy. This is to reduce the super structure weight. Figure 3.21 shows the final drawing of the main steel structure at the amidships.

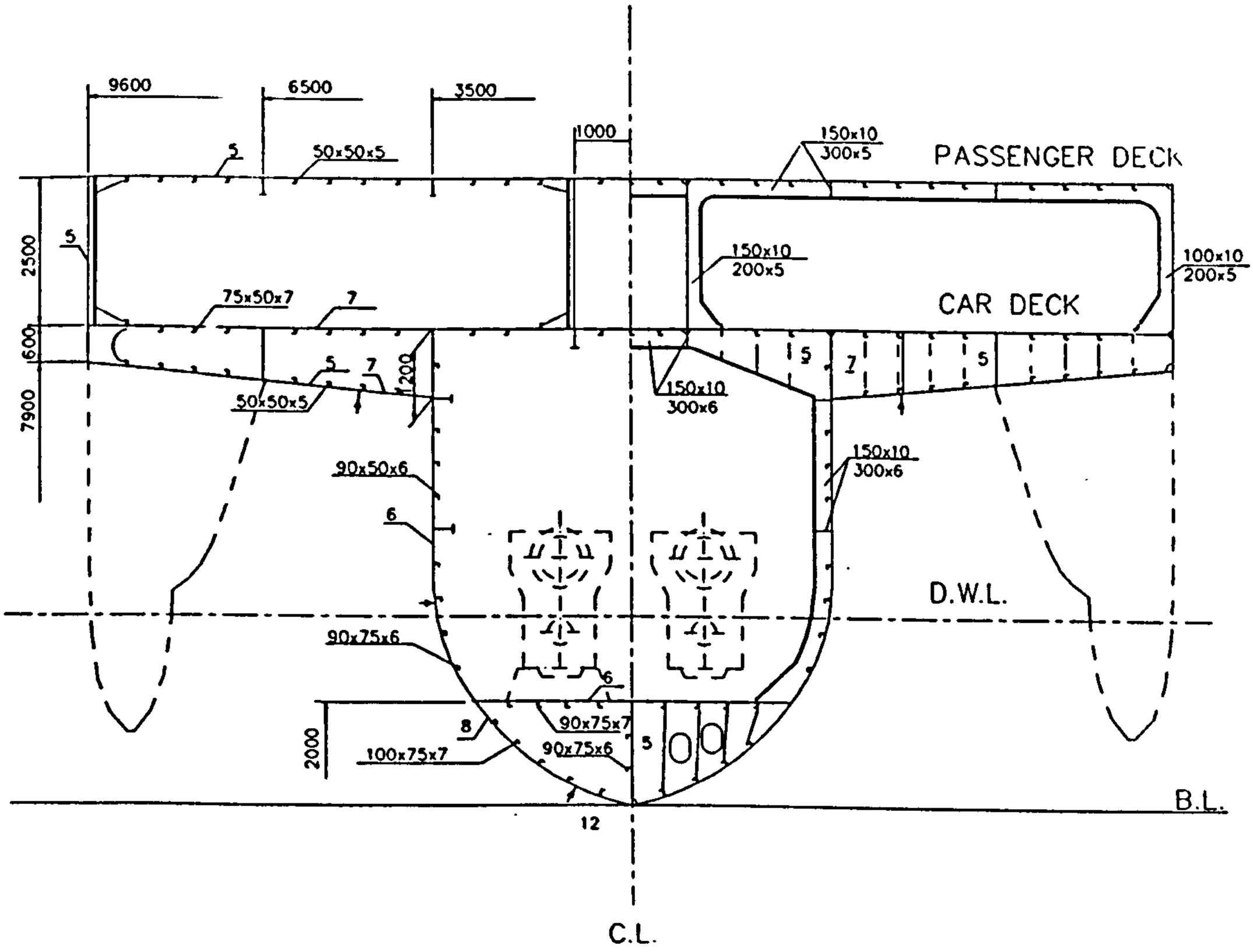

Figure 3.21 Midship section drawing

3.9 Comparison and Discussion

Potential advantages of the trimaran ship over other ship type have been generally discussed in Chapter 2. In addition, the trimaran ferry design has further demonstrated some of these possibilities.

Speed

It is commonly claimed that the modern marine vessels can only achieve high speed by using lightweight structural materials and light propulsion machinery **(Philips 1993)**. The trimaran ferry uses mild steel in its main structure but has achieved similar high speed as that of those lightweight material constructed ferries. This is mainly because the trimaran ferry has better resistance performance and higher structure efficiency.

It is clear from Figure 2.8 that the trimaran ship is superior to conventional monohull ships in resistance. This is also the same case when comparing the trimaran ferry with a catamaran ferry of the same displacement. Figure 3.22 shows the effective power curve of a 700 tonne catamaran ferry, derived from the dimensions of the 74m SEACAT **(Jane's 1991)**, comparing with that of a trimaran ship of the same displacement. The trimaran ship shows less resistance over the whole speed range. The main dimensions of the two ships are listed in Table 3.4.

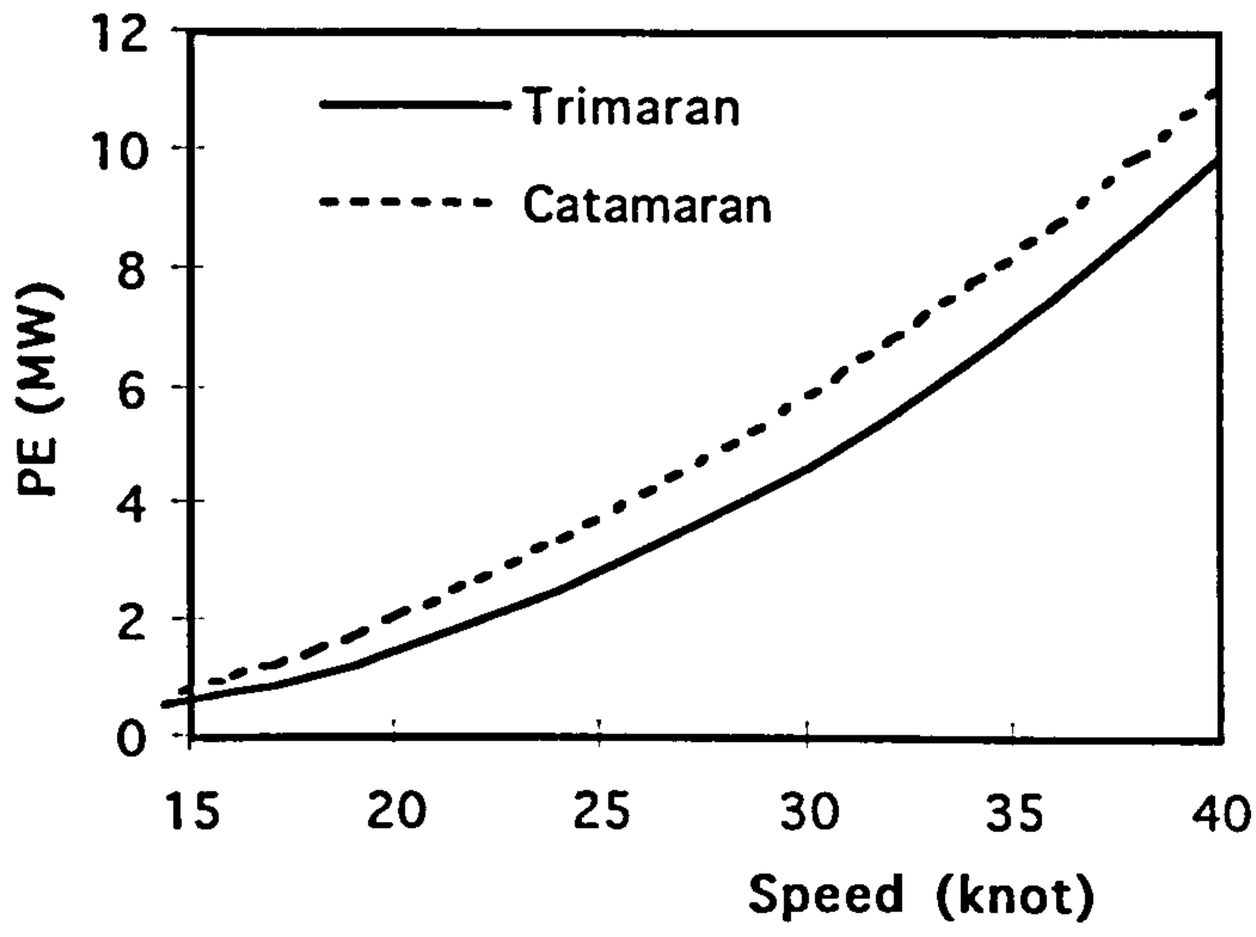

Figure 3.22 Resistance comparison between a trimaran and a catamaran with equivalent displacements (700t)

Table 3.4 Parameters of the trimaran and the catamaran in comparison

Parameter	Catamaran	Trimaran	
	Demi-hull	Centre hull	Side hull
Length WL (m)	60.0	85.0	30.0
Beam WL (m)	4.4	5.7	1.4
Draught (m)	2.4	2.9	1.4
Total Displacement (t)	700	700	

Structure

The structure efficiency of the trimaran ferry is less than that of monohull but greater than that of catamarans and SWATH ships, because, the long and deep centre hull forms a very strong hull girder as the monohull; the smaller span of the cross structures reduces the transverse loads; and the small size of the side hulls makes them subject to less hydrodynamic loads. These factors make the trimaran ship structure lighter than a twin hull ship of the same construction material. However, to clarify this issue, extensive investigation into the dynamic load on the trimaran hull is needed.

Layout

Similar to twin hull ships, the trimaran ferry provides a large car deck area with a wide beam which is most desirable feature for a car ferry and is not achievable for monohull ferries of similar size. The open space on the passenger deck would also be very attractive to passengers.

The narrow centre hull causes difficulties in the layout of propulsion machinery, but the asymmetric main engine arrangement pattern used in the trimaran ferry design showed that the problem could be readily solved by effectively utilising the space of the long centre hull.

Safety

The safety of car ferries has been high on the agenda in recent years after several ferry disasters, centred on the issue of preventing water flooding the car deck and causing capsize. The trimaran ferry possesses the following advantages in this respect:-

- The stability can be tuned by varying the side hull configuration to achieve a level of stability not practical for a monohull ferry

- The car deck is further away from the water surface than a monohull ferry thus reducing the possibility of water entering the car deck

- The wide car deck beam allows passenger cars to U turn for easy loading/unloading, therefore, the bow door can be eliminated as shown in the design (Figure 3.17). The Estonia type of disaster (**RINA 1995**), where the water entered the car deck from the damaged bow door, can therefore be avoided.

In addition, the steel structured car deck of the trimaran ferry provides better fire protection compared with aluminium ferries.

CHAPTER 4

TRIMARAN MODEL EXPERIMENTS

4.1 Aims of the Experiments

As summarised in Chapter 2, the initial studies on the trimaran ship hydrodynamic performance were mostly qualitative rather than quantitative, mainly by exploiting the knowledge obtained by the trimaran designs carried out at UCL. A series of discrete investigations were undertaken into various aspects of trimaran naval architecture, including initial seakeeping analysis designs **(Zhang 1992)** **(Pearson & Schild 1992)**, resistance model experiments **(Cudmore 1992)**, and manoeuvring model tests **(Bowman 1993)**, but the extent of these investigations were very limited due to the lack of analytical tools and test facilities at the time.

The seakeeping analyses in the trimaran designs **(Zhang 1992)** **(Pearson & Schild 1992)**, were performed using monohull strip theory programs, either ignoring the side hulls or 'bulging' the main hull to incorporate the small additional displacement. This was necessary because UCL lacked seakeeping computer tools for multihull ships. This simplification is probably to a reasonable degree acceptable for symmetric modes of motion, pitch and heave, but for asymmetric motion modes, especially for the roll motion, this is not acceptable because in this mode the interactions between three hulls could be very significant.

The model tests to investigate trimaran resistance conducted by **Cudmore (1992)** produced initial results on the interference of the three hulls by finding the change in resistance when the centre hull and side hulls were towed separately and then together and showed varying detrimental interference up to a maximum of about 10 percent of total resistance of the ship. However the results could only be taken as an initial indication of the resistance characteristics of the trimaran ship because, firstly, the model was based on the very first trimaran design, the Advanced Technology Frigate **(Bastisch & Peters 1990)**, of which the hull form design (particularly the side hull design) was not up to the current knowledge of the trimaran concept (the side hulls were relatively short and fat); secondly, the model was very small, only 1.5 metres in length. The experiments on manoeuvrability **(Bowman 1993)**, using the same 1.5 m model, indicated that the trimaran configuration had excellent directional stability as expected for a long slender monohull, but the accuracy of the tests was limited as with the resistance tests, due to the small scale model and the limitation of the UCL testing facilities. There had been no theoretical predictions and analyses in both aspects apart from the equivalent monohull approach.

It was necessary to undertake more comprehensive and rigorous investigations than were possible solely using the University's experimental facilities. From discussions with

DRA Haslar, it was decided that DRA Haslar and UCL's Naval Architecture Research Group (NARG) would commence a programme of ship model tests and analytical prediction work proposed by UCL **(Pattison & Zhang 1993)**.

From the preliminary investigations it was felt that the first area to be studied in depth would be that of seakeeping performance. The greatest uncertainty was seen to be in the rolling motion where no analysis had been possible. This implied a full set of seakeeping model tests using a free running, fully instrumented and controlled ship model. This was undertaken in the main Haslar Manoeuvring Tank (60m by 120m) where a range of wave headings and frequencies could be imposed on the model. In addition, there was a need to carry out conventional towing tank resistance tests to better predict the hull resistance. There was also a need to address the manoeuvrability aspect.

A detailed hull form design for a 5000 tonnes trimaran ship was carried out **(Zhang 1993)**, as described in the following sections, to provide a proper trimaran hull form for the model experiments and subsequent theoretical work. Although the primary purpose of the hull form design was to provide a model ship for the experimental and analytical work, the design process described in the subsequent sections also revealed some general considerations in the development of the trimaran hull forms.

4.2 Basic Requirements to the Trimaran Model Ship

The decision to design a new trimaran hull form **(Pattison & Zhang 1993)** rather than adopting an existing one was made because the existing trimaran designs were mostly concentrated on initial sizing and feasibility studies of the trimaran concept and lacked detailed consideration of the hull form design, particularly on the size and the shape of the side hulls. The flexibility and the sophistication of a trimaran hull form lies largely in the side hull configurations which offers the designer more choices of design variables compared with other types of hull forms and consequently demands more consideration. Side hull design has important effects primarily on intact stability, damaged stability , seakeeping, resistance, and the building cost of the ship. All of these aspects need to be taken into account in the hull form design.

In selecting the characteristics of the ship on which the model tests should focus, it was decided the design should be based on the likely requirement for which the trimaran might be considered, if its apparent potential could be demonstrated. The next major class of naval surface ship being considered for the Royal Navy is the Future Escort

(Betts 1996). This vessel is likely to lie in the 4,500 to 6,500 tonne size range as described by **Andrews & Zhang (1995)**. It was therefore decided to take one of the existing UCL designs, a 5000 tonne AAW Destroyer **(O'Brien & Russell 1993)**, as the basis for the trimaran hull form design. Operational requirements to the destroyer are shown in Appendix 4.

The critical ship dimensions, as far as the design of the trimaran hull form was concerned, were the waterline length of 150m, corresponding to a model length of 6m, and the ship's overall beam. To determine the effects of the trimaran hull form variations, it was decided that as well as an overall beam of 25m, as in the AAW Destroyer study, a second set of side hulls would be designed to fit a model with an equivalent ship overall beam of 30m. This would then give some indication of the effect of significantly different hull separations on the seakeeping behaviour of a trimaran frigate. It was important to ensure that the two sets of outrigger hulls were designed to the same set of criteria so that the two trimarans were comparable in a clear manner. The criteria and the logic behind the two designs were:

(1) *The same centre hull.*

This meant that any variation in the performance between the two designs would be due to the different side hulls and their separation. It is envisaged that the effects due to slightly varying the centre hull parameters on the hydrodynamic performance of a trimaran ship would more or less similar to that of a monohull ship and it was not seen as an objective to be explored in this experiment.

(2) *The same length for the side hulls.*

The function of the side hull is to provide the ship with extra waterplane area and volume to meet the stability requirements. The length of the side hull is normally dominated by the stability requirement, particularly the damaged stability. With the same overall ship length the two trimaran configurations would be subject to the same damaged length in case of damages.

(3) *The same GM value.*

The value of metacentric height in the deep condition was to be the same for the two variant models. This was set to find out if the roll period in particular was governed by $\sqrt{GM}$ in the same manner as for a monohull. This meant that the side hulls in the case of the 30m equivalent beam would have reduced waterplane area relative to that of the 25m equivalent beam model.

(4) *The same heeling angle.*

The draughts of the side hulls were chosen to allow the two hull configurations to reach the same heeling angle when the keel of one side hull emerged from the still water surface. This was also imposed to ensure the effect of the side hulls in roll were at least comparable in this regard. When this constraint is taken with the GM constraint, it means that the displacement contribution of the side hulls in the 30m equivalent beam case is considerably less than in the 25m equivalent beam model. That is each side hull contributes only 2.7% of ship displacement compared to 4.2% in the 25m equivalent beam design.

4.3 Details of the Trimaran Model Hull Form Design

4.3.1 Hull Form Design Considerations

With the overall requirements of the model ship defined in the previous section and the need to produce two sets of outrigger hulls to meet the constraints listed, it was possible to design the hull forms. For a trimaran, this has to be done in three distinct but related parts, namely the centre hull, the two side hulls and the cross deck structure joining the three hulls. The final principal characteristics of the full scale ships on which the 6m model would be based are given in Table 4.1.

Centre hull

In order to meet the raison d'être of a trimaran, the centre hull must be extremely slender. The parametric study carried out in the design study of the fast ferry (Chapter 3) showed that the advantage of the trimaran ship on resistance can be achieved with a centre hull length beam ratio between 14 to 15. In the case of this model ship the length to beam (L/B) was taken as 14. The beam to draught ratio (B/T) was about 2.0. This was chosen to achieve minimum wetted surface area of the submerged hull to reduce the frictional resistance.

Table 4.1 Principal particulars of the trimaran hull forms

	Ship 1	Ship 2
Centre Hull:		
Length WL	150.00m	150.00m
Beam WL	10.80m	10.80m
Draught Deep	5.50m	5.50m
Displacement	4289t	4289t
Cm	0.803	0.803
Cp	0.581	0.581
Side Hulls:		
Length WL	60.00m	60.00m
Beam WL	1.80m	1.14m
Draught	2.80m	3.50m
Displacement	198t	126t
% Total Displacement	4.2	2.7
Overall Ship:		
Overall Length	160.00m	160.00m
Overall Beam	25.00m	30.00m
Depth	11.70m	11.70m
Displacement	4685t	4541t
Side Hull Span	11.14m	13.97m
WL Hull Separation	4.84m	8.00m
Air Gap	3.50m	3.50m
LCG	-3.77m	-3.44m
VCG (Fluid)	8.10m	8.21m
KM_T	10.60m	10.71m
GM (Fluid)	2.50m	2.50m
Pitching radius of gyration	39.16m	39.16m
Rolling radius of gyration	4.77m	5.11m

The methodical hull series data for such slender hulls is limited. The Series 64 **(Yeh 1965)** was produced specifically to address very high L/B ratios and was used for power prediction for some of the UCL design studies in Table 2.1. However, it was found that a Series 64 derived form would give too penalising a powering requirement at the frigate cruise speed of 18 knots **(Pattison 1993)**. Whereas a high speed merchant ship would

operate at a high design speed, naval ships spend considerable time at cruise speeds which therefore governs endurance and hence fuel consumption. It was therefore considered that a more appropriate series on which to base the hull form development and resistance prediction was the Taylor-Gertler Series (**Gertler 1954**). This series covers L/B up to 14 and B/T down to 2.25. The hull form was then developed with a B/T of 2.0 and a midship section coefficient of 0.81 both slightly beyond the minimum Taylor-Gertler values. The lines plan of the centre hull is shown in Figure 4.1. To ease the hull fairing required at the model manufacturing stage, the final form consisted of a distortion of an existing monohull ship (**DRA 1995**) but had the same hull parameters as the UCL design.

Side hulls

The side hulls were designed from several considerations:

a. *Minimum side hull length.*

This obviously results in reduced structural weight for the whole vessel and decreases the wetted surface area, keeping down installed power and fuel carried. The limiting factor on the side hull length was primarily meeting the stability requirements and to a lesser extent the cross deck area.

b. *Minimum acceptable metacentric height (GM).*

In comparison with a catamaran which has inherently a high transverse GM and consequently stiff rolling characteristics, the trimaran's GM can be tuned. It was decided to design the side hulls' waterplanes to produce a GM = 2.5m in the ship's deep condition for both sets of side hulls. Whilst this was larger than a typical monohull (1 - 1.5m) it was the minimum required GM obtained from stability analysis. Further discussion on the choice of GM for trimaran ships will be found in Chapter 9.

c. *Stability requirement.*

This largely dominated the choice of the side hull form. From previous design studies it was expected that the critical stability condition was likely to be the most extreme damage case of the four discussed in Section 3.5, namely damage to a side hull with the main and other side hull remaining intact. A minimum damage length of 15% of ship's length (i.e. 22.65m) was imposed assuming flooding without

vertical limit **(NES 109 1989)**. This resulted in five adjacent compartments of the side hull being flooded giving a flooded length of 28.5m. Under this substantial loss of side hull buoyancy the ship will heel towards the damaged side, the other side hull will then come out of the water and the resultant righting lever (GZ) would reduce in value. This dominates the choice of the side hull length and flare. The necessary amount was determined by applying the NES (Naval Engineering Standard) stability criteria **(NES 109 1989)**. This approach was used with the GODDESS CASD system to systematically increase the flare of the side hulls until an acceptable design of side hull was achieved for both the 25m and 30m equivalent beam designs. Finally, with regard to stability, having designed the side hulls for the deep condition of the ship, stability in the light condition was checked. This showed that ballast was required in the side hulls to meet the same NES damage stability criteria in this light condition, which assumed some 800 tonnes of variables consumed. The resultant ballast requirement was found to be 80 tonnes per side hull for the 25m equivalent beam design and 50 tonnes per side hull for the 30m equivalent beam design. The results of the stability calculation are given in Appendix 5

d. *Cost considerations.*

Even within the design constraints above there remained the choice of the precise lines of the side hulls. It was considered appropriate to reduce the extent of hull curvature in the side hulls. This was done to ease production in an eventual ship programme in order to reduce construction cost and time. At this stage, without any detailed hull resistance analysis and model testing, it was not possible to say whether this would have any detrimental effect on resistance. Once the size of the side hull is determined, any small change of the side hull shape should have little effect on the total resistance of the ship. Flat surfaces were therefore adopted in the above and underwater form of the side hulls. This led to two sets of knuckle lines giving a hard chine, flat bottom and flat sides below and above the deep waterline. Since it was assumed that twin shafts would be fitted to the main hull, it was further assumed that no propulsive or even manoeuvring devices would be fitted in either side hull. This meant the side hulls could be symmetric, about their midlength, again for ease of construction and definition. Figures 4.2 and 4.3 show the lines plans of the side hull forms of the two model ships respectively.

e. *Other considerations*

Other considerations were, to a degree, arbitrarily introduced within the constraints of the above issues, however, they were thought to be consistent with the likely design evolution of a future frigate project. Thus a flare of some 7° from the vertical was

incorporated in the outboard side of the side hulls to meet the perceived radar signature reduction requirement. It is relevant that, unlike a monohull, this does not lead to a reduction in the righting lever (GZ) curve at high heel angles as this loss of waterplane due to flare can be compensated by the flare on the inboard sides of the side hulls. A rise of floor of 30° was incorporated into the lines of the side hulls to reduce the slam induced pressures on the side hulls in extreme sea states. The bows and sterns of the side hulls were given similar rakes to those for the centre hull. This was an essentially aesthetic consideration in the absence of any clear hydrodynamic investigations to date.

Finally, the midship section of both side hulls was located 0.1L aft of amidships. This was a little arbitrary but was consistent with the frigate upper deck and internal layout, together with a concern to reduce the extent to which the cross structure was likely to be exposed to wave action in the forward portion of the main hull. The effects of side hull position on hydrodynamic performance, with regard to the wavemaking resistance and the turning ability, are discussed in Chapters 7 and 8.

Cross structure

Following the practice in the UCL frigate design studies, the cross deck structure had the same length at its maximum width as the side hulls. Thus there was no consideration of either overhanging or reduced length of the cross deck, as can occur with SWATH vessels. Again, this followed on from the configuration of the frigate design study and seemed logical as regards structural design considerations prior to any specific structural design investigations. Finally, as far as the cross deck was concerned, an air gap of 3.5m was adopted from the underside or wet deck of the cross structure to the design waterline. This value was chosen from the preliminary seakeeping analysis described in Section 4.3.2 below.

The final configurations of the two ship designs are shown in Figures 4.4 and 4.5.

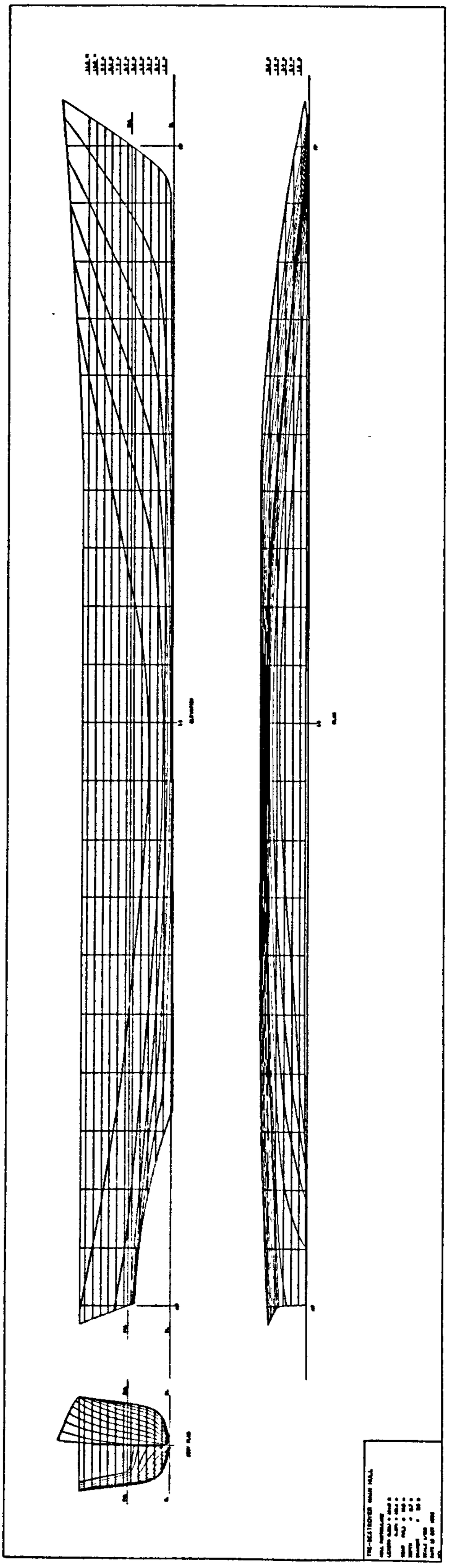

Figure 4.1 Centre hull lines plan

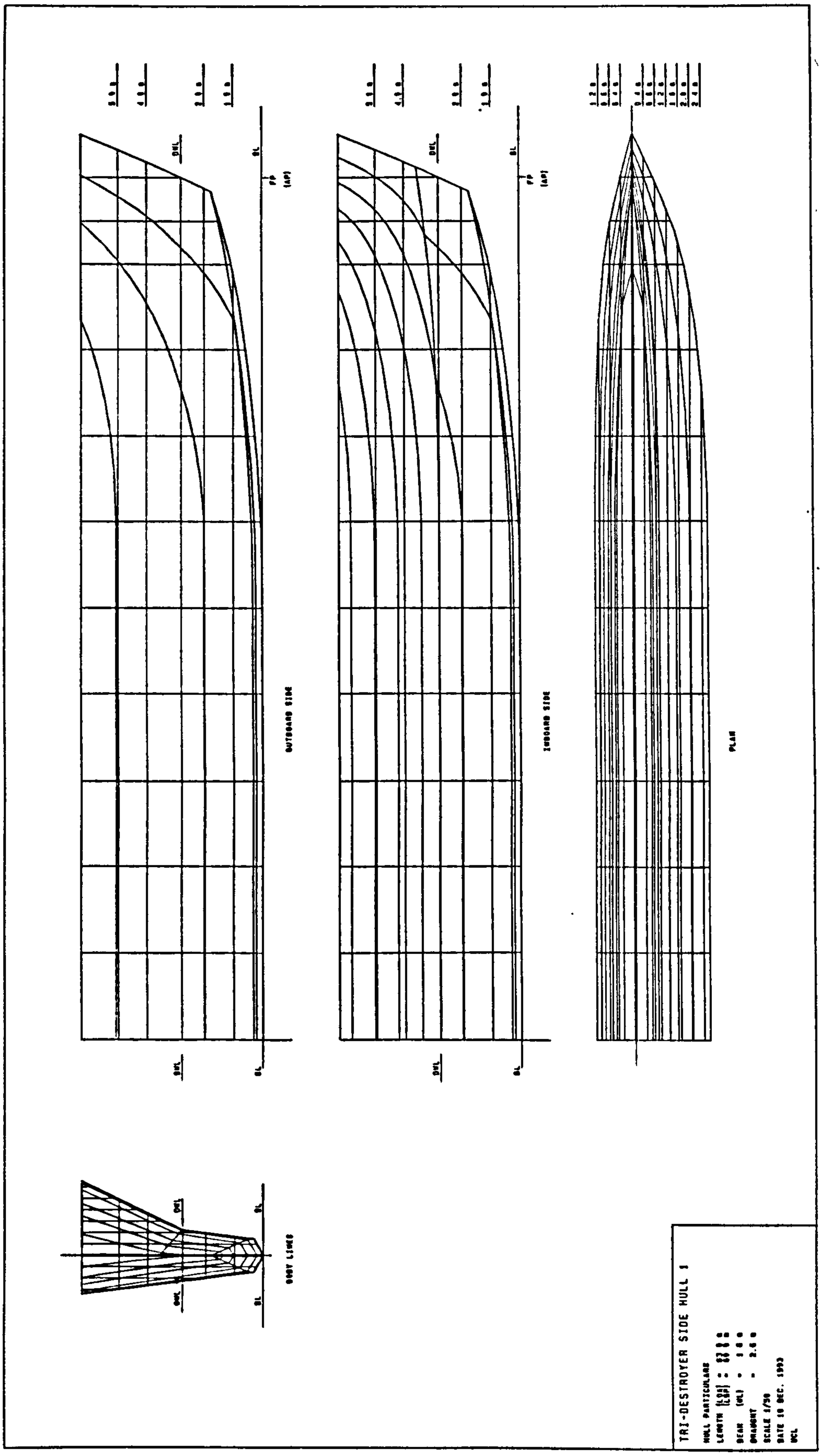

Figure 4.2 Side hull lines plan for Ship 1

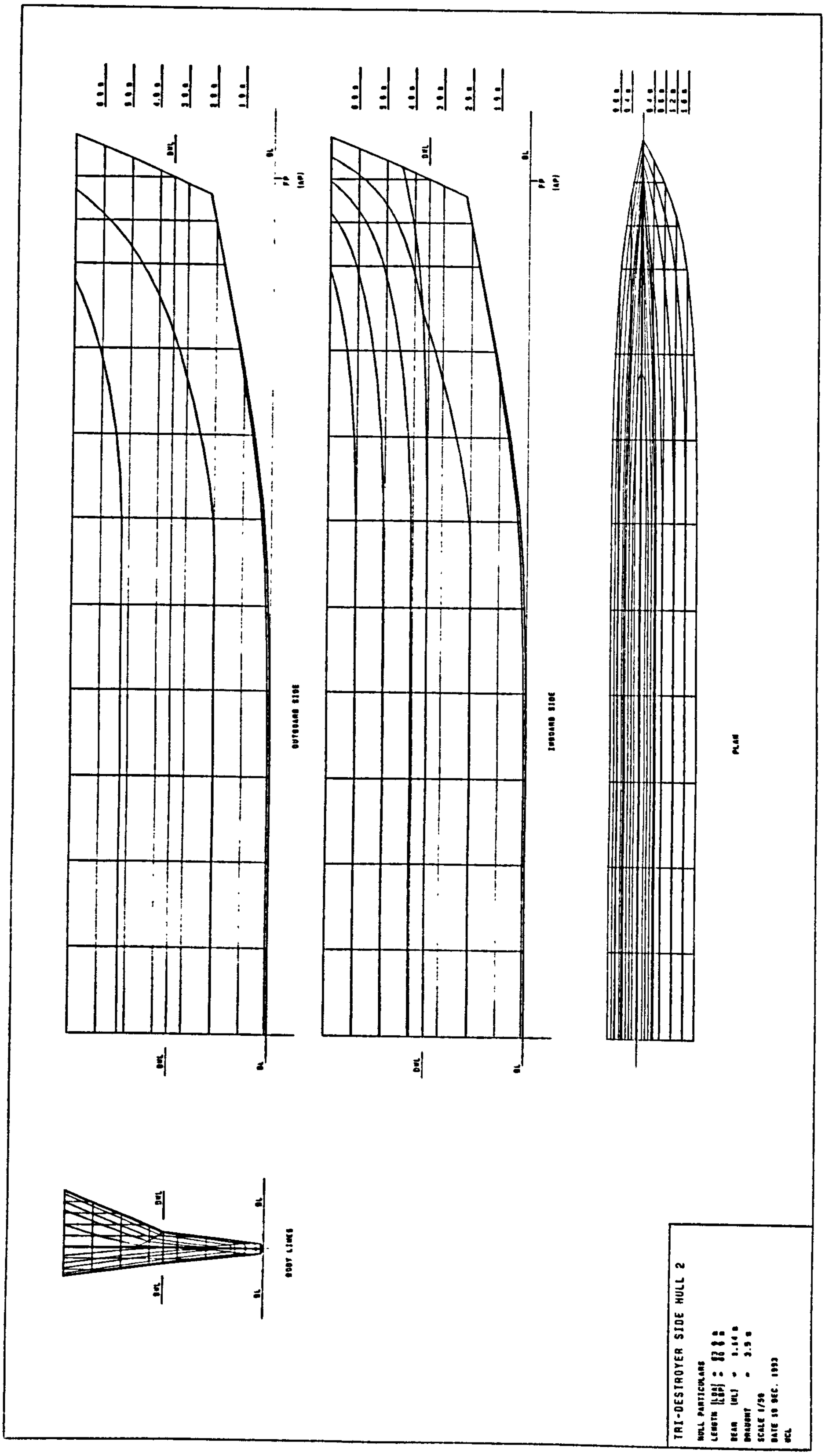

Figure 4.3 Side hull lines plan for Ship 2

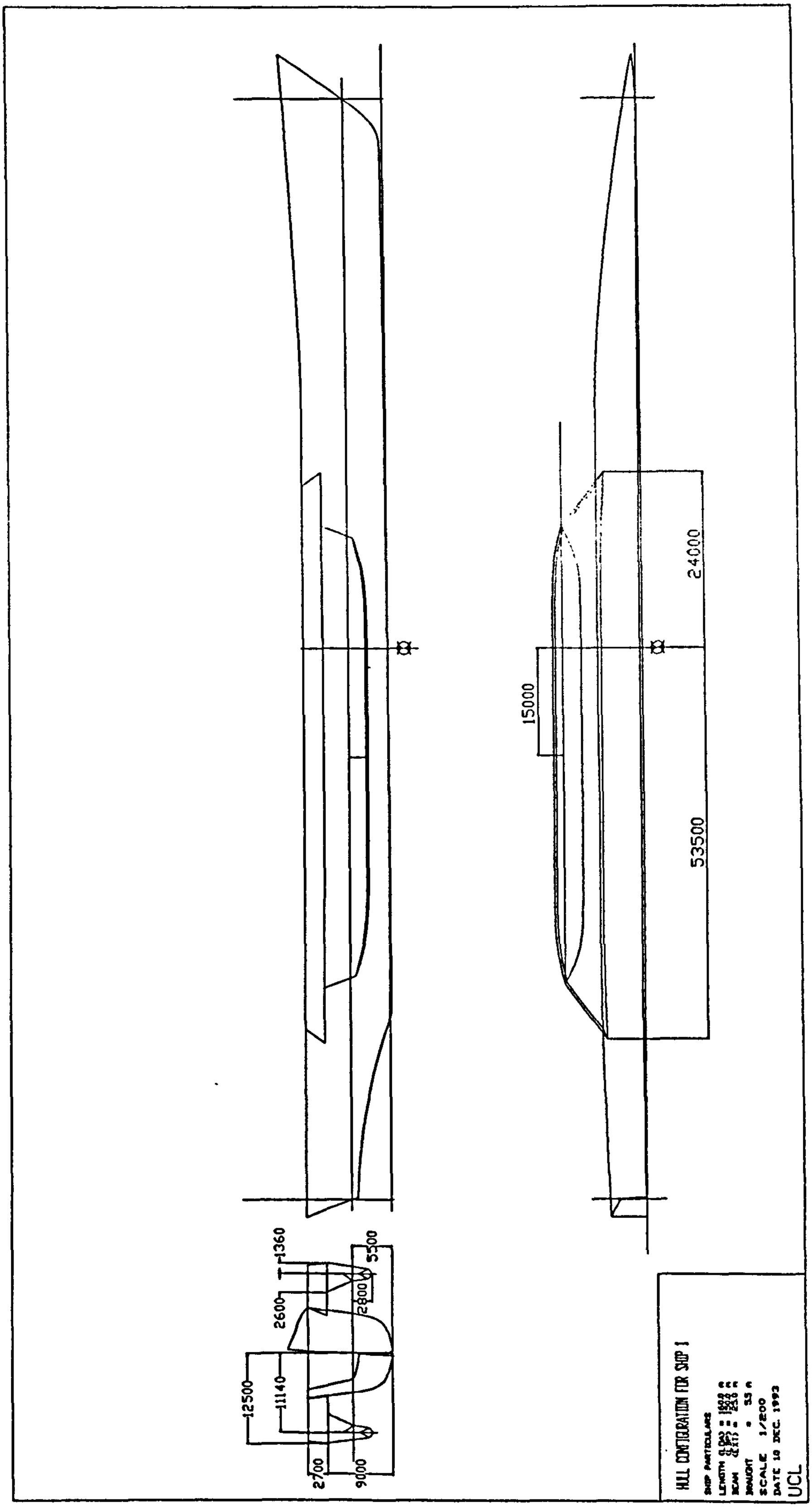

Figure 4.4 Hull form configuration of Ship 1

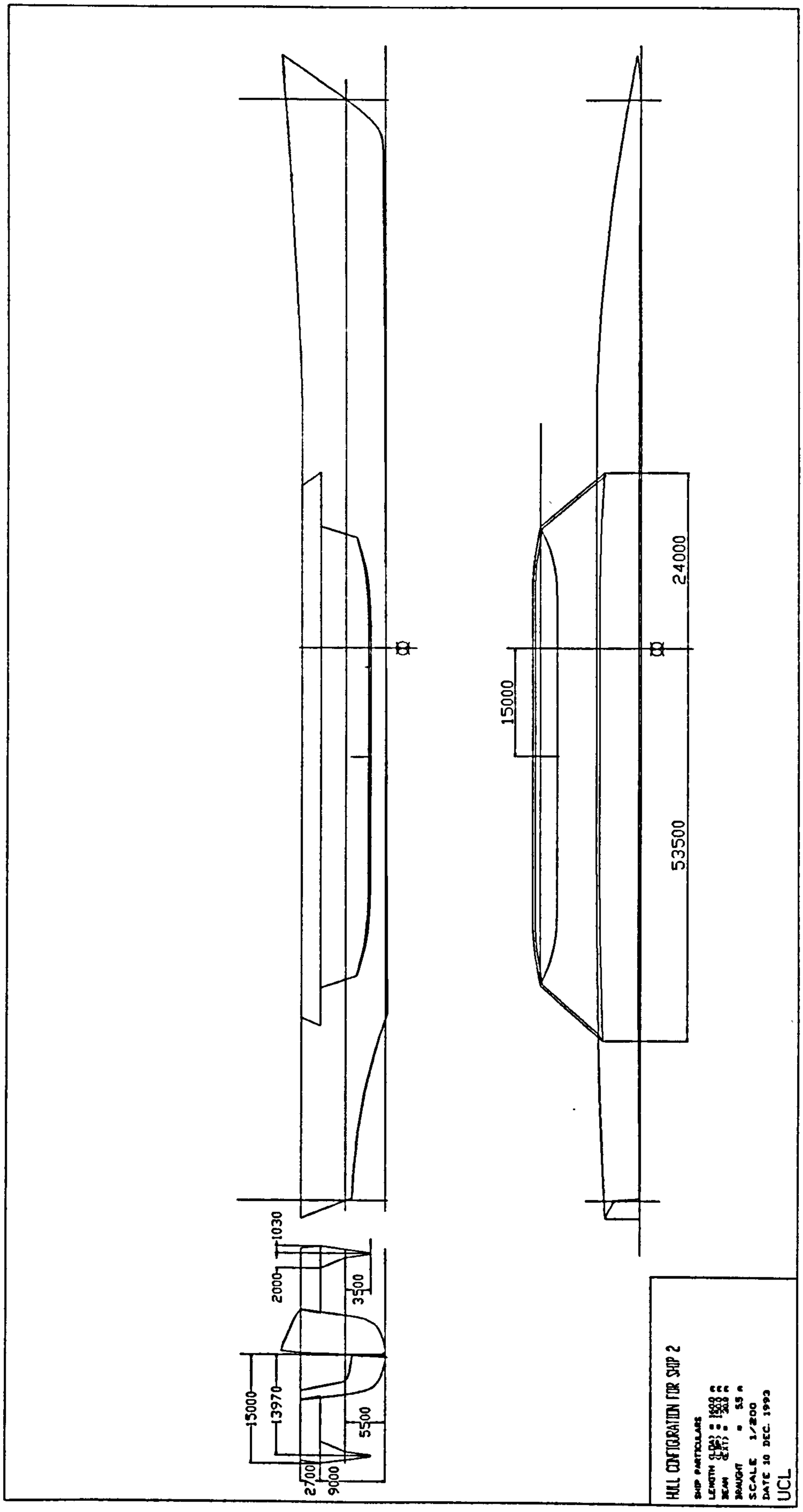

Figure 4.5 Hull form configuration of Ship 2

4.3.2 Initial Seakeeping Analysis

At the stage that the hull form was being selected for the trimaran model, the *GODDESS* strip theory seakeeping program (PAT-86) was used for the symmetric (pitch and heave) motion analysis of the model hull. This gave some insights into the likely overall behaviour of the trimaran. This program **(Andrews, Loader & Penn 1984)** is based on the SCORES program **(Raff 1972)**. The sea states considered were specifically for head seas as the extreme case for pitch and heave motions. For asymmetric motions, a three dimensional theory program is developed and described in Chapter 5.

The seakeeping criteria adopted for this preliminary indication of the behaviour of the model hull was based on the criteria for naval ships proposed by **Comstock et al. (1982)** and listed in the following Table 4.2 .

Table 4.2 Seakeeping criteria adopted in the model ship design

Slamming at keel	<	20 events per hour
Deck wetness	<	20 events per hour
Acceleration at bridge	<	$2.0m/sec^2$
Acceleration at flight deck	<	$1.0m/sec^2$
Slapping on wet deck	<	20 events per hour

The choice of the hull form parameters (see Table 4.1) was based on the *GODDESS* analysis of the seakeeping performance of the trimaran model ship. Presented in Figure 4.6 are the plots of the limiting speeds for the hull form for a range of sea states to meet the five criteria listed above. The impact on the design to meet the five criteria differs for each criteria. For example, to reduce the slapping at the bottom of the fore body of the ship demands deeper draught, while to reduce the deck wetness and slamming on the wet deck under the cross-structure demands higher freeboard. The best result for the design would be when the five criteria are meet which means the ship will reach a similar speed limit at the same sea state for all the five criteria.

Of the five criteria, the slamming on the bottom of the fore body of the centre hull appears to be the limiting one between the sea state 5 to 7. Slamming is affected by two major factors, draught of the hull and the dead rise of the ship's bottom. The centre hull of the trimaran ship is very slender that the dead rise of along the ship's bottom is higher than that of a monohull as shown in Figure 4.7, which would be advantageous in terms of slamming to compensate for the effects of the increased relative motion at the ship ends

due to increased hull length. A small beam draught ratio (B/T=2.0), as described in a previous section, was also chosen to increase the draught to reduce the slamming.

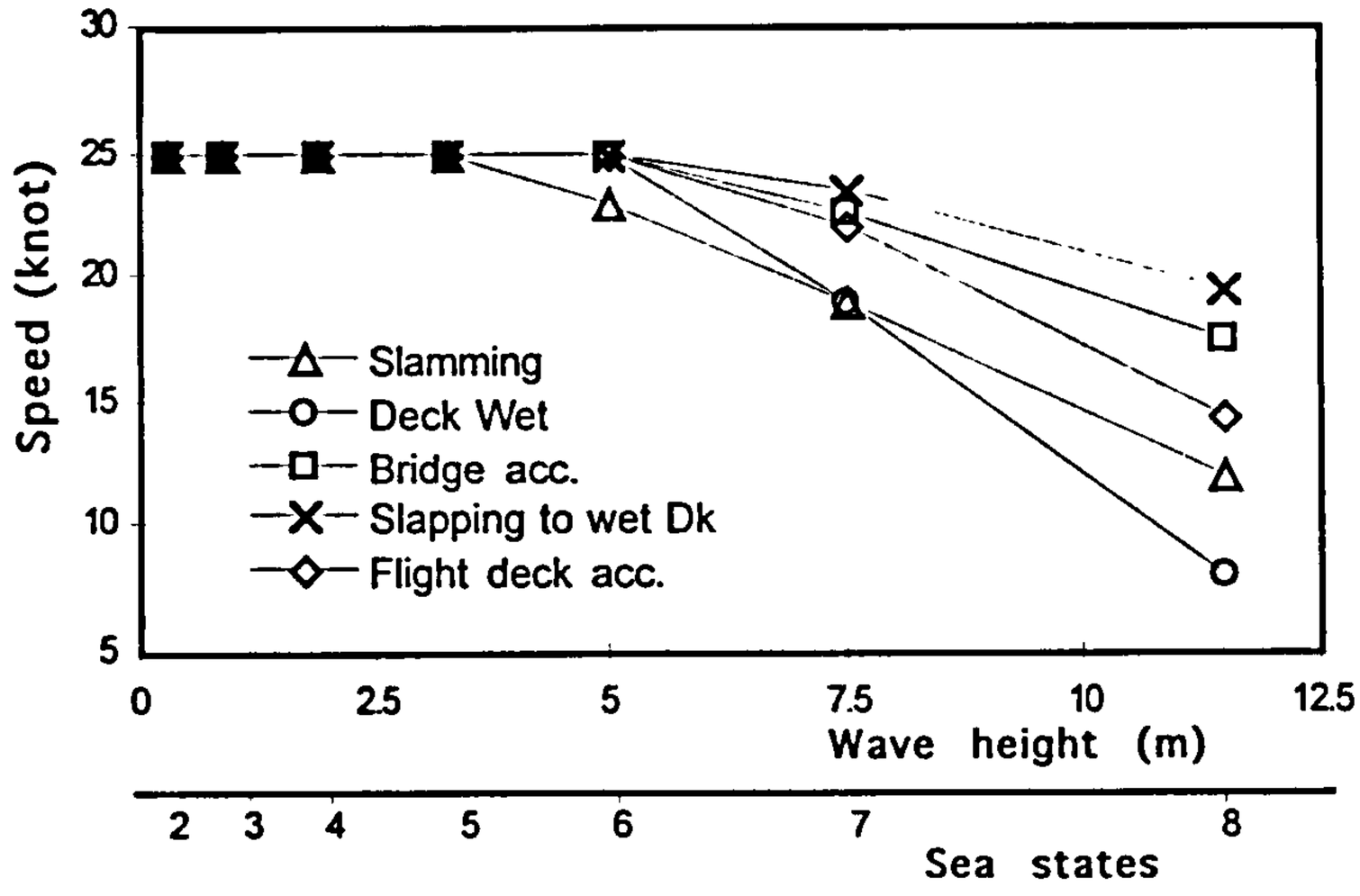

Figure 4.6 Speed reduction by seakeeping criteria

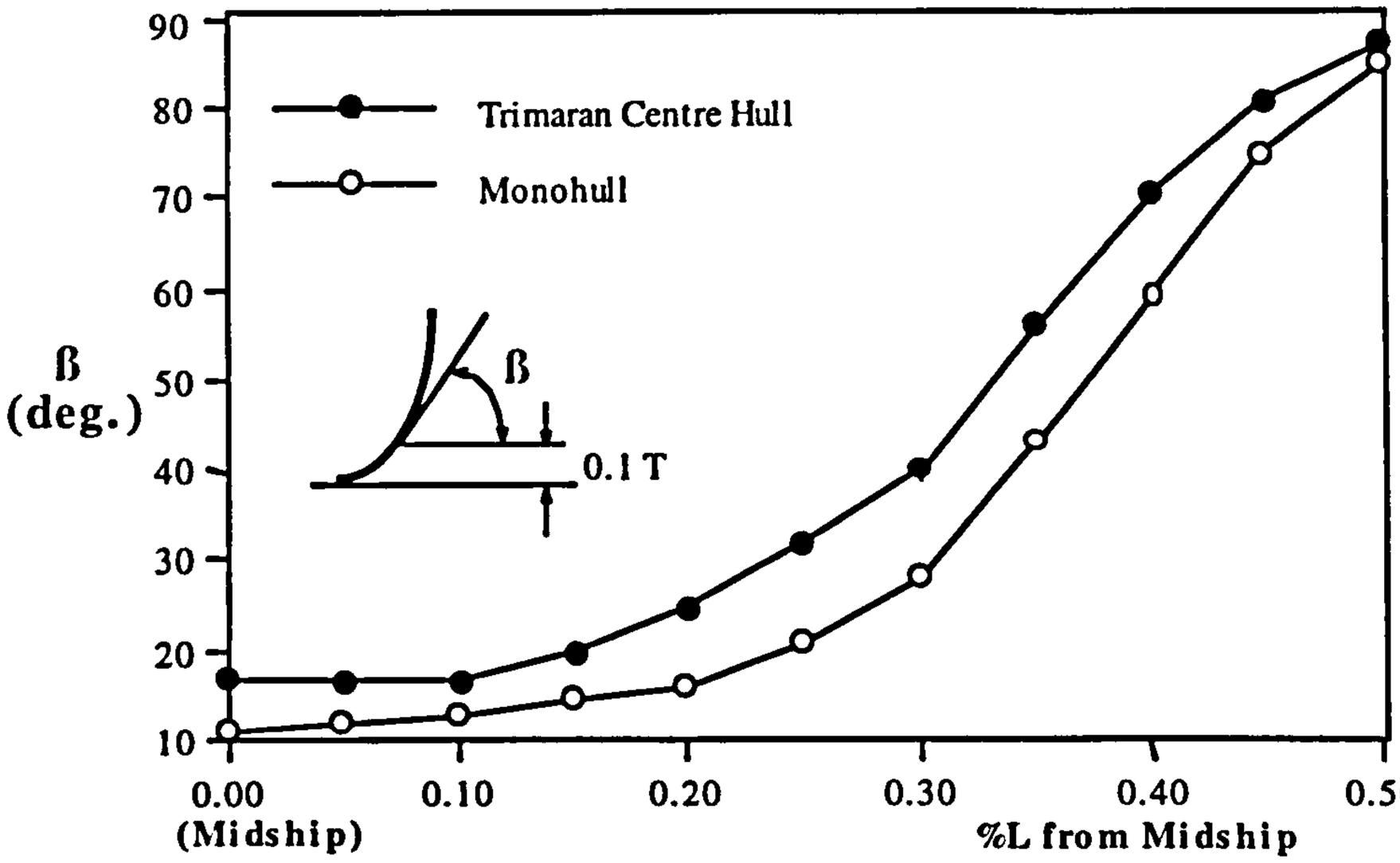

Figure 4.7 Section deadrise of forebody

Figure 4.8 shows the speed reduction due to deck wetness at the fore perpendicular of the centre hull at various freeboards. Of the three speed reduction curves, that for depth=14.0m is most close to that of the slamming curve as shown in Figure 4.6. An

upper deck sheer at the fore body of the centre hull is arranged to allow the depth of the hull reach 14 metres at the fore perpendicular. However, there is a doubt about the relevance of the forecastle deck wetness for the trimaran ship due to the narrow forecastle deck near the bow. In fact, a forecastle may not be needed, given the large deck area amidships provided suitable anchor arrangement can be provided. This is discussed in Chapter 9 together with discussion of wave piercing bows for trimaran ships.

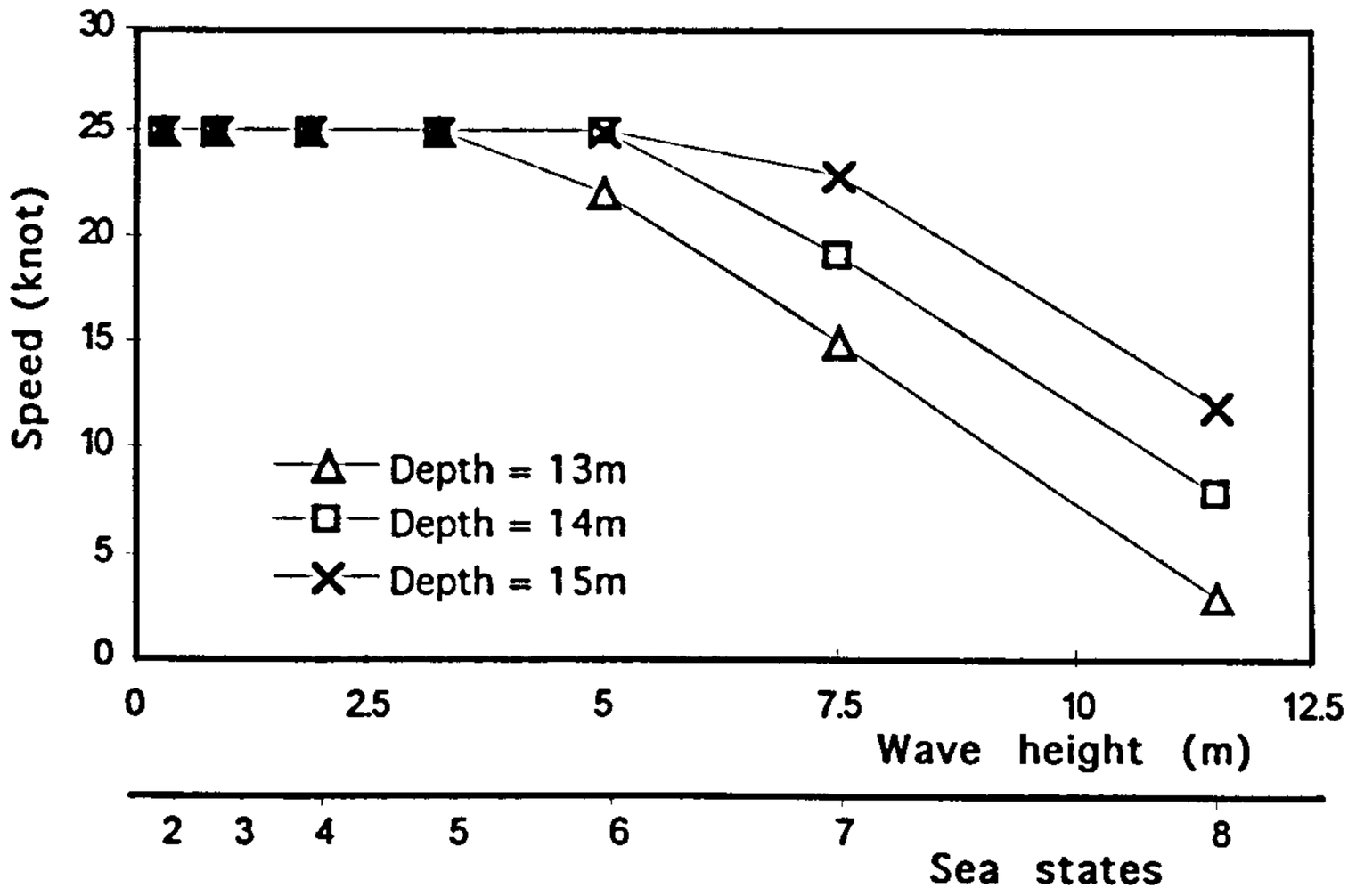

Figure 4.8 Speed reduction due to deck wetness

Finally, the remaining criterion of slamming on the wet deck under the cross deck structure was considered for the trimaran central hull analysis. Figure 4.9 shows the comparison of the reduction in ship speed necessary to meet this slamming criterion for air gaps of 2.5, 3.0 and 3.5m. The final figure was chosen as the decrements in speed at sea states 7 and 8 for a 3.5m air gap were comparable with the other criteria, whereas the smaller air gaps showed considerably greater decrements and earlier onsets of slapping to the bottom of the wet deck.

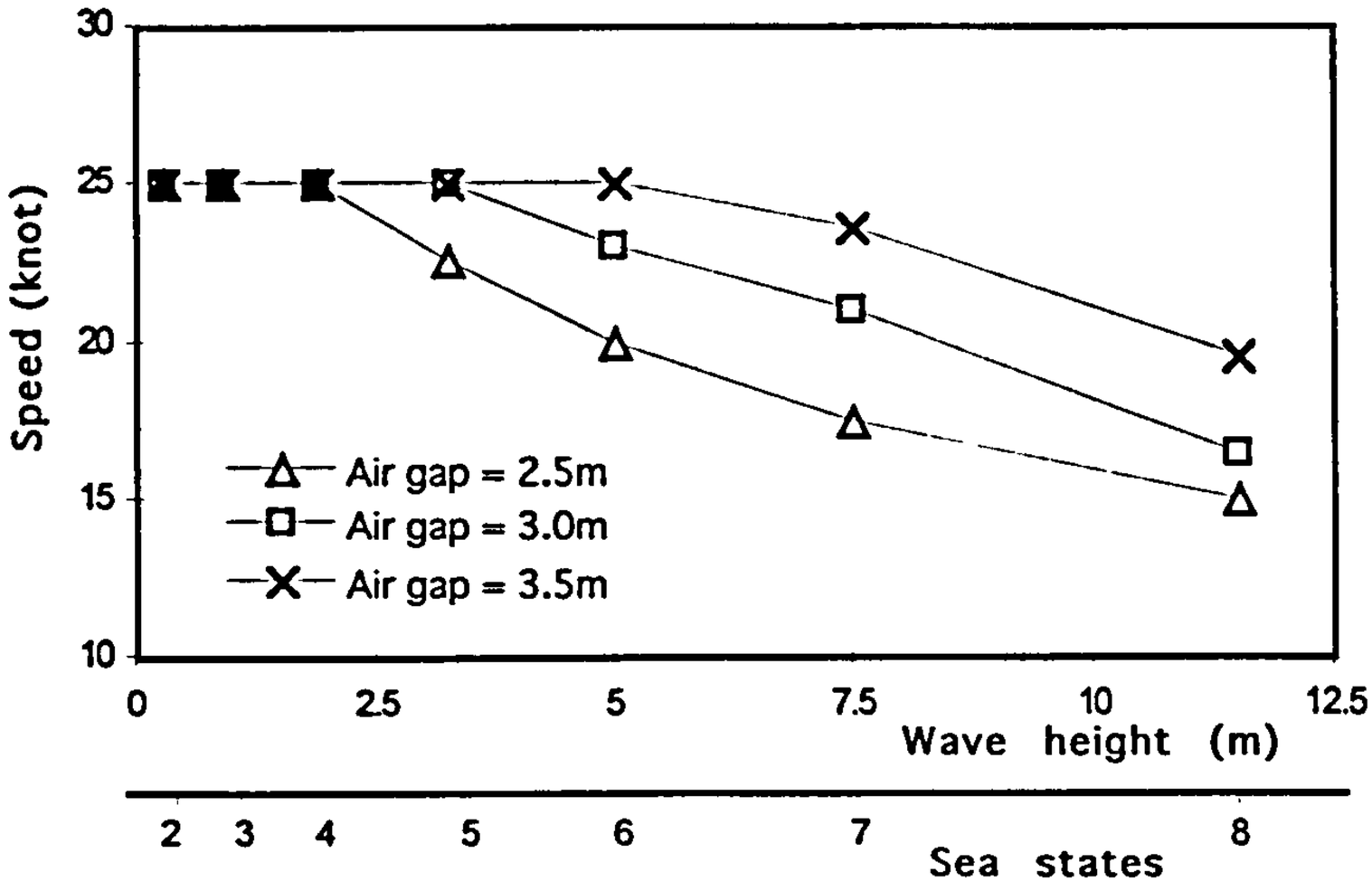

Figure 4.9 Speed reduction due to slapping to wet deck

4.3.3 Initial Power Prediction

Although the seakeeping and stability considerations were the primary factors in determining the hull forms for the two trimaran models, there were other aspects investigated to ensure the design produced was as representative of a realistic frigate design as possible. The primary additional considerations were associated with propulsion .

As already mentioned, the design did not exploit the likely propulsive advantage of a single main shaft. Given a more traditional two shaft arrangement in the main hull, it was necessary to design both the propellers and the twin rudders fitted abaft the screws. The rudders were balanced spade rudders and the propellers were designed using the GODDESS CASD suite for a 4.3m equivalent diameter at 170rpm giving an open water efficiency of 0.76. Powering prediction was achieved using the Taylor-Gertler methodical series **(Gertler 1954)** for both sets of outrigger hulls and the centre hull. An additional 10% was included for typical appendages and the further 10% previously mentioned was incorporated for a possible wave interference effect between the three hulls due to their proximity. This addition was provided as no attempt was made to eliminate detrimental wave interference or exploit a potential wave cancellation effect. From this analysis a power speed curve was produced for both hull configurations to compare with the subsequent towing tank resistance tests plus the estimates of the propulsive elements. Figures 4.10 and 4.11 show the power curves of the two trimaran

hull forms respectively. The details of the powering calculation and the propeller design can be found in Appendix 6.

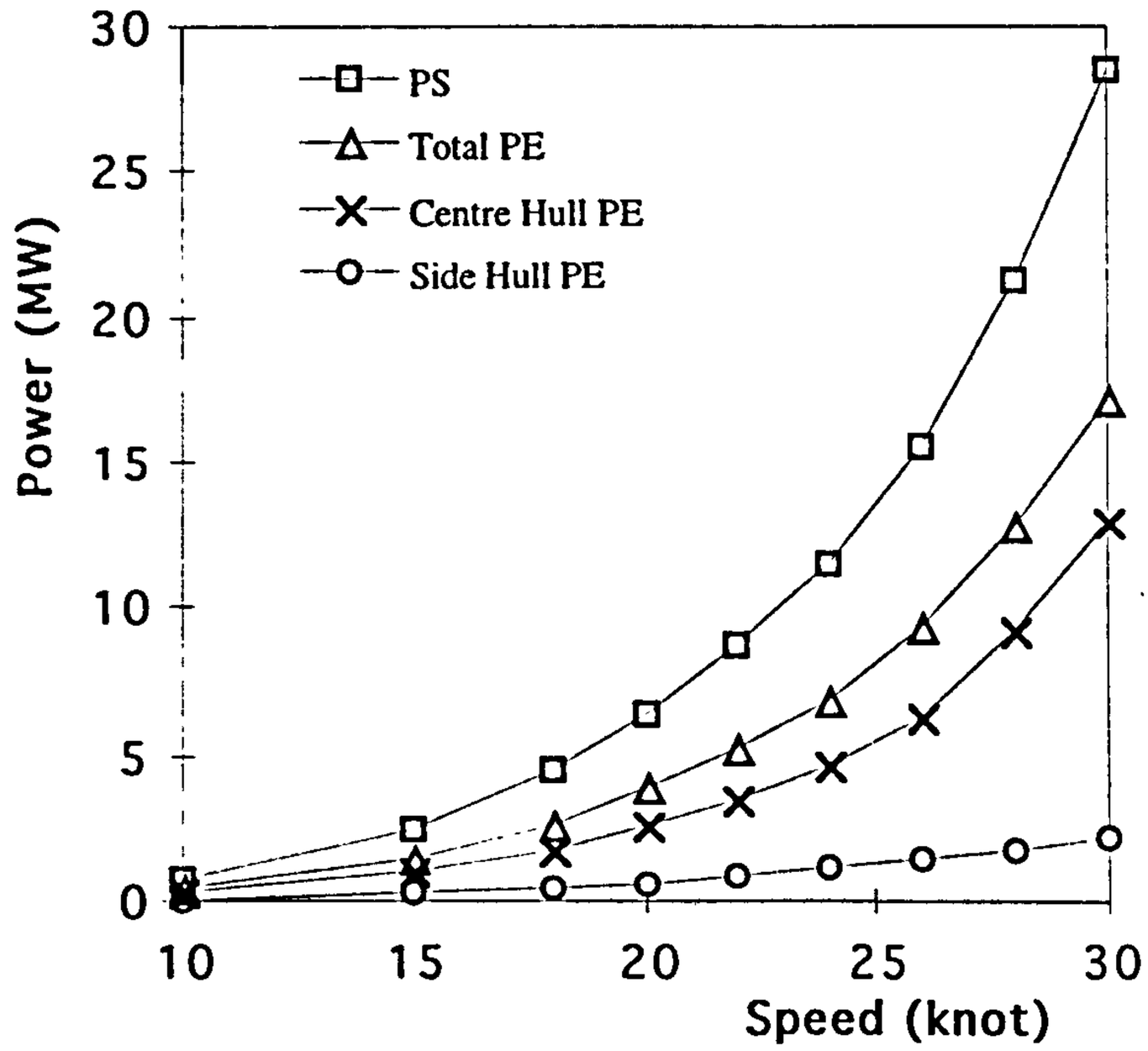

Figure 4.10 Power curves for Ship 1

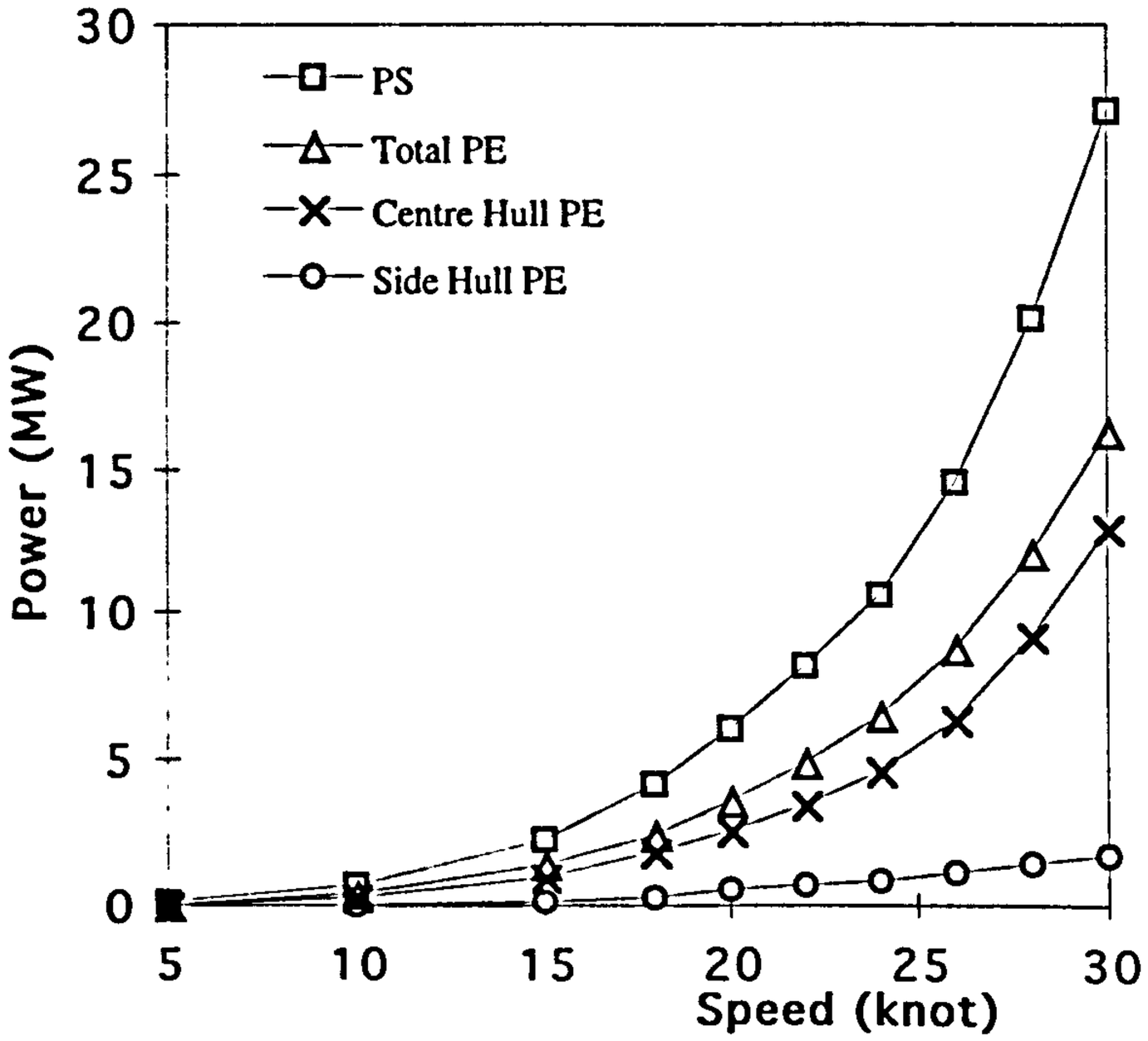

Figure 4.11 Power curves for Ship 2

4.3.4 Mass Inertia

It was also necessary to provide estimates of both the pitching and rolling inertias of the ship design so that the models could be set up correctly for the seakeeping tests. Firstly, the longitudinal mass distribution for the frigate ship design was taken from that produced by the student design team **(O'Brien & Russell 1993)** This was then used with the modified side hull inertias for the two configurations to produce an estimated pitch radius of gyration in the deep condition for both configurations.

At this preliminary design stage it was not possible to directly determine the transverse mass distribution of the frigate design. It was therefore decided to estimate this by considering:

a. The rolling inertia of the centre hull as though it were a monohull. The formula provided in **(Lewis 1989)** was then used which gave a rolling radius of gyration of 0.36 of the centre hull beam.

b. Using a degree of judgement, the structure and outfit in the cross deck structure outboard of the central hull and in the side hulls was estimated and the likely weight distribution judged to give lumped additions to the rolling inertia for the central hull. This gave full scale rolling radii of inertia of 4.77m and 5.11m for the 25m and 30m equivalent beam hull designs respectively.

Detailed calculations of the pitch and roll inertias for the two ship configurations are given in Appendix 7.

4.4 Model Set Up for Seakeeping Experiments

The model was manufactured, installed, and tested by DRA Haslar. The model to ship scale was set to be 1/25 which led a model length of 6 metres. One centre hull and two sets of side hulls were manufactured. Five sets of model configurations were set up known as Models A, B, C, D, and E, using the combinations of the centre hull and the side hulls. The details of the models are listed in Table 4.3. The corresponding full scale ships' details are listed in Table 4.4.

Table 4.3 Details of the trimaran models as tested

		Model A	Model B	Model C	Model D	Model E
Centre Hull:						
Length WL	(m)	6.00	6.00	6.00	6.00	6.00
Beam WL	(m)	0.432	0.432	0.432	0.432	0.432
Draught	(m)	0.247	0.247	0.247	0.252	0.252
Side Hulls:						
Length WL	(m)	2.40	2.40	2.40	2.40	2.40
Beam WL	(m)	0.072	0.0456	0.0456	0.0456	0.0456
Draught	(m)	0.119	0.147	0.147	0.152	0.152
Overall Model						
Overall Beam	(m)	1.01	1.21	1.21	1.21	1.21
Displacement	(t)	0.338	0.341	0.346	0.348	0.348
Roll Gyr. Radius	(m)	0.295	0.317	0.317	0.286	0.292
Pitch Gyr. Radius	(m)	1.21	1.21	1.21	1.21	1.21
GM	(m)	0.061	0.076	0.076	0.122	0.156
Bilge Keels		No	No	Yes	Yes	Yes

Table 4.4 Details of the corresponding full scale trimaran ships

		Model A	Model B	Model C	Model D	Model E
Centre Hull:						
Length WL	(m)	150.00	150.00	150.00	150.00	150.00
Beam WL	(m)	10.80	10.80	10.80	10.80	10.80
Draught	(m)	6.18	6.18	6.18	6.30	6.30
Side Hulls:						
Length WL	(m)	60.00	60.00	60.00	60.00	60.00
Beam WL	(m)	1.80	1.14	1.14	1.14	1.14
Draught	(m)	3.00	3.68	3.68	3.80	3.80
Overall Ship						
Overall Beam	(m)	25.00	30.00	30.00	30.00	30.00
Displacement	(t)	5281	5328	5406	5438	5438
Roll Gyr. Radius	(m)	7.38	7.93	7.93	7.15	7.30
Pitch Gyr. Radius	(m)	30.25	30.25	30.25	30.25	30.25
GM	(m)	1.50	1.90	1.90	3.00	3.90
Bilge Keels		No	No	Yes	Yes	Yes

Model A is based on Ship 1 (see Table 4.1), with narrow overall beam (25m in full scale) and large side hulls. Model B is based on Ship 2, with wide overall beam (30m in full scale) and small side hulls. Due to excessive weight of on board test equipment, the models manufactured were heavier than the design weight. This error resulted in:-

- the draughts of the models being deeper than that designed. The draught of the central hull in each model configuration was deeper than the design draught (5.5m in full scale) comparing Table 4.3 with Table 4.1;

- the GM values being smaller than that designed. The GM is 1.5m for Model A, and 1.9m for Model B. Both models have lower GM values than the designed value of 2.5m for both Ship 1 and Ship 2.

Models C is the same configuration as for Model B, but fitted with bilge keels. The bilge keels are fitted onto the inner bottom knuckle lines of the side hulls as shown in Figure 4.12.

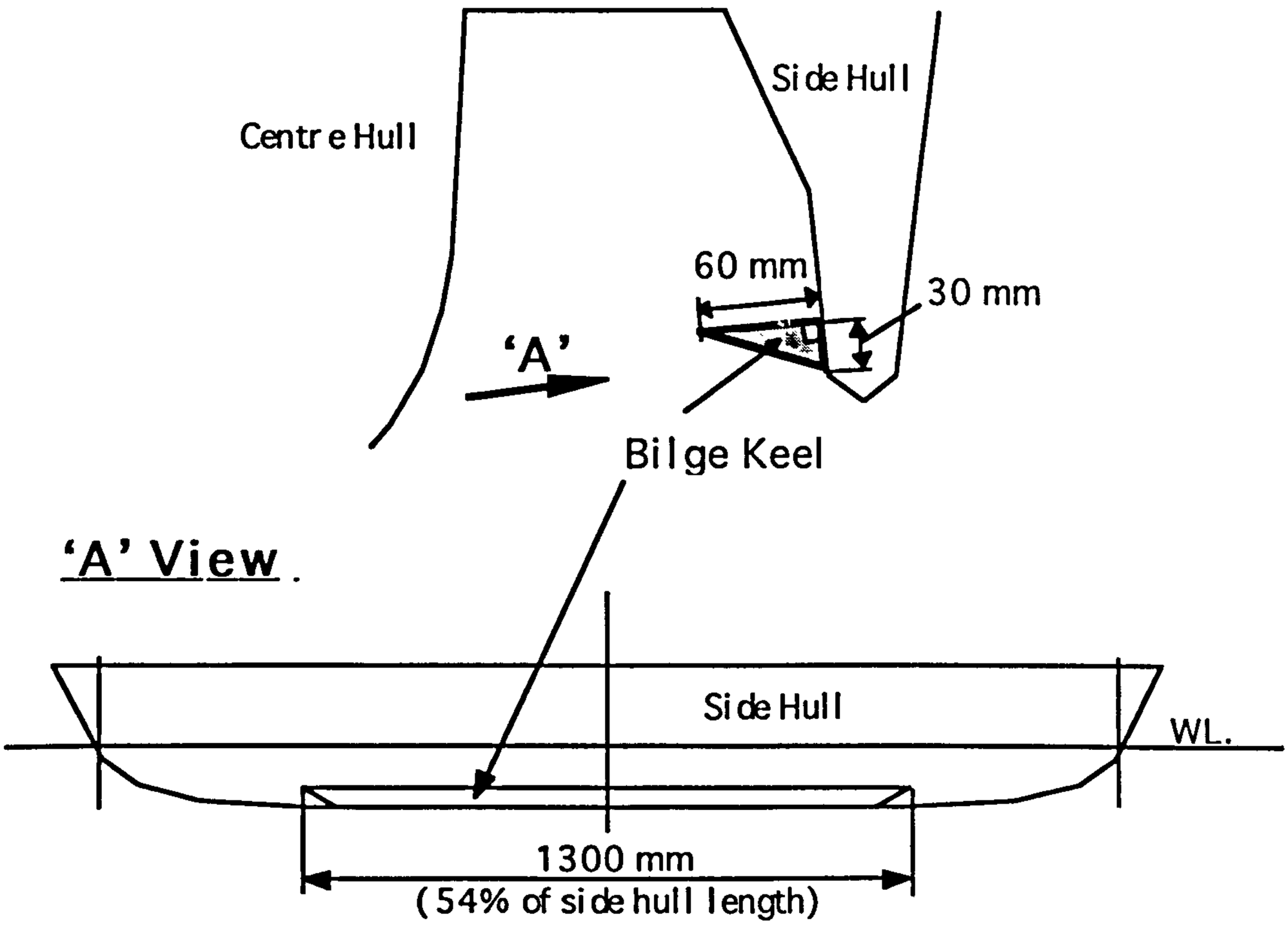

Figure 4.12 Bilge keel for Models C, D, and E

Having experienced excessive roll amplitudes for the models in following quartering seas during the seakeeping experiments, as will be discussed in Section 4.5, it was decided to raise the GM values to the designed value by re-arranging the on board equipment. This resulted two more model configurations, Models D and E, based on Model C but with higher GM values.

Figure 4.13 shows one of the completely installed model ready for experiments (photograph). Each model is self propelled with twin screws and rudders. It is fitted with a remotely controlled autopilot to maintain it on any set heading and speed during the experiments.

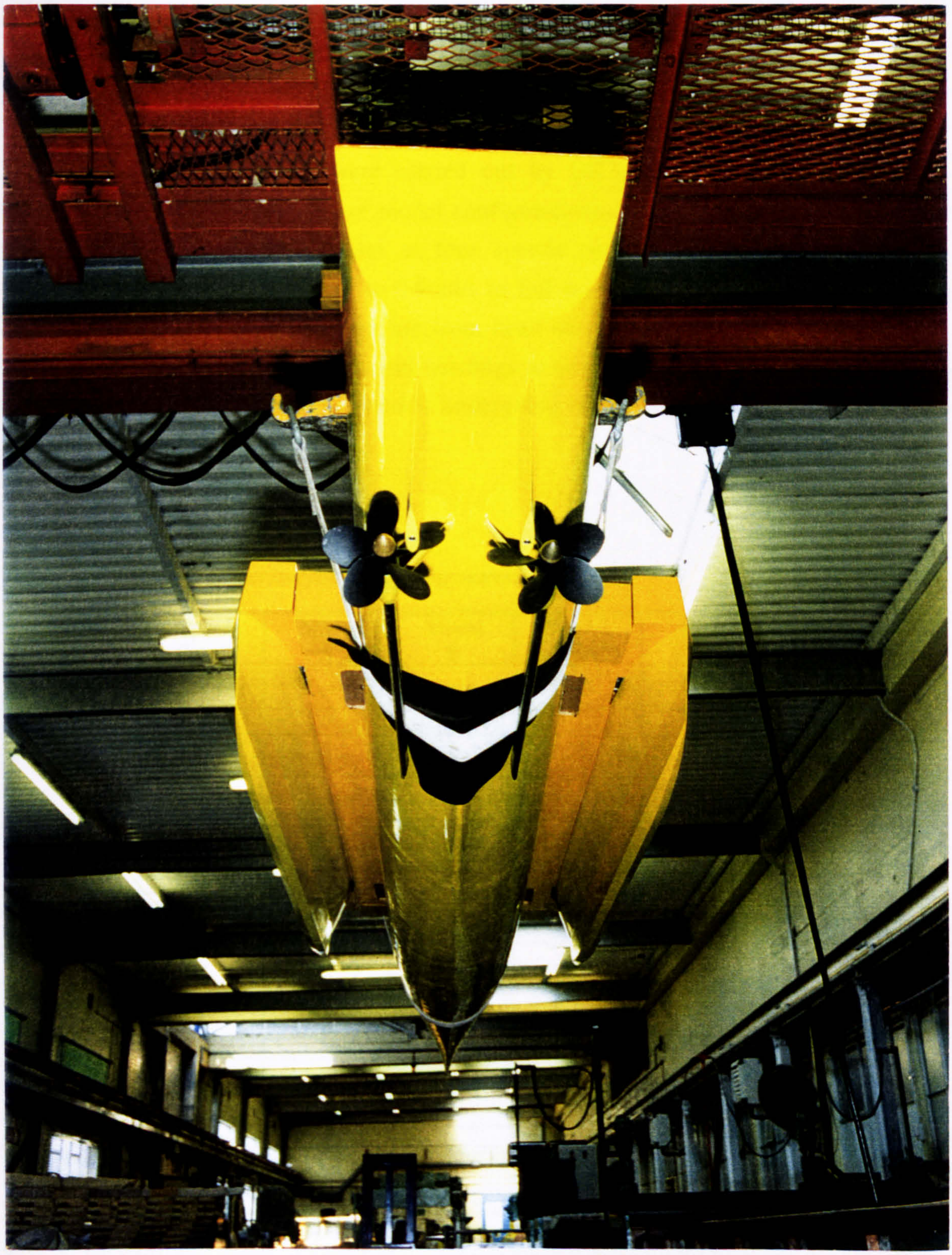

Figure 4.13 Photograph for one of the complete set up models

4.5 Seakeeping Experiments

4.5.1 Motion Experiments in Regular Waves

The seakeeping experiments were carried out by DRA Haslar in the 60m x 120m Manoeuvring Tank for all the five model configurations. The model was run in regular waves of seven wave frequencies at four speeds and seven headings. The wave frequencies covered are from 0.4 to 0.9rad/s in full scale. The four speeds are 0, 5, 18, and 30 knots. The seven headings are from head seas to following seas in 30 degrees steps. Table 4.5 lists the speeds and headings tested in the experiments. Figure 4.14 shows a photograph of one of the models undergoing motion experiment in regular waves at speed of 30 knots (full scale).

Table 4.5 Motion experiments in regular waves

Heading (degree)	Speed (knot)	Model A	Model B	Model C	Model D	Model E
0	0					
	5					
	18	√	√	√		
	30	√				
30	0					
	5					
	18	√	√	√	√	√
	30			√		
60	0					
	5		√	√		
	18	√	√	√	√	√
	30	√	√	√	√	√
90	0		√	√		
	5		√	√		
	18	√	√	√	√	√
	30	√	√	√	√	√
120	0					
	5					
	18	√	√	√	√	√
	30					
150	0					
	5					
	18	√	√	√	√	
	30					
180	0					
	5		√	√		
	18	√	√	√	√	
	30	√	√	√		

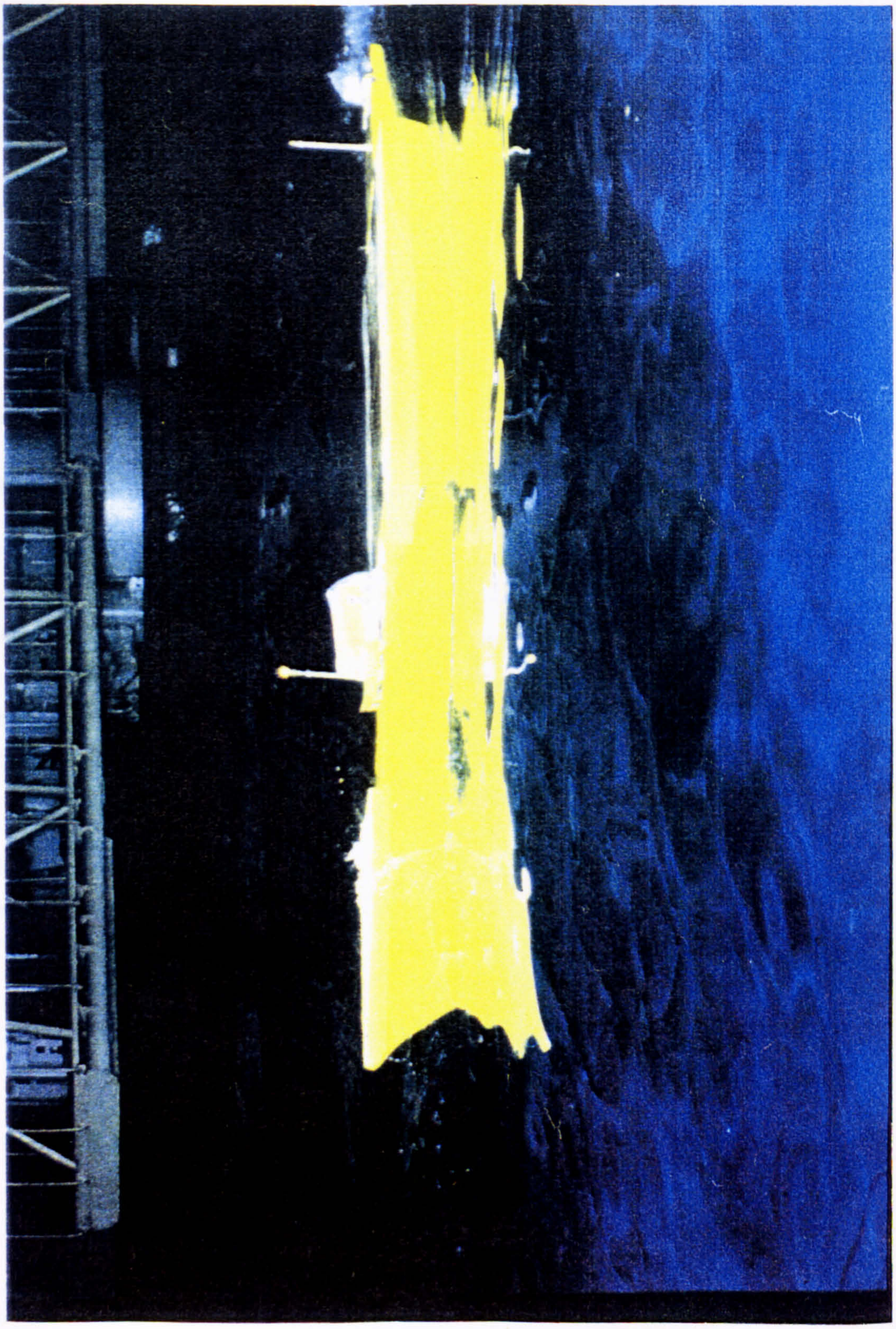

Figure 4.14 Photograph of the trimaran model under seakeeping experiment at 30 knots equivalent speed

As interest focused mostly on the roll motion of the trimaran, the motion measurements of the models were categorised **(Pattison and Zhang 1993)** as follows:-

- *First priority:* Roll response
- *Second priority:* Heave response
  Pitch response
  Yaw response
  Sway response
- *Third priority:* Surge response

Roll motion

The roll motion of trimaran Models A and B showed similar characteristics as that of the monohull ship except for the case of following quartering seas (at a heading of 60 degrees) around wave frequencies between 0.4 and 0.8rad/sec, where excessive roll motions were recorded for both the models at a speed of 18 knots. The corresponding wavelength at this wave frequency is about the length of the ship. Figure 4.15 shows the roll motion Response Amplitude Operator (RAO) of Model B at various headings.

In order to reduce the roll motion, a pair of bilge keels, as show in Figure 4.12 were fitted on to the inner side of the side hulls of Model B, in the belief that the excessive roll motion was due to the lack of roll damping devices. The new configuration was taken as Model C. Experiments on Model C showed a certain degree of improvement in roll motions compared with Model B at the same heading and the same speed. The comparison of roll motions for model B and Model C are plotted in Figure 4.16

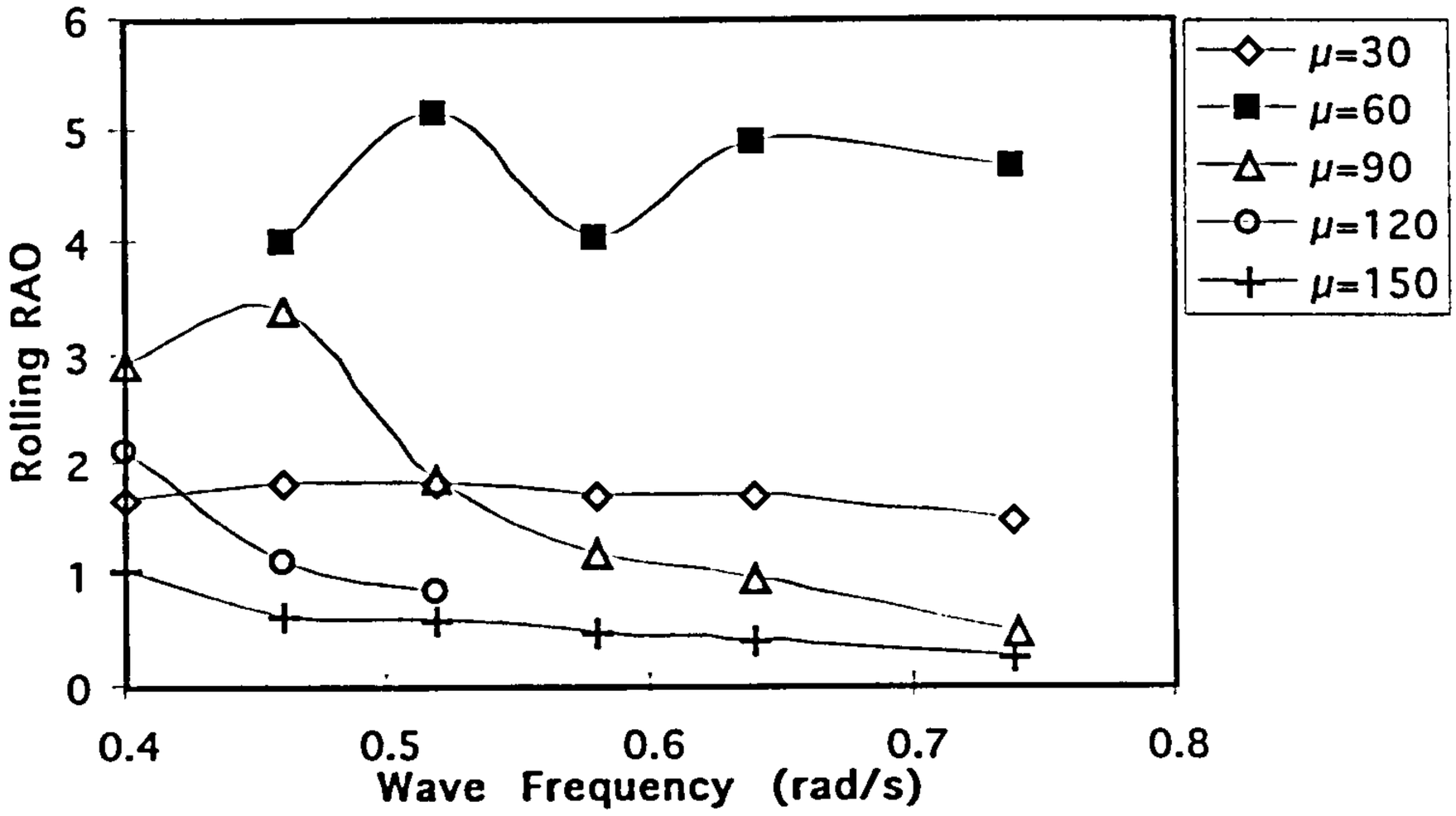

Figure 4.15 Recorded roll motion for Model B at 18 knots

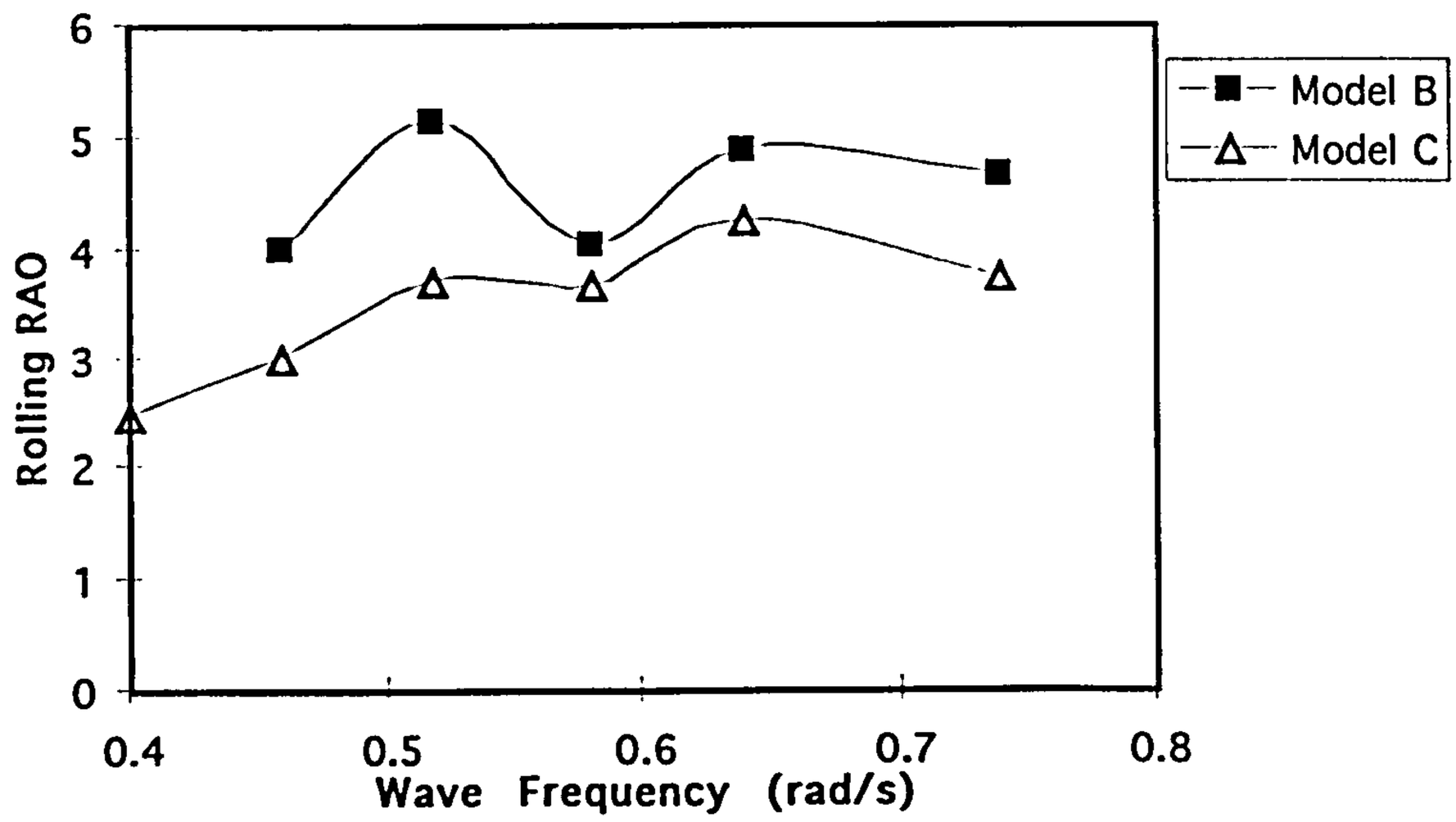

Figure 4.16 Comparison of roll motions between models B and C at 60° heading and 18 knots

The comparisons between Models B and C in Figure 4.16 actually shows the effects of the bilge keels on roll motions. Though the sizes of the bilge keels are significant, 1.5m wide in full scale, the improvement on roll motions was not as big as would be expected for a monohull ship fitted with bilge keels.

The roll damping moment produced by a bilge keel of a monohull is governed mainly by three factors, area of the bilge keel, distance from the centre of gravity to the bilge keel, and the water depth (distance from waterline to the bilge keel) **(Kato, 1966)**. The length of bilge keel of a monohull ship is normally in an average of 35% of the ship's waterline length. The length of the bilge keel of the trimaran model, restricted by the length of the side hull, is 22% of the waterline length of the centre hull, i.e. 37% shorter than that of a monohull. However, the distance from the bilge keel to the centre of gravity of a trimaran ship is much greater than that of a conventional monohull, in a range of 50 ~ 100% greater. This last factor should have provided a greater level of roll damping than the reduction due to the first factor (shorter bilge keels) based on monohull practice. The fact that the contribution of bilge keels to trimaran roll damping is not as great as for a monohull indicates that the experience derived from monohull bilge keels can not be wholly used to explain the effects of the bilge keels of a trimaran ship.

Due to the complexity of the flow around a bilge keel, it would be extremely difficult to derive an explicit numerical model for the fluid mechanics effects of a bilge keel. However, if we look into the possible pattern of fluid streamlines around the bilge keels, as shown in Figure 4.17, an explanation to the model experimental results may be provided. The roll damping effects of a bilge keel are dependent on the energy it dissipates in disturbing the fluid flow around the hull surface. The fluid streamlines around the bilge keel of a trimaran side hull are quite different from that of a monohull. It appears that the fluid around the bilge of the side hull is 'escaping' to the other side around its bottom, whilst the fluid around the bilge of the monohull is more restricted by the continued surface of the hull. Thus, for the same roll velocity, the energy dissipated by the bilge of the side hull to disturb the fluid may be less than that by the bilge keel of the monohull.

The roll damping calculations presented in Chapter 6 suggests a wider and shorter damping device to take the place of the long and narrow bilge keel. This is because a damping device of higher aspect ratio produces greater damping moment due to lift force, which is the dominant damping force when the ship is at speeds. Thus, this wider damping device, when fitted on a trimaran side hull, could take full advantage of its greater distance to the ship's centre of gravity compared with a monohull.

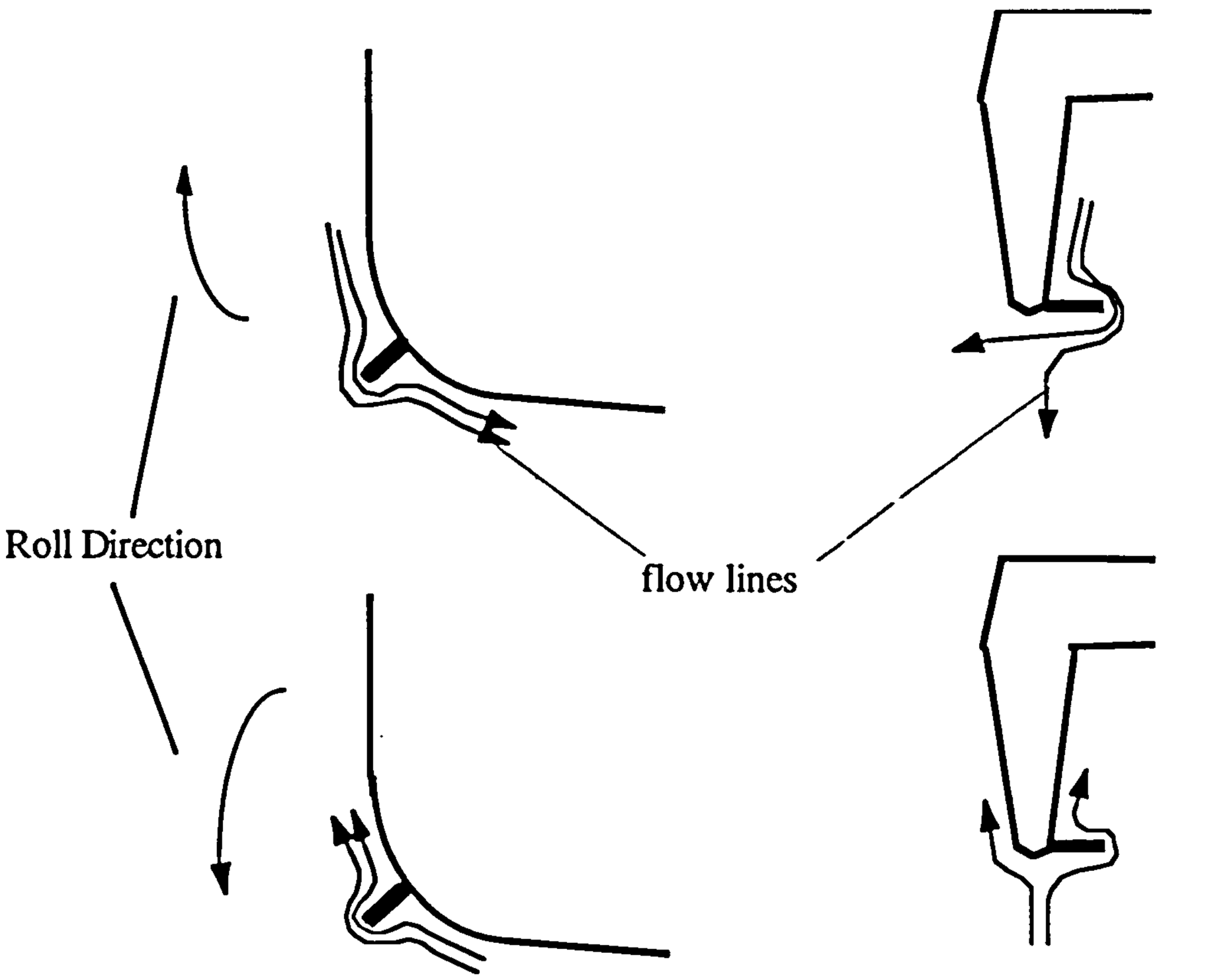

Figure 4.17 Fluid flow lines around the bilge keels of a monohull and a trimaran side hull

As already described, the GM value (1.9m) for Models B and C as manufactured were both lower than that of the designed 2.5 metres due to excessive equipment weight (the actual GM values of the models could be even lower as will be discussed in Chapter 5). It was then decided to increase the GM value by removing and re-arranging some of the equipment. A GM of 3.0m was achieved which resulted in a new model configuration, the Models D. Experiments on Models D showed significant improvements in roll motions in stern quartering seas compared with Model C as shown in Figure 4.18. This demonstrates that the GM parameter of a trimaran ship has a major effect on its roll motions.

Another model with an even higher GM, 3.9m, was also tested as Model E. The results are also plotted in Figure 4.18 where it can be seen that the roll amplitude differences between Model E and Model D are marginal compared with the difference between Model D and Model C. Also, this increase of GM resulted in an increase of RAO for Model E in bow quartering seas in the frequency range above 0.6rad/s compared with that of Model D, as shown in Figure 4.19. This indicates that any further increase of GM is not appropriate, bearing in mind that an unnecessary high GM would also result in an

unfavourable stiff roll motion. The relationship between the roll motion and GM values for trimaran ships will be further discussed in Chapter 9 where a recommended procedure for the choice of GM at the initial design stage for the trimaran ship is presented.

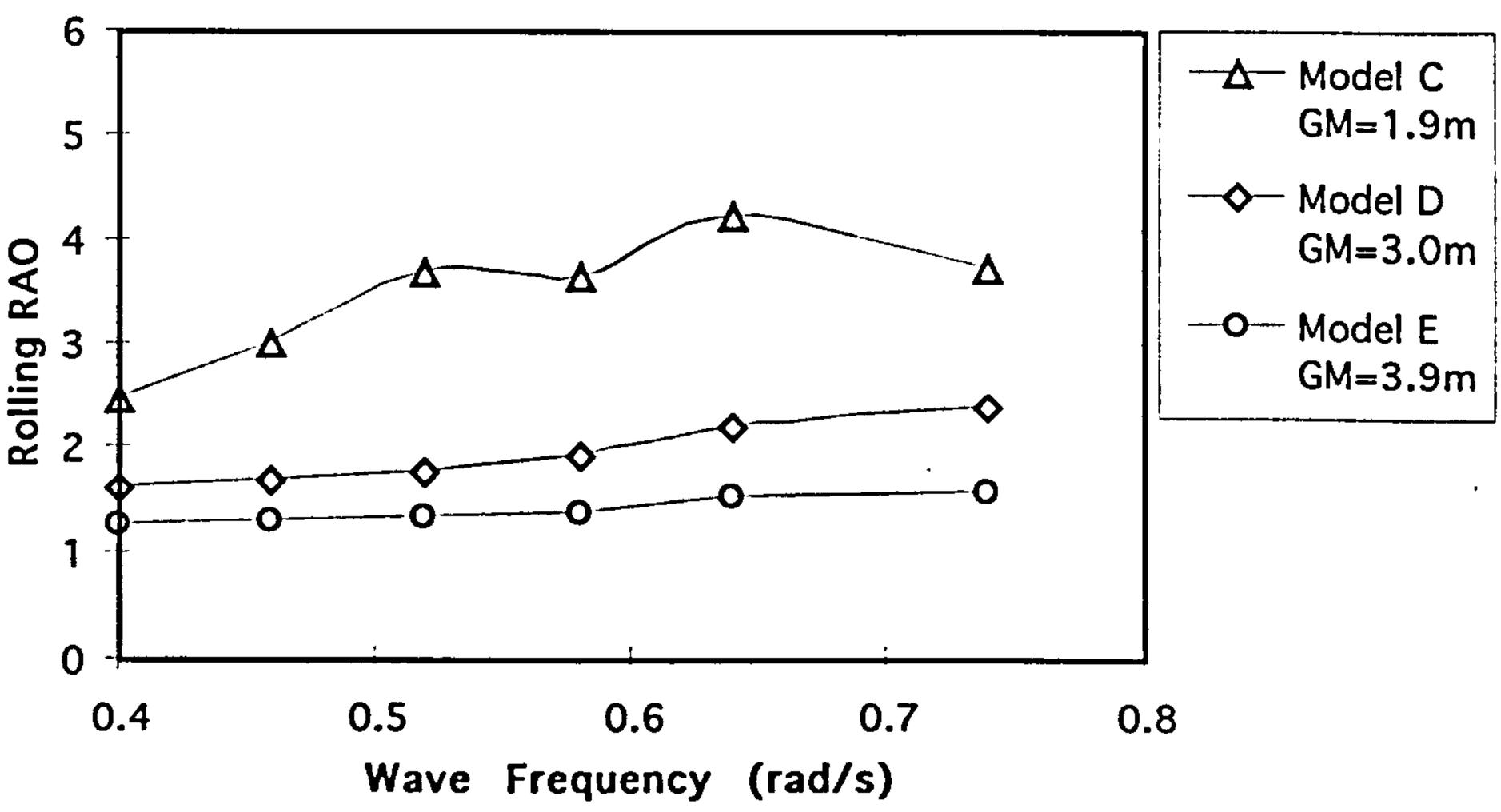

Figure 4.18 Effects of GM on roll motions at 60° heading and 18 knots

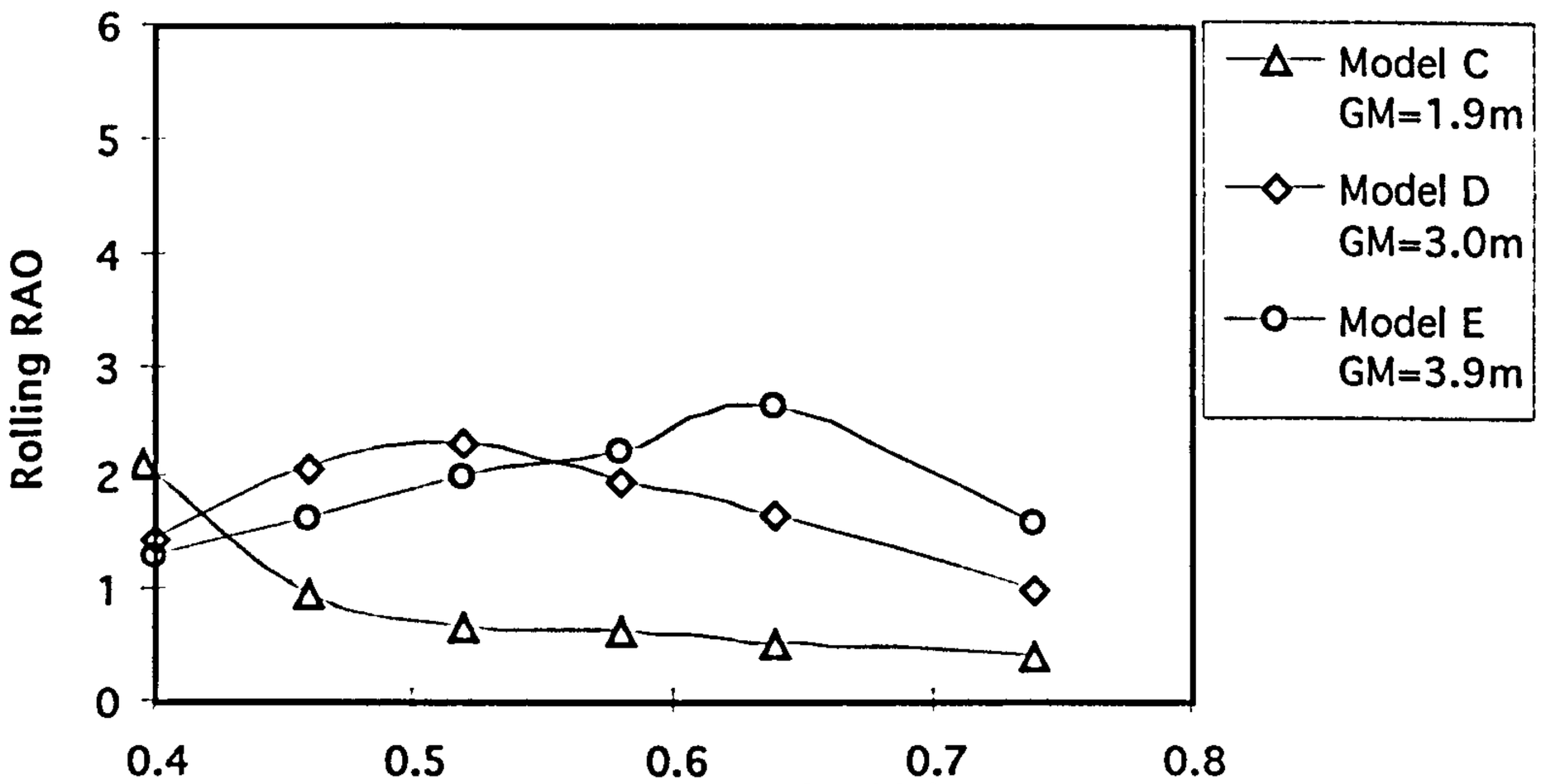

Figure 4.19 Comparison of roll motions between models C, D and E at 120° heading and 18 knots

Heave and pitch motions

The recorded heave and pitch motions of the models at various headings and speeds showed slightly better or similar results in comparison with the experimental results of an equivalent monohull ship **(DRA 1995)**. The comparison between the model experiments and the theoretical prediction are presented in Chapter 5. It can be concluded from the test results that there are no unexpected heave and pitch motions for the trimaran ships.

4.5.2 Free Roll Decay Experiments

Free decay experiments were carried out at various speeds in calm water at DRA Haslar for the trimaran models. The purpose of these tests was to determine the roll damping coefficients for use in the motion predictions and to identify the roll damping characteristics of the trimaran ship. For the zero forward speed case, an initial heeling moment to give 15° heel was applied to the model, and the decay curves were then recorded after the model was released for free rolling. For cases with forward speeds, a weight was added on the top of one side hull of the model to give an initial heel angle. When the model reached the required speed, the weight was removed from the model leaving the model to roll freely at constant forward speed while the decay in roll was recorded.

Tests were conducted for all the five model configurations at equivalent ship's speeds of 0 knot, 18 knot, and 30 knot. Figure 4.20 shows the recorded free decay data for one of the models, Model D. Table 4.6 gives the decay coefficient for each model provided by DRA Haslar, which is a linear fitting to the roll decay equation in the form of:-

$$\eta_4 = \eta_{40} e^{-kt} \cos(\omega t + \theta)$$

where η_4 is the rolling amplitude, ω is rolling frequency, and k is the roll decay coefficient.

Since roll damping is a crucial factor in the prediction of roll motions, the results of free decay experiments are analysed in Chapter 6 using a nonlinear method to derive roll damping coefficients to improve roll motion predictions.

Table 4.6 Free decay coefficients for the trimaran models

Model	Speed (knots)	ω (rad/s)	*k*	Roll Period (s)
B	0	2.38	0.10	2.64
B	18	2.17	0.28	2.90
B	30	2.06	0.35	3.05
C	0	2.29	0.13	2.74
C	18	2.12	0.34	2.96
C	30	1.80	0.40	3.49
D	0	3.32	0.13	1.89
D	18	3.30	0.48	1.90
D	30	3.14	0.49	2.00
E	0	3.89	0.22	1.62
E	18	4.00	0.42	1.57
E	30	3.77	0.49	1.67

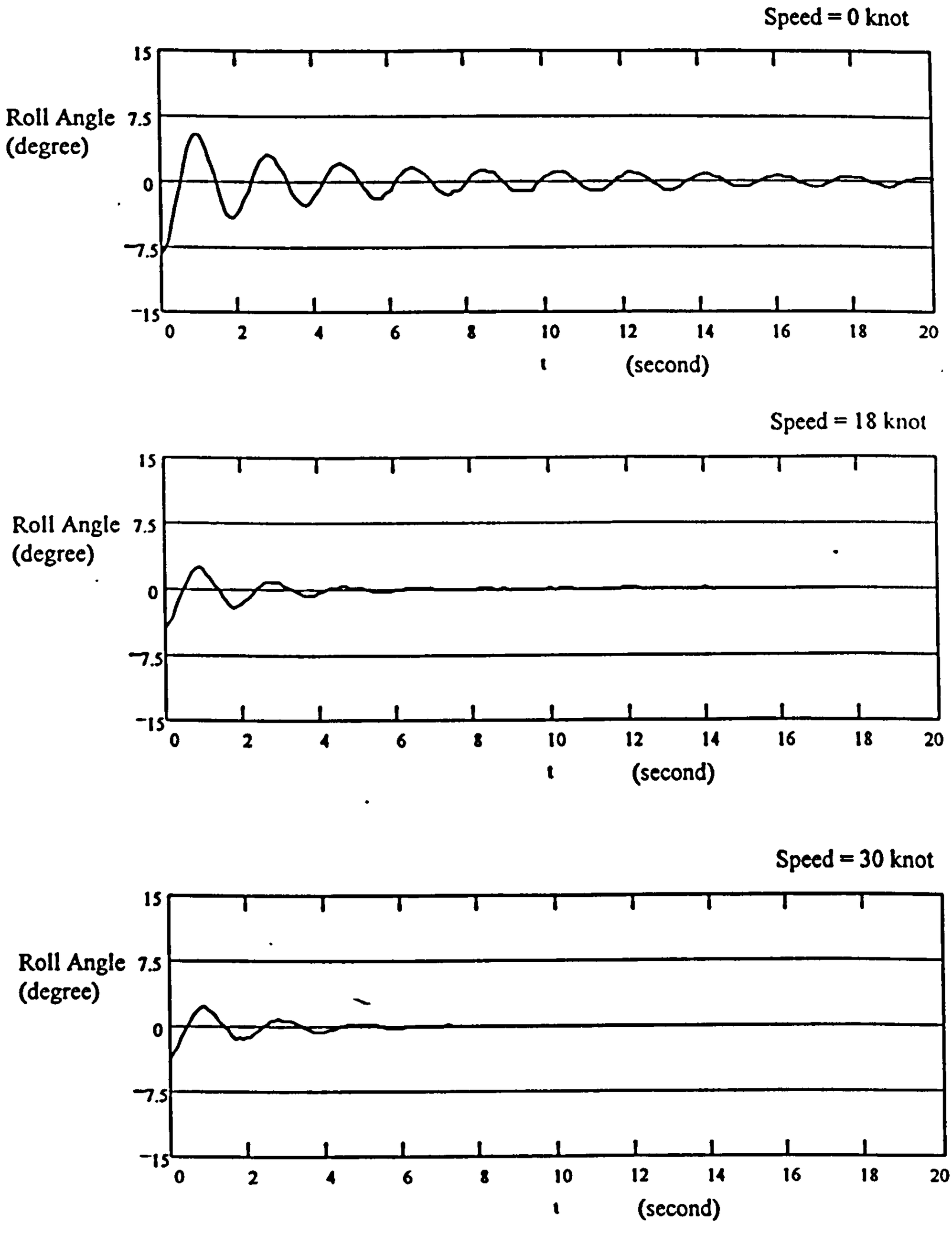

Figure 4.20 Recorded free decay test data for Model D

4.6 Other Experiments

Experiments in resistance and manoeuvrability were also carried out by DRA Haslar for the trimaran models. As these results will be used for the validation of theoretical predictions to be presented in later chapters, only brief descriptions of these experiments follows.

4.6.1 Resistance Experiments in Calm Water

Two sets of models were restored to the original designed configurations as Ship 1 and Ship 2 (Table 4.1). The measured resistances in DRA Haslar Towing Tank for the two models in calm water are plotted in Figure 4.21.

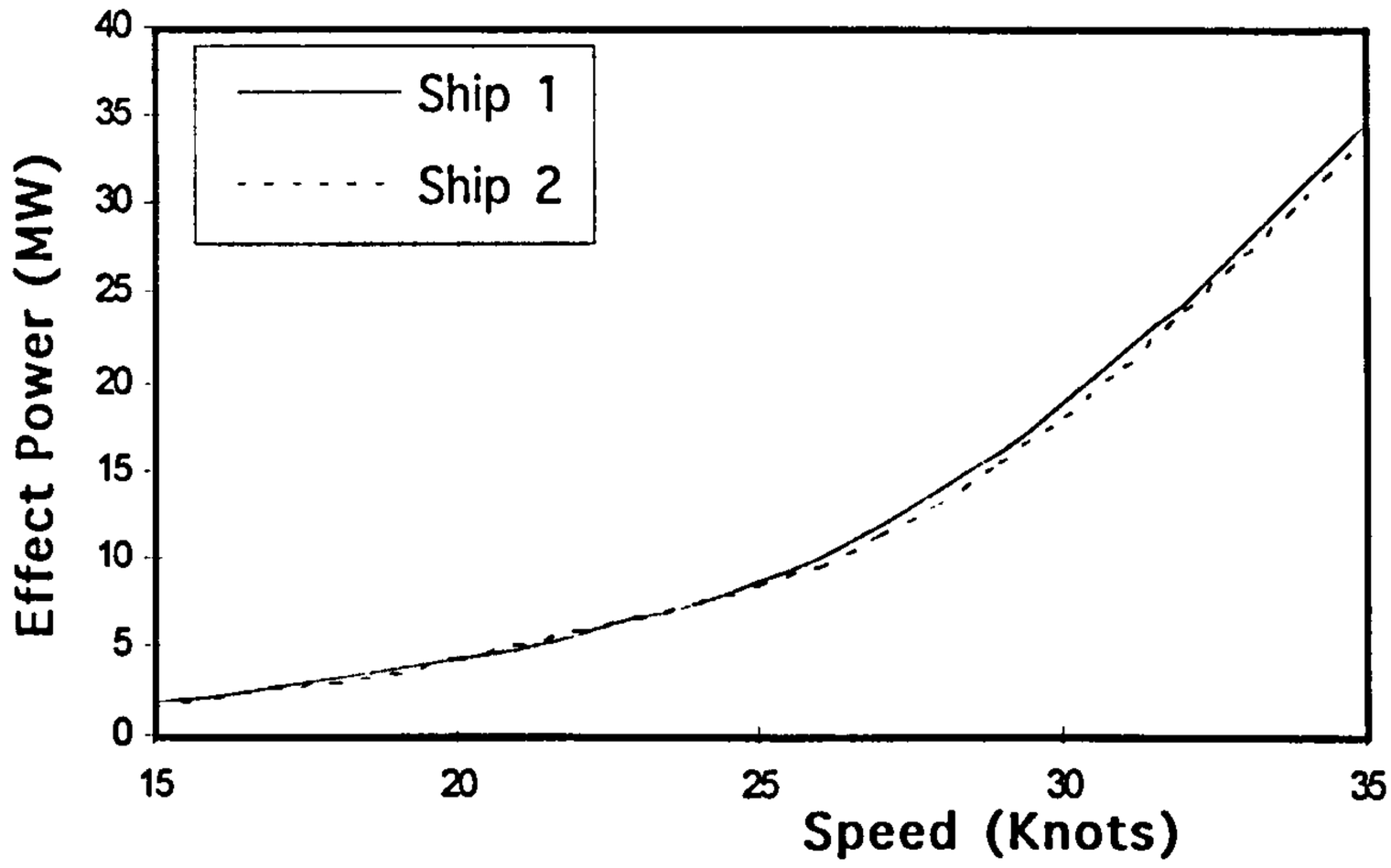

Figure 4.21 Calm water resistance of the trimaran Ships 1 & 2

It can be seen that the resistance for Ship 2 (wide beam with smaller side hulls) is slightly less than that of the Ship 1 (Narrow beam with larger side hulls). This does not reflect the differences in residuary resistance of the two ships. The total wetted surface of Ship 2 is slightly larger, 1.6%, than that of Ship 1, as the side hull draught of Ship 2 is deeper. This should mean a bigger frictional resistance for Ship 2. Using the procedure to be described in Chapter 7, residuary resistance coefficients are extracted from the total resistance for the two ships, and plotted in Figure 4.22. It shows less residuary resistance for Ship 2 because its side hulls are narrower and with less displacement, 36% less than

the side hulls of Ship 1. This leads to that the overall resistance of Ship 2 is marginally less than that of Ship 1 as shown in Figure 21.

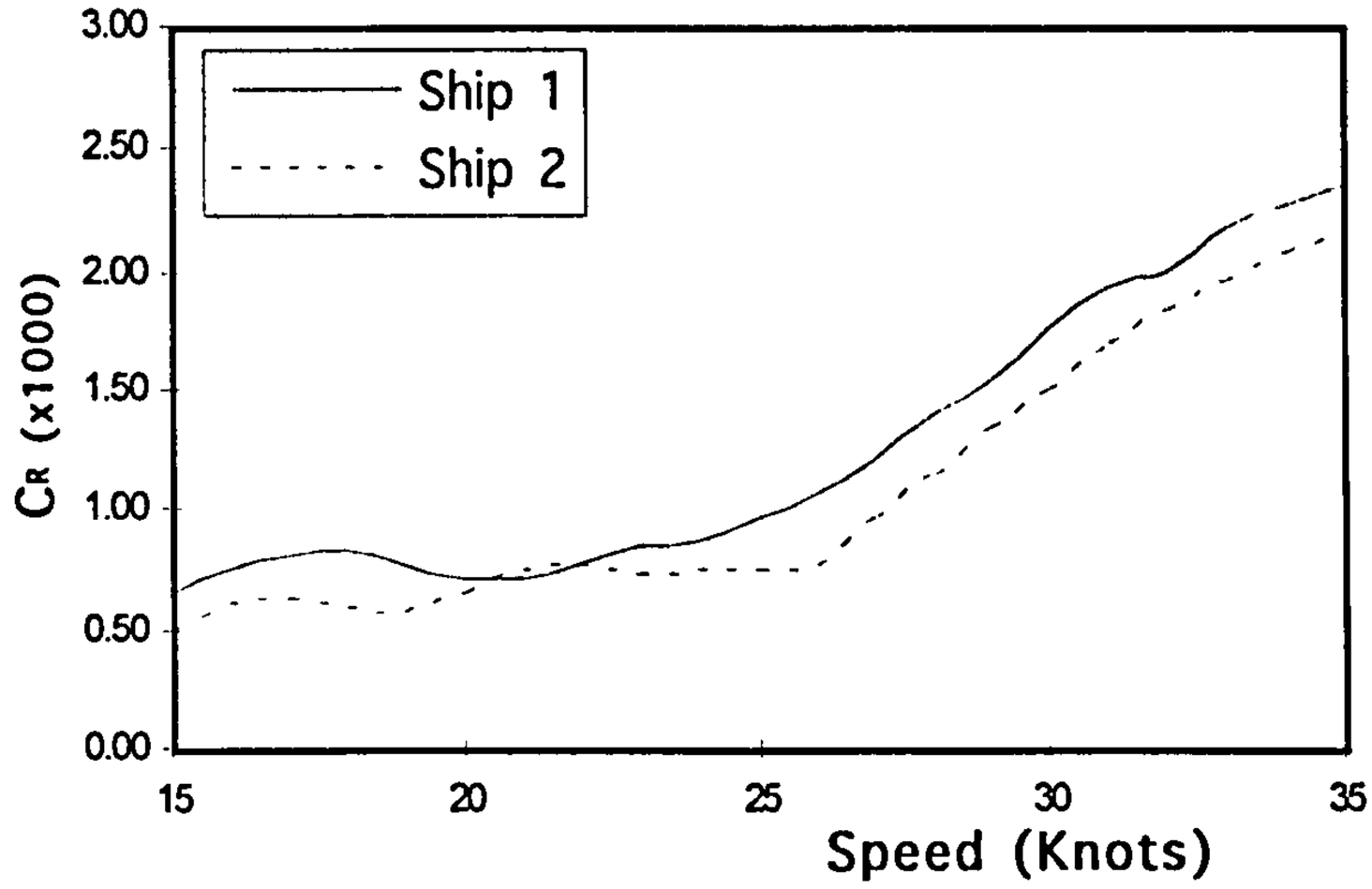

Figure 4 22 Residuary resistance of the models

The centre hull and the side hulls of the two models were also towed separately in the experiments to identify the effects of wave interactions between the hulls. Plotted in Figure 4.23 are the percentages of the residuary resistance, due to wave interactions, to the total residuary resistance of the models. The curves fluctuate with the model's speed around zero interference for both the models. The fluctuating amplitudes for Ship 1 are generally larger than that of Ship 2 because the gap between its centre hull and side hulls is smaller. However, this does not necessarily mean the wave interference of Ship 1 is worse than that of Ship 2. Though the positive wave interference for Ship 1 around 18 knots is larger, it also shows a larger negative interference around 22 knots. No reasonable judgements can be made without taking into account of operational profiles of the ship.

One of the most important variations which is not investigated in the experiments is the longitudinal position of the side hulls. The investigation on this issue using theoretical methods is presented in Chapter 7, where the resistance characteristics of the trimaran ship is analysed.

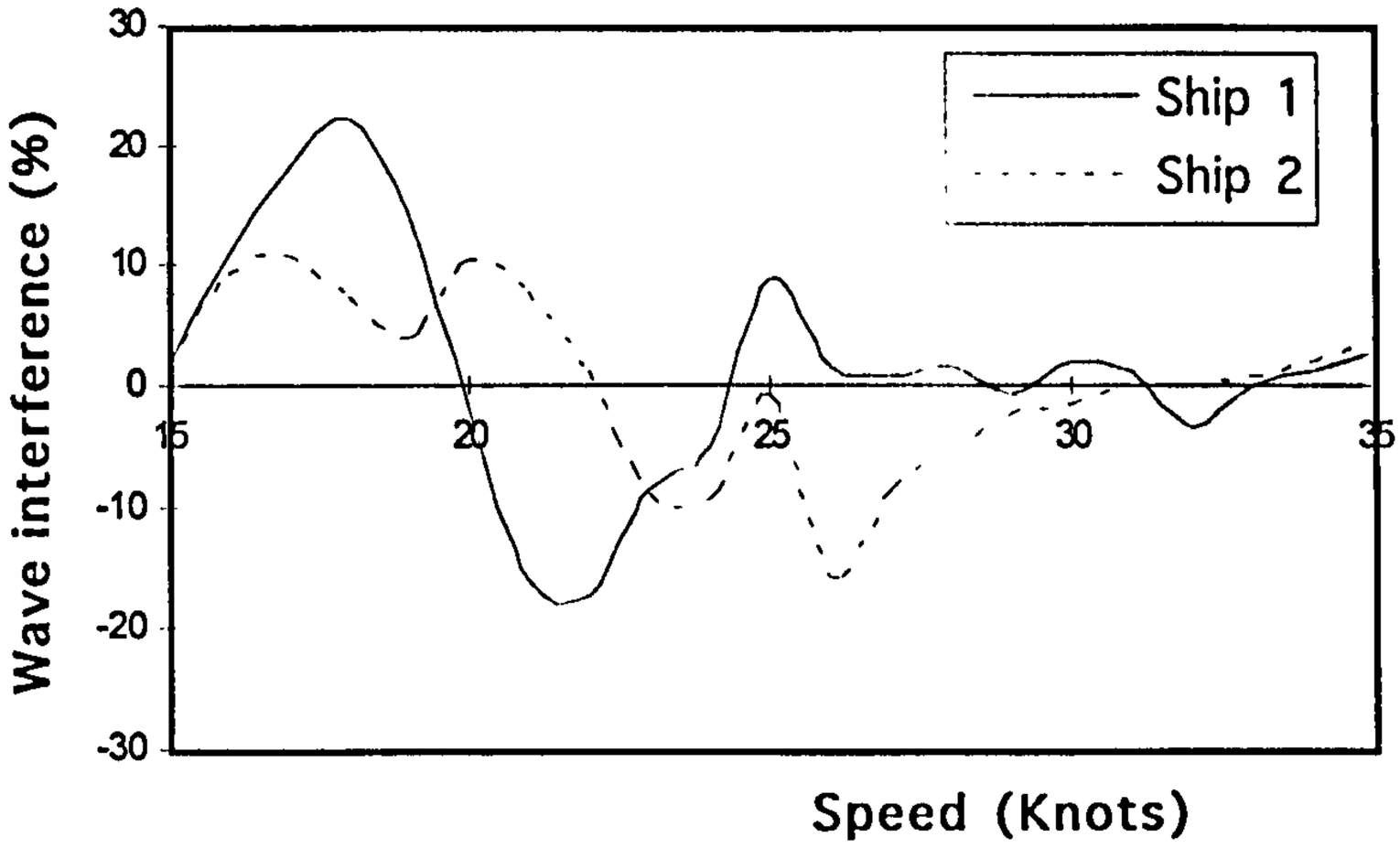

Figure 4.23 Wave interference

4.6.2 Turning Ability Experiments

A limited number of runs of circle trials were also conducted by DRA Haslar **(DRA 1995)** in the Manoeuvring Tank for model Ship 2 only. The aim of the tests was to identify the steady turning ability of the trimaran ship. The method of experiments was the standard DRA free model testing procedure **(Burcher 1971 & 1972)**. The model was tested with two rudder angles, 20° and 35°. Only the tactical diameters of the runs were recorded. The control of the model is the same as described in Section 4.3.

The test results are used for validating theoretical predictions of trimaran turning abilities which are discussed in Chapter 8, where the effects of trimaran configurations and side hull propulsion on its turning ability are also considered.

CHAPTER 5

TRIMARAN MOTION PREDICTION

5.1 Introduction

Although testing ship models is the most reliable way to gain the performance data for a new ship type, it can only be conducted for a very limited number of cases due to its high cost in time and resources. In parallel with the trimaran model experiments described in Chapter 4, systematic theoretical analyses of the hydrodynamic performance for trimaran ships have been carried out. These aimed at achieving the following objectives:-

- develop a theoretical method for trimaran hydrodynamic performance assessment;
- provide computer tools for naval architects to use in future trimaran ship designs;
- verify that the new trimaran concept has the predicted advantages in hydrodynamic performance over other types of ships;
- clarify the effect of varying the configuration of the trimaran on its performance.

This chapter, through to Chapter 8, presents the methods used in the analysis of the trimaran ship motion in waves, wavemaking resistance, and manoeuvrability. As already indicated priority is given to the assessment of the trimaran seakeeping performance, with the theoretical trimaran motion prediction dealt with in this chapter followed by the roll damping analysis in Chapter 6.

In this Chapter, firstly, the current ship motion theories are briefly reviewed in Section 5.2, both for strip theory and three dimensional theory. Although linear strip theory has been successfully used in motion predictions for monohull ships as well as for twin hull ships, the three dimensional theory appears to be more suitable because the centre hull length and the side hull length are quite different and the flow around a trimaran ship would be more complicated than for monohull and twin hull ships. A numerical model of the three dimensional theory used for trimaran motion predictions is presented in Section 5.3.

Motion predictions and comparisons with the trimaran model experiments are presented in Section 5.4. Some computational considerations are explained and discussed regarding the roll damping coefficients and side hull flare effects. The comparisons between the predictions and the model experiments show good agreement for heave and pitch motions. Roll motion predictions also show good agreement with model tests when free decay data are used for estimating roll damping.

Finally, a comparison of predicted seakeeping performance between a trimaran ship and an equivalent displacement monohull ship is given in Section 5.5. The trimaran ship is shown to have a better operability in waves than the monohull ship for the chosen seakeeping criteria.

5.2 Ship Motion Theories

Pioneering work on ship motion can be traced back as early as to the work of William **Froude (1861)** for the roll motions of a ship and the work of **Krylov (1898)** for the pitching and heaving motions with considerable subsequent effort to develop theoretical methods for ship motion predictions. However, these were not widely used in ship designs until the development of linear strip theory by **Korvin-Kroukovsky & Jacobs (1957)**. Their strip theory was based on intuitive analysis rather than on a rigorous mathematical derivation, but provided very good agreement with experiment results. After that, there were extensive modifications made to strip theory. Among them, **Salvesen, Tuck & Faltinsen (1970)** presented a most popular theory which satisfied the **Timman-Newman (1962)** relation for the cross coupling added mass and damping terms. One common limitation to strip theories is that they are not valid for low frequencies or high speeds, and thus may fail to give satisfactory results for fast ships or following seas and quartering seas. To remove the low frequency limitation, **Newman (1978)** developed a unified strip theory, which was claimed to be valid for all frequencies. His theory takes some account of wave interactions between different cross sections of the ship. Numerical results of the unified theory for heave and pitch motions showed improved agreement with experimental results for zero forward speed **(Sclavounos 1985)**.

Strip theory has been used successfully for many monohull designs and also in motion analyses for twin hull ships, both catamaran and SWATH ships. Typically, **Lee & Curphey (1977)** used the Salvesen strip theory for the motion and wave load predictions for a SWATH ship with forward speeds. The two dimensional hydrodynamic properties were solved assuming two infinitely long, semi-submerged, horizontal cylinders having cross-sections identical to a cross-section of the SWATH ship undergoing heave, pitch, and roll oscillations. By taking into account viscous damping, the theoretical predictions of heave and pitch of the ship showed good agreement with model experiments for head seas and beam seas, as well as for roll motions in beam seas, though no predictions for following quartering seas were presented. Similar work has been done by **Nordenstrom, Faltinsen & Pederson (1971)** for catamarans, and by **McCreight (1987)** for SWATH ships.

Nevertheless, the strip theory has its inherent limitations. It requires the ship to be slender and the magnitudes of forward speed and encounter frequency to be in a certain range. This is because the strip theory converts the three dimensional ship body into hydrodynamically independent two dimensional sections. It follows, firstly, that the component of the hull normal to the x-direction is assumed much smaller than the normal components in the y and z directions. Secondly, it follows that the frequency of encounter is assumed high, i.e., $\omega >> V\frac{\partial}{\partial x}$, to reduce the free surface condition:-

$$\left[\left(i\omega + V\frac{\partial}{\partial x}\right)^2 + g\frac{\partial}{\partial z}\right]\phi_j = 0 \qquad on \quad z = 0 \tag{5-0}$$

where ω is the encounter wave frequency, V is the speed of the ship, $j=1,2,...6$ represents six modes of motions, and ϕ_j is the velocity potential due to jth mode of motion. These assumptions made the theoretical justification for the strip theory somewhat questionable in low frequency and high speed ranges **(Salvesen, Tuck & Faltinsen 1970)**.

The trimaran ship has slender hulls, both the side hulls and the central hull, which should make it suitable for strip theory applications. The section properties of the trimaran could be derived assuming three infinitely long, semi-submerged, horizontal cylinders having cross sections identical to a cross section of the ship undergoing heave, pitch, or roll oscillations, as is the case for twin hull ships. However, there is a difference between the trimaran and twin hull ships, the two demi-hulls of a twin ship are of the same length, but the centre hull and the side hulls of a trimaran ship are of quite different lengths. Thus, the lengthwise discontinuity of the trimaran hull sections could make the numerical model for ship motions more complicated than that for monohull and twin hull ships, and may also hamper the accuracy of the strip theory which assumes that lengthwise interactions could be neglected. Furthermore, the encounter frequency limitation of strip theory made it an unfavourable tool for motion predictions for following quarter seas as discussed above. The initial experiments on trimaran motions carried out at Haslar showed that critical motions occurred specifically in following quarter seas **(DRA 1995)**. Taking into account all of these factors, it was considered that strip theory may not be as suitable for the trimaran motion prediction as is the case for the monohull and twin hull ships.

Therefore, a three dimensional analysis was pursued for trimaran motion predictions, particularly, for asymmetric motion predictions, since some of the limitations of the strip theory could be removed by using the three dimensional approach. Three dimensional

theories have been routinely used for the last 20 years by researchers for the offshore industries in solving the linear and zero speed problem for vessels in regular waves **(Garrison 1974) (Faltinsen & Michelsen 1975)**, because the geometry of many offshore vessels precludes the use of strip theory. **Chang (1977)** was the first to use a three dimensional approach to solve the ship motion in waves with forward speed. She used a source distribution which contains a body surface integral and a waterline integral. The disturbance of the steady potential is neglected in the procedure for solving the unsteady motion, but is retained for the pressure force. Better agreement between the computed hydrodynamic coefficients and experimental data was obtained than with strip theory. A similar method is also applied by **Guevel & Bougis (1982)** using a source distribution and a combination of source and dipole distribution. Satisfactory results were obtained using a small number of panels.

Inglis & Price (1982) examined the effect of the steady potential disturbance in the body surface condition and the effect of the forward speed in the free surface condition. As expected, the computation results showed that the first factor is insignificant. They also showed that the longitudinal convective term $V\frac{\partial}{\partial x}$ is significant at higher speeds and lower frequencies, particularly on the heave and pitch damping coefficients. These results confirmed the limitation of the strip theory that neglects the convective term under the assumption that the encounter frequency is far great than the convective term, i.e., $\omega >> V\frac{\partial}{\partial x}$. Similar conclusions were also obtained by **Hearn et al. (1987)**, when they used a simplified three dimensional method neglecting the longitudinal convective term and found satisfactory results could be achieved over the intermediate frequency range and at small Froude numbers.

Wu & Eatock Taylor (1987) presented an efficient method by coupling the finite element formulation with a boundary integral formulation to solve the motion problem for a ship with forward speed. Their results for a submerged circular cylinder compared very well with the semi-analytical solutions. They also showed how the second derivatives of the steady potential in the body surface condition can be reduced to the first derivatives by applying an integral theorem derived by **Ogilvie & Tuck (1969)**. Further improvement to the three dimensional method was made by **Wu & Eatock Taylor (1989)** using higher order elements instead of plane constant panels.

Alongside the research into the use of three dimensional theory for the motion analysis of monohulls, there have been several efforts made to use the theory for multihull vessels, mainly the twin hull ships. **Chan (1993)** used a three dimensional linearised potential

theory in the motion and wave load predictions for a catamaran and a SWATH ship. Good agreement between theory and experiments was obtained except for some discrepancies that could have been caused by the neglect of forward speed effects on the free surface.

Though the three dimensional methods developed vary in detail, the basic task is to find a source distribution method and solve for source strength to derive the velocity potential. Since the three dimensional approach evaluates the hydrodynamic force on the ship by small panels rather than by sections, as in the case of the strip theory, this means the interactions between the panels can be taken into account both transversely and longitudinally. The requirement for longitudinal continuity of the section shape for the ship, therefore, can be removed. Thus, the three dimensional model allows the interactions between centre hull and the side hulls to be taken into account in the motion calculation. The three dimensional theory is therefore more suitable for the trimaran motion analysis than strip theory. The method used for motion predictions reported in this thesis is a three dimensional linearised potential theory based on the theory developed by **Wu & Eatock Taylor (1987 & 1989)** with some computational considerations accounting for the special characteristics of the trimaran ship as is discussed in Section 5.4.

5.3 Numerical Model for Trimaran Motion

5.3.1 Basic Equations

Consider a trimaran ship travelling at constant forward speed V and arbitrary heading μ relative to oblique regular waves of frequency ω_o, and $oxyz$ is defined as a right handed coordinate system which is translating with the same speed as the ship. The x axis is on the central plane of the centre hull and in the direction of the ship's forward speed; the xy plane on the undisturbed water surface; and z axis passing through the centre of gravity of the ship. Figure 5.1 illustrates the coordinate system. The frequency of encounter between the ship and the waves is:

$$\omega = \omega_o - V\frac{\omega_o^2}{g}\cos\mu \tag{5-1}$$

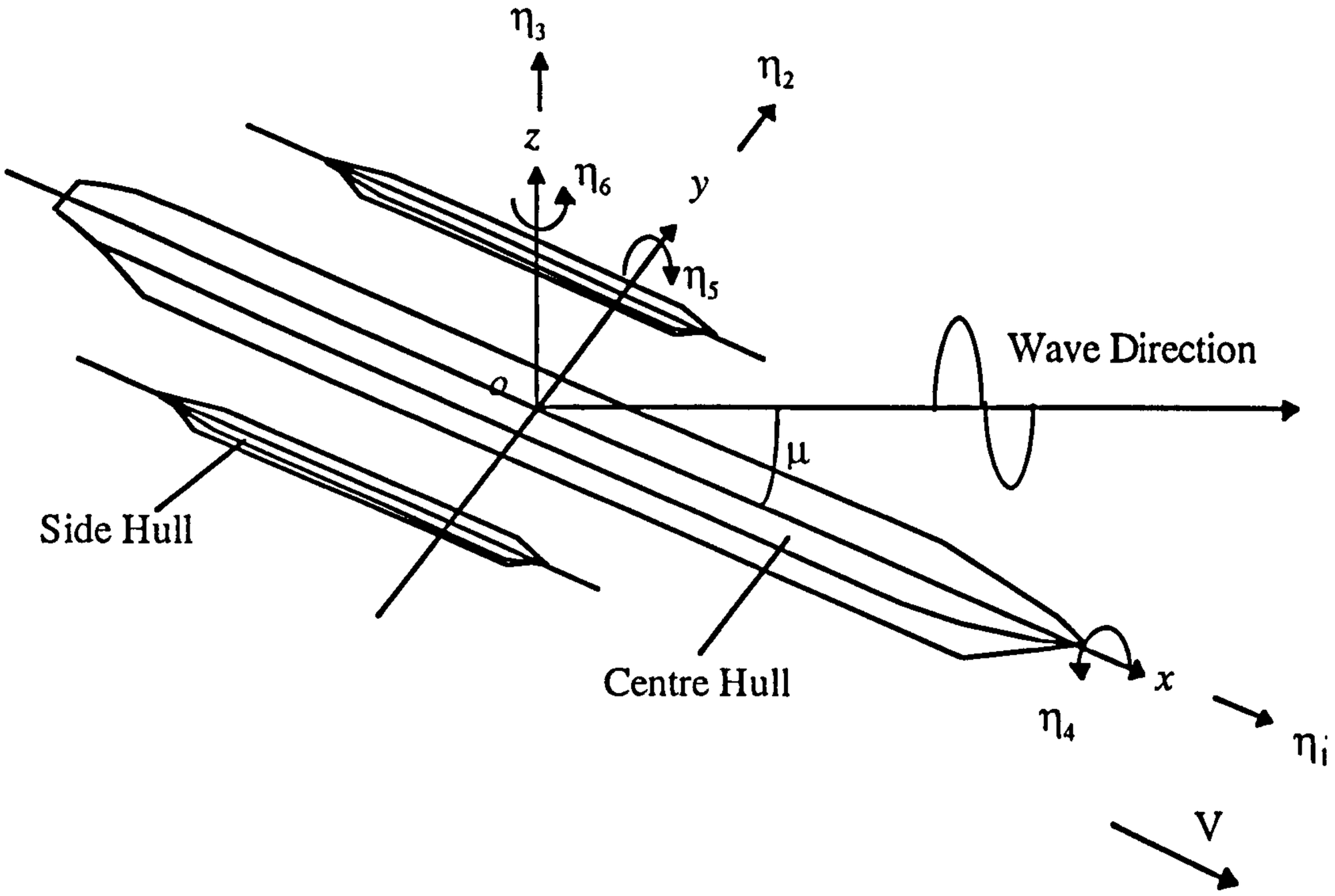

Figure 5.1 Coordinate system of the trimaran ship

Assuming the ship is a rigid body undergoing oscillatory motions in ideal and incompressible fluid, the total velocity potential will consist three parts, the ship's forward speed, steady potential, and unsteady potential:-

$$\Phi = -Vx + \bar{\phi}(x,y,z) + \tilde{\Phi} \tag{5-2}$$

where $\bar{\phi}(x,y,z)$ is the steady perturbation potential due to forward speed, and $\tilde{\Phi}$ is the unsteady potential. **Haskind (1952)** found that the linearised ship motion equation can be solved by decomposing the velocity potential into a form consisting a diffraction potential and six radiation potentials for the six modes of oscillations. The unsteady potential can then be written as:-

$$\tilde{\Phi} = \mathrm{Re}\left\{\left[\eta_0(\phi_0 + \phi_7) + \sum_{j=1}^{6} \eta_j \phi_j\right]\exp(-i\omega t)\right\} \tag{5-3}$$

where η_0 is the incoming wave amplitude, ϕ_0 is the potential of incident waves, ϕ_7 is the potential of diffraction waves, η_j (j=1,...,6) are the motion amplitudes of six modes,

and ϕ_j are the radiation potentials corresponding to the six modes of oscillations of the ship.

The incident wave potential ϕ_0 is:-

$$\phi_0 = \frac{ig}{\omega_0} \exp k(z - ix\cos\mu + iy\sin\mu) \tag{5-4}$$

where g is gravitational acceleration, and k is the wave number.

The diffraction wave potential is related to the incident wave potential by the following condition (**Newman 1977**):-

$$\frac{\partial \phi_7}{\partial n} = \frac{\partial \phi_0}{\partial n} \tag{5-5}$$

on the body surface S_0, where n is the outward normal vector of the body surfaces.

5.3.2 Boundary Conditions

The total velocity potential must satisfy the Laplace's equation and a suitable far-field radiation condition. Based on the assumptions of the linearised theory, the steady perturbation potential is small compared with the radiation potential and can be neglected. The free surface condition is:-

$$\left[\left(i\omega + \frac{V\partial}{\partial x}\right)^2 + \frac{g\partial}{\partial z}\right]\phi_j = 0 \qquad (j = 1,...,7) \tag{5-6}$$

where $\phi_j (j=1,2,...6)$ are radiation potentials corresponding to the six modes of oscillations of the ship, and ϕ_7 is the potential of diffraction waves.

Following **Ogilvie & Tuck (1969)**, the boundary condition for the unsteady potential can be expressed as:-

$$\frac{\partial \phi_j}{\partial n} = i\omega n_j + V m_j \qquad (j = 1,...,6) \tag{5-7}$$

on the submerged surface of the ship, where the components are:

$$\left.\begin{aligned}
&(n_1,n_2,n_3) = (n_x,n_y,n_z)\\
&(n_4,n_5,n_6) = r \times n\\
&V(m_1,m_2,m_3) = -(n\cdot\nabla)W\\
&V(m_4,m_5,m_6) = -(n\cdot\nabla)(r\times W)
\end{aligned}\right\} \qquad (5\text{-}8)$$

with $n = (n_1,n_2,n_3)$ is a unit normal vector outward from the wetted surface S, $r = (x,y,z)$ is a position vector of a point on S, and W is a steady velocity vector relative to the moving reference frame as:-

$$W = V\nabla(\bar{\phi} - x) \qquad (5\text{-}9)$$

The radiation and diffraction potentials also satisfy the kinematic boundary condition on the sea bottom of infinite water depth as:-

$$\frac{\partial \phi_j}{\partial n} = 0 \qquad j = 1,\ldots,7 \qquad (5\text{-}10)$$

5.3.3 Source Distribution

Having defined the boundary conditions for the velocity potentials, a source distribution technique is required to solve the problem. **Brard (1972)** has shown that the unknown potential at a point p of a surface piercing body with forward speed can be represented by integrating a source distribution σ over the body surface S and waterline C as:-

$$\phi(p) = \frac{1}{4\pi}\left[\iint_S \sigma(q)G(p,q)ds + \frac{V^2}{g}\oint_C \sigma(q)G(p,q)n_x(q)dy\right] \qquad (5\text{-}11)$$

where the Green function $G(p,q)$ is a source function at the field point p due to a source of unknown strength σ at the field point q. A form of Green function has been developed by **Wu & Eatock Taylor (1987)**.

In equation (5-11), the term $G(p,q)n_x(q)$ should be integrated along the waterline C, but in practice this is achieved by evaluating this term at the centroid of a element and simply multiplying the component dy in Oy direction **(Inglis & Price 1982)**.

From equation (5-11) we have on the wetted surfaces:-

$$\frac{\partial\phi(p)}{\partial n(p)} = \frac{1}{4\pi}\left[\iint_S \sigma(q)\frac{\partial G(p,q)}{\partial n(p)}ds + \frac{V^2}{g}\oint_C \sigma(q)n_x(q)\frac{\partial G(p,q)}{\partial n(p)}dy\right] \qquad (5\text{-}12)$$

The unknown source strength can then be determined by substituting boundary condition equations (5-5) and (5-7) into the above equation.

Due to the complexity of the Green function, the boundary integral equation (5-12) has to be solved numerically. Let the submerged ship surfaces be represented by N surface elements of which the elements number 1 to M are at the free surface. The discretised form of equation (5-12) can be expressed as **(Inglis & Price 1982)**:-

$$\frac{\partial\phi(p)}{\partial n(p)} = \frac{1}{4\pi}\left[\sum_{k=1}^{N}\sigma_k\iint_{\Delta S_k}\frac{\partial G(p,k)}{\partial n(p)}ds + \sum_{k=1}^{M}\sigma_k\oint_{l_k} n_x\frac{\partial G(p,k)}{\partial n(p)}dy\right] \qquad (5\text{-}13)$$

where ΔS_k is the area of the *kth* element, l_k is the length of *kth* element *($k \le M$)* at the waterline, l_k is the strength of the source density on the *kth* element, and *G(p,k)* is the Green's function at the point p due to a unit source on the *kth* element.

5.3.4 Method of Solution

The velocity potential can be derived by discretising equation (5-11) in the form:-

$$\phi(p) = \frac{1}{4\pi}\left[\sum_{k=1}^{N}\sigma_k\iint_{\Delta S_k}G(p,k)ds + \frac{V^2}{g}\sum_{k=1}^{M}\sigma_k\oint_{l_k}G(p,k)n_x dy\right] \qquad (5\text{-}14)$$

The total oscillatory force on the ship hulls is obtained by integrating the fluid pressure over the hull surfaces as:-

$$F_j = \iint_S Pn_j ds \qquad (5\text{-}15)$$

where *Fj (j = 1,2,3)* represent the total hydrodynamic components of force in the x, y, z directions respectively, F_j *(j = 4,5,6)* represent the moment about these axes, and P is the pressure on the hulls given by the linearised Bernoulli equation:-

$$P = -\rho(\frac{\partial \phi}{\partial t} + W \cdot \nabla \phi + \frac{1}{2} W \cdot W + gz) \tag{5-16}$$

in which the last two terms on the right hand side are time independent and do not enter the oscillatory force calculation(**Inglis & Price 1982**) and can be omitted. Equation (5-15) can be rewritten as:-

$$F_j = -\rho \iint_S n_j \left(\frac{\partial \phi}{\partial t} + W \cdot \nabla \phi \right) ds \quad j = 1,...,6 \tag{5-17}$$

From equation (5-3), the total force can be split into two terms, one is the exciting force due to incident wave and diffraction wave potentials and the other is the hydrodynamic force due to radiation potential as:-

$$F_j = F_j^{EX} + F_j^R \tag{5-18}$$

where the exciting force is

$$F_j^{EX} = -\rho \iint_S n_j (i\omega + W \cdot \nabla)(\phi_0 + \phi_7) \exp(-i\omega t) ds \tag{5-19}$$

and the hydrodynamic force due to forced motion of the ship can be expressed by the following equation:-

$$\begin{aligned} F_j^R &= -\rho \iint_S n_j (i\omega + W \cdot \nabla) \sum_{k=1}^{6} \eta_k \phi_k \exp(-i\omega t) ds \\ &= \sum_{k=1}^{6} T_{jk} \eta_k \exp(-i\omega t) \end{aligned} \tag{5-20}$$

where T_{jk} denotes the hydrodynamic force and moment in the *jth* direction due to unit oscillatory motion amplitude in the *kth* mode. By separating the complex force T_{jk} into real and imaginary parts, the added mass and damping coefficients are then revealed as:-

$$\begin{aligned} T_{jk} &= -\rho \iint_S n_j (i\omega + W \cdot \nabla) \phi_k ds \\ &= \omega^2 A_{jk} - i\omega B_{jk} \end{aligned} \tag{5-21}$$

where A_{jk} and B_{jk} are added mass and damping coefficients respectively.

Now, the motion responses of a trimaran ship in regular waves can be calculated using the motion equation:-

$$\sum_{k=1}^{6}(-\omega^2(M_{jk}+A_{jk})-i\omega\, B_{jk}+C_{jk})\eta_k = F_j^{EX} \qquad (5\text{-}22)$$

$$j = 1, ..., 6$$

where ω is the encounter frequency between the ship and waves when the ship is travelling with a forward speed *V*, M_{jk} is the mass matrix of the ship, C_{jk} is the restoring force coefficient matrix and η_k represents the motion amplitude of the ship in the *kth* mode of motion.

5.4 Computation and Comparisons

5.4.1 Some Computation Considerations

Slender Hull Assumption

Computations for the trimaran model ships have been performed using a modified version of an existing UCL 3D boundary element program (**Wu & Eatock Taylor 1989**). The three dimensional theory described in the previous section has been simplified by neglecting the line integral term in equation (5-11), which is a function of the derivative of the steady potential, under the assumption that the trimaran hulls are very slender. Both **Inglis et al. (1982)** and **Wu et al.(1989)** have used the simplification for the motion calculation of slender monohulls. **Chan (1993)** also made similar simplifications in the motion computations for catamaran and SWATH ships. Though this may affect motion predictions at the low encounter frequency range, as in the case for strip theory, the effects are expected to be smaller than that for strip theory. This is because interactions of the three hulls, interactions between hull sections, and end effects, which are significant at low frequencies **(Chan 1993)**, are all taken into account in the three dimensional computation.

Viscous Roll Damping Effects

Another important aspect is the effect of viscous damping on the trimaran motions. The damping coefficients derived from the above linearised potential theory are wavemaking damping only, that is, due to the oscillating hulls radiating waves away from the ship. For vertical motions, (i.e. heave and pitch), the damping is dominated by the wavemaking

damping. But, for roll motions, the wavemaking damping may only be a small fraction of the total damping **(Lloyd 1989)**. Therefore, the viscous roll damping due to hull friction, eddy making, appendage lift and drag need to be taken into account for predicting roll motions.

At first, the linearised rolling damping coefficients obtained from free decay experiments **(DRA 1995)** were used in roll motion predictions. The free decay experiment gives the damping coefficient of the ship at its natural rolling frequency and consists of both the wavemaking damping and the viscous damping. This could not be used directly for roll motion predictions over all range of frequencies since the wavemaking damping is frequency dependent. To solve this problem, the difference between the free decay damping coefficient and the calculated wavemaking damping coefficient at the resonance frequency was calculated. This difference was then added to the wavemaking damping coefficients over the whole range of encounter frequencies.

Although the use of the linearised free decay damping coefficients improved the roll motion predictions, as is shown below, questions still remain:-

- What would the viscous damping effects be if the damping coefficients are taken into account in a more appropriate form, such as including a non-linear term?

- How could the viscous roll damping coefficients for a trimaran ship be determined when there are no free decay experimental data?

Because of the importance of understanding the rolling characteristics for the new trimaran ship, these two questions certainly require to be investigated. Detailed roll damping analysis of the trimaran ship and the methods to estimate viscous roll damping coefficients are discussed in Chapter 6 since it is an extensive topic.

The viscous damping coefficients, estimated using the methods described in Chapter 6, depend on the amplitudes of motion responses. Thus, the equations of motion are solved interactively until a satisfactory convergence of the motion amplitudes (to 1% of the non-dimensional RAO function) is obtained.

Effects of Side Hull Flare on Restoring Force

To meet the stability requirements, the side hulls would normally have flare above the design waterline as illustrated in Chapters 3 and 4. Both the three dimensional theory and strip theory for motion predictions are normally based on the assumption that the hull

sections above the still waterlines are wall sided. This may be justified for monohull ships since their flares above the waterline are usually small along the most part of the hulls and have little influence on the hydrostatic restoring forces when the ships oscillate in waves. However, the wall sided assumption may not be justified for the trimaran ship because the flares of the side hulls may be too big to be neglected. In addition, the motion response of a ship at low frequencies, when ω is small in motion equation (5-22), would be largely controlled by the hydrostatic restoring force. An increased waterplane area will increase the restoring force and hence reduce the motion amplitudes.

For heave motions, when the ship moves downwards there is an increased heave restoring force due to the side hull flare. Assuming the waterplane area of a side hull at the design waterline is A_{ws} and the deck area of the side hull at the top of the side hull is A'_{ws} as shown in Figure 5.2, then the increased heave restoring force coefficient is:

$$C_{33}^{\cdot} = \rho g \frac{A_{ws}^{\cdot} - A_{ws}}{H_a} \eta_3 \tag{5-23}$$

where H_a is the vertical distance between the still waterline and the top of the side hull, and η_3 is the heave motion amplitude.

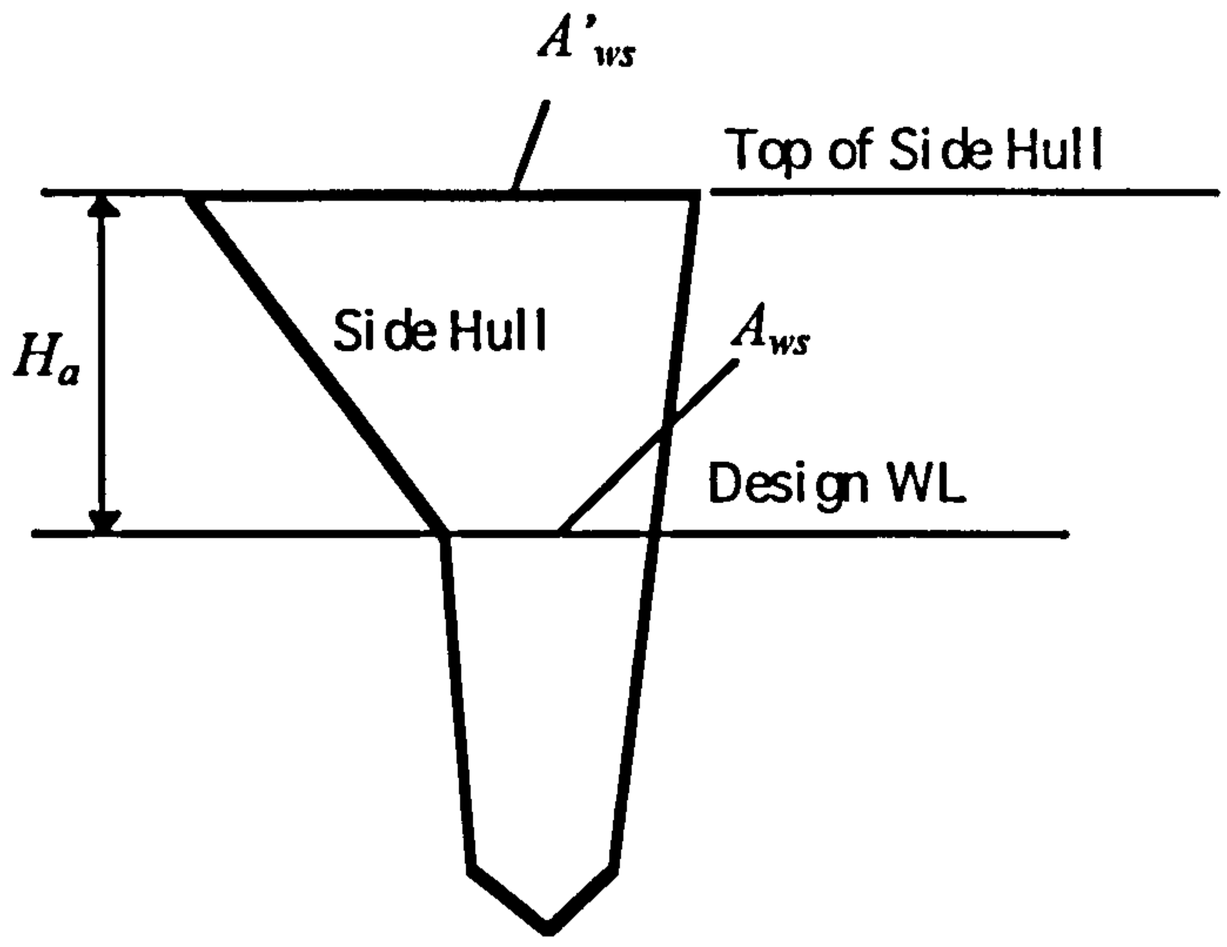

Figure 5.2 Side hull flare

Thus the total heave restoring force coefficient is:

$$C_{33} = C_{33}^{*} + C_{33}^{'}$$
$$= \rho g\left(A_w + \varepsilon \frac{A_{ws}^{'} - A_{ws}}{H_a} \eta_3 \right) \tag{5-24}$$

where C_{33}^{*} is the heave restoring coefficient calculated at the design waterline, C'_{33} is the heave restoring coefficient due to side hull flare, and the operator $\varepsilon = 0$ for $\eta_3 \geq 0$ and $\varepsilon = 1$ for $\eta_3 < 0$. It must be noted that this restoring force is no longer a linear term but depends on the heave amplitude η_3. Again, the motion equation needs to be solved interactively in the same way as the roll motion with its viscous roll damping term.

The increased waterplane area due to side hull flare would also effect the restoring forces in pitch motion. Because the trimaran ships studied in this thesis all have their side hulls close to amidships, the pitch effect can be considered as small and is therefore disregarded here.

The side hull flare would not have much effect on the roll motion restoring force, which can be verified by examining the shape of the GZ curves for trimaran ship. Figure 3.11 (Chapter 3) shows that the heeling restoring force of a trimaran ship with side hull flares can be considered approximately as linear up to an angle of heel up to 30 degrees. The reason for this is that whilst flare of the immersing side hull increases the waterplane area, the other (emerging) side hull causes a corresponding decrease in waterplane area.

5.4.2 Comparisons with Trimaran Model Experiments

The suitability of the theory for the motion predictions of the trimaran ship had to be verified. Due to the lack of the trimaran motion data at the early stage of the project and given that strip theory is well established for monohull motion predictions, the 3D computer program was firstly compared against the results from the GODDESS strip theory program SEAKPG for an existing 4,000t monohull ship **(Zhang 1995b)**.

Having achieved satisfactory agreements with the strip theory for monohull vertical motion predictions, and incorporated the roll viscous damping into the 3D program (see Chapter 6), computations for the trimaran model ships were carried out and the results were compared with the model experiments. The computations of the trimaran motion in regular waves were conducted for the ships corresponding to the tested Models A, B, C,

D, and E, which are detailed in Table 4.3. Surface meshes were generated using a UCL computer program **(Mateus 1994)** for all of the model ships. Figure 5.3 shows one of the meshes. Since the ships are symmetrical about the centrelines, only half of the central hull mesh and one side hull mesh were used in the calculations for each of the model ships. The surface mesh of each trimaran ships consists 796 triangle elements.

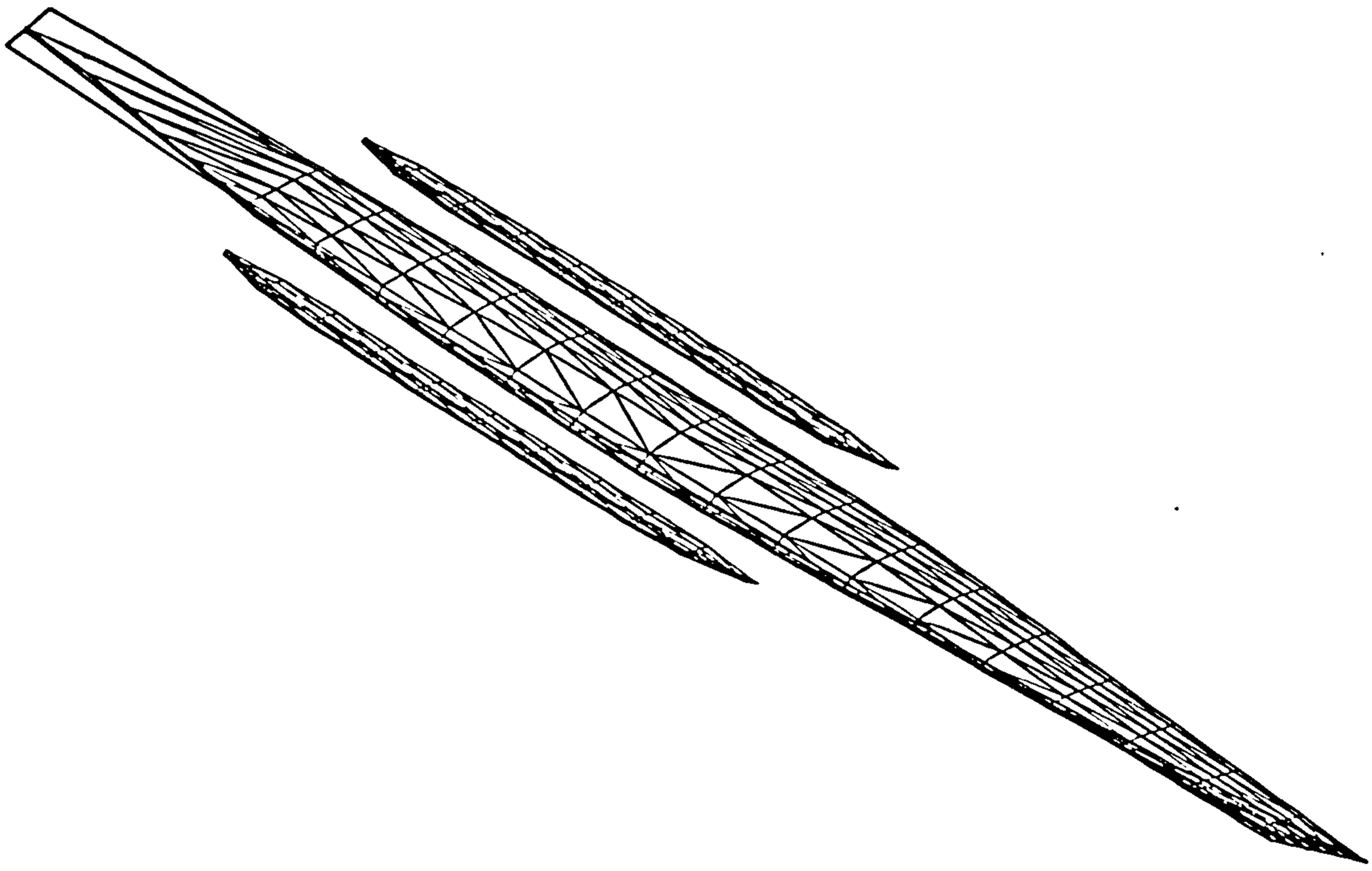

Figure 5.3 3D mesh of a trimaran model

The calculations covered wave frequencies between 0.2 to 2.0 rad/s. The ships' headings and the forward speeds were set corresponding to the tested cases. Given the model experiment data available from the tests conducted by DRA Haslar, the comparison between the predictions and the model data was limited to the heave, pitch, and roll motions only. The results of the computation and the comparison between the predictions and the model data are discussed below. The calculated results are shown in the form of response amplitude operator (RAO) plotted against wave frequencies. The response amplitude operator is the ratio of the amplitude of the ship's response to the regular wave amplitude for heave and pitch motions, and to the wave slope for the roll motions as:-

$$RAO = \begin{cases} \left|\frac{\eta_j}{\zeta_o}\right| & \textit{for heave and pitch motions} \\ \left|\frac{\eta_j}{k\zeta_o}\right| & \textit{for roll motions} \end{cases} \qquad (5\text{-}25)$$

where η_j is the motion amplitude, ζ_o is the wave amplitude, and k is the wave number.

In total 84 cases for the five model configurations were calculated (**Zhang 1995b & 1995c**) corresponding to the tested cases listed in Table 4.5. Presented below are the motion predictions for Models C and D in comparison with the DRA model experiment results (**DRA 1995**).

Heave and Pitch Motions

Heave motion predictions for Model C at various headings and speeds are shown in Figure 5.4 and pitch motion predictions in Figure 5.5 compared with model experiment results. Figures 5.6 and 5.7 give the heave and pitch motion predictions compared with experimental results for Model D.

These figures show the heave and the pitch motions predicted for the model ships agreed well with the model test results over the frequency ranges for which the test data are available. This indicates that the three dimensional theory described above is a suitable tool for trimaran heave and pitch motion predictions.

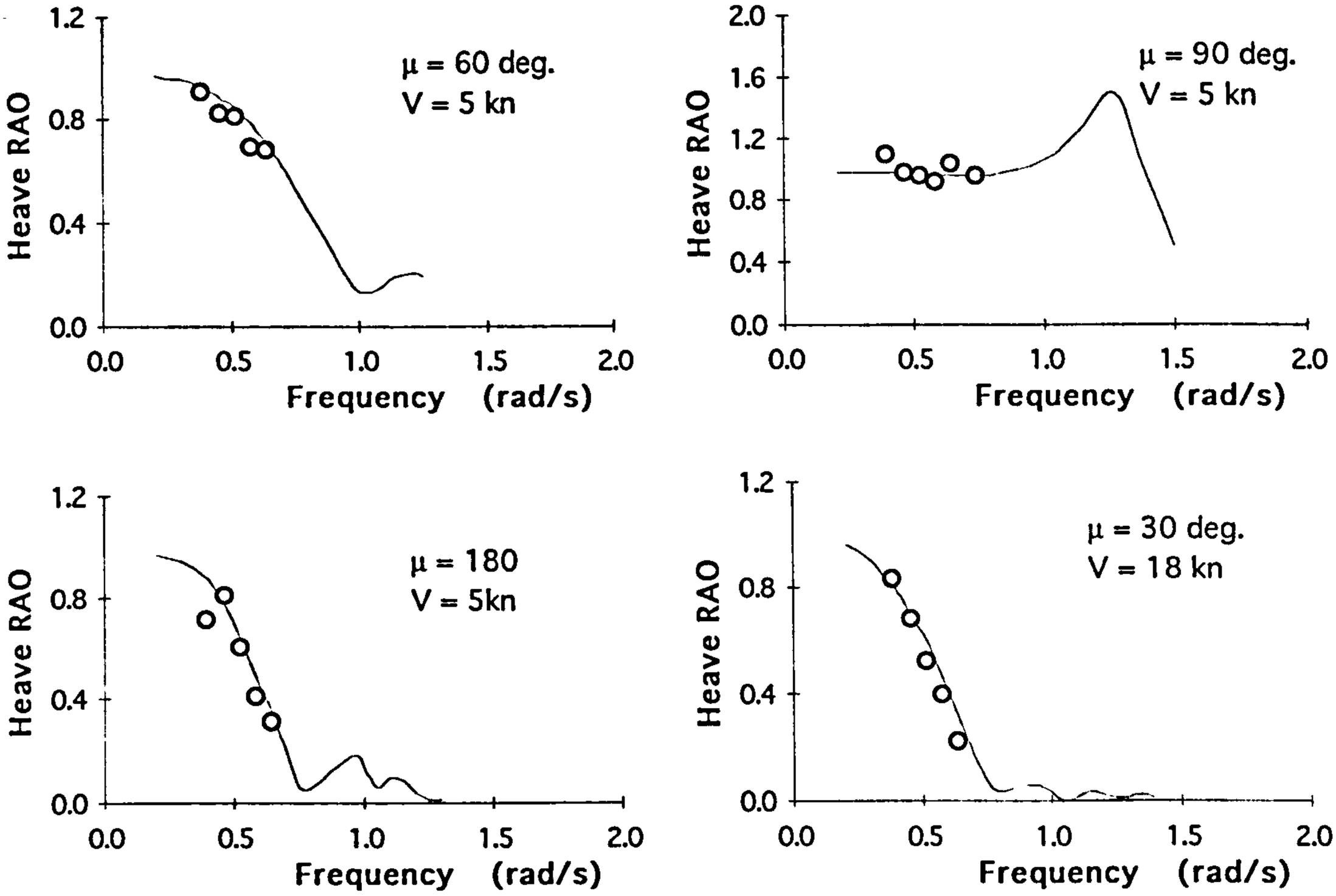

Figure 5.4 Heave motion prediction for Model C

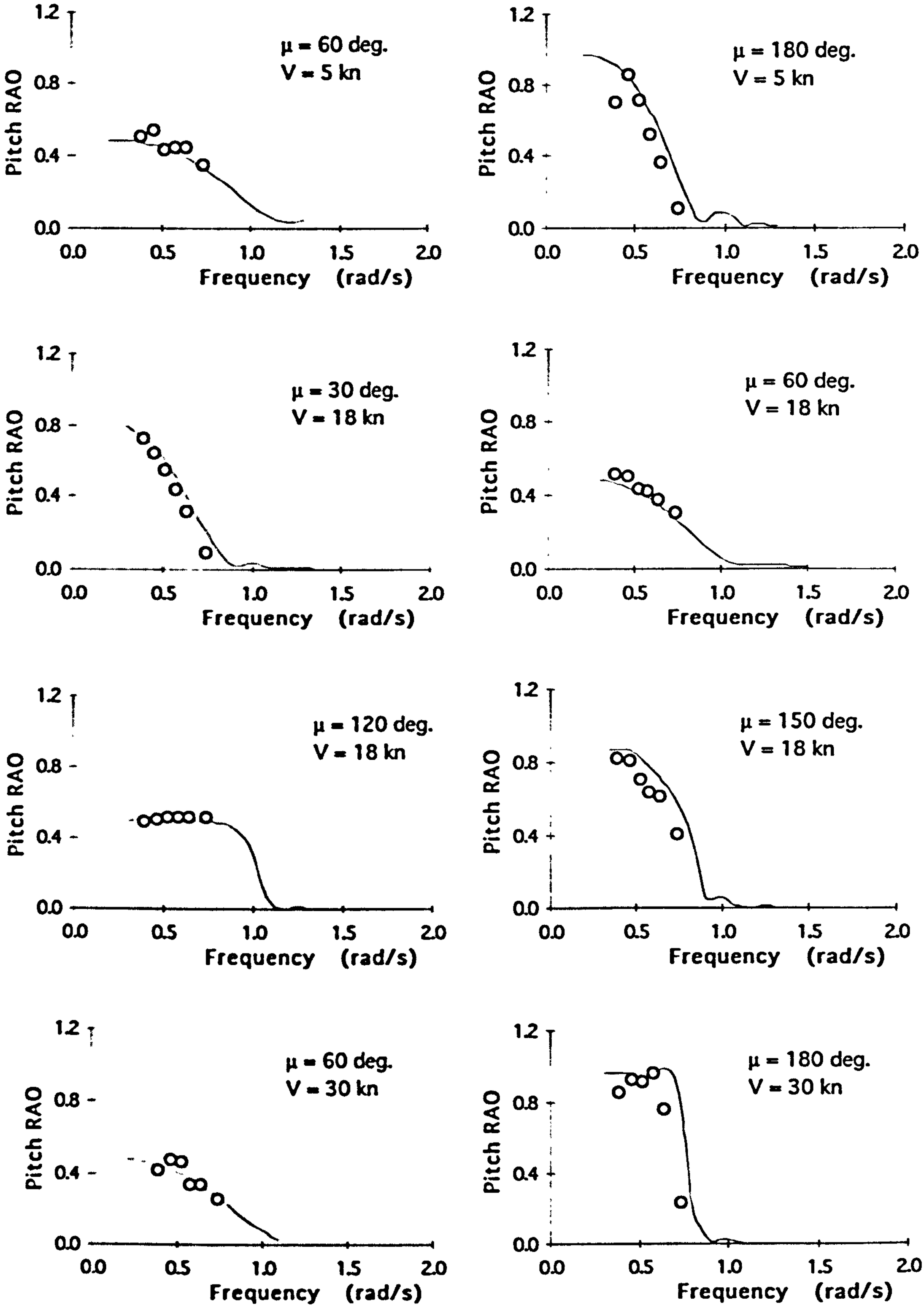

Figure 5.5 Pitch motion predictions for Model C

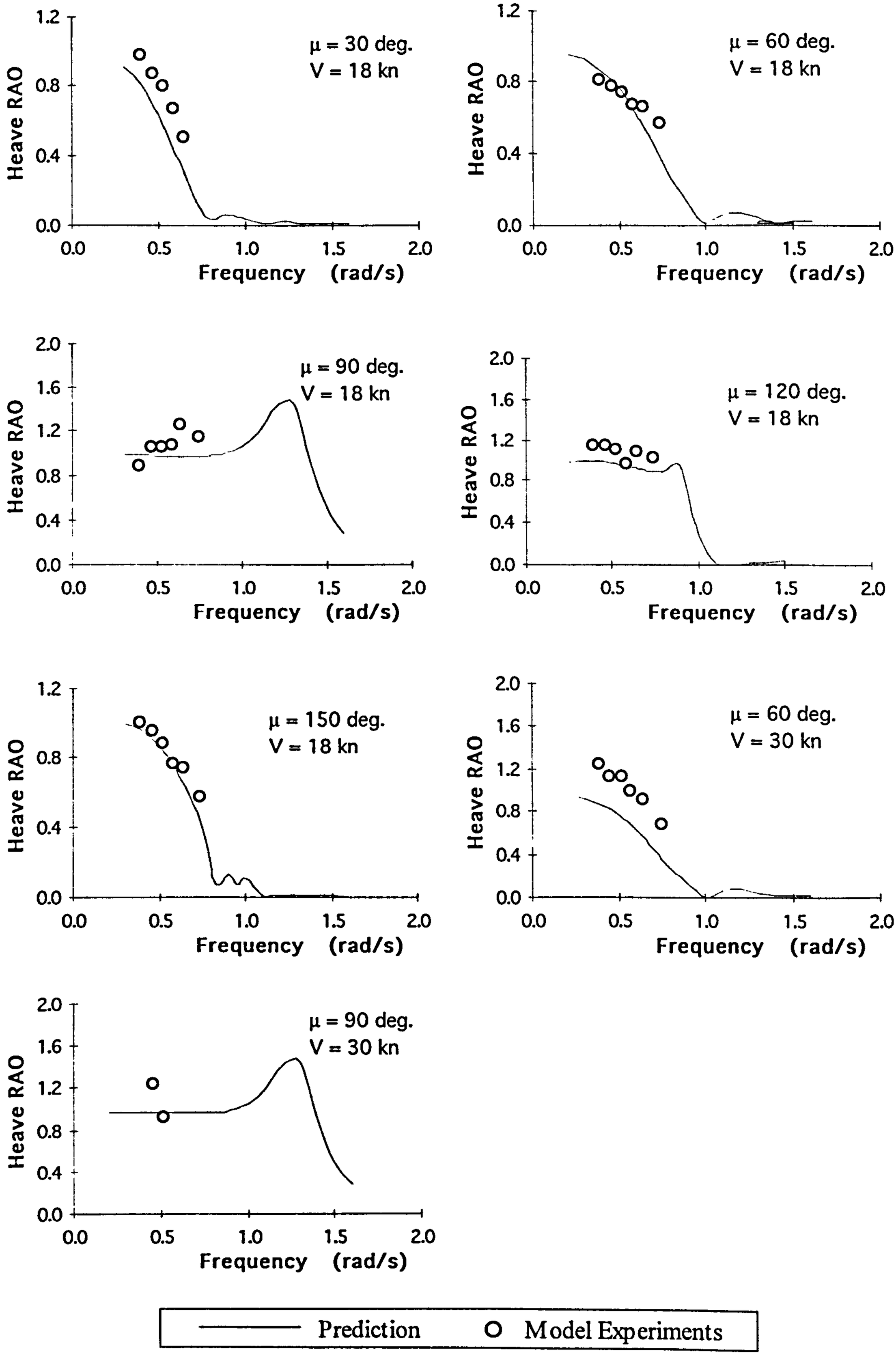

Figure 5.6 Heave motion prediction for Model D

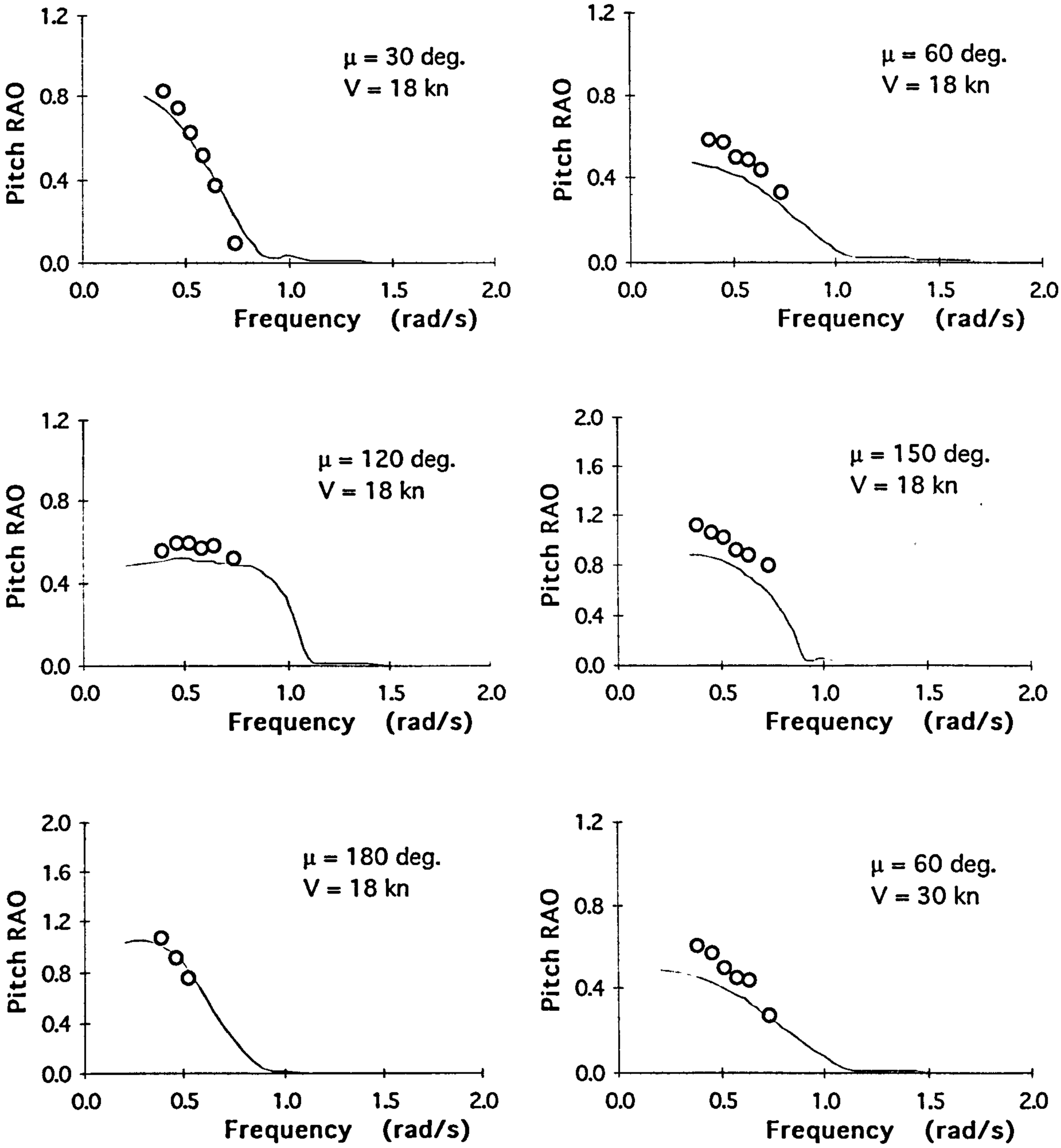

Figure 5.7 Pitch motion predictions for Model D

Roll Motion

Generally, the predicted roll motions of the trimaran models are quite close to the model experiment results as shown in Figures 5.8 and 5.9. Particularly, the predicted roll motion of the models at bow quartering seas and beam seas showed good agreement with the measured data. An exception is for Model C at a heading of 60 degrees and a speed of 30 knots, where the predicted roll motions are lower than the model data (See Figure 5.8). This is hard to explain as Figure 5.9 for Model D at the same heading and speed does not support this. However this indicates a need for a further verification to the program to be used in roll motion predictions for high speed trimaran ships.

For Model C, the predicted resonance frequencies of the roll motion are slightly higher than that of the model test results for most cases, particularly in beam seas. This could be due to some small errors which might exist in the measurement of *GM* and/or roll inertia during the model test. Either an over-measured *GM* value or under-measured roll inertia would result in a higher resonance frequency. The possible measurement error seemed to exist when the measured *GM* values were checked against the *GM* values derived from free decay data. For example, the measured *GM* value for Model C was 1.9 metres equivalent, while if the roll inertia measurement was correct then the *GM* value derived from the free decay test was equivalent to 1.6 metres. Vice versa, if the measured *GM* value was correct, this would mean the actual roll inertia would have been higher than the measured value. To check the effects of *GM* errors on roll motion prediction, attempts have been made to use *GM* values corrected by free decay data for roll motion predictions. Figure 5.10 illustrated the roll motion predictions using the corrected *GM* value, which revealed improved agreement between the predictions and the model test results.

The effects of *GM* value on roll motion can also been seen from the calculated results between the model ships of different *GMs*. As model D has a higher *GM* (3.0m) compared with model C (1.9m), the roll motion of model D is smaller than that of model C as shown in Figure 5.11, at the heading of 60 degrees and with forward speed of 18 knots. Comparisons of the predicted roll motion between the models in beam seas can be seen from Figure 5.12. Model ship C reveals some lower resonance frequency due to its lower *GM*, and higher resonant rolling amplitudes compared with model ship D. In addition, Figures 5.11 and 5.12 also show roll RAO curves for the other two models at a forward speed of 18 knots. The reduction in roll motion from Model B to Model C is due to the effects of bilge keels fitted on Model C which increased the roll damping coefficient. The reductions in roll motion from C to D and E are mainly due to the higher *GM* values which resulted in increased hydrostatic restoring forces.

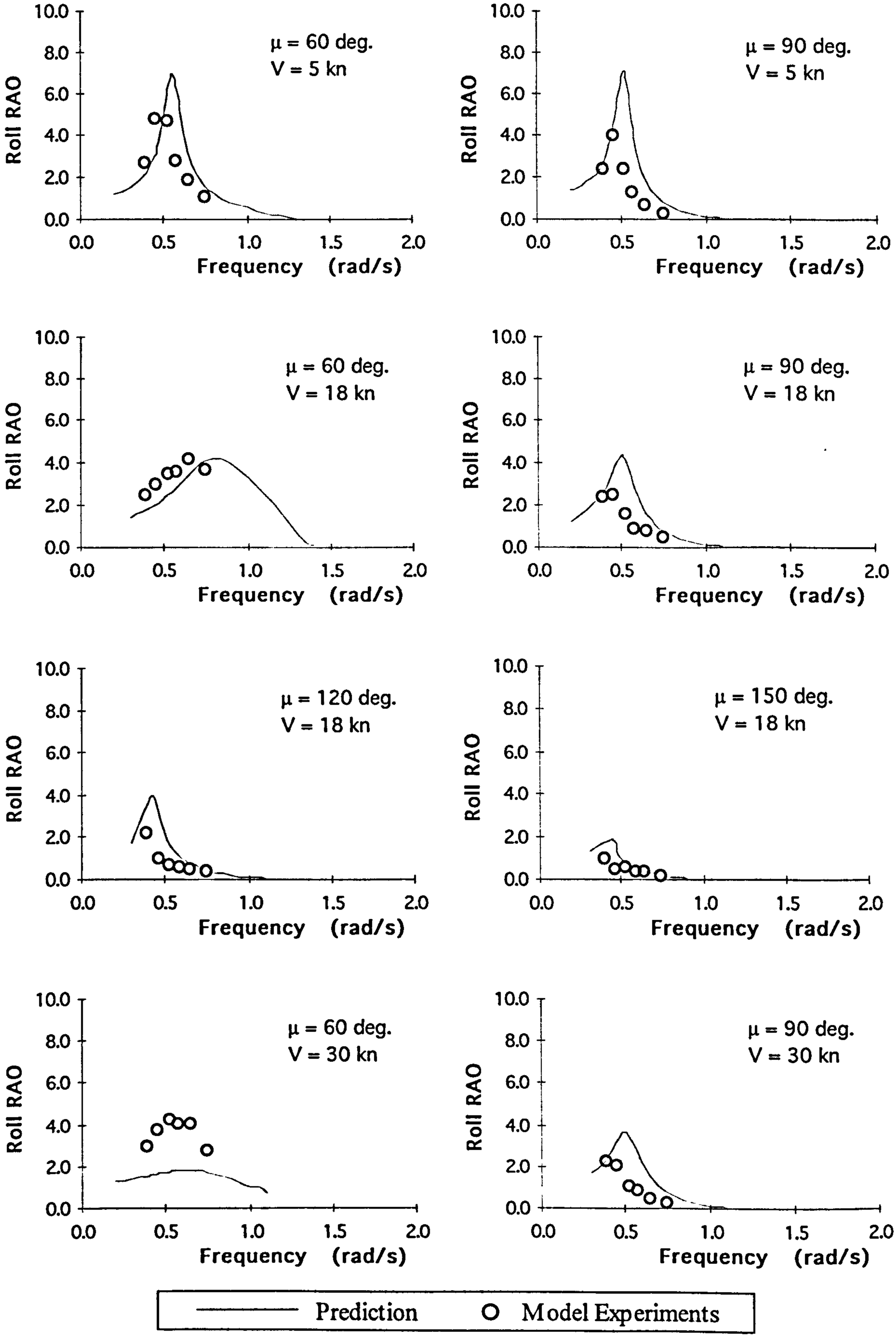

Figure 5.8 Roll motion predictions for Model C

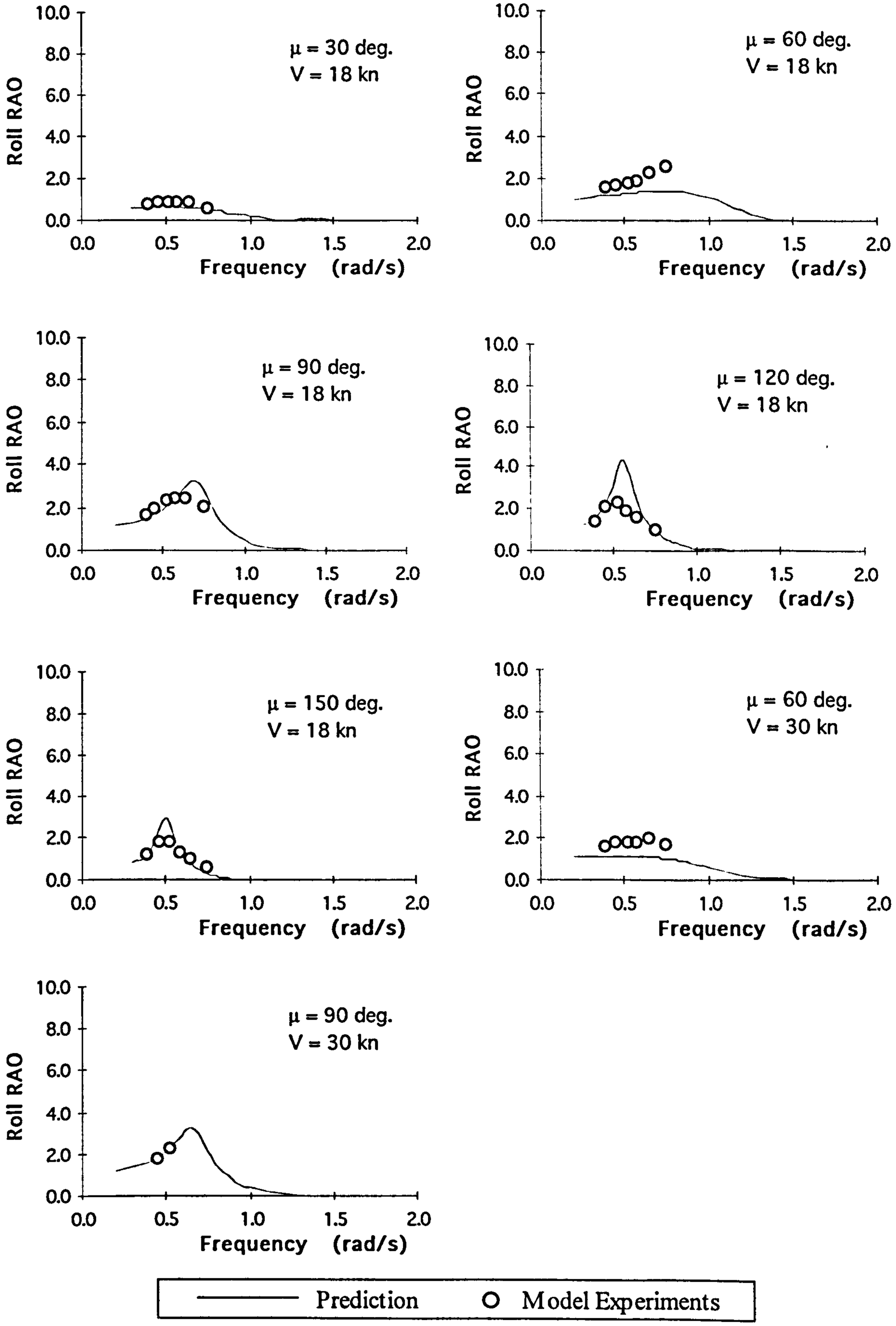

Figure 5.9 Roll motion predictions for Model D

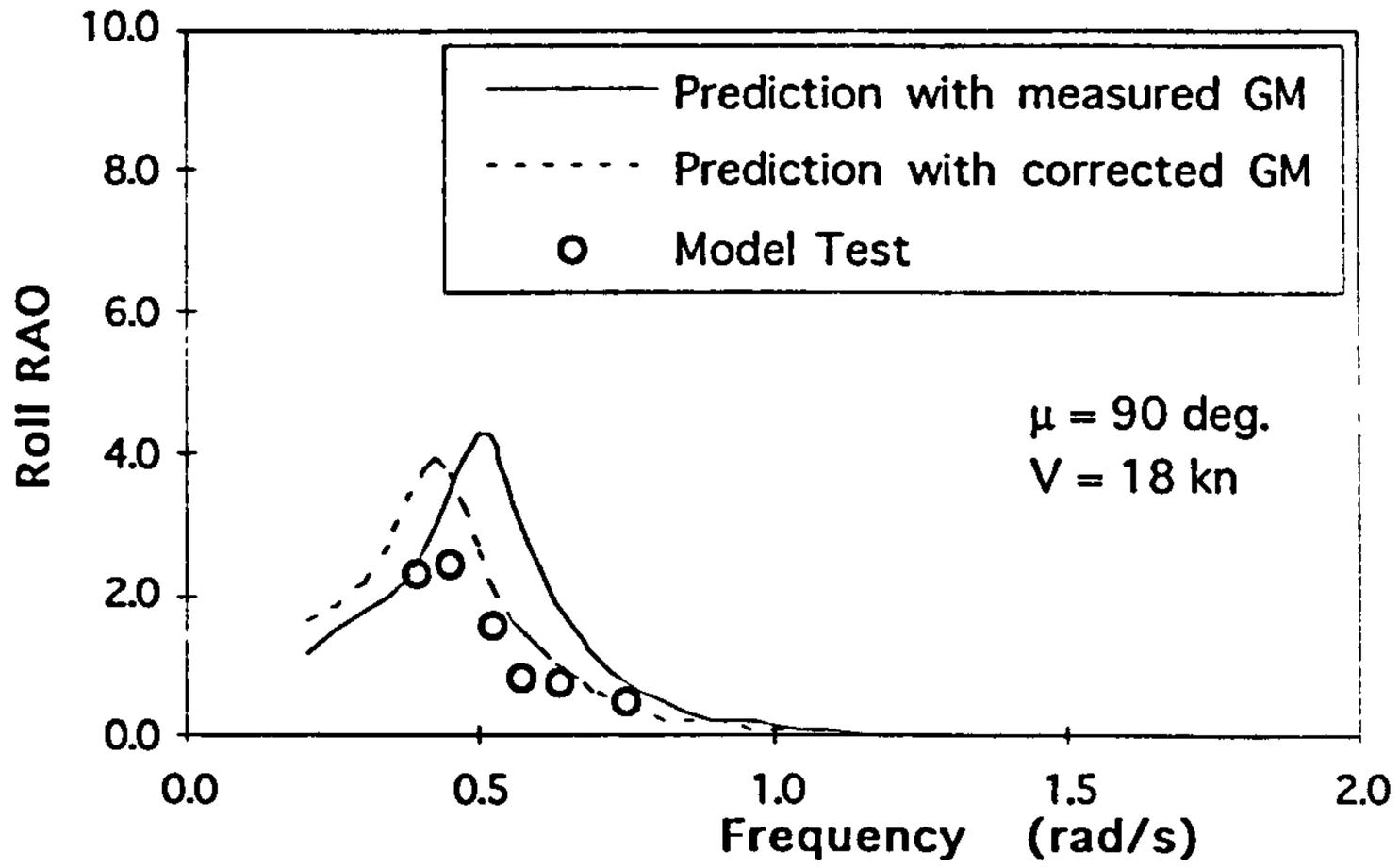

Figure 5.10 Roll motion of Model C with corrected GM

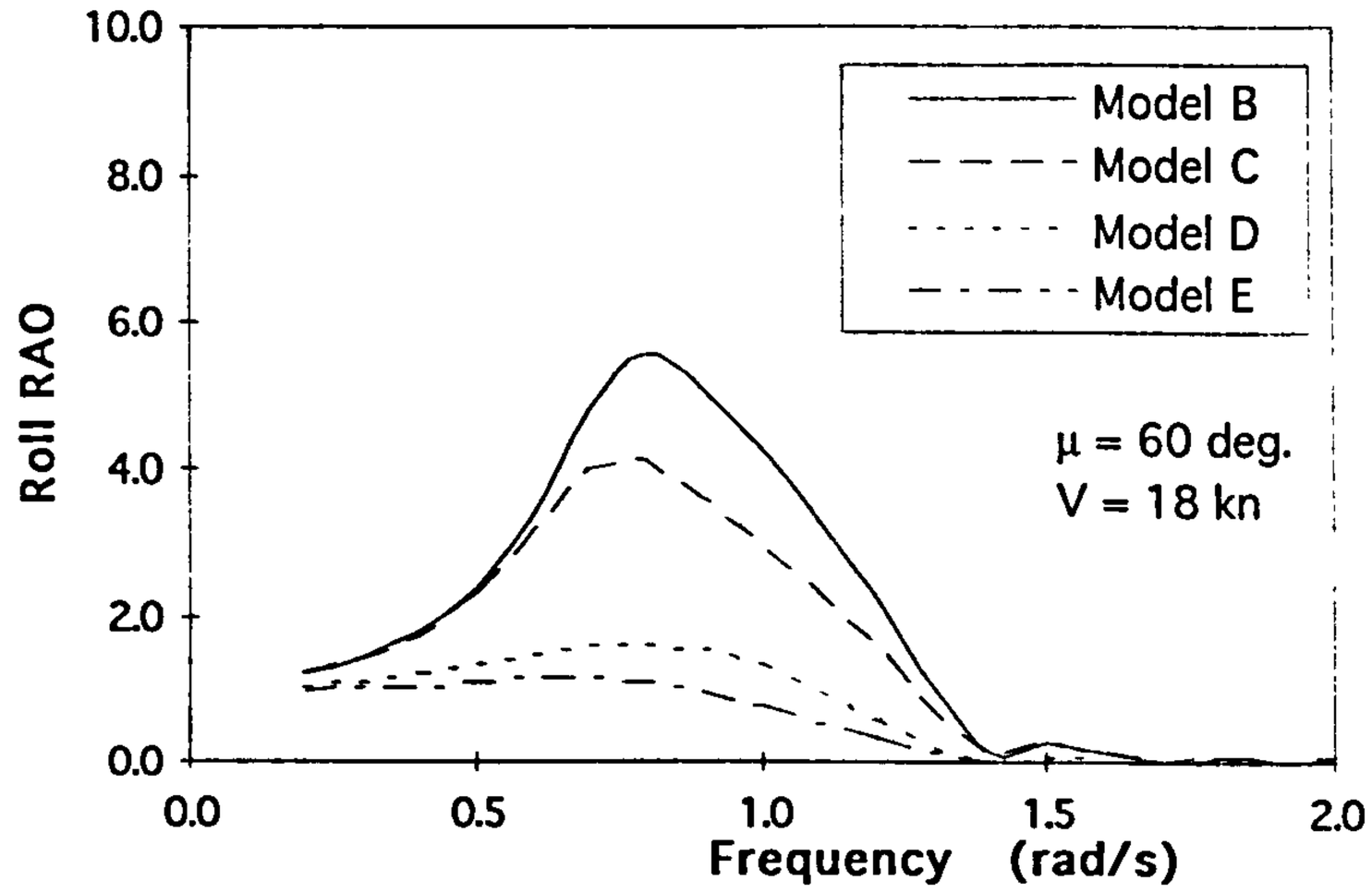

Figure 5.11 Roll predictions for the models in following quartering sea

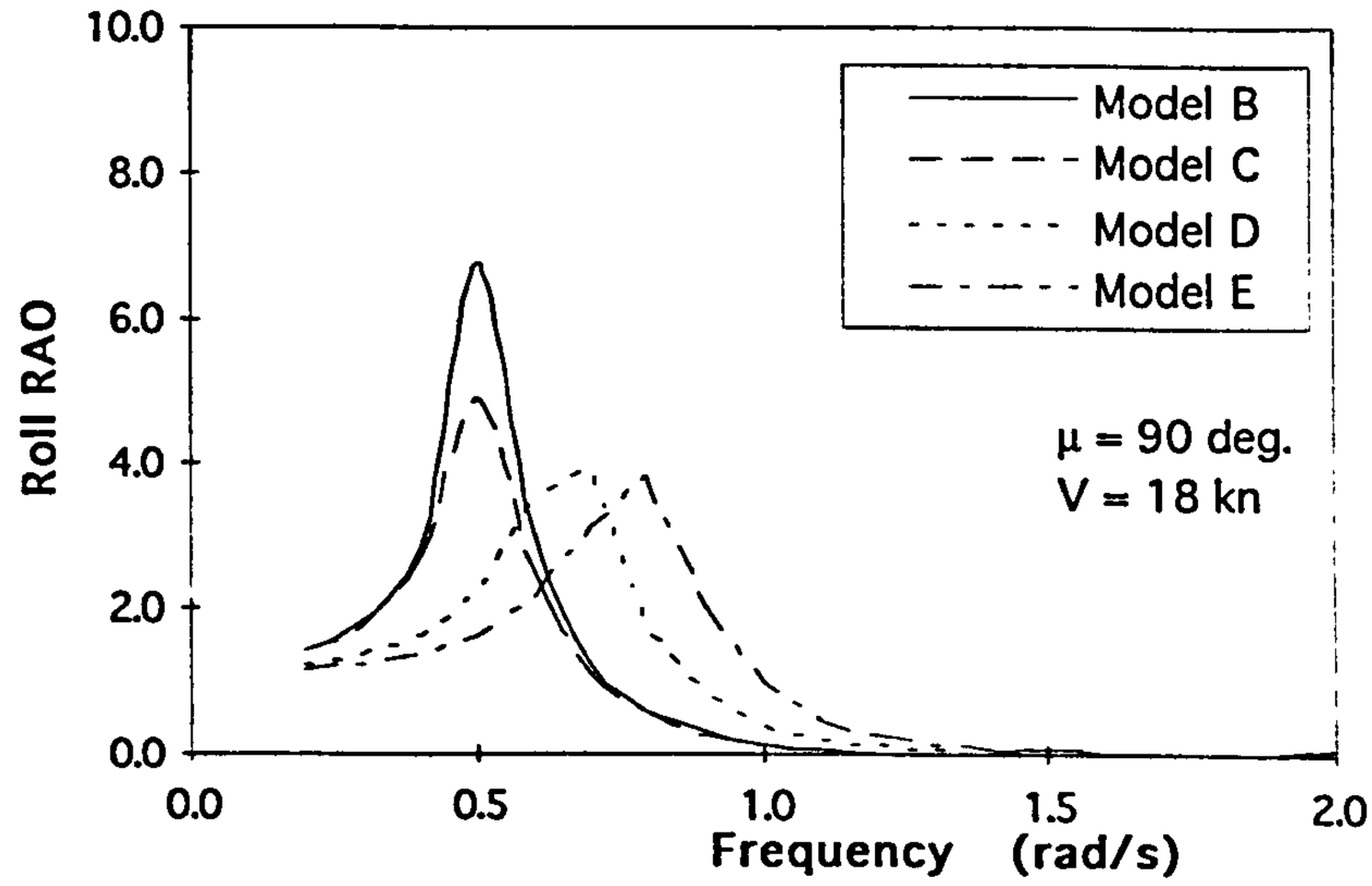

Figure 5.12 Roll motion predictions for the models in beam sea

5.5 Seakeeping Performance Compared with a Monohull

A comparison of seakeeping performance was performed between a trimaran ship and an typical frigate monohull form **(Zhang 1993)** using the GODDESS seakeeping program . The monohull form chosen was that of an existing frigate of 4000 tonnes displacement. The comparative hull dimensions and form parameters for these two ships is given in Table 5.1.

Table 5.1 Parameters of the two forms compared

Parameter	Monohull	Trimaran (centre hull)
Length (m) (L)	125	148
Beam (m) (B)	14.75	10.52
Draught (m) (T)	4.3	5.0
L/B	8.47	14.07
B/T	3.43	2.06
Total Displacement (t)	4000	4000

The comparison is made on the operability of the ships in waves against the four criteria listed in Table 4.2 (Chapter 4), namely, bow slamming, deck wetness, bridge deck acceleration, and flight deck acceleration. The plots for a range of sea states compare the limiting speeds for the two hull forms as shown in Figures 5.13 to 5.16. As would be expected, the much longer trimaran central hull maintains ship speed for longer at higher sea states than the conventional monohull. This is least marked for the deck wetness criterion (Figure 5.14) and most obviously in the flight deck acceleration case (Figure 5.16). The latter is accentuated by the far more favourable location of the flight deck in the trimaran design, close to the centre of pitch.

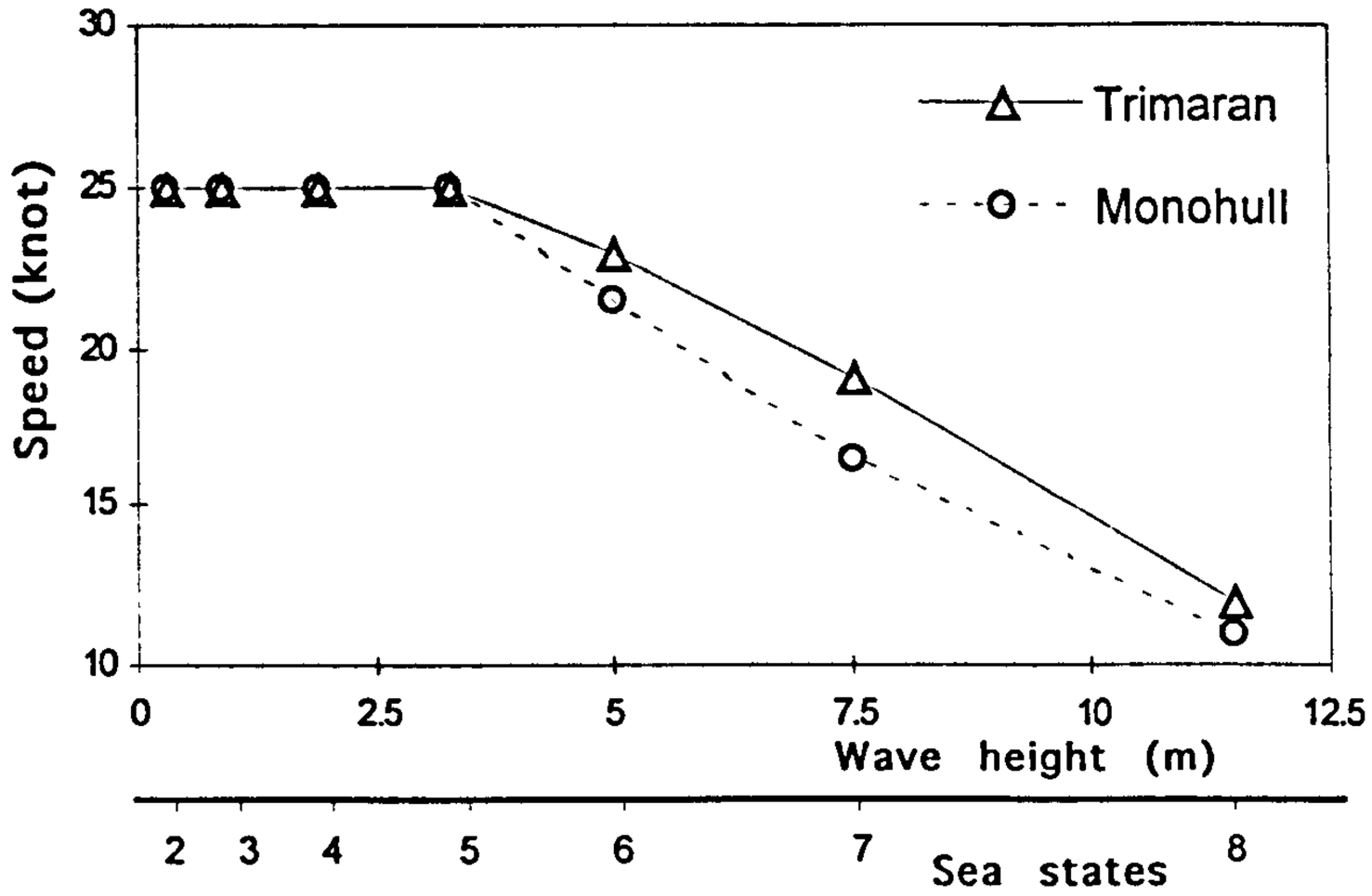

Figure 5.13 Speed reduction due to bow slamming

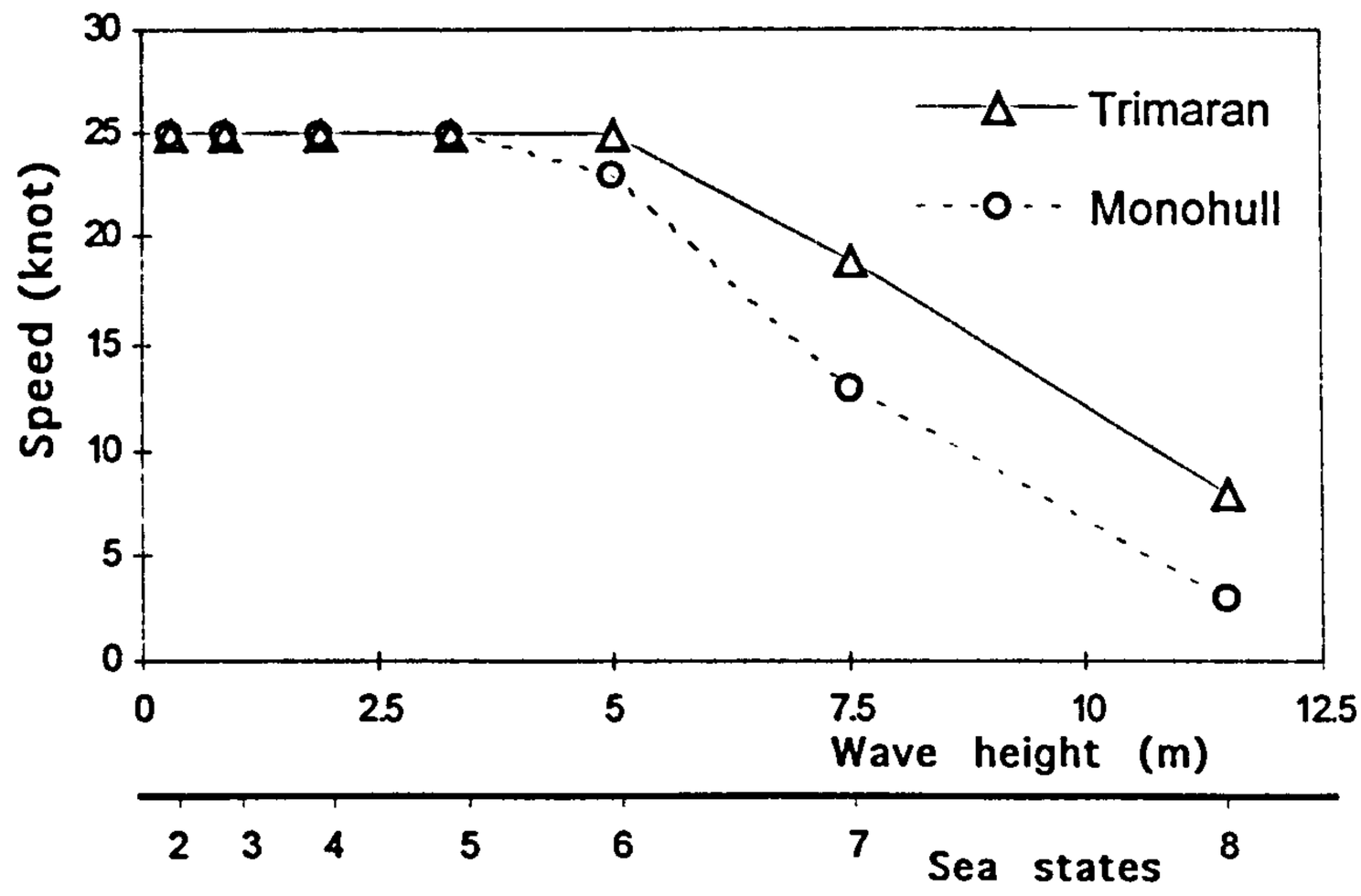

Figure 5.14 Speed reduction due to deck wetness

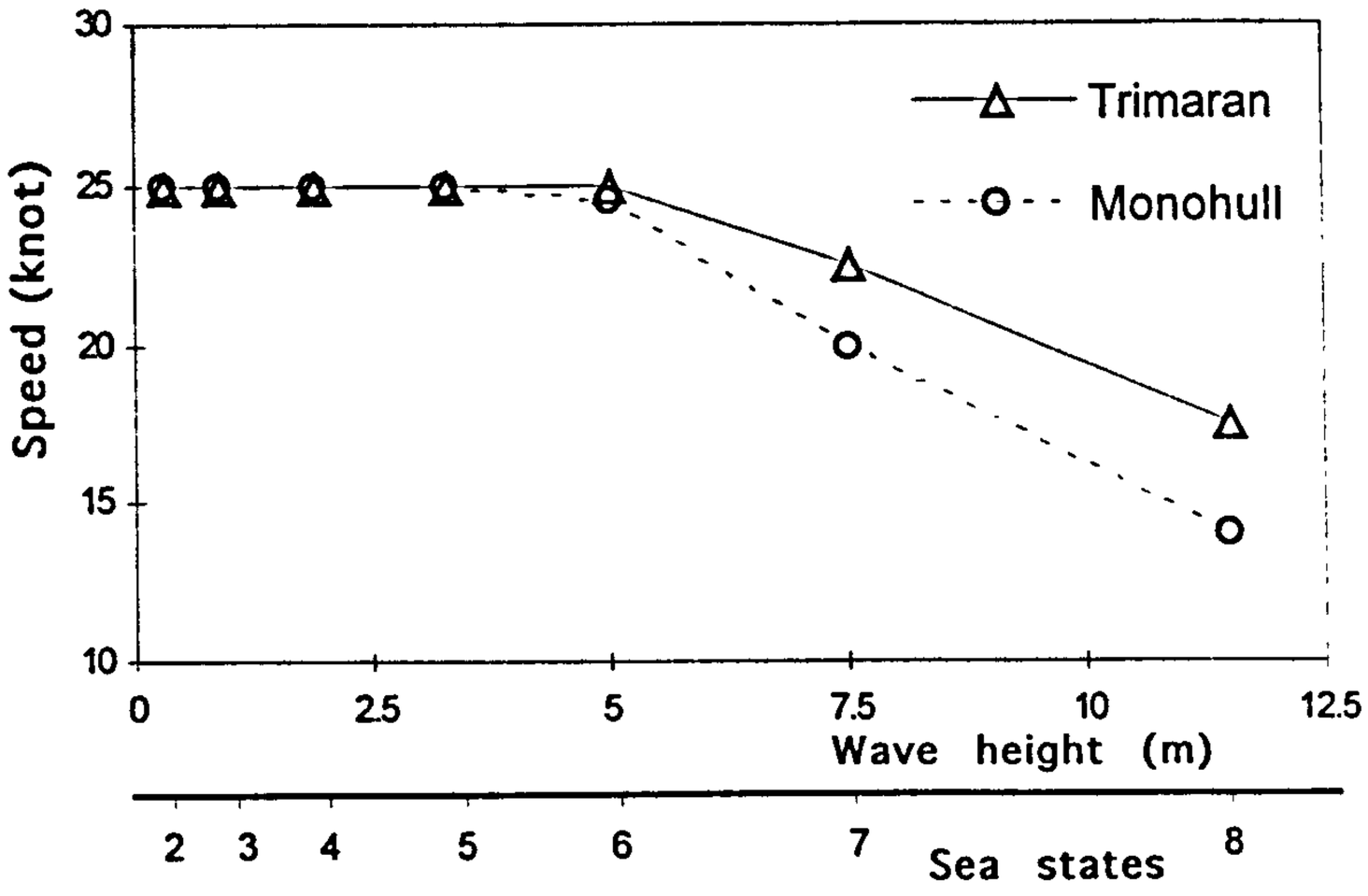

Figure 5.15 Speed reduction due to bridge deck acceleration

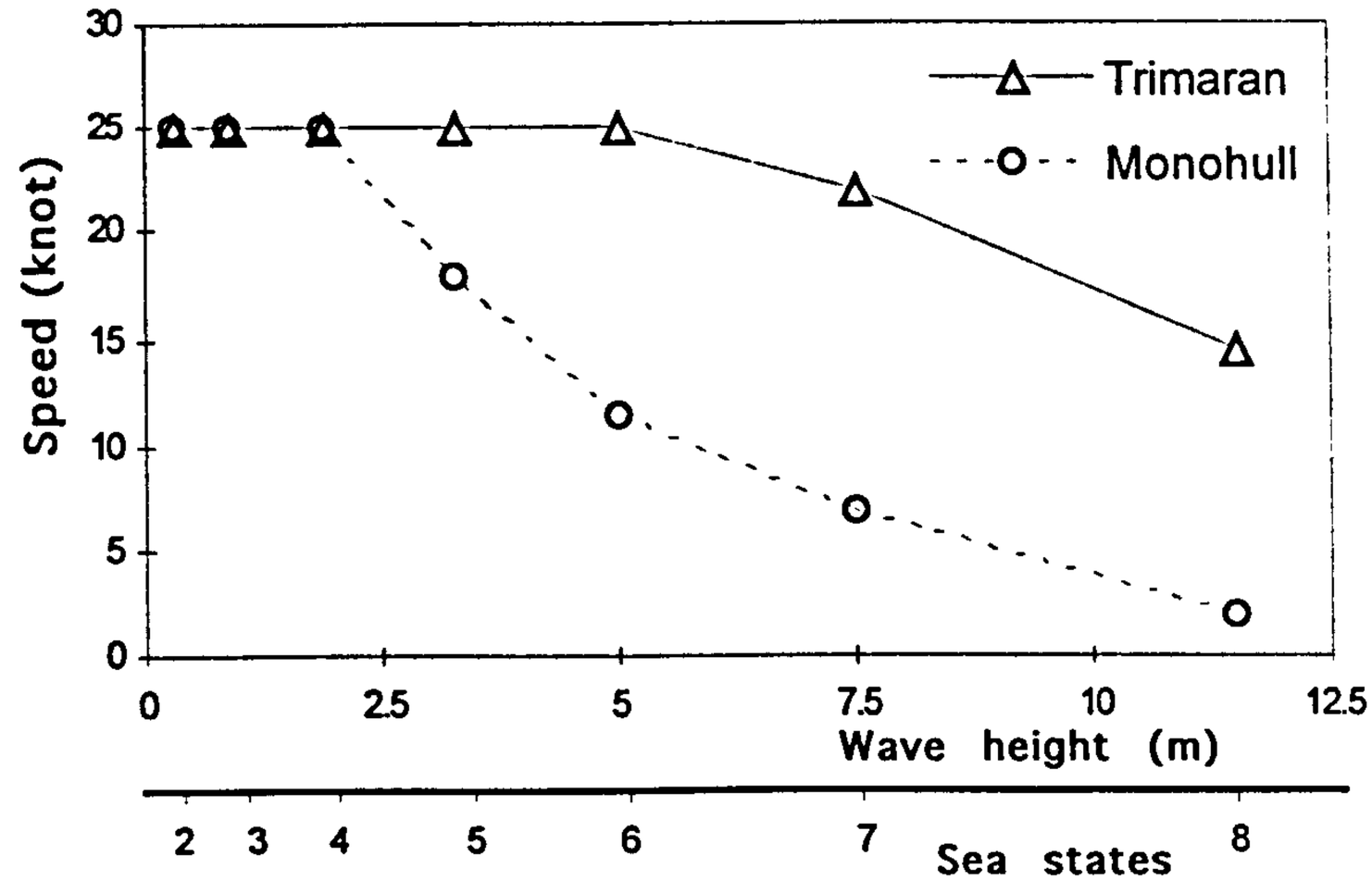

Figure 5.16 Speed reduction due to flight deck acceleration

5.6 Conclusions and Discussions on Seakeeping

The trimaran ship motion predictions with ship's forward speed using a computer program employing the three dimensional theory generally show good agreement when compared with experimental results, both for symmetric and asymmetric motions. It can be concluded that agreement is sufficient for the program to be used with some confidence to predict the motion of trimaran ships which have configurations similar to those of the models tested by DRA Haslar.

The effects of viscous roll damping and side hull flare need to be taken into account in the trimaran motion prediction. The viscous roll damping coefficients used for roll motion prediction in this chapter are derived from the results of free decay experiments. Nevertheless, a method for direct estimation of these coefficients applicable to trimaran ships needs to be developed for situations when free decay test data is unavailable. A method for such prediction is proposed in Chapter 6.

The comparison between a trimaran ship and an equivalent displacement monohull ship shows a generally superior seakeeping performance for the trimaran ship. It is also worth mentioning that, unlike the monohull, the trimaran concept allows the designer a wide range of choices on hull form variables to achieve a desirable seakeeping performance. The predominant parameters are seen to be the side hull displacement ratio, the waterplane areas of the centre hull and the side hulls, and the relative positions of the three hulls. Certainly, to comprehensively understand the effects of these variables on trimaran seakeeping performance requires more extensive investigations than those to date.

CHAPTER 6

ROLL DAMPING OF TRIMARAN SHIPS

6.1 Introduction and Aims

Roll damping estimation is an area, even for monohull ships, where adequate methods of prediction have yet to be developed. Thus special efforts are required to investigate the methodology for roll damping prediction and to analyse its effects on trimaran roll motions. This chapter describes the investigation **(Zhang 1996a)** into the two questions raised earlier (see Section 5.4.1) about the effects of viscous roll damping on the roll motion of the trimaran ship.

Previous studies have emphasised that viscous damping plays a very important role in the roll motion **(Schmitke 1978) (Lloyd 1989)**. In some cases the wave making damping is only a small fraction of the total roll damping. The viscous damping to be accounted for in the roll motion prediction includes that due to eddy shedding, skin friction and the appendage drag/lift forces.

Two types of approaches have been used in the trimaran roll damping analysis. The first approach is to estimate nonlinear roll damping coefficients from free decay experimental data using the energy loss method. The theory for this method is described in Section 6.2. Comparisons between the linear and nonlinear results are illustrated in Section 6.4. The simulation of the free decay curve using the nonlinear damping coefficients showed better results than those obtained with the linear coefficients at low forward speed.

The second approach is direct computation of the components of the viscous roll damping coefficients and is described in Section 6.5. The aim of this approach is to develop a method for the prediction of the roll damping of a trimaran ship with just its design data when no free decay data are available. The components of roll damping coefficients are computed theoretically with some empirical approximations.

In addition, the roll damping coefficients were separately calculated for the central hull and the side hulls to examine the contribution of the side hulls to roll damping. Some damping coefficients were also calculated for side hulls in different transverse positions and these are presented in Section 6.6

6.2 Estimation of Roll Damping Coefficients from Free Decay Data

6.2.1 Basic Theories and Mathematical Models

There are generally three types of mathematical models for extracting roll damping coefficients from free decay data: linear roll damping, linear plus quadratic damping, and linear plus cubic damping.

The uncoupled *linear* equation of the ship undergoing free rolling can be expressed as:-

$$A\ddot{\eta}_4 + B\dot{\eta}_4 + C\eta_4 = 0 \tag{6-1}$$

where A is the mass inertia of the ship, B is the roll damping coefficient, C is the hydrostatic coefficient, and η_4 is the rolling angle. A general solution to this ordinary linear differential equation is in the form of

$$\eta_4 = \eta_{40} e^{-kt} \cos(\omega t + \theta) \tag{6-2}$$

where η_{40} is the initial roll amplitude, k is the decay coefficient, ω is the rolling frequency, and θ is the phase angle. Using appropriate curve fitting techniques, these coefficients can be obtained by fitting equation (6-2) with the recorded free decay experiment data. The damping coefficient can then be calculated from the decay coefficient k, mass inertia A, and hydrostatic coefficient C.

The linear method has been routinely used for analysing free decay data as indicated by **Conolly (1969)** and **Lloyd (1989)**. The decay coefficients derived in this way for the trimaran model ships have been supplied by DRA Haslar **(DRA 1995)** as described in Section 4.5.2, and will not be further discussed here.

The *linear plus quadratic* roll damping coefficient has to be obtained by solving the following nonlinear roll motion equation:-

$$A\ddot{\eta}_4 + B_1\dot{\eta}_4 + B_2\dot{\eta}_4|\dot{\eta}_4| + C\eta_4 = 0 \tag{6-3}$$

where, B_1 is the linear damping coefficient and B_2 is a quadratic damping coefficient.

Similarly, the *linear plus cubic* roll damping coefficient can be obtained by solving the following nonlinear roll motion equation:

$$A\ddot{\eta}_4 + B_1\dot{\eta}_4 + B_3\dot{\eta}_4^3 + C\eta_4 = 0 \qquad (6\text{-}4)$$

where B_3 is the cubic roll damping coefficient.

Unlike the linear differential equation (6-1), these nonlinear equations (6-3)(6-4) can not be solved directly. A numerical method has to be adopted in deriving the damping coefficients.

For solving the nonlinear damping coefficients, **Dalzell (1978)** investigated the quadratic and cubic models by using the method of slowly varying parameters and a least squares technique to find an equation for the rate of decay curve as a function of the damping moment parameters. **Roberts (1982 & 1985)** investigated a general approach to the analysis of decay tests, including nonlinearities both for damping and restoring terms. He related the parameters of the roll damping moment, including the amplitude of rolling motion, to a loss function using a parametric identification procedure. A spline fitted to the peaks of the roll decay curve was used to obtain experimental estimates for the loss function. Because of the presence of the nonlinear restoring moment, this method can be used for free decay data resulting from very large initial roll amplitude.

Both methods require the use of just the peak values of the roll decay curve for fitting the roll damping moment, thus to get a reasonable accurate fitting the use of a large number of cycles of roll decay records is required. These long records are usually difficult to obtain, especially for multihull vessels. The roll damping of a trimaran ship is expected to be larger than an equivalent monohull ship due to the large span of the side hulls and any roll damping devices fitted on to the side hulls are further away from the roll centre of the ship, and so would make the roll amplitudes decay very rapidly. In addition, the roll decay experiments conducted for the trimaran model ships included cases with ship's forward speeds that made the decay data records even shorter, such that only two or three cycles of record could be obtained in some cases. The accuracy of the estimation would be significantly affected if only the peak values of these records could be used.

Mathisen & Price (1984) used a perturbation method to estimate roll damping coefficients from both free and forced rolling decay tests of a vessel. The method assumes that the nonlinear response is a small perturbation of the linear response which makes the method valid only for small nonlinearities.

Bass & Haddara (1988) introduced an energy method for estimating roll damping coefficients from decay data. It does not use the peak values of the free decay curve for deriving the rolling moment. Instead, it is based on the concept that the rate of change of the total energy of a ship undergoing free rolling equals the rate of energy dissipated by the damping and utilises the full range of the recorded decay curve. Such a method allows the analysis of very short decay records and can be used to estimate roll damping coefficients from decay data for ships with large roll damping and with forward speeds.

This energy method is used for the analysis of the free decay experiment data for the trimaran model ships as described in the following subsection. However, **Bass & Haddara (1988)** did not present any methods to eliminate the measured 'noise' in decay curves which is a vital part of the analysis as indicated by **Roberts (1985)**, particularly when the derivatives of the decay curves have to be used for energy calculations. A method of analysing free decay data to eliminate the 'noise' has been developed and is presented in subsection 6.2.3.

Of the two types of nonlinear forms, the quadratic and the cubic, only the quadratic has been considered in the thesis. **Mathisen et al. (1984)**, **Roberts (1985)**, and **Haddara et al. (1992)** all examined the difference between the linear plus quadratic and linear plus cubic approaches. The results showed that better or similar results can be obtained in the estimation of roll damping from free decay data using linear plus quadratic approach compared with that of the linear plus cubic approach. Therefore, the roll damping coefficients of the trimaran ship are analysed using the linear plus quadratic approach from the free decay data.

6.2.2 Energy Method

The method used in the estimation of the nonlinear roll damping coefficients is the Energy Method **(Haddara & Cumming 1992)**. The concept of this method is that the rate of change of the total energy in roll motion equals to the rate of energy dissipated by the roll damping. It is assumed that the ship is under uncoupled roll motion during the free decay experiments because the coupling terms between roll, sway and yaw can be assumed to be small **(Mathisen & Price 1985)**. However, it should be noted that in applying nonlinear roll damping coefficients to predict the ship motion in waves, the coupling terms due to sway and yaw have been added to the calculation using the wave diffraction method.

The uncoupled roll motion equation (6-3) of the ship in free decay tests can be written in another form as:-

$$\ddot{\eta}_4 + N(\dot{\eta}_4) + D(\eta_4) = 0 \tag{6-5}$$

where η_4 is the roll angle, $N(\dot{\eta}_4)$ is the damping moment per unit mass inertia, $D(\eta_4)$ is the restoring moment per unit mass inertia. To simplify the problem, the restoring moment here is considered as a linear term, assuming the rolling angle is moderate and hence the GZ curve can be taken as linear over the range. This assumption can be justified by examining the shape of the GZ curves of the trimaran ship.

Let $E(t)$ be the total energy of the ship per unit mass as:-

$$E(t) = \frac{1}{2}\dot{\eta}_4^2 + \int_0^t D(\eta_4)\dot{\eta}_4 dt \tag{6-6}$$

In the decay test, from time t_i to t_{i+1} , the loss of total ship energy per unit mass equals to the energy dissipated by the damping moment. Thus:-

$$E(t_{i+1}) - E(t_i) = -\int_{t_i}^{t_{i+1}} N(\dot{\eta}_4)\dot{\eta}_4 dt \tag{6-7}$$

The damping moment is defined in a form of linear plus quadratic terms as:-

$$N(\dot{\eta}_4) = B_1\dot{\eta}_4 + B_2\dot{\eta}_4|\dot{\eta}_4| \tag{6-8}$$

where B_1 is the linear damping coefficient, and B_2 is the quadratic damping coefficient.

After substituting Equation (6-8) into Equation (6-7), and letting

$$Q_i(t) = E(t_{i+1}) - E(t_i) \tag{6-9}$$

Equation (6-7) becomes:-

$$Q_i(t) = B_1\int_{t_i}^{t_{i+1}} \dot{\eta}_4^2 dt + B_2\int_{t_i}^{t_{i+1}} \dot{\eta}_4^2|\dot{\eta}_4|d \tag{6-10}$$

The left hand side of the equation $Q_i(t)$ represents rate of change of the total ship energy per unit mass from time point t_i to time point t_{i+1}. The right hand side of the equation represents the energy dissipated by the damping moment. $Q_i(t)$ and the integrals of the right hand side of the equation can be calculated using the rolling angle and the velocity derived from the free decay experiments.

6.2.3 Preparation of Free Decay Data

A vital task in the estimation of the energy function is to eliminate measurement error from recorded decay data. The error, normally regarded as a "noise" **(Roberts 1985)**, is superimposed on the true decay data. Though the noise is not very apparent when one looks at the decay curve of rolling angle, it results in a serious error in obtaining the derivative of the curve, i.e. the rolling velocity, as shown in Figures 6.1 and 6.2.

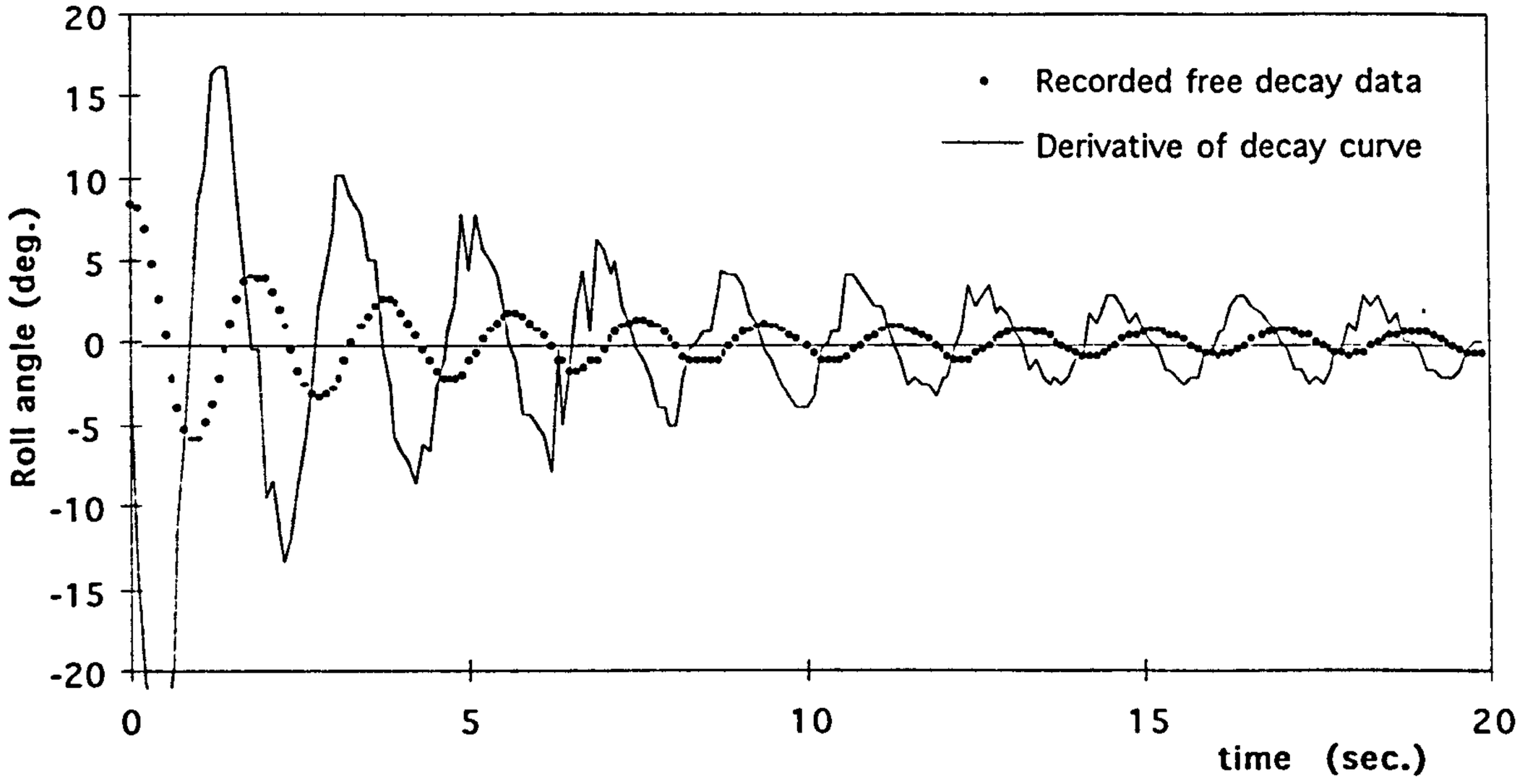

Figure 6.1 Recorded decay curve and its derivative for Model C, V=0kn

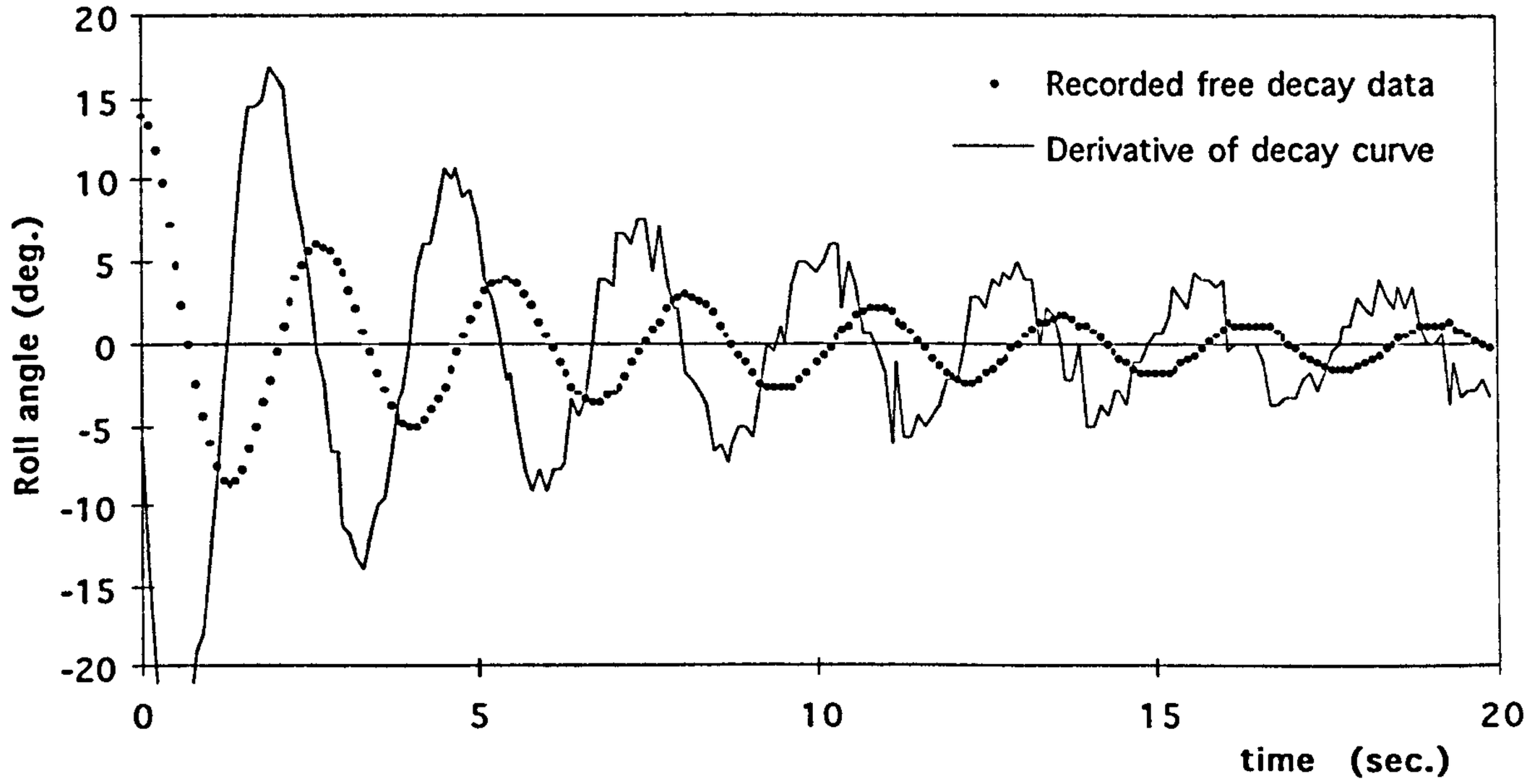

Figure 6.2 Recorded decay curve ant its derivative for Model D, V=0kn

Since the energy calculation is based on the derivative of the decay curve, such noise can produce a very significant scatter in the final estimate.

Many sophisticated methods exist for dealing with various sorts of test data noise, such as the "Parametric Identification" procedure used by **Roberts (1985)**. Roberts calculated the energy loss function from a cubic-spline fitted decay curve of the peak roll amplitude, and then varying a particular parameter form for the damping to obtain curve fitting between the chosen form and the first estimate of the function.

The method used in this work is a simplified approach. Firstly, a parameter form is chosen to represent the decay curve directly. Secondly, a least-squares fit between the chosen form and the recorded decay curve is performed to "identify" the true decay curve. Then the "identified" decay curve can be used to estimate the energy functions. It is believed that the advantage of this method, apart from the simplicity, is that the treated decay curve and its derivative can be visually checked directly with the original recorded decay data with some degree of confidence. More importantly, the resultant true decay data is not only for the peak values but for the complete free decay curve.

The first task is to find a proper parameter form which would not eliminate the nonlinearity of the decay curve. If we compare equation(6-2), solution of the linear differential equation (6-1), it basically contains two terms, a harmonic rolling angle term $\eta_{40}\cos(\omega t+\theta)$ and a decay term e^{-kt}. To fit the decay curve and retain the nonlinearity, terms involving the rolling velocity have to be added. Several forms were tried and finally, assuming that in the decay test the ship rolls with a constant frequency, the following form was found to fit the roll decay curves very closely:-

$$\tilde{\eta}_4(t)=a_1e^{-k_1t}\cos(\omega t+\theta_1)+a_2e^{-k_2t}\sin(\omega t+\theta_2) \tag{6-11}$$

where a_1, a_2, k_1, k_2, ω, θ_1, *and* θ_2 are seven unknown parameters, and $\tilde{\eta}_4(t)$ represents the fitted true roll decay curve. A least-squares curve fit method is used to evaluate these parameters, and to minimise the error function between the estimated true decay curve and the recorded decay curve:-

$$e=\sum_{i=1}^{N}[\eta_4(t_i)-\tilde{\eta}_4(t_i)]^2 \tag{6-12}$$

where, e is the error function, N denotes the number of rolling cycles in the measured decay record, $\eta_4(t_i)$ is the recorded decay curve, and $\tilde{\eta}_4(t_i)$ is the estimated true decay curve.

A computer program was written in **MATLAB (1992)** to carry out the calculation with a standard least-squares function used in the computation. Figures 6.3 to 6.5 show the fitted roll decay curves and their derivatives compared with the recorded decay data for one of the models. Good agreement between the fitted decay curves and the experiment data was obtained. Table 6.1 gives a listing of the resultant parameters for all the fitted free decay curves.

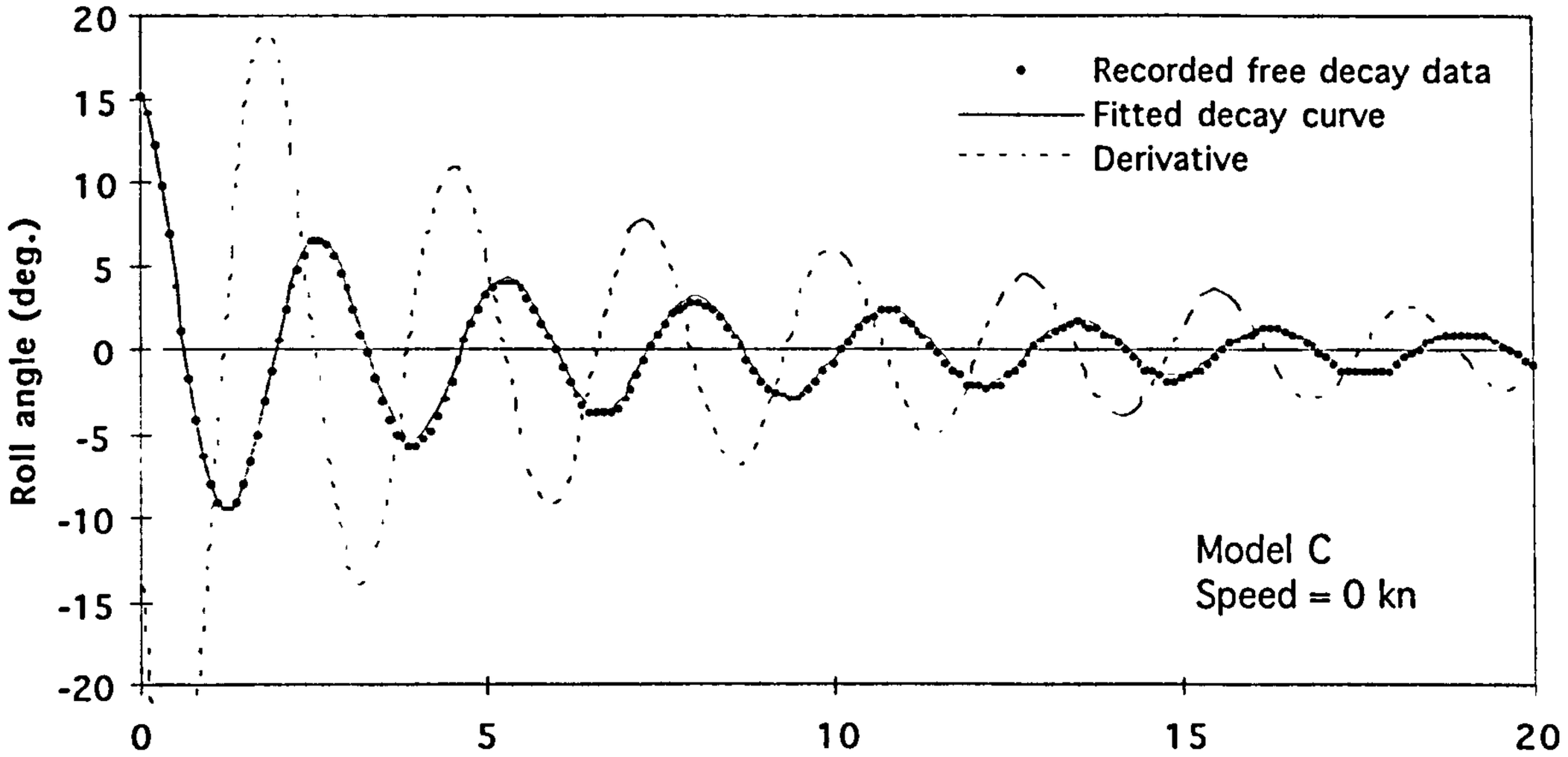

Figure 6.3 Identified true decay curves for Model C at V=0kn

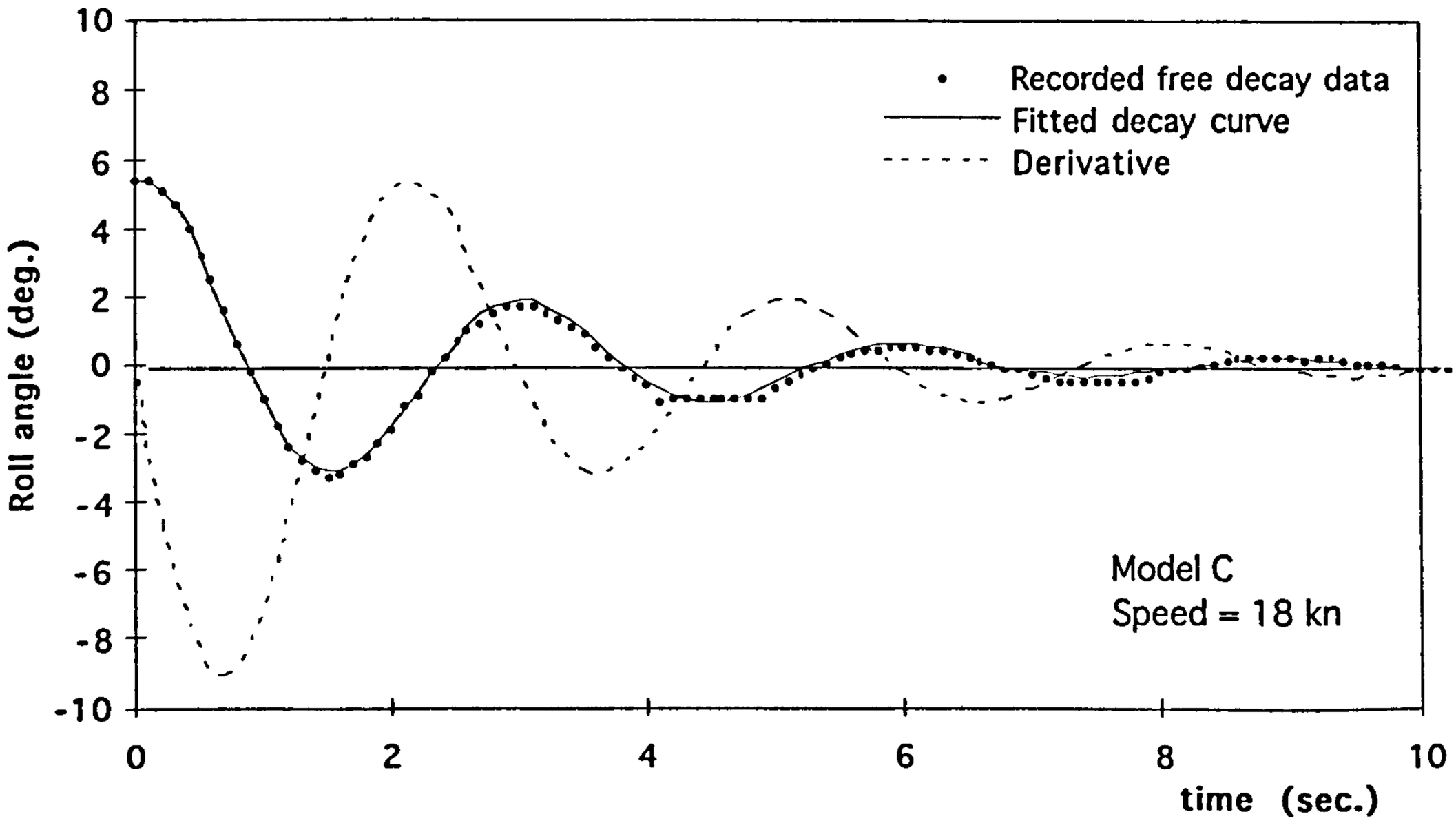

Figure 6.4 Identified true decay curves for Model C at V=18kn

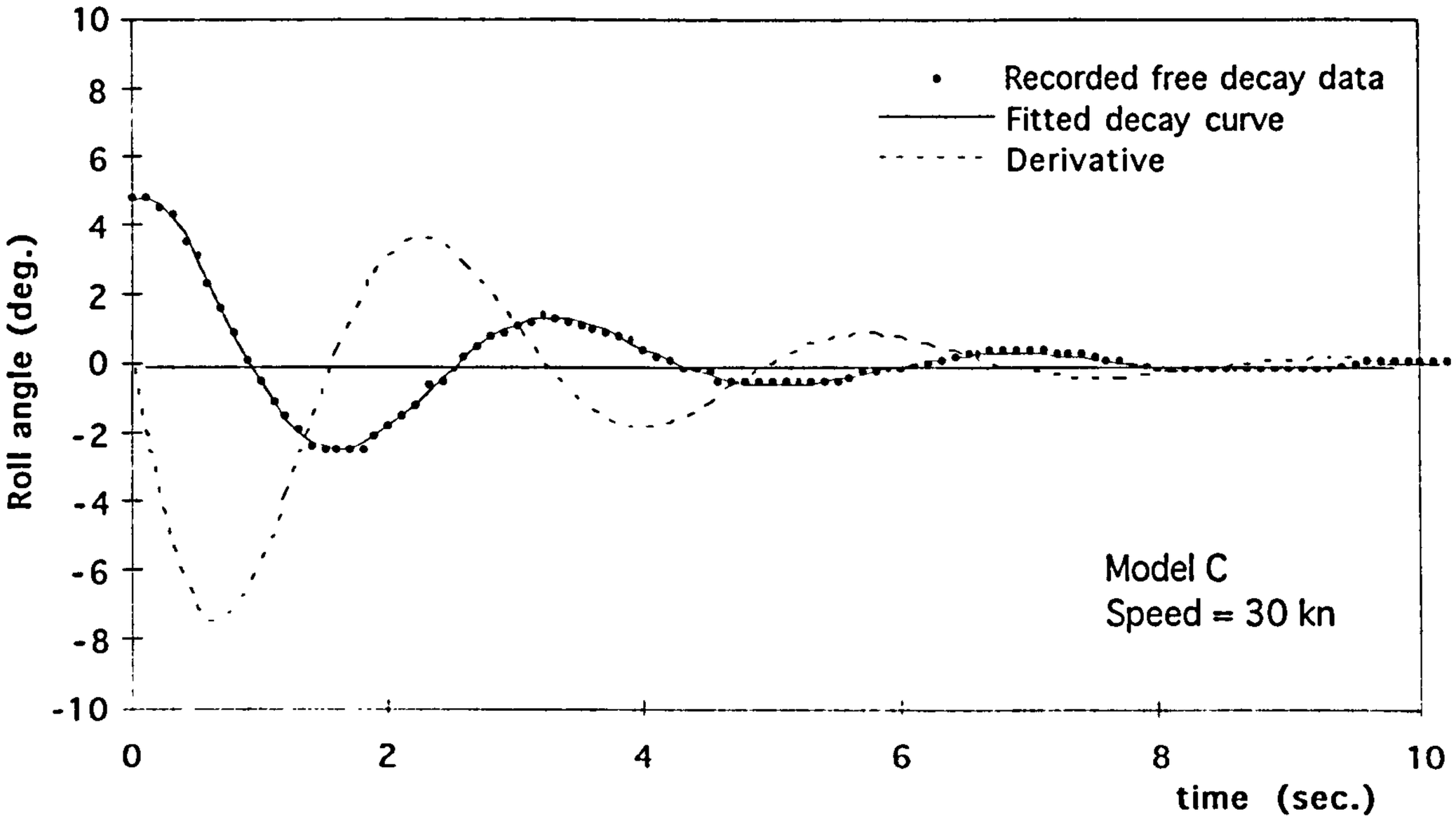

Figure 6.5 Identified true decay curves for Model C at V=30kn

Table 6.1 Coefficients for The Fitted Free Decay Curves

Model	*Speed (knot)*	a_1	k_1	$\|\omega\|$	θ_1	a_2	k_2	θ_2
A	0	8.07	0.047	2.297	0.783	8.370	0.201	0.651
A	18	2.735	1.127	2.118	1.131	5.815	0.273	1.600
A	30	7.194	0.663	1.940	0.458	0.209	0.664	-0.887
B	0	12.07	0.074	2.343	1.123	-18.559	0.268	-2.382
B	18	20.20	0.341	2.036	1.263	19.466	0.427	0.026
B	30	3.379	0.375	2.072	0.283	-3.289	0.375	-1.402
C	0	6.994	0.097	2.290	0.415	9.191	0.680	1.364
C	18	0.995	11.659	2.131	-1.473	5.510	0.356	1.286
C	30	5.366	0.404	1.735	-0.512	-4.693	0.990	0.002
D	0	5.715	0.619	3.320	-0.271	-2.808	0.088	-1.496
D	18	1.852	3.043	3.290	-1.331	-3.831	0.454	-1.429
D	30	16.189	0.733	2.959	-1.606	-16.867	0.639	-0.253
E	0	2.410	0.980	3.867	-0.523	-5.359	0.230	-1.513
E	18	7.811	0.696	4.038	-3.451	-0.113	0.596	-1.787
E	30	5.232	0.502	3.784	-0.859	-3.644	0.502	-0.212

6.2.4 Computation and Verification

Equation (6-10) can not be solved directly because there are two unknowns in one equation. It can be rewritten as:-

$$Q_i(t) = B_1 u_{i1} + B_2 u_{i2} \tag{6-13}$$

where

$$u_{i1} = \int_{t_i}^{t_{i+1}} \dot{\eta}_4^2 dt \quad and \quad u_{i2} = \int_{t_i}^{t_{i+1}} \dot{\eta}_4^2 |\dot{\eta}_4| dt \tag{6-14}$$

and a least squares method can used for the calculation of values of the damping coefficients B_1 and B_2.

Figures 6.6 to 6.8 show the calculated rates of change of the total ship energy $Q_i(t)$ and the energy dissipated by the damping moment $B_1 u_{i1} + B_2 u_{i2}$ for all the models at various speeds. Table 6.2 gives a listing of the calculated roll damping coefficients for all the model ships.

Now, it is necessary to use the experimental data to verify the accuracy of the estimation. The procedure of verification is a reversed sequence to the way the coefficients were estimated. Once damping coefficients B_1 and B_2 have been calculated, Equation (6-3) becomes a nonlinear ordinary differential equation with known constant coefficients. A Runge-Kutta numerical integration, as used by **Mathisen & Price(1984)**, has been employed to solve the equation numerically to simulate the roll motion of the ship in the decay tests.

A computer program for this simulation was written in **MATHCAD (1995)**. Firstly, an initial value for roll angle η_4 and its derivative had to be defined as a vector. Then another vector was defined containing the functions of the first order and the second order derivatives of the expression. The differential equation can then be solved numerically starting with the initial values at the specified intervals. Thus the roll decay curve is simulated. The detail of the Runge-Kutta method will not be discussed further since a standard function from MATHCAD was used in the calculation. Figures 6.9 to 6.13 display the simulated decay curves using the estimated roll damping coefficients which show very good agreement with the recorded decay curve. This gives confidence to use the estimated nonlinear roll damping coefficients in roll motion predictions.

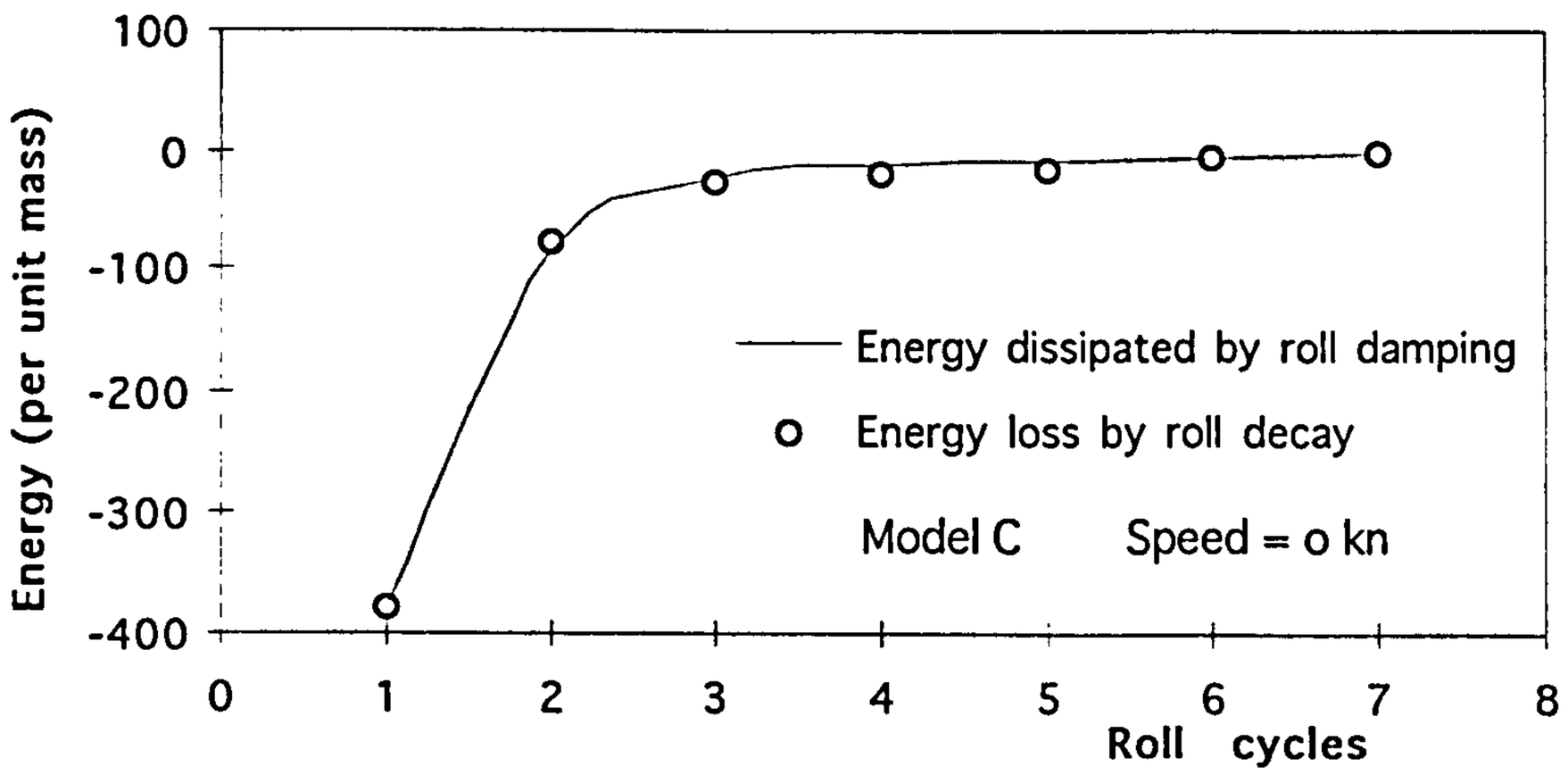

Figure 6.6 Energy dissipation for Model C at V=0kn

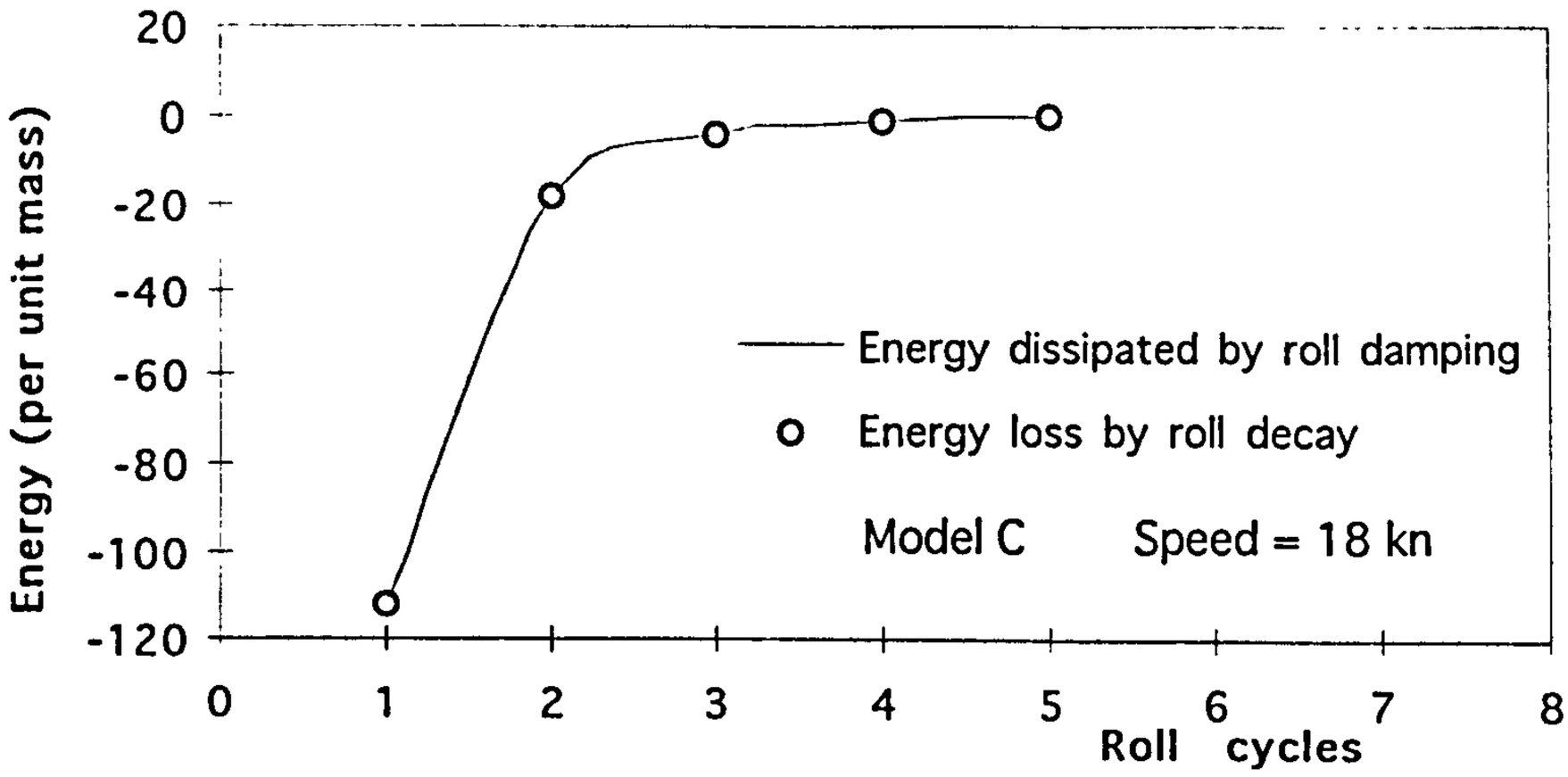

Figure 6.7 Energy dissipation for Model C at V=18kn

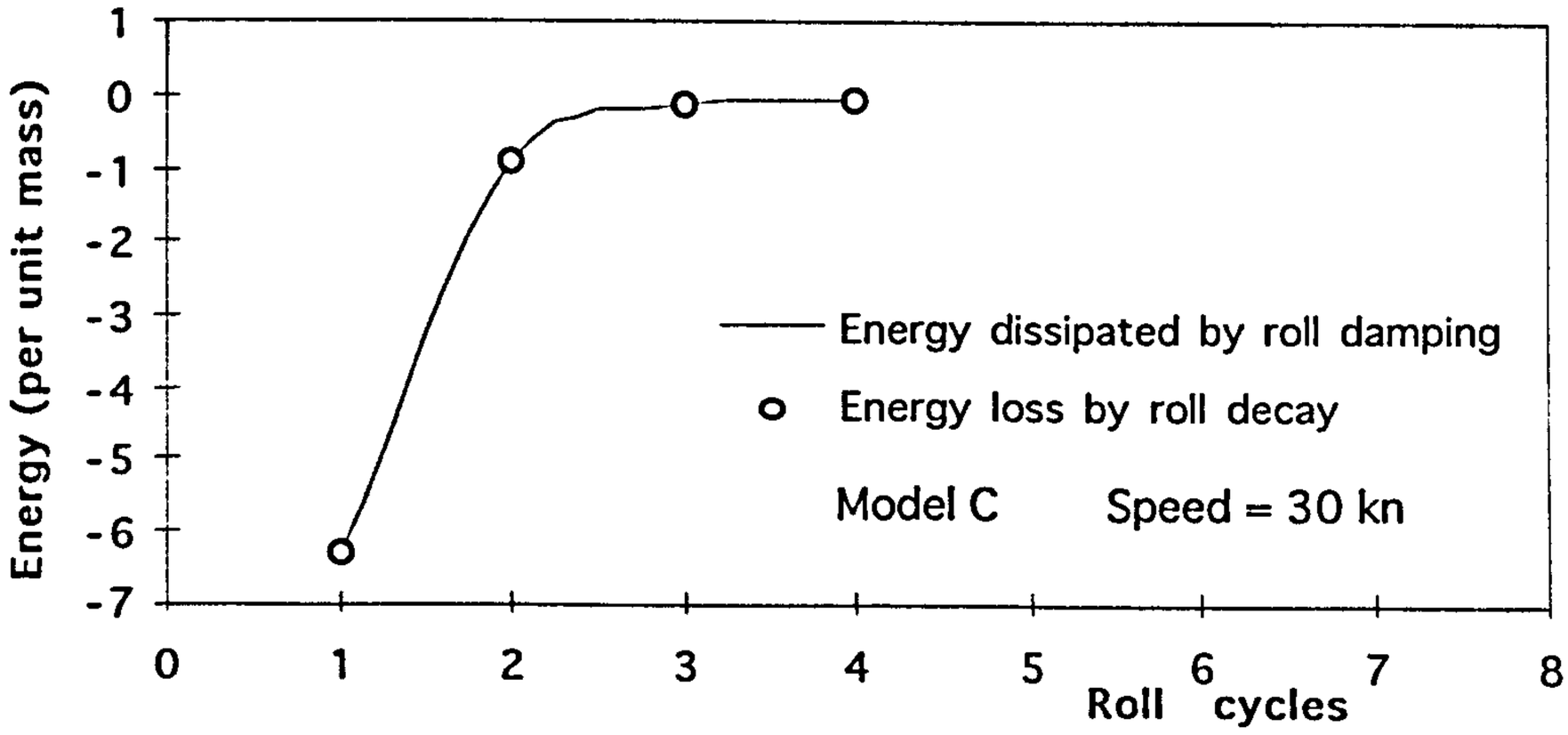

Figure 6.8 Energy dissipation for Model C at V=30kn

Table 6.2 Estimated Roll Damping Coefficients

Model	Speed (knot)	B_1	B_2
A	0	0.011	0.013
	18	0.600	0.020
	30	1.430	0.000
B	0	0.023	0.015
	18	0.512	0.010
	30	0.681	0.000
C	0	0.056	0.036
	18	0.710	0.011
	30	1.010	0.000
D	0	0.221	0.042
	18	0.890	0.008
	30	0.868	0.000
E	0	0.381	0.026
	18	0.910	0.000
	30	1.236	0.000

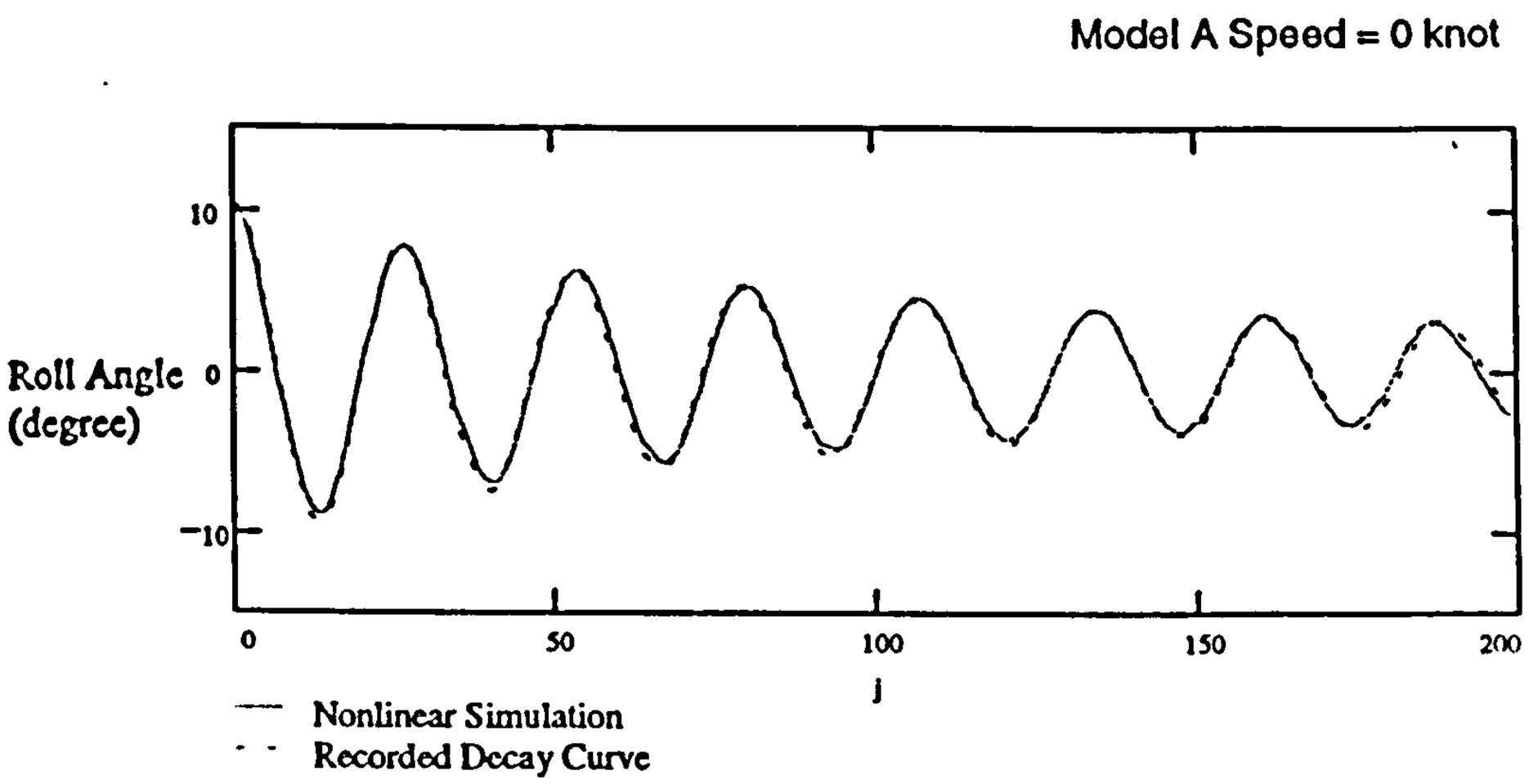

Figure 6.9 Nonlinear simulation of free decay curve for Model A

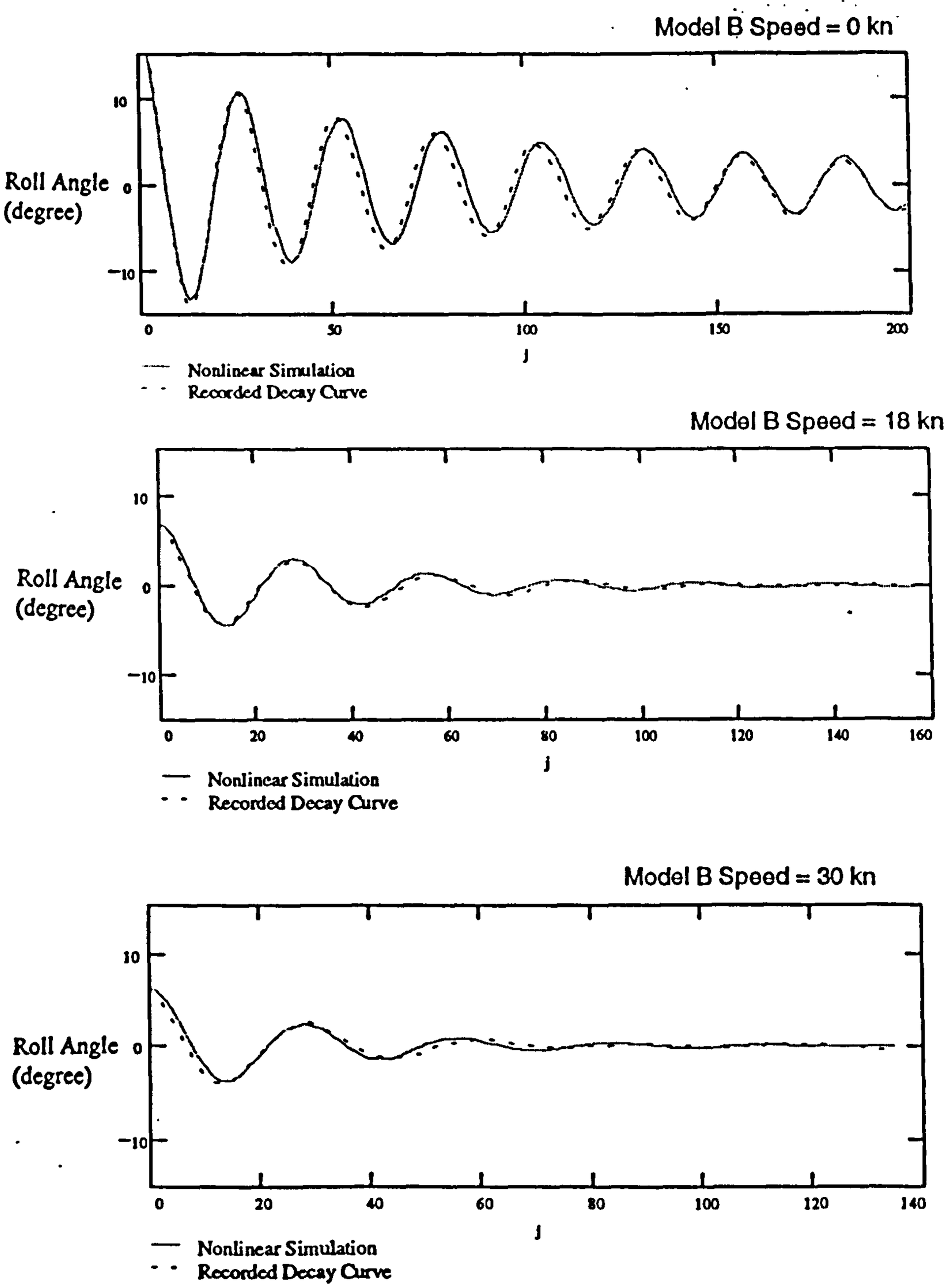

Figure 6.10 Nonlinear simulation of free decay curve for Model B

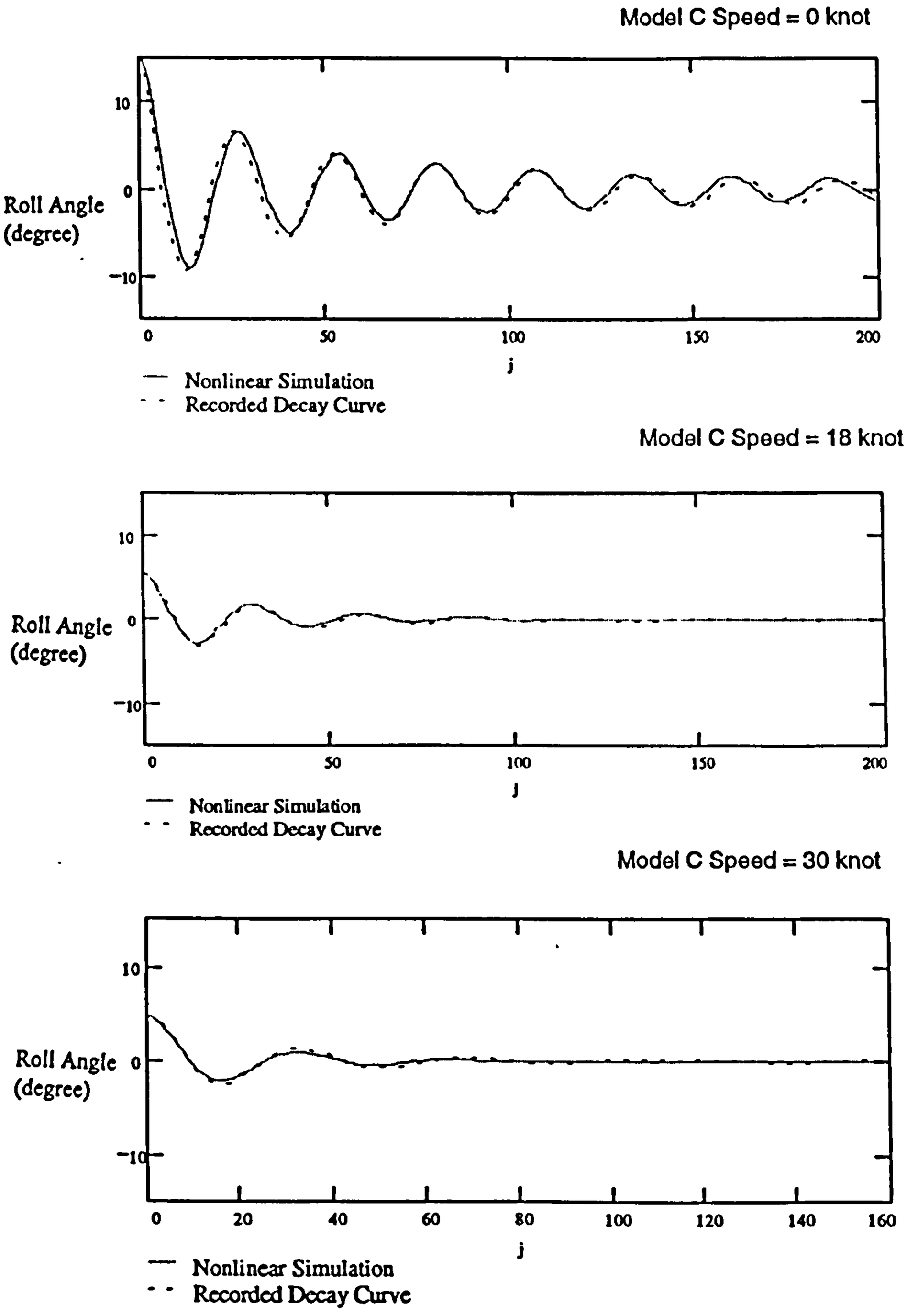

Figure 6.11 Nonlinear simulation of free decay curve for Model C

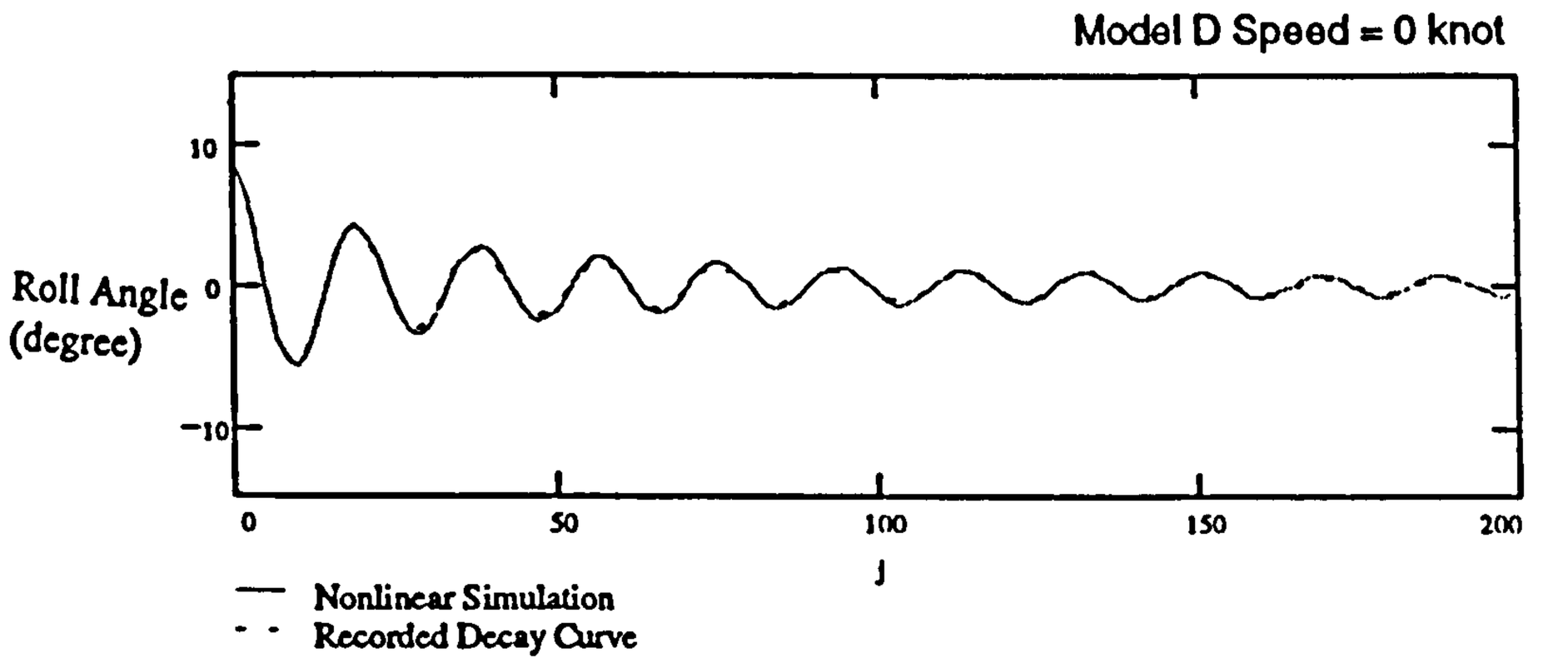

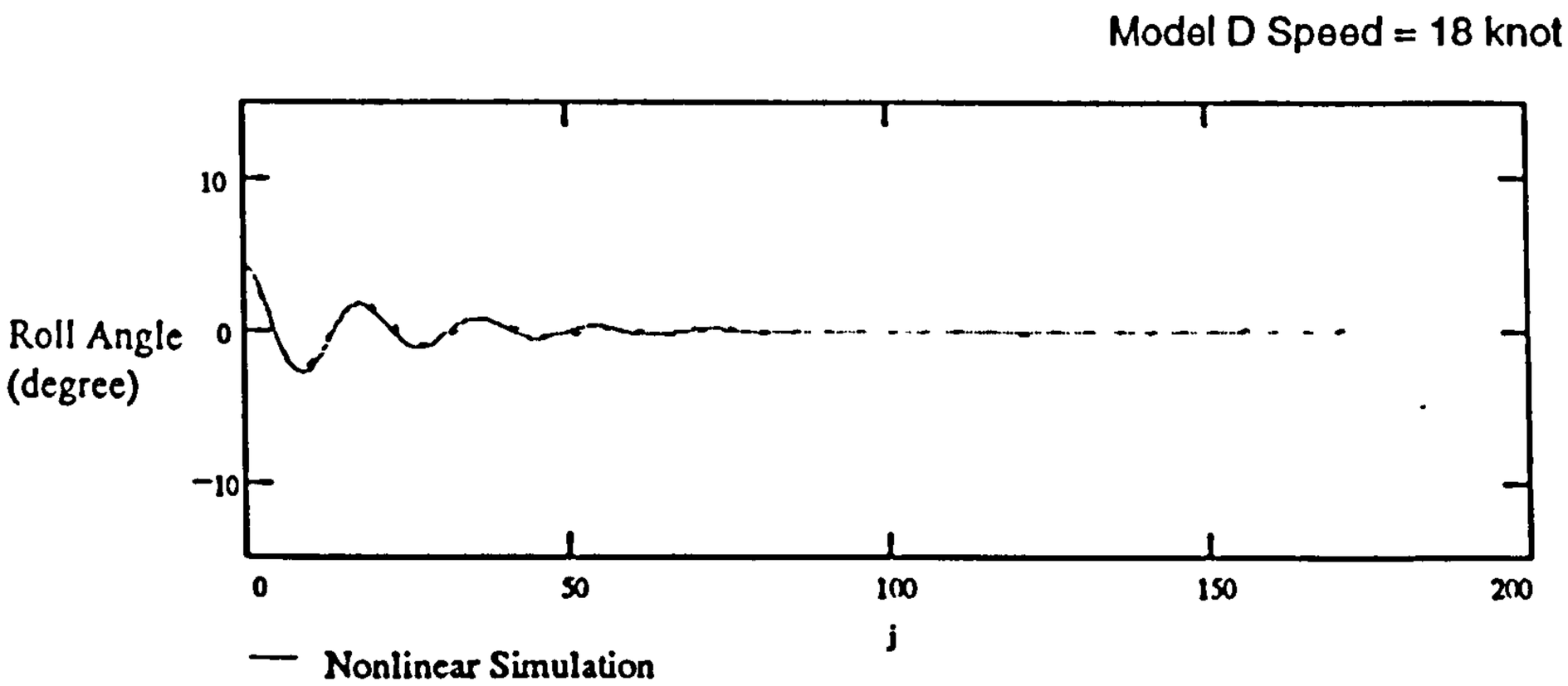

Figure 6.12 Nonlinear simulation of free decay curve for Model D

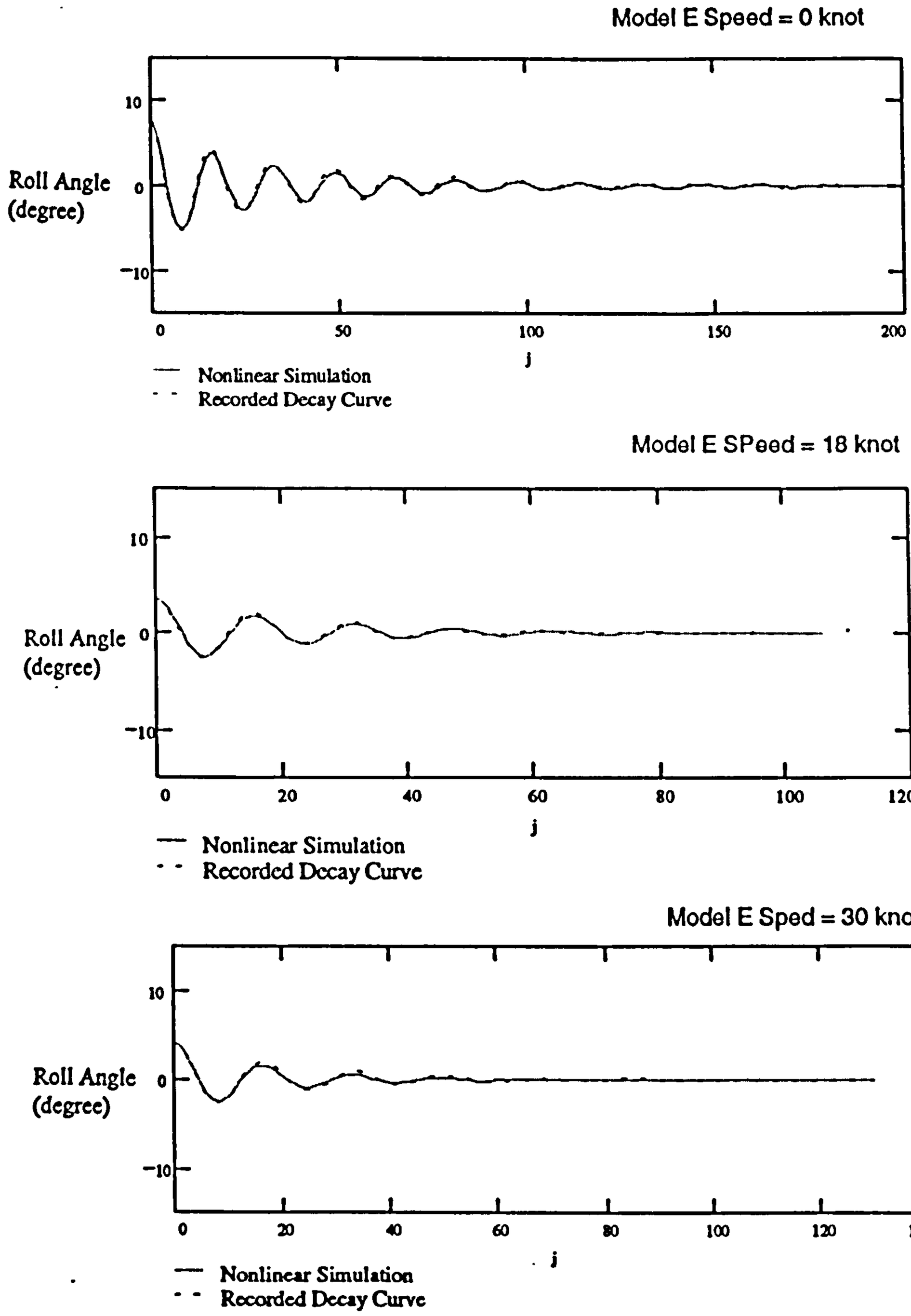

Figure 6.13 Nonlinear simulation of free decay curve for Model E

6.3 Method of Using Nonlinear Damping Coefficients for Roll Motion Predictions

The nonlinear roll damping coefficients as described above contain both the wavemaking damping and the viscous damping. If the nonlinear damping effect is included in the motion equation (5-22) to predict motions for the trimaran ship, the roll damping coefficient B_{44} will become:-

$$B_{44} = B_1 + B_2|\dot{\eta}_4| \tag{6-15}$$

and equation (5-22) will become a nonlinear equation, thus making the equation very difficult to solve. A method is therefore required to incorporate the nonlinear damping term into the linear motion equation to make it possible to be solved.

Lloyd (1989) showed that the nonlinear viscous damping moment terms could be treated using an equivalent linearisation concept. It was based on the assumption that an equivalent linear damping coefficient could be chosen so that the calculated energy dissipated by this term in the equation of motion is the same as that which is actually dissipated by the nonlinear effects. This allows continued use of the linear equation of motion including the effects of nonlinear damping coefficients.

If the rolling motion is given by

$$\eta_4 = \eta_{40}\sin(\omega t) \tag{6-16}$$

the work done by linear roll damping in one roll cycle will be the integral of the moment times the angular distance moved as **(Lloyd 1989)**:-

$$\begin{aligned} E &= 4\int_0^{\eta_{40}} B_{44}\dot{\eta}_4 dx \\ &= 4\omega^2 B_{44}\eta_{40}^2\int_0^{\pi/2\omega}\cos^2(\omega t)dt \\ &= \pi\omega B_{44}\eta_{40}^2 \end{aligned} \tag{6-17}$$

The equivalent linearised roll damping coefficient is therefore related to the dissipated energy by:-

$$B_{44} = \frac{E}{\pi\omega\eta_{40}^2} \tag{6-18}$$

Therefore, for nonlinear the roll damping moment, the work done by the damping moments $B_1\dot{\eta}_4$ and $B_2\dot{\eta}_4|\dot{\eta}_4|$ can be given as:-

$$\begin{aligned} E &= 4\int_0^{\eta_{40}} (B_1\dot{\eta}_4 + B_2\dot{\eta}_4|\dot{\eta}_4|)dx \\ &= \omega\pi B_1\eta_{40}^2 + \frac{8}{3}\omega^2 B_2\eta_{40}^3 \end{aligned} \tag{6-19}$$

Substitute Equation (6-19) into Equation (6-18), the equivalent roll damping coefficient can be expressed as:-

$$B_{44(eq)} = B_1 + \frac{8}{3\pi}B_2\eta_{40}\omega \tag{6-20}$$

It should be noticed that the equivalent roll damping coefficient contains a term of roll amplitude η_{40} as shown in Equation (6-20). In the computer program an initial rolling angle is assumed for the calculation of the equivalent B_{44} term. When the rolling angle η_{40} has been calculated, the new value of η_{40} is used to recalculate a new B_{44} term for the next loop of the rolling angle calculation. The process is repeatedly carried out until a satisfactory agreement between the current η_{40} and the previous η_{40} is achieved, $1.0\text{x}10^{-3}$ of the roll amplitude is set in the program as an acceptable agreement.

6.4 Effects of Nonlinear Roll Damping

It is commonly acknowledged that better roll motion predictions can be obtained if nonlinear roll damping coefficients are included in the calculation instead of just using linear roll damping coefficients **(Robert 1982) (Lloyd 1989)**. However, previous studies were normally for roll predictions of the monohull ships whereas the trimaran displacement ship is a new type of hull form concept. The contribution of nonlinear roll damping to roll motions was one of the unknown aspects about the trimaran ship. In order to get a better understanding of the trimaran motion characteristics it is necessary to find out the effects of nonlinear roll damping on the predictions of roll motions. This section discusses the preliminary results of the nonlinear roll damping coefficient estimations and their application to motion predictions compared with the results of the linear-only method.

6.4.1 Relationship with Ship's Forward Speeds

Having developed and verified the method of estimating the nonlinear roll damping coefficients, as described in the previous sections, the roll damping coefficients for all the five model ship configurations were estimated from the free decay data at various speeds as shown in Table 6-2.

It was found that the significance of the nonlinear damping coefficients depends very much on the ship's forward speed. At zero forward speed, the nonlinear roll damping coefficient B shows significant values for each of the models compared with the linear term B_1. As the speed increases, the value of the nonlinear roll damping coefficient decreases while the linear term increases. Figure 6.14 shows the ratio between nonlinear and linear damping coefficients with speed for Model C. At zero forward speed, the ratio of nonlinear and linear roll damping coefficients is about 0.6, and it quickly reduces to zero at as the speed approaches 30 knots.

Bearing in mind that the nonlinear roll damping moment is proportional to the square of the roll angular velocity as shown in Equation (6-3), the results suggest that the dominant roll damping coefficient for trimaran ship at low speed is the nonlinear roll damping. The results also suggest that the linear roll damping become dominant at higher speeds. In other words the roll damping of the trimaran ship at medium or high speeds can be simulated using just the linear damping coefficients. This may be explained as: (a) when the ship's speed increases the roll damping produced by lifting surfaces increases and gradually become the dominant damping force when the ship reaches medium speeds; (b) the roll damping moment due to the forces on the lifting surfaces is actually a linear damping moment as shown in Section 6.5.3 (equation 6-40).

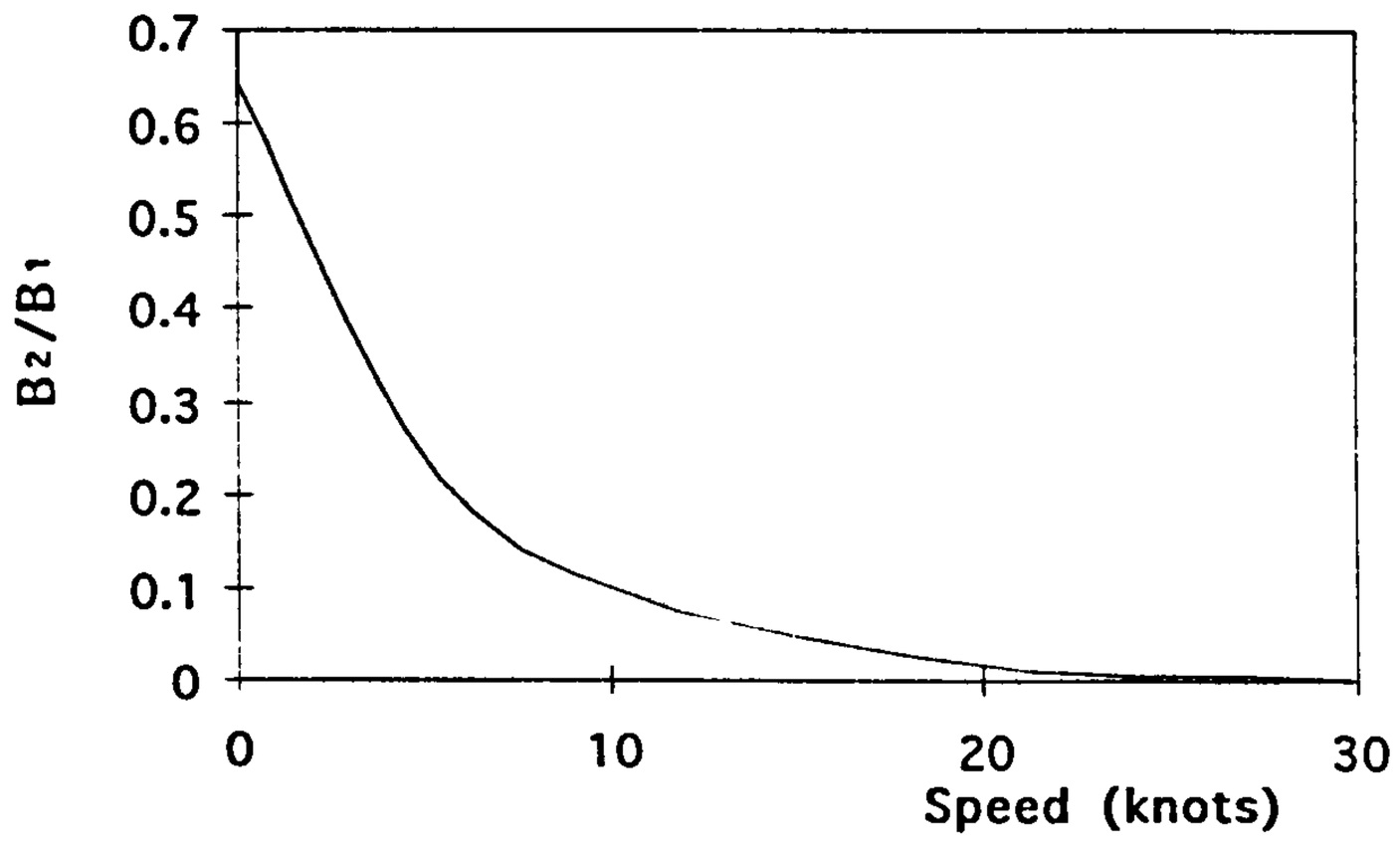

Figure 6.14 Ratio of nonlinear to linear roll damping coefficients

6.4.2 Roll Free Decay Simulation

Since the effects of the nonlinear roll damping coefficients on the roll motion at high ship speeds are very small as discussed above, the comparisons between the roll decay simulation using linear and nonlinear methods were only made for the low speed cases. As none of the models were tested at a speed below 18 knots, it was only possible to compare the results of the free decay simulations by the two methods at zero forward speed.

Figures 6.15 and 6.16 show results of the nonlinear simulation comparing with the linear fitted free decay curves. The linear fitted free decay curves are the fitted data provided by DRA Haslar using Equation (6-2). The nonlinear free decay curves are simulated using the linear plus quadratic damping coefficients derived in this chapter. The results show improvement in the decay simulations, particularly at the initial rolling angles. This suggests that the nonlinear effects are very important at large rolling amplitudes.

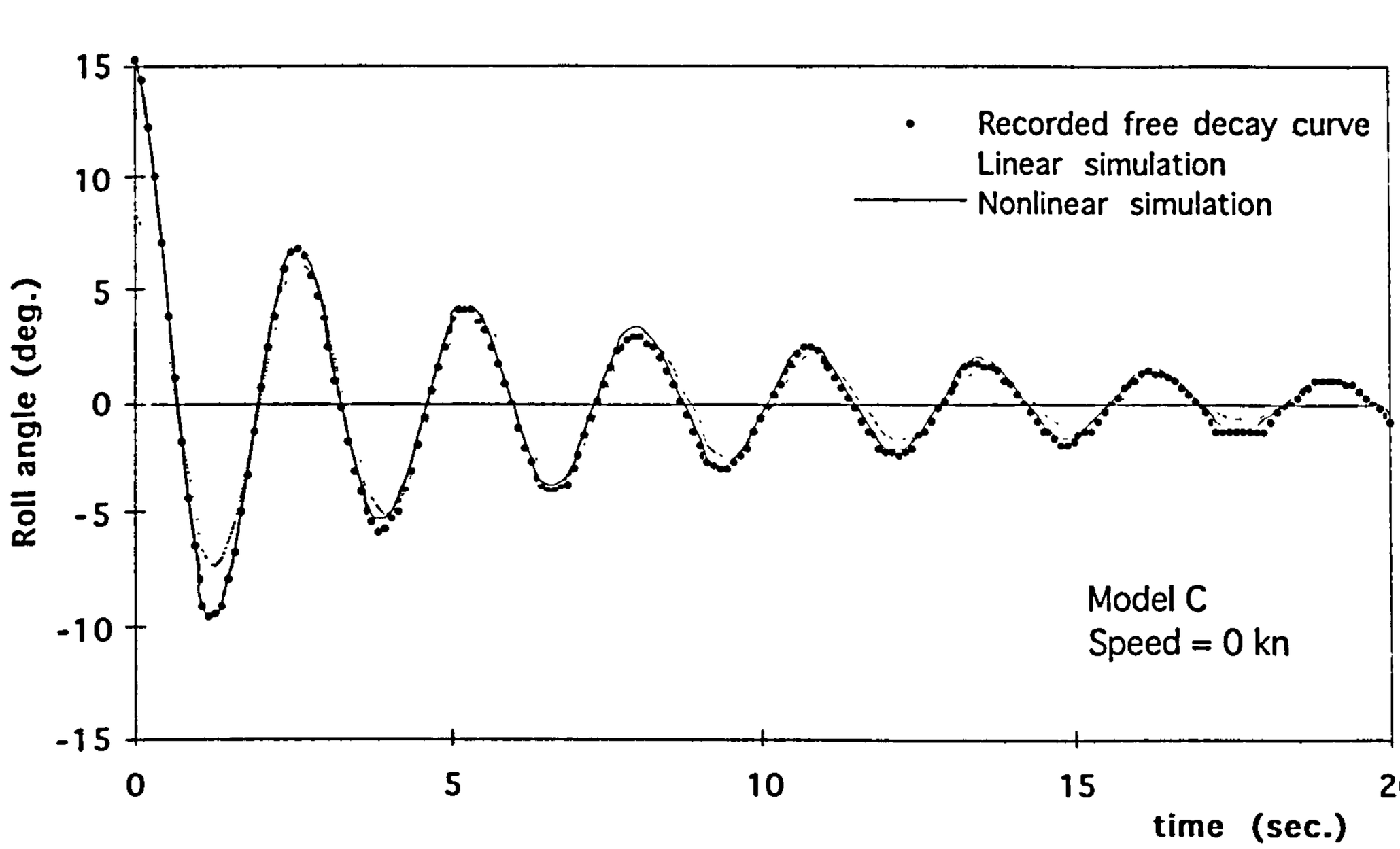

Figure 6.15 Comparison of free decay simulation for Model C

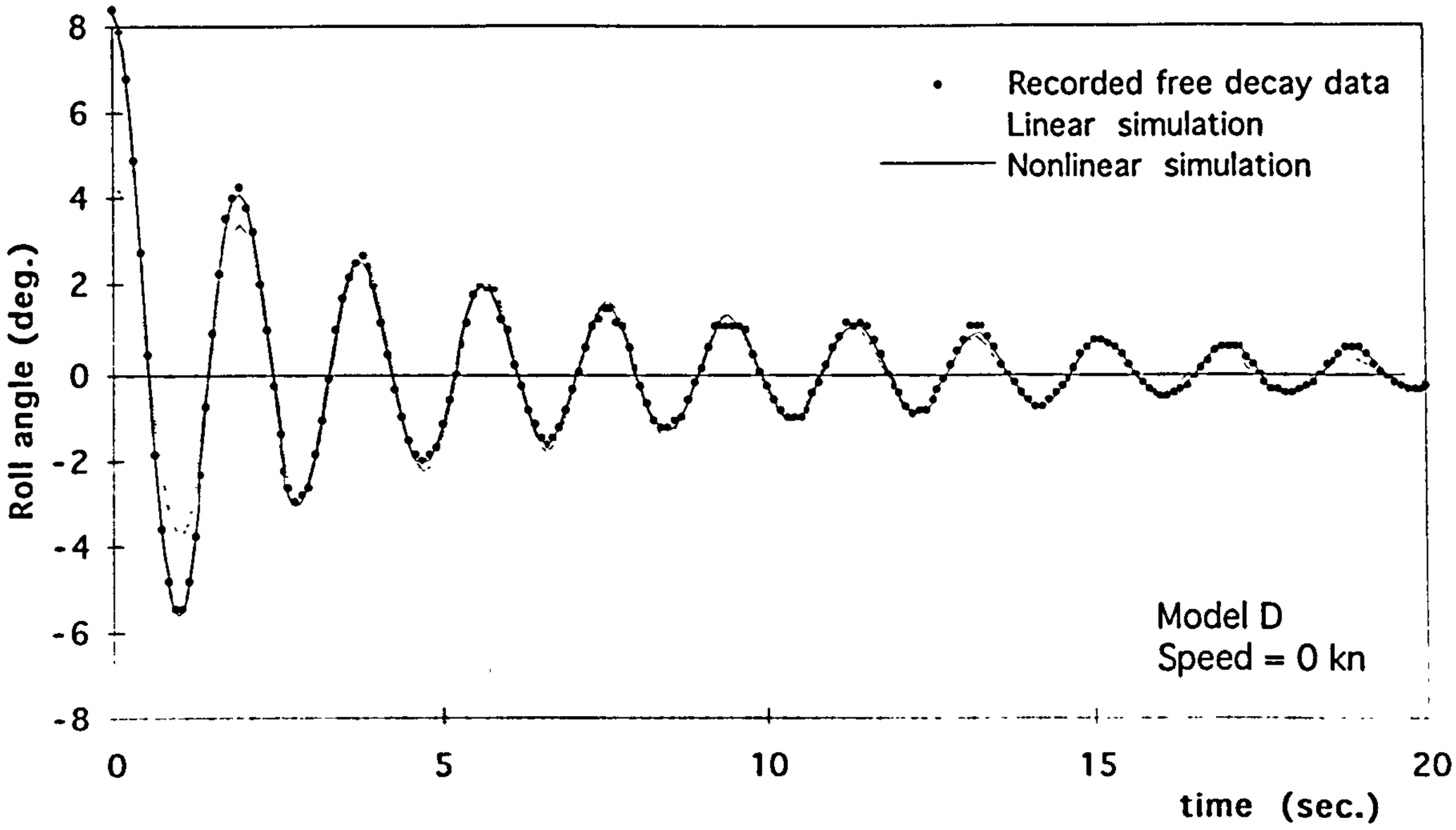

Figure 6.16 Comparison of free decay simulation for Model D

6.4.3 Comparison in Roll Motion Prediction

As the 3D trimaran motion program has been modified to include the nonlinear roll damping effects as described in the previous Chapter 5, the roll motions of the models were also calculated using linear damping coefficients, and linear plus quadratic damping coefficients, separately.

The predictions of trimaran roll motions are shown in Figure 6.17 for the models with zero forward speed in beam seas. It can be seen that improved predictions of the roll motion around the resonance wave frequencies have been achieved compared with the previous linear predictions. Figure 6.18 show the roll motion prediction for the models at 18 knots forward speed. There are marginal differences between the results using the two methods because the nonlinear damping coefficients at this speed are relatively small.

The results indicate roll motion predictions for trimaran ships using the nonlinear damping technique at low speeds, say below 18 knots for a frigate, would provide better results than using the linear-only method. For higher forward speeds, the linear technique is adequate for motion predictions as is the case in free decay simulations.

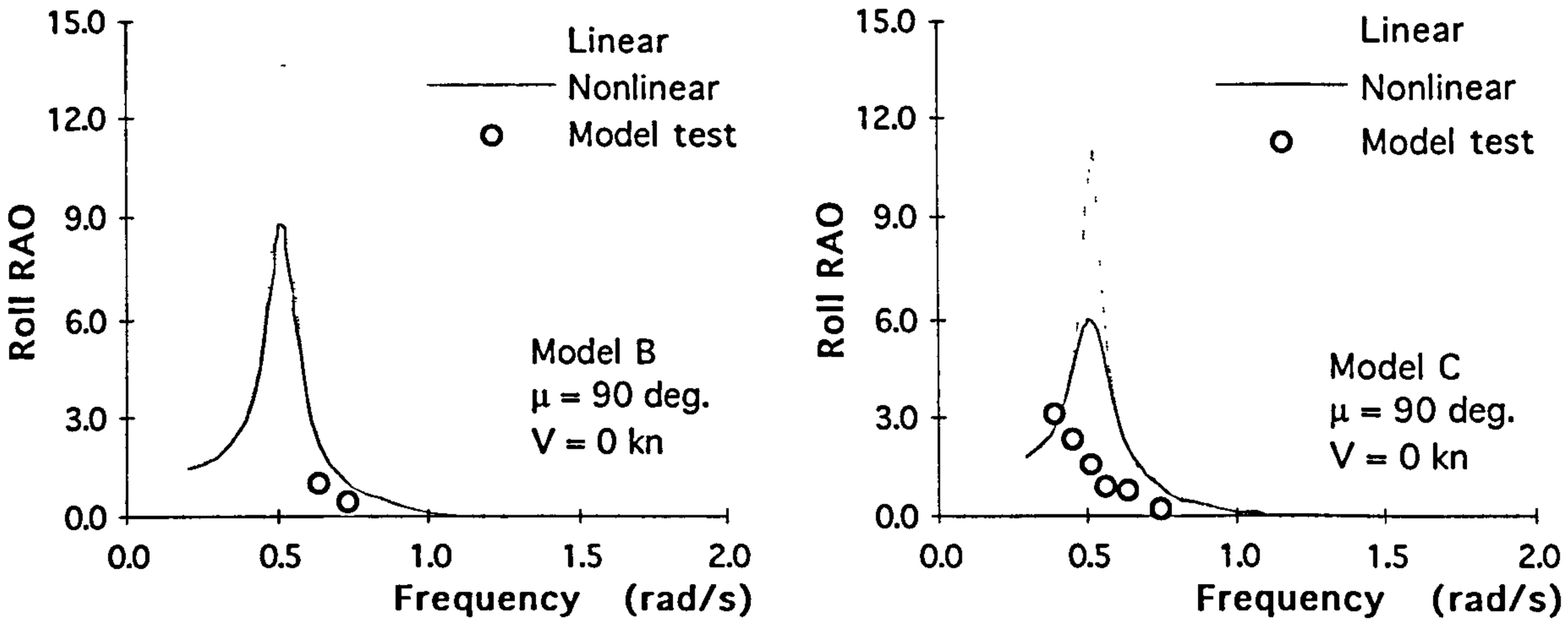

Figure 6.17 Comparison of roll motion predictions at zero speed

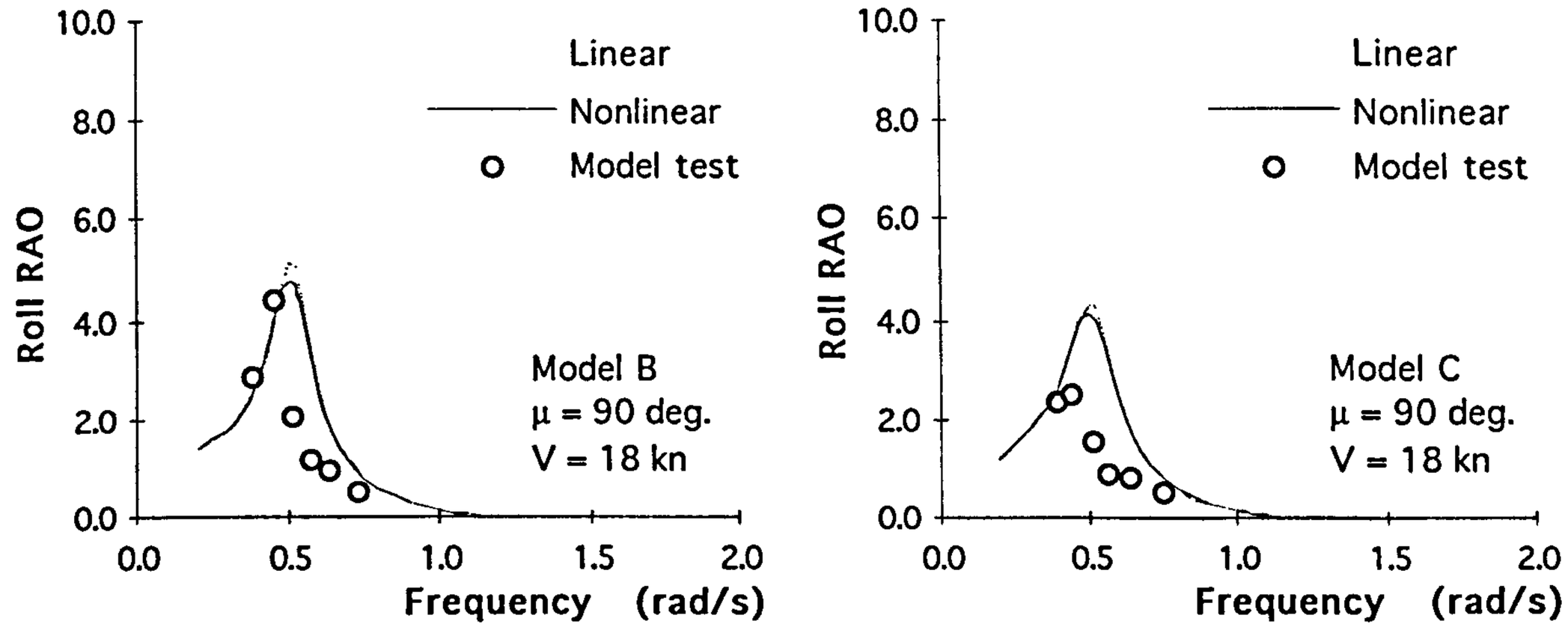

Figure 6.18 Comparison of roll motion predictions at V = 18 kn

6.5 Computational Predictions of Trimaran Roll Damping Coefficients

The estimations of roll damping coefficients described in the previous sections are based on the data derived from free decay experiments of the trimaran models. The roll motion predictions showed good agreement compared with the model experiments. However, for a trimaran design at an early design stage free decay experiment data may not be available. It is therefore necessary to develop a method for estimating roll damping coefficients without free decay data. This section details the methods that have been used

in the calculation of the roll damping coefficients and provides some results for motion prediction using these coefficients.

The roll damping of a ship consists wavemaking damping B_w, skin frictional damping B_f, eddy damping B_e, and appendage damping B_a. The total roll damping B_{44} is the summary of those damping coefficients as:-

$$B_{44} = B_w + B_f + B_e + B_a \tag{6-21}$$

The wavemaking roll damping coefficient B_w can be calculated using the potential theory described in Chapter 5. This section focuses on the development of the method for theoretical prediction of the remaining roll damping coefficients.

The development of a satisfactory theoretical procedure for estimation of roll damping has been consistently identified as the single most important task in ship motion theory **(Schmitke 1978) (Lloyd 1989)**. This is mainly because the complex features of the fluid dynamics around the parts of a ship, bilge keels, rudders, propellers, and shaft brackets, etc., which contribute substantially to the total roll damping. This complexity makes mathematical modelling more difficult than in the case of a bare hull for which both the strip theory and the three dimensional theory show success. Thus, the methods developed so far for the prediction of roll damping of monohull ships are all combinations of theoretical methods and empirically based model experiments. This would also be the case for trimaran ships. The title of this section, as 'computational' rather than 'theoretical', reflects this.

Bilge keels are normally considered to be the most important damping devices for monohull ships and receive most attention. **Kato (1966)** studied the effect of bilge keels on roll damping and developed an empirical method for calculating the bilge keel roll damping after analysing considerable monohull experiment data. The formula includes the effects of bilge keel area, breadth, aspect ratio, and a long list of coefficients reflecting the hull form and the rolling Reynolds number. This can be used for a trimaran ship if there are bilge keels fitted on to the centre hull. As for the cases with bilge keels attached to the bottom of the side hulls, such as the case of the model ship described in Chapter 4 and believed to be most likely for trimaran ships, the method is obviously not suitable.

Tanaka (1960) conducted rolling experiments with various monohull sections to assess the effect of section shape on eddy making roll damping. He developed empirical equations for the prediction of eddy making damping based on the experimental data and

related the coefficients in the equations with the section beam, flare at the water line, radius of the keel, and roll amplitudes.

Schmike's (1978) theoretical work on the mechanics of the roll damping emphasised the effect of the lifting surface terms on roll damping and he developed a method for the prediction of roll damping due to lifting surfaces. He also incorporated the methods developed by Kato and by Tanaka for the viscous roll damping into his motion prediction and achieved good agreement between roll motion predictions and experimental data. In addition, he also studied the contributions of lifting surfaces to added mass and exciting forces.

All the work on roll damping prediction methods described above are based on monohull ships' properties and experiments and can not be simply applied to the trimaran ship. The theoretical methods have to be adjusted to suit the geometry of the trimaran ship, and the empirical data can not be applied to the trimaran ship as a whole but could be used for the three hulls separately where appropriate. The following subsections describe and discuss methods for predicting the roll damping components for trimaran ships.

6.5.1 Skin Frictional Roll Damping

The skin fictional roll damping is due to the frictional forces exerted on the hull surfaces by the water when a ship rolls. Consider a panel ds on the hull surfaces as shown in Figure 6.19, there is a skin friction drag force dF acting on the panel as a result of the rolling velocity $\dot{\eta}_4$. The frictional torque dT resulting from dF about the rolling axis can be expressed as **(Schmitke 1978)**:-

$$dT = -\frac{1}{2}\rho r(yn_2 + zn_3)^2 \dot{\eta}_4 |\dot{\eta}_4| C_{DF} ds \tag{6-22}$$

where, r is the distance from the panel to the rolling axis, n_2 and n_3 are the components of unit outward force normal to the hull surface of the panel ds corresponding to its coordinates y and z, and C_{DF} is a skin friction drag coefficient.

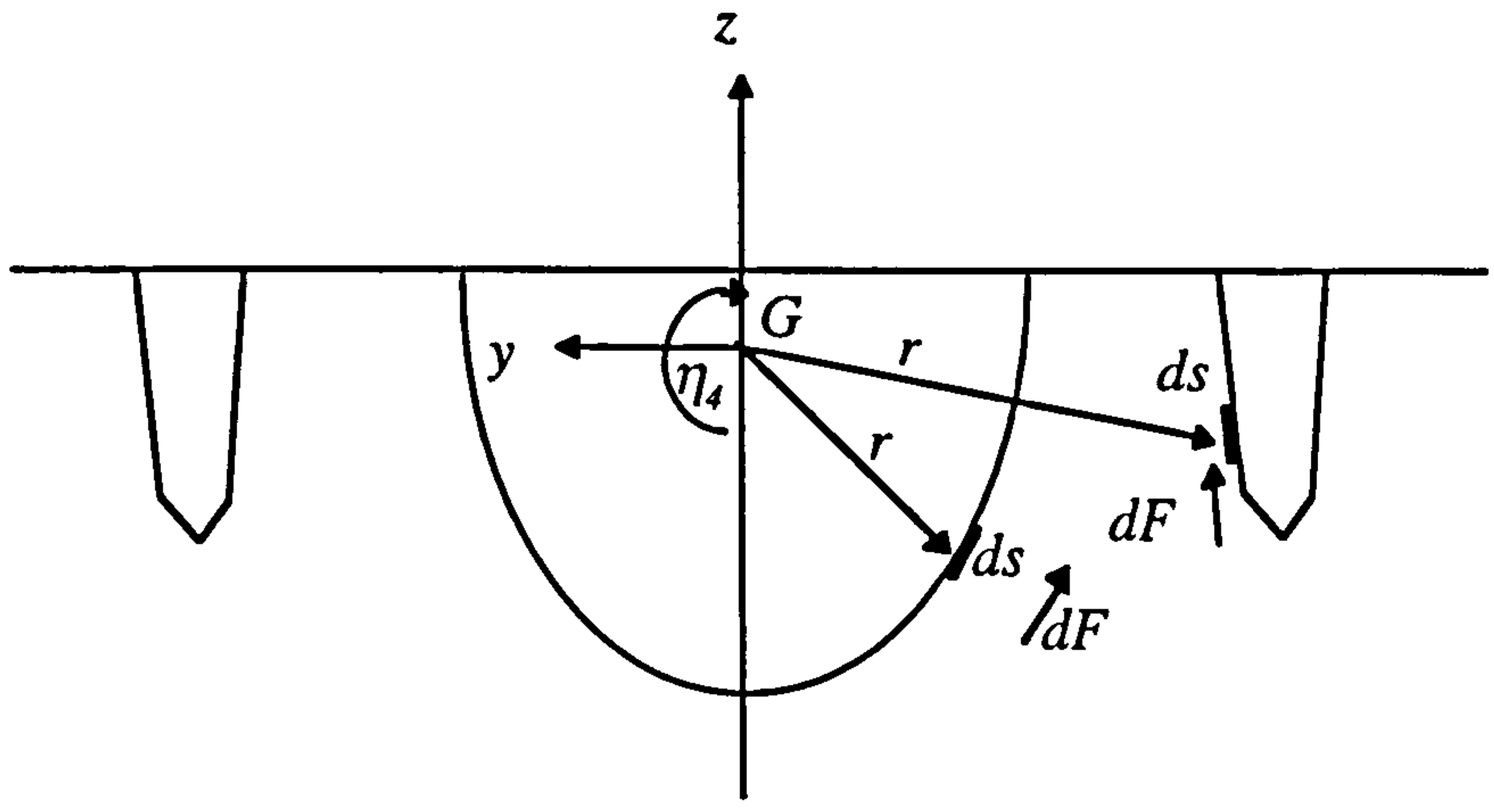

Figure 6.19 Roll Damping due to skin friction

Skin friction damping is a nonlinear function of roll amplitude. It needs to be linearised for use in the linear ship motion equations. Again, the linearisation technique described in Section 6.3 can be used here to derived the linearised frictional roll damping coefficient. From equation (6-22), the energy dissipated by torque dT during one cycle of roll is:

$$dE = 4\int_0^{\frac{\pi}{2}} dT d\eta_4 = \frac{4}{3}\rho r(yn_2 + zn_3)^2 \omega \eta_{40}^3 C_{DF} ds \tag{6-23}$$

Integrating the energy term over the whole hull surfaces, and using Equation (6-18), we get the roll damping coefficient due to skin friction as:-

$$B_f = \frac{4}{3\pi}\rho \omega x_{40} \int_S C_{DF} r(yn_2 + zn_3)^2 ds \tag{6-24}$$

The drag coefficient C_{DF} is determined using the Schoenherr formula based on smooth turbulent flow as suggested by **Schmitke (1978)**:-

$$C_{DF} = 0.0004 + (3.46\log(R_n) - 5.6)^{-2} \tag{6-25}$$

where R_n is the appropriate Reynolds numbers based on forward speed, V, and the lengths of the central hull and the side hulls separately.

At zero forward speed, the drag coefficient C_{DF} is obtained using **Kato's (1958)** formula:-

$$C_{DF} = 1.328R_{n0}^{-0.5} + 0.014R_{n0}^{-0.114} \tag{6-26}$$

where R_{n0} is now a Reynolds number associated with rolling motion at zero forward speed:-

$$R_{n0} = \frac{0.512\rho(r\eta_{40})^2\omega}{\mu_v} \tag{6-27}$$

where μ_v is the coefficient of dynamic viscosity, and r is the actual distance from the panel to the roll centre.

6.5.2 Eddy Making Damping

The eddy making damping coefficient was calculated using the method developed by **Schmitke (1978).** The roll resistance force due to eddy making can be expressed as-

$$F = \frac{1}{2}\rho U_h^2 S C_{DE} \tag{6-28}$$

where U_h is the horizontal linear velocity of the point on the hull where the eddies are generated, S is the wetted surface of the hull section, and C_{DE} is a drag coefficients. U_h can be expressed as:-

$$U_h = \begin{cases} r_c\dot{\eta}_4 & \text{for central hull} \\ r_s\dot{\eta}_4\sin\beta & \text{for side hulls} \end{cases} \tag{6-29}$$

where β, r_c and r_s are defined in Figure 6.20.

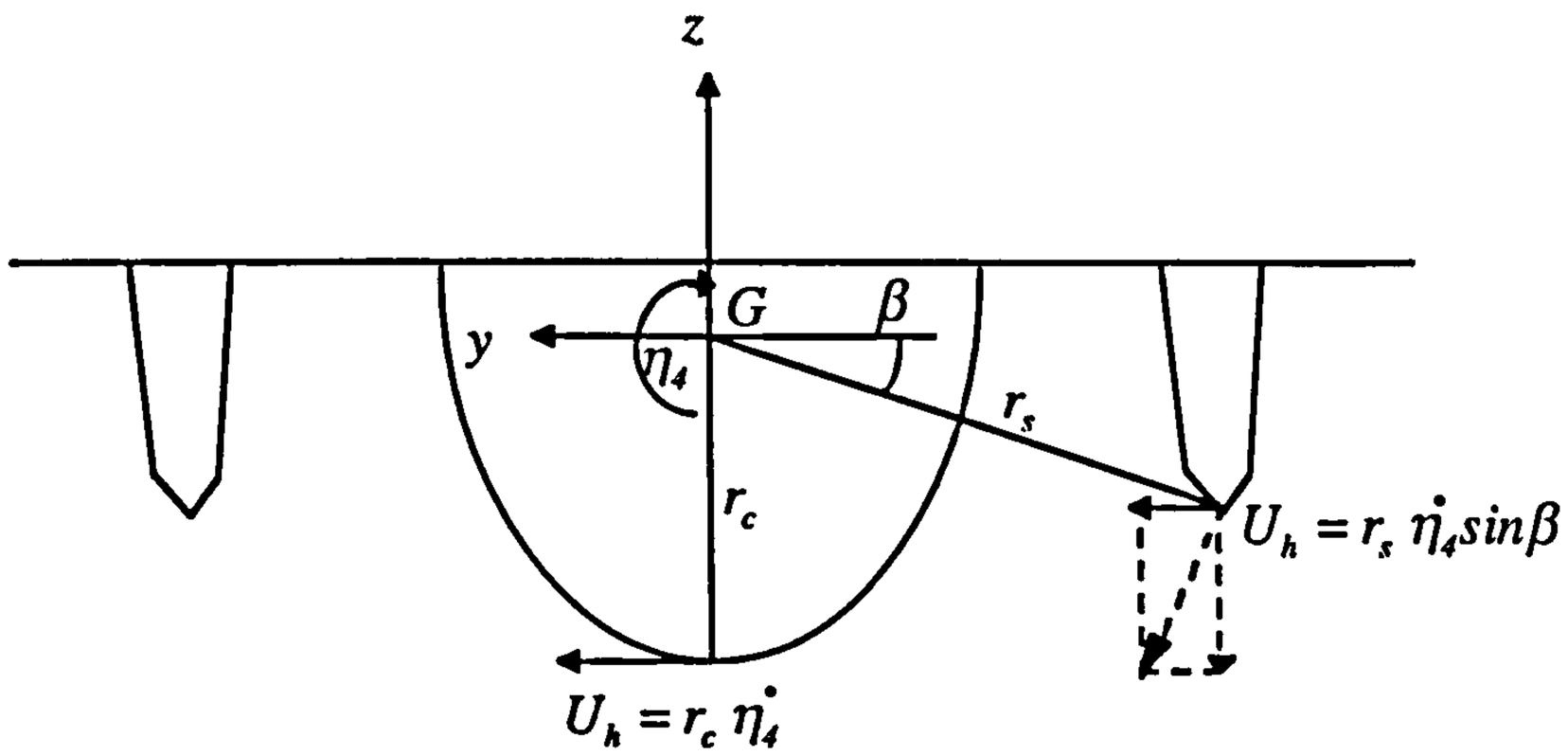

Figure 6.20 Roll damping due to eddy making

The force F exerts a torque about the roll centre as:

$$T = rF = \frac{1}{2}\rho r U_h^2 S C_{DE} \tag{6-30}$$

The energy dissipated by this torque during one cycle of roll is:-

$$E = 4\int_0^{\eta_{40}} T d\eta_4 = \begin{cases} \frac{4}{3}\rho r_c^3 \omega^2 \eta_{40}^3 S_c C_{DE} & \text{for central hull} \\ \frac{4}{3}\rho r_s^3 \omega^2 \eta_{40}^3 \sin^2\beta S_s C_{DE} & \text{for side hull} \end{cases} \tag{6-31}$$

Using equation (6-18) the eddy making damping coefficients for each section of each hull are:-

$$\left.\begin{aligned} b_{ec} &= \frac{4}{3\pi}\rho\omega\eta_{40} r_c^3 S_c C_{DE} && \text{for central hull} \\ b_{es} &= \frac{4}{3\pi}\rho\omega\eta_{40} r_s^3 \sin^2\beta S_s C_{DE} && \text{for side hull} \end{aligned}\right\} \tag{6-32}$$

The drag coefficient C_{DE} is calculated using the empirical formulas based on the sectional beam and draft of the hull. The formula are not listed here as they can be found in **(Lloyd 1989)**. The central hull can be treated as a deep V hull shape. The side hulls can be treated as triangular shapes.

The total eddy making damping coefficients B_e of the ship will be the integration of the sectional damping coefficients over the length of each hulls:-

$$B_e = \int_0^{L_c} b_{ec} dl + 2\int_0^{L_s} b_{es} dl \tag{6-33}$$

where the integrals are over the length of the central hull L_c and the side hull L_s separately.

6.5.3 Appendage Roll Damping

The appendages considered in the roll damping estimation are rudders and bilge keels fitted on the side hulls. Bilge keels for most trimaran ships are expected to be positioned on the inner side bottom of the side hulls and therefore are not expected to behave in the same way as those fitted to monohulls. This excludes the use of **Kato's (1966)** method

which is based on monohull ships. Thus, the bilge keel is treated in the same way as other appendages. The roll resistant forces produced by these appendages can be considered as drag forces and lift forces. The appendage roll damping coefficient will be the sum of the drag force damping and the lift force damping as:-

$$B_a = B_{aD} + B_{aL} \tag{6-34}$$

Damping due to drag forces

When the roll velocity is $\dot{\eta}_4$ and the appendage is located at radius r_a as shown in Figure 6.21, the induced torque about the roll centre due to the drag force on an appendage is:-

$$T = \frac{1}{2}\rho C_{DA} r_a^3 \dot{\eta}_4^2 A \tag{6-35}$$

where A is the total area of the appendage, and C_{DA} is the drag coefficient.

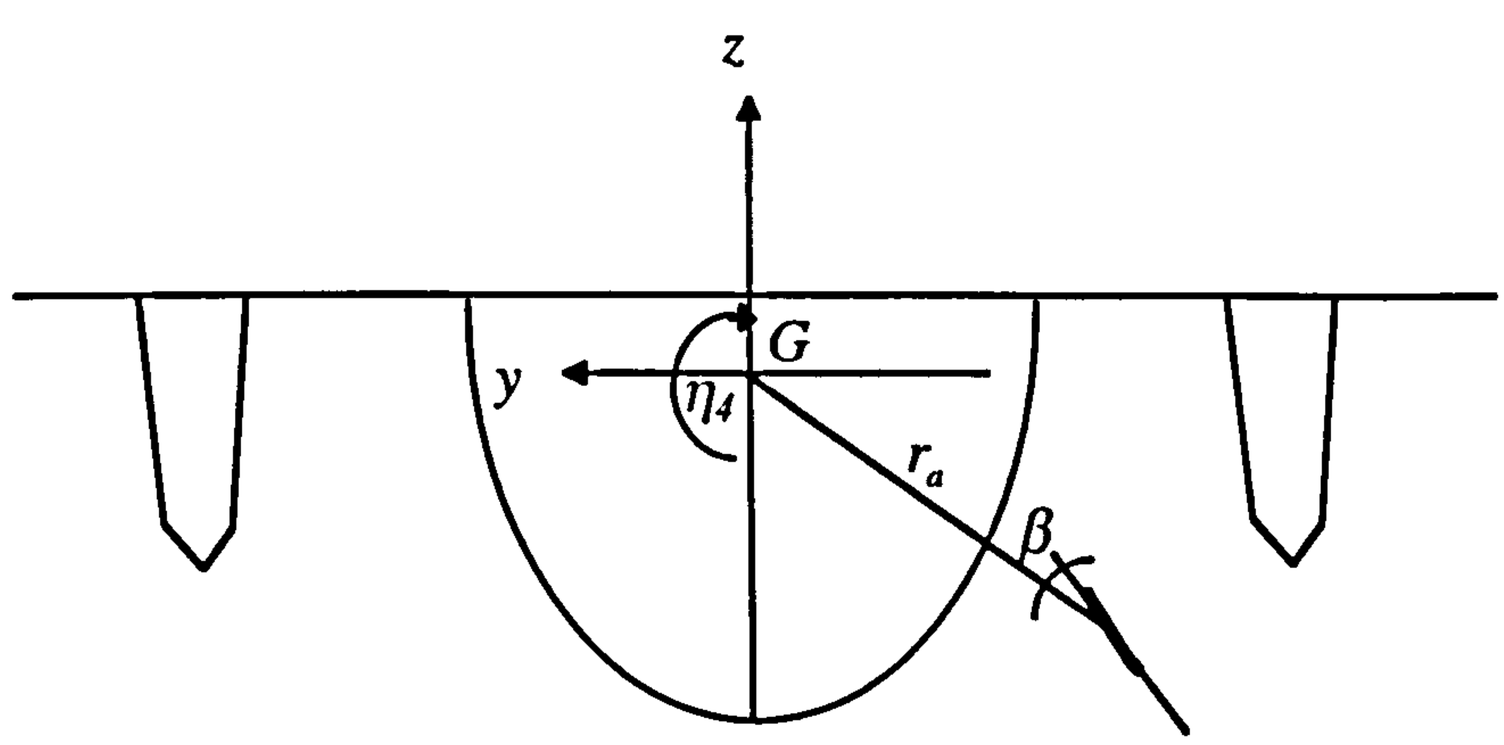

Figure 6.21 Roll damping due to appendages

The energy dissipated during in a roll cycle is:-

$$E = 4\int_o^{\eta_{40}} T d\eta_4 = \frac{4}{3} C_{DA} \rho r_a^3 \eta_{40}^3 \omega^2 A \tag{6-36}$$

Again, using equation (6-18), the damping coefficient for all of the appendages due to drag forces can be expressed as:-

$$B_{aD} = \frac{4}{3\pi}\rho\eta_{40}\omega\sum C_{DA}Ar_a^3\sin\alpha \tag{6-37}$$

where α is the angle between appendage surface and the velocity of the flow with $\tan\alpha = \frac{\dot{\eta}_4}{V}$. The value of sin$\alpha$ equals 1 when the forward speed V is zero. The summation $\sum$ is for all appendages accounted in the calculation.

The drag coefficients C_{DA} is given as:-

$$C_{DA}=1.17\cos\beta$$

where β is the angle between the radial line from roll centre and the appendage surface. The value *1.17* is given by **Hoerner & Borst (1975)** as the drag coefficient for a plane normal to the flow direction.

Damping due to lift forces

When the ship has forward speed, the roll resistant torque due to lift forces on an appendage can be expressed as:-

$$T = \frac{1}{2}\rho\frac{dC_L}{d\alpha}V\cos\alpha Ar_a^2\dot{\eta}_4 \tag{6-38}$$

The lift curve slope can be determined by:-

$$\frac{dC_L}{d\alpha} = \frac{1.8\pi a}{1.8+\sqrt{(a^2+4)}} \tag{6-39}$$

where a is the aspect ratio of the appendage.

Then, the damping coefficient due to lifting forces is:-

$$B_{aL} = \frac{T}{\dot{\eta}_4} = \frac{1}{2}\rho V\sum\frac{dC_L}{d\alpha}A\,r_a^2\cos\alpha \tag{6-40}$$

The summary Σ is for all appendages.

6.5.4 Comparison of Roll Damping Components

The roll damping prediction method described above has been implemented into the trimaran motion prediction program described in Chapter 5. The components of the roll damping coefficients were calculated for the model ships. Firstly, it was found the frictional roll damping coefficient B_f in all of the calculated cases was very small compared with the other components of roll damping. It can barely be seen when plotted on a damping coefficient diagram as shown in Figure 6.22. This is mainly due to the skin frictional drag coefficient C_{DA} being so small when the ship rolls.

In beam seas, the wavemaking damping coefficient B_w is significant when the wave frequencies are beyond the resonance frequencies as shown in Figures 6.22 and 6.23, but is very small around and below the resonance frequencies where the roll motion response is significant.

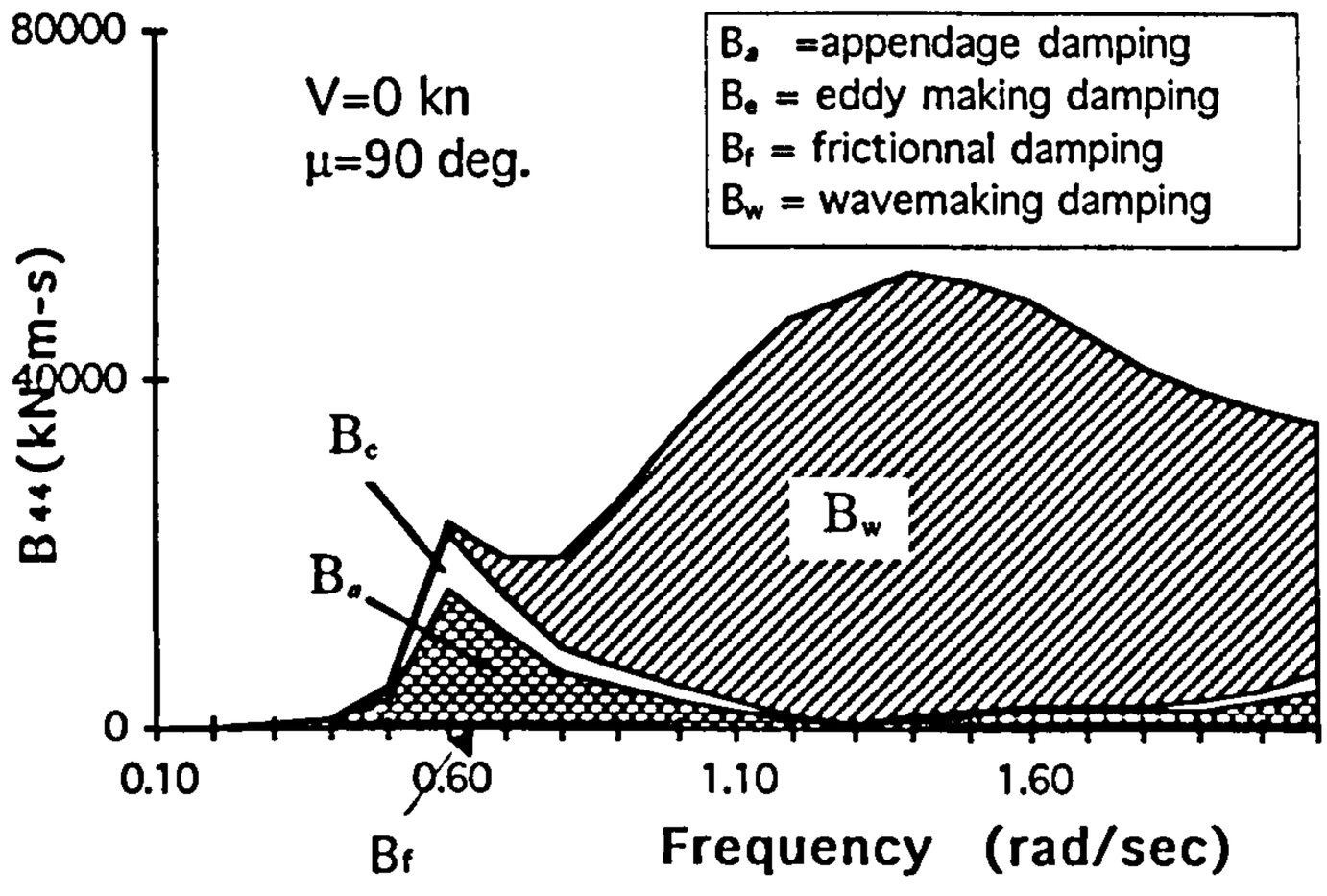

Figure 6.22 Roll damping components of Model C at zero speed

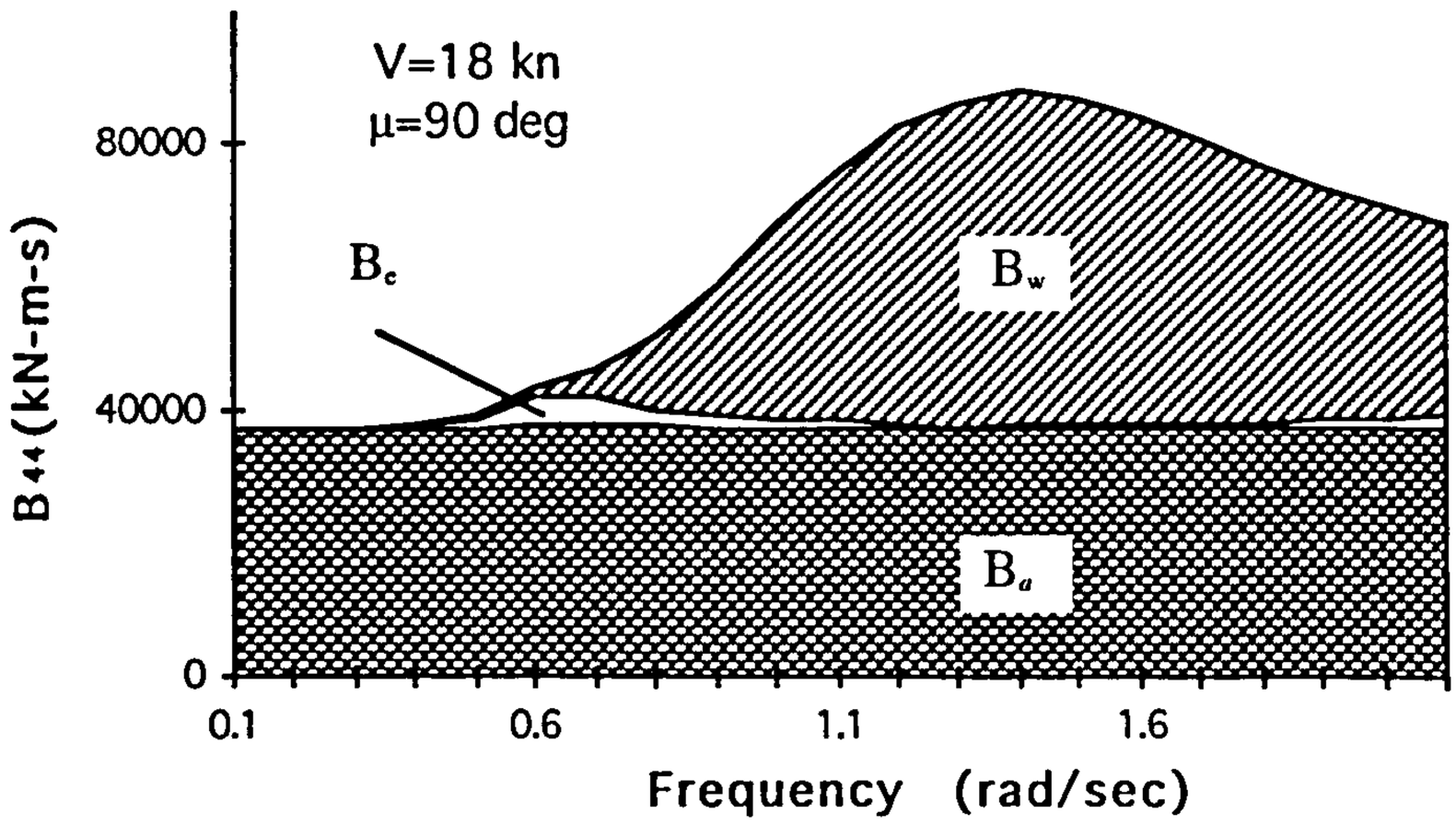

Figure 6.23 Roll damping components of Model C at 18 knots

In following quartering sea with forward speeds, as shown in Figure 6.24, the wavemaking roll damping is reduced because of smaller encounter frequencies. This demonstrates that wavemaking roll damping is not playing a very significant part in the roll motion in following quartering seas where the roll motions are of most concern.

The highest values of the eddy making roll damping coefficient B_e for all of the cases occurred at the resonant frequencies. This shows the important role of eddy damping to the resonant roll amplitudes of the ship.

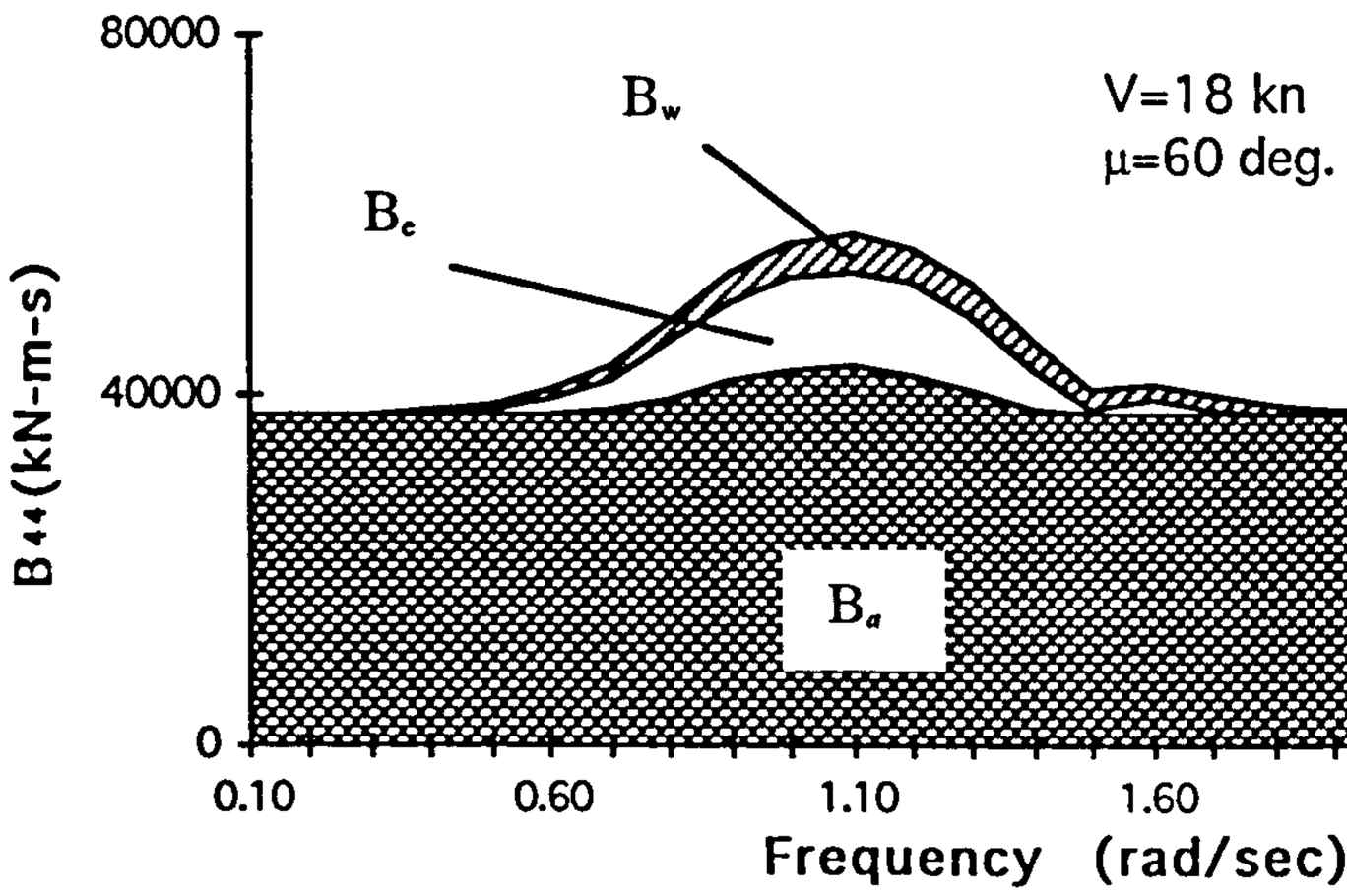

Figure 6.24 Roll damping components of Model C in following quartering sea

Of all the roll damping components, the most significant one is appendage roll damping B_a, as shown in all the cases through Figures 6.22 to 6.24. At ship's zero forward speed, the appendage damping coefficient B_a is mainly due to the drag forces on the long and narrow bilge keels fitted on the inner side of the side hulls. At a forward speed of 18 knots, the dominant appendage roll damping is produced by the lift forces exerted on the appendages. As the lifting forces are independent of roll amplitude, the appendage roll damping coefficients are almost constant over the whole range of the wave frequencies, as shown in Figures 6.23 and 6.24. Two types of appendages have been accounted for in the current calculation, the rudders and the bilge keels fitted on the side hulls. Though the total lift surface area of the bilge keels is three times that of the rudders, and the locations of the former are further away from the roll centre, the roll damping coefficient of the former is less than half of the total lift force damping coefficient. This is because the bilge keels are very narrow compared with the rudders and their lift curve slopes are very small. It is therefore anticipated that a wider but shorter bilge keel or fin (i.e. higher aspect ratio) located on each of the side hulls will be more effective to reduce the roll motions of the trimaran ship at speed.

6.5.5 Validation on Roll Motion Predictions

The predictions of roll motion using the computed damping coefficients were carried out for some of the model ships. Figure 6.25 shows the predicted roll RAO functions for the model ships at a forward speed of 18 knots. The ships' headings are beam seas and following quartering seas. The results show reasonably good agreement between the theoretical predictions and the model experiments.

The roll motion predictions using the damping data derived from the free decay data are also plotted as dotted lines on the diagrams. It can be seen that the roll RAO curves predicted using the two methods are quite close to each other. This demonstrates that the computer tools presented here can be used in the assessment of the trimaran ship's roll behaviour when free decay data are not available.

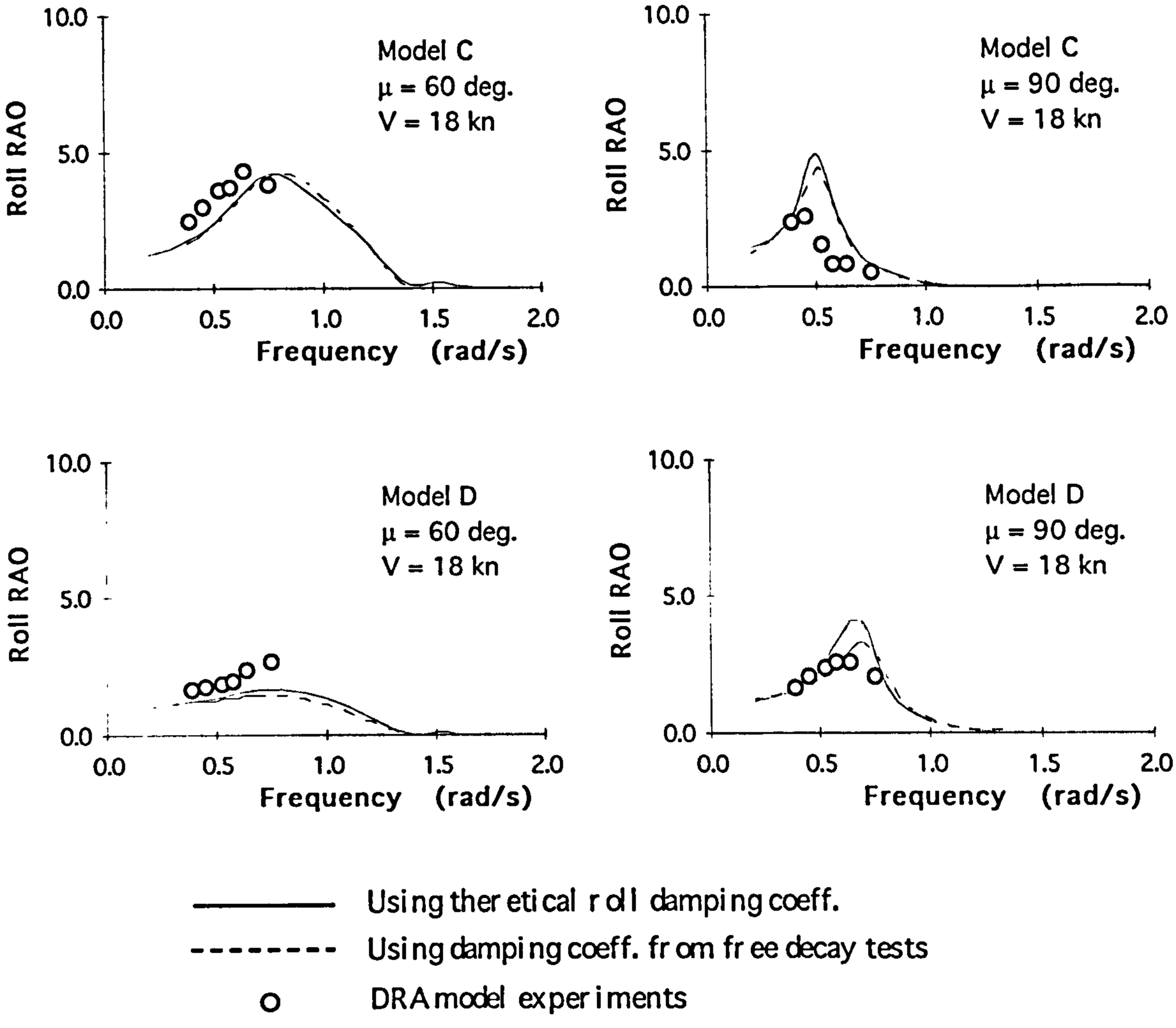

Figure 6.25 Roll motion predictions using estimated damping coefficients

6.6 Effects of Side Hulls on Roll Damping

Any differences in the motion behaviour of a monohull ship and a trimaran ship would be mainly due to the latter having a very slender central hull and two additional side hulls. The effect of a longer central hull on the motion behaviour of a ship is relatively easy to anticipate, as it would normally result in reduced pitch and heave motions as the ship's length increases. In contrast, the effects of side hull on the ship motion behaviour would be much more difficult to predict as there is no experience. Since more than 90 per cent of the total displacement lies in the central hull which is essentially a normal monohull, except it is slender, the small side hulls would have very limited effects on the vertical motion of the trimaran ship. It was envisaged that the influence of the side hull would be mainly on the transverse motions of the ship, particularly the roll motion.

In order to get an initial insight into the effects of the side hulls on the trimaran ship's roll motion behaviour, the damping coefficients of the central hull and the side hulls were calculated separately for some cases. The calculations were carried out using the 3D program. The hull surface meshes for the central hull and the side hulls were generated separately for the calculations. Once the central hull and the side hulls have been separated, the resulting centres of gravity and the metacentric centre would also be altered. In order to make the calculated damping coefficients comparable, an identical artificial centre of roll was imposed on the central hull model and the side hull model. Since this centre of roll is not the real centre of roll either for the central hull model or for the side hull model, the calculated roll motion amplitudes are not strictly correct. However, this does not affect the calculation of wavemaking roll damping coefficients which are independent of the rolling velocity.

It should also be noticed that the roll damping coefficients calculated in this way ignore the interaction between the side hulls and the central hull compared with the coefficients calculated for the three hulls as a whole ship. Therefore, the roll damping coefficients calculated here are only for comparison purpose.

Figure 6.26 shows a calculated sample of roll damping coefficients for Model C at zero forward speed in beam seas. Over most of the wave frequencies, the damping effect of the side hulls is still a small proportion compared with the damping effect of the central hull. However at the lower band of wave frequencies, the roll damping coefficients of the side hulls are larger than that of the central hull. This indicates the contribution of the side hulls to roll damping is more significant than that of the centre hull over a certain low wave frequency band, although for the total wavemaking roll damping of the three hulls it is still very small compared with the appendage damping as shown in Figures 6.23 and 24.

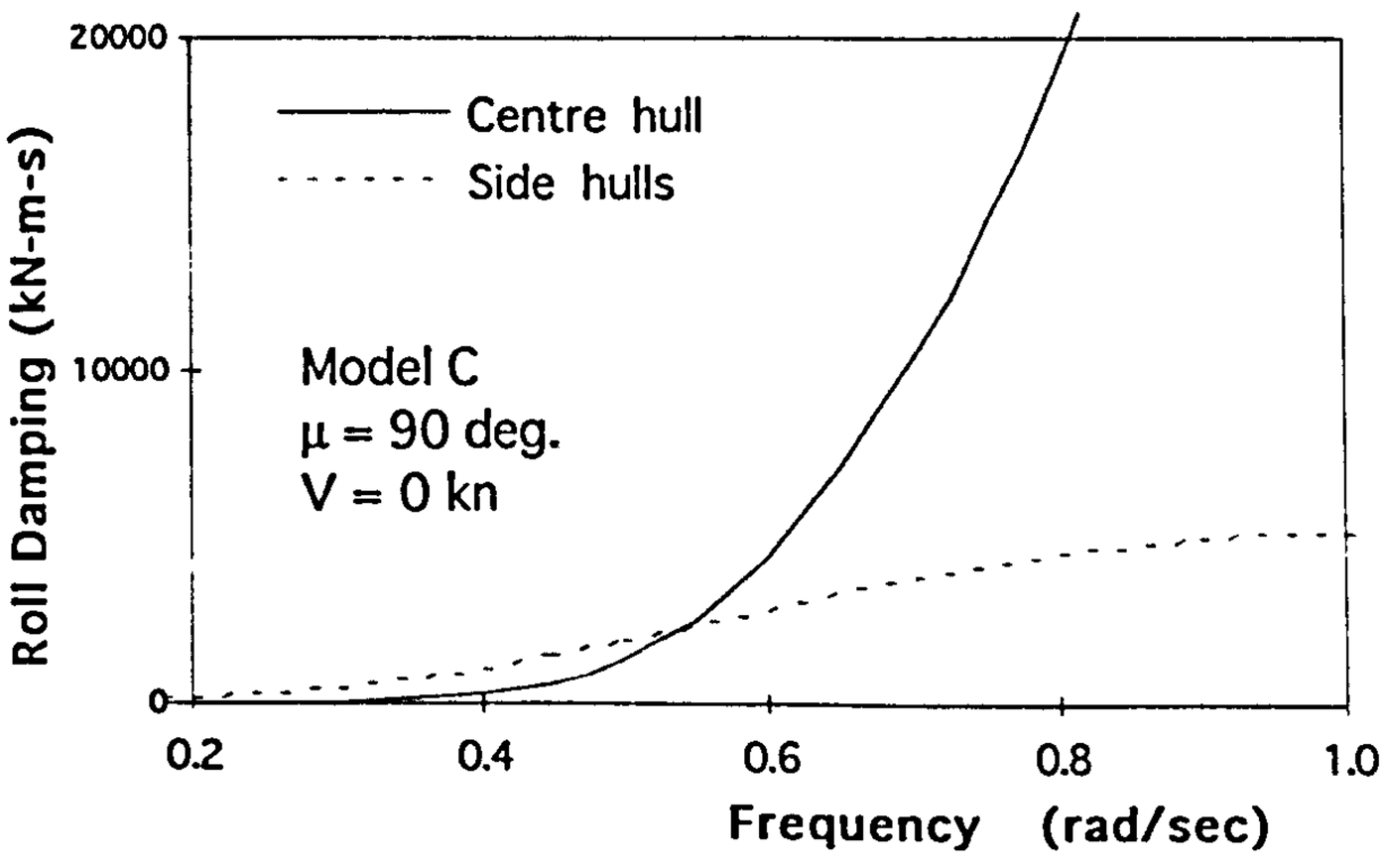

Figure 6.26 Side hull contribution to roll damping

The effects of the side hull span were also checked by trial calculations. Figure 6.27 shows the calculated results. The side hull model was based on a 30 metre overall beam and was increased by 10, 20, and 30 per cent. The results show the side hull roll damping increased as the span increased. These are very straightforward to explain. As the damping moment is proportional to the distance from the side hull to the roll centre, the damping coefficients would increase linearly as the span increases.

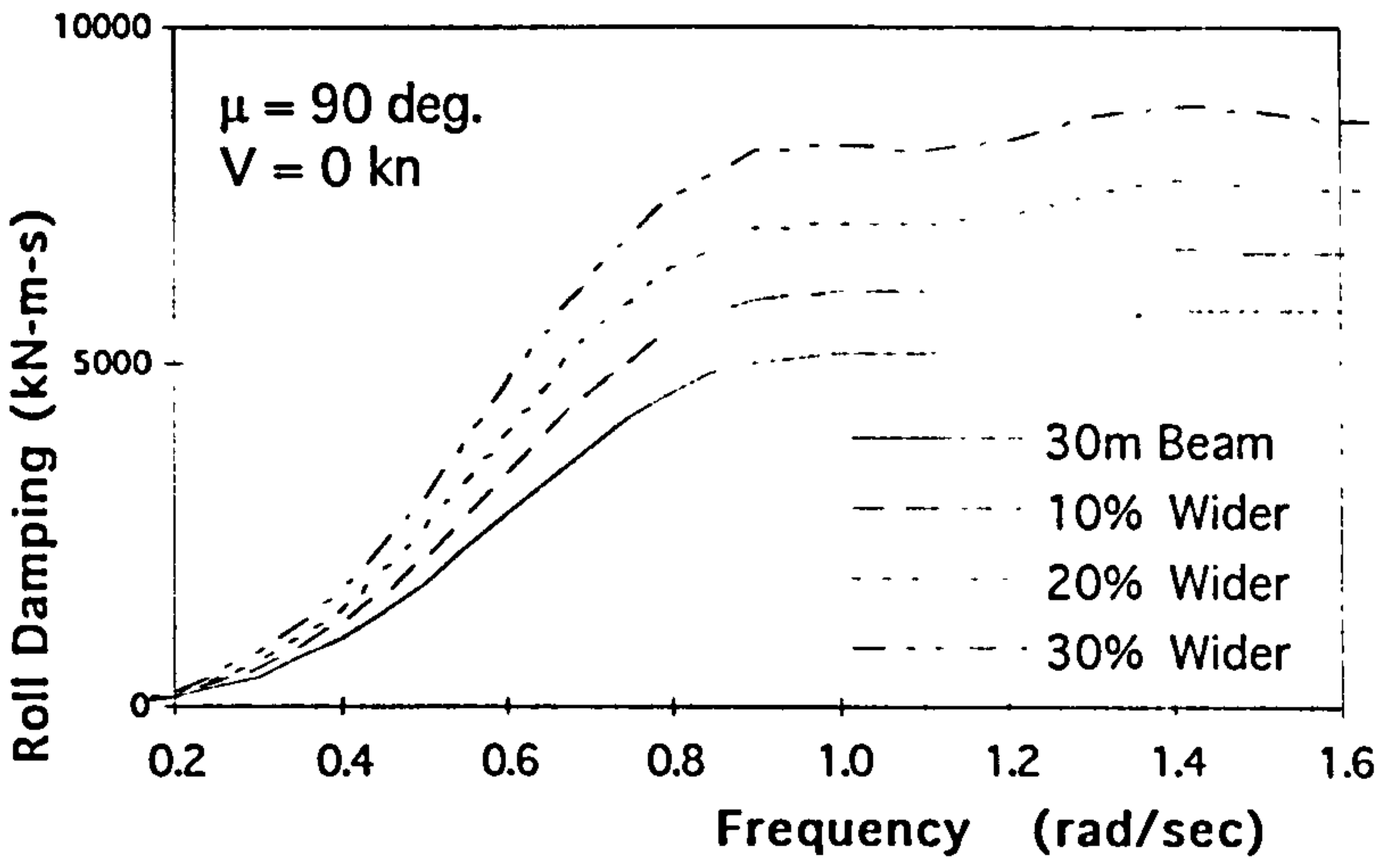

Figure 6.27 Effects of side hull span on roll damping

The above outlines an investigation into effects of the side hulls on roll damping. There are more side hull variations which can be explored. For example, varying the side hull shape may produce a significant impact on the roll damping of the trimaran ship, akin to increasing the beam and reducing the draft of the side hulls. This would be a good project for future research.

However, the investigation described in the previous section has shown the importance of the appendage damping on the roll motions for trimaran ships. Effort should be spent to explore the configuration of the bilge keels to improve trimaran roll motions while the configuration of the side hulls could be focused on reducing the resistance to enhance the propulsive advantages of the trimaran ship.

6.7 Conclusions on Roll Damping

1. A method for estimating nonlinear roll damping coefficients of trimaran hull forms from free decay data has been developed. Good agreement was achieved using the estimated nonlinear roll damping coefficients to simulate the free decay curves. The study shows that for trimaran roll motions calculated at low forward speed, the use of nonlinear roll damping coefficients gives a better prediction. For the medium and high speed cases, the simpler linear roll damping calculation is sufficient for roll motion predictions.

2. Theoretical methods to estimate the trimaran roll damping coefficients have been developed and examined. Good agreement was achieved for roll motion prediction when compared with calculations using free decay data and with the model experiment results. This provides some confidence that this tool can be used for future research work into the configuration of trimaran ships.

3. Initial calculations of the side hull contribution to trimaran roll damping showed the important role of the side hulls for a particular band of wave frequencies. Further research work is needed in this area. For example, model tests could be carried out for the central hull and the side hulls separately to identify the damping effects of the side hull. Additionally, the effects of varied side hull shapes on roll damping need to be studied.

4 The study has shown the importance of appendage damping. Effort should be spent exploring the configuration of the bilge keels or fins on the side hulls for improving trimaran roll motions while the configuration of the side hull itself could be focused on reducing the contribution of the side hulls to the resistance of the trimaran ship.

CHAPTER 7

RESISTANCE CHARACTERISTICS OF TRIMARAN SHIPS

7.1 Introduction

Chapter 2 discussed briefly the potential resistance advantage of the proposed displacement trimaran ship at high speed compared with conventional monohull ships. The slender hulls deployed for the trimaran ship would produce less wavemaking resistance at high speeds. However, there are more hull form variables in the design of a trimaran ship which affect the resistance performance than in the design of a monohull. Thus, the resistance characteristics of the trimaran need to be further explored to gain a better understanding of this new ship concept, since its resistance advantages can only be achieved when the trimaran ship is appropriately configured.

The work described in this chapter is based a research project (**Zhang 1996b**) which was specified by DRA Haslar and UCL (**Andrews & Zhang 1995b**), which investigated the effects of the trimaran configuration on its wavemaking resistance a major consideration in the hydrodynamic performance of trimaran ships .

The components of the trimaran resistance are assumed to be similar to that of the monohull and are usually said to consist of three parts, frictional resistance R_F, residual resistance R_R, and appendage resistance R_A, in accordance with **ITTC (1957)**. Thus the total resistance R_T of a trimaran ship can be expressed as:-

$$R_T = R_F + R_R + R_A \tag{7-1}$$

Of the three components, the characteristics of the trimaran frictional resistance is briefly explained in section 7.2, with some discussion about the effects of trimaran configuration on the wetted surface area. The residuary resistance R_R consists of the wavemaking resistance and the form resistance. Since trimaran hulls are very slender, the form resistance is very small, and therefore the focus in this chapter is on the wavemaking resistance and how the configuration of the trimaran influences it. A thin ship theory (**Wehausen 1973**) is used in the computation of wavemaking resistance for the trimaran ship and the theoretical model is explained in Section 7.3. In Section 7.4, computation results are compared with the model test results measured at DRA Haslar (**DRA 1995**) for two trimaran model ships.

The two additional side hulls of the trimaran ship provide the ability to reduce the wavemaking resistance by varying the configuration to achieve wave cancellation effects. The effects of the side hull longitudinal position on the wavemaking resistance and the

relative magnitudes of the components of wavemaking resistance for the trimaran ships are presented in Section 7.5.

7.2 Frictional Resistance

The method used to estimate the frictional resistance of the trimaran ships described in Chapters 3 and 4 is that normally used for monohulls ships, namely, the standard friction line proposed in the 1957 International Towing Tank Conference **(ITTC 1957)**. This is expressed as a function of the total wetted surface area and the Reynolds number of the ship as:-

$$R_F = C_F \frac{1}{2} \rho S V^2 \tag{7-2}$$

with

$$C_F = \frac{0.075}{(\log_{10} R_n - 2)^2} \tag{7-3}$$

where C_F is the frictional resistance coefficient, R_n is the Reynolds number, and S the wetted surface area.

The length of the centre hull of a trimaran ship is normally different from that of the side hulls. This will result in different Reynolds numbers for the centre hull and the side hulls, and hence different frictional resistance coefficients. Individual lengths of the centre hull and the side hulls are used in deriving different Reynolds numbers and hence the separate resistance coefficients. The total frictional resistance of a trimaran ship, therefore, is expressed as:-

$$R_F = (C_{FC} S_C + 2 C_{FS} S_S) \frac{1}{2} \rho V^2 \tag{7-4}$$

where C_{FC} and C_{FS} are the frictional resistance coefficients for the centre hull and two identical side hulls, S_c and S_s represent the wetted surface areas for the centre hull and one side hull.

The wetted surface area has been obtained:-

- For the centre hull, the wetted surface area can be estimated using slender monohull series data. In this study, Taylor-Gertler series data **(Gertler 1954)** were used for the trimaran destroyer, and Series 64 data **(Yeh 1965)** were used for the fast ferry.

- For the side hulls, the narrow and deep side hulls prevent the use of existing monohull data and formulas for the estimation of the wetted surface due to the beam to length ratio of the side hulls generally being very small *(B/L = 0.03 ~ 0.06)*. The wetted surface area of the side hulls therefore has to calculated directly from the side hull forms.

One of the penalties of a trimaran ship, in comparison with a equivalent monohull, is that the trimaran ship is likely to have a larger wetted surface area. For the trimaran ships described in this thesis, their wetted surface areas are about 30% larger than that of a monohull with the same displacement. It is worth pointing out that this is still better than that of an 'equivalent' SWATH ship which would generally be some 60% larger **(Kennell 1992)**. Figure 7.1 shows wetted surface areas of some trimaran ships compared with that of monohulls and SWATH ships. As a result, the frictional resistance of a trimaran is greater than that for an equivalent monohull. This is particularly an important issue at low and medium speeds, where frictional resistance is the dominant component of the total resistance. Therefore, minimising the wetted surface area is one of the basic considerations in trimaran hull form design.

The primary hull form parameters which influence the wetted surface area of the centre hull are the length, beam and draught. Other principal parameters which would also effect the wetted surface area are, block coefficient (C_B), midship section coefficient (C_M), and the fore and aft body shapes of the hull forms. The length of the centre hull is required to meet the slenderness requirement. Therefore, in this preliminary study, only the centre hull beam and draught are discussed below as they are likely to have more influence on wetted surface area than the remaining parameters.

In a general discussion about conventional monohull hull forms, Mannen **(Lewis 1989)** indicated that the optimum value of beam draught ratio to achieve the minimum wetted surface area for a given displacement, is about 2.25 for a block coefficient of 0.80 and about 3.0 at 0.5. Because the centre hull of a trimaran ship is a much more slender hull form compared with conventional monohulls, DRA Haslar **(Hall 1995)** has conducted specific studies which revealed that the minimum wetted surface area occurred at a beam

draught ratio of about 2.4. This is confirmed by the results of direct calculations shown in Figure 7.2, where the wetted surface areas have been calculated with constant hull slenderness at a block coefficient of 0.5 and with varied beam to draught ratios based on the centre hull of the UCL designed trimaran model **(Zhang 1993).** The calculation was carried out using the regression formula developed by **Holtrop et al (1984)** which included slender hull form data for the Series 64 models **(Yeh 1965).** This shows that the favourable beam draught ratio lies in between 2.0 and 2.5 for minimising frictional resistance.

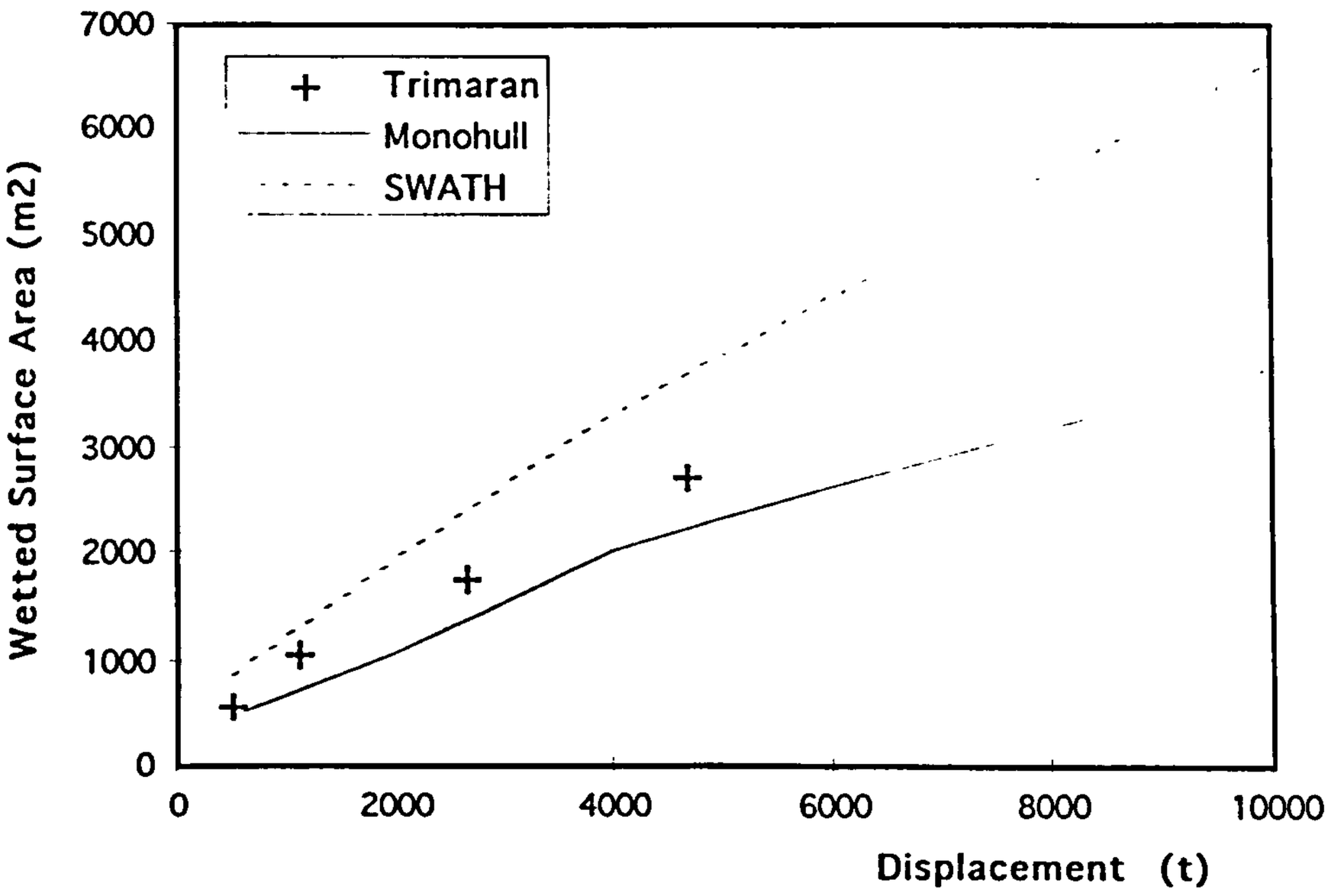

Figure 7.1 Wetted surface area

Note: Monohull and SWATH data are based on Fig. 6.2 in **(Kennell 1992)**
Trimaran data are based on UCL designs.

The side hulls contribute a large portion to the wetted surface area of a trimaran ship, approximately 30% of the total area in the case of the Haslar models. Therefore, reducing the side hull wetted surface area is one of the major considerations in the side hull configuration choice. The dominant side hull parameters for wetted surface area are length and draught. As the side hull configuration is a very complicated issue influenced by considerations in stability, seakeeping, resistance, as well as by manoeuvrability, this issue is discussed further in Chapter 9 where trimaran general design procedures and considerations for side hull configurations are explored.

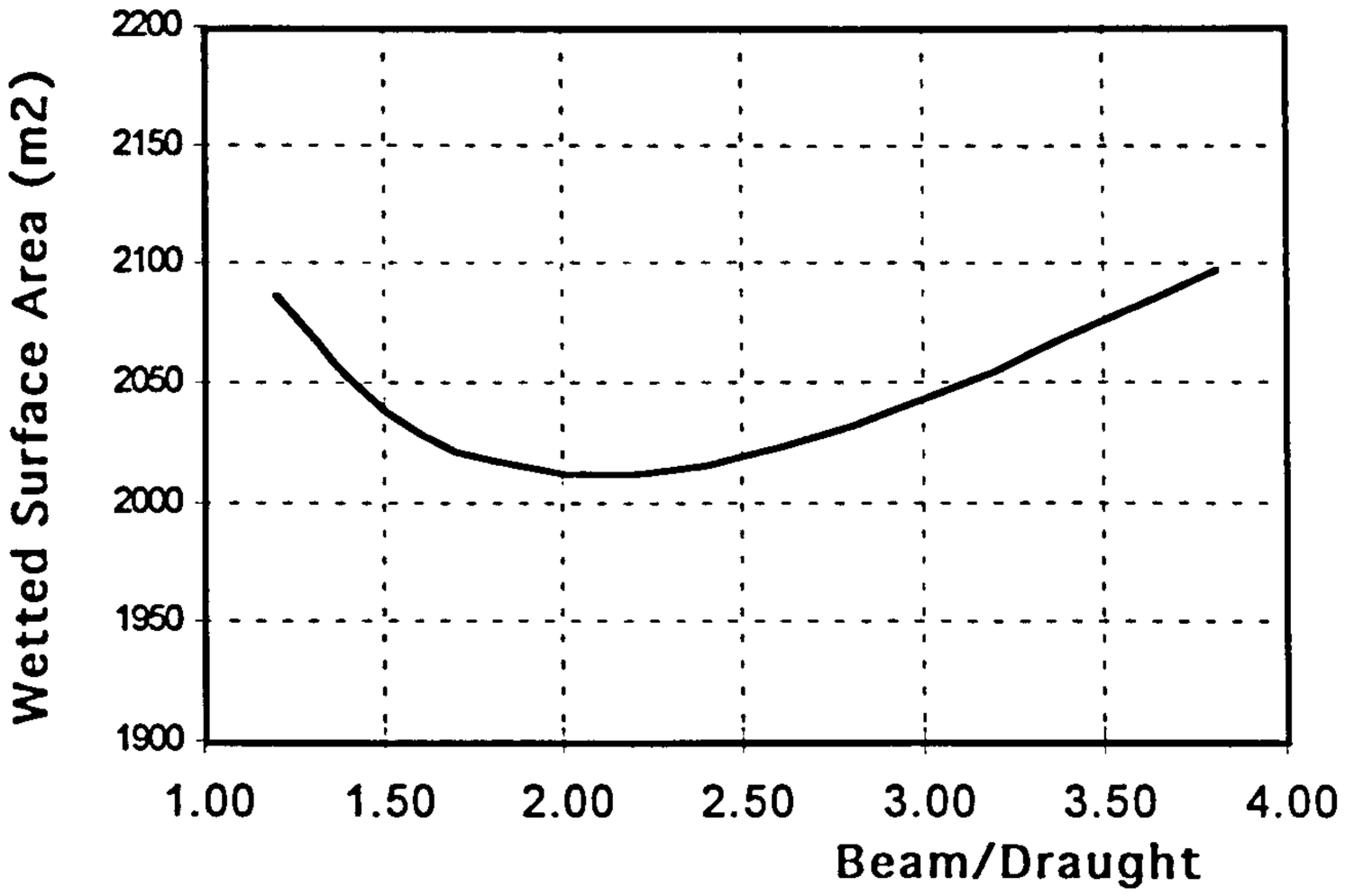

Figure 7.2 Wetted surface area of the centre hull of constant slenderness

7.3 Wavemaking Resistance

The three hulls of a trimaran ship will produce more complex wave patterns than a monohull ship as the waves produced by the hulls will interfere with each other. Thus the wavemaking resistance of a trimaran ship will not only depend on the sizes and shapes of the hulls but will also strongly depend on the relative positions of the hulls **(Everest 1968)**. Though the model experiment is conceived as a very reliable method for predicting wavemaking resistance, it was only possible to conduct a limited number of tests because of the high cost. To investigate the effects of the various trimaran configurations on the wavemaking resistance, a more cost effective theoretical method was sought for the computation of the wavemaking resistance. The previous research work **(Lunde 1951) (Noblesse 1983) (Wilson & Hsu 1992)** has showed that a thin ship theory is a valuable tool for computing the wavemaking resistance of monohull and multihull ship complement any model experiments. Under the thin ship assumption **(Wehausen 1973)**, a computer program has been developed at UCL by Wu recently based on his previous work on a three dimensional potential flow theory **(Wu 1988)** and has been used for predicting the trimaran wavemaking resistance **(Zhang 1996b)**. This theory is not explained in detail here, since the author has not been involved in the development of the computer program but has just used it as an analytical tool.

wavemaking drag will equal the energy dissipated by the wave system. To describe the wave system, the velocity potential can be simulated by suitable singularity distributions. Based on these, using the thin ship approximation, the wavemaking resistance of a ship can be expressed as **(Wehausen 1973)**:-

$$R_w = \frac{\rho k^2}{\pi} \int_0^{\frac{\pi}{2}} |H|^2 \sec^3 \theta d\theta \tag{7-5}$$

where $k = g/V^2$, g is gravity acceleration, V is the speed of the ship, ρ is the density of water, and H is the Kochin Function **(Wehausen 1973)** defined as:-

$$H = 4\pi \int_S \sigma \exp(zk \sec^2 \theta + i(x \cos\theta + y \sin\theta) k \sec^2 \theta) ds \tag{7-6}$$

where σ is the source strength function, and the integral S is over the whole of the submerged surfaces of the three hulls. The coordinate system of the trimaran ship used in the formulation is the same as that used in Chapter 5 (Figure 5.1).

In most of the previous studies **(Wilson & Hsu 1992)(Hanhirrova 1995)** on the application of the thin ship theory, the sources were distributed on the central plane of the ship. For multihull ships, the Kochin function needed to have different source strength expressions for the three hull form components. The method used here is to place the sources on the hull surfaces to deal with the added complexity of the multihulls. By distributing the sources over the hull surfaces, the wave system generated by each of the hulls and the wave system generated between the hulls are all accounted for in the calculation. Furthermore, the "thin ship" restriction to the method can be eliminated when the sources are placed on the hull surface. The boundary element technique has been used in the integration of the Kochin function instead of the traditional method which requires the hull geometry to be described mathematically **(Wilson & Hsu 1992) (Hanhirrova 1995)**. This allows the program to be used for more complex hull forms.

7.4 Comparisons between Computations and Model Experiments

The wave making resistance prediction method described in the previous section and the computer program were first verified. The two trimaran hull forms **(Zhang 1993)** designed for the DRA Haslar model experiments were used for the validation of the program. Table 4.1 (Chapter 4) gives a list of the full scale principal particulars of the two trimaran ships designated as Ship 1 and Ship 2.

Surface meshes

To use the computer program which calculates the wavemaking resistance for a trimaran ship, surface meshes need to be generated for the hulls as input to the program. As in the seakeeping analysis (Chapter 5), triangular panels were used in generating the meshes. The sensitivity of the surface mesh density was checked. It was found that the surface meshes required for the wavemaking calculations are much denser than the meshes required by previous seakeeping calculations, particularly in way of the bow of the ship. This led to three thousand panels being required for each of the trimaran ships. With this number of panels the computation showed 'steady' results. An AutoLISP program **(Zhang 1996b)** was also written which read the mesh data and produced 3D drawings of the mesh for a visual check of the mesh generated. Figure 7.3 shows a mesh generated for one of the Ship 2 configurations.

Presentation of resistance coefficients

The residuary resistance coefficient C_R of the tested model is derived by subtracting the frictional resistance from the total measured resistance. The frictional resistances for the central hull and the side hulls are calculated separately using the "ITTC 1957 model-ship correlation line". C_R is then in the form of:-

$$C_R = \frac{R_T - R_{FC} - 2R_{FS}}{\frac{1}{2}\rho V^2 (S_C + 2S_S)} - C_A \tag{7-7}$$

where R_T is the total resistance of the model, R_{FC} is the calculated frictional resistance for the centre hull, R_{FS} is the calculated frictional resistance for each side hull, S_C is the

wetted surface area of the central hull, S_s is the wetted surface area of a side hull, and C_A is the correlation factor of 0.0004 **(Lewis 1989)**

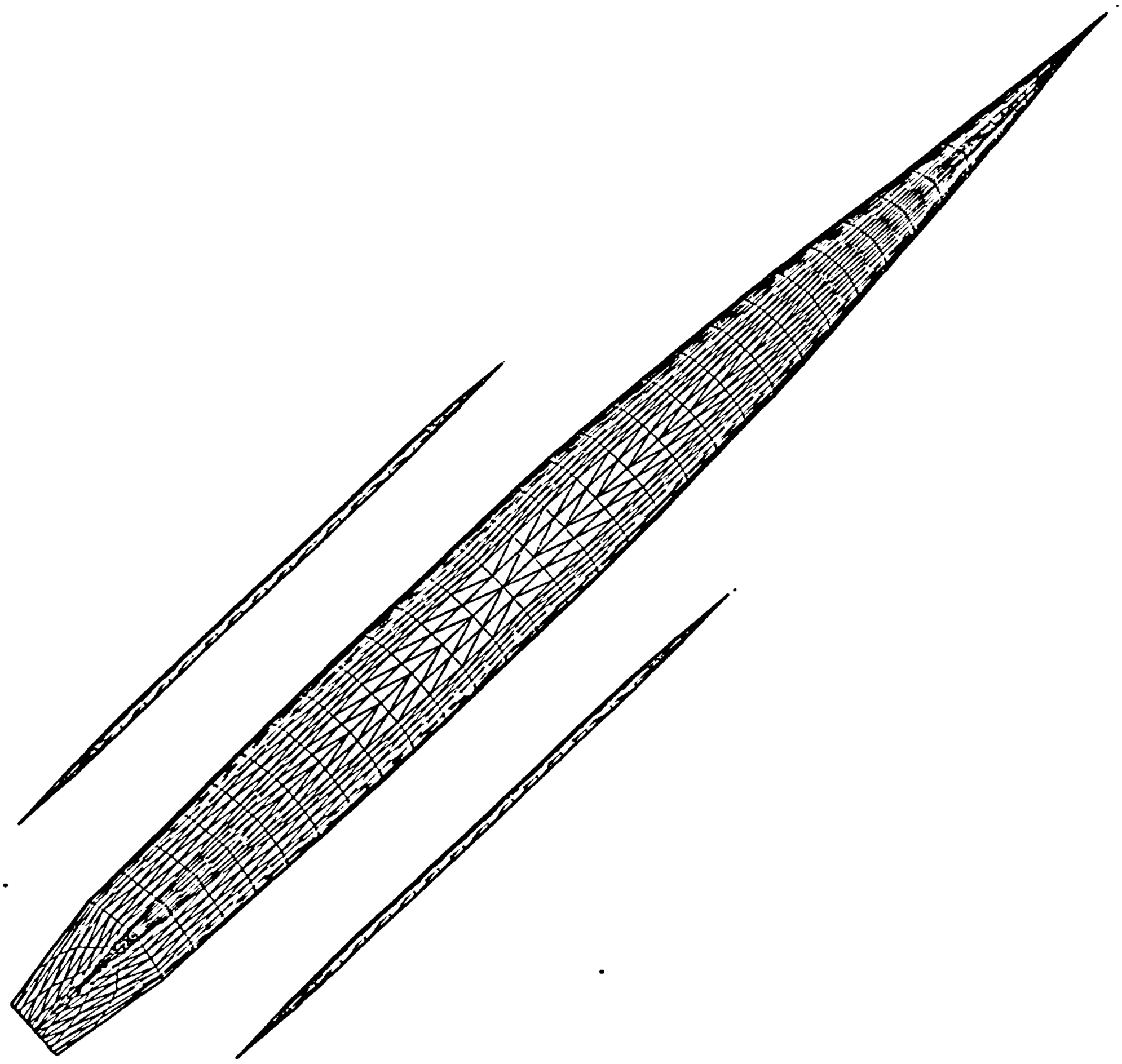

Figure 7.3 A 3D mesh generated for resistance computation

For slender ship hulls, the form resistance is very small, so the measured residuary resistance is dominated by wavemaking resistance. The following comparisons are between the computed wavemaking resistance and the measured residuary resistance of the model ships. The nondimensional coefficient of the computed wavemaking resistance is:

$$C_w = \frac{R_W}{\frac{1}{2}\rho V^2 (S_C + 2S_S)} \tag{7-8}$$

where R_W is the computed wavemaking resistance. For clear plotting, all the wavemaking resistance coefficients in the following diagrams have been multiplied by 10^3.

Verification

Figure 7.4 shows the calculated wavemaking resistance coefficient C_W for Ship 2 (wide beam and small side hulls configuration) compared with the results of the model experiments **(DRA 1995)**. The computed wavemaking resistance coefficients show good agreement between the computation and the model experiments up to a ship's speed of 25 knot. The computed C_w is higher than that of the model test result in the speed range between 25 knot and 35 knot. Figure 7.5 is the same diagram for Ship 1 (narrow beam and big side hulls configuration) which shows a similar trend to Figure 7.4.

The computed C_w has then been corrected using the model experiment data by multiplying by a correction coefficient. A better agreement between the computations and the model tests has been shown in Figures 7.6 and 7.7. As the merit of the theoretical computation of wavemaking resistance would be its relative nature rather than the absolute nature, the good agreement in Figures 7.6 and 7.7 after the correction shows the method as a valuable comparison tool to be used in the trimaran configuration investigation. However, further improvements to the computation model or to the program are necessary if the program is to be used for a wider range of trimaran ships for which the simple correction method used above may not be appropriate, due to the limited available model experiment data. For the speed range between 35 and 40 knots, significant added resistance due to wave interference was shown in the model experiments **(DRA 1995)**, but was not predicted by the theoretical computation. This could be another area where more investigations should been conducted in the future research if the required top speed of a trimaran exceeds 35 knots.

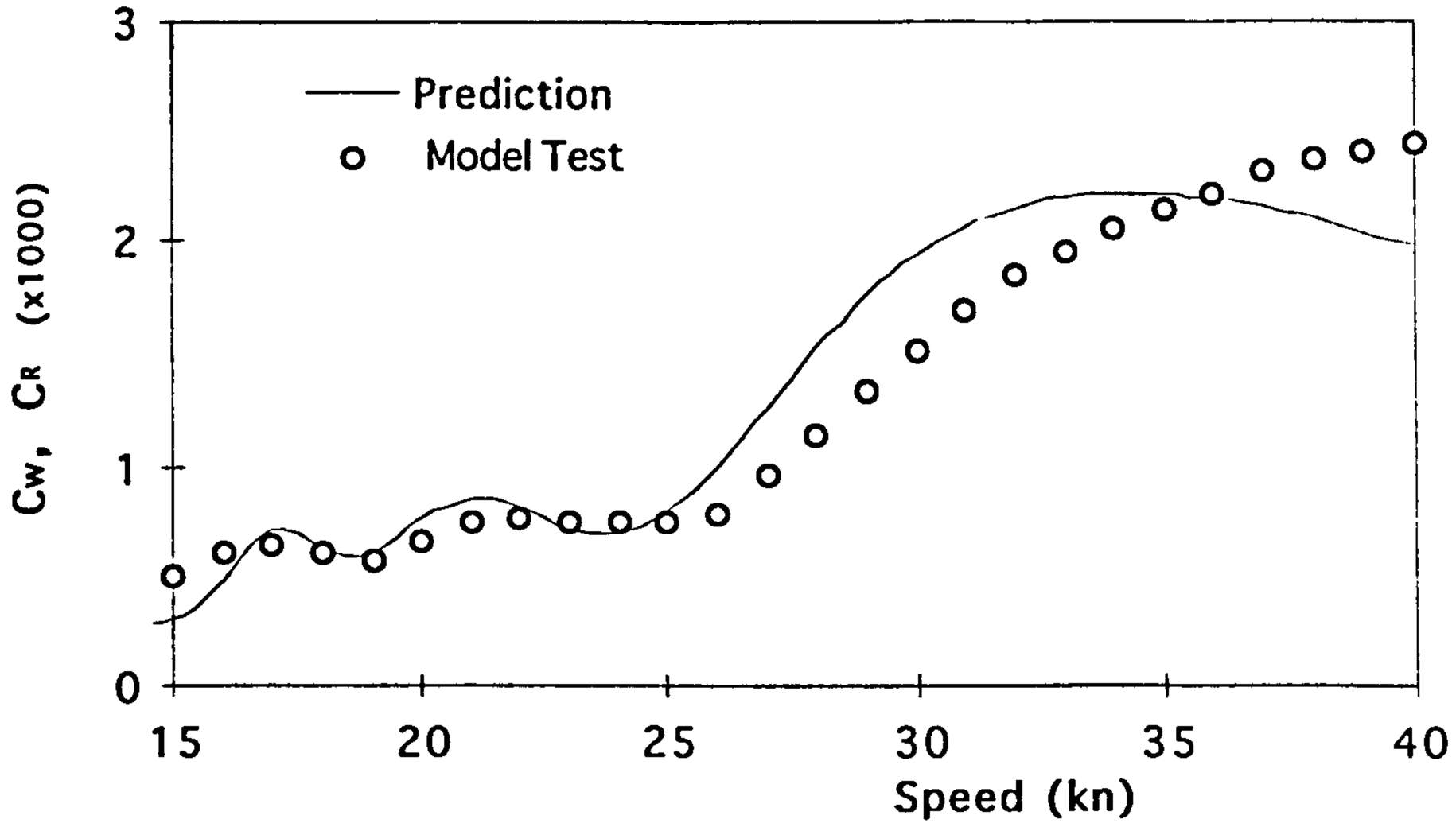

Figure 7.4 Comparison between predictions and experimental results for DRA model Ship 2

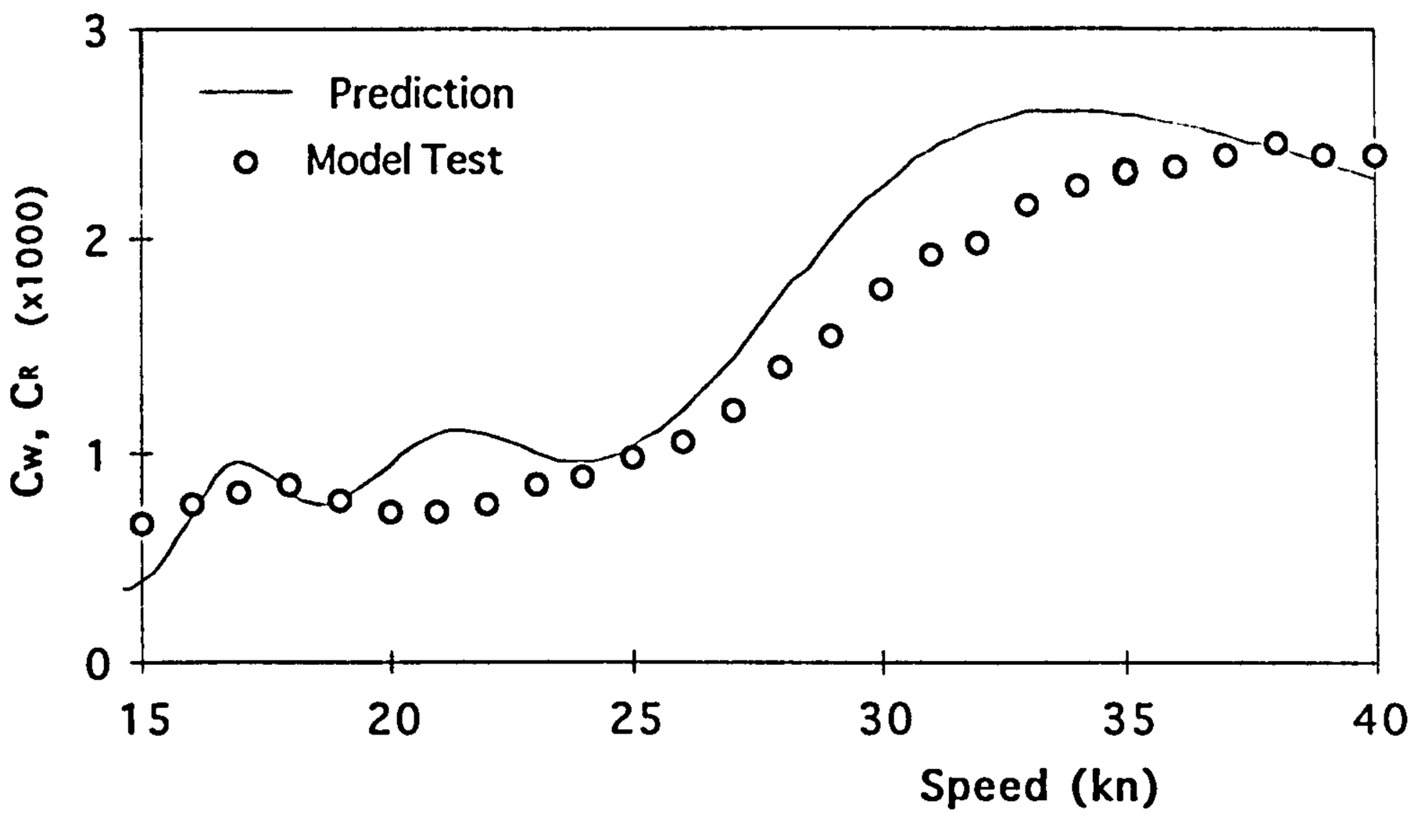

Figure 7.5 Comparison between predictions and experimental results for DRA model Ship 1

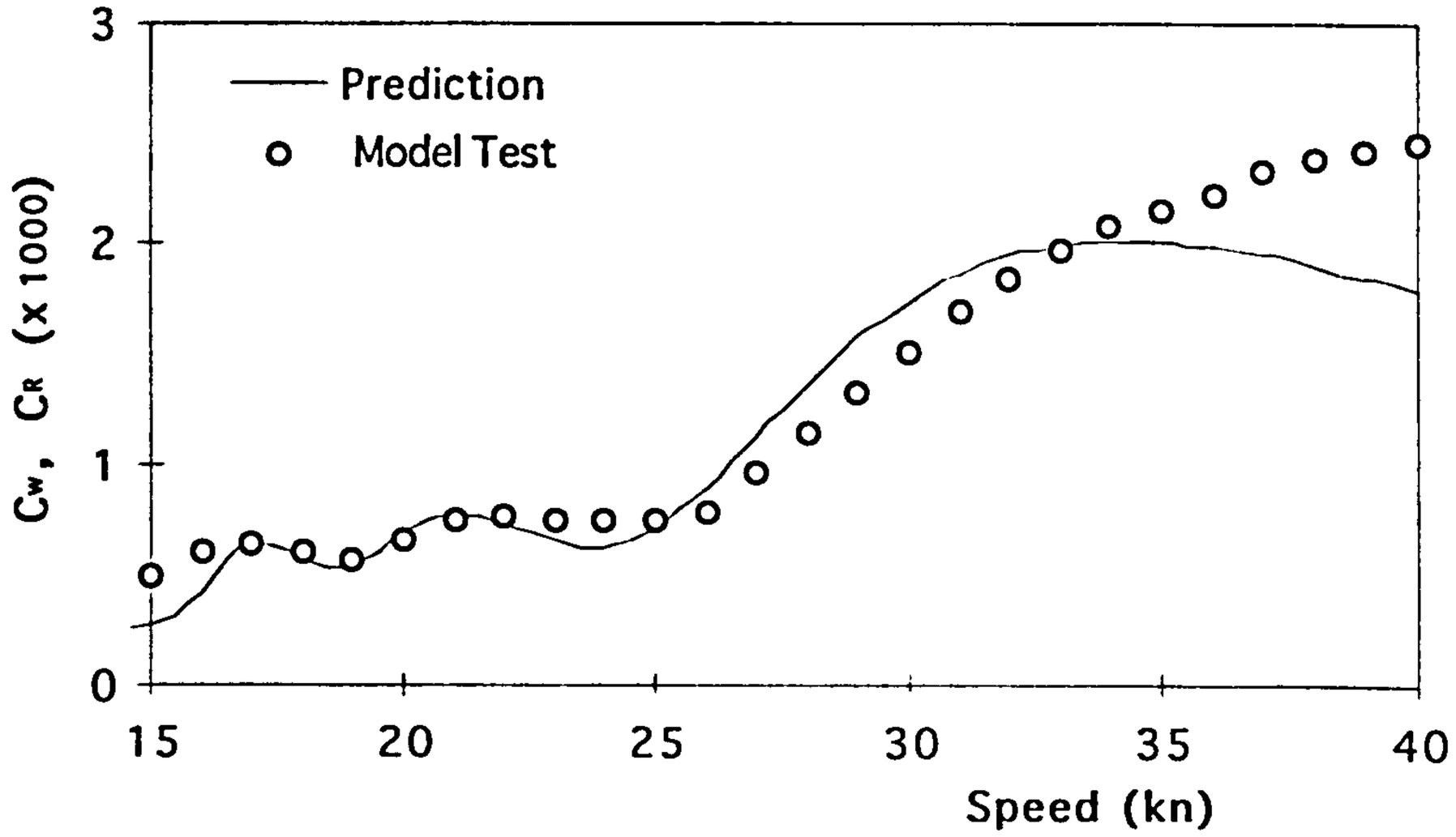

Figure 7.6 Wavemaking resistance corrected for DRA model test (ship 2)

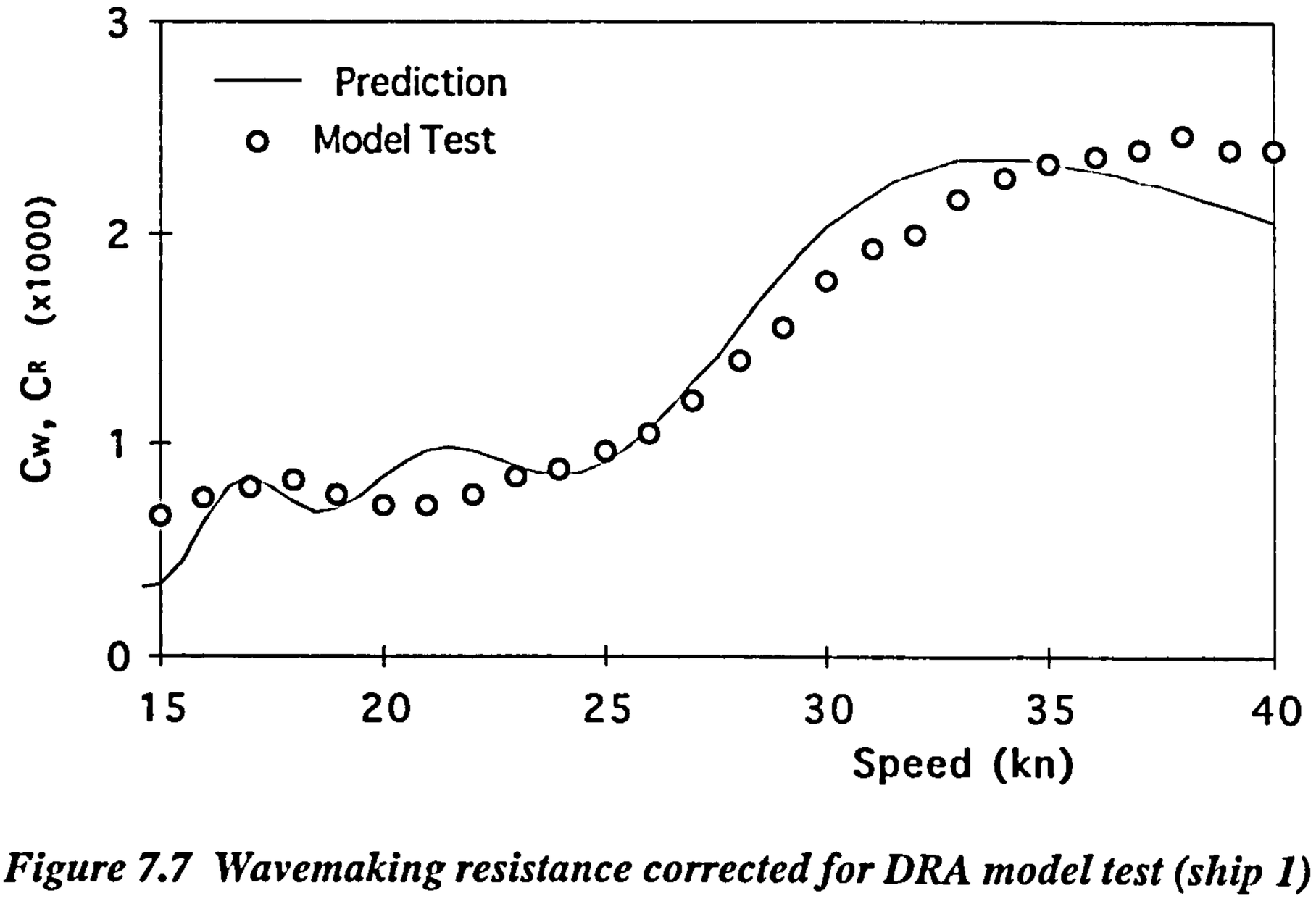

Figure 7.7 Wavemaking resistance corrected for DRA model test (ship 1)

7.5 Effects of Side Hull Configuration on Wavemaking Resistance

In an early study, **Everest (1968)** conducted a series of model experiments to investigate the wavemaking resistance for multihull vessels. One of his experiments, on an equal length triple hull model, showed that the wave making resistance could be reduced when the three hulls were positioned such that wave cancellation effects occurred. To find out whether this phenomena exists for the trimaran ship, the computations of wavemaking resistance were carried out varying the configurations of the side hulls of model ship 2 (with a centre hull length L_c=*150m* and side hull length L_s=*60m*).

Initially, the variations were limited to the longitudinal position of the side hulls. Figure 7.8 indicates the variations of side hull position investigated. Varying the shape and the transverse position of side hulls may also effect the wavemaking resistance of a trimaran ship. As the side hulls are so narrow and slender, with a Ⓜ of 10.3 for Ship 1 and 12.0 for Ship 2, any minor changes in hull shapes would have little influence on wavemaking resistance. The transverse location of the side hulls could normally be restricted by other design considerations, such as, stability, operational maximum beam restriction, and layout requirements. Therefore, the analysis was focused the longitudinal side hull position variations in this study.

The following is a list of the side hull configurations investigated, where the side hull set back l_s is the distance from the fore perpendicular of the side hulls to the fore perpendicular of the central hull:-

l_s = 30 metres;
l_s = 45 metres, (i.e. the side hulls are at amidships);
l_s = 60 metres, (i.e. the designed side hulls position for the DRA 1995 model tests);
l_s = 75 metres, (i.e. fore ends of the side hulls are at amidships);
l_s = 90 metres, (i.e. aft ends of the side hulls are in line with the stern of the central hull).

An additional configuration has also been calculated with l_s = 120 metres, where half length of the side hulls is behind the stern of the centre hull. Obviously, this is not a realistic design configuration from the layout and structural points of view, but was

included to show the trend of the wavemaking resistance due to the locations of the side hulls.

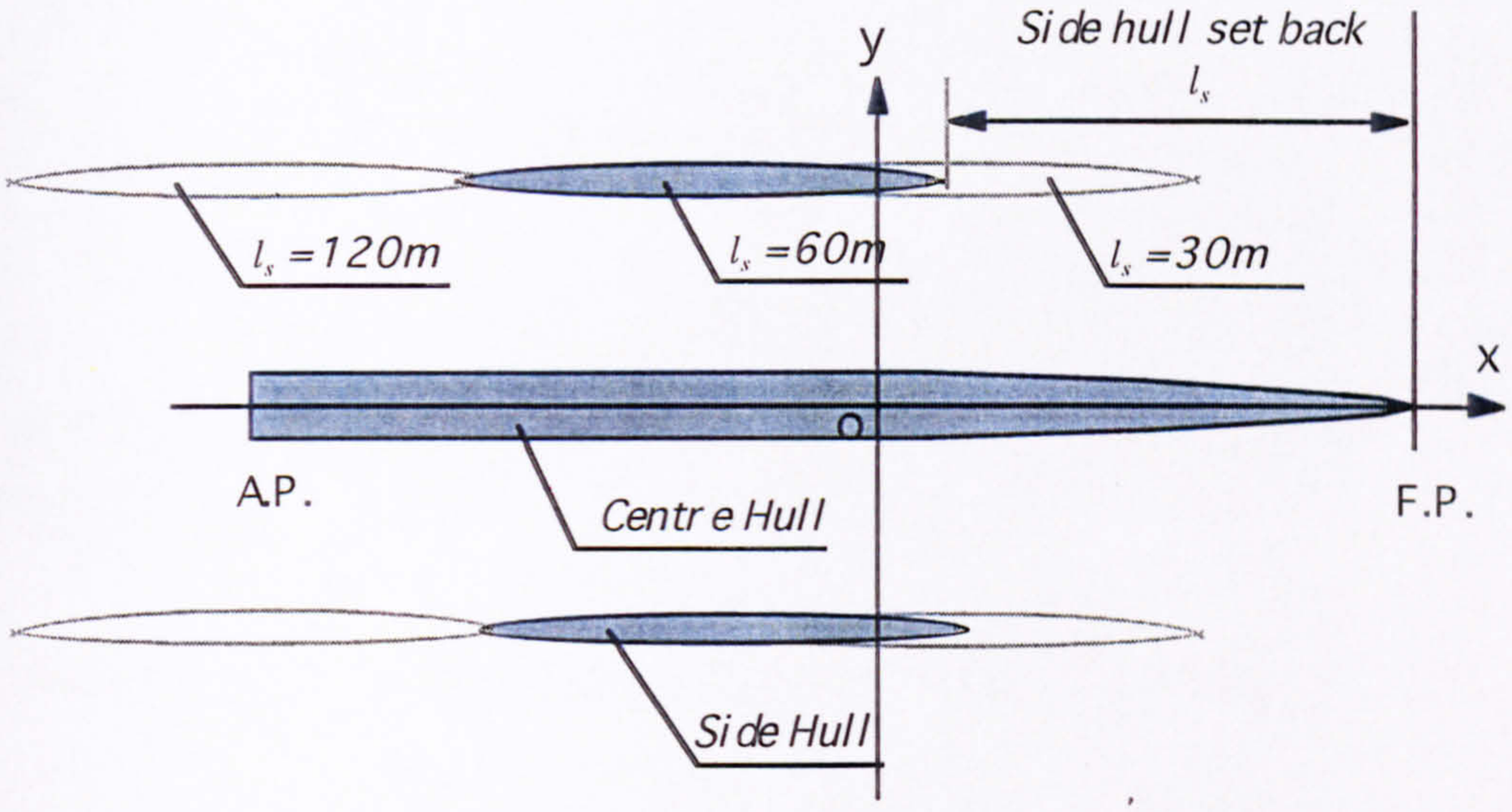

Figure 7.8 Variations of side hull locations

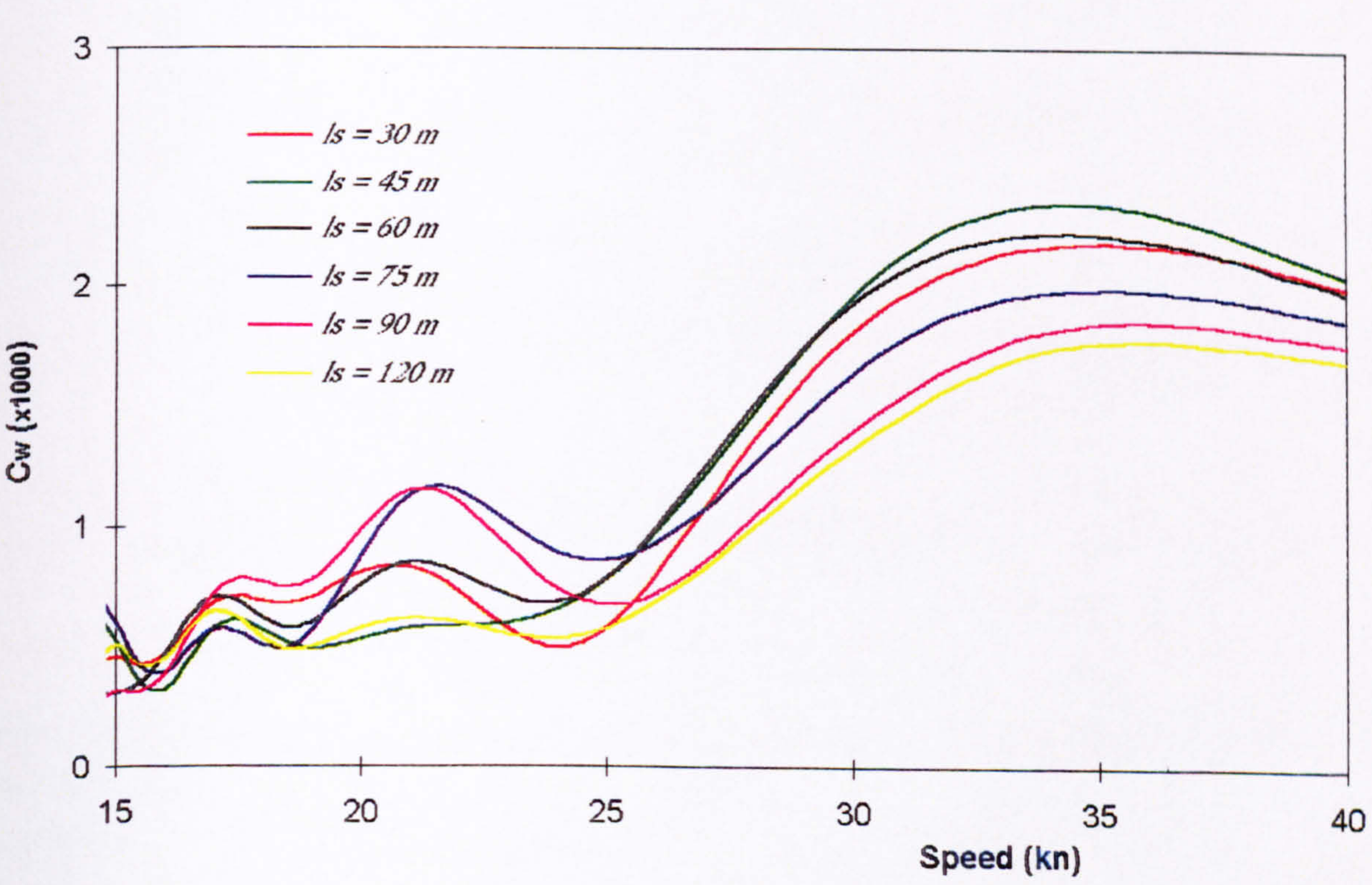

Figure 7.9 Effects of side hull location on C_w for DRA model Ship 2 from wavemaking resistance computation

Wavemaking resistance coefficient C_w curves were computed for all of the configurations and are plotted on Figure 7.9. At speeds higher than about 25 knots, i.e., beyond the second hump of each curve, it is clear that the wavemaking resistance reduces as the side hulls are moved towards the stern of the ship. To show the trend more clearly, the C_w curves of the trimaran Ship 2 at 30 and 40 knots are plotted against the side hull positions in Figure 7.10. At the speed of 30 knots, high C_w occurred when the side hull are located at the positions between $l_s = 45$ metres and $l_s = 60$ metres. Lower value of C_w is achieved when the side hull is located at the position of $l_s = 90$ metres where the aft ends of the side hulls are in line with the stern of the central hull. A similar trend can be noticed for the ship at the speed of 40 knots but the highest C_w occurred when the side hulls are at the fore most position of the variations around $l_s = 45$ metres.

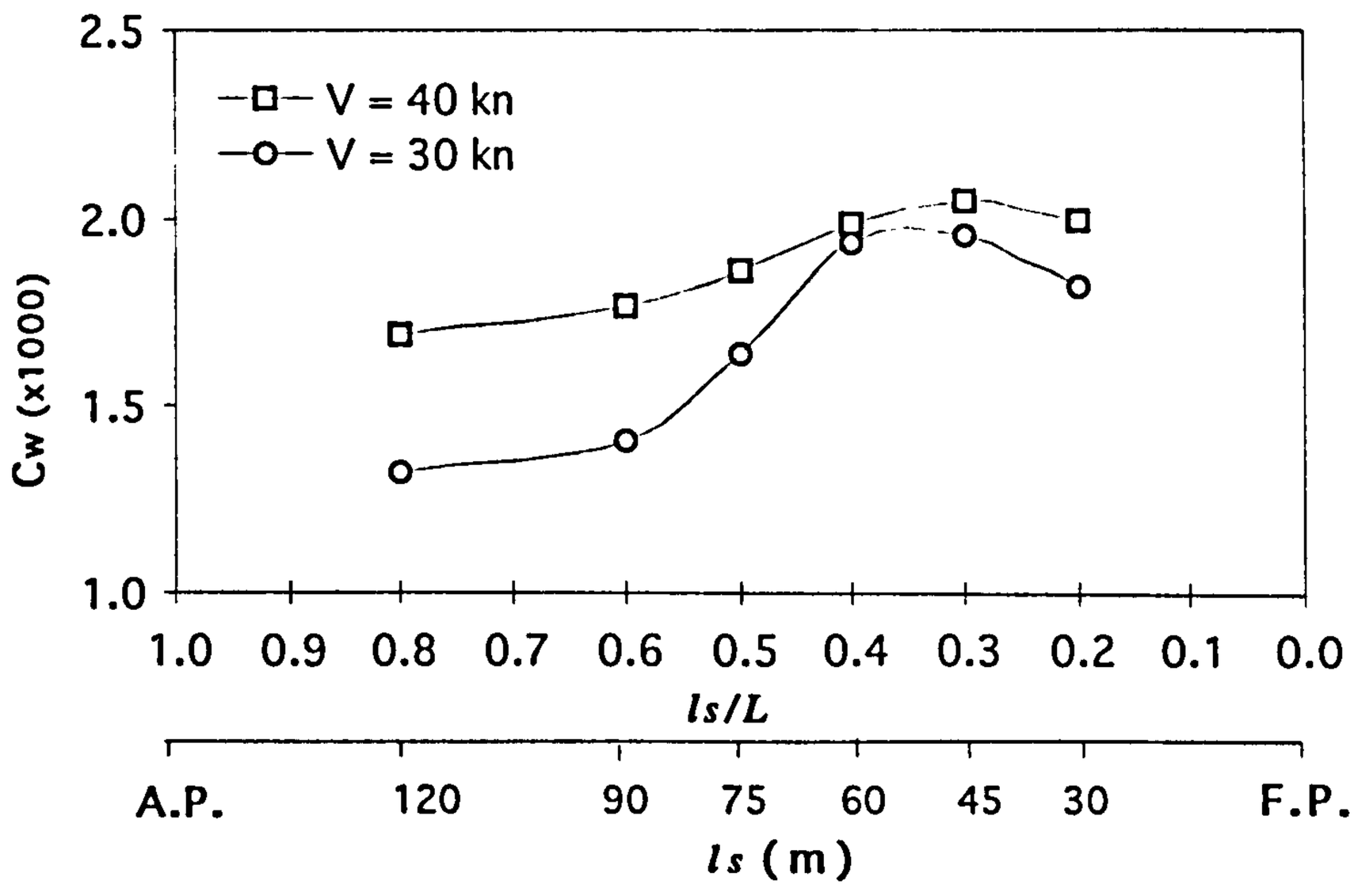

Figure 7.10 C_w vs. location of the side hulls for DRA model Ship 2

The wavemaking resistance of the trimaran ship at speeds below 25 knot varies depending on the position of the side hulls and the design speed. Different side hull locations give different shape of humps in the speed range as shown in Figure 7.9. The highest C_w hump for most of the variations occurs at the speed around 22 knots which is the second hump in the speed range covered . Figure 7.11 shows the C_w curve with variation in the position of the side hulls at the speed of 22 knots and the highest value of C_w occurs between $l_s = 75$ metres and $l_s = 90$ metres. This is the speed which should be

avoided if possible when choosing operational speeds for a trimaran ship of a similar configuration if the side hulls are positioned to achieve the maximum wave cancellation effect at the design speed of 30 knots.

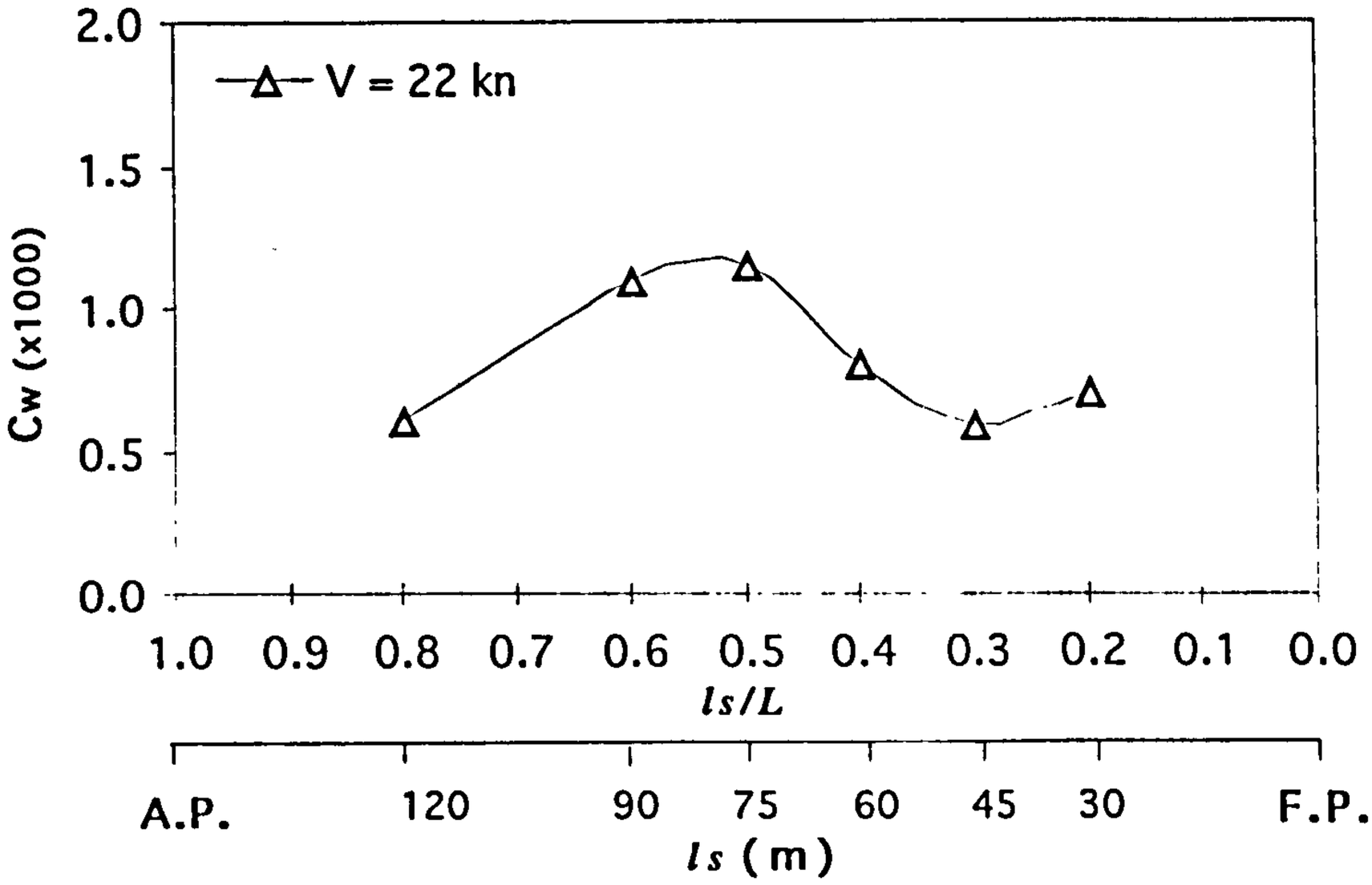

Figure 7.11 C_w vs. location of the side hulls for DRA model Ship 2 at V=22kn

It is also of interest to identify the components of wavemaking resistance of a trimaran ship. Firstly, wavemaking resistance calculations are carried out for the central hull and the side hulls separately. The resulted wavemaking resistance coefficients C_{w0} excluding the wave interference between the hulls is:-

$$C_{w0} = \frac{R_{WC} + 2R_{WS}}{\frac{1}{2}\rho V^2 (S_C + 2S_S)} \qquad (7\text{-}9)$$

where R_{WC} is the wave making resistance of the central hull alone, and R_{WS} is the wavemaking resistance of a side hull alone.

Then the wavemaking resistance coefficient C_{wi} due to the wave interaction effects of the three hulls will be:-

$$C_{wi} = C_w - C_{w0} \qquad (7\text{-}10)$$

A positive C_{wi} represents added wavemaking resistance due to wave interference between the central hull and the side hulls. A negative C_{wi} means a reduction in total wavemaking resistance due to wave cancellation effects between the hulls.

Figures 7.12 shows the wavemaking resistance component curves for DRA model Ship 2 where the side hulls are located with l_s = 30 metres to l_s = 120 metres. The wave interaction coefficients (C_{wi}) are positive over most of the speeds ranges with l_s between 30 m to 75 m. These show added wavemaking resistance due to wave interference. In contrast, the wavemaking resistance component curves for the same ship with the side hulls are located at l_s = 90 metres, show the wave interaction coefficients to be negative over the speed range above 25 knots. This indicates a reduction in total wavemaking resistance due to wave cancellation effects between the hulls. A even greater wave cancellation effect can be seen when the side hulls are positioned at l_s = 120 metres.

These results demonstrate that the longitudinal position of the side hulls has a significant influence on the wavemaking resistance. Generally, at higher speeds, the ship will benefit by moving the side hulls toward the stern of the ship because of the wave cancellation effects.

In addition to the investigations into the effects of the longitudinal position of the side hull on wavemaking resistance, Figure 7.13 shows the wavemaking resistance comparison between the two DRA model configurations (Ship 1 and Ship 2), reflecting the effects of the side hull transverse position on wavemaking resistance. These two configurations have the same side hull longitudinal location but different side hull beams and transverse locations. The side hulls of Ship 2 are narrower (1.1 m in side hull beams) with a smaller displacement than that of Ship 1 (1.8 m in side hull beams). The span from side hull to the central hull is about 14 metres for Ship 2, and about 11 metres for Ship 1. As shown by Figure 7.13, Ship 2 has a lower wavemaking resistance than Ship 1 over all the speed range. This can be explained as the side hulls of Ship 2 are smaller and produce less waves than that of Ship 1.

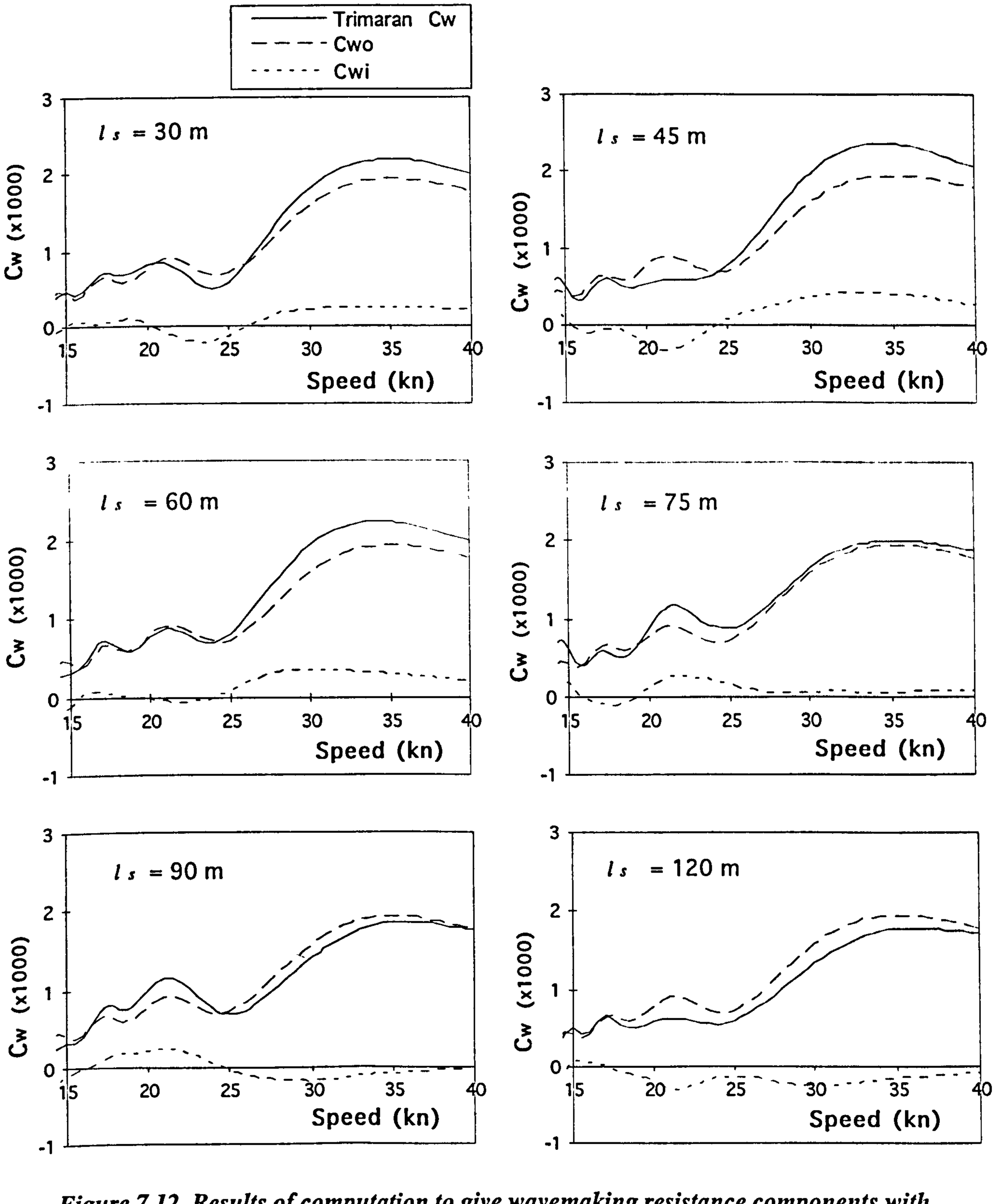

Figure 7.12 Results of computation to give wavemaking resistance components with varied side hull positions based on DRA model Ship 2

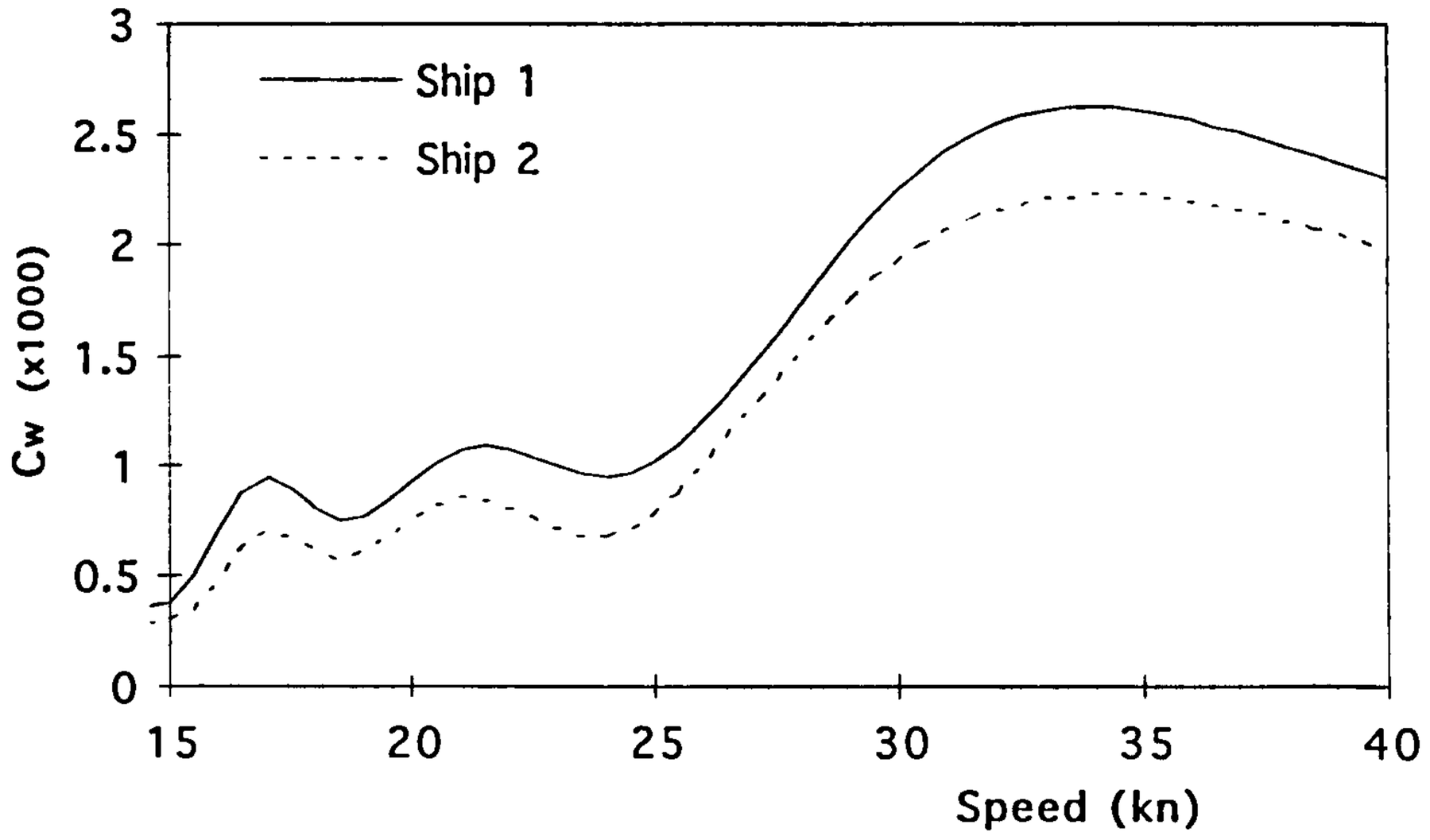

Figure 7.13 Comparison between Ship 1 and Ship 2

7.6 Conclusions

Initial investigations into the trimaran configurations have been conducted with regard to the characteristics of trimaran resistance. The results show that the resistance advantages of trimaran ships over conventional monohull ships particularly at top speed could be enhanced if the side hulls are positioned to achieve maximum wave cancellation effects.

Reasonably good agreement has been achieved between the computation results and the model experiment measurements. The analytical results show that the side hull position of the current model ships **(Zhang 1993)** designed for the DRA Haslar experiments is not the most favourable position in term of minimising wavemaking resistance. Less wavemaking resistance can be achieved if the side hulls are moved towards the stern of the ship where there would be better wave cancellation effects at the designed maximum speed of 30 knots.

Further research work is necessary to investigate the effects on the resistance of the trimaran ships of the side hull transverse position and the side hull shape. The objective is seen to be the determination of the best side hull configuration resulting in minimal wavemaking resistance as well as frictional resistance at design top speed while satisfying the stability requirements.

CHAPTER 8

MANOEUVRABILITY PREDICTION

8.1 Statement of Problems

Manoeuvrability is another area which needs to be explored for the new trimaran displacement ship. The trimaran ship, as revealed in the previous chapters, consists some new features not occurred to conventional monohull ships, including

- the use of an extremely slender centre hull,
- the adoption of two narrow side hulls,
- the possibility of adopting wing propulsion facilitated by the presence of the side hulls.

These features, which are not present in traditional monohull ships, would have certain effects on the manoeuvrability of the ship. As part of the justification of trimaran concept, the following questions have to be answered,

- To what extent does the new trimaran hull form affect its manoeuvrability?
- When considering the possibility of wing propulsion for trimaran ships, would the wing propellers alone be able to turn the ship effectively and eliminating the use of rudders?

In considering the above questions, we first need to identify what are the crucial criteria when examining the manoeuvrability of a trimaran ship. **Clark, Gedling & Hine (1982)** suggested three criteria for assessing manoeuvrability of a ship: the turning ability, course stability, and manual steering ability. The third one is more related to navigational needs and is not discussed further here. Of the first two criteria, it was felt that the turning ability of a trimaran ship needed to be more closely examined than the course stability. This is because the characteristics of the trimaran ship of a long slender hull and the two additional narrow side hulls which act like two fixed fins when manoeuvring, are likely to have positive effects on course stability and adverse effects on turning ability of the ship from the knowledge of monohull ships **(Burcher 1972) (Lewis 1989)**. On this basis, the course stability of a trimaran ship is expected to be better than that of an equivalent monohull ship. Therefore, when a preliminary investigation into the manoeuvrability of the trimaran ship was carried out by UCL in co-operation with DRA Haslar **(Zhang 1995a)**, it was decided that the key issue for the trimaran ship in this area was turning ability. The work presented in this chapter is on the prediction of turning ability for trimaran ship.

As there were no existing prediction methods for the manoeuvrability of the trimaran ship, a suitable method had to be developed. This is described in the following sections. The investigation starts with the effect of the new trimaran configuration on its turning ability when just using rudders, and then the turning ability of a trimaran just using wing propellers. The predictions are compared with available results from the model experiments carried out by DRA Haslar **(DRA 1995)**. The effects of varying the side hull configuration on turning ability are also examined.

8.2 Equations of Turning Motion

8.2.1 Basic Equations

The motion of a trimaran ship on the water surface can be described using Newton's equation of motion. From a fixed coordinate system $x_o O y_o$ as shown in Figure 8.1 the equations of motion of the ship can be written as:-

$$\begin{aligned} X_o &= m\ddot{x}_o \qquad \text{(surge)} \\ Y_o &= m\ddot{y}_o \qquad \text{(sway)} \\ N &= I_z\ddot{\psi} \qquad \text{(yaw)} \end{aligned} \tag{8-1}$$

where X_0 and Y_0 are total forces in x_0 and y_0 directions respectively, N is the total yaw moment, m is the mass of the ship, I_z is the mass inertia of the ship about the yaw axis, and ψ is the yaw angle.

By transferring the equations into a coordinate system xoy fixed on the ship, and neglecting surge, the equations of motion can be written as **(Clark, Gedling & Hine 1982)**:-

$$\begin{aligned} Y &= m(\dot{v} + ur + x_G\dot{r}) \\ N &= I_z\dot{r} + mx_G(\dot{v} + ur) \end{aligned} \tag{8-2}$$

where, Y is total forces in the sway direction y, x_G is the longitudinal distance from amidships to the centre of gravity of the ship, u and v are the longitudinal and lateral velocities, and r is the yaw rate of the ship.

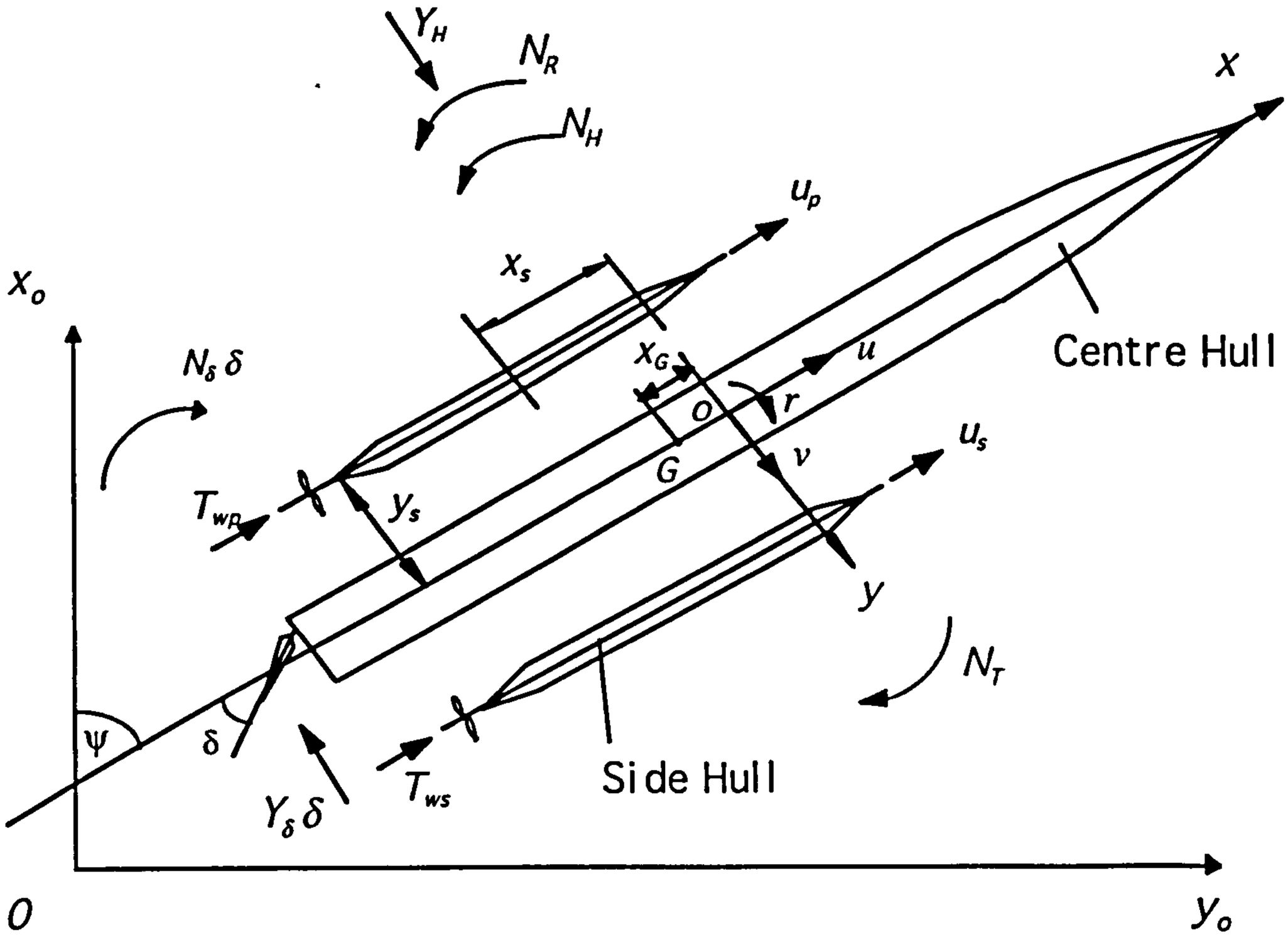

Figure 8.1 Orientation system and external forces

8.2.2 Forces Exerted on the Ship

To establish the equations for the turning motion for a trimaran ship, the forces acting on the ship need first to be identified. Assuming a trimaran ship fitted with rudders and wing propellers is under steady turning motion at a constant speed, the forces and moments acting on the ship, i.e. the left hand side of equations (8-2), can be expressed as:-

$$\begin{aligned} Y &= Y_H + Y_\delta \delta \\ N &= N_H + N_T + N_R + N_\delta \delta \end{aligned} \tag{8-3}$$

where, Y_H and N_H are hydrodynamic force and moment, N_T is moment produces by the wing propellers due to the differential in the port side propeller thrust force T_{wp} and the starboard side thrust force T_{ws}, N_R is the moment induced by the resistance differential of

the two side hulls, and the rudder force and moment are presented by the products of their control derivatives Y_δ and N_δ with the rudder angle δ.

It has to be noted that only the forces related to the turning moment are considered here as the equations to be derived are only for the turning motion of the ship.

Hydrodynamic forces due to ship motion

The hydrodynamic force Y_H and moment N_H are due to the motion of the ship body. These forces and moments can be expressed as linear functions of the velocities and accelerations of the ship **(Burcher 1971)**. When the ship is on a steady turn, the accelerations will be zero. The forces are then the linear functions of the velocities only as:-

$$\begin{aligned} Y_H &= Y_v v + Y_r r \\ N_H &= N_v v + N_r r \end{aligned} \tag{8-4}$$

where $Y_v, N_v, Y_r, N_r,$ are the linear coefficients which are the partial derivatives of the forces with respect to the velocities.

Thus the calculation of the hydrodynamic forces depends on the determination of these derivatives. The method for estimating velocity derivatives for trimaran ships is discussed in Section 8.3.

Turning moment by wing propellers

The turning (yaw) moment induced by the wing propellers is due to a thrust force differential of the two wing propellers when the ship is manoeuvring. This turning moment can be calculated as:-

$$N_T = \left(T_{wp} - T_{ws}\right) y_s \tag{8-5}$$

where T_{wp} and T_{ws} are the thrust force of wing propeller of port side and starboard side respectively, and y_s is the distance of the wing propeller shaft to the centre line plane of the ship.

Moment due to side hull resistance differential

When a trimaran ship is under a steady turning motion, the advance speed of the two side hulls will be different which are:-

$$\begin{aligned} u_p &= u + ry_s \quad \text{for port side hull} \\ \text{and} \quad u_s &= u - ry_s \quad \text{for starboard side hull} \end{aligned} \tag{8-6}$$

where u_p and u_s are the advance speeds of the port and the starboard side hulls respectively.

The difference in advance speeds results in different resistances for the two side hulls. This resistance differential tends to resist the turning of the ship and its resultant turning moment can be calculated as:-

$$N_R = -\left(X_{RP}(u_p) - X_{RS}(u_s)\right)y_s \tag{8-7}$$

where $X_{RP}(u_p)$ and $X_{RS}(u_s)$ are the resistance of the port side hull and the starboard side hull respectively. In the computation, the resistance X_{RP} and X_{RS} were taken in a form of regression equation of the calculated resistance as a function of the advance speed of the side hull as:-

$$X_R(u) = a_0 + a_1 u + a_2 u^2 + a_3 u^3 \tag{8-8}$$

where a_0, ..., a_3 are regression coefficients.

8.2.3 Steady Turning Radius

Having derived the forces acting on the ship, the equations of motion for a steady turn of the trimaran ship can be derived from the basic motion Equation (8-2) by eliminating acceleration terms as:-

$$\begin{aligned} mur - Y_v v - Y_r r &= Y_\delta \delta \\ mx_G ur - N_v v - N_r r &= (T_{wp} - T_{ws})y_s - (X_{RP} - X_{RS})y_s + N_\delta \delta \end{aligned} \tag{8-9}$$

Then the turning rate r of the ship can be derived from the above equation as:-

$$r = \frac{(T_{wp} - T_{ws})y_s - (X_{RP} - X_{RS})y_s + \frac{N_v Y_\delta \delta}{Y_v} + N_\delta \delta}{mx_G u - \frac{N_v}{Y_v}(mu - Y_r) - N_r} \tag{8-10}$$

Finally, the radius R of steady turning of the ship is:-

$$R = \frac{u}{r} \tag{8-11}$$

8.3 Estimate of Velocity Derivatives

In the turning ability calculation, the crucial task is to find an appropriate method for the estimate of velocity derivatives. The turning motion prediction largely depends on the determination of the derivatives. This section describes the method used in the calculation of the derivatives for the trimaran.

There are no existing analytical methods for the prediction of the hydrodynamic coefficient for trimaran ships or formal experimental data available on the manoeuvrability of trimarans, except for the brief experiment conducted at DRA Haslar on a trimaran model **(DRA 1995)**. However, decades of monohull manoeuvring research have produced some theoretical and empirical methods for the prediction of those derivatives, including empirical formulae from model tests **(Inoue, Hirano & Kijima 1981)**, strip theory **(Clark 1972)**, 3D potential flow analysis, and regression analysis **(Clark, Gedling & Hine 1982)**. To utilise this knowledge developed for monohull ships, the derivatives of the trimaran ship have therefore not been calculated as a whole but produced separately for the centre hull and the side hulls, ignoring the interaction effects between the hulls.

Centre Hull

The derivatives of the centre hull are calculated using the empirical formula developed by **Inoue, Hirano & Kijima (1981)** from experiments, which covered a wide range of hull forms at various loading conditions. The formulae are listed as follows:-

$$Y_{vc} = -\frac{1}{2}\rho LTu\left(\pi\frac{T}{L} + 1.4C_B\frac{B}{L}\right)\left(1.0 + 2\frac{\Delta T}{3T}\right)$$

$$Y_{rc} = \frac{1}{2}\rho L^2 Tu\left(\frac{\pi}{2}\frac{T}{L}\right)\left(1.0 + 0.8\frac{\Delta T}{T}\right)$$

$$N_{vc} = -\frac{1}{2}\rho L^2 Tu\left(\frac{2T}{L}\right)\left(1.0 - 0.27\frac{\Delta T}{T}\right) \qquad (8\text{-}12)$$

$$N_{rc} = -\frac{1}{2}\rho L^3 Tu\left(0.54\frac{2T}{L} - \left(\frac{2T}{L}\right)^2\right)\left(1.0 + 0.3\frac{\Delta T}{T}\right)$$

where, L, B and T are the length, beam, and draught of the hull, C_B is the block coefficient, and ΔT is the trim of the ship.

Side Hulls

In the absence of experimental or real ship data, there are two possible ways to estimate the velocity derivatives for the side hulls. One is to treat the side hull in the same way as the centre hull described above, using empirical monohull formula to calculate the derivatives for the side hulls and then adding them to give the total derivatives of the ship. Another way is to treat the side hulls as fixed fins and to calculated the derivatives directly from the lifting forces produced by these fins

Jacobs (1964) showed that the hydrodynamic derivatives of the bare hull and deadwood combination can be computed with reasonable accuracy by simply adding the contributions of the appropriate fixed fins to the bare hull derivatives, neglecting the interference effect between the hull and the fins. Based on this concept, the computation of the trimaran derivatives can be done by adding the derivatives of the side hulls to the derivatives of the centre hull. Considering the characteristics of the side hulls of the trimaran Ship 2 as shown in Table 4.2, with a length to beam ratio of 52 and a beam to draught ratio of 0.33, the side hulls are extremely narrow and deep compared with a normal monohull. Thus, it is considered more appropriate to use the fixed fin concept for the estimation of the side hull derivatives.

The derivatives for the narrow side hulls are therefore can be calculated using equations given by **Jacobs (1964)** for fixed fins. The sway velocity derivative Y_{vs} of a side hull is:-

$$Y_{vs} = -\left|\left(\frac{\rho}{2}\right)A_f u^2\left(\frac{\partial C_L}{\partial \beta}\right)\right| \qquad (8\text{-}13)$$

where A_f is the profile area of the side hull, and $\partial C_L/\partial\beta$ is the slope of lift coefficient curve. The negative sign in the equation indicates the derivative Y_{vs} is always negative as the lifting force acting on the fin is always in the opposite direction to the lateral velocity v.

Since the effective aspect ratio of the side hulls of a trimaran ship is very low, a simple formula developed for slender wings **(Hoerner & Borst 1975)**, which is suitable for fins of very low effective aspect ratio with $a<1.0$, can be used to solve the value of lift-curve slope $\partial C_L/\partial\beta$ for the side hulls as:-

$$\frac{\partial C_L}{\partial \beta} = \frac{\pi}{2} a \tag{8-14}$$

where a is the effective aspect ratio of the fin-like side hull:

$$a = \frac{2T_s}{L_s} \tag{8-15}$$

where L_s is the length of the side hull, and T_s is the draught.

Now, the other velocity derivatives of the side hull can be readily derived from the sway derivative Y_{vs} of the side hull as:-

$$\begin{aligned} Y_{rs} &= Y_{vs}\, x_s \\ N_{vs} &= Y_{vs}\, x_s \\ N_{rs} &= Y_{vs}\, x_s^2 \end{aligned} \tag{8-16}$$

where x_s is the distance from the middle point of the side hulls to amidships of the centre hull as shown in Figure 8.1.

The Whole Ship

Noting the assumption of no interference effects between hulls, the velocity derivatives of the trimaran ship can then be obtained by adding that of the centre hull and side hulls together as:-

$$
\begin{aligned}
Y_v &= Y_{vc} + 2Y_{vs} \\
Y_r &= Y_{rc} + 2Y_{rs} \\
N_v &= N_{vc} + 2N_{vs} \\
N_r &= N_{rc} + 2N_{rs}
\end{aligned}
\qquad (8\text{-}17)
$$

8.4 Turning Ability Using Rudders

The turning ability of the trimaran ship can now be examined using the method described in the last two sections. The aim is to find out how the trimaran hull form will significantly affect the turning ability of the ship. In order to compare calculated results with the model experiment, also to investigate the effects of the trimaran configuration on the ship's turning ability compared to conventional monohull ships, only rudder forces are considered in this section. The effects of any possible side hull propulsion on turning ability are discussed in Section 8.5.

8.4.1 Rudder Forces

The rudder forces present during the turning of the ship can be derived by means of evaluating the control derivatives as in equation (8-3). The derivatives are calculated from the following equations **(Clark, Gedling & Hine 1982)**:-

$$
\left.
\begin{aligned}
Y_\delta &= \frac{1}{2}\rho u^2 A_R \left(\frac{\partial C_L}{\partial \delta}\right) \\
N_\delta &= x_r Y_\delta
\end{aligned}
\right\} \qquad (8\text{-}18)
$$

where A_R is the rudder area, x_r is the distance of the rudder from amidships, and the other terms are as previously defined. The lift curve slope $(\partial C_L/\partial \delta)$ of the rudder is computed using a semi-empirical formula derived by **Whicker & Fehlner (1958)** from extensive experimental data as:-

$$
\left(\frac{\partial C_L}{\partial \delta}\right) = \frac{1.8\pi a}{(\cos\lambda)\sqrt{\dfrac{a^2}{\cos^4\lambda} + 4 + 1.8}} \qquad (8\text{-}19)
$$

where a is the effective aspect ratio of the rudder, λ is the sweep angle of the quarter-chord line

The trimaran ship and its rudder arrangement are the same as Ship 2 designed (see Table 4.1) for DRA Haslar model experiments (**DRA 1995**). Two balanced rudders are located right behind the twin propellers at the stern of the centre hull. The characteristics of the rudders used in the computation are the same as of the rudders fitted on to the model as shown in Figure 8.2. Table 8-1 gives major coefficients of the rudders.

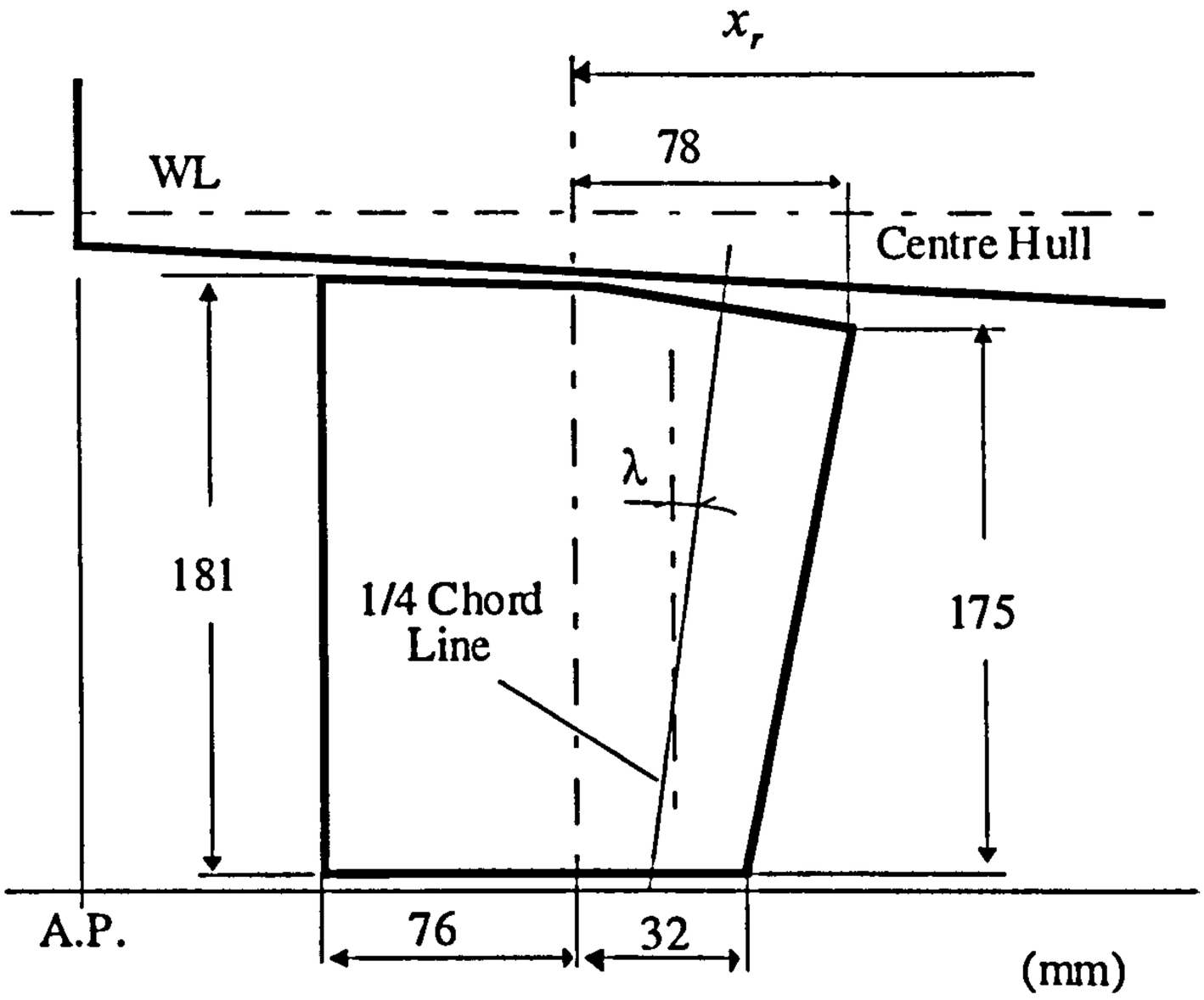

Figure 8.2 Sketch of the rudder (model scale)

Table 8.1 Details of the rudders

Type	Balanced rudder
Total area (%LT)	3.57
Effective aspect ratio a	0.276
Sweep angle λ(rad)	0.248

8.4.2 Computation and Verification

The turning ability prediction method has been implemented into a computer program using MATHCAD. Steady turning radii have been computed for the DRA model Ship 2 at various rudder angles for a range of rudder areas, from $A_R = 1\%LT$ *to* $A_R = 5\%LT$, as

shown in Figure 8.3. A_R denotes the rudder area as a percentage of the ship's profile area which is the product of the length *(L)* and draught *(T)* of the ship.

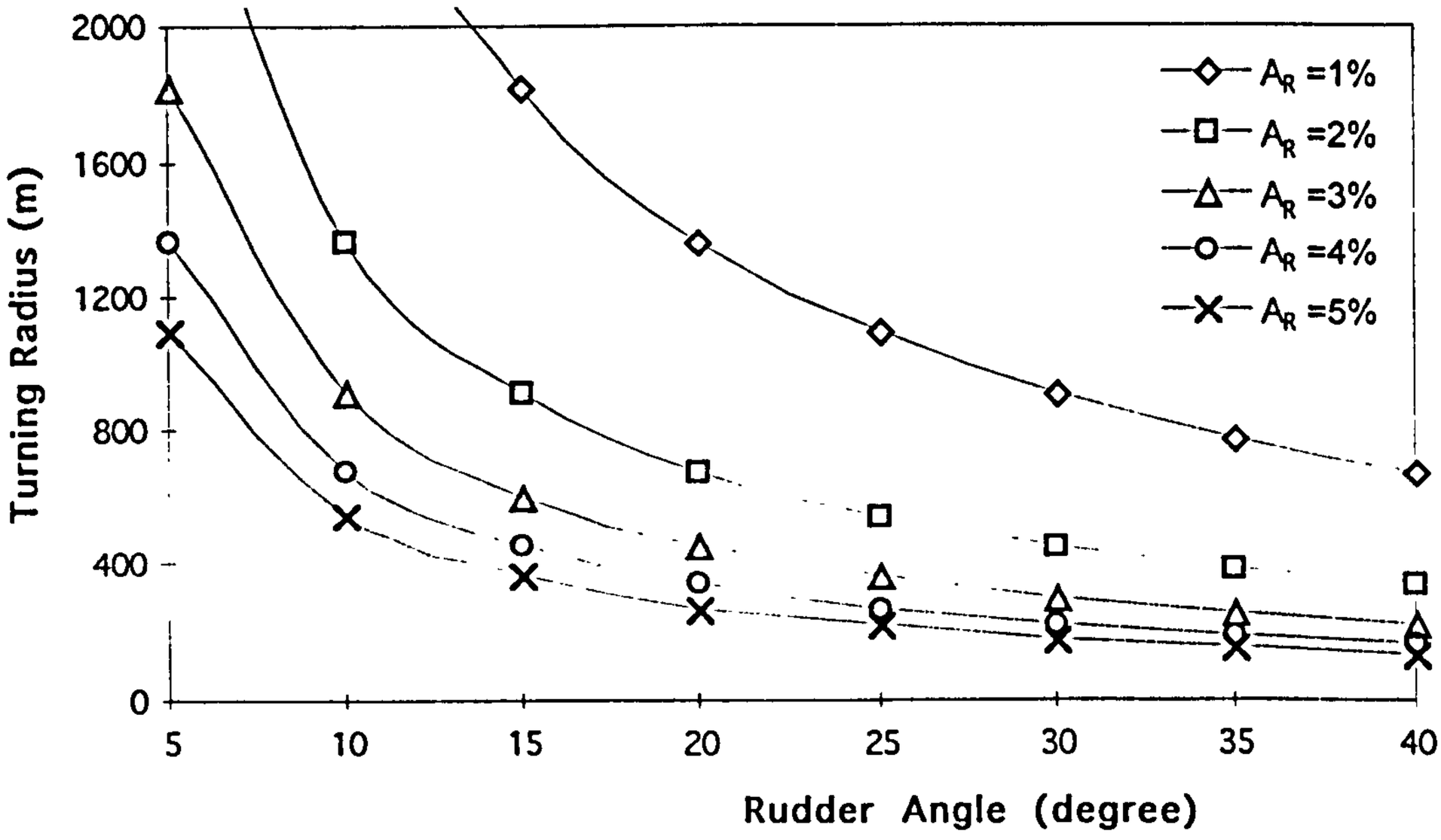

Figure 8.3 Steady turning calculation for trimaran Ship 2

In order to assess the validity of the computation method, the steady turning is computed for Ship 2 in the same conditions as in the model experiments. The computed results are plotted in Figure 8.4 together with the results of the model experiments. It can be seen that reasonable good agreement has been achieved for both 20 and 35 degrees of rudder angles. However, the computation had not revealed effects of the ship's speed on turning radius unlike the model experiments (see Figure 8.4). This is because the hydrodynamic derivatives are assumed to be in a linear relationship with the ship's speed. However, the effects of ship's speed on steady turning radius are not very significant.

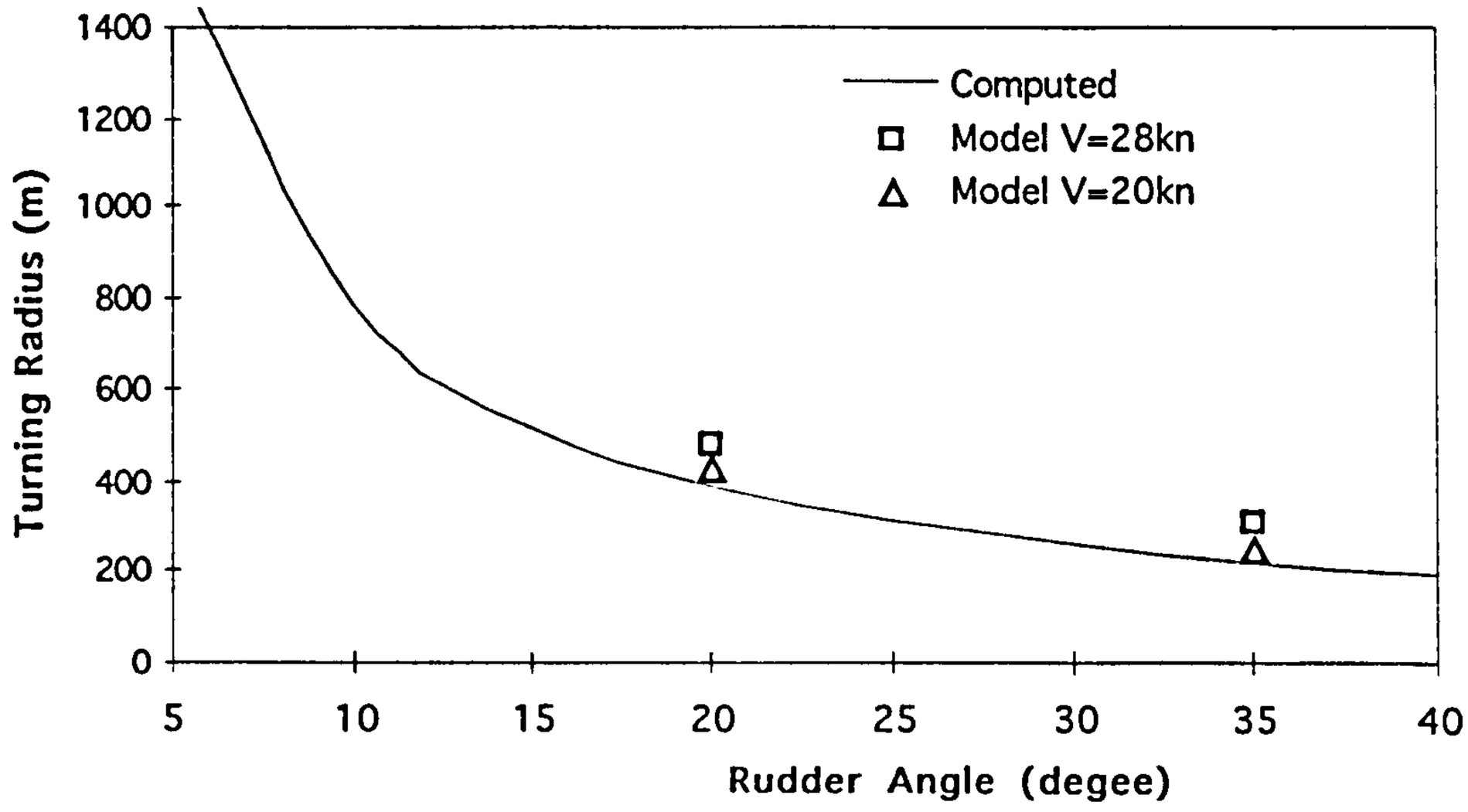

Figure 8.4 Comparison between computation and experiment

8.4.3 Comparison with a Monohull Ship

Since the aim of this section is to investigate the characteristics of the new trimaran ship in its turning ability, the question which needs to be answered is whether the trimaran ship can meet operational requirements in manoeuvrability. Ideally, this can be done by comparing the trimaran's ability with certain manoeuvring criteria. The difficulty is it is very hard to find applicable manoeuvrability criteria as the requirements varies significantly for various ship roles. Therefore, the method used here is to compare the trimaran ship with a typical monohull ship to see whether the trimaran ship could achieve the similar standard as the monohull ship and to identify the differences. The monohull ship of equivalent displacement is derived from Type 22 Frigate **(Jane's 1991)** by keeping its slenderness (the same length to beam ratio and length to draught ratio). Table 8.2 gives the principal particulars of the monohull ship used in comparison with the trimaran.

Table 8.2 Principal particulars of the ships for comparison

	Monohull	Trimaran (DRA model Ship 2)
Length (m) (L)	136.2	150
Beam (m) (B)	16.0	30
Draught (m) (T)	4.6	5.5
Total Displacement (t)	5400	5400

The following two comparisons between the trimaran and the monohull were made:

- *Tactical turning diameter*

  Comparative turning diameter curves for the trimaran and the monohull ship are shown in Figure 8.5 with a rudder angle of 35 degrees. This shows that a large rudder area is required for the trimaran ship if it is to achieve the same level of turning ability as the monohull. Assuming that the total rudder area is 2.0%LT for the monohull with a tactical diameter about 500 metres, then the required total rudder area for the trimaran ship will be 3.25%LT which is about 63% larger to achieve the same tactical diameter.

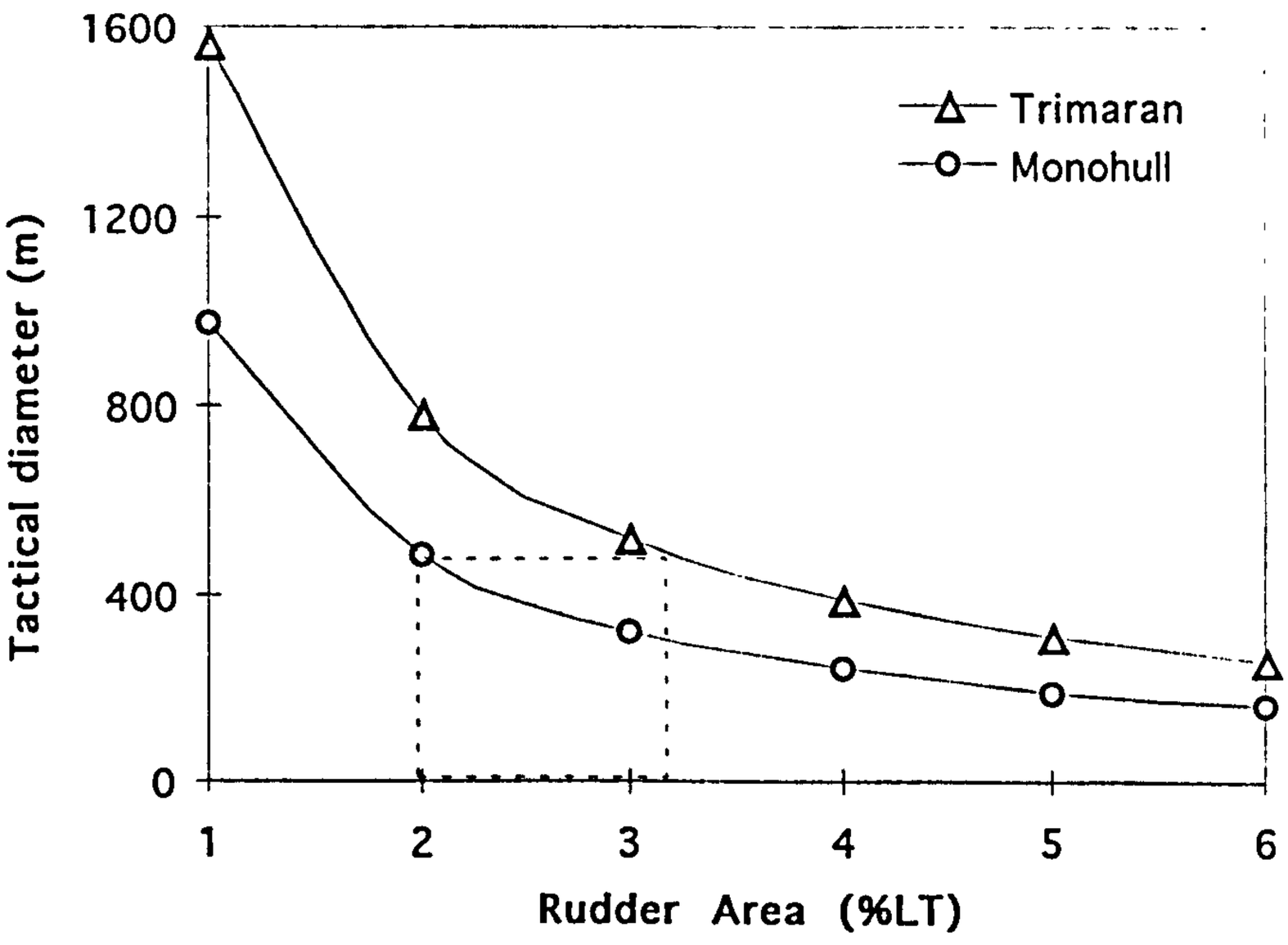

Figure 8.5 Steady turning tactical diameter vs rudder areas($\delta = 35^{o}$)

- *Tactical diameter to ship length ratio*

  If we repeat the comparison using the turning Diameter and ship Length ratio (D/L), as usually a longer ship is expected to have a larger turning diameter, a D/L=3.6 has been achieved by the monohull with A_R=2.0%LT, whilst an A_R=2.8%LT is required for the trimaran to achieve the same level of D/L as shown in Figure 8.6. In this case the required rudder area for the trimaran is about 40% larger than that of the monohull.

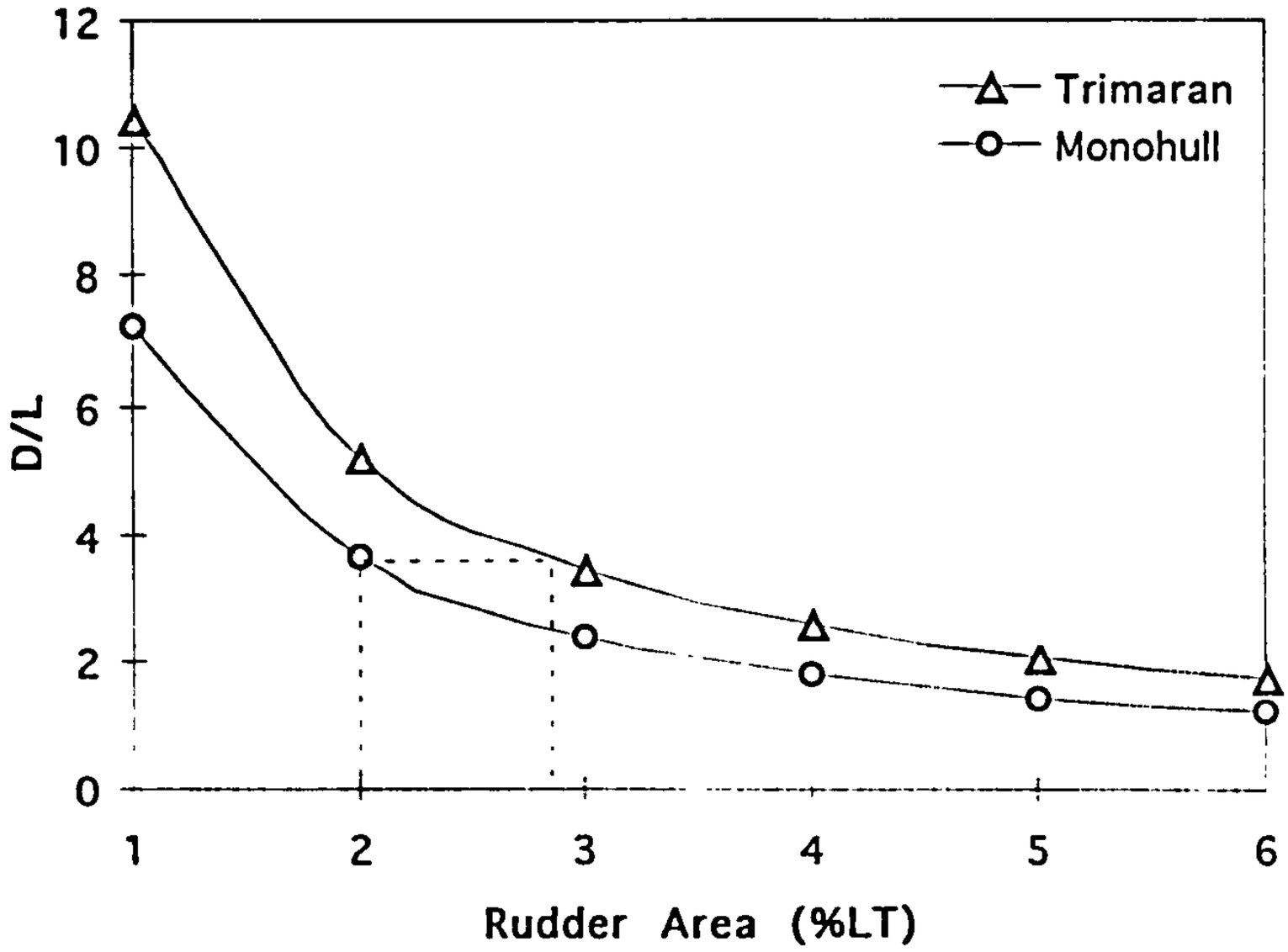

Figure 8.6 Tactical diameter to ship length ratio vs rudder area ($\delta = 35^{o}$)

This increased requirement in the rudder area for the trimaran ship is mainly due to the increase in the hydrodynamic forces and moment acting on the ship. Since the centre hull of a trimaran ship is longer than an equivalent monohull ship it will be subjected to greater hydrodynamic forces and moments resisting turning. The side hulls also give additional hydrodynamic forces and moment. Among the terms in the numerator of Equation (8-8), the dominant term is N_r. It is found from the calculated data that the extra component of N_{rs} due to the side hulls added about 12 percent to the value due to the centre hull alone.

8.4.4 Effects of Side Hull Configurations on Turning Ability

The analysis has also shown that the side hull configuration has a definite effect on the turning ability of a trimaran ship. The major factors are the side hull draught and the side hull location. It is apparent from considering equations (8-13) and (8-16), that the velocity derivatives of the side hulls are dependant on the longitudinal location of the side hull x_s and the effective aspect ratio a which is a function of the side hull draught and length. Figure 8.7 shows the turning ability of the trimaran ship with side hulls located at $x_s = -30\%L$ (aft amidships), compared with a side hull location of the original design with $x_s = -10\%L$. About 15% of additional rudder area is required to maintain the same level

of turning ability at the point of A_R = 3%LT. This suggests that if the side hulls are moved further towards the stern of the ship the turning ability will be reduced in the same way as would occur if vertical fins on a monohull were similarly moved.

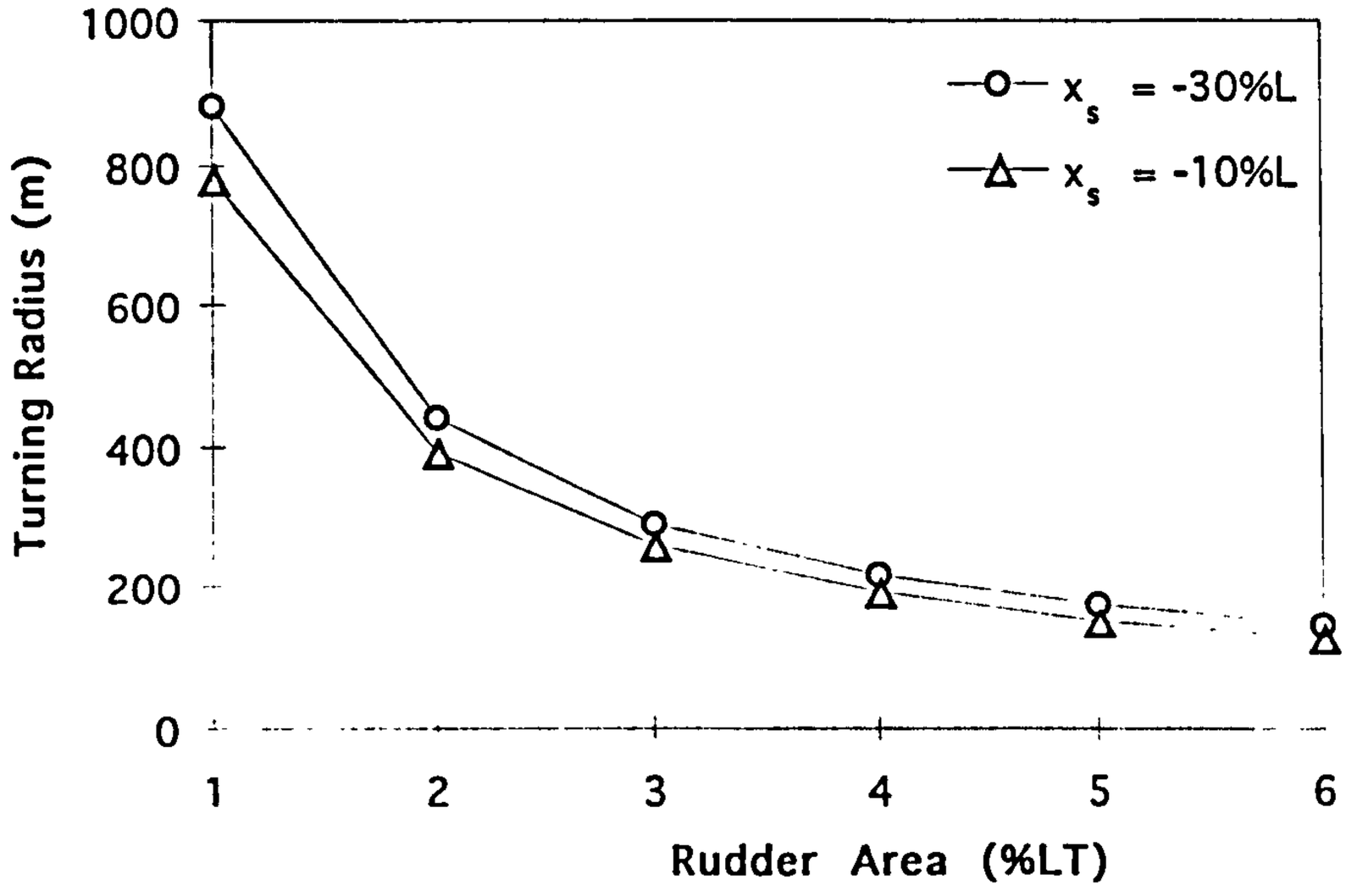

Figure 8.7 Effects of side hull location on turning ability ($\delta = 35^o$)

The side hull draught also has a definite effect on the turning ability of a trimaran ship. A reduced side hull draught will result in an increased turning ability as shown in Figure 8.8, where the turning ability of the ship with a reduced side hull draught of T_s = 2.5m is compared with that of the designed side hull draught of T_s = 3.5 m. Although the major considerations in deciding the side hull draught of a trimaran ship would be those of stability, resistance, and seakeeping requirements, the manoeuvrability should also be part of the overall consideration in balance with the other considerations.

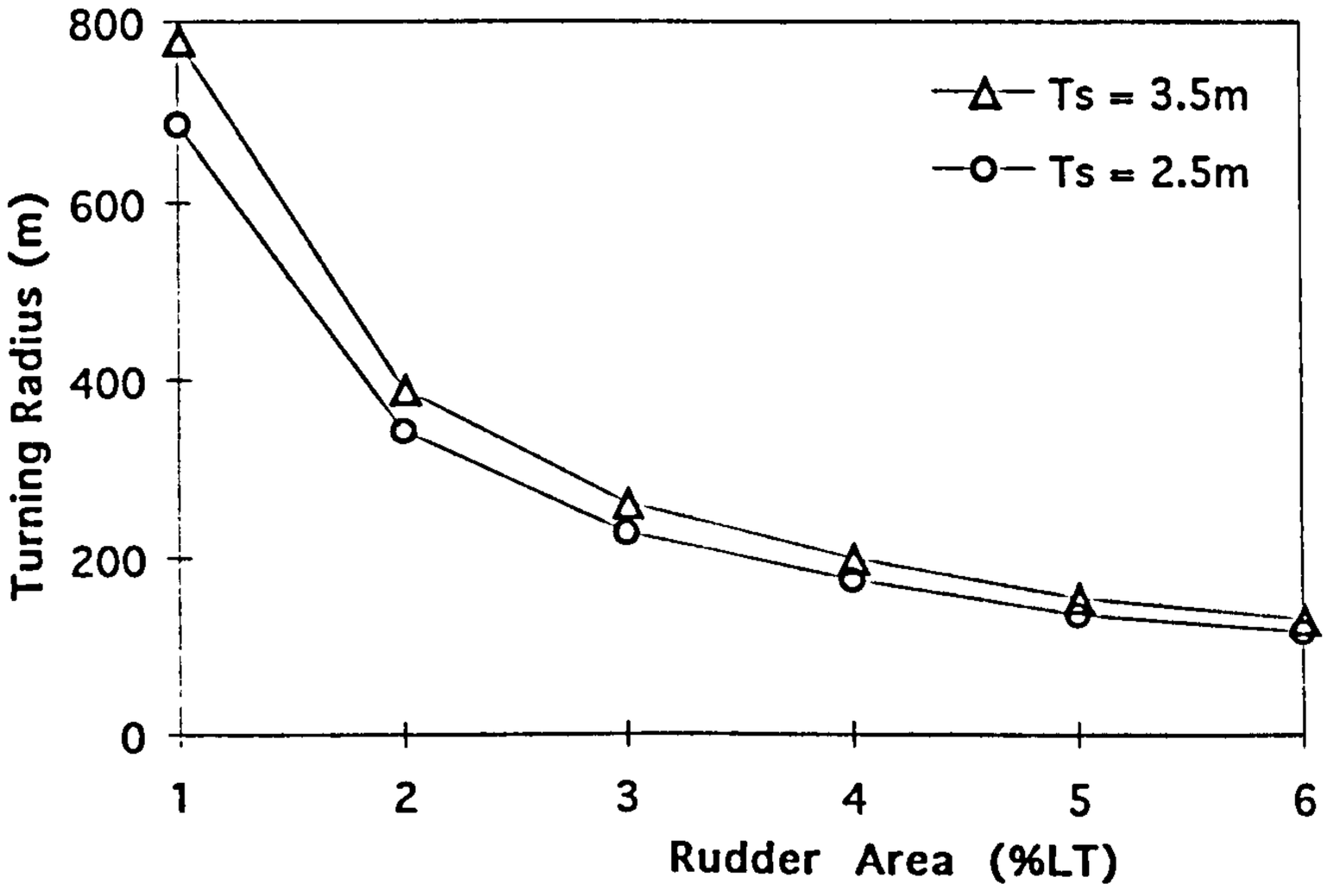

Figure 8.8 Effects of side hull draught on turning ability ($\delta = 35^o$)

8.4.5 Influence of Side Hull Resistance Differential

When a trimaran ship is under steady turning, the advance speeds of the two side hulls are not the same thus giving different resistances for the two sides. This resistance differential forms a yaw moment which tends to resist the turning. The effect of this side hull resistance differential on the turning motion of the trimaran ship has also been examined. The resistance yaw moments $(X_{RP}\text{-}X_{RS})y_s$, (as in equation 8-7) at various speeds, divided by the rudder turning moments $N_\delta\delta$, have been plotted in Figure 8.9. It shows this resistance yaw moment is less than *0.1%* of the rudder moment over the whole speed range. Therefore the effects of this resistance differential are very small and negligible.

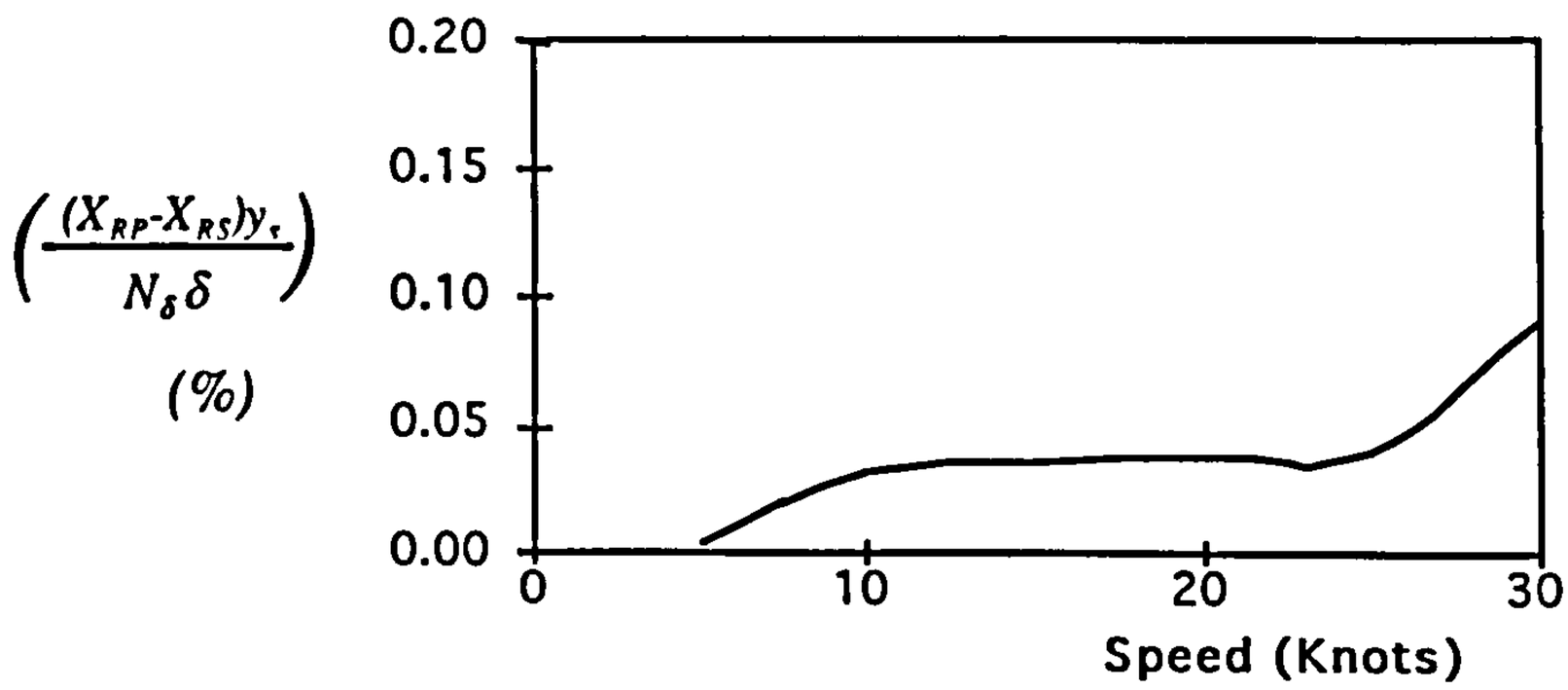

Figure 8.9 Moment of side hull resistance differential to rudder moment ratio

8.5 Turning Ability Using Wing Propellers

In order to identify the effects of wing propellers, this section assesses the turning ability with just wing propellers acting to answer the question raised in Section 8.1, namely whether the turning moment provided by the wing propellers would be sufficient for the ship to be manoeuvred without using rudders.

Wing propellers

Prior to calculating the wing propeller turning ability, the design of the wing propellers and the arrangement of the wing propulsion system must be decided. For the choice of the wing propulsion system, it was decided to use electrical motors and fixed pitch propellers **(Zhang 1995a)**. Because the DRA model Ship 2 was configured without side hull propulsion, the side hulls have to be reconfigured for wing propulsion arrangement. Detailed considerations for wing propulsion arrangement and the procedure used for wing propeller design are discussed in Chapter 9.

In the wing propeller design, initially an attempt was made to design a single propeller for each side hull. This required a propeller diameter bigger than acceptable considering general ship design restrictions. It was therefore decided to use contra-rotating propellers for the wing propulsion, as this should give a smaller diameter and higher propeller efficiency. In the absence of a specific contra-rotating methodical propeller series, an approximate design method was to use the 20 inch AEW **(Gawn 1952)** series with the thrust for each pair of propellers assumed to be equally apportioned. The resultant wing propeller characteristics are given in Table 8.3.

Table 8.3 Wing propeller characteristics

	V =20 knots	V =30 knots
D (m)	3.5	3.5
BAR	0.8	0.8
P/D	1.68	1.68
J	1.39	1.59
rpm	127	166
η_o	0.76	0.71
QPC	0.745	0.696
PS per wing (MW)	3.38	4.35

Operation of the wing propellers on turning

To calculate the turning ability of the ship using wing propellers, it was necessary to clarify first how the wing propellers are to be operated. On turning the ship at various speeds, the wing propellers could be operated in the following modes to provide the necessary turning moment:-

(a) One wing propeller keeps thrusting forward whilst the other wing propeller idles producing no thrust,
(b) One wing propeller keeps thrusting forward whilst the other wing propeller is stopped providing a braking effect,
(c) One wing propeller keeps thrusting forward whilst the other wing propeller is put in reverse producing negative thrust.

Modes (a) and (b) can be considered as possible manoeuvring evolution when the ship is at speed. Mode (c) is not considered as a normal at speed manoeuvre as it would take a considerable time for the propeller to reverse, and the ship would be subjected to a violent vibration as a sudden reverse of a propeller would be akin to an emergency stop. Mode (c) is however relevant to harbour manoeuvring when the ship is at stationary or very low speed.

Turning moments

When the rudder is not in use (zero rudder angle), the turning moments acting on the ship are produced by the thrust differential and the hydrodynamic forces as indicated in the right hand side of equation (8-3).

The forward thrust force produced by a wing propeller is:-

$$T_w = \rho\, n^2\, D\, K_T \tag{8-20}$$

where n is the propeller revolutions, D is the propeller diameter, and K_T is the thrust coefficient which can be obtained from propeller design diagrams related to the advance coefficient of the propeller **(Gawn 1952)**. To simplify the problem, the negative thrust force produced by a reversing wing propeller is assumed to be the same magnitude as the maximum thrust produced by the propeller at zero speed.

When a wing propeller is stopped, $J = \infty$ and the brake force can be expressed as **(Gutsche & Schroeder 1963)**:-

$$T_w = -C_t \rho\, V^2\, D^2 \tag{8-21}$$

where C_t is the brake coefficient.

Computation results

The turning rate and the turning radius of the ship in the three turning operation modes are plotted in Figure 8.10. It is found that when the ship's speed exceeds 10 knots the turning rates are very low, even for the case when one of the wing propellers is in reverse. These low turning rates at speed are caused by insufficient turning moments produced by the wing propellers. For the same output power of the wing propulsion, the higher the ship speed, the less thrust force it would produce. Additionally, the turning moment lever, from the wing propeller to the centre line of the ship, 13.25 metres, is only 17 percent of the moment lever of a rudder when fitted at the stern of the centre hull.

However, as could be intuitively expected, the results demonstrate a good turning ability for the ship using the wing propellers at low speed. Stationary turning is possible using the wing propellers. This could be highly desirable coming alongside in harbour or manoeuvring at low speed in confined waters. This capability could be a significant advantage over a monohull, since the latter could only achieve this by additional lateral thrusters.

8.6 Conclusions

In considering the criteria for trimaran manoeuvrability, turning ability is seen to be crucial. This is because of the trimaran ship characteristics of a long slender hull and the two additional narrow side hulls acting like two fixed fins when manoeuvring which are likely to have positive effects on course stability and adverse effects on ship turning ability drawing on the knowledge of monohull ship behaviour **(Burcher 1972) (Lewis 1989).**

A method for analysing the ability of a trimaran to turn has been developed using a combination of theoretical and empirical methods **(Jacobs 1964).** This treats the trimaran ship as a combination of a slender hull with two fixed fins whilst ignoring the interaction between the hull and the fins. Good agreement has been achieved between the predictions and the DRA model tests.

To achieve the same turning ability as an equivalent monohull, a trimaran ship requires a larger rudder area. The comparison between the DRA model Ship 2 and an equivalent displaced monohull has shown that the rudder area of that trimaran needs to be 63%

larger to achieve the same tactical diameter as that of the monohull, and 40% larger to achieve the same tactical diameter to ship length ratio.

The side hull draught and longitudinal position are two important parameters of a trimaran ship, influencing its turning characteristics. A small side hull draught and a forward location appear to be favourable to the turning ability.

Wing propellers fitted to the side hulls can give the trimaran ship excellent low speed manoeuvring characteristics, including the capability of stationary turning. However, it is not possible to achieved a satisfactory turning rate at medium and high speeds using the wing propellers without the use of rudder(s).

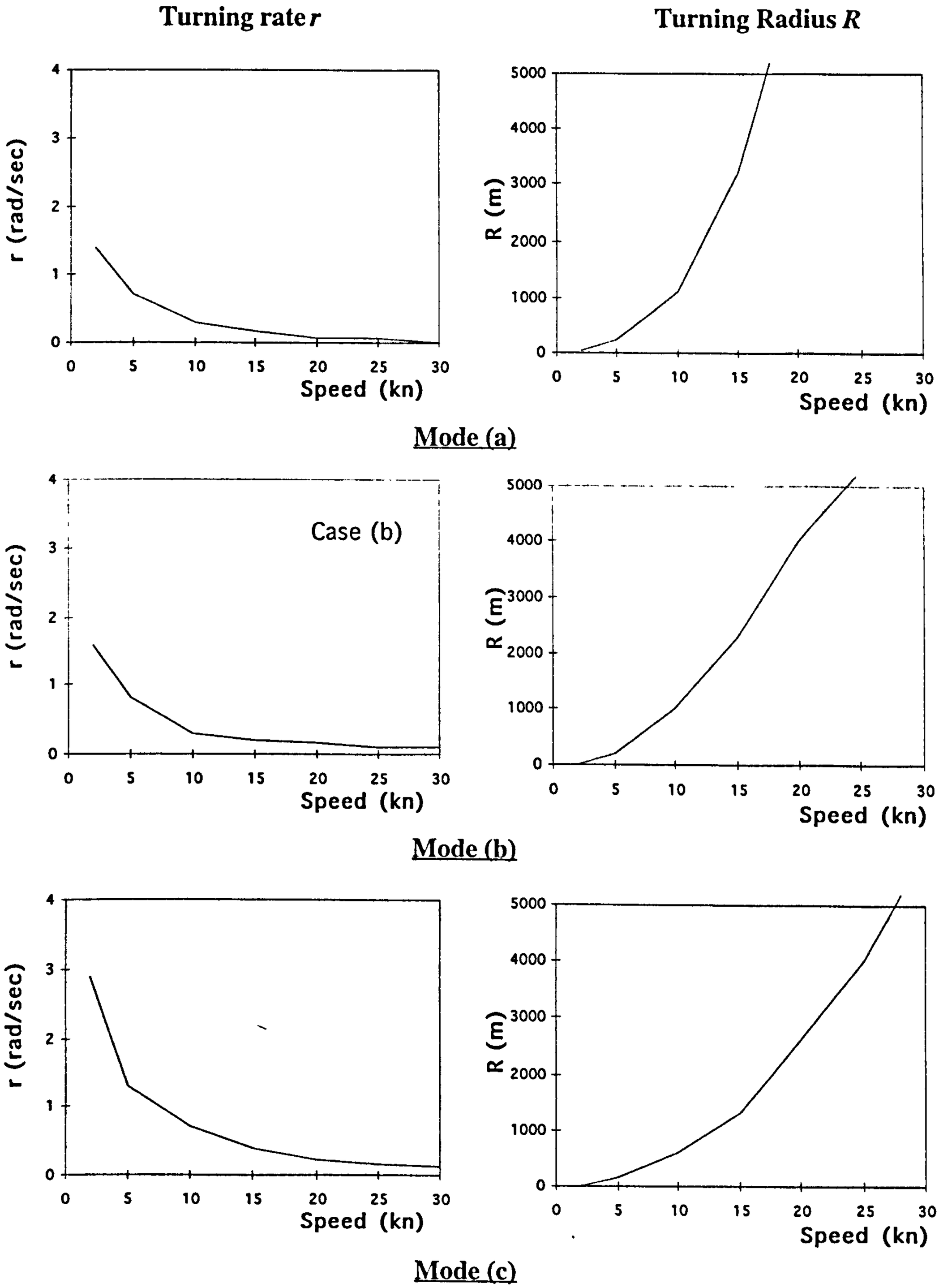

Figure 8.10 Turning ability of the trimaran ship using wing propellers only for three modes: (a) one propeller stopped, (b) one propeller braking, (c) one propeller in reverse

CHAPTER 9

GENERAL DISCUSSIONS ON TRIMARAN DESIGN PROCEDURES AND CONSIDERATIONS

9.1 Introduction and Aims

Having investigated the hydrodynamic performance of the trimaran ship through model experiments and theoretical analyses, it is now possible to discuss further on general procedures and considerations in trimaran design. The design process for trimaran ships has been indicated in Chapters 3 and 4 through the initial design study of the fast trimaran ferry and the design of the trimaran model hull forms. Because these designs were performed for specific tasks, the discussions on design procedures and possible design options were limited to those cases. Furthermore, some aspects which have not been covered in previous chapters need to be addressed.

Firstly, in Section 9.2, trimaran design procedure is discussed focusing on considerations in side hull configurations for stability and hydrodynamic performance. The trimaran design process, particularly for the side hull configuration, is more involved the stability consideration than that of the monohull. An appropriate procedure is required and as such would benefit the designer in deriving a design solution for a trimaran ship with superior hydrodynamic and stability performance.

As study of the trimaran is still at its early stages, all design options are open to be investigated for improving the ship's performance. In Section 9.3, the design philosophy and design options for the centre hull are discussed. The side hull draught is considered as a very important parameter affecting the resistance performance of the trimaran ship but has not been thoroughly examined in the trimaran studies to date. An initial discussion on this issue is presented in Section 9.4.

Stability criteria used in trimaran ship design studies are examined and discussed in Section 9.5 with some recommendations considered appropriate to the special needs of trimaran ships.

Finally, a design procedure for trimaran wing propulsion is presented in Section 9.5, based on the experience gained in design of wing propulsion for the manoeuvrability analysis presented in Chapter 8. The procedure covers wing propeller arrangements and design conditions.

Not all the considerations discussed in this chapter have been applied in the trimaran designs described early in the thesis. The aim of this chapter is to reveal some considerations based on these design studies as well as broader issues to be considered in future trimaran ship designs.

9.2 Stability Procedure for Side Hull Configuration

Design to achieve acceptable stability is one of the crucial parts in the design process of a trimaran ship, since the basic parameters for the side hulls largely depend on the stability considerations albeit moderated by hydrodynamic considerations. The more involved configuration of the trimaran ship, compared with the monohull ship, gives the designer more choices with which to achieve the stability requirements. This then means that in form determination more detailed attention needs to be addressed to meet the stability condition for a trimaran ship than in the case for a monohull ship. This section discusses the stability procedure and considerations for trimaran ship design, particularly in the configuration of the side hulls.

The discussion commences with the differences between the trimaran ship and the monohull ship in stability design to highlight the significance of stability design in the design process of the trimaran ship. For this purpose the concept process for a trimaran ship can be considered in two stages, the initial sizing stage, concentrating on the sizing of the centre hull, and then the detailed side hull configuration stage. It has to be noted that the trimaran concept is still at its early stage, and the extent of the design studies are limited to date, so the suggested values used in the following procedure are based on limited information.

9.2.1 Differences between Trimaran and Monohull in Stability Procedure

The stability check in the initial sizing stage for a monohull ship is comparatively straightforward. The hull parameters are usually derived from empirical data which are based on an enormous number of existing ship types and experience of their performance. A check of the *GM* value is usually sufficient justification to adjust the ship's beam. The subsequent detailed stability assessment decides the extent of the subdivision of the ship required within the broad hull size achieved from this initial sizing **(Taggart 1980)**.

For the trimaran ship, stability considerations are not that straightforward due to the more complex configuration and to the lack of existing data and experience. A simple *GM* check is not sufficient to size the three hulls. The same *GM* value for a trimaran ship can be achieved by a range of side hull configurations with totally different sizes, hull shapes, and relative positions, which may result in totally different large angle and damage

stability characteristics of the ship and also different hydrodynamic performance. In giving the designer more choices the trimaran concept demands more initial attention than is required for a monohull. Thus, the large angle and damage stability of a trimaran ship can only be assessed through relatively detailed stability calculations.

Therefore, as already discussed briefly in Chapter 3, the stability design procedure for a trimaran ship is best divided into two stages, the initial centre hull sizing and the detailed refinement of the side hull configuration. At the initial sizing stage, the trimaran form design is largely a process of obtaining the parameters of the centre hull with the parameters of the side hull normally considered fixed. At the second stage the parameters of the side hulls are obtained from essentially an assessment of stability. The full stability assessment of a trimaran ship is not just concerned with the subdivision of the ship but also the size and the shape of the side hulls. The tasks in this stage are, final refinement of the side hull size, detailing the side hull shape, and identifying additional measures such as required flare and ballast. The final configuration results from an interactive consideration of all of these three tasks.

The resistance performance of a trimaran ship is very much affected by the configuration of the side hulls, i.e. their size and location. Reduced side hull displacement ratio would result in reduced resistance for the trimaran ship. Thus the objective of this process is to find a side hull configuration with minimum effect on ship resistance whilst satisfying stability requirements.

9.2.2 Initial Sizing Stage

At the initial sizing stage of a trimaran ship design, the parameters of the centre hull can be determined independently from the stability requirements, since the side hulls would provide extra waterplane area and buoyancy to make the ship meet the intact and damaged stability requirements. Thus the design balance can result in a very slender centre hull, with length beam ratio above 14 and Ⓜ greater than 9.0 **(Zhang 1992)**.

Initial parameters for the side hulls are required at this stage to contribute to the design balance of weight and space. This requires a first estimate of the size of the side hulls. Given it is premature to carry out a detailed stability calculation at this stage, the side hull parameters are derived approximately to meet particular values of *GM*, damaged length, and governing heeling angle.

The initial parameters of the side hulls can be determined by the following major factors.

a Damaged length of the ship

The length of the side hulls can be derived from the damaged stability requirements for the ship. If we denote the damaged extent of the ship calculated from the chosen stability criteria as *'Damaged Length'*, and the total length of the flooded compartments in the hull as *'Flooded Length'*, then the side hull length can be derived from the *flooded length*. Based on the experience gained from the trimaran design studies carried out at UCL, when a side hull is subjected to damage, about half of its length is required to remain intact to provide sufficient waterplane area and buoyancy for the ship meet typical warship stability criteria **(NES 109 1989)**. Thus, the length of the side hull required can be initially selected as approximately twice that of the expected flooded length for a warship stability standard.

b Size and location of the cross structure

The size and location of the cross structure are largely dominated by the layout and structural considerations emerging from the vessel's broad operational requirements such as payload capacity or flight deck arrangements. In addition, any dock or canal restrictions on the overall beam of the ship could also be a limiting factor in the determining the side hull span.

c Choice of GM

With the initial length and span of the side hulls, it is now necessary to obtain the beam of the side hulls. This is significantly influenced and driven by the value of transverse metacentric height because it has to meet intact stability and damage stability requirements and has also to be checked to avoid undesirable roll motions. While it may be still too early in the understanding of trimaran design to conclude on an acceptable criterion for the desired *GM* value, the following considerations are currently seen as most appropriate.

i *Minimum GM for stability*

The value of *GM* required to achieve the necessary stability of a trimaran ship is normally higher than that of an equivalent monohull ship. This arises from

consideration of a side hull of a trimaran ship being damaged, since lost of waterplane area results in a larger initial heeling angle and wind heeling angle compared with an equivalent monohull of the same *GM*. In addition, adoption of a larger value for *GM* would also help to reduce the side hull length requirement discussed above.

As an initial guidance, if the value of *GM* for a trimaran ship is selected to retain the same value of *GM* as the equivalent monohull once it has lost half the waterplane area of one of its side hulls, then the metacentres of the two ships can be related as:-

$$BM = 1.20(GM_E + KG - KB) \tag{9-1}$$

where *BM* represents required value of the distance of metacentre above the centre of buoyancy for the trimaran ship, *KG* and *KB* are the distances from the keel to the centre of gravity and centre of buoyancy of the trimaran ship, and GM_E is metacentre height of an equivalent monohull ship. The coefficient 1.20 is derived from the fact that half the length of side hull if in the middle portion normally provides about 20% of the total waterplane area inertia for a trimaran ship. Should the flooded length assumption differ from this, then the coefficient would have to be varied accordingly.

The *GM* values of the two ship configurations can be expressed as:-

$$\begin{aligned} GM &= BM - (KG - KB) && \text{for trimaran} \\ GM_E &= BM_E - (KG_E - KB_E) && \text{for equivalent monohull} \end{aligned} \tag{9-2}$$

where KG_E and KB_E are the distances from the keel to the centre of gravity and centre of buoyancy respectively for an equivalent monohull.

Then the relationship between the *GM* and GM_E becomes:-

$$GM = \left(1 + \frac{0.20\left(BM_E - (KG_E - KB_E) + (KG - KB)\right)}{BM_E - (KG_E - KB_E)}\right) GM_E \tag{9-3}$$

Equation (9-3) can be simplified by cancelling the denominator of the second term in the bracket with the GM_E term. The reason of retaining the denominator is to show the relationship between GM and GM_E.

For a first estimate, the distance from the centre of buoyancy to the centre of gravity for the trimaran can be assumed to be the same as that of the equivalent monohull (the trimaran ship would have a higher KG, but also a higher KB), as this can be updated in the subsequent estimates.

To give a quantitative indication of the relationship between GM and GM_E, assuming the value of $(KG_E - KB_E)$ of the equivalent monohull (a typical 5000t monohull frigate with $KB_E=3m$, $KG_E=7m$, *and* $BM_E=5.5m$) is approximately $0.7BM_E$, then from equation (9-3) the required GM will be:-

$$GM = 1.7\, GM_E$$

Thus the required minimum GM for a trimaran ship can be roughly estimated from GM_E of an equivalent monohull ship.

ii *Seakeeping considerations in the choice of GM*

The above discussion relates to the minimum required GM to achieve necessary stability. However, model experiments described in Chapter 4 have shown that the choice of GM for a trimaran ship has a significant influence on its seakeeping performance, particularly roll motions. Therefore, the trimaran designer also faces a task to validate the GM at the early design stage to avoid unfavourable roll motions.

Roll motions of a ship are governed by many factors including ship's speed, heading, the range of wave frequencies, roll damping characteristics, and, of course, the ship's size and configuration. In what follows not all the considerations which would actually effect the choice of GM in a given design are discussed, however, this addresses the most significant issues in general.

Avoidance of too stiff a roll motion

Stiff roll motion is one of the problems which would occur in a typical catamaran ship which possesses an extremely high GM **(Alaez 1989)**. Some modern

catamarans have been forced to install ride control devices to overcome this problem **(Hercus 1991)** to reduce pitch motions as well as the roll motions. The trimaran ship, has the advantage that it can be tuned to avoid stiff roll motions. It is likely to require a relative low value of *GM* compared with a catamaran to give a longer roll period, and hence provide the minimum required *GM* as discussed above.

Avoidance of synchronous roll motion

Not only must the stiff motion mentioned above be avoided, but also roll motion near likely resonance frequencies has to be checked to avoid severe synchronous roll motion. This means that the natural roll period of the ship needs to be tuned away from the likely encounter wave periods.

The natural roll period of a ship is determined by three factors, mass inertia, restoring moment, and roll damping. Since roll damping has little effect on the roll period of a ship it is usually neglected and the resonant roll period T_n is given by the following expression **(Lewis 1989)** :-

$$T_n = \frac{2\pi\sqrt{I + I'}}{\sqrt{g\Delta \cdot GM}} \tag{9-4}$$

where I is the mass moment of inertia of the ship about the rolling axis, I' is added mass inertia about the rolling axis, and Δ is the displacement of the ship.

The encountered wave period T_e is determined by:-

$$T_e = \frac{L_w}{\sqrt{\frac{gL_w}{2\pi}} - V\cos\mu} \tag{9-5}$$

where L_w is the wave length, V is the ship's speed, and μ is the ship's heading.

If we define a tuning factor as:-

$$\Lambda = \frac{T_n}{|T_e|} \tag{9-6}$$

when the tuning factor Λ becomes close to unity, i.e. the ship roll period T_n approximates to the encounter wave period T_e, the ship is then close to synchronous roll motion. Thus, the chosen *GM* for a trimaran ship must be a sensible value which ensure the tuning factor is not close to unity.

The choice of the encounter wave periods in the calculations is affected by the following issues:-

1) The areas where the ship is to be operated and the sea states the ship is designed for. These give the likely wave periods at which the tuning factors are to be examined.
2) The speeds of the ship which are to be sustained at the above sea states.
3) The likely wave headings which are of most concern.

The difficulties of applying this tuning factor approach would be:

1) The possible combinations of the above three issues are very large. It would be very difficult to identify all possible cases in a early ship design stage.
2) The resulting tuning factors could widely vary in value when the chosen range of values those for the above three operational issues are other than very narrow. This makes the choice of GM to avoid unfavourable roll motions rather difficult.

The designer has therefore to narrow these ranges using judgement on the operational profile of the ship and the likely critical situations the ship may encounter. The following is a example of using this approach for a trimaran destroyer design in which the ship speed and wave heading are fixed allowing only the wave periods to vary in a narrow band.

The trimaran destroyer, designed for DRA model tests (Table 4.1, Ship 2), is to operate in the Atlantic Area (see appendix 4). Sea State 6, with a significant wave height of about 5 metres, is considered as the critical sea state for the ship's operations. The likely wave periods to be encountered are from 8 to 11 seconds (wave frequency $\omega = 0.6 \sim 0.8$ *rad/s* and wave length $L_w = 96m \sim 171m$) **(Hogben & Lumb 1967)**. A speed of 18 knots is chosen as the critical speed for the ship to operate in this sea state.

The critical wave heading is chosen at 60 degrees (following quartering seas) for which the DRA Haslar model test results (**DRA 1995**) showed severe roll motions with an unfavourable choice of *GM* (see Figure 5.11, $\mu = 60^{o}$, *V=18 knots*). It is believed that following quartering seas would normally be the critical wave heading for trimaran ships when considering roll motions. This is not only demonstrated by the DAR trimaran model tests but is also similar to that of monohulls (**Lloyd & Crossland**). A further explanation could be that:-

(a) when the ship is travelling in following quartering seas, the frequency dependent roll damping effects are greatly reduced since the encounter wave frequency is reduced;

(b) the hydrostatic restoring force is then the major source to resist roll motions, thus the roll motion behaviour of the ship is more dependent on *GM* at this wave heading.

Figure 9.1 shows the relationship between *GM* and tuning factor Λ for the ship at various headings. The wave frequency used in the calculation is 0.8rad/s (L_w = 96m). Figure 9.2 shows the tuning factor of the ship at various encountered wave lengths. These results are then used to check the chosen GM for the ship. The GM values which resulting in a tuning factor close to unit should be avoided (the orange and pink zones in the figure). As the minimum GM required for stability has to be met first, the blue zones are also ruled out where the GMs are less than the minimum required. Thus, the choice of GM for the ship has to be made in the zone where the GM value is no less than 2.5 metres.

The approach illustrated here can be used as an initial check in the early stage of a trimaran ship design to identify undesirable GM values. However, the tuning factor calculation is very sensitive to the accuracy of the ship's mass moment inertia of roll, which is difficult to be estimated very accurate at the early design stage. The assumptions of neglecting roll damping effects and the choice of a narrow wave frequency band may also limit the accuracy and extent of the predictions. Therefore, this simple GM check is not to take the place of a full seakeeping analysis in a later stage which would be required to cover the whole range of wave frequencies, ship speeds, and headings.

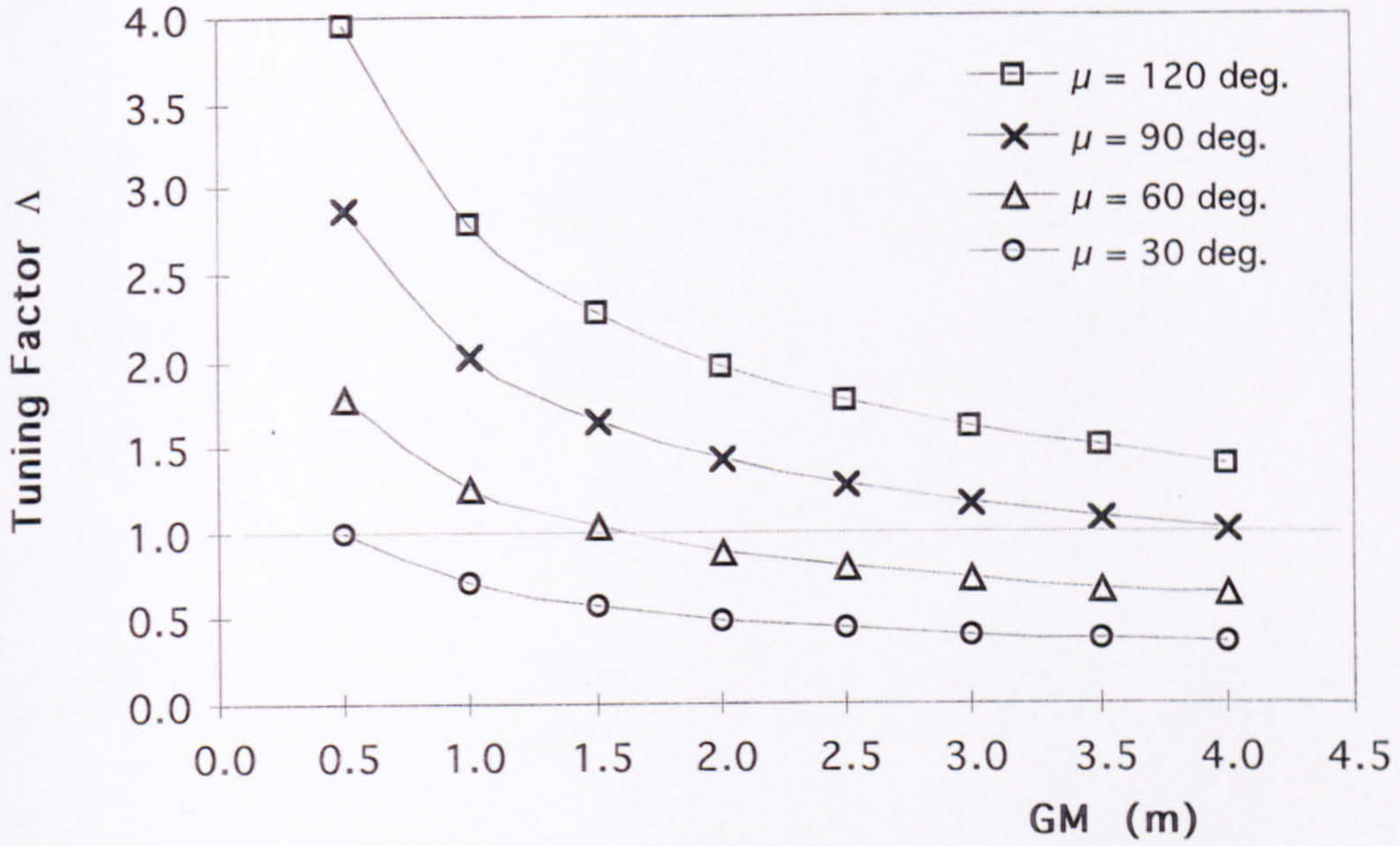

Figure 9.1 Relationship between GM and tuning factors of different headings (L_w=96m)

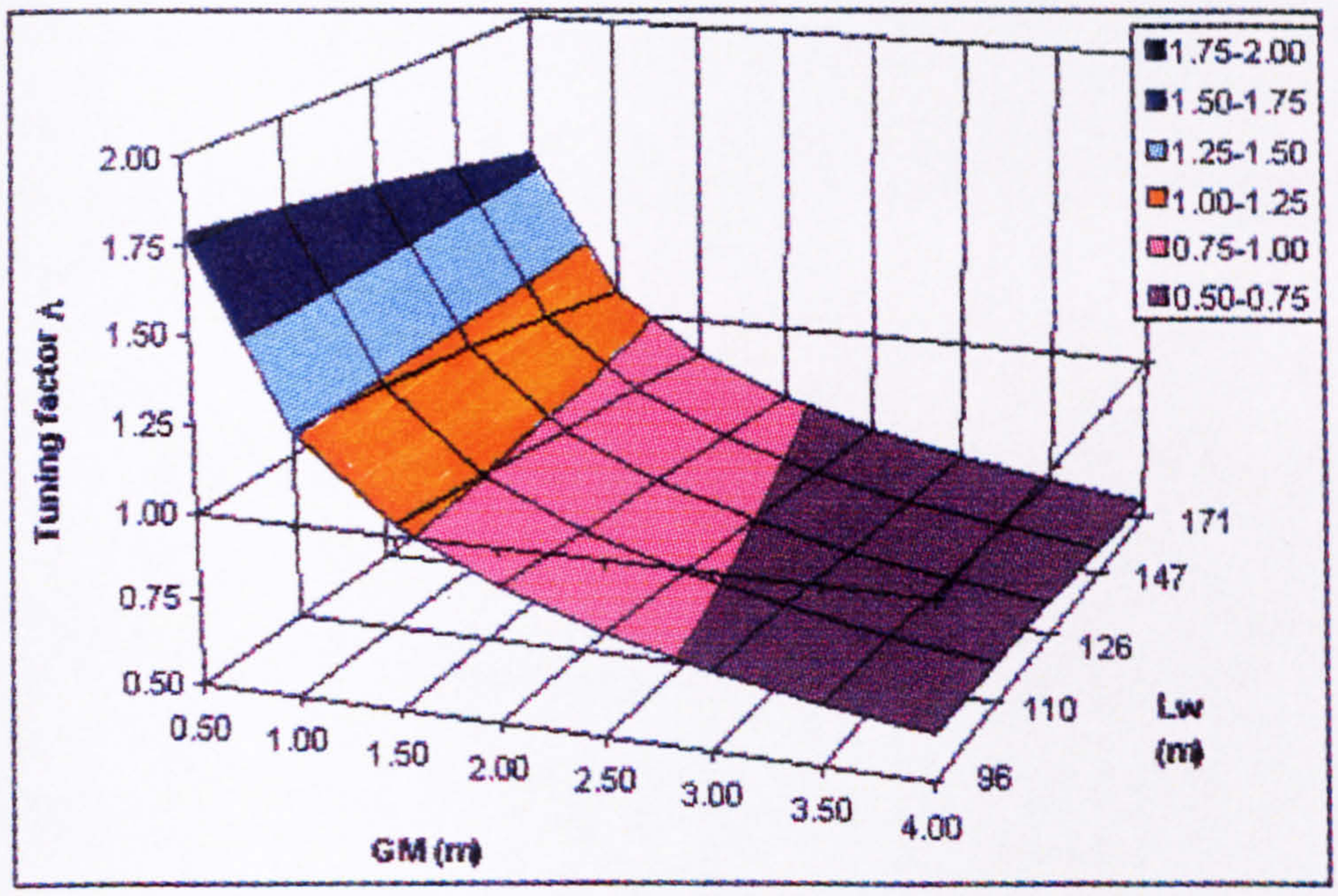

Figure 9.2 Relationship between GM and tuning factor of different wave length (μ=60°)

9.2.3 Detailed Side Hull Configuration Stage

Once the main ship parameters have been largely determined it is necessary to refine the parameters of the side hulls and this is best carried out in conjunction with the detailed stability assessment. The stability assessment of a trimaran ship is relevant not just to the extent of subdivision of the ship but also to the size and shape of the side hulls. The tasks involving the side hull design can be summarised:-

a) Identify the extreme damaged cases for the ship to survive

Detailed intact and damaged stability calculations need to be carried out at this stage for all the loading conditions and the possible damaged cases required by the relevant stability codes. For damage stability the possible conditions of damage as mentioned in the ferry study (Chapter 3) should be checked. The worst damaged cases need to be identified, and to be used as baselines in the refinement of the side hull parameters. As already discussed, one side hull damaged only is normally the worst damaged case, particularly if the middle section of the side hull is flooded. This is due to the heavy loss of waterplane area and buoyancy in the flooded side hull. At the same time the opposite, unflooded side hull would begin to emerge from the water as the ship heels. Unlike monohull ships, the increased waterplane area at the centre hull due to heeling has less influence on the total inertia of the waterplane area because of its narrow beam.

b) Carry out subdivision assessments

The subdivision of the centre hull and the side hulls can be carried out and refined throughout the stability assessment process. The subdivision of the centre hull should be broadly similar to that of a monohull ship although longer compartment lengths are acceptable from a stability stance because, firstly, the freeboard of a trimaran ship is usually higher than that of an equivalent monohull, and secondly the cross structure provides substantial buoyancy as the ship heels at the new deeper draught due to flooding.

For side hull subdivision, assuming any machinery located in these hulls does not demand excessively long compartments then short compartments are advantageous. Such an approach would allow the side hull length to be minimised. In a study about stability criteria for SWATH ships **(John Brown 1988)**, it was suggested that the boundaries between the deck box and the struts could be considered watertight when

the struts are floodable. If this can be shown to be applicable to a trimaran ship then fitting watertight boundaries between the side hulls and the cross structure means the damage stability criteria could be more readily met, although this might prove unattractive for layout reasons in a given design.

c) Adjust the side hull size

The side hull length obtained in the initial sizing stage would be based on initial consideration of the flooded length of the side hulls. However the side hull length is also governed by the shape of the side hulls and other design issues. The side hull configuration can be refined when the subdivision of the side hulls is determined, their shape configured, and the critical damaged cases have been identified, when the side hull length can be adjusted accordingly. The design intent is to reduce both the length and the displacement of the side hulls as far as possible. Unfortunately, the side hull length may have to be increased if this proves insufficient to provide required stability. According to the trimaran stability investigations and the design studies **(Zhang 1992 & 1993)** **(Masson 1993)**, a side hull length of up to 40 percent of the centre hull length would appear necessary to meet the MOD stability standard **(NES 109 1989)**, whilst initial studies suggest a side hull length of under 35 percent would meet commercial standards **(DTp 1991 & IMO 1995)**.

d) Side hull displacement ratio

In defining the shape of the side hulls and determining other measures to reduce the side hull length and the side hull displacement ratio, an eye needs to be kept on the effect this has on building cost whilst ensuing the stability requirements continue to be met. As discussed by **Andrews & Zhang (1995)** with regard to the specific DRA Haslar model design, it is necessary to consider the design of the side hulls not just for the deep condition but also for the light or, at least, the worst seagoing condition as well. Meeting the criteria, particular the MOD damage stability requirements, may prove difficult and as in the DRA model design (Chapter 3), recourse may have to be made to incorporating ballast in the side hulls in the light condition.

As in any ship design, the above considerations are inter-related to a greater or less degree and the final configuration will be the result of the usual interactive process. Thus the resistance performance is very much affected by the configuration of the side hulls, i.e., their size and location. Reduced side hull displacement ratio would result in reduced resistance for the trimaran ship. The objective in design is thus to find a side hull

configuration with least side hull displacement whilst satisfying the stability requirements.

9.3 Some Considerations in the Design of the Centre Hull

9.3.1 Design Arguments

The hull forms of the centre hulls in the existing trimaran studies at UCL (Table 2.2) are either based on the Series 64 **(Yeh 1965)** or the Taylor-Gertler Series **(Gertler 1954)**. Though both these series are well established for slender monohull ships, they may not be the right hull forms for trimaran ships, as the philosophy behind their designs is not necessarily the same. There are differences in the design requirements between the two hull forms. Based on the design studies and the hydrodynamic analysis of trimaran ships described in previous chapters, the design philosophy for the hull form of the centre hull may be summarised as:-

a) The centre hull needs to be slender (long) enough to achieve low wavemaking resistance at speeds.

b) To achieve a minimum frictional resistance, the centre hull should be designed with a minimum wetted surface area.

c) The centre hull can be designed regardless of the requirement to achieve directional stability as side hulls produce sufficient directional stability. Instead, measures to increase the turning ability should be taken to reduce required rudder area.

d) The centre hull can be designed regardless of stability requirements as the side hulls can provide the required extra buoyancy and waterplane area. However, a wider beam (larger beam to draught ratio), provided it did not affect slenderness, would help to improve the hydrodynamic performance of the whole ship, because, it would reduce the extra waterplane area from the side hulls and hence reduce the side hull size.

e) There is unlikely to be a direct requirement in upper deck area for the centre hull, as the cross structure deck provides a large enough deck area for accommodation and deck equipment.

f) As the centre hull of a trimaran ship is longer than an equivalent monohull, the improved pitch motion eases the demand for the flare at the bow of the centre hull compered with a monohull. The forebody flare of the DRA model is very small and the increase in motion is not expected to be significant

g) A deeper forebody draught would be favourable for delaying slamming onset.

h) An increased beam would be favourable for easing the difficulty in propulsion machinery arrangement.

It can be appreciated that there is no lack of conflict and constraint arising from these various issues. Therefore, designing a hull form to meet every aspect in the above list is most unlikely. The designer's task in a ship design is to find a balanced design solution considering the relative merits of individual performance requirements. Fortunately, they are not always in direct conflict, and in the case of a trimaran some of them actually reduce the design constraints compared with the design of a monohull.

9.3.2 An 'Ideal' Centre Hull Shape

If the above listed design issues are considered in determining the shape of the centre hull, an 'ideal' hull shape would be: a high slenderness to reduce wavemaking resistance; a deep draught for the forebody to reduce slamming; a relatively large beam to draught ratio for the aftbody to favour the turning ability, stability, main engine arrangement, and wetted surface area. Thus, the shape of the resultant centre hull could be like the one shown in Figure 9.3.

The hull form has a deep narrow forebody and a wide shallow aftbody. The term 'Fore Cutup' corresponds to the term 'After Cutup' used for monohulls as the cutup has been moved to the forebody. Certainly, this may make some of the conventional propeller and shaft arrangements for monohulls, as used in the current trimaran studies, unsuitable for this hull form due to the shallow draught of the aftbody, but there would be no difficulty in finding a solution using prospective electrical propulsion. A major draw back would be the uneven keel of the hull which makes docking more complicated than for an even keel.

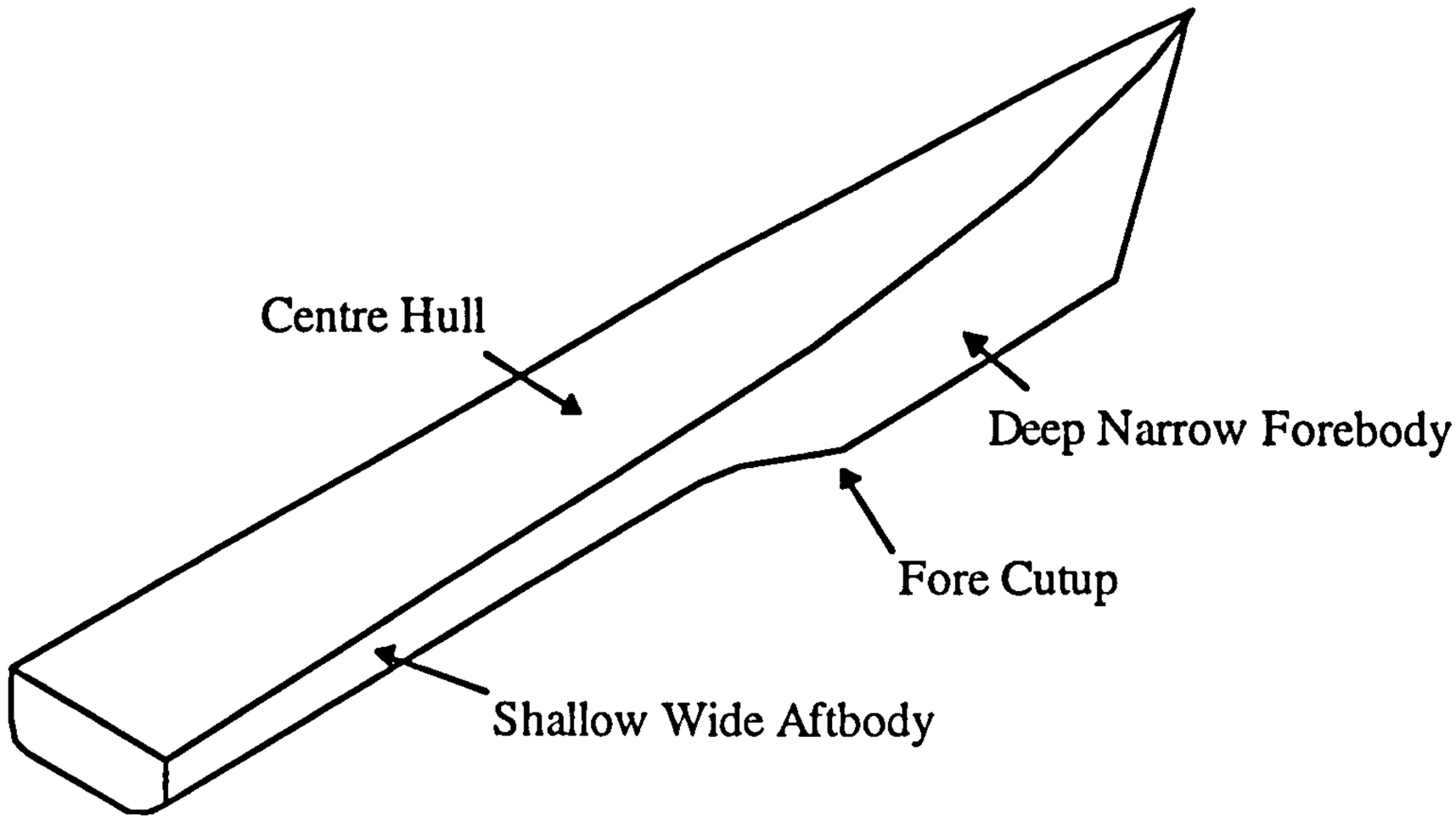

Figure 9.3 An ideal hull form for the centre hull

One of the reasons why the evolution of the monohull ship did not result in this proposed hull shape could be that it would lack directional stability. This would not pose a problem for the trimaran centre hull, as it already has sufficient directional stability due to the presence of the side hulls.

9.3.3 Wavepiercing Bow

The large deck area of a trimaran ship makes the bow deck area not as essential as for a monohull in the deck layout. This provides the possibility to us a wavepiercing bow for the centre hull. Based on the DRA model ship **(Zhang 1993)**, a trimaran ship with a wave piercing bow has been designed as shown in Figure 9.4.

The benefits gained from the wave piercing bow hull form are seen to be:-

- A saving in space, about 5% of the centre hull volume, has been suggested by calculation.
- It is estimated that this will lead to a saving in the structural weight of the centre hull of at least 5%.
- The bow deck has been shifted further aft, hence the deck wetness could be reduced.

- A saving in power is expected because the ship's light weight is reduced and possibly

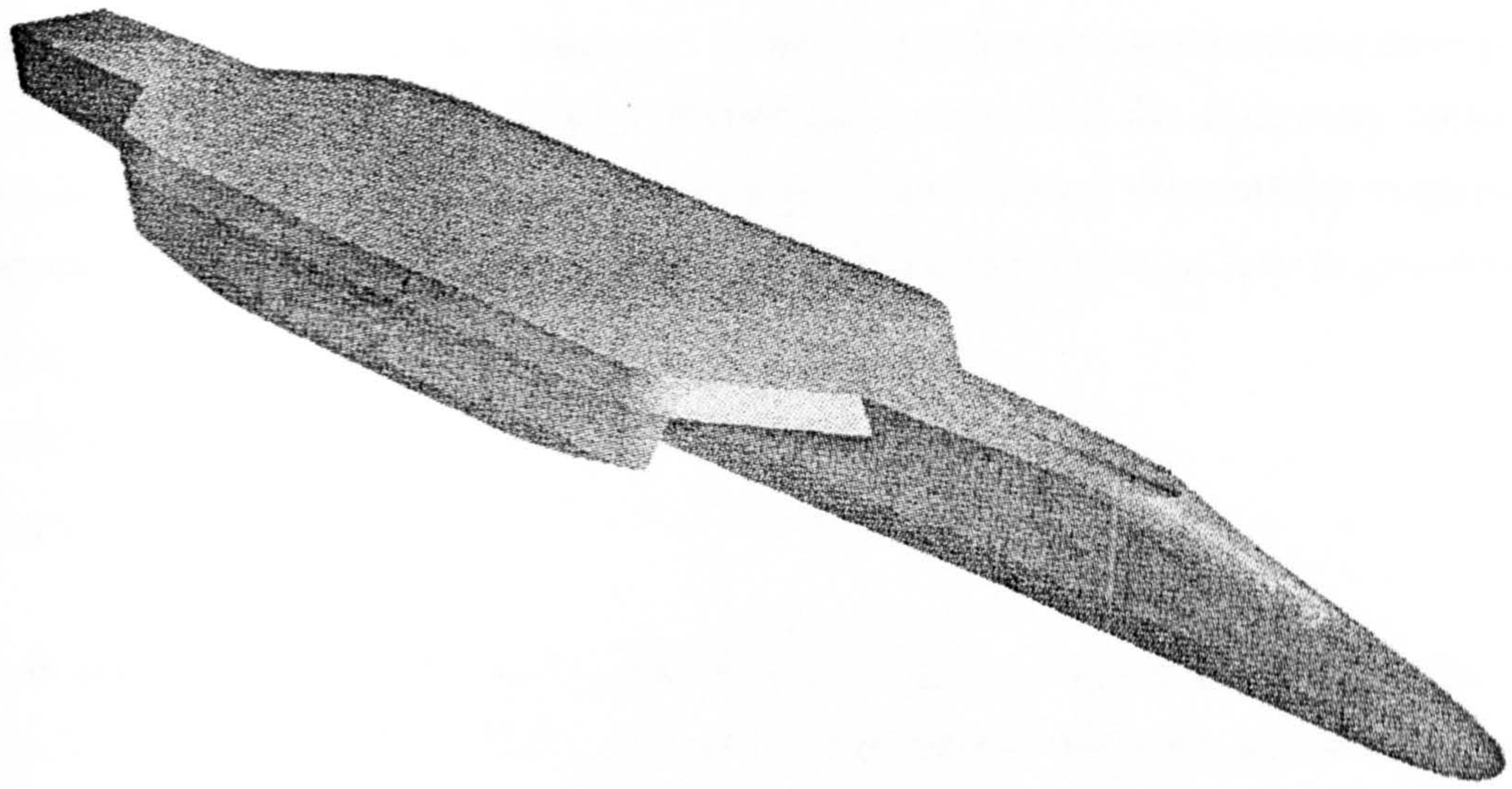

Figure 9.4 Applying wave piercing bow to the centre hull of a trimaran ship

The possible penalties due to a wave piercing bow are seen as:-

- The complete absence of the forebody flare would have an adverse effect on the relative motion of the bow. The comment in the paragraph f) of Section 9.3.1 only refers to the fact that flare is relatively less important on a non-wavepiercing trimaran compared with monohulls.

- The foremost end of the ship is under the water not visible to the captain, and there is no reference point above the waterline; This is unfavourable for harbour manoeuvring in a manner akin to a submarine.

- Mooring equipment have to be arranged further away form the bow, special attention would be required to design an efficient anchoring system.

The choice of bow shape for the centre hull may also be influenced by other factors including the artistic style of the ship and mission requirements. However, the above listed advantages have shown it as a potential option to be considered for the centre hull design.

9.4 Discussions on Side Hull Draught

The resistance performance of a trimaran ship is very much affected by the configuration of the side hulls, i.e., size and location. A reduced side hull displacement ratio results in reduced ship resistance. The design studies have suggested the following measures, as discussed in previous chapters, can be used as means to meet the stability requirement of the trimaran ship whilst keeping the side hull displacement ratio as low as possible:

- Side hull flare
- Side hull ballast water.
- Side hull foam filling

One of the side hull parameters which has not been discussed in detail is the draught. The side hull draught can significantly affect the wetted surface area of a trimaran ship which is larger than that of the monohull. The wetted surface area of the side hulls can be up to 30% of the total wetted surface area of the trimaran ship. The length and beam of the side hulls are largely determined by the stability requirements as shown in Section 9.2. Appropriate use of the above measures may reduce the length of the side hulls, however the reduction achievable normally is limited unless a significant change in stability criteria can be justified.

The constraint on draught applied in existing designs is that the bottom of the side hulls should not emerge when the ship heels to an angle of 15 degrees to prevent slamming occurring in anything but extreme conditions. This restriction was somewhat arbitrary in the absence of actual trimaran ship experience. The trimaran seakeeping model experiments **(DRA 1995)** successfully avoided any slamming on the side hulls or emergence of the side hulls when the ship rolls in high sea states. But, the following questions remain:-

- Is the 15 degree heeling restriction an excessive requirement? If so, what should be the minimum required heeling angle to avoid side hull emergence?

- Will slamming at the bottom of the side hull occur if the side hull draught is reduced to the extent that the side hull emerges when the ship rolls in modest sea states. If so, what would be the effect of the slamming, both locally and on the fatigue of the cross structure?

If the side hull draught can be reduced significantly, the side hull resistance will be significantly reduced as the side hull wetted surface area reduces. If this can be achieved without compromising the seakeeping performance, it will be a significant step to improve the hydrodynamic performance for the trimaran ship. The side hull draught of the trimaran model Ship 2 designed for the Haslar experiments is 3.5 metres (see Table 4.1). If the draught can be reduced to 2 metres or even less, as shown in Figure 9.5, the reduction in side hull resistance will be very significant. The limitation to this side hull draught variation is the waterline of the ship's light condition as the dotted line showed in the figure.

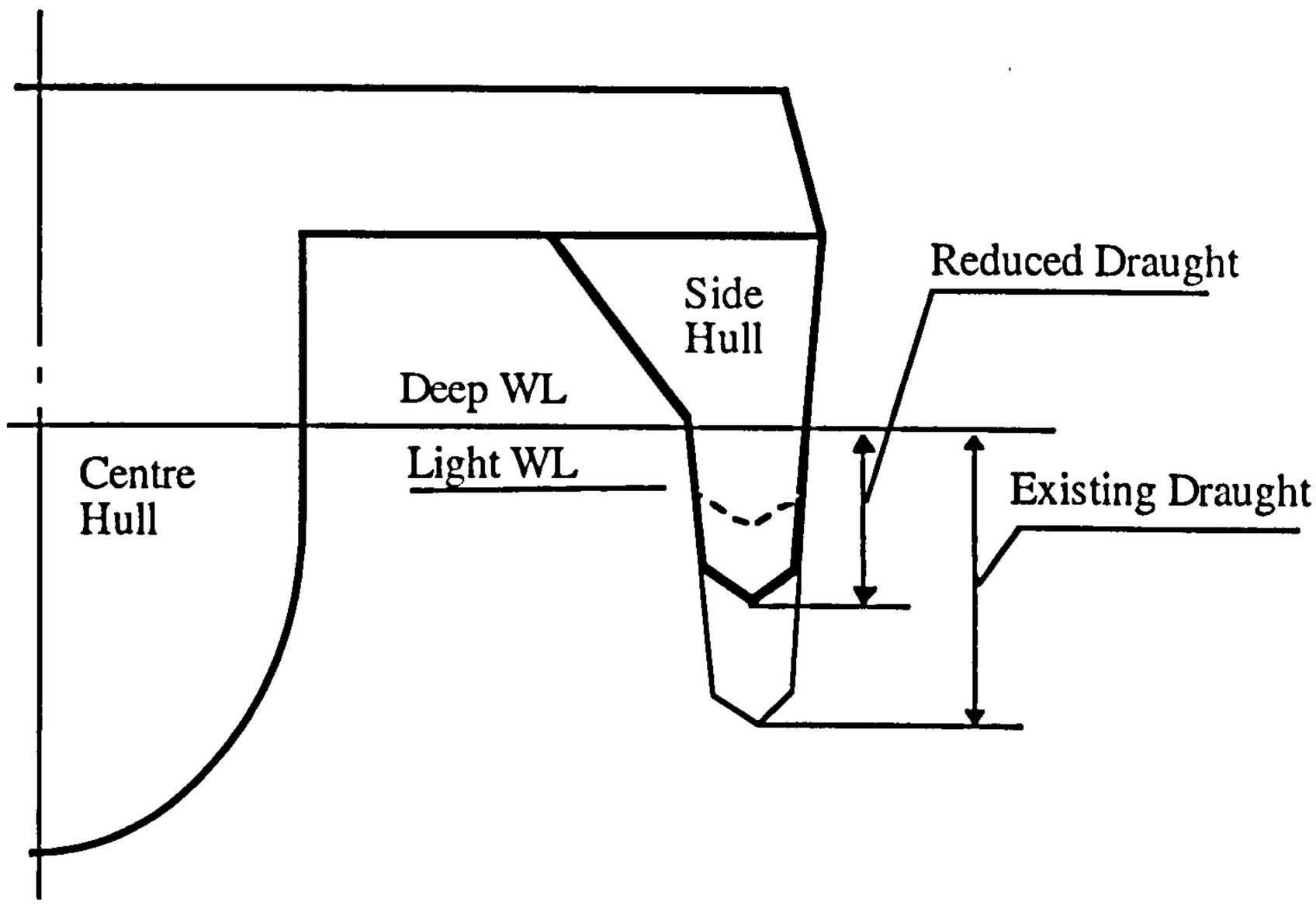

Figure 9.5 Reduced side hull draught

In considering a reduction in the side hull draught, the following two aspects need to be addressed:-

a) A reduced side hull draught will result in a reduction of roll damping contributed by the side hulls. To compensate for this, a set of roll damping fins can be fitted underneath of the side hulls as shown in Figure 9.6 which should be very efficient since, as in the roll damping study (Chapter 6), the roll damping produced by the lifting forces on the appendages is a major damping source when the ship is at moderate to high speeds.

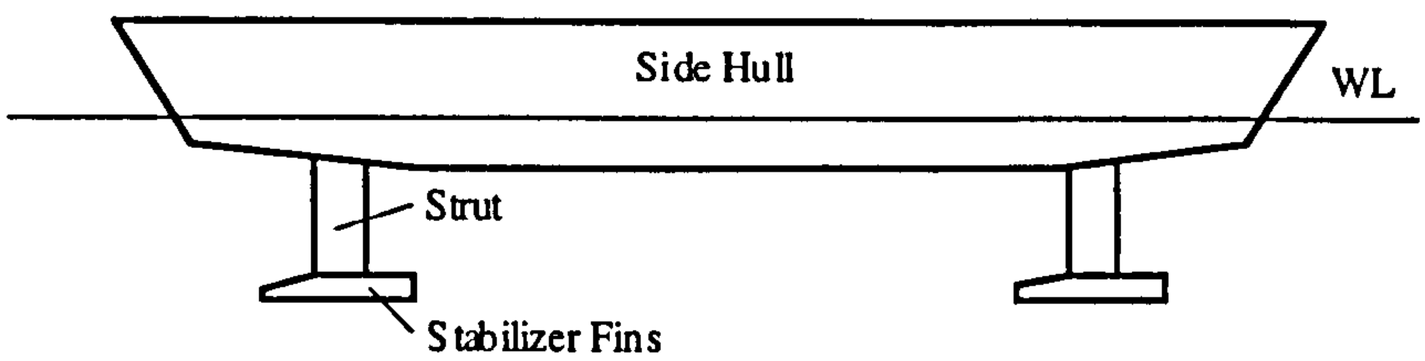

Figure 9.6 Roll stabiliser fins

b) A reduced side hull draught will also affect the stability performance of the trimaran ship. Because the change of the side hull draught would not change the waterplane area of the side hulls, threfore would have little effects on initial intact stability. However, large angle stability and damage stability will be affected. The decrease in the displacement of the side hulls would have adverse effects on the damaged stability, as the damage stability of a trimaran ship largely depends on the buoyancy remaining in the side hulls after damage. Conversely, the loss of the under water volume in the side hull may not have as severe an effect as the majority of the volume in the side hulls is located above the waterline when the ship heels. And also, less side hull displacement would result in a smaller initial heeling angle of the ship when one side hull is damaged. Certainly, the actual effects on damage stability require a more extensive stability assessment.

However, to justify a significant reduction in side hull draught, more detailed analytical work together with model experiments is required. As slamming is an area where an adequate theoretical prediction tool is yet to be developed, the most reliable way to assess this would be through conducting model experiments. Model experiments, therefore, need to be undertaken to observe the slamming occurrence and record the rolling angles. A research proposal has been put foreword to investigate the possibility of reducing the side hull draught by model experiments and theoretical analysis **(Zhang 1996c)**.

9.5 Stability Criteria for Trimaran Ships

Because there are no designated stability criteria for the trimaran ship yet, stability criteria for other ship types have had to be used in the trimaran ship studies discussed

earlier in the thesis. It is therefore necessary to examine the suitability of these criteria to the trimaran ship. As it would be arbitrary to abandon any aspects in the current criteria at this early stage of the trimaran study, when there is little experimental work and no full scale trimaran experience, the following discussion provides some preliminary recommendations as to where additional criteria and considerations might be pursued.

9.5.1 Stability Criteria for Naval Ships

The stability criteria used in the previous UCL naval trimaran ship designs were based on the MOD standard **(NES 109 1989)** with the assumption that the stability of a trimaran ship would be adequate if it could achieve the same level of stability as a monohull ship. In view of the lack of real trimaran ship data and sea experience, the current criteria are still deemed as most appropriate for trimaran ship design. However, the NES 109 criteria have been designed for monohull ships and may prove to be less appropriate for the trimaran ship. Some terms in the criteria might be redundant and the others might be inadequate or more than adequate. The following aspects have to be addressed.

i *Weight Growth*

For a ship to meet stability criteria throughout its life, a margin for weight growth has to be considered in the initial stability calculations. NES 109 requires a 3% increase of lightship KG, together with an increase in displacement for monohull ships.

The displacement of a trimaran ship is expected to increase in a similar manner to a monohull ship with the same role, but the rise in KG due to growth may be greater than that of a monohull as growth is expected to occur at higher locations in the case of trimarans **(Cole 1992)**. Though the actual growth data can only be obtained through sea service of real trimaran ships, a slightly higher percentage increase in KG for trimaran ships should be used for current trimaran designs. An increase to 5% is deemed sufficient.

ii *GZ curve shape criteria*

NES 109 criteria specifies the minimum area under the GZ curve up to 30 degrees and an area between 30 and 40 degrees to ensure an increasing righting arm with an increasing heel angle for the monohull ship. No minimum area under the GZ curve between 10 to 30 degrees is specified. This seems adequate for the monohull ship as

the GZ curve of a monohull ship would increase steadily until the heeling waterline reaches the deck edge, normally a heeling angle of at least 30 degrees.

However, this may not be adequate for all trimaran ships. For a trimaran ship without significant side hull flare, the GZ curve would tend to flatten out or even decrease as early as at a heeling angle of 10 degrees. Figure 9.7 shows the GZ curve of such a trimaran ship compared with that of a similar monohull. This may cause a progressive heeling of the ship beyond 10 degrees unless GM is exceptional high. Thus the ship may fail to meet the stability criteria or passengers/crew may start to panic. Therefore additional criteria seem necessary to define the GZ curve shape for heeling angles between 10 degrees to 30 degrees to prevent this happening.

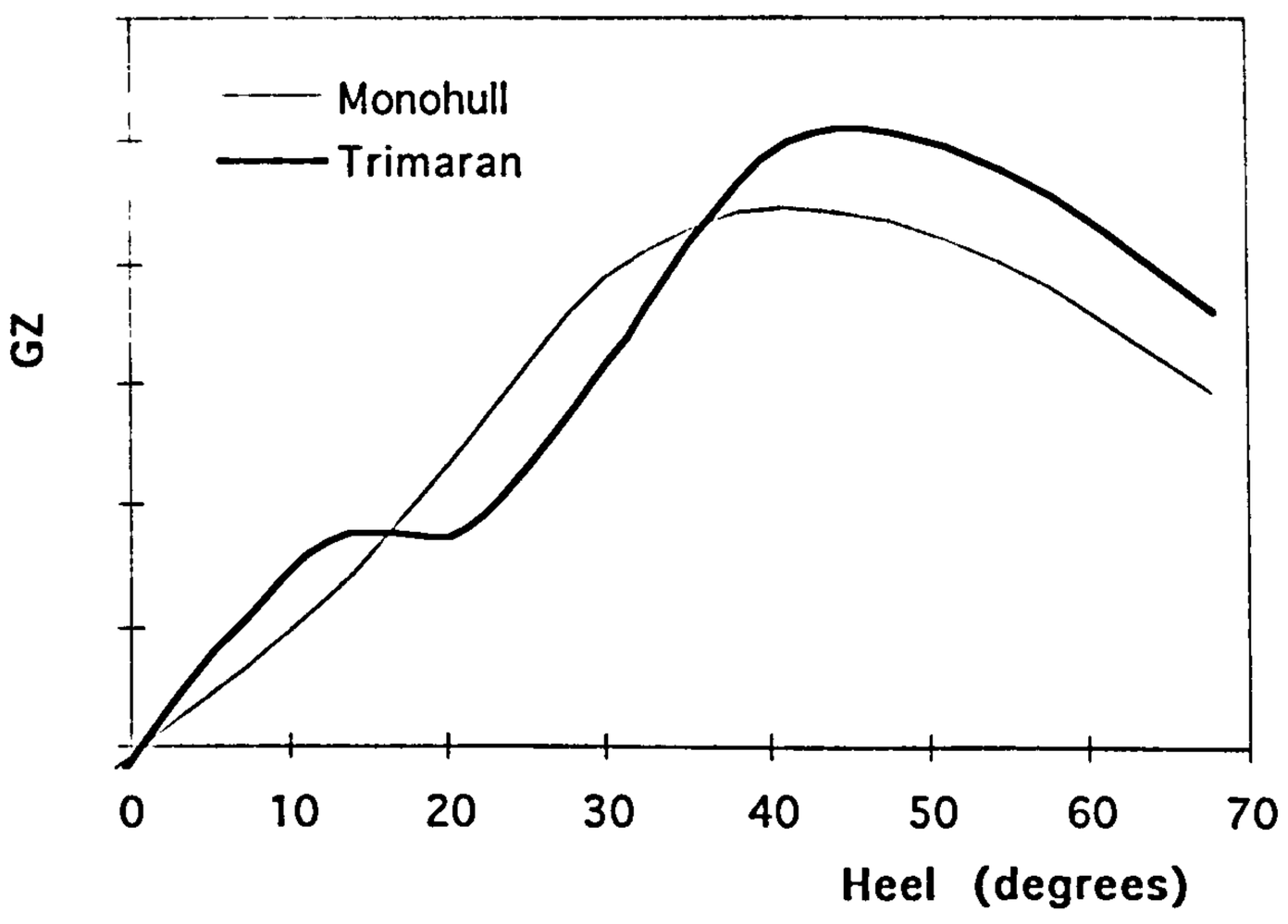

Figure 9.7 Undesirable GZ flatten out for a trimaran ship without side hull flare

There are two ways to achieve this:-

(a) Require a minimum area under GZ curve between the heeling angles of 15 to 30 degrees for the trimaran ship, for example, a minimum 2.5 times the area of GZ curve up to 15 degrees, or,

(b) Require the values of the GZ curve up to 30 degrees to be not less than a virtual GM line which is a percentage of the real GM line as shown in Figure 9.8, for example, 80 per cent.

Obviously, further investigations are required to validate the necessity and values for these criteria.

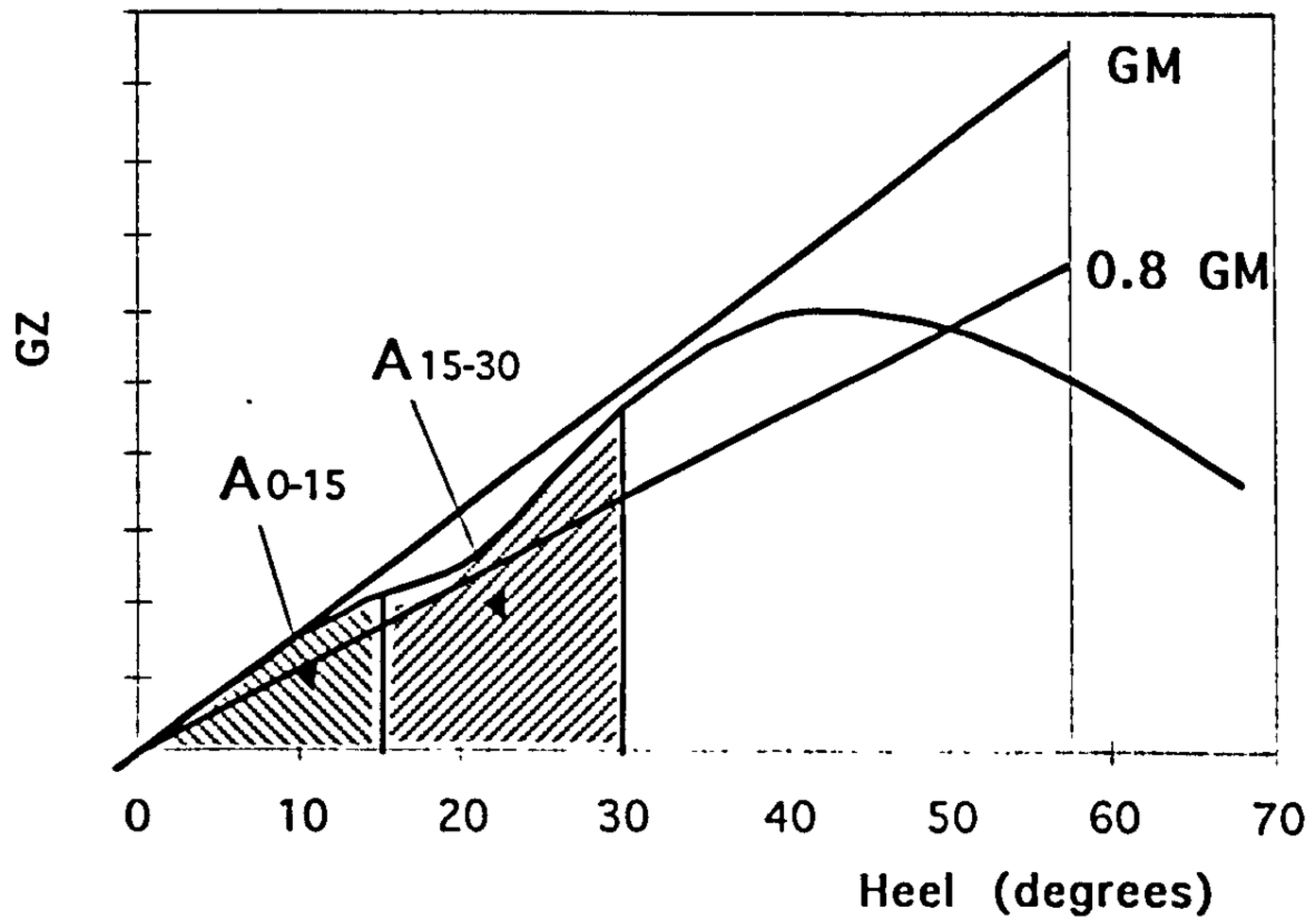

Figure 9.8 Proposed restrictions to GZ Curve between 15-30 degrees

iii *Wind heeling arm*

NES 109 criteria requires the maximum wind heel moment of a monohull to be calculated at the ship's upright condition with beam wind, and the heeling moment is then assumed to reduce with angle of heel at a rate of $cos^2\theta$, where θ is the heel angle. Wind tunnel experiments have shown that the worst wind heeling moment for a catamaran does not occur at 90 degree beam wind and 0 degree heel but at 60 degree off the bow and 40 degree of heel **(Roberts 1990)**.

Though it is still not clear whether the trimaran would have a similar wind heeling moment trend as the catamaran, because this would require wind tunnel experiments on trimarans, more effort should be spent in the calculation of the wind heeling moment. The recommendation made by **Cole (1992)** should be considered, that is, to perform calculations for various angles of heel using the true waterline of free trim.

9.5.2 Stability Criteria for Fast Ferries

The fast trimaran ferries **(Zhang 1992) (Hill & Merchant 1993)** were designed to comply with the criteria proposed by the Department of Transport for the revision of Chapter 2 - Buoyancy, Stability and Subdivision of the IMO Code of Safety for Dynamically Supported Craft **(DTp 1991)**. The proposal covers not just dynamically supported craft but also the stability criteria for multihull ships which have now been slightly modified and incorporated into the new IMO code for High Speed Craft (HSC) **(IMO 1995)**. The code for multihulls is clearly based on the experience with twin hull ships. Again, since there is no full scale experience of the trimaran yet, this remains the only code currently appropriate for commercial fast trimaran ships. However, based on the characteristics of the trimaran ship, the following aspects need to be considered in applying the current HSC code for trimaran ship design.

i *The minimum GM requirement*

The HSC code has eliminated the requirement for the minimum initial metacentric height *GM* as most twin hull ships possess a very high value of *GM* and this makes this requirement redundant. Considering the characteristics of the trimaran ship as discussed above, as the *GM* value of a trimaran ship is normally much lower than that of a twin hull ship, the rolling behaviour of the trimaran ship should be more akin to the monohull ship rather than the twin hull ship. Therefore, this suggests that the minimum *GM* requirement is retained for trimaran ships. The minimum GM requirement designated for monohull ship **(IMO 1977)** used for trimaran ferry studies, which is the same as in the current HSC code, can be applied to the trimaran ship, namely

Liquid *GM* > 0.15m

ii *The angle of Maximum GZ occurs*

The HSC code has also reduced the angle at which the maximum *GZ* occurs to 10° because for some twin hull ships it is impractical to achieve larger angles because the maximum *GZ* occurs very early due to their extreme high *GM* which results in a steep initial *GZ* curve. In contrast, this is not the case for the trimaran ship which possess a much lower *GM*, a smooth and sufficient *GZ* curve for the trimaran ship is as essential as for the monohull ship, the requirement proposed by **DTp (1991)** has been retained in the trimaran fast ferry studies, namely

Angle of maximum *GZ* occurs > 20°

iii *GZ curve shape criteria*

Similar considerations as for naval ships discussed in 9.6.1 (ii) should be taken into account for commercial trimaran designs for the reason already discussed.

9.5.3 Damage Stability Criteria

The NES and HSC damage stability criteria could generally be considered to be adequate for use in the design of naval and commercial trimaran ships respectively. No additional criteria is deemed necessary according to the current knowledge of the trimaran ship.

However, some terms in these damage criteria currently adopted for trimaran ships might be excessive, for example:-

i The longitudinal damage extent is calculated as a proportion of the ship's length. The ship's length for monohull ships is the hull length, for twin hull ships is the demi hull length, whilst for the trimaran ship is the centre hull length. For the current calculation of the trimaran side hull damage extent is also based on the ship's length, i.e., the centre hull length, though the side hulls are much shorter compared with the centre hull. This would seem rather penalising.

ii There is no vertical limit specified for side hull damages, though the boundaries between the side hulls and the cross structure, when there are no machinery systems in the side hulls, could be made more watertight than any horizontal boundaries in a monohull ship. The vertical damage limit suggested in a SWATH ship stability investigation **(John Brown 1988)** could be considered for the trimaran ship, i.e., using the wet deck between the side hull and the cross structure as a horizontal watertight boundary instead of allowing unlimited vertical extent of flooding.

However, it would be premature to suggest any changes to current damage stability criteria, as these criteria were produced from extensive experiments and sea experience on monohulls and catamarans. Any suggested changes have to be supported by experiments and sea experience. The above comments show the need for future

investigations as any changes in these criteria could have significant impact on the configuration and performance of the trimaran ship.

9.6 Wing Propulsion Design Procedure

The trimaran configuration has provided the opportunity for installing wing propulsion units in the side hulls which provides the trimaran ship with some enhanced operating abilities not possible for monohull ships:-

- An increased survivability, should the main propulsion system in the centre hull fail to operate in cases of engine room fire or flood, the wing propulsion could still be used to propel the ship.

- An increased manoeuvrability at low speed using the wing propulsion, as well as for stationary turning described earlier.

The following discussion reveals some considerations for the design of the trimaran wing propulsion system by presenting the process of the wing propulsion design carried out during the trimaran turning ability analysis presented in Chapter 8

9.6.1 Wing Propulsion Arrangement

The trimaran ship used for the turning ability analysis in Chapter 8 is based on Ship 2, the 150m length and 30m beam destroyer, designed for DRA Haslar model experiments (Table 4.1 in Chapter 4). Ship 2 was designed with twin shafts in the main hull only, and so the design has to be reconfigured to accommodate wing propellers. As it was decided to use electrical motors and fixed pitch propellers for wing propulsion **(Zhang 1995a)**, the following design changes have been made to the side hulls to accommodate the wing propulsion system:-

a) A motor compartment of 3 metres diameter has been added on to the stern of each side hull to accommodate the propulsion motor and gear box.

b) The transverse position of the side hulls was adjusted to make sure neither the wing propeller nor the wing motor compartments would exceed the maximum beam of the ship. The shape and above water flare of side hull has been modified accordingly.

c) The side hulls are vertically sided below the waterline to provide a fairer connection between side hull body and motor compartment. In addition, the increased bottom width of side hulls would provide an increased roll damping effect and improve the GZ curve as is demonstrated in the stability calculation (**Zhang 1995a**).

d) The displacement of the side hulls has been increased due to the change of the section shape and the added motor compartment. As a general principle, the side hull displacement of a trimaran is to be kept as small as possible, provided the ship continues to meet the stability requirements, to achieve minimum resistance. Therefore the draught of the side hulls has been reduced from 3.5 metres as for Ship 2 to 3.0 metres to the side hull keel. The side hull draught to the bottom of the motor compartment is 4.5 metres, whilst the centre hull draught is 5.5 metres.

Figure 9.9 shows the section drawing of the new configuration, and Figure 9.10 is a 3D model of the ship created using GODDESS.

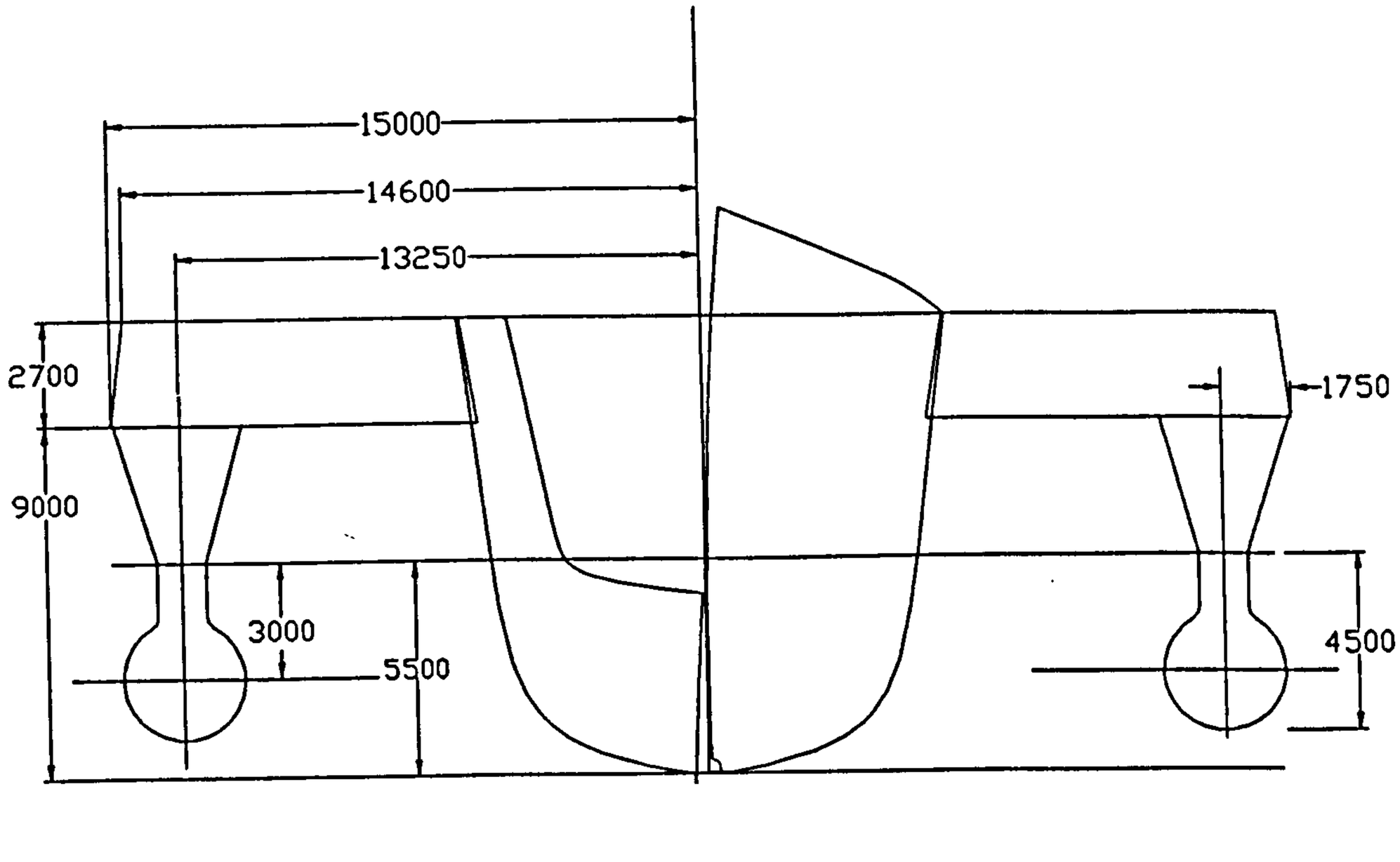

Figure 9.9 Configuration of the trimaran with wing propellers (dimensions in mm)

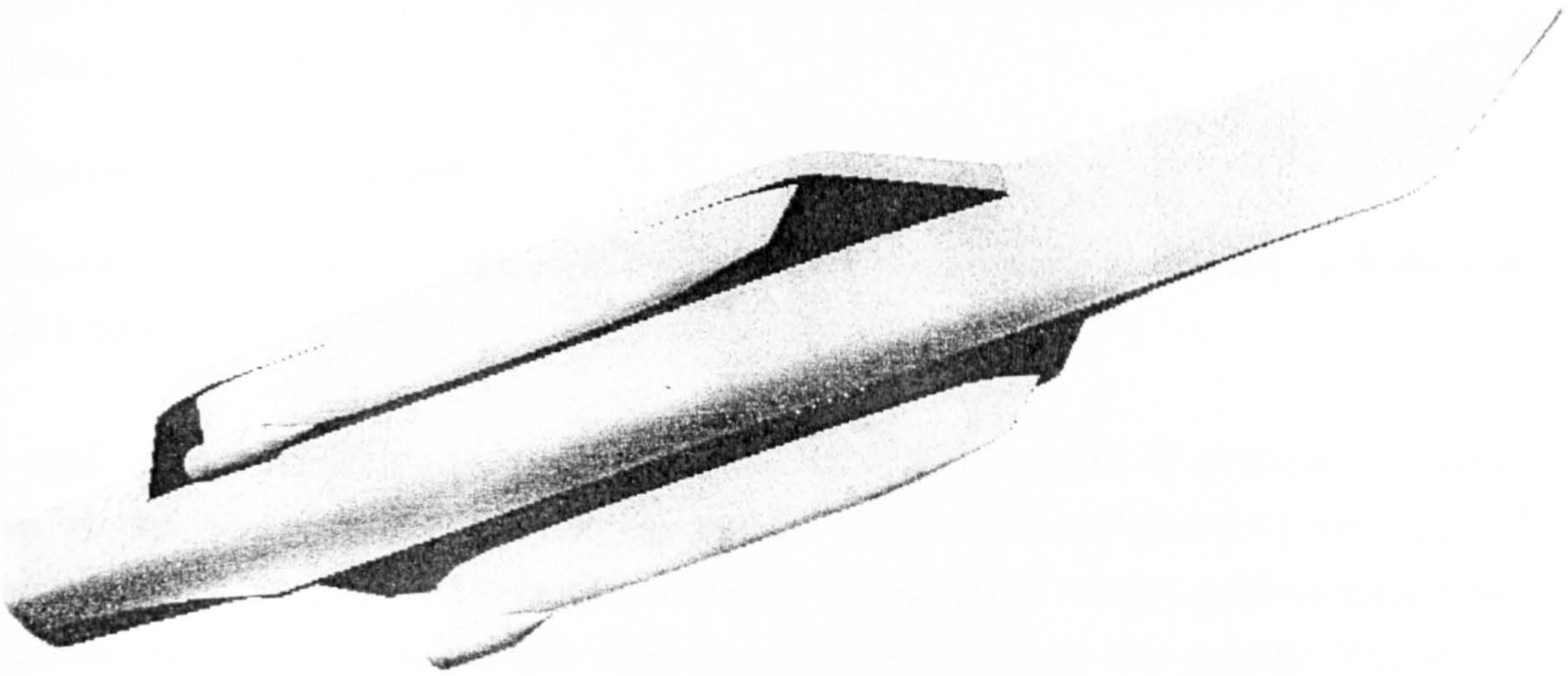

Figure 9.10 3D modelling of the trimaran with wing propulsion compartments

9.6.2 Wing Propeller Design

In considering design conditions for the wing propellers, there are normally two speed requirements for a naval ship, the cruise speed and the maximum speed. A cruise speed of 20 knots and a maximum speed of 30 knots, as is the case in DRA model design, were set for the trimaran wing propeller design. The wing propellers are therefore required to work in the following two modes,

a) Operating alone to drive the ship up to 20 knots

b) Operating with the central propeller to drive the ship up to 30 knots.

The optimum design point for the wing propellers was chosen at 20 knots which is considered as the main operating condition. The objective is therefore to design the wing propeller at the chosen speed (20 knots) with highest possible efficiency, and with minimal lost of efficiency at the other speed (30 knots). There are two design approaches which can be used:-

a) *Equivalent thrust approach.*

Assuming the propeller will produce the same amount of thrust power at 30 knots as it does at 20 knots.

b) *Constant torque approach.*

Assuming the propulsion motor will produce the same torque at 30 knots as it does at 20 knots.

The equivalent thrust method means the propulsion motors need to produce the same power at two different propeller rotating speeds. This can be achieved by altering the input voltage of the electric propulsion motors. The constant torque method means the propulsion motor would produce the same torque at two different ship speeds. The thrust power produced at the higher speed will be more than that at the lower speed. For both methods, there would be a certain amount of propulsion efficiency lost when the ship runs at her maximum speed of 30 knots rather than at 20 knots which is the propeller design speed.

In comparing the two methods, the constant torque method showed a slightly better result in terms of the propeller efficiency at the higher speed condition **(Zhang 1995a)**. It was also envisaged that it would be easier to make the propulsion motors meet a constant torque requirement rather than constant power at various motor speeds. The constant torque method was thus adopted in the wing propeller design.

There are also some restrictions that need to be taken into account in considering the wing propeller diameter. The wing propellers are located at the sterns of the side hulls. Whilst the tips of the wing propeller would extend below the keel of the side hulls, it is not desirable for the tips to extend below the keel of the centre hull since this would make the propeller vulnerable and make docking more difficult. A minimum draught is also required for the propeller tips below the water line to avoid cavitation occurring when the ship rolls in the seaway. Finally, the tips of the wing propellers should not project outside of the maximum beam of the ship.

The actual procedure of the wing propeller design is as the follows:-

(1) Firstly, design a propeller at the power required to drive the ship at her cruise speed of 20 knots. The propeller geometry data including propeller diameter and blade area ratio can be derived with the design considerations discussed above. This step is essentially the same as that used for monohull propeller design. The optimum

efficiency point of the propeller and pitch ratio are found. The propeller design point (P_1) is determined as shown in Figure 9.11. The propeller torque at 20 knots is then obtained from the corresponding torque coefficient K_{Q20kn}.

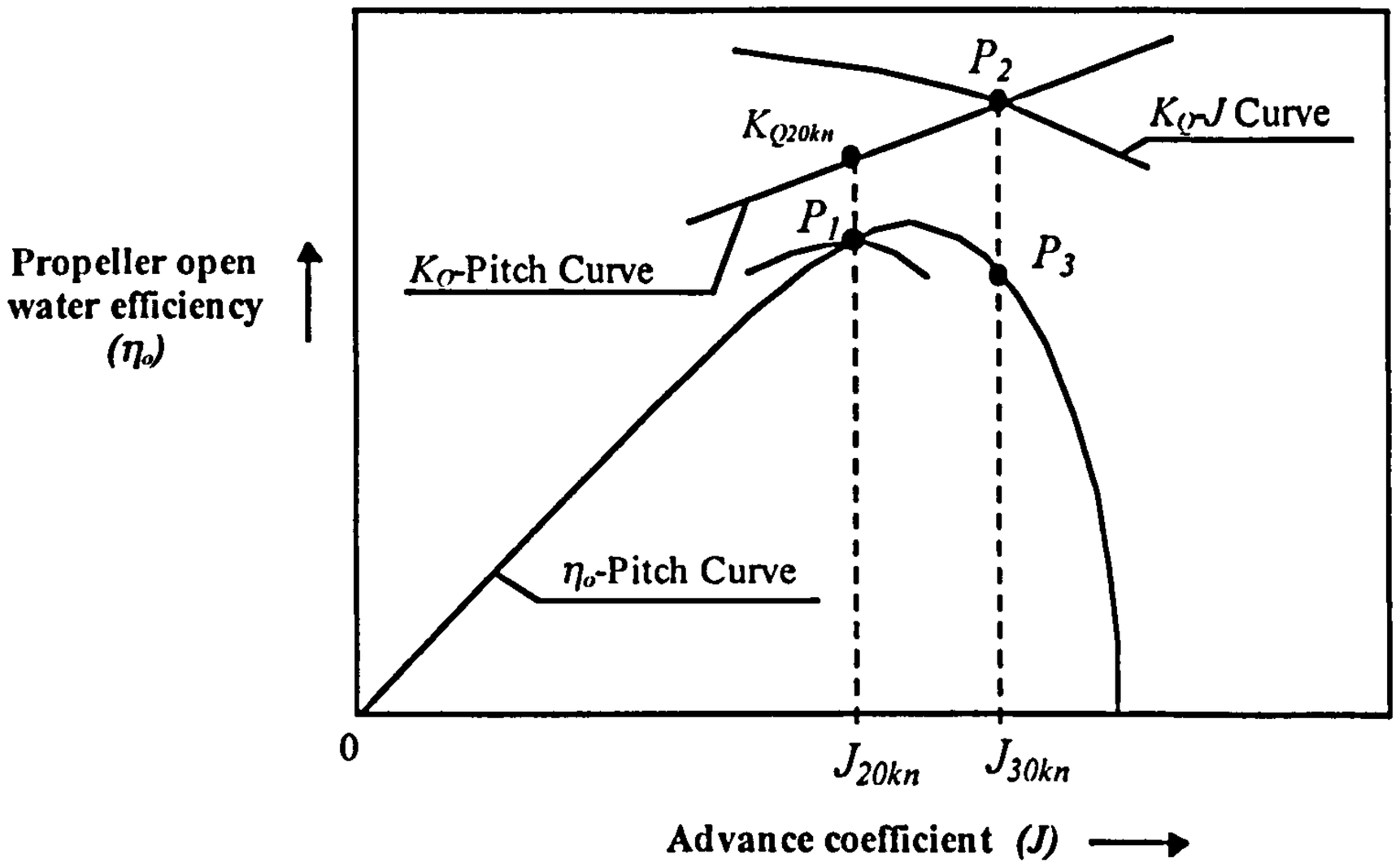

Figure 9.11 Wing propeller design procedure

(2) The propeller condition at the maximum speed of the ship at 30 knots is then calculated. Using the propeller torque derived at step (1), the K_Q-J curve is calculated by the following constant torque equation:-

$$\frac{K_Q}{J^2} = \frac{Q}{\rho D^3 V_A^2} \qquad (8\text{-}17)$$

where K_Q is the torque coefficient, J is the advance coefficient, Q is the torque, D is the propeller diameter, and V_A is the advance speed. The value of torque Q is given from Step (1). The advance speed V_A is now 30 knots. Using the propeller diagram as in Figure 9.11, the intersection of the K_Q-J curve and the constant *Pitch*-K_Q curve (P_2) gives the working condition of the propeller at the speed of 30 knots. The corresponding advance coefficient, propeller rpm, and propeller efficiency point (P_3) are then obtained.

(3) Now the propeller working condition at 30 knots needs to be checked, if the point P_3 falls too far from the peak of the efficiency curve, the wing propellers will be unstable at 30 knots should any slight change of the ship condition occurred. In this case, step (1) needs to be repeated to re-select the design point (P_1) for 20 knots. This process is repeated until satisfactory propeller working condition for both 20 knots and 30 knots are obtained.

9.7 Summary

This chapter has discussed some special procedures and considerations in the design of trimaran ships, which have not been encountered in the designs of other marine vessels, and has focused on the configuration of the side hull and the centre hull of the trimaran ship.

1 The presence of the side hulls has made the design procedure and considerations in the trimaran initial sizing stage more involved than that in the design of a conventional monohull ship. A practical procedure is proposed in this chapter to divide the side hull configuration process into two stages, the initial sizing stage, and the detailed side hull configuration stage. Thus the centre hull can be optimised in the first stage with the side hull parameters simply approximated. Then the side hull configuration can be refined through a comprehensive stability analysis.

2 The discussion of the philosophy behind the choice of the centre hull shape reveals that the requirements for the hull form of the centre hull and that for a monohull are significantly different. These differences may lead to a completely new type of hull form for the centre hull as illustrated in Section 9.3.2. Obviously, this would require to be refined by more extensive analytical and experimental work.

3 The stability criteria for naval ships and commercial ships are discussed with some recommendations on the criteria which need to be pursued for the trimaran ship. An additional GZ curve shape criteria to the current codes is recommended. This is to avoid inadequate GZ value at the heeling angle of 10° and 20° which may occur if the side hulls are not properly configured.

4 The proposed design procedure for wing propellers shows the general considerations in propulsion arrangements and the choice of working conditions. Since the wing propellers of a trimaran ship are likely to work under two different speeds, the

design example presented in Section 9.6 has provided a design method to make the wing propeller achieve satisfactory efficiencies for both speeds whilst being designed primarily for the cruise condition.

CHAPTER 10

CONCLUSIONS AND RECOMMENDATIONS

10.1 General

The thesis has presented the study of the design and the hydrodynamic performance for a novel ship type, the trimaran displacement ship. The work has demonstrated that this new trimaran ship concept offers the naval architect a multihull configuration which,

1) provides the possibility to exceed the speed power limitation encountered by existing monohull ships by using slender hull forms which reduce wavemaking resistance, and effectively decouples the desire to minimise installed power from direct conflict with the need to achieve sufficient beam to meet stability standards;

2) provides the flexibility for the designer to tune up the hull form configurations to achieve better hydrodynamic performance, namely seakeeping, resistance, and stability, to an extent not possible for monohull and twin hull ships;

3) provides a wider beam on the upper deck (larger deck area) allowing a flexible layout compared with monohulls.

The design process and major design considerations for the trimaran displacement ship have been explored. Theoretical models and computer tools have been developed for the analysis of the trimaran hydrodynamic performance, and good agreement with the first extensive model experiments have been achieved.

Both experimental and theoretical studies so far have found no fatal flaws in this new concept though more extensive research is required to explore a wider range of configuration variations for the new ship type.

The studies to date suggest that the trimaran ship concept is a potential contender for future marine transportation and naval applications, and that present day design technology is up to the job of transferring this novel concept into real ships.

10.2 Design Process

The design process for a trimaran ship is, in principle, similar to that for the design of monohull displacement ships. However, the more involved configuration of the trimaran ship, compared with the monohull ship, gives the designer more choices in achieving stability requirements, lower resistance, and better seakeeping performance. Thus, more

detailed considerations need to be addressed in the early design stage than that for the monohull. The design procedure for determining the hull form parameters for a trimaran ship is best carried out in two stages which have been broadly demonstrated in the design studies presented in the thesis:

1) *Initial sizing stage.* At this stage, the trimaran form design is largely a process of obtaining the parameters of the centre hull with the parameters of the side hull fixed. The process focuses on optimising the centre hull to achieve minimum resistance regardless of the stability requirements. However, the side hull parameters need to be brought into the design balance. This can be done by approximating the side hull parameters simply from the damaged length of the ship and a GM value chosen from stability requirements and the considerations to avoid unfavourable roll motions.

2) *Detailed side hull refinement stage.* The tasks in this stage are, refining the side hull size, detailing the side hull shape, and identifying additional measures such as required flare and ballast, through full stability assessment. Because a reduced side hull displacement ratio would result in reduced resistance for the trimaran ship, the objective of this process is to find a side hull configuration with minimum displacement ratio whilst satisfying stability requirements. A favourable side hull location needs also to be found to minimise the wavemaking resistance in conjunction with ship layout considerations.

Given that stability, resistance and seakeeping further interact with other issues which are not addressed in the thesis, such as structural strength and internal configuration, it is important to appreciate the procedure outlined above must be seen in the overall design context and the particular drivers of a given ship design.

10.3 Seakeeping

Current studies have shown that the seakeeping performance of a trimaran ship can be expected to be generally be better than that of a monohull of equivalent displacement, and the stiff roll motions encountered by the catamaran ship can be avoided in the new trimaran configuration.

The motion prediction using the three dimensional wave potential theory gave good agreement with the model experiment results for heave and pitch motions of the trimaran

ship. Good agreement for trimaran roll motion predictions with model experiments has also been achieved when viscous roll damping is taken into account.

Methods for estimating roll damping coefficients both from roll free decay data and direct computation have been developed which show good agreement with the experiment results in simulating the free decay curves as well as for roll motion predictions. The roll damping analysis has shown that the lift forces produced by appendages contribute most of the damping effects when the ship is at speed, particularly in following quartering seas at which the wavemaking roll damping has little effect due to reduced encounter frequencies. This indicates the importance of finding appropriate configurations of the bilge keels or fins on the side hulls for improving the roll motions in a trimaran design.

Although the trimaran ship has a much lower metacentre compared with the catamaran ship to avoid stiff roll motions, the results of model experiments and theoretical analysis have suggested that a slightly higher GM value compared with the monohull may have to be selected for a trimaran ship to avoid unfavourable roll motions in following quartering seas. An appropriate approach needs to be used at the early side hull sizing stage to check the tuning factor of the ship, as is illustrated in Chapter 9, to avoid unfavourable roll motions .

10.4 Resistance

It is shown that the resistance of a trimaran ship is lower than that of an equivalent displaced monohull ship at high speed due to the reduction in wavemaking resistance. The ferry design study has also shown that the resistance of a trimaran is lower than that of a catamaran of the same displacement over the whole speed range.

The wetted surface areas of the current trimaran ships are generally 30% larger than those of equivalent monohulls. This has an adverse effect on the resistance of trimaran ships at low speed where the frictional resistance is dominant. Therefore, reducing wetted surface is one of the principal objectives in the trimaran hull form design, for both the centre hull and the side hulls, in order to reduce the frictional resistance.

Initial investigations into the effects of trimaran configurations on the wavemaking resistance shows that the advantage of trimaran ships over conventional monohull ships can be enhanced if the side hulls are advantageously located to achieve maximum wave cancellation effects. For the trimaran destroyer analysed in the thesis, the optimum side hull position appeared to be at the stern of the ship for its top speed.

The theoretical prediction of wavemaking resistance for trimaran ships has shown a reasonably good agreement with the model experiment measurements. The program has merit as a comparison tool in the investigation although further improvement are needed to improve the computer program for use with a wide range of trimaran configurations and for high speed trimarans.

Further research work is necessary to investigate the effects of the side hull transverse position and side hull shape on the resistance of trimaran ships. The objective should be to find the best side hull configuration which would result in less wavemaking resistance as well as frictional resistance whilst satisfying stability and other practical requirements.

10.5 Manoeuvrability

Investigation into the trimaran manoeuvrability has suggested that, to achieve a same level of turning ability, a trimaran ship requires a larger rudder area than that required by an equivalent monohull. This also means the trimaran ship has superior directional stability. Therefore the hull form design of a trimaran ship can be conducted without immediate concern for its directional stability. The directional stability measures adopted by monohull ships, such as the deadwood, vertical fins, and after cut up, are not necessary in the trimaran hull form design. Instead, a flat bottom in the aft body, and reduced side hull draught, all of which will also be favourable in reducing resistance, can be adopted to reduce the requirement for the rudder area.

The study into effects of side hull configurations on turning ability shows that the side hull draught and longitudinal position are two important parameters of a trimaran ship which influences its turning characteristics. A small side hull draught and a forward location appear to be favourable to the turning ability provided these do not conflict with other considerations.

Wing propellers can give the trimaran ship excellent low speed manoeuvring characteristics, including the capability of stationary turning. However, it would seem that a satisfactory turning rate at medium and high speeds cannot be achieved using the wing propellers alone.

10.6 Stability

The design studies have shown that satisfactory stability can be achieved for a trimaran ship to meet the current stability criteria, although a more extensive stability procedure has to be carried out for a trimaran ship than for other ship types. This extra effort is required due to the flexibility in the configuration of the side hulls which plays a key role for stability and also has definite effects on the hydrodynamic performance of the ship.

Stability criteria

The existing stability criteria are generally applicable for trimaran ships as demonstrated in the design studies. However, extra care needs to be taken for the GZ curve shape between the heeling angles of 10 degrees and 20 degrees to avoid abrupt 'flattening out'. This can be done by imposing an additional GZ curve shape criteria for the trimaran ship as suggested in Chapter 9. It is also suggested that the minimum GM requirement, which has been eliminated in the current HSC Code (**IMO 1995**) for multihull vessels, should be retained in the trimaran fast ship design for the reasons already discussed.

Intact stability

The trimaran ships designed at UCL showed no difficulties in meeting the intact stability criteria of the current safety codes, except the above mentioned concern over the GZ curve shape criteria. Side hull flare, as shown in the thesis, or equivalent measures are normally required which would provide extra buoyancy in the side hull above the waterline, thus avoiding excessive heeling angles when the ship is under a steady wind and/or at high speed turning.

Damage stability

The damage stability requirement is the driving factor in determining the size of the side hulls of a trimaran ship, as discussed in the design procedure. The critical dimension for meeting damage stability requirements is the length of the side hulls. It has also been identified that the critical damaged case for a trimaran ship is when one side hull only is damaged. This tends to induce an excessive heeling angle if there is insufficient reserved buoyancy in the side hull. Thus the side hulls need to have a length of about 40% of the centre hull length for naval ships and about 35% for commercial ships to meet the requirements of existing stability criteria. To minimise the side hull length, which is advantageous for reducing its resistance, close side hull subdivision and adequate side hull flare above the waterline should be considered.

Pre-ballast water in side hulls at light sea going conditions is a very efficient way of reducing the heeling angle after damage.

10.7 Recommendations for Future Work

Seakeeping

The seakeeping analysis presented in the thesis is limited to a particular trimaran design, the DRA Haslar trimaran model (**Zhang 1993**). Effects of further variants in the trimaran configuration on seakeeping performance need to be investigated. A set of variations that could be explored have been already proposed (**Andrews & Zhang 1995a**):-

a. Further variations in side hull separation from the central hull.

b. Further variations in the longitudinal position of the side hulls relative to the centre hull.

c. Further variations in side hull size relative to centre hull.

d. Further variations in side hull shape.

e. Further variations in ship displacement.

Since the seakeeping performance of a trimaran ship cannot be isolated from other considerations, any of these variations, whilst being explored to see whether they provide a more hydrodynamically efficient configuration, will need to be checked in detail to see that the stability, resistance and other primary naval architecture aspects are not degraded beyond the level that is deemed necessary for the given ship applications.

Resistance

It is believed that further research into trimaran resistance should focus on reducing the frictional resistance, particularly the side hull frictional resistance. It is recommended to conduct systematic experiments and theoretical analyses on reducing the side hull wetted surface. One of the possible solutions is to reduce the side hull draught as discussed in Chapter 9. Again, this would also require extensive analysis work to check the effect of change in side hull draught on other aspects, particularly on stability and seakeeping.

For wavemaking resistance, although the effect of side hull configuration has been investigated using a computer tool, systematic experiments in this area are deemed necessary to validate the theoretical results. To improve the computer tool for use in future trimaran designs, the theoretical method for the prediction of trimaran wavemaking resistance needs to be further developed for use with high speed trimaran ships.

Structural analysis

There is a need to analyse the hydrodynamic loads on trimaran ship structures and structural responses, since this is still an area where very little has been investigated concerning the trimaran ship, although the existing structural designs **(Zhang 1992)** **(Pearson & Schild 1992)** and structural efficiency studies using a simplified model **(Ash 1993)** or a conventional method **(Putnam 1995)** have broadly investigated the characteristics of the trimaran structures.

Theoretical analyses on the hydrodynamic loads on the trimaran ship should focus on the lateral loads on the side hulls and the cross structure due to ship motion in waves, slamming forces on the bottom of the side hulls, and impact forces on the wet deck. This can be done using the three dimensional ship motion theory and needs to be validated using the stress data measured by DRA Haslar during the trimaran seakeeping model experiments **(DRA 1995)**.

Structural responses of the trimaran ship can then be analysed using an finite element methods with the hydrodynamic loads obtained in the above analysis. The modelling of the structure can start with one of the existing trimaran structural designs. The result of this analysis will lead to the design of a more realistic and more efficient trimaran structure than the existing design studies. The studies about the air gap between the cross structure and waterline (Chapter 4) are so far based on the occurrence frequencies of the water exceeding the wet deck. This is referred as *slapping* rather than *slamming* in the thesis because a threshold value of relative motion between the ship and the wave surface has to be exceeded for the slamming to occur **(Ochi & Motter 1973)**. In order to predict the frequency of slamming occurrence and the magnitude of impact pressure for the cross structure, experimental and theoretical studies have to be carried out to establish threshold values for slamming to occur and to impact the wet deck.

One of the major benefits of the above analysis is to obtain more accurate estimates of trimaran structural weights, particularly the weight of the cross structures. Studies into the slamming loads on the wet deck of the cross structure and side hulls will also

provide necessary data for the determinations of the required air gap and side hull draught which have significant effects on the overall design of a trimaran ship.

Stability

It is believed that further investigations into stability should focus on identifying suitable damage stability criteria for trimaran ships as none are designated for trimaran ships as yet. Current trimaran ship studies have indicated that damage stability is the design driver for the side hull length and the objective in side hull sizing is to find the shortest possible side hulls whilst satisfying the stability requirements. If the damage extent defined in the current stability criteria can be shown to be excessive for the trimaran ship, any justified reduction in this would result in significant improvements in hydrodynamic performance. This investigation can be done through model experiments and theoretical analyses akin to work that has been done for twin hull ships **(John Brown 1988 & 1991) (Roberts 1990)**.

Layout

The unique feature of the trimaran hull form configuration demands a new layout methodology to be developed.

Firstly, as discussed throughout the thesis, the side hull location has a definite effect on the hydrodynamic performance of a trimaran ship, both for resistance and seakeeping as well as for manoeuvrability. The side hull location would influence the size and position of the cross structure, and subsequently influence the strategy of upper deck layout. As the demands on the side hull position due to hydrodynamic performance and ship layout requirement may not always be consistent, the best compromise between the two should be explored. This can be done by carrying out a systematic exploration into trimaran layout variations alongside the systematic investigation into seakeeping and resistance mentioned above.

Secondly, although the wider upper deck area of a trimaran ship allows more efficient layout than for a monohull ship, excessive void spaces may exist in the long and narrow centre hull near the bow and also in the side hulls, and this would need to be addressed. One approach would be to find efficient ways to utilise these spaces by varying layout strategies, particularly for utilising the space in the side hulls above the waterline where a significant flare would normally exist and considerable internal spaces may be available. Another approach is to explore the possibility of reducing these void spaces by varying hull form configurations, for example, to further explore

the possibility of applying a wavepiercing bow to the centre hull as explored in Chapter 9.

10.8 Concluding Remarks

With regard to the choice of type of marine vessel, the naval architect's success depends on two major factors, a good understanding of the basic characteristics of the chosen ship type, and a good grasp of all design constraints existing on that ship type. It is believed that the thesis has made an initial contribution in these two aspects for the new trimaran ship type and will benefit the future trimaran designers. The basic characteristics of the trimaran ship is revealed through hydrodynamic performance analysis, and the design constraints are those design considerations discussed throughout the thesis. Design and analysis methods have been developed during the study and provided preliminary tools for further development of this trimaran ship concept.

In conclusion, the thesis has demonstrated some of the potential superior qualities of the trimaran ship with regard to high speed, less motions, and flexible layout. However, this significant potential requires of the ship designer a much greater open mindedness in manipulating the configuration, particularly of the side hull design, to achieve the desired performance. Although more detailed development work is still required for the trimaran ship concept, the author is confident in believing that this new concept will be transferred into real ships in the near future, as the world shipping industry will not ignore the potential benefits of this trimaran displacement ship for long.

REFERENCES

Alaez, J.A. (1989) 'Preliminary Design Considerations for Fast Catamarans', Lecture No. 5, Thirteenth WEGEMT School on 'Design Techniques for Advanced Marine Vehicles and High Speed Displacement Ships', Oct.

Andrews, D.J. (1982) 'Creative Ship Design', Trans. RINA 1982

Andrews, D.J. (1984) 'Synthesis in Ship Design', PhD Thesis, University College London.

Andrews, D.J. & Zhang, J.W. (1995a) 'Trimaran Ships - The Configuration for the Frigate of the Future', ASNE Day 95, Washington DC, May.

Andrews, D.J. & Zhang, J.W. (1995b) 'Considerations in the Design of a Trimaran Frigate', Inter. Symposium., 'High Speed Vessels for Transport and Defence' RINA, London, Nov.

Andrews, D.J. & Zhang, J.W. (1995c) 'Proposal for Research Work on Hydrodynamics of Trimaran Displacement Ships - Initial Investigation into the Configuration of Trimaran Displacement Ship', UCL NARG Report No. 1027/95, London, Dec.

Andrews, D.J. & Zhang, J.W. (1996) 'A Novel Design Solution to Stability - The Trimaran Ship', Inter. Conf, 'Watertight Integrity & Ship Survivability' RINA, London, Nov.

Andrews, R.N., Loader, P.R. & Penn, V.E. (1984) 'The Assessment of Ship Seakeeping Performance in Likely to be Encountered Wind and Wave Conditions', Int. Sym. on Waves and Wind Climate Worldwide, RINA, London.

Ash, M.W. (1993) 'An Investigation of The Structural Efficiency of The Trimaran Hull Form'. MSc in Naval Architecture Dissertation Report, Mech. Eng. Dept., UCL.

Bales, N.K. & Cummins, W.E. (1970) 'The Influence of Hull Form on Seakeeping', Trans. SNAME, Vol. 78.

Bass, D.W. & Haddara, M.R. (1988) 'Nonlinear Models of Roll Damping', Int. Shipbuilding Prog.

Bastisch, C. & Peters, T. (1990) 'Advanced Technology Frigate - Mk. II'. MSc in Naval Architecture Ship Design Exercise Report, Mech. Eng. Dept., UCL.

Bastisch, C. (1992) 'An Advanced Technology ASW Frigate for The Year 2000', RINA Int. Symposium on Affordable Warships, London.

Betts, C.V. (1988) 'A Review of Developments in SWATH Technology', International Conference on SWATH Ships And Advanced Multi-Hulled Vessels II, RINA, Nov.

Betts, C.V. (1996) 'Development in Warship Deign and Engineering', Proceedings of IMechE, Sixty-eighth Thomas Lowe Gray Lecture, London.

Bhattacharyya, R. (1978) 'Dynamics of Marine Vehicles', John Willey & Sons, New York.

Bishop, R.E.D, Price, W.G. & Tam, P.K.Y. (1977) 'A Unified Dynamic Analysis of Ship Response to Waves', Trans. RINA, Vol. 119.

Bowman, J. (1993) 'An Investigation of the Manoeuvrability of Trimaran Hull Forms'. 3rd Year project report for BSc in NAOE, Mech. Eng. Dept., UCL.

Brard, R. (1972) 'The Representation of a Given Ship Form by Singularity Distribution When the Boundary Condition on the Free Surface is Linearized', J. of Ship Research, Vol. 16, No. 1.

Brown, D.K. (1988) 'The Naval Architect of Surface Warships', Trans. RINA.

Burcher, R.K. (1971) 'Developments in Ship Manoeuvrability', Trans. RINA.

Burcher, R.K. (1972) 'Model Testing', J. Mech. Eng. Science, Vol. 14, No. 7.

Chan, H.S. (1993) 'Prediction of Motion and Wave Loads of Twin-Hull Ships', J. of Marine Structures, Vol. 6.

Chang, M.S. (1977) 'Computation of Three-Dimensional Ship-Motions with Forward Speed', 2nd Int. Conf. on Numerical Ship Hydrodynamics, Hiroshima, Univ. of California, Berkeley.

Clark, D. (1972) 'A Two-Dimensional Strip Method for Surface Ship Hull Derivative: Comparison of Theory with Experiments on a Segmented Tanker Model'. Jour. Mech. Eng. Sci.

Clark, D., Gedling, P., & Hine, G. (1982) 'The Application of Manoeuvring Criteria in Hull Design'. Trans. RINA.

Cole, C.J.P. (1992) 'Trimaran Stability, A Criteria Review', MSc in Naval Architecture Dissertation Report, Mech. Eng. Dept., UCL.

Comstock, E.N., Bales, S.L. & Gentile, D.M. (1982) 'Seakeeping Performance Comparison of Air Capable Ships', NEJ.

Conolly, J.E. (1969) 'Rolling and Its Stabilisation by active fins', Trans. RINA, Vol. 111.

Cudmore, A. & Best, G. (1992) 'Small Aircraft Carrier', MSc in Naval Architecture Ship Design Exercise Report, Mech. Eng. Dept., UCL.

Cudmore, A. (1992) 'Resistance of Trimaran', MSc in Naval Architecture Dissertation Report, Mech. Eng. Dept., UCL.

Dalzell, J.F. (1978) 'A Note on the Form of Ship Roll Damping', Journal of Ship Research, Vol. 22, September, 1978.

Davis, J. & Jones, E. (1987) 'Design of the O'Neill Hull Form', 13.461 New Construction Naval Ship design, Department of Ocean Engineering, Massachusetts Institute of Technology.

DNV (1985) 'Rules for Classification of High Speed Light Craft', Det Norske Veritas.

DNV (1992) 'Rules for Classification of Ships Newbuildings Part 3 Chapter 2 - Hull Structural Design with Length less Than 100 metres', Det Norske Veritas.

DRA (1995) 'Results of Trimaran Model Experiments', DRA Haslar, Restricted Report.

DTp (1991) 'Proposed Review of Res. A.373(X) Chapter 2 - Buoyancy, Stability and Subdivision', The Chamber of Shipping, Oct.

Engineering, (1959) 'Boat Show', Engineering Vol. 240, pp 86, Jan.

Everest, J.T. (1968) 'Some Research on the Hydrodynamics of Catamarans and Multi-hulled Vessels in Calm Water'. Trans. N.E.C.I.E.S. May.

Faltinsen, O.M. & Michelsen, F.C. (1974) 'Motions of Large Structure in Waves at Zero Froude Number', Int. Sym. on Dynamics of Marine Vehicles in Waves, University College London.

Farrar, A. (1989) 'Ilan Voyager: a Prototype for the Future'. *Small Craft*, RINA 1989.

Frost, P. & Palios, S. (1996) 'A Trimaran Cruise Liner', MSc in Naval Architecture Ship Design Exercise Report, Mech. Eng. Dept. UCL, June.

Froude, W. (1861) 'On the Rolling of Ships', Trans. RINA 1861.

Fry, E.D., & Graul, T. (1972) 'Design and Application of High Speed Catamaran', Marine Technology, July.

Galtiev, B. (1994) 'Carenes-Le Magazine due Bassin D'Essais des Carenes', The Highly-Streamlined Monohull with Lateral Wings', Volume No. 2, December 1994, DGA/DCN Paris.

Garrison, C.J. (1974) 'Hydrodynamics of Large Objects in the Sea', J. of Hydronautics, Vol. 8.

Gawn, R.W.L. (1952) 'Effect of Pitch and Blade Width on Propeller Performance'. Paper No. 6, RINA Autumn Meeting, September.

Gertler, M. (1954) 'A Reanalyses of the Original Test Data for the Taylor Standard Series'. DTMB Report 806.

Gifford, E.W.H. (1995) 'The Design, Testing and Operating of Low-wash, High Speed Trimaran Passenger Ferries to Class VB', Inter. Symposium., 'High Speed Vessels for Transport and Defence' RINA, London, Nov.

Gore, J.L. (1985) 'SWATH Ships', Naval Engineers Journal, Special Edition on modern Ships and Craft, Vol. 97, Feb.

Graham, C. (1985) 'The Modern Monohull', Naval Engineers Journal, Special Edition on modern Ships and Craft, Vol. 97, Feb.

Guevel, P. & Bougis, J. (1982) 'Ship Motions with Forward Speed in Infinite Depth', Int. Shipbuilding Prog., Vol. 29.

Gutsche, F. & Schroeder, G. (1963) 'Open Water Tests on Propellers with Fixed and CP Blades Running Ahead and Astern'. BSRC Transaction No 2565.

Haddara, M.R. & Cumming, D. (1992) 'Experimental Investigation into the Physics of Roll Damping of a Long Slender Hull Form,' Int. Shipbuilding Prog., 1992.

Hall, J.H (1995) Investigations into Wetted Surface Area of Slender Hulls. DRA Haslar Report.

Hall, J.H. (1988) Unpublished ARE(H) Report.

Hanhirrova, K. (1995) 'Preliminary Resistance Prediction Method for Mono- and Multihull Vessels', Inter. Symposium., 'High Speed Vessels for Transport and Defence' RINA, Nov.

Haskind, M.D. (1952) 'The Hydrodynamic Theory of Heaving and Pitching of a Ship', SNAME.

Hearn, G.E., Tong, K.C. & Lau, S.M. (1987) 'Hydrodynamic Models and Their Influence on Added Resistance Predictions', Proceedings of PRADS 87, Trondheim.

Helasharju, H. (1994) 'Performance of Fast Multi Hull Vessels Model Tests for the "TELAKKA 200" R&D Project', Maritime Research News, Vol. 8.

Hercus, P. (1991) 'INCAT Designs Reviews Wavepiercer Experience', Fast Ferry International, Sept.

Hill, C.J.R. & Merchant, A.A. (1993) 'Trimaran Ferry for West Coast Canadian Services'. MSc in Naval Architecture Ship Design Exercise Report, Mech. Eng. Dept., UCL.

Hoerner, S.F. & Borst, H.V. (1975) 'Fluid-Dynamic Lift', Hoerner Fluid Dynamics, Brick Town, N.J. 08723.

Hogben, N. & Lumb, F.E. (1967) 'Ocean Waves Statistics', Her Majesty's Stationary Office, London.

Holtrop, J. & Mennen, G.G.J. (1984) 'A Statistical Re-Analysis of Resistance and Propulsion Data', ISP, Vol. 31.

Hornell, J. (1946) 'Water Transport, Origins and Early Evolution'. Cambridge Univ. Press.

IMO (1977) 'Code for Dynamically Supported Craft', IMO Resolution A.373(X), Nov.

IMO (1995) 'International Code of Safety for High Speed Craft', IMO Resolution MSC.36(63).

Inglis, R.B. & Price, W.G. (1982) 'A Three Dimensional Ship Motion Theory-Comparison Between Theoretical Predictions and Experimental Data of Hydrodynamic Coefficients with Forward Speed', Trans. RINA, Vol. 124.

Inoue, S., Hirano, M. & Kijima, K. (1981) 'Hydrodynamic Derivatives on Ship Manoeuvring'. Inter. Ship. Prog., Vol.28, May.

ITTC (1957) Proceedings of the 8th ITTC, Madrid, Spain.

Jacobs, W. R. (1964) 'Estimation of Stability Derivatives and Indices of Various Ship Forms and Comparison with Experimental Results'. Davidson Lab. R1035, September.

Jane's (1991) 'Fighting Ships 1991-1992', Ed by Sharpe R., Jane's Information Group.

Jane's, (1991) 'High Speed Marine Craft', Edited by Trillo, R.L., Jane's Information Group.

John Brown, (1988) 'SWATH Stability Standard Study', Document 6047/2033/002, John Brown Engineering & Construction.

John Brown, (1991) 'Proposed Criteria For SWATH Vessels', John Brown Engineering and Construction.

Kamil, M.S. & Burrows, J. (1994) 'Trimaran Corvette', MSc in Naval Architecture Ship Design Exercise Report, Mech. Eng. Dept. UCL, June.

Kato, H. (1958) 'On the Frictional Resistance to the Roll of Ships', J. Soc. Naval Arch. Japan, Vol. 102.

Kato, H. (1966) 'Effects of Bilge Keels on the Rolling of Ships', Memories of The Defence Academy, Japan, Vol. 4.

Kennell, C.G. (1992) 'SWATH Ships Technical and Research Bulletin', No 7-5, SNAME.

Kennell, C.G. (1995) Discussion on the Paper 'Trimaran Ships - The Configuration for the Frigate of the Future', ASNE Day 95, Washington DC, May.

Kennell, C.G., White, B. & Comstock, E.N. (1985) 'Innovative Naval Designs for North Atlantic Operation', SNAME Transaction, Vol. 93, pp. 261-281.

Korvin-Kroukovsky, B.V. & Jacobs, W.R. (1957) 'Pitching and Heaving Motions of a Ship in Regular Waves', SNAME Transactions, Vol. 65.

Krylov, A. (1898) 'A New Theory of the Pitching Motion of Ships on Waves, and of The Stresses Produced by this Motion', Trans., INA, London.

Lang, T.G., Hightower, J.D. & Strickland, A.T. (1974) 'Design and Development of the 190ton Stable Semi-Submerged Platform(SSP)', Trans. of ASME, Journal of Engineering for Industry, December.

Lee, M.C. & Curphey, R.M. (1977) 'Prediction of Motion, Stability, and Wave Loads of Small-Waterplane Area, Twin-Hull Ships', SNAME Transactions, Vol. 85.

Lewis, E.V. (1989) (ED) 'Principles of Naval Architecture'. Vol III, SNAME, Nov.

Lloyd, A.R.J.M. (1989) 'Seakeeping: Ship Behaviour in Rough Weather', Ellis Horwood Series in Marine Technology.

Lloyd, A.R.J.M. (1991) 'The Seakeeping Design Package', Trans. RINA.

Lloyds Register of Shipping (1988) 'Report of the Enquiry into Hull Forms for Warships'. HMSO.

Lunde, J.K. (1951) 'On The Linearized Theory on Wave Resistance for Displacement Ships in Steady and Accelerated Motion', Trans. SNAME, Vol. 59.

Machin, S. (1992) 'OPV Monohull'. MSc in Naval Architecture Ship Design Exercise Report, Mech. Eng. Dept., UCL.

Masson, T. A. (1993) 'Trimaran Stability Investigation'. 3rd Year project report for BSc in NAOE, Mech. Eng. Dept., UCL.

Mateus, S.R. & Whatley, A. (1995) 'A Trimaran LPH', MSc in Naval Architecture Ship Design Exercise Report, Mech. Eng. Dept. UCL, June.

Mateus, S.R. (1994) 'Mesh Generation for Ship Hulls', E441-Project Report, Mech. Eng. UCL.

MATHCAD (1994) 'Mathsoft MATHCAD 5.0 Plus' Mathsoft, Inc.

Mathisen, J.B. & Price, W.G. (1984) 'Estimation of Ship Roll Damping Coefficients', Trans. RINA 1984.

MATLAB (1992) 'MATLAB Reference Guide', The Math Works, Inc.

McCreight, K.K. (1987) 'Assessing The Seaworthiness of SWATH Ships', Trans. SNAME 1987.

Moor, D.I. (1966) 'Resistance and Motion of High Speed Single-Screw Cargo Liner', Trans. NECIES 1966.

NES 109 (1989) 'Stability Standards for Surface Ships'. Naval Engineering Standard 109, Issue 3. Sea Systems Controllerate, MoD.

Newman, J.N. (1977) 'Marine Hydrodynamics', MIT Press, Cambridge, Mass.

Newman, J.N. (1978) 'Theory of Ship Motions', Advances in Applied Mechanics, Vol. 18.

Newton, R.N. & Rader H.P. (1960) 'Performance Data of Propellers for High-Speed Craft', Trans RINA, Nov.

Noblesse, F. (1983) 'A Slender Ship Theory of Wave Resistance', J. Ship Research, Vol. 27.

Nordenstrom, N., Faltinsen, O. & Perdersen, B. (1971) 'Prediction of Wave-Induced Motions and Loads for Catamarans', Offshore Technology Conference, Dallas, Texas 75206.

O'Brien, P. & Russell, M. (1993) 'Trimaran AAW Destroyer'. MSc in Naval Architecture Ship Design Exercise Report, Mech. Eng. Dept., UCL.

O'Neill, W.C. (1986) 'A New Small Waterplane Area Ship Concept', Paper No. AIAA-86-2382, 8th AIAA Advanced Marine System Conference, San Diego, Sept.

Ochi, M.K. & Motter, L.E. (1973) ' Prediction of slamming Characteristics and Hull Response for Ship Design'. Trans SNAME, Vol. 81.

Ogilvie, T.F. & Tuck, E.O. (1969) 'A Rational Strip Theory for Ship Motion part 1', Report No. 013, University of Michigan, Ann Arbor.

Oossanen, P.van (1989) 'Characteristics and Relative Merits of the Different Vehicle Types'', Lecture No.1, Thirteenth WEGENT School on 'Design Techniques for Advanced Marine Vehicles and High Speed Displacement Ships', Oct.

Oxford (1986) 'A Supplement to the Oxford English Dictionary', Edited by Burchfield, R.W., Vol. IV Se-Z, Oxford at The Clarendon Press.

Parsons, C.H. (1897) 'The Application of the Compound Steam Turbine to the Purpose of Marine Propulsion', Trans. RINA, Vol. 38.

Pattison, D.R. & Zhang J.W. (1994) 'The Trimaran Ships'. Paper No. 1, RINA Spring Meeting, April.

Pattison, D.R. & Zhang, J.W. (1993) 'Proposal for Research Work on Hydrodynamics of Trimaran Displacement Ships', Naval Architecture Research Group, Mech. Eng. Dept., UCL.

Pattison, D.R. (1993) Presentation on UCL Research into Trimaran Ships, UCL.

Pattison, D.R., Moores, N., & van Griethuysen, W.J. (1986) 'Computer Aided Structural Design in GODDESS', International Conference on Advances in Marine Structures, Dunfermline, Scotland.

Pearson, K.G. (1991) 'Proposed Trimaran Study', Letter from Three Quays Marine Services, Oct.

Pearson, S & Schild, W. (1992) 'OPV Trimaran'. MSc in Naval Architecture Ship Design Exercise Report, Mech. Eng. Dept., UCL.

Philips, S. (1993) 'Advanced Marine Vehicles', Lecture Notes, UCL.

Putnam, N. (1995) 'Trimaran Support Vessel', MSc in Naval Architecture Ship Design Exercise Report, Mech. Eng. Dept. UCL, June.

Raff, A.I. (1972) 'Program SCORES - Ship Structural Response in Waves', US Coastguard Ship Structure Committee Report, SSC-230.

RINA (1995) 'Loss of The ESTONIA: A Technical Interim Appraisal', Naval Architects RINA, July/Aug.

Roberts, J.B. (1982) 'A Stochastic Theory for Nonlinear Ship Rolling in Irregular Seas', J. Ship Res. Vol. 26. Dec.

Roberts, J.B. (1985) 'Estimation of Nonlinear Ship Roll Damping Coefficients from Free Decay Data', J. Ship Res. Vol 29.

Roberts, S.A. (1990) 'An Investigation into the Stability and Survivability of Passenger Carrying Catamaran Craft', Trans. RINA, Vol. 133 pp 363-387.

Ruston (1992) 'Ruston Diesel Power', Ruston Diesels Ltd.

Salvesen, N., Tuck, E.O. & Faltinsen, O. (1970) 'Ship Motions and Sea Loads', SNAME Transactions, Vol. 78.

Schmitke, R.T. (1978) 'Ship Sway, Roll, and Yaw Motion in Oblique Seas', Trans. SNAME., Vol. 86.

Sclavounos, P. (1985) 'The Unified Slender-Body Theory: Ship Motions in Waves', Proceedings, Sym. Naval Hydrodynamics, University of Michigan, Ann, Arbor.

Scott, R. (1995) 'UK Studies Trimaran Hull for Future ASW Frigate', Jane's Navy International, March/April.

Smith, S. (1996) 'Trimaran ASW Frigate', MSc in Naval Architecture Ship Design Exercise Report, Mech. Eng. Dept. UCL, June.

Summers, A. & Eddison, J. (1995) 'A Design Study for a Trimaran Frigate', IMDEX 95, RNC Greenwich, March.

Taggart, R. (1980) 'Ship Design and Construction', SNAME, New York, N.Y. 10048,

Tanaka, N. (1960) ' A Study on The Bilge Keels', J. Soc. Naval Arch. Japan, Vol. 109.

Timman, R. & Newman, J.N. (1962) 'The Coupled Damping Coefficients of Symmetric Ships', J. Ship Research, Vol. 5, No. 4.

Watson, D.G.M. & Gilfillan, A.W. (1976) 'Some Ship Design Methods', RINA, London, Nov.

WEGEMT (1989) 'Design Techniques for Advanced Marine Vehicles and High speed Displacement Ships', Thirteenth Graduate School, Delft university of Tech., Netherlands.

Wehausen, J.V. (1973) 'The Wavemaking Resistance of Ships', Advances in Applied Mechanics, 13, 1973, Academic Press, N.Y.

Whicker, L.F. & Fehlner, L.F. (1958) 'Free Stream Characteristics of a Family of Low Aspect Ratio Control Surfaces for Application to Ship Design', DTRC Report 993.

Wilson, M.B. & Hsu, C.C. (1992) 'Wave Cancellation Multihull Ship Concept', Proc. of The High Performance Marine Vehicle Conf., June 1992, Arlington.

Woodcroft, B. (1848) 'A Sketch of the Origin STEAM NAVIGATION from Authentic Documents by Bennet Woodcroft, Professor of Machinery - University College London with Illustrations', London: Taylor, Walton and Mabely.

Wu, G.X. & Eatock Taylor, R. (1987) 'A Green's Function Form for Ship Motions at Forward Speed', Int. Shipbuilding Prog., Vol. 34.

Wu, G.X. & Eatock Taylor, R. (1989) 'The Numerical Solution of The Motions of a Ship Advancing in Waves', 5th Int. Conf. on Numerical Ship Hydrodynamics, Hiroshima.

Wu, G.X. (1988) 'Hydrodynamic Forces on Oscillating Submerged Bodies at Forward Speed', PhD Thesis, UCL.

Yeh, H.Y.H. (1965) 'Series 64 Resistance Experiments on High Speed Displacement Forms', Marine Technology, July.

Zhang, J.W. (1992) 'Design and Hydrodynamic Performance of a High Speed Trimaran Passenger/Car Ferry', NARG Report No. 1015/92, Mech. Eng. Dept., UCL. November.

Zhang, J.W. (1993) 'Hull form Design of a Trimaran Destroyer', NARG Report No. 1017/93, Mech. Eng. Dept., UCL. December.

Zhang, J.W. (1995a) 'Investigation into Trimaran Tractor Propulsion', NARG Report No. 1018/95, Mech. Eng. Dept., UCL. April.

Zhang, J.W. (1995b) 'Preliminary Prediction of Ship Motion for Trimaran Hull Forms', NARG Report No. 1020/93, Mech. Eng. Dept., UCL. May.

Zhang, J.W. (1995c) 'Comparison of Trimaran Motion Prediction with Model Experiment', NARG Report No. 1024/95, Mech. Eng. Dept., UCL. Sept.

Zhang, J.W. (1996a) 'Investigation into Roll Damping of Trimaran Ships', NARG Report No. 1026/96, Mech. Eng. Dept., UCL. Feb.

Zhang, J.W. (1996b) 'Initial Investigation into Trimaran Configurations', NARG Report No. 1029/96, Mech. Eng. Dept., UCL. Feb.

Zhang, J.W. (1996c) 'Investigation into Effects of Side Hull Draught', Trimaran Research Proposal, Mech. Eng. Dept., UCL. Sept.

APPENDIX 1 A TRIMARAN FERRY CONCEPT DESIGN COMPUTER PROGRAM - TRIDES

This Appendix illustrates the basic algorithms and functions of the trimaran ferry design program TRIDES (Chapter 3) as follows with a listing of its menus and a sample output in the next two sections. It has to be noted that the algorithms and design procedure embedded in the program are produced by means of some broad assumptions, aimed to reveal the design trend of trimaran ferries rather than provide a complete trimaran design package. And also, it is not aimed to produce an automated parametric analysing tool as it would be prudent to predetermine which parameters should be varied in design studies at the trimaran's initial design stage. Instead, the program gives a list of the trimaran parameters to allow interactive uses in trimaran design studies.

1 Algorithms for The Trimaran Ferry Design Program

1.1 Design Balance

Generally speaking, a ship initial sizing procedure should involve two balance equations , one would be a weight balance, and the other would be a space balance. A satisfactory design can only be achieved when these two balances are properly accomplished:-

$$Total\ displacement = \Sigma Weights \tag{A1-1}$$

$$Total\ space = \Sigma Required\ spaces \tag{A1-2}$$

The weight balance starts from a designer's choice of side hull displacement ratio, from which the required displacement in the centre hull and the side hulls are determined as:-

$$\Delta_c = \Delta\,(1 - 2\gamma) \tag{A1-3}$$

where Δ_c is the displacement of the centre hull, Δ is the total displacement of the ship, and γ is the side hull displacement ratio.

Since the driving factor in the hull form design of a trimaran ship is its slenderness, dimensions of the centre hull can be derived from length to beam ratio and beam to draught ratio, and satisfying the balanced displacement as:-

$$L_c = \left[\frac{1}{\rho C_{bc}} \Delta_c \left(\frac{L_c}{B_c} \right)^2 \left(\frac{B_c}{T_c} \right) \right]^{\frac{1}{3}} \qquad \text{(A1-4)}$$

where L_c, B_c, T_c are the length, beam, draft of the centre hull, and C_{bc} is the block coefficient of the centre hull. The dimensions of the side hulls are derived in a similar way.

However, whereas the weight balance for the trimaran ferry design program can be achieved in the ship's *total* displacement-weight balance, the space balance has to be carried out for *individual* required spaces rather than a total space of the ship, because the total space of a trimaran ferry is not simply a function of the required spaces of the payload as most monohull ships would be. Thus, the internal space of a trimaran ship can be divided into two categories, *payload driven spaces*, and *performance driven spaces*. They have to be addressed separately. The space of a car deck is a function of car numbers; and the space of a passenger deck is a function of passenger numbers which also determines the crew number and crew accommodation spaces. The spaces of the centre hull and the side hulls are not determined merely by space considerations but depends more on the seakeeping and stability requirements. The depth of the centre hull is governed by the required air gap below the wet deck which is represented by a user input minimum freeboard in the program. The total space in the side hulls is governed by stability requirements, particularly the damage stability requirements, which is too complicated to be included in an initial sizing program. In the program, the space in the side hulls under the waterline is determined by the side hull displacement ratio which represents broadly the stability requirements. The side hull space above the waterline is considered to have no significant influence on the overall design balance and can be determined later in the detailed side hull configuration stage.

1.2 Weight Estimation

The development of the algorithms for trimaran weight estimation is a crucial part of the design program, particularly the structural weights, since the structural

model of a trimaran ship is fundamentally different from any existing ship types. In view of the lack of existing data, though as an initial sizing program, the weight for the trimaran ferry has to be broken down as far as possible to minimise any estimation errors.

The total weight of a trimaran ship can be broken down into four categories as:-

$$W_t = W_s + W_m + W_o + W_d \qquad \text{(A1-5)}$$

where W_t is the total weight of the ship, W_s is the structural weight, W_m is the machinery weight, W_o is the outfitting weight, and W_d is the deadweight of the ship.

Structural weights

Referring to Figure 3.21 (Chapter 3), the structural weight of a trimaran ferry can be further broken down as the follows:-

$$W_s = W_{hc} + 2W_{hs} + 2W_{cross} + W_{cardk} + W_{sup} \qquad \text{(A1-6)}$$

where W_{hc} is the structural weight of the centre hull, W_{hs} is the structural weight of one side hull, W_{cross} is the weight of one side cross structure excluding the car deck, W_{cardk} is the structural weight of the car deck, and W_{sup} is the superstructure weight. These structural weight items are estimated separately as follows.

The method of estimation of the structural weight for the centre hull can be derived referring to the monohull formula developed by **Watson & Gilfillan (1976)** in the form of

$$W_s = K E^{1.36} \qquad \text{(A1-7)}$$

where W_s is the structural weight of the ship, K is a factor which depends on the ship type, and E is a parameter defined by main dimensions of the hull and the superstructure. The factor K can not be used directly for the centre hull of a trimaran because a very slender centre hull is very much outside of the range of the sample ships used by Watson in deriving the formula.

Based on equation (A1-7), the structural weight of the centre hull can be expressed as:-

$$W_{hc} = \gamma K_{sc} L_c^{1.36} B_c D_c [1+0.5(C_{bc}'-0.7)] (1+ K_f) \qquad \text{(A1-8)}$$

where γ is the specific gravity of the material, K_{sc} is the structural weight coefficient for the centre hull, D_c is the hull depth, C_{bc}' is the block coefficient of the centre hull measured at $0.8D_c$, and K_f is an added weight factor for fire protection due to the use of light materials with $K_f = 0$ when steel structures are used.

In order to derive a realistic structural weight coefficient K_{sc} for the centre hull, and also for the verification of the following formulae for other structures, a basic midship section structure for a 100m trimaran ferry was designed using the DNV rules (**DNV 1992**). The weight of the centre hull of the basic ship was estimated from the midship section data by approximately distributing the weight along the hull. This weight was then used in equation (A1-8) to drive the coefficient K_{sc}. This approximation restricts the program being only valid for the design of trimaran ferries of similar sizes.

The structural weight of a side hull can be expressed in a similar way as:-

$$W_{hs} = \gamma K_{ss} L_s^{1.36} B_s D_s [1+0.5(C_{bs}'-0.7)] (1+K_f) \qquad \text{(A1-9)}$$

The structural coefficients derived from the basic trimaran ferry for the centre hull and the side hulls are:-

$K_{sc} = 0.0073$ for the centre hull

and $K_{ss} = 0.0107$ for the side hulls.

The structural weights for the car decks, superstructures, and cross structures can be estimated directly using the user defined geometry of the decks and the panel thickness of the structure derived from **DNV (1992)** rules. The formula for the structural weight of the car deck is:-

$$W_{cardk} = \Sigma \gamma [t_1 A_{cardk}+2 t_2(L_{cardk}+B_{cardk})H_{cardk}] (1+K_f) (1+K_{frame}) \qquad \text{(A1-10)}$$

where W_{cardk} is the structural weight of car decks, t_1 is the plate thickness of car deck panels, A_{cardk} is the area of car deck, t_2 is the plate thickness of wall structures, L_{cardk} is the length of car deck, B_{cardk} is the beam of car deck, H_{cardk} is the height of car deck (3 metres in this ferry study), K_{frame} is the frame factor of the structure taken as 50% of the plating weight, and Σ represents the summation for all car decks.

Similarly, the weight of the superstructure/passenger decks can be expressed as:-

$$W_{sup} = \Sigma \gamma [t_3 A_{pasdk} + 2 t_4 (L_{pasdk} + B_{pasdk}) H_{pasdk}] (1+K_f) (1+K_{frame}) \qquad \text{(A1-11)}$$

Finally, the weight of the cross structure can be estimated as:-

$$W_{cross} = \gamma t_5 L_{cardk} (B - B_c/2) (1+K_f)(1+K_{frame}) \qquad \text{(A1-12)}$$

where B is the extreme beam of the ship, and B_c is the beam of the centre hull.

The steel plate thickness of the structural panels derived from the basic ship is shown in the following Table A1.1. The limit for plate thickness of deck walls and passenger decks were taken as the minimum manufacturable thickness (advice sought from ship builders). Since no detailed structural design was carried out for trimaran ferries using light materials, the increase of plate thickness and insulation meterials due to the use of light materials was reflected in the fire protection factor K_f. An approximated fire protection factor of 0.5 for aluminium alloy was used in the program by examining existing aluminium vessels. It was believed this simplification would not effect the accuracy of the estimation very much as the major structures of the trimaran in the study were of steel. However, this method would need further verification if any trimaran ships with major structure being built in light materials were to be studied.

Table A1.1 Steel plate thickness

Symbol	Location	Plate thickness (mm)
t_1	car deck	7.0
t_2	car deck wall	5.0
t_3	passenger deck	5.0
t_4	passenger deck wall	5.0
t_5	cross structure wet deck	6.0

Machinery weights

The machinery weight W_m of a trimaran can be broken down into the weights of main engine W_{eng}, propulsion system W_{prop}, and auxiliary machinery W_{aux} as:-

$$W_m = W_{eng} + W_{prop} + W_{aux} \tag{A1-13}$$

Considering the trimaran ferry to be designed would have no side hull propulsion, the formulae developed by **Watson & Gilfillan (1976)** were used for deriving the machinery weight formulae for the trimaran ferry. The machinery weights of a trimaran ferry can be estimated from the required shaft power of the ship as:-

$$W_{eng} = K_{eng} P_s^{0.84} \tag{A1-14}$$
$$W_{prop} = K_{prop} P_s^{0.84} \tag{A1-15}$$
$$W_{aux} = K_{aux} P_s^{0.7} \tag{A1-16}$$

where P_s is the shaft power of the ship, K_{eng} is weight coefficient of the main engine type, K_{prop} is the weight coefficient effected by propulsion types, and K_{aux} is the weight coefficient of the auxiliary machinery which is 15.54 in the program. The weight coefficients for main engine and propulsion system are listed in Tables A1.2 and A1.3.

Table A1.2 Weight coefficients of main engines

Engine Type	K_{eng}
High speed diesel	8.50
Medium speed diesel	9.25
Gas turbines	3.31

Table A1.3 Weight coefficients of propulsion systems

Propulsion Type	K_{prop}
Fixed pitch propeller	1.50
Controlled pitch propeller	2.25
Water jet	3.91

It has to be noted that the performance of engines and propulsion systems have been constantly improved over recent years, particularly for gas turbines and water jets. The weight coefficients listed in the above tables and also the fuel consumption rates in the following formulae only represent the data available at the time when the program was developed **(Zhang 1992)**.

Outfit weight

It was assumed that there were no equipment allocated in the side hulls apart from piping systems of which the weight has been included in the auxiliary machinery weight. The outfit weight of a trimaran ferry can therefore be considered as a function of the car deck area, passenger deck area, and the size of the centre hull as:-

$$W_o = 0.02\,(A_{pasdk} + A_{cardk}) + 0.1\,L_c\,B_c \qquad \text{(A1-17)}$$

Deadweight

The deadweight is basically the summary of the weights of cars, passengers, crew, stores, fuel, and fresh water. These weights are simple functions of car number, passenger number, range of the ship, and the fuel consumption rate of engines. The fuel consumption rate of main engines are listed in Table A1.4.

Table A1.4 Fuel consumption rate

Engine Type	***Rate (kw/hour)***
Medium speed diesel	200g
High speed diesel	250g
Gas turbines	300g

1.3 Resistance

The resistance prediction in the computer program is based on Series 64 model experiment data **(Yeh 1965)**. Three parameters, beam-draught ratio, displacement-length ratio, and block coefficient are used to derive the coefficients of residuary resistance at various speed-length ratios. The friction resistance is calculated from ITTC 1957 line. An allowance of 0.0004 is added to the coefficient of total resistance in keeping with normal practice **(Lewis 1989)**. The effects of wave interaction between hulls were not taken into account at this stage of the trimaran study, although a early model test on multihull ships showed some wave cancellation effects **(Everest 1968)**. The added resistance due to appendages is taken as 10% for fixed pitch propellers, 12% for controlled pitch propellers, and 6% for water jet propulsions.

1.4 Initial metacentric height

At the initial sizing stage of a trimaran ship, the initial metacentric height of the ship has to be checked to verify the beam of the side hulls. Without detailed hull form, the metacentric centre can only be approximated from the principal dimensions and the positions of the three hulls. The metacentric centre of a trimaran ship above the centre of buoyancy is:-

$$BM = \frac{I_c + 2(I_s + A_s y_s^2)}{\Delta} \qquad \text{(A1-18)}$$

where I_c is the waterplane area inertia of the centre hull, I_s the waterplane area inertia of one side hull about its own centre line, A_s is the waterplane area of one side hull, and y_s is the span of the side hulls.

The centre of buoyancy of the ship can be estimated from the centre of buoyancy of the three hulls as:-

$$K_B = \frac{\Delta_C K_{BC} + 2(T_C - (T_S - K_{BS}))\Delta_S}{\Delta} \qquad \text{(A1-19)}$$

where Δ_C is the displacement of the centre hull, Δ_S is the displacement of a side hull, K_{BC} and K_{BS} are the centres of buoyancy of the centre hull and a side hull respectively, and T_C and T_S are the draughts of the centre hull and the side hulls respectively.

Finally, the metacentric height *(GM)* of a trimaran ship is:-

$$GM = BM + K_B - K_G \qquad \text{(A1-20)}$$

where K_G, the centre of gravity of the ship derived in the weight estimations described above.

1.5 Layout Model

The layout model of the trimaran ferry in the program is defined by the following parameters:

- Number of passenger decks
- Number of car decks
- Side hull span
- Side hull set back
- Length to width ratio of passenger decks

2 Menu of the Trimaran Ferry Design Program -TRIDES

```
                    MAIN MENU

1.  INPUT PAYLOAD AND GENERAL DATA
2.  INPUT PROPULSION REQUIREMENTS
3.  SELECT HULL PARAMETERS
4.  SELECT MATERIALS
5.  DEFINE ARRANGEMENT MODEL
6.  CALCULATE MAIN DIMENSIONS
7.  POWER ESTIMATION
8.  DISPLAY RESULTS
9.  SAVE DATA
10. DISPLAY INPUT DATA
11. EXIT PROGRAM

  SUBMENU 1.  INPUT PAYLOAD AND GENERAL DATA

  1.1. NAME OF THE SHIP
  1.2. NUMBER OF PASSENGERS
  1.3. NUMBER OF CARS
  1.4. OTHER PAYLOAD IN TONNES
  1.5. RANGE OF THE FERRY
  1.6. MAX. SPEED
  1.7. SERVICE SPEED

  SUBMENU 2. PROPULSION REQUIREMENTS

  2.1. NUMBER OF PROPULSION UNITS
  2.2. SELECT TYPE OF MAIN ENGINES
       HIGH SPEED DIESEL ENGINES
       MEDIUM SPEED DIESEL ENGINES
       GAS TURBINES
  2.3. SELECT PROPULSION TYPE
       FIXED PITCH PROPELLERS
       CONTROLLED PITCH PROPELLERS
       WATER JETS
```

SUBMENU 3. SELECT HULL PARAMETERS

3.1. LENGTH BEAM RATIO OF MAIN HULL
3.2. BEAM DRAFT RATIO OF MAIN HULL
3.3. MIN. FREEBOARD OF MAIN HULL
3.4. BLOCK COEFFICIENT OF MAIN HULL
3.5. PRISMATIC COEFFICIENT OF MAIN HULL
3.6. DISPLACEMENT RATIO OF MAIN HULL AND SIDE HULLS
3.7. LENGTH BEAM RATIO OF SIDE HULLS
3.8. BEAM DRAFT RATIO OF SIDE HULLS
3.9. BLOCK COEFFICIENT OF SIDE HULLS
3.10. PRISMATIC COEFFICIENT OF SIDE HULLS
3.11. FINISH PARAMETERS INPUT

SUBMENU 4. SELECT MATERIALS

MILD STEEL ------ 1
HY STEEL ------ 2
AL. ALLOY ------ 3

4.1. MATERIAL FOR MAIN HULL
4.2. MATERIAL FOR CROSS STRUCTURE
4.3. MATERIAL FOR SIDE HULLS
4.4. MATERIAL FOR SUPERSTRUCTURE

SUBMENU 5. DEFINE ARRANGEMENT MODEL

5.1. NUMBER OF CAR DECKS ABOVE MAIN DECK (0 FOR DEFAULT ONE DK)
5.2. NUMBER OF PASSENGER DECKS (0 FOR DEFAULT ONE DK)
5.3. LENGTH BEAM RATIO OF SUPERSTRUCTURE (0 FOR DEFAULT 3)
5.4. SPAN OF SIDE HULL TO MAIN HULL /BEAM (0 FOR DEFAULT BOX WIDTH)
5.5. LONGITUDINAL POSITION OF SIDE HULLS FROM AP.

3 Sample Output of The TRIDES Program

```
>>OUTPUT OF TRIDES<<      TIME OF RUN: 11-MAY-1992 17:40:

SHIP NAME:    TRIFERRY

1. PRINCIPAL PARTICULARS:

LENGTH OVERALL          109.67 m
BEAM MAX.                19.70 m
DRAFT                     3.32 m
DEADWEIGHT              258.22 t
DISPLACEMENT           1104.10 t

PASSENGERS                450
CARS                       90
CREW                       18

PROPULSION UNITS            2 sets
TYPE OF ENGINE              2    (1.H DIESEL 2.M DIESEL 3.GAS T.)
MCR                  18624.15 KW
PROPULSION                  1    (1.FPP. 2.CPP. 3.W.JET)
MAX. SPEED APPROX.      38.00 knots
RANGE                  200.00 miles

2. MAIN HULL:

WATER LINE LENGTH       99.70 m
WATER LINE BEAM          6.65 m
DEPTH (TO MAIN DK)       7.36 m
DRAFT (DESIGN)           3.32 m
CB                       0.45
CP                       0.63
DISPLACEMENT          1015.77 t
```

3. SIDE HULLS:

WATER LINE LENGTH		35.06 m
WATER LINE BEAM		2.34 m
DRAFT (DESIGN)		1.17 m
CB		0.45
CP		0.63
DISPLACEMENT	2 x	44.16 t

4. LIGHT WEIGHT BREAKDOWN:

HULL STRUCTURE	539.94 t
MACHINERY	245.79 t
OUTFIT	111.94 t
LIGHT WEIGHT	897.68 t

5. DEAD WEIGHT BREAKDOWN:

PASSENGER + LUGGAGE	54.00 t
CARS	112.50 t
CREW + EFFECTS	2.16 t
STORES	4.50 t
DUTY_FREE GOODS	6.75 t
FUEL	21.56 t
FRESH WATER	6.75 t
DEAD WEIGHT	208.22 t

6. BUILDING MATERIALS

MAIN HULL	1	
CROSS STRUCTURE	1	
SIDE HULLS	3	
SUPERSTRUCTURE	3	(1. MS. 2. HY. 3. A.AL.)

7. ARRANGEMENT :

NUMBER OF PASS DKS	1
NUMBER OF CAR DKS	1
LENGTH OF SUP_STRUC	63.83 m
WIDTH OF CAR DECK	19.70 m
WIDTH OF PASS. DECK	14.50 m
LONGL POSIT. OF BOX	
FROM AP. (TRIM=0)	49.95 m
SPAN OF SIDE HULL	8.68 m
CLEAR SPAN	4.19 m
GM	1.90 m
LONGL POSITION OF SIDE HULLS	
FROM AP. (TRIM=0)	43.27 m
DECK AREA	
CAR DECK	1358 m^2
PASSENGER. DECK	925 m^2

APPENDIX 2 IMO STABILITY CRITERIA FOR MULTIHULLS

This appendix summarises the stability criteria used in the trimaran fast ferry design described in Chapter 3. The criteria was the proposed revision by DTp (1991) to the existing IMO Resolution A.373(X) *Code of Safety for Dynamically Supported Craft* **(IMO 1977).** This revision has now become part of the new code *'International Code of Safety for High Speed Craft'* **(IMO 1995).** The application of this criteria to trimaran ships has been discussed in Chapter 9 of the thesis.

Intact stability

A multihull vessel has to meet the requirements in the code for the area under the *GZ* curve, taking into the effect of wind heeling and either passenger crowding or high speed turning, which are:

• Area under *GZ* curve	A_1	>	0.55 x 30°/θ° m-rad
• Angle of maximum *GZ* occurs		>	20°
• Residual area of *GZ* curve	A_2	>	0.028m-rad
• Heeling angle due to passenger crowding		<	10°
• Heeling angle due to steady wind		<	16°
• Wind pressure		=	500pa

where A_1 is the area under GZ curve up to an angle of downflooding, 30°, or the angle at which the maximum GZ occurs, whichever is the least. Figure A2.1 illustrates the definition of the above criteria.

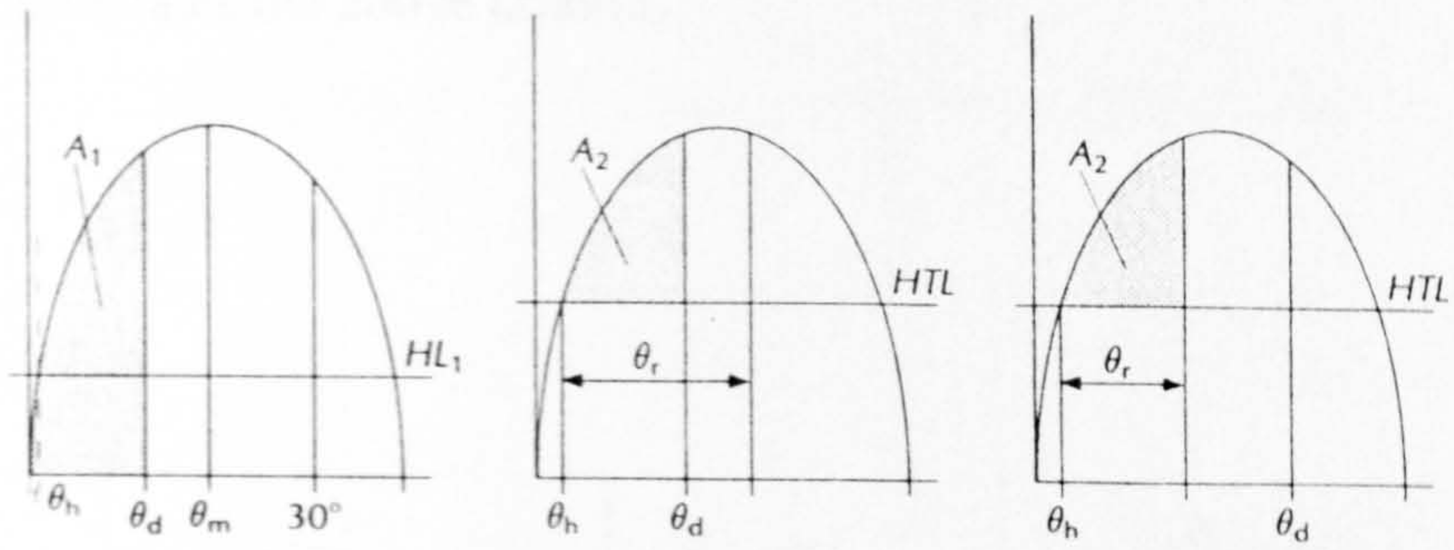

Figure A2.1 IMO definition of intact stability criteria for multihulls

where HL_1 = heeling lever due to wind

HTL = heeling lever due to wind + gusting + (passenger crowding or turning)

θ_h = angle of heeling

θ_d = downflooding angle

θ_m = angle of maximum GZ

θ_r = angle of roll

Damage stability

The extents of damage to the hulls are as follows,

- Longitudinally, (3 m + 0.03L) or 11 metres whichever is the least.
- Transversely, 0.2B or 5 metres whichever is the least for side damages; 12.0 metres for bottom damage.
- Vertically, full depth of the ship for side damages and 0.9 metre for bottom damage.

The vessel in the final condition after damage should be considered to have adequate standard of residual stability if it meet following criteria :

The final waterline below any opening > 100 mm

Angle of inclination	<	8°
Angle of heel due to steady wind	<	20°
Residual area of *GZ* curve A_2	>	0.028 m-rad

Figure A2.2 illustrates the above criteria.

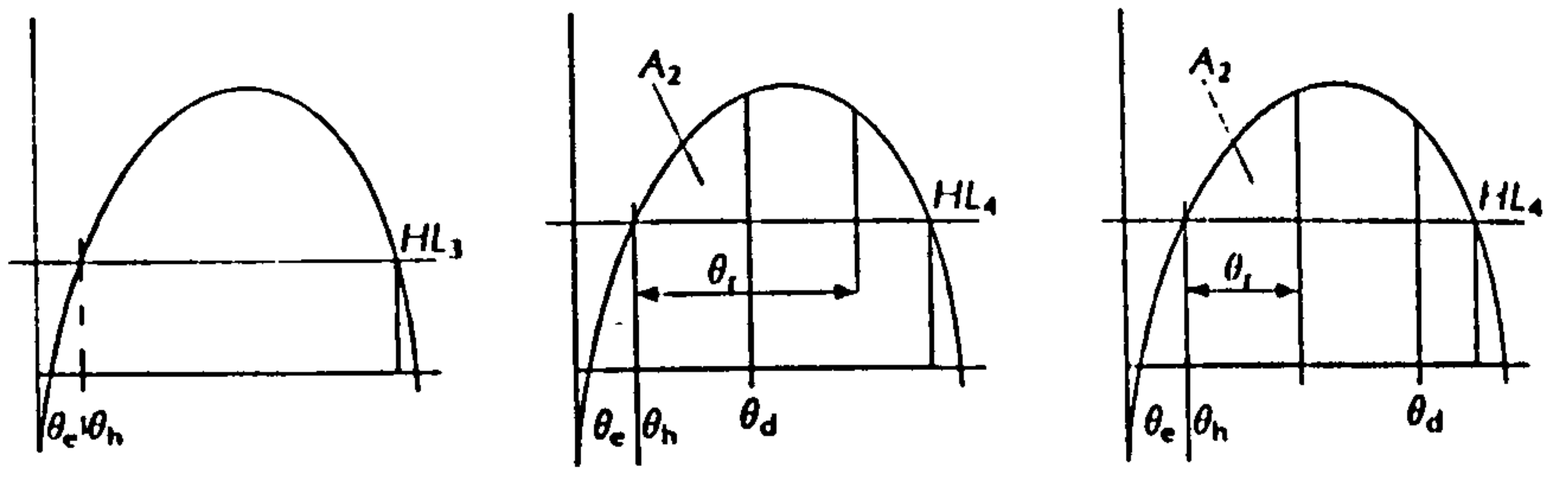

Figure A2.2 IMO definition of damage stability criteria for multihulls

where HL_3 = heeling lever due to wind

HL_4 = heeling lever due to wind + gusting + (passenger crowding or turning)

θ_e = angle of equilibrium after damage.

APPENDIX 3 LONGITUDINAL LOADING CALCULATIONS FOR THE TRIMARAN FERRY

Table A3.1 GODDESS output of the wave balance calculation for the trimaran ferry (sagging)

SHIP CONDITION	: DEEP	CURVE FILE(S)	: DR1:HULLOO.SRP
SHIP CONDITION LCG	: -8.81 METRES	WAVE TYPE	: TROCHOIDAL
SHIP LENGTH	: 99.00 METRES (B.P.)	WAVE CONDITION	: SAGGING
FINAL DRAUGHT (AMIDSHIPS)	: 1.551 METRES	WAVE HEIGHT	: 4.95 METRES (L/20)
FINAL TRIM (BASELINE B.P.)	: -1.703 METRES	WAVE LENGTH	: 99.00 METRES (100.00 %LBP)
		CREST POSITION	: 0.00 %LBP FROM FORE PERP

SEGMENT	LENGTH(M)	DRAUGHT(M)	WEIGHT(TONNES)	BUOYANCY(TONNES)	LOAD(MN)
1	1.980	7.363	0.878	8.297	-0.073
2	4.950	7.267	5.795	24.661	-0.185
3	4.950	6.855	5.795	42.073	-0.356
4	4.950	6.185	5.795	53.637	-0.469
5	4.950	5.363	7.397	58.827	-0.506
6	4.950	4.494	25.344	57.611	-0.316
7	4.950	3.662	54.052	51.477	0.025
8	4.950	2.925	54.918	42.774	0.119
9	4.950	2.324	55.970	34.325	0.212
10	4.950	1.883	68.821	28.019	0.400
11	4.950	1.616	83.702	25.090	0.575
12	4.950	1.531	96.657	25.553	0.697
13	4.950	1.627	99.745	28.537	0.698
14	4.950	1.898	99.485	35.099	0.631
15	4.950	2.329	97.588	44.664	0.519
16	4.950	2.895	81.169	57.468	0.232
17	4.950	3.558	59.823	73.037	-0.130
18	4.950	4.256	59.762	88.646	-0.283
19	4.950	4.908	57.329	101.003	-0.428
20	4.950	5.407	31.858	107.309	-0.740
21	4.950	5.649	22.948	80.619	-0.566
22	0.990	5.639	1.669	7.797	-0.060

STATION	SHEAR FORCE(MN)	BENDING MOMENT(MN)
1	-0.073	-0.216
2	-0.258	-1.049
3	-0.614	-3.220
4	-1.083	-7.432
5	-1.587	-14.054
6	-1.903	-22.707
7	-1.878	-32.081
8	-1.759	-41.098
9	-1.547	-49.295
10	-1.147	-55.976
11	-0.572	-60.243
12	0.125	-61.363
13	0.824	-59.028
14	1.455	-53.402
15	1.974	-44.929
16	2.207	-34.596
17	2.077	-24.008
18	1.794	-14.442
19	1.366	-6.637
20	0.626	-1.724
21	0.060	-0.041

Table A3.2 GODDESS output of the wave balance calculation for the trimaran ferry (hogging)

```
SHIP CONDITION              :  DEEP                          CURVE FILE(S)   : DEI:HULLOO.GRP
SHIP CONDITION LCG          :    -0.01 METRES                WAVE TYPE       : TROCHOIDAL
SHIP LENGTH                 :    99.00 METRES (B.P.)         WAVE CONDITION  : HOGGING
FINAL DRAUGHT (AMIDSHIPS)   :   5.066 METRES                WAVE HEIGHT     :    6.95 METRES (LOSS)
FINAL TRIM (BASELINE B.P.)  :   6.792 METRES                WAVE LENGTH     :  99.00 METRES (100.00 %LBP)
                                                            CREST POSITION  :  50.00 %LBP FROM FORE PERP
```

SEGMENT	LENGTH(M)	DRAUGHT(M)	WEIGHT(TONNES)	BUOYANCY(TONNES)	LOAD(MN)
1	1.980	0.000	0.878	0.000	0.009
2	4.950	0.000	5.795	0.000	0.057
3	4.950	0.000	5.795	0.000	0.057
4	4.950	0.000	5.795	0.000	0.057
5	4.950	0.000	7.397	0.000	0.073
6	4.950	0.547	25.344	0.933	0.239
7	4.950	1.534	54.052	11.595	0.416
8	4.950	2.557	54.918	34.759	0.198
9	4.950	3.533	55.970	65.429	-0.093
10	4.950	4.357	68.821	96.617	-0.273
11	4.950	4.923	83.702	123.495	-0.390
12	4.950	5.163	96.657	138.990	-0.415
13	4.950	5.075	99.745	139.917	-0.394
14	4.950	4.730	99.485	130.180	-0.301
15	4.950	4.232	97.588	110.568	-0.127
16	4.950	3.688	81.169	85.345	-0.041
17	4.950	3.180	59.823	59.966	-0.001
18	4.950	2.767	59.762	37.718	0.216
19	4.950	2.491	57.329	22.054	0.246
20	4.950	2.374	31.858	12.675	0.188
21	4.950	2.432	22.948	6.309	0.163
22	0.990	2.554	1.669	0.658	0.010

STATION	SHEAR FORCE(MN)	BENDING MOMENT(MN)
1	0.009	0.010
2	0.066	0.196
3	0.123	0.666
4	0.180	1.419
5	0.253	3.093
6	0.493	4.341
7	0.910	7.813
8	1.108	12.807
9	1.015	18.063
10	0.741	22.415
11	0.353	25.138
12	-0.061	25.849
13	-0.456	24.570
14	-0.756	21.571
15	-0.883	17.518
16	-0.924	13.044
17	-0.918	8.469
18	-0.708	4.427
19	-0.362	1.779
20	-0.174	0.483
21	-0.010	-0.001

APPENDIX 4 OPERATIONAL REQUIREMENTS TO THE TRIMARAN DESTROYER

The operational requirements to the original destroyer design **(O'Brien & Russell 1993)** area summarised as the follows :

(1). SHIP ROLE

a) Sea Control. To provide support and escort to a task force with 'high value' units or a resupply and reinforcement convoy.

b) Naval Presence. To contribute to 'low key' operations world wide.

c) Projection of Power Ashore. To provide aerial support to tactical amphibious landings.

(2). PRIMARY TASKS

a) To detect and prosecute hostile airborne targets. To provide the primary area air defence capability against regimental attack when operating in support or escort roles.

b) To provide the area air defence needed in support of beach landing operations

c) To provide command, control and communications facilities when operating as flag ship.

(3) AREA OF OPERATIONS AND DURATION

a) Wartime: Eastern and Western Atlantic Area.

b) Peace and tension:World wide area.

c) Duration of mission: 60 days

(4) SIGNATURES

Design features must aim to produce the lowest practicable levels of relevant signatures.

(5). SPEEDS

A maximum sustainable speed of 30 knots is required and with a cruise speed of 20 knots.

Table A4.1 provides information on the vessel such as the intended weapon fit, complement, machinery fit, and cost estimate.

Table A4.1 Ship Characteristics of UCL 1993 Destroyer Design Study

Weapon Fit	2 x 32 FAMS [1], 1 x 5" Gun, 1 x Goalkeeper, 2 x 2 - 40mm, 2 x 20mm 1 Merlin Helicopter, 4 x AUV, 1 Towed Sonar, 1 x Type 2050 Hull Sonar
Machinery Fit	2.x WR21 Gas Turbine Generators, 2 x PA6V Diesel Gen. 2 x 16 MW AC Electric Motors, 2 x 0.5MW Salvage Gen.
Hull Form Characteristics	Main Hull C_B = 0.56 Air Gap = 3.65m Side Hull C_B = 0.56 Hull Sep = 4.0m
Complement	28 Officers, 67 Senior Rates, 133 Junior Rates = 228
Cost	£215m Unit Procurement Cost

Note: [1] FAMS -Family of Anti Air Missiles

APPENDIX 5 STABILITY ASSESSMENTS FOR THE TRIMARAN DESTROYER

1. Loading Conditions

Table A5.1 Loading conditions for the trimaran destroyer

Loading Condition	Displacement (t)	LCG (m)	VCG (m)
Ship 1			
Deep	4980	-4.00	7.70
Light	4205	-3.5	8.72
Ship 2			
Deep	4980	-4.00	7.70
Light	4205	-3.5	8.72

2. Stability Criteria (NES 109 1989)

Intact Stability

Area under GZ curve up to 30°	> 0.080 m-rad
Area under GZ curve up to 40°	> 0.133 m-rad
Area between 30° and 40°	> 0.048 m-rad
Maximum GZ	> 0.300 m-rad
Angle of Max. GZ	< 30 degrees
Liquid GM	> 0.30 m

Steady wind speed = 90 knots (ocean going vessel)

Wind heeling moment $M = M_o \cos^2\theta$

(where M_o is the upright heeling moment)

Angle of heel	< 30 degrees
GZ at Intersection	< 60% Maximum GZ
Area1/Area2	> 1.4

Damage Stability

Extent of damage - a minimum length of 15 % of the ship length of 22.65 metres, extending vertically without limit. This amounted to five adjacent compartments of one side hull to be flooded, each with a length of 5.7 metres, total 28.5 metres.

Steady wind speed = 32.56 knots	
Angle of list or loll	< 20 degrees
GZ at intersection	< 60 % GZ max.
Area1/Area2	>1.4

3. Calculated Cases

For Ship 1

Case 1. Intact stability at deep condition, Figure A5.1

Case 2. One side hull damaged at deep condition, Figures A5.2 & A5.3

Case 3. Intact stability at light condition Figure A5.4 .

Case 4. One side hull damaged at light condition, with 80 tonnes of ballast water in each side hull Figures A5.5 & A5.6.

For Ship 2

Case 5. Intact stability at deep condition, Figure A5.7

Case 6. One side hull damaged at deep condition, Figures A5.8 & A5.9

Case 7. Intact stability at light condition, Figure A5.10

Case 8. One side hull damaged at light condition, with 50 tonnes of ballast water in each side hull, Figures A5.11 & A5.12.

STABILITY FILENAME: DAMD00 DEMAND NAME: INTLNG

INITIAL CONDITION KG : 7.70 METRES
ANALYSIS CONDITION KG: 7.70 METRES
DISPLAYED KG : 7.70 METRES

CRITERION TYPES	VALUE	REQUIRED VALUE	RESULT
1	7.410	30.000	PASS
2	0.204	0.600	PASS
3	4.670	1.400	PASS
7	2.370	0.300	PASS
8	0.364	0.080	PASS
9	0.645	0.133	PASS
10	0.281	0.048	PASS

PARAMETERS

GZ CURVE	INTERACTION
θ_1 = 0.00	θ_A= 7.41
θ_2 =70.00	θ_B=70.00
θ_3 =43.73	θ_C=17.59
A = 1.485	A_1= 1.228
GZ_{MAX}= 1.762	A_2= 0.263
	H_{MAX}= 0.364

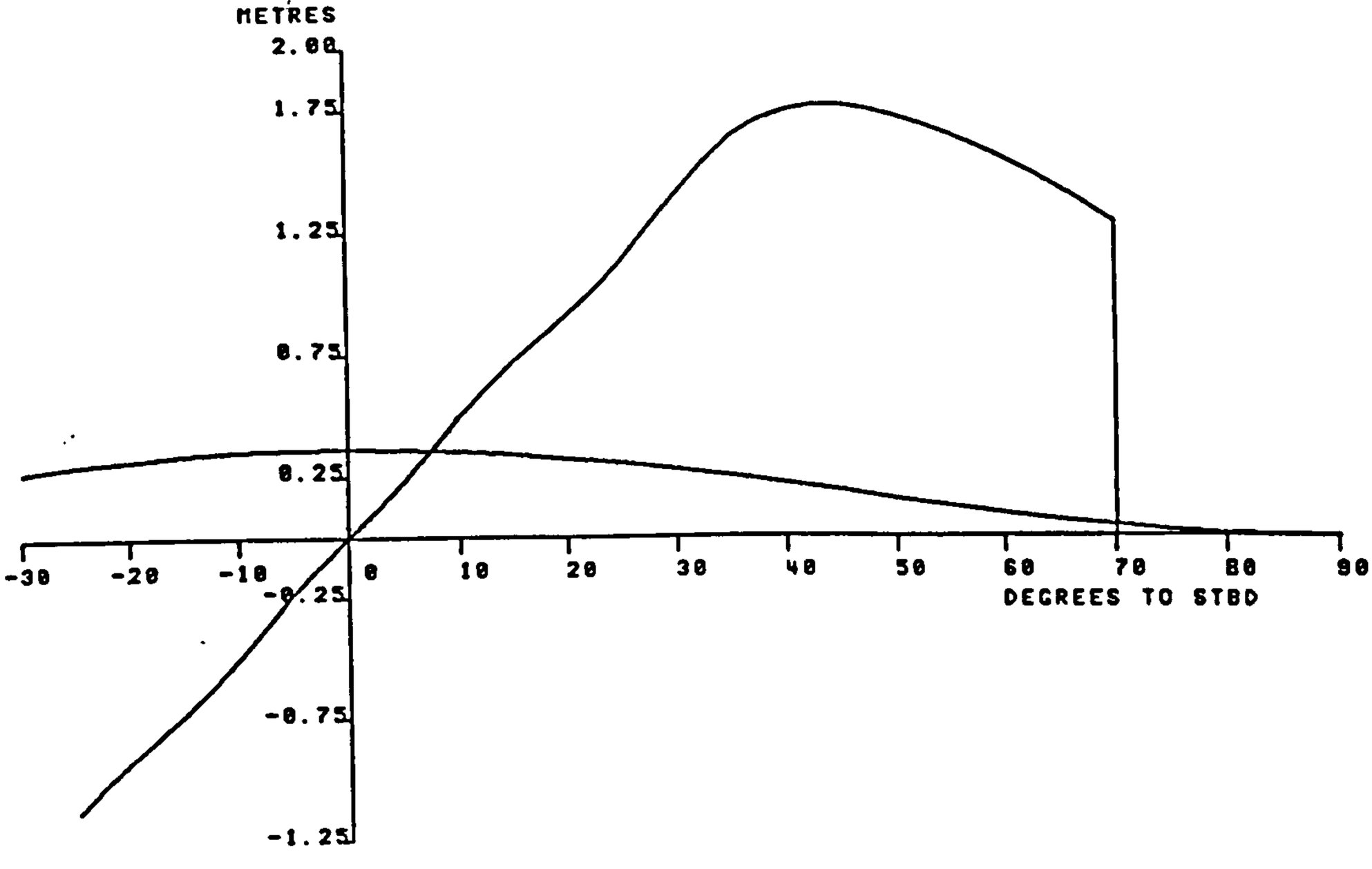

Figure A5.1 Intact GZ curve (Ship 1 at deep condition)

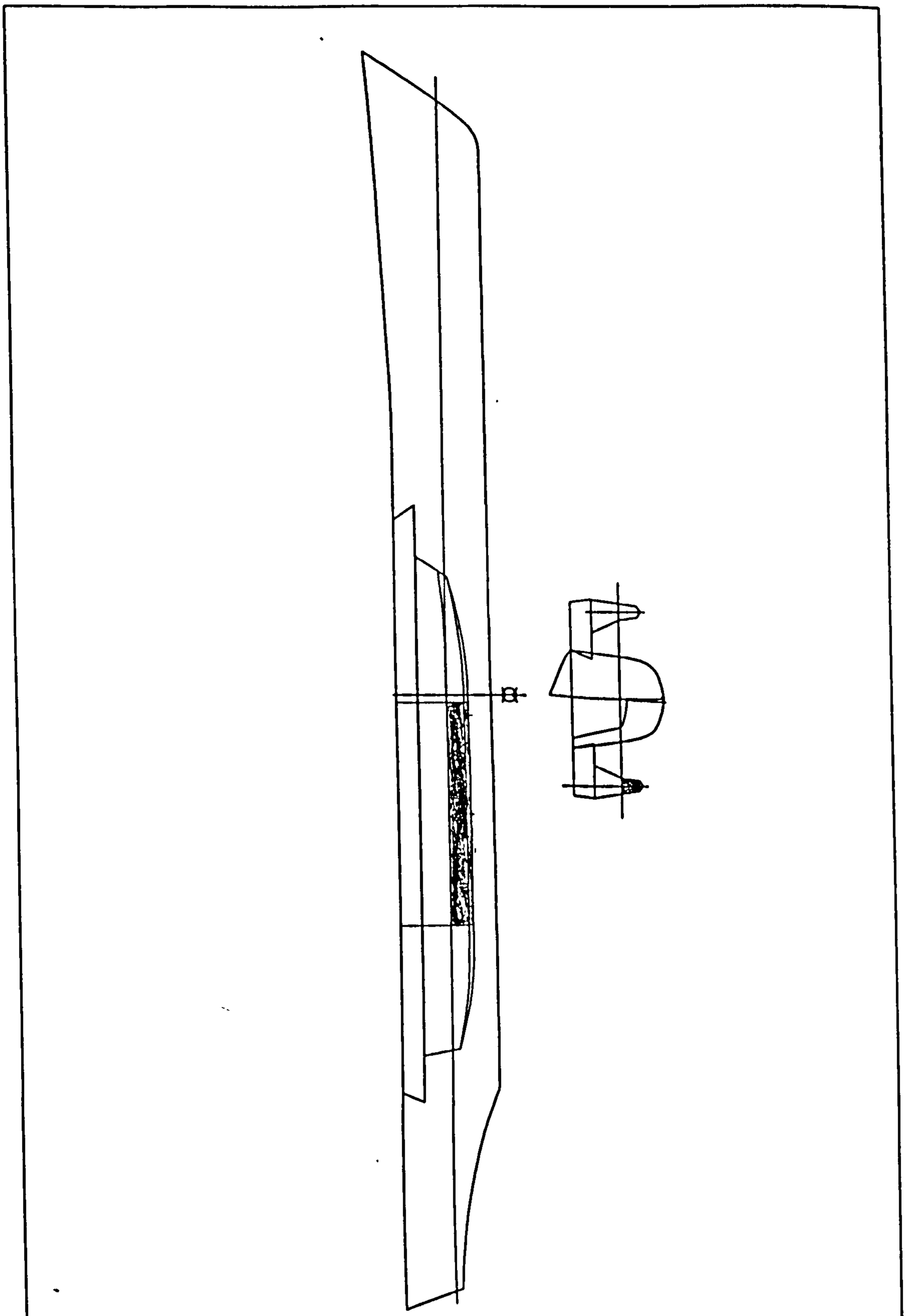

Flooded compartments

Figure A5.2 One side hull damaged (Ship 1 at deep condition)

STABILITY FILENAME: DAMD00 DEMAND NAME: DAMLNG

INITIAL CONDITION KG : 7.70 METRES
ANALYSIS CONDITION KG: 7.70 METRES
DISPLAYED KG : 7.70 METRES

CRITERION TYPES	VALUE	REQUIRED VALUE	RESULT
2	0.083	0.600	PASS
3	3.456	1.400	PASS
12	8.395	20.000	PASS

PARAMETERS

GZ CURVE	INTERACTION
θ_1 = 8.39	θ_A= 10.99
θ_2 =45.00	θ_B= 45.00
θ_3 =48.05	θ_C= -4.01
A = 0.208	A_1= 0.187
GZ_{MAX}= 0.538	A_2= 0.054
	H_{MAX}= 0.046

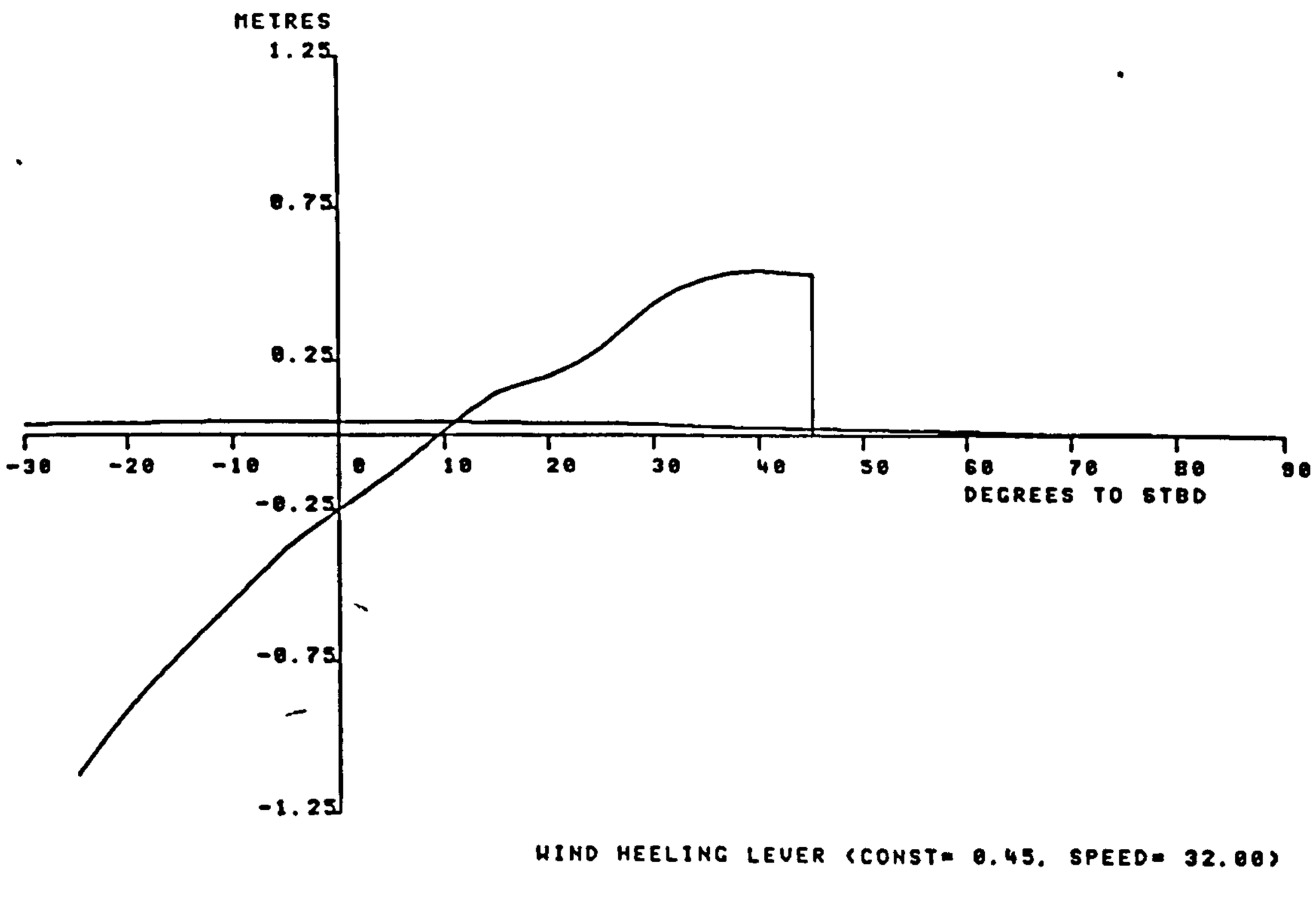

Figure A5.3 GZ curve after one side hull damaged (Ship 1 at deep condition)

STABILITY FILENAME: INTL90 DEMAND NAME: INTLNG

INITIAL CONDITION KG : 8.70 METRES
ANALYSIS CONDITION KG: 8.51 METRES
DISPLAYED KG : 8.51 METRES

CRITERION TYPES	VALUE	REQUIRED VALUE	RESULT
1	13.510	30.000	PASS
2	0.307	0.600	PASS
3	4.302	1.400	PASS
7	1.685	0.300	PASS
8	0.243	0.080	PASS
9	0.454	0 133	PASS
10	0.211	0 048	PASS

PARAMETERS

GZ CURVE	INTERACTION
θ_1 = 0.00	θ_A= 13.51
θ_2 =70.00	θ_B= 70.00
θ_3 =42.90	θ_C=-11.49
A = 1.055	A_1= 0.762
GZ_{MAX}= 1.371	A_2= 0.177
	H_{MAX}= 0.445

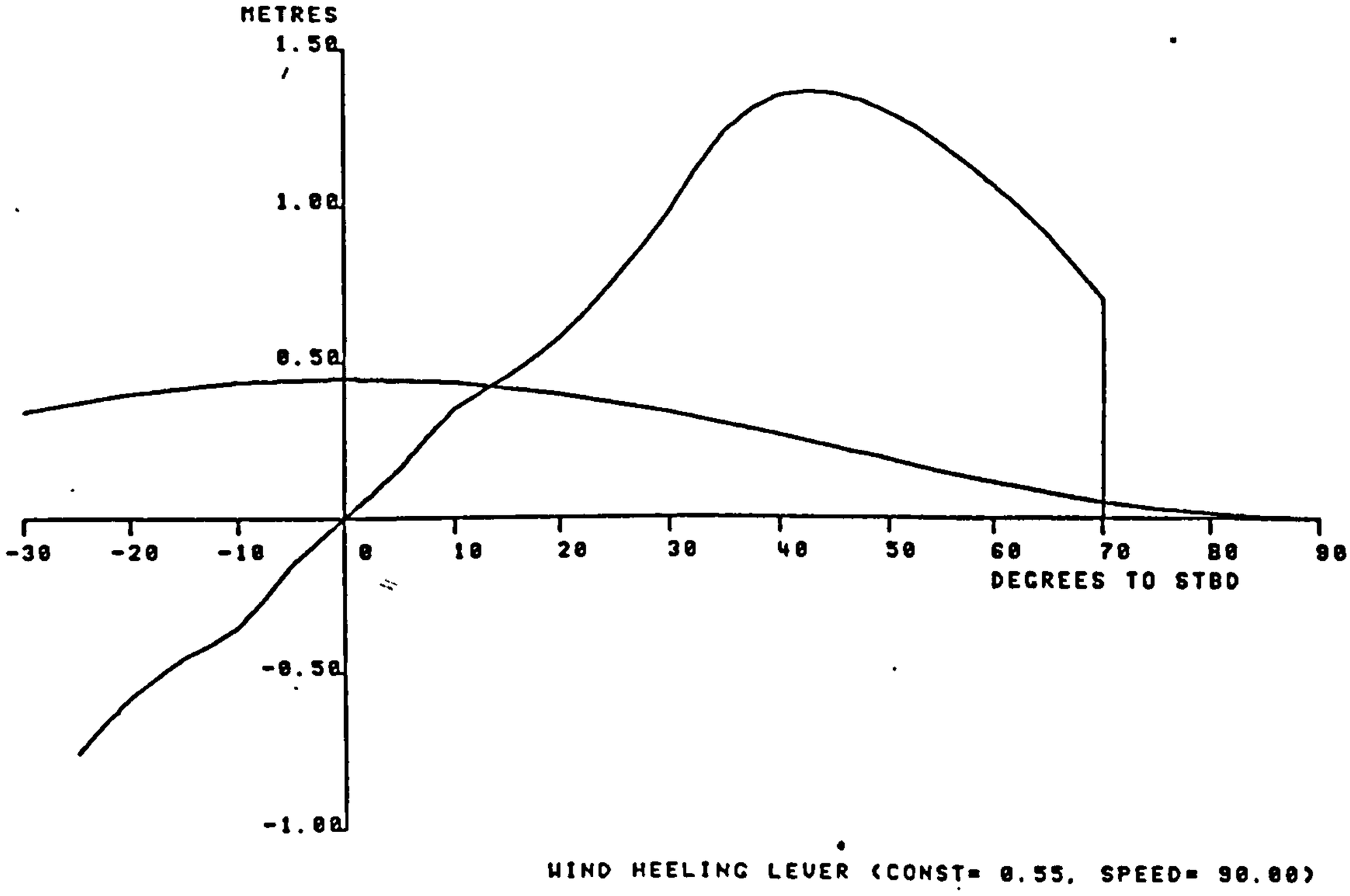

Figure A5.4 Intact GZ curve (Ship 1 at light condition)

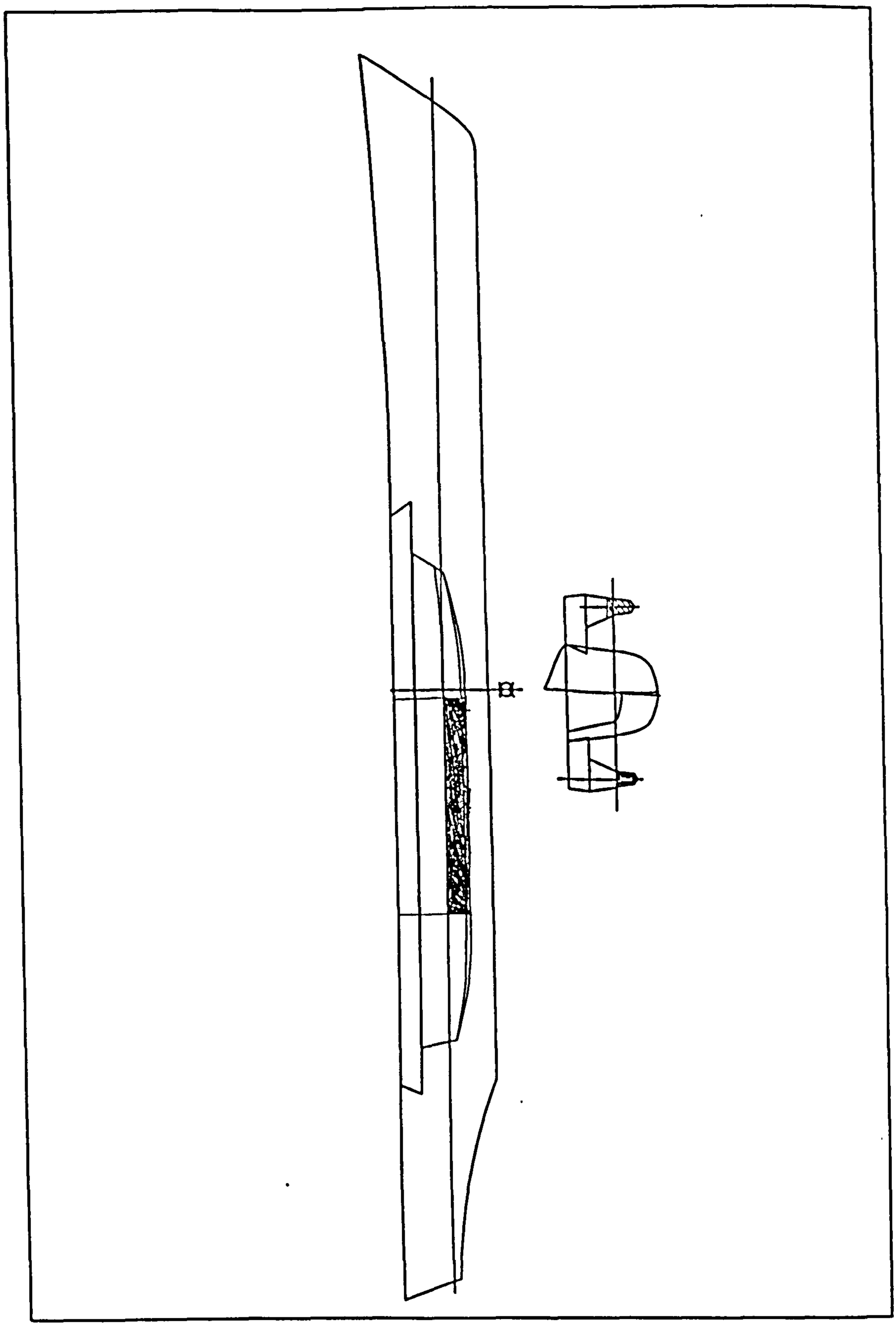

Figure A5.5 One side hull damaged and with 80t ballast water in the other side hull (Ship 1 at light condition)

STABILITY FILENAME: DAML90 DEMAND NAME: DAMLNG

CRITERION TYPES	VALUE	REQUIRED VALUE	RESULT
2	0.229	0.600	PASS
3	3.301	1.400	PASS
12	-1.605	20.000	PASS

INITIAL CONDITION KG : 8.70 METRES
ANALYSIS CONDITION KG: 8.60 METRES
DISPLAYED KG : 8.56 METRES

PARAMETERS

GZ CURVE	INTERACTION
θ_1 = -1.60	θ_A = 5.91
θ_2 = 45.00	θ_B = 45.00
θ_3 = 36.90	θ_C = -9.09
A = 0.089	A_1 = 0.057
GZ_{MAX} = 0.231	A_2 = 0.017
	H_{MAX} = 0.053

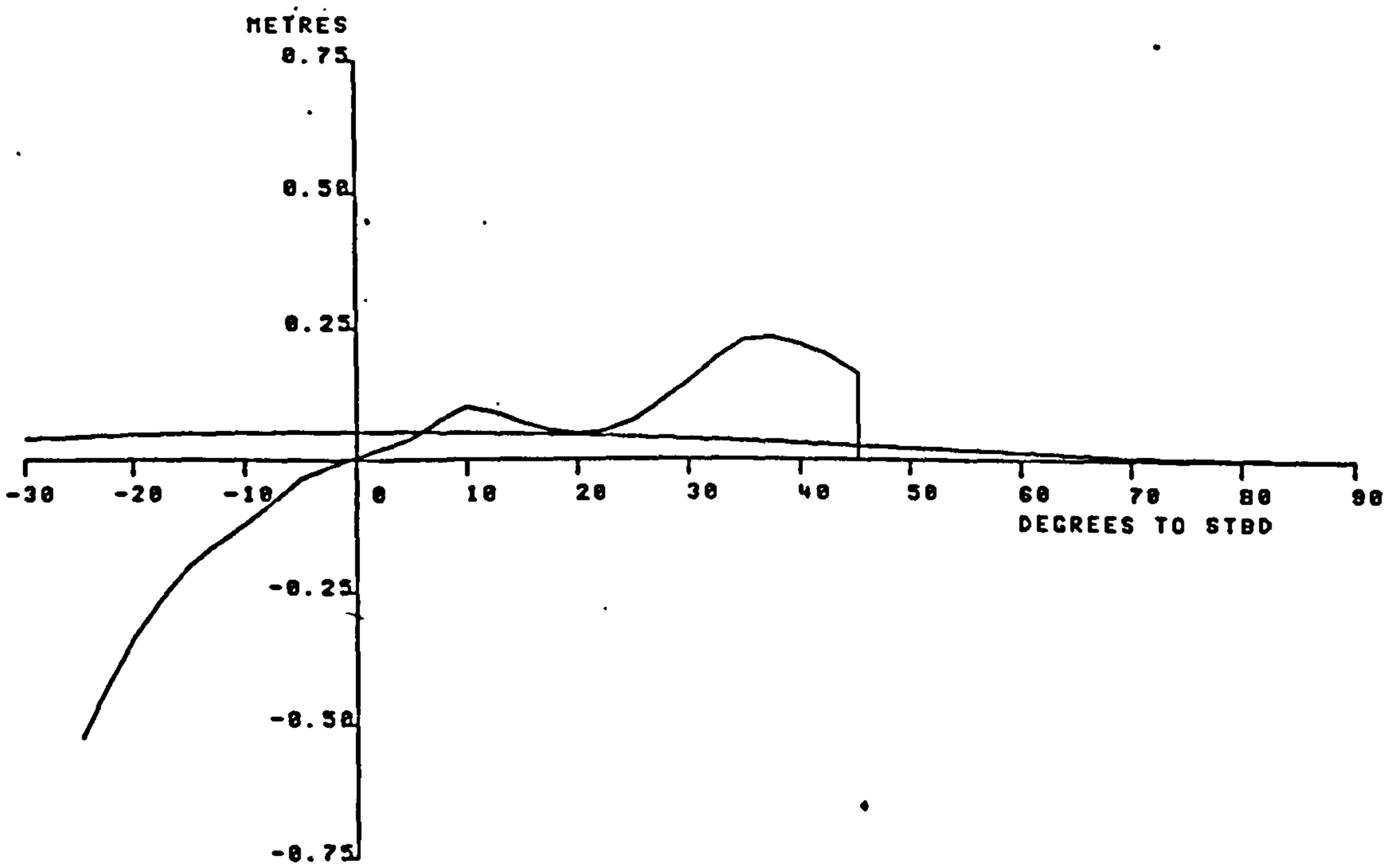

Figure A5.6 GZ curve after one side hull damaged and with 80t ballast water in the other side hull (Ship 1 at light condition)

STABILITY FILENAME: DAM2D1 DEMAND NAME: INT2D1

INITIAL CONDITION KG : 7.71 METRES
ANALYSIS CONDITION KG: 7.71 METRES
DISPLAYED KG : 7.71 METRES

CRITERION TYPES	VALUE	REQUIRED VALUE	RESULT
1	6.860	30.000	PASS
2	0.135	0.600	PASS
3	6.631	1.400	PASS
7	2.582	0.300	PASS
8	0.508	0.080	PASS
9	0.949	0.133	PASS
10	0.441	0.048	PASS

PARAMETERS

GZ CURVE	INTERACTION
θ_1 = 0.00	θ_A= 6.86
θ_2 =70.00	θ_B= 70.00
θ_3 =42.46	θ_C=-18.14
A = 2.210	A_1= 1.951
GZ_{MAX}= 2.670	A_2= 0.294
	H_{MAX}= 0.364

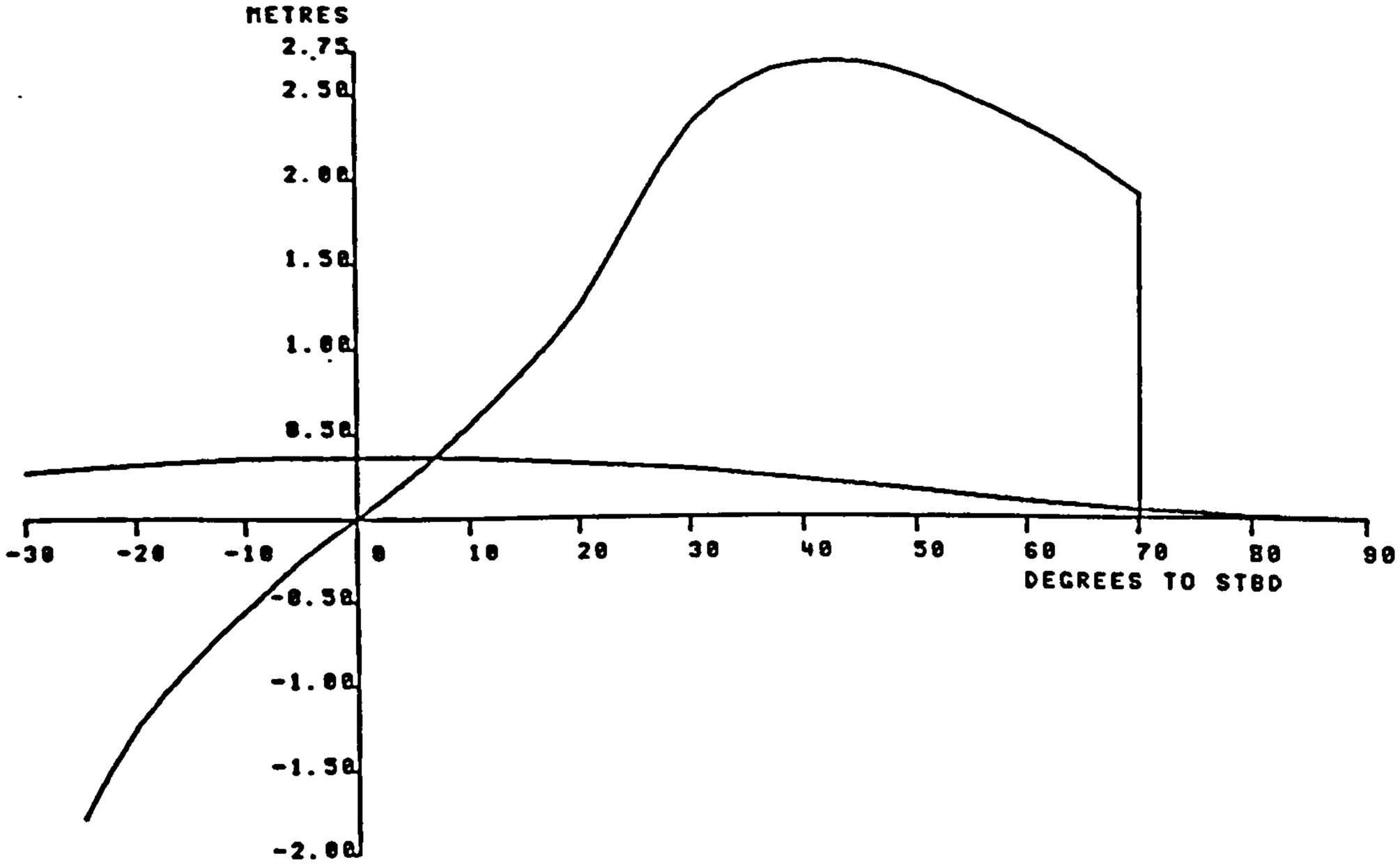

Figure A5.7 Intact GZ curve (Ship 2 at deep condition)

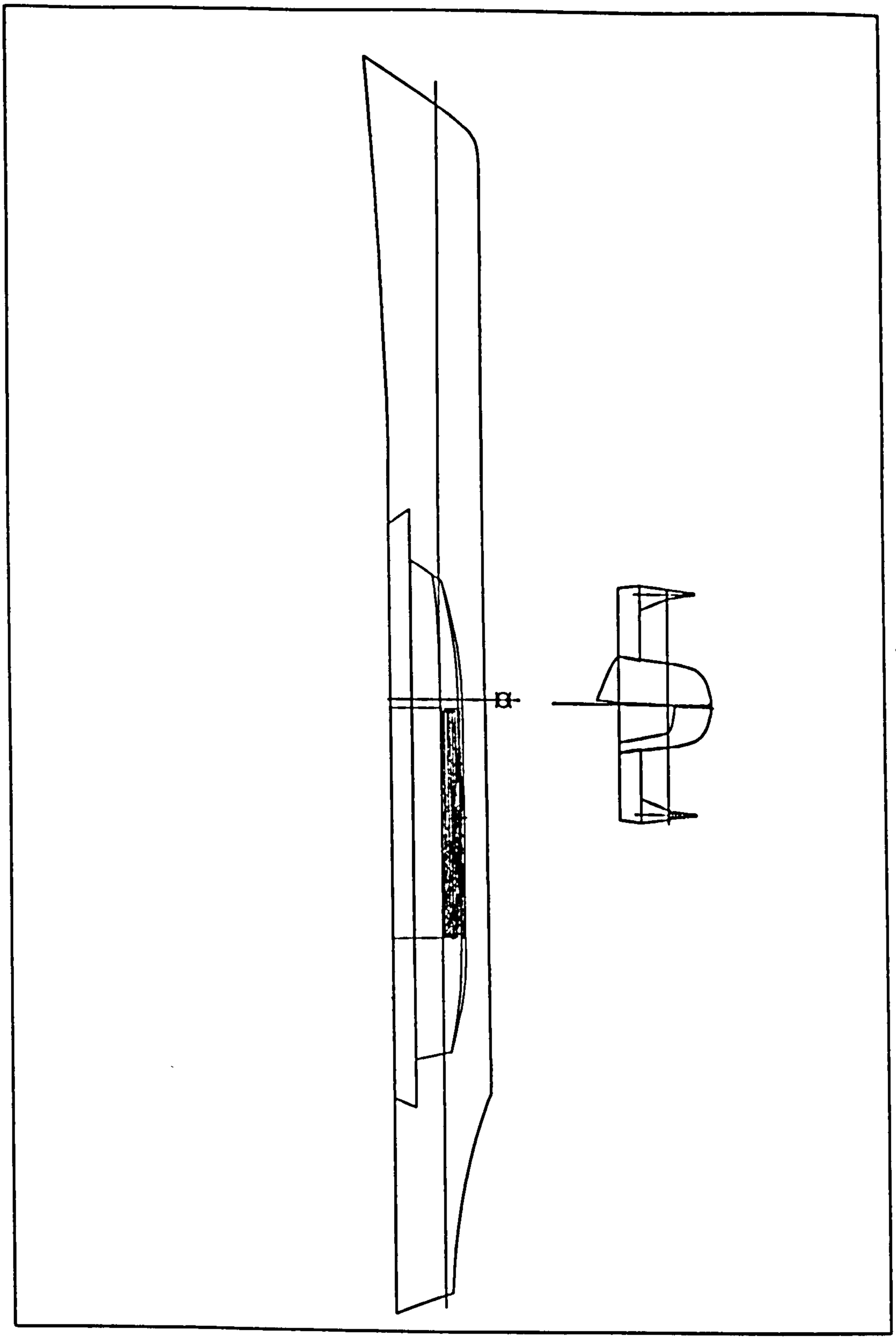

Flooded compartments

Figure A5.8 One side hull damaged (Ship 2 at deep condition)

STABILITY FILENAME: DAM2D1 DEMAND NAME: DAM2D1 INITIAL CONDITION KG : 7.71 METRES
ANALYSIS CONDITION KG: 7.71 METRES
DISPLAYED KG : 7.71 METRES

CRITERION TYPES	VALUE	REQUIRED VALUE	RESULT
2	0.043	0.600	PASS
3	7.555	1.400	PASS
12	7.395	20.000	PASS

PARAMETERS

GZ CURVE	INTERACTION
θ_1 = 7.39	θ_A= 9.82
θ_2 =45.00	θ_B= 45.00
θ_3 =39.17	θ_C= -5.18
A = 0.423	A_1= 0.401
GZ_{MAX}= 1.051	A_2= 0.053
	H_{MAX}= 0.046

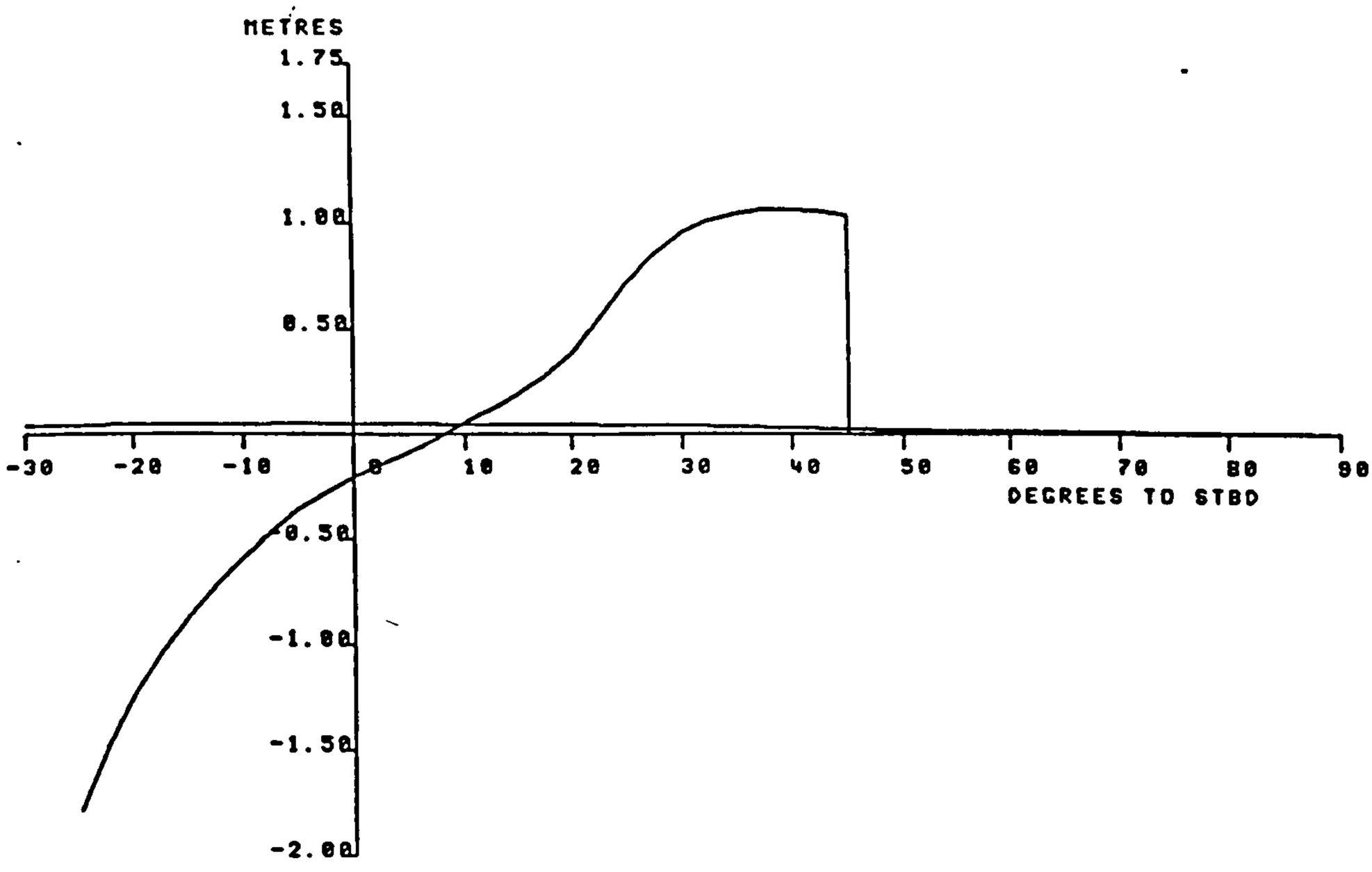

Figure A5.9 GZ curve after one side hull damaged (Ship 2 at deep condition)

STABILITY FILENAME: INT2L1 DEMAND NAME: INT2L1 INITIAL CONDITION KG : 8.72 METRES
ANALYSIS CONDITION KG: 8.60 METRES
DISPLAYED KG : 8.60 METRES

CRITERION TYPES	VALUE	REQUIRED VALUE	RESULT
1	11.410	30.000	PASS
2	0.184	0.600	PASS
3	7.175	1.400	PASS
7	1.653	0.300	PASS
8	0.377	0.080	PASS
9	0.760	0.133	PASS
10	0.382	0.040	PASS

PARAMETERS

GZ CURVE	INTERACTION
θ_1 = 0.00	θ_A= 11.41
θ_2 =70 00	θ_B= 70.00
θ_3 =41.38	θ_C=-13.59
A = 1.798	A_1= 1.502
GZ_{MAX}= 2.332	A_2= 0.209
	H_{MAX}= 0.445

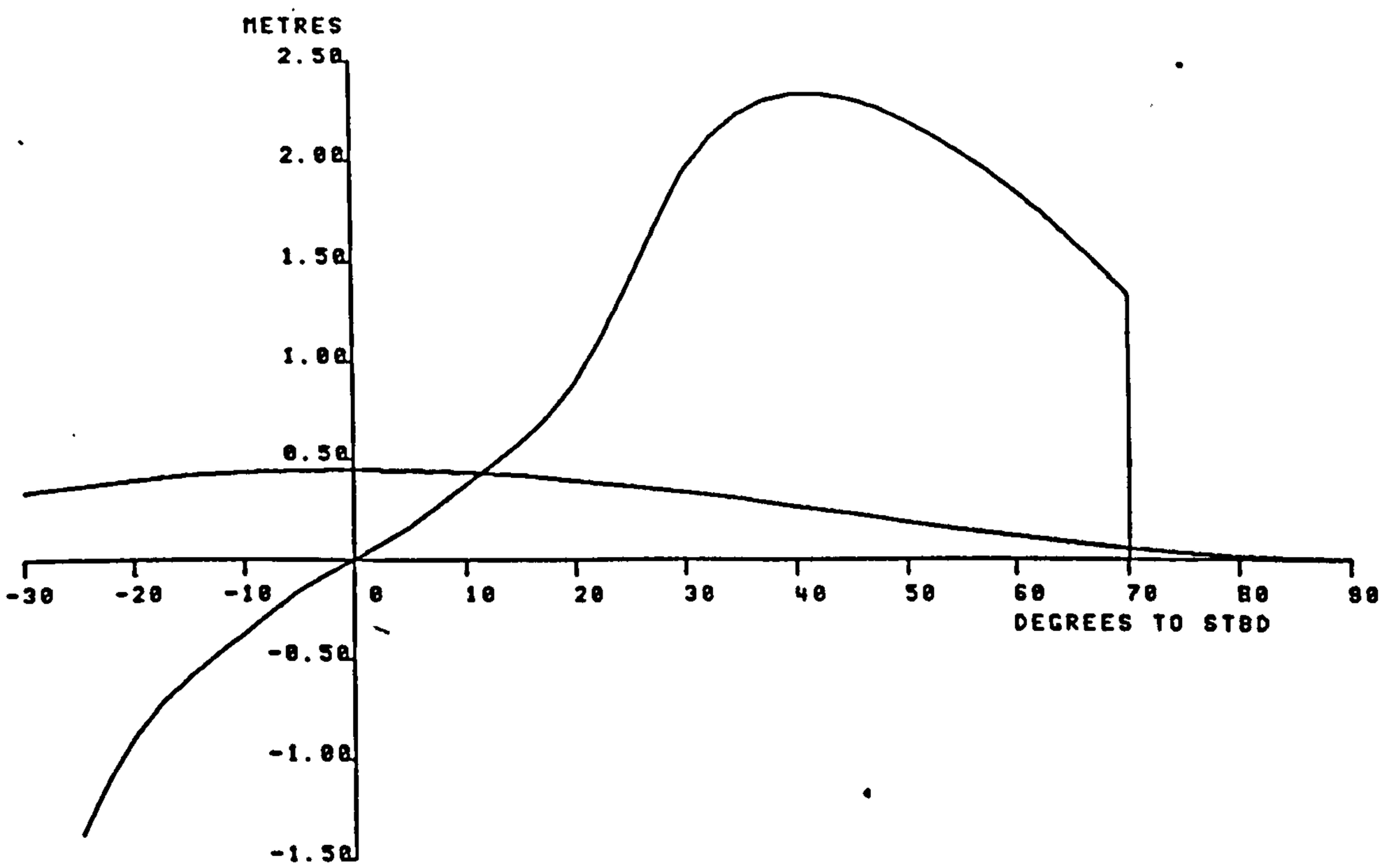

Figure A5.10 Intact GZ curve (Ship 2 at light condition)

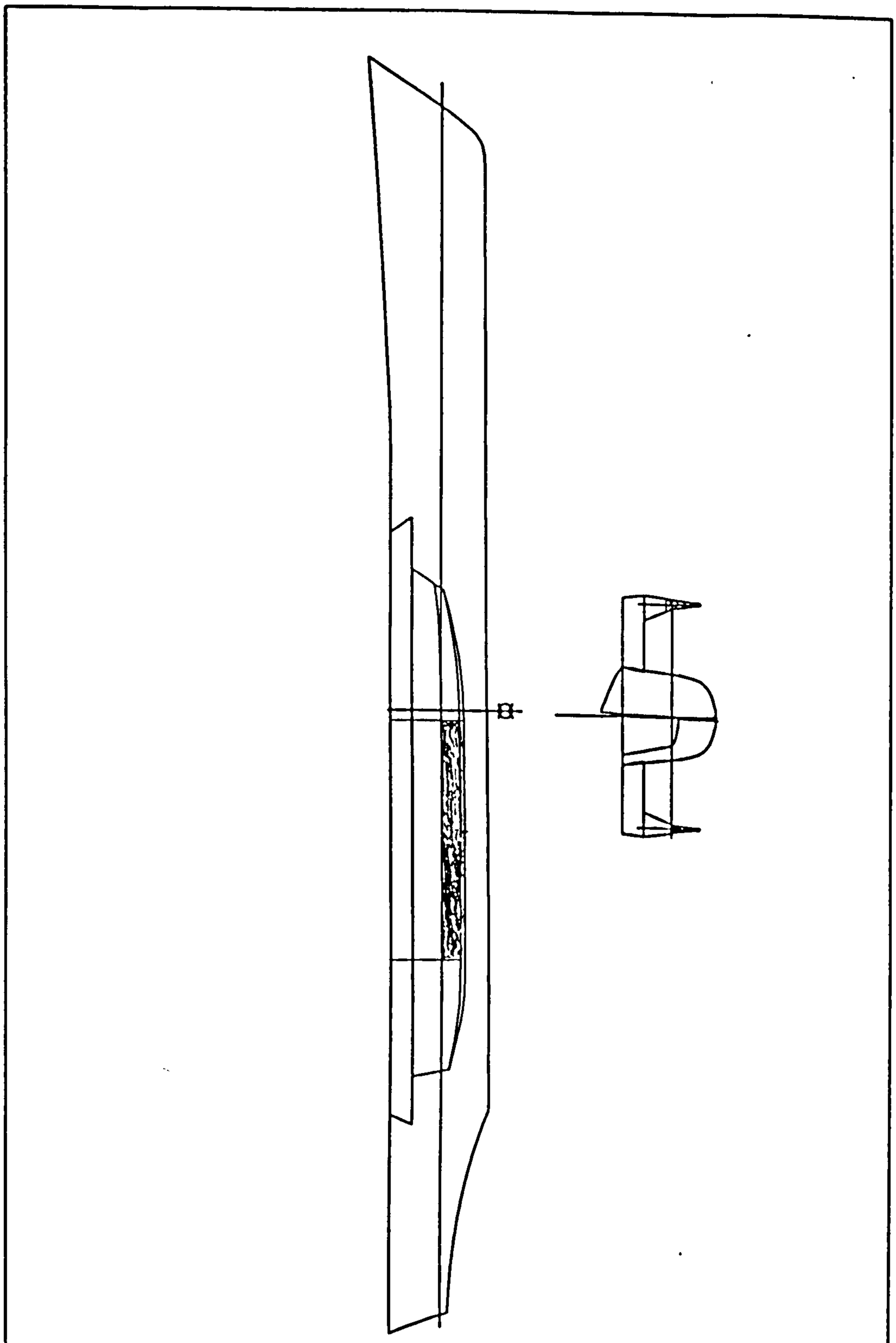

Flooded compartments

Ballast water

Figure A5.11 One side hull damaged and with 50t ballast water in the other side hull (Ship 2 at light condition)

STABILITY FILENAME: DAM2L1 DEMAND NAME: DAM2L1

INITIAL CONDITION KG : 8.72 METRES
ANALYSIS CONDITION KG: 8.66 METRES
DISPLAYED KG : 8.66 METRES

CRITERION TYPES	VALUE	REQUIRED VALUE	RESULT
2	0.069	0.600	PASS
3	21.978	1.400	PASS
12	5.395	20.000	PASS

PARAMETERS

GZ CURVE	INTERACTION
θ_1 = 5.39	θ_A= 15.73
θ_2 =45.00	θ_B= 45.00
θ_3 =36.17	θ_C= 0.73
A = 0 256	A_1= 0.232
GZ_{MAX}= 0.715	A_2= 0.011
	H_{MAX}= 0.053

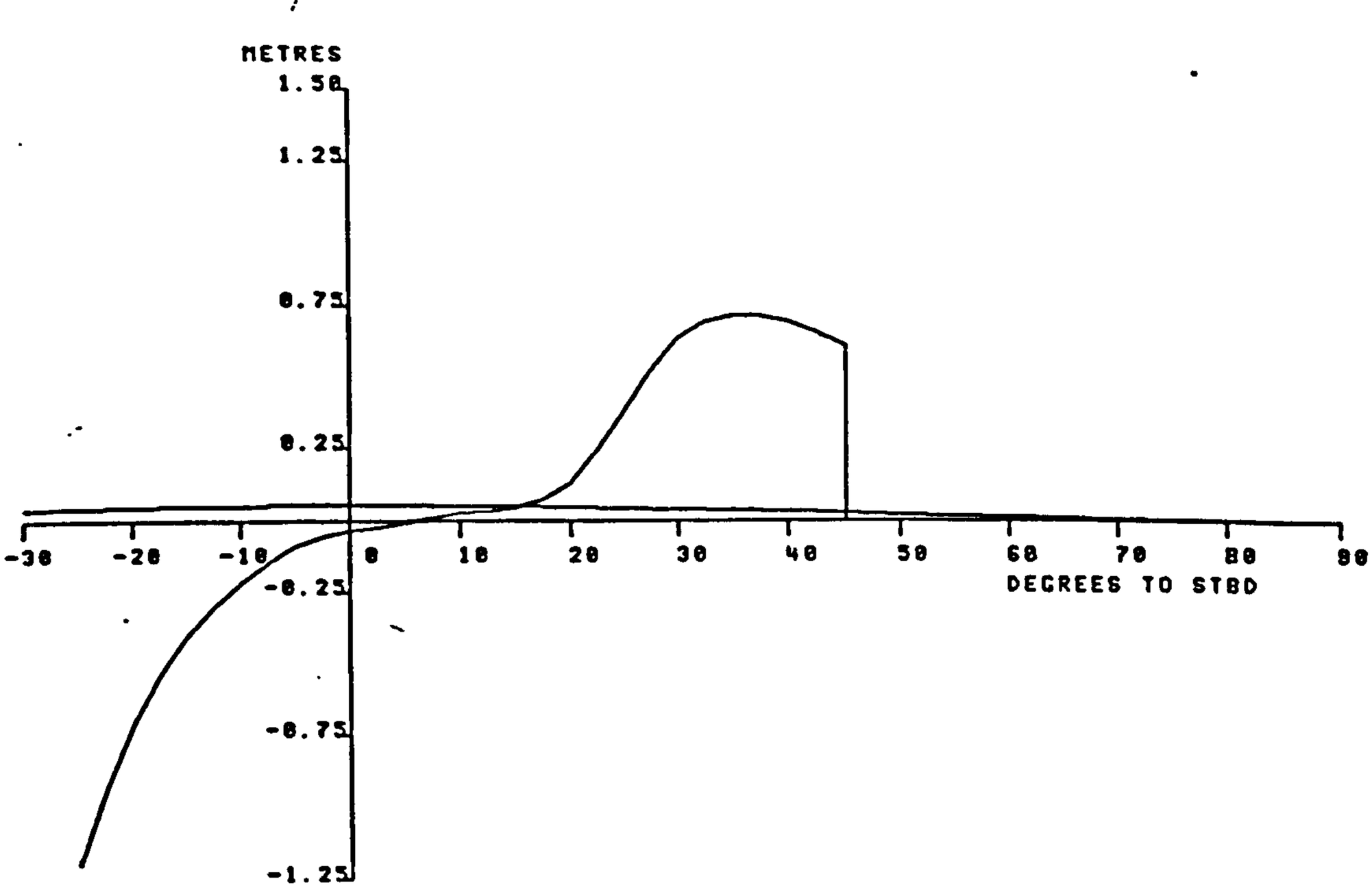

Figure A5.12 GZ curve after one side hull damaged and with 50t ballast water in the other side hull (Ship 2 at light condition)

APPENDIX 6 RESISTANCE CALCULATIONS & PROPELLER DESIGN FOR MODELS SHIP 1 & SHIP 2

The trimaran model ship is propelled by two fixed pitch propellers located at the stern of the centre hull. No propulsion devices are to be fitted to the side hulls. Two rudders are also located behind the propellers onto the centre hull.

The resistance of the hulls were determined using the Taylor-Gertler Series (**Gertler 1954**) as shown in Tables A6.2 to A6.4. The total powering data and curves are shown in Tables A6.5 and A6.6 for the two ships (models Ship 1 and Ship 2). The resistance of the centre hull was increased by 10 % to allow for appendages. Another 10% resistance was added to the ship to account for the wave interface effect between the centre hull and the side hulls

The GODDESS POWSPD program (based on 20 inch propeller) (**Gawn, 1952**) was used to perform the propeller design for the ship as shown in Table A6.7 and Figure A6.1. The arrangement of the propellers and the rudders is shown in Figure 6.2. The propeller characteristics are given in the following Table 6.1,

Table A6.1 Propeller characteristic for DRA model ships

Blades	3
Diameter	4.3 m
rpm	170
BAR	0.71
η_o	0.76

Table A6.2 Resistance calculation for the centre hull

Centre Hull Data

Hull Length	150.00	m
Hull Beam	10.80	m
Hull Draft	5.50	m
Displacement	4289.00	tonnes
L/B	15.85	
B/H	1.96	

Vc	0.001236	
Cp	0.581	
Wet Surf. Coeff.	2.546	
Wet Surf.	2014.287	m^2
Propul. coeff.	0.6	
Kinematic Visc.	1.61E-06	m^2/s
Density	1.02783	tonnes/m^3
Roughness Coeff.	0.0004	

1	2	3.00	4	5	6	7	8	9
Ship Speed (knot)	Fn	CR x 10^3		CR x10^3	Rn /10^6	CF x10^3 ITC 57	CT x10^3	PE (MW)
		B/H=2.25	B/H=3.00					
5	0.07	0.25	0.31	0.23	239.63	1.84	2.47	0.04
10	0.13	0.25	0.31	0.23	479.25	1.68	2.31	0.33
15	0.20	0.25	0.31	0.23	718.88	1.60	2.22	1.06
18	0.24	0.30	0.48	0.23	862.66	1.56	2.19	1.80
20	0.27	0.42	0.65	0.33	958.51	1.54	2.27	2.56
22	0.30	0.49	0.72	0.40	1054.36	1.52	2.32	3.48
24	0.32	0.59	0.91	0.47	1150.21	1.50	2.37	4.62
26	0.35	0.76	1.02	0.66	1246.06	1.49	2.55	6.32
28	0.38	1.13	1.22	1.10	1341.91	1.48	2.97	9.19
30	0.40	1.58	1.72	1.53	1437.76	1.46	3.39	12.90

Table A6.3 Resistance calculation for the side hull of Ship 1

Side hull Data

Hull Length	60.00	m
Hull Beam	1.80	m
Hull Draft	2.80	m
Displacement	198.00	tonnes
L/B	33.98	
B/H	0.64	

Cv	0.00089	
Cp	0.83	
Wet Surf. Coeff.	2.54	
Wet Surf.	273.075	m^2
Propul. coeff.	0.6	
Kinematic Visc.	1.61E-06	m^2/s
Density	1.02783	tonnes/m^3
Roughness Coeff.	0.0004	

1	2	3	4	5	6	7	8	9
Ship Speed (knot)	Fn	CR x 10^3		CR x10^3	Rn /10^6	CF x10^3 ITC 57	CT x10^3	PE (MW)
		B/H=2.25	B/H=3.00					
5	0.11	0.26	0.37	0.02	95.85	2.10	2.52	0.01
10	0.21	0.33	0.45	0.07	191.70	1.90	2.37	0.05
15	0.32	1.58	1.75	1.22	287.55	1.80	3.41	0.22
18	0.38	2.05	2.16	1.81	345.06	1.75	3.97	0.44
20	0.42	2.52	2.7	2.13	383.40	1.73	4.26	0.65
22	0.47	2.61	2.75	2.19	421.74	1.71	4.30	0.87
24	0.51	2.77	3.02	2.23	460.08	1.69	4.32	1.14
26	0.55	2.63	2.73	2.42	498.42	1.67	4.49	1.51
28	0.59	2.45	2.55	2.24	536.77	1.66	4.29	1.80
30	0.64	2.3	2.4	2.09	575.11	1.64	4.13	2.13

Table A6.4 Resistance calculation for the side hull of Ship 2

Side hull Data

Hull Length	60.00	m
Hull Beam	1.14	m
Hull Draft	3.50	m
Displacement	126.00	tonnes
L/B	52.96	
B/H	0.33	

Cv	0.00057	
Cp	0.79	
Wet Surf. Coeff.	2.54	
Wet Surf.	217.838	m^2
Propul. coeff.	0.6	
Kinematic Visc.	1.61E-06	m^2/s
Density	1.02783	tonnes/m^3
Roughness Coeff.	0.0004	

1	2	3	4	5	6	7	8	9
Ship Speed (knot)	Fn	CR x 10^3		CR x10^3	Rn /10^6	CF x10^3 ITC 57	CT x10^3	PE (MW)
		B/H=2.25	B/H=3.00					
5	0.11	0.26	0.37	-0.02	95.85	2.10	2.47	0.00
10	0.21	0.33	0.45	0.02	191.70	1.90	2.32	0.04
15	0.32	1.58	1.75	1.14	287.55	1.80	3.34	0.17
18	0.38	2.05	2.16	1.77	345.06	1.75	3.92	0.35
20	0.42	2.52	2.7	2.06	383.40	1.73	4.19	0.51
22	0.47	2.6	2.75	2.15	421.74	1.71	4.26	0.69
24	0.51	2.77	3.02	2.13	460.08	1.69	4.22	0.89
26	0.55	2.63	2.73	2.37	498.42	1.67	4.45	1.19
28	0.59	2.45	2.55	2.19	536.77	1.66	4.25	1.42
30	0.64	2.3	2.4	2.04	575.11	1.64	4.08	1.68

Table A6.5 Powering calculation for Ship 1

Ship Particulars

Ship Length	150.00	m	Propul Coeff.	0.6
Ship Beam	25.00	m		
Ship Draft	5.50	m	L/B	10.55
Displacement	4685.00	tonnes	B/H	4.55

1	2	3	4	5	6
Ship Speed (knot)	PE Main Hull (MW)	PE Side Hull (MW)	PE Total (MW)	PS (MW)	PS + APP & W Int. (MW)
5	0.04	0.01	0.06	0.09	0.11
10	0.33	0.05	0.42	0.69	0.82
15	1.06	0.22	1.50	2.49	2.94
18	1.80	0.44	2.68	4.47	5.25
20	2.56	0.65	3.86	6.44	7.55
22	3.48	0.87	5.23	8.72	10.23
24	4.62	1.14	6.90	11.51	13.50
26	6.32	1.51	9.33	15.55	18.26
28	9.19	1.80	12.79	21.32	25.14
30	12.90	2.13	17.16	28.59	33.82

Table A6.6 Powering calculation for Ship 2

Ship Particulars

Ship Length	150.00	m	Propul Coeff.	0.6	
Ship Beam	30.00	m			
Ship Draft	5.50	m	L/B	10.45	
Displacement	4537.00	tonnes	B/H	5.45	

1	2	3	4	5	6
Ship Speed (knot)	PE Main Hull (MW)	PE Side Hull (MW)	PE Total (MW)	PS (MW)	PS + APP & W Int. (MW)
5	0.04	0.00	0.05	0.09	0.11
10	0.33	0.04	0.40	0.66	0.79
15	1.06	0.17	1.40	2.33	2.76
18	1.80	0.35	2.50	4.16	4.91
20	2.56	0.51	3.58	5.97	7.03
22	3.48	0.69	4.87	8.11	9.56
24	4.62	0.89	6.40	10.66	12.58
26	6.32	1.19	8.70	14.50	17.10
28	9.19	1.42	12.04	20.06	23.75
30	12.90	1.68	16.26	27.10	32.17

Table A6.7 GODDESS output of propeller design data

GODDESS Program: POWSPD VERSION: A-01.04/VAX Username: J_ZHANG

Listing Title: HULL RESISTANCE RESULTS Listing Created: 11-NOV-1993 13:09

Study Reference: Study Title:
Ship dimensions: LBP: 55.000 m Maximum Beam at Design Waterline: 2.000 m Depth at Sides Amidships: 6.000 m

LENGTH BETWEEN PERPENDICULARS	151.0 METRES	TRIPLET	20
WATERLINE BEAM	10.8 METRES	PARENT	40
DRAUGHT	5.5 METRES	APPENDAGES	0
CHOSEN DISPLACEMENT	4980.0 TONNES		
PRISMATIC COEFFICIENT	0.000		

CONDITION: CLEAN---------(K= 0.00) TEMPERATE-----(K= 0.00) TROPICAL------(K= 0.56)

SPEED KNOTS	FROUDE NO	FROUDE DIS NO	PENH KW	PEAPP KW	PET KW	PENH KW	PEAPP KW	PET KW	PENH KW	PEAPP KW	PET KW	SPEED KNOTS
18	0.2406	0.7186	3240.	0.	3240.	3240.	0.	3240.	4013.	0.	4013.	18
19	0.2540	0.7586	3950.	0.	3950.	3950.	0.	3950.	4853.	0.	4853.	19
20	0.2674	0.7985	4660.	0.	4660.	4660.	0.	4660.	5706.	0.	5707.	20
21	0.2807	0.8384	5490.	0.	5490.	5490.	0.	5490.	6694.	0.	6694.	21
22	0.2941	0.8783	6310.	0.	6310.	6310.	0.	6310.	7687.	0.	7687.	22
23	0.3075	0.9183	7320.	0.	7320.	7320.	0.	7320.	8885.	0.	8885.	23
24	0.3208	0.9582	8330.	0.	8330.	8330.	0.	8330.	10099.	0.	10099.	24
25	0.3342	0.9981	9800.	0.	9800.	9800.	0.	9800.	11789.	0.	11789.	25
26	0.3476	1.0380	11270.	0.	11270.	11270.	0.	11270.	13497.	0.	13497.	26
27	0.3610	1.0780	13400.	0.	13400.	13400.	0.	13400.	15883.	0.	15883.	27
28	0.3743	1.1179	15530.	0.	15530.	15530.	0.	15530.	18287.	0.	18287.	28
29	0.3877	1.1578	18220.	0.	18220.	18220.	0.	18220.	21270.	0.	21270.	29
30	0.4011	1.1977	20910.	0.	20910.	20910.	0.	20910.	24273.	0.	24273.	30

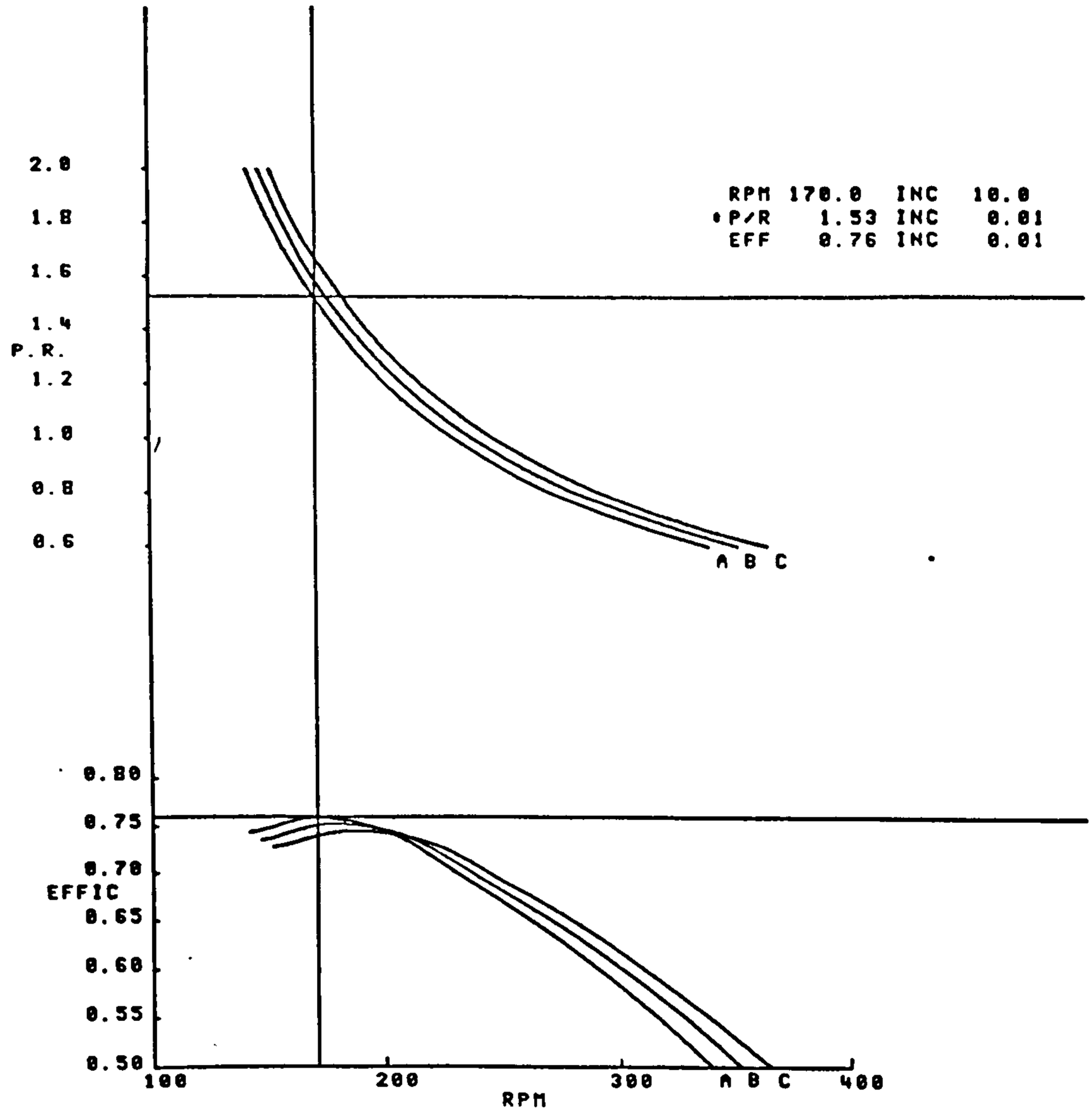

Figure A6.1 Propeller design curves

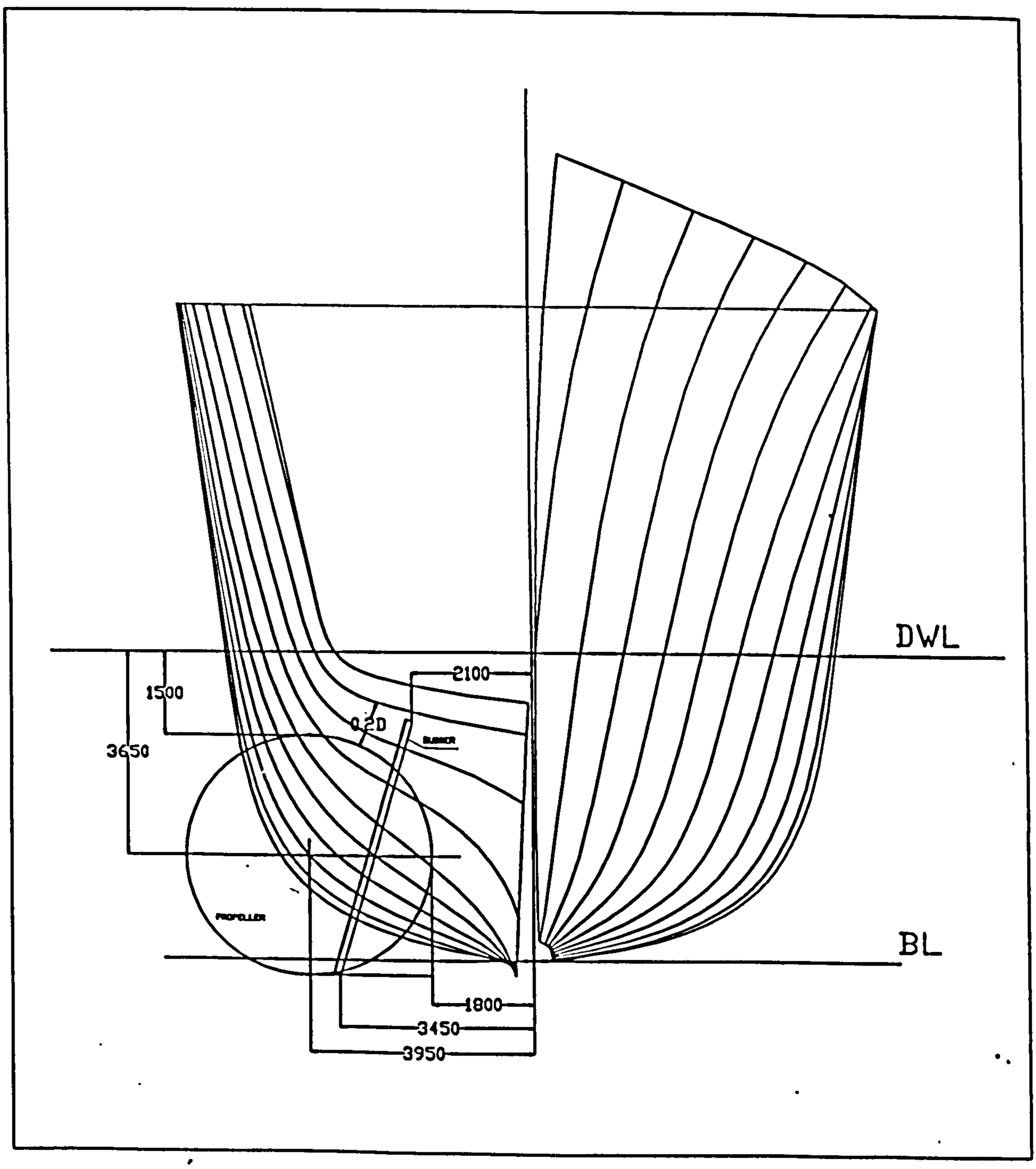

Figure A6.2 Propeller and rudder arrangement in the centre hull of DRA models

APPENDIX 7 MASS INERTIA CALCULATION FOR MODELS SHIP 1 & SHIP 2

The tables in this appendix show the mass inertia calculation for models Ship 1 and Ship 2 regarding to the description in Section 4.3.4.

Table A7.1 Pitching Inertia of Ship 1 (Deep Condition)

Station	Mass (tonne)	Location (metre)	Longl. Mom. tonne-m	Iyy tonne-m^2
21	159.00	-75.50	-12005	906340
20	111.00	-67.95	-7542	512509
19	122.00	-60.40	-7369	445076
18	208.00	-52.85	-10993	580969
17	414.00	-45.30	-18754	849565
16	240.00	-37.75	-9060	342015
15	276.00	-30.20	-8335	251723
14	261.00	-22.65	-5912	133899
13	283.00	-15.10	-4273	64527
12	241.00	-7.55	-1820	13738
11	315.00	0.00	0	0
10	358.00	7.55	2703	20407
9	234.00	15.10	3533	53354
8	380.00	22.65	8607	194949
7	146.00	30.20	4409	133158
6	275.00	37.75	10381	391892
5	171.00	45.30	7746	350907
4	139.00	52.85	7346	388244
3	136.00	60.40	8214	496150
2	110.00	67.95	7474	507892
1	106.00	75.50	8003	604227
		LCG		
SUM	4685.00	-3.77	-17644	7241541
		To the centre of gravity		7175090
Pitching radius gyration of the ship				39.13 m

Table A7.2 Pitching Inertia of Ship 2 (Deep Condition)

Station	Mass (tonne)	Location (metre)	Longl. Mom. tonne-m	Iyy tonne-m^2
21	148.00	-75.50	-11174	843637
20	107.73	-67.95	-7320	497390
19	118.40	-60.40	-7151	431946
18	201.86	-52.85	-10669	563831
17	389.70	-45.30	-17653	799699
16	232.92	-37.75	-8793	331926
15	267.86	-30.20	-8089	244297
14	253.30	-22.65	-5737	129949
13	274.65	-15.10	-4147	62623
12	233.89	-7.55	-1766	13332
11	308.71	0.00	0	0
10	347.44	7.55	2623	19805
9	227.10	15.10	3429	51780
8	368.79	22.65	8353	189198
7	147.00	30.20	4439	134070
6	266.89	37.75	10075	380331
5	165.96	45.30	7518	340556
4	134.90	52.85	7129	376791
3	131.99	60.40	7972	481513
2	111.20	67.95	7556	513433
1	102.87	75.50	7767	586402
		LCG		
SUM	4541.15	-3.44	-15638	6992509
		To the centre of gravity		6938661
Pitching radius gyration of the ship				39.09 m

Table A7.3 Rolling Inertia of Ship 1 (Deep Condition)

1. Displacement of the ship	4685	tonnes	**VCG**	8.10	metre
			LCG	-3.77	metre

2. Mass and inertia of side hulls and cross structures:

Item	Mass	Location (metre)			Size (metre)		Ixx
	(tonne)	X	Y	Z	width	height	t-m^2
Structure							
Side Hulls	172.44		10.80	6.00	2.40	6.50	27011
Cross Box	123.00		8.95	10.35	6.70	2.70	23564
Fittings							
Boats	10.32		10.00	12.90			2749
Personnel							
Officers II	6.68		9.05	10.20	6.70	2.70	1271
Officers III	7.65		9.05	10.20	6.70	2.70	1456
CPO's	6.53		9.05	10.20	6.70	2.70	1243
PO's	6.59		10.10	10.20	6.70	2.70	1387
JR Messes	11.18		7.50	10.20	6.70	2.70	1841
Payload							
40mm Guns	15.00		11.00	12.90			4311
SUM	359.39						64832
						Inertia to the centre of gravity	41252

3. Centre hull

Mass of the centre hull	4326	tonnes
Radius of Gyration of centre hull	3.89	meter
Rolling Inertia of The Centre Hull	65456	tonnes-m

4. The ship

Mass of the ship	4685	tonnes
Rolling inertia of the ship	106708	tonne-m^2
Radius of gyration of the ship	4.77	metre

Table A7.4 Rolling Inertia of Ship 2 (Deep Condition)

1. Displacement of the ship	4541	tonnes	**VCG**	8.21			
			LCG	-3.44			
2. Mass and inertia of side hulls and cross structures:							
Item	Mass	Location (metre)			Size (metre)		Ixx
	(tonne)	X	Y	Z	width	height	t-m^2
Structure							
Side Hulls	111.80		13.60	6.00	2.00	7.00	25197
Cross Box	161.00		10.50	10.35	8.80	2.70	36134
Fittings							
Boats	10.32		12.00	12.90			3203
Personnel							
Officers II	6.68		10.60	10.20	8.80	2.70	1493
Officers III	7.65		10.60	10.20	8.80	2.70	1709
CPO's	6.53		10.60	10.20	8.80	2.70	1459
PO's	6.59		10.80	10.20	8.80	2.70	1501
JR Messes	11.18		9.50	10.20	8.80	2.70	2251
Payload							
40mm Guns	15.00		12.20	12.90			4729
SUM	336.75						77676
						Inertia to the centre of gravity	54978
3. Centre hull							
Mass of the main hull	4204	tonnes					
Radius of Gyration of main hull	3.89	metre					
Rolling Inertia of The Main Hull	63619	tonne-m^2					
4. The ship							
Mass of the ship	4541	tonnes					
Rolling inertia of the ship	118597	tonne-m^2					
Radius of gyration of the ship	5.11	metre					